MICROCOPY RESOLUTION TEST CHART

NAVAL POSTGRADUATE SCHOOL
Monterey, California

DTIC

S

JUN 1 5 1988

H

D

THESIS

Design Considerations for the ORION Satellite:
Structure, Propulsion and Attitude Control
Subsystems for a Small, General Purpose Spacecraft

by

Austin Walker Boyd, Jr.

March 1988

Thesis Advisor: Allen E. Fuhs

Approved for public release: distribution is unlimited.

88 6 14 013

REPORT DOCUMENTATION PAGE

1a REPORT SECURITY CLASSIFICATION UNCLASSIFIED	1b RESTRICTIVE MARKINGS NONE
2a SECURITY CLASSIFICATION AUTHORITY ---	3 DISTRIBUTION/AVAILABILITY OF REPORT APPROVED FOR PUBLIC RELEASE; DISTRIBUTION IS UNLIMITED
2b DECLASSIFICATION/DOWNGRADING SCHEDULE NONE	
4 PERFORMING ORGANIZATION REPORT NUMBER(S)	5 MONITORING ORGANIZATION REPORT NUMBER(S)

6a NAME OF PERFORMING ORGANIZATION NAVAL POSTGRADUATE SCHOOL	6b OFFICE SYMBOL (If applicable) CODE 72	7a NAME OF MONITORING ORGANIZATION NAVAL POSTGRADUATE SCHOOL
6c ADDRESS (City, State, and ZIP Code) MONTEREY, CALIFORNIA 93943-5000		7b ADDRESS (City, State, and ZIP Code) MONTEREY, CALIFORNIA 93943-5000

8a NAME OF FUNDING/SPONSORING ORGANIZATION HEADQUARTERS, US AIR FORCE	8b OFFICE SYMBOL (If applicable) AFTAC/TXO	9 PROCUREMENT INSTRUMENT IDENTIFICATION NUMBER

8c ADDRESS (City, State, and ZIP Code) AFTAC/TXO PATRICK AFB, FLORIDA 32925-6011	10 SOURCE OF FUNDING NUMBERS			
	PROGRAM ELEMENT NO	PROJECT NO	TASK NO	WORK UNIT ACCESSION NO

11 TITLE (Include Security Classification) DESIGN CONSIDERATIONS FOR THE ORION SATELLITE: STRUCTURE, PROPULSION AND ATTITUDE CONTROL SUBSYSTEMS FOR A SMALL, GENERAL PURPOSE SATELLITE

12 PERSONAL AUTHOR(S) JUSTIN W. BOYD

13a TYPE OF REPORT MASTERS THESIS	13b TIME COVERED FROM _____ TO _____	14 DATE OF REPORT (Year, Month, Day) 1988 MARCH	15 PAGE COUNT 626

16 SUPPLEMENTARY NOTATION THE VIEWS EXPRESSED IN THIS THESIS ARE THOSE OF THE AUTHOR ONLY AND DO NOT REFLECT THE POLICY OR POSITION OF THE DEPARTMENT OF DEFENSE OR US GOVERNMENT.

17	COSATI CODES		18 SUBJECT TERMS (Continue on reverse if necessary and identify by block number)
FIELD	GROUP	SUB-GROUP	SATELLITE, LIGHTSAT, GETAWAY SPECIAL, ORION, SPIN STABILIZATION, ATTITUDE CONTROL, GENERAL PURPOSE, HYDRAZINE, LOW COST, NAVY, NAVAL POSTGRADUATE SCHOOL

19 ABSTRACT (Continue on reverse if necessary and identify by block number)

A general purpose satellite (ORION) has been designed which will launch from the Space Shuttle using a NASA Get-Away-Special (GAS) canister. The design is based on the use of a new extended GAS canister and a low profile launch mechanism. The satellite is also configured to launch as a dedicated payload on SCOUT or commercial expendable launch vehicles. The satellite is cylindrical, measuring 19 inches in diameter and 35 inches long. The maximum spacecraft mass is 250 pounds, of which 32 pounds are nominally dedicated to user payloads. The remaining 218

20 DISTRIBUTION/AVAILABILITY OF ABSTRACT ☑ UNCLASSIFIED/UNLIMITED ☐ SAME AS RPT ☐ DTIC USERS	21 ABSTRACT SECURITY CLASSIFICATION UNCLASSIFIED	
22a NAME OF RESPONSIBLE INDIVIDUAL ALLEN E. FUHS	22b TELEPHONE (Include Area Code) 408-646-2958	22c OFFICE SYMBOL Code 72

DD FORM 1473, 84 MAR
83 APR edition may be used until exhausted
All other editions are obsolete

1

pounds encompass the satellite structure and support elements, which include a hydrazine propulsion subsystem and a spin stabilized attitude control subsystem. The propulsion subsystem provides sufficient impulse to enable circular orbits as high as 835 nm or elliptic orbits with apogees at 2200 nm, leaving a nominal Shuttle orbit of 135 nm. Four stabilizing booms or active nutation control techniques are employed for spin stabilization about the longitudinal axis of the spacecraft. Attitude control accuracies on the order of 1° are attainable for a total mission duration of 90 days to 3 years. Total satellite cost is $1.5 million. The thesis outlines the history of general purpose spacecraft, the ORION design criteria, and the design of the major subsystems.

Accession For

NTIS GRA&I	☑
DTIC TAB	☐
Unannounced	☐
Justification	

By

Distribution/

Availability Codes

| Dist | Avail and/or Special |
| A-1 | |

DTIC
COPY
INSPECTED
4

Design Considerations for the ORION Satellite:
Structure, Propulsion, and Attitude Control
Subsystems for a Small, General Purpose Spacecraft

by

Austin Walker Boyd, Jr.
Lieutenant Commander, United States Navy
B.A., Rice University, 1978

Submitted in partial fulfillment of the requirements for the degree

MASTER OF SCIENCE IN ELECTRICAL ENGINEERING

from the

NAVAL POSTGRADUATE SCHOOL
March 1988

Author: _____
Austin Walker Boyd, Jr.

Approved by: _____
Allen E. Fuhs, Thesis Advisor

_____
Harold A. Titus, Second Reader

_____
John P. Powers, Chairman
Department of Electrical and Computer Engineering

_____
Gordon E. Schacher
Dean of Science and Engineering

ABSTRACT

A general purpose satellite (ORION) has been designed which will launch from the Space Shuttle using a NASA Get-Away-Special (GAS) canister. The design is based on the use of a new extended GAS canister and a low profile launch mechanism. The satellite is also configured to launch as a dedicated payload on SCOUT or commercial expendable launch vehicles. The satellite is cylindrical, measuring 19 inches in diameter and 35 inches long. The maximum spacecraft mass is 250 pounds, of which 32 pounds are nominally dedicated to user payloads. The remaining 218 pounds encompass the satellite structure and support elements, which include a hydrazine propulsion subsystem and a spin stabilized attitude control subsystem. The propulsion subsystem provides sufficient impulse to enable circular orbits as high as 835 nm or elliptic orbits with apogees at 2200 nm, leaving a nominal Shuttle orbit of 135 nm. Four stabilizing booms or active nutation control techniques are employed for spin stabilization about the longitudinal axis of the spacecraft. Attitude control accuracies on the order of 1° are attainable for a total mission duration of 90 days to 3 years. Total satellite cost is $1.5 million. The thesis outlines the history of general purpose spacecraft, the ORION design criteria, and the design of the major subsystems. (These

TABLE OF CONTENTS

8

10

.

ACKNOWLEDGEMENTS

Dedicated to Dr. Dea Bailey Calvin who lovingly inspired us to create.

When a thesis exceeds 600 pages in length, there are likely to have been many contributors to its completion. That is certainly so in the case of this tome. Nearly one hundred engineers, professors, military officers, astronauts, public officials, writers, scientists, students, graphic artists and friends have contributed to this work directly. Their inputs span a period of two years since the gestation of the ORION concept in September 1985. Wherever possible, I have sought to recognize contributors in the body of this work. However, I apologize in advance for the many tidbits of knowledge for which originators are not cited. ORION was born in concept during a time when small satellites were visionary, but not marketable. It began to mature as a viable research program when the US space launch crisis made spaceflight alternatives imperative. The excited forecasting, dreaming and engineering that went into ORION is thus a conglomerate of many thinkers. Thanks to all of you who shared in this creation.

Credit for the ORION general purpose satellite concept is due to Dr. Allen E. Fuhs, Distinguished Professor at the Naval Postgraduate School, whose vision as early as 1983 led to this work. His leadership, enthusiasm and technical expertise is directly responsible for much of America's small satellite research effort. Particular thanks are due to CAPT Joe Nicholas (USAF) and the US Air Force Headquarters whose support for ORION generated the first research funding, bringing the concept to life. Finally, I wish to thank Mr. Marty Mosier who expertly guided the ORION engineering effort through many critical phases during 1987-1988.

The completion of this work is attributable, not to engineers or typists, but to my wife. Enduring a never-ending onslaught of thesis interruptions, she carried the load of two parents for three years while I researched, travelled and typed. Without her support, none of this immensely enjoyable and rewarding project would have been possible. This is your thesis too, Cynthia... Thank you.

I. INTRODUCTION

A wealthy man is supposed to have once commented that if you have to
ask the price of a yacht, you can't afford one. To some extent it seems that
this same philosophy has been applied to the satellite business. Scientists
developed mission requirements. These, in turn, were handed to engineers
who prepared specifications to meet the mission requirements. The
specifications were issued for contractors to bid on. When the final bills
were totaled, the cost was sometimes an unpleasant surprise.

Today space budgets in science and applications are facing reduced
Government priorities. Military space programs are also facing increased
cost scrutiny. Finding ways to reduce satellite costs (is) becoming a
necessity. (Keyes, 1982)

No nation should structure its spacecraft fleet solely upon the use of high

cost satellites and a single launch system. Without the balanced use of

spacecraft which span a wide range of cost profiles, the development of

space may be doomed to a flawed future. The present status quo of high

cost satellites denies the general public, the business entrepreneur, and the

military the widespread access to space that is required to ensure a vital and

energetic development of space resources. Public access to space is

effectively denied through the lack of low cost, competitive launch services

and inexpensive but dependable low earth orbit spacecraft. Tactical use of

space is hampered because, with only a few high value space systems, there

are no space assets dedicated to the operational commander. Like public

access to space, the tactical use of space cannot develop without the

provision of low cost space systems.

Figure 1-1

ORION General Purpose Satellite

Opening the realm of low earth orbit to a wider audience of space users requires that low cost, generic spacecraft be developed which are readily adapted to a variety of missions. Such satellites provide new opportunities for space based research, communication, and commercial access that are presently available to only a select group of government and industrial entities. For example, small communication transponders, miniature earth imaging systems and platforms for basic science research could all be profitably implemented on small satellites. The technology to develop such vehicles has existed for twenty years, yet the concept of inexpensive generic spacecraft has not been emphasized widely in the public space program or the US military. It is proposed, therefore, that a small general purpose spacecraft be designed to demonstrate the feasibility of inexpensive vehicles as effective workhorses in the exploitation of near Earth space. The purpose of this thesis is to report on just such a spacecraft concept. A small spin stabilized satellite known as ORION (Fig. 1-1) has been designed to launch from the Space Shuttle as part of the "Get-Away-Special" (GAS) program. Pending final funding arrangements, the first such spacecraft is anticipated to be ready for launch in 1990 carrying a military payload.

A. BACKGROUND

There are currently three United States spacecraft and one European Space Agency (ESA) spacecraft dedicated to the transportation of small satellite payloads. In the US inventory, the SPARTAN, NUSAT, GLOMR, and LDEF satellites carry payloads ranging in mass from ounces to thousands of pounds. However, each of these vehicles is limited to operations at the

16

deployment altitude, being unable to transit to higher orbits. SPARTAN is a free flyer platform, deployed from Shuttle, with a payload capability of up to 1000 pounds. The box-like spacecraft is launched in a formation flight with the Shuttle for missions of up to 2.5 days. The vehicle is retrieved prior to the Shuttle's return to Earth. Although it uses a highly accurate cold gas attitude control system, SPARTAN has no orbital propulsion capability. One SPARTAN spacecraft has flown, and a second was destroyed in the Challenger (STS 51-L) explosion. (Cruddace and Fritz, 1985).

LDEF (Long Duration Exposure Facility) is an experimenter platform capable of transporting 57 experimenter payloads for the investigation of materials subjected to long duration exposure within the space environment. Weighing up to 20,000 pounds, the LDEF represents a significant payload transportation capability. Unfortunately, LDEF has no propulsion or attitude control capability and cannot maneuver to satisfy the needs of individual payloads. Without propulsion, LDEF cannot climb to higher altitudes.

NUSAT (Northern Utah Satellite) is a small spacecraft ejected from a 5.0 cubic foot Get-Away-Special (GAS) canister using a special launch mechanism. The first NUSAT was dedicated to a radar signal calibration mission for the FAA. This vehicle was launched in 1984 and operated without propulsion at Shuttle altitudes (135 nm) for more than two years. It reentered the atmosphere with its 5.0 pound payload in late 1986. This type of satellite does not possess an attitude control capability and cannot maneuver to higher orbits. GLOMR (Global Message Relay) is based upon the NUSAT design and uses the NUSAT launch mechanism. This Defense

Advanced Research Project Agency (DARPA) satellite was launched in 1985 and reentered the atmosphere with its small classified payload in February 1987.

The European spacecraft, EURECA, is a derivative of the SPARTAN satellite with the incorporation of an ion engine for slow transits to higher altitudes following deployment from the Ariane expendable booster. A serviceable EURECA platform that uses cold gas (nitrogen) and hydrazine is also being developed for launch in the early 1990's. EURECA has not flown, but is scheduled for its first launch in the late 1980's.

In summary, no spacecraft in the United States inventory is dedicated to the low cost transportation of small payloads to altitudes above Shuttle orbital altitudes. SPARTAN is a very short-lived vehicle incapable of autonomous operation for periods greater than four days. NUSAT and GLOMR were unpropelled and unable to transport payloads larger than 5 lbm. Finally, LDEF is an untended giant that is best suited to passive experimental roles rather than active operational uses. Although each of these spacecraft have played a vital role in the future of low cost spacecraft development, none of them has successfully integrated the needs of a sufficiently wide audience of users in their design. In particular, they lack propulsive systems capable of propelling payloads to orbits above Shuttle altitudes.

Specifically, a vehicle which can operate in the regime of low Earth orbit between the very low orbits of 100 nm and the lower extremity of the Van Allen radiation belts (850 nm) is required. Propulsive systems which enable such orbits also provide operational flexibility, such as orbital stationkeeping

propulsion for extended satellite lifetimes. None of the US satellites listed provide the autonomous attitude control needed of a long lived vehicle. Only the European spacecraft, EURECA, will provide such control. Although SPARTAN and LDEF each are capable of transporting large payloads, neither can maneuver to higher orbits. Hence, the US inventory does not possess a general purpose spacecraft with propulsion which provides a solution to the needs of a vast number of potential users. These users require a low cost and standardized spacecraft to access low earth orbit for extended periods. The time has come to build upon the successes of the aforementioned systems integrating the needs of today's users with an eye for tomorrow's applications.

B. HISTORY OF GENERAL PURPOSE SPACECRAFT

The history of the development of general purpose spacecraft dates to the beginning of the Space Shuttle era. With the introduction of the Shuttle, scientists and payload managers saw a means of deploying a wide variety of spacecraft from the relatively standardized Shuttle. The Shuttle also acted as an impetus for the development of competing launch systems such as the French Ariane and thus, development of spacecraft that could capitalize upon the use of that launch vehicle. The Shuttle inspired a renaissance in spacecraft design as engineers began to explore new forms of spacecraft optimized for Shuttle use. These spacecraft were as different from their rocket-based predecessors as the Shuttle was from Apollo-era launch systems. Payload bay geometries on the Shuttle led to new spacecraft designs that had been impossible in previous years. In many ways the

Space Transportation System (STS) was linked to efforts on several horizons to develop cost effective, multi-mission spacecraft.

The earliest concept in general purpose spacecraft is traced to the Explorer series of satellites that composed the first of the United States' spacecraft. These satellites saw use in over forty five missions during the 1960's and early 1970's. The Explorer spacecraft was not initially conceived as a general purpose, standardized vehicle, although the designs tended to rely heavily upon those of proven satellites. It represented the first attempt to produce a large number of spacecraft whose designs were roughly similar.
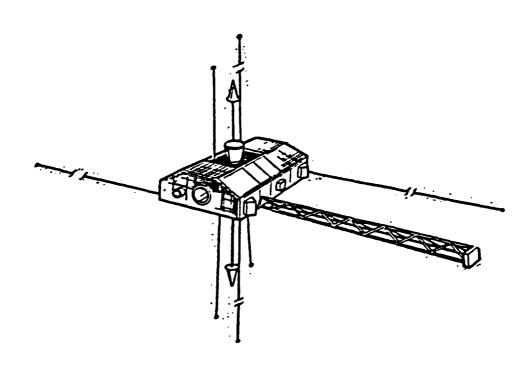
Figure 1-2

Boeing Co. Small Satellite (S-3)
(Boeing Aerospace Co., 1981, p. 10)

As early as 1970, the Department of Defense (DoD) began to perceive the need for standardization of spacecraft design in some missions. DoD promoted the need for improved knowledge of the influence of atmospheric properties and dynamics on Earth orbiting satellites. To that end, the government supported the development of the Boeing Small Satellite (S-3). The S-3 project was initiated to support earth atmospheric investigations using small, low cost ($5 million, 1971) spacecraft that could be launched in conjunction with other missions on a space-available basis. A common spacecraft bus was developed and instrumented for three specific missions covering orbit regimes out to 280 nm. The three S-3 spacecraft (Fig. 1-2) carried a total of 34 experiments. Each spin stabilized S-3 weighed approximately 700 pounds and occupied a volume of 10 cubic feet. Using off-the-shelf technology and minimally redundant designs, the S-3 achieved lifetimes of up to 6 months following expendable booster launches between 1973 and 1976. Although few of the S-3 spacecraft were flown, this vehicle represented an important first step toward a general purpose satellite for a variety of experiments. By Apollo standards, the S-3 was also quite affordable.

The first Shuttle-based spacecraft proposed as a general purpose experiment bus was the Naval Research Laboratory SPEAR vehicle (Fig 1-3).

During the early 1970's some scientists and engineers, becoming aware of the dwindling return from sounding rocket flights, started thinking of ways of using the Shuttle, then in development, to obtain more time for their instruments in space. They wanted to retain the proven sounding rocket organizations, with their accent upon economy, flexibility, fast response to opportunities, and acceptance of reasonable risks, for the preparation of scientific payloads. What emerged should, to a first approximation, replace the sounding rocket booster with the Shuttle. In March of 1975, the Naval

21

Research Laboratory (NRL) made its first proposal along these lines. Called SPEAR (Small Payload Ejection and Recovery), the proposed payload looked very much like a rocket payload. The basic goals, which have not changed during the evolution of the ... program were:

1) The reduction of interfaces with the Shuttle to a bare minimum.
2) The use of sounding rocket experience and hardware and the standardization of subsystems in order to support a variety of missions.
3) Using the minimum of documentation.

The payload was conceived as an autonomous free flyer, containing its own pointing system, data encoder, on-board data storage system, and battery power system. It would be deployed by the orbiter, using the remote manipulator system (RMS), and then would perform its prearranged tasks for a day or more. Finally, it would be recovered by the orbiter, containing data equivalent to the product of several hundred rocket flights. The mission cost, however, would be equivalent to one or two rocket flights. (Cruddace and Fritz, 1985, p.1).

As the SPEAR concept was being developed at NRL, similar ideas were given consideration at the Sounding Rocket Division of the Goddard Space Flight Center and the Space Test Program of the US Air Force Space Division. At approximately the same time as the SPEAR proposal, the USAF Space Division contracted a preliminary design study of a Space Test Program Standard Satellite (STPSS) to Rockwell International and the Aerospace Corporation. (Space Test Program Standard Satellite Launch Optimization Study, 1975). This satellite (Fig. 1-4) was intended to provide a standardized spacecraft to transport various payloads for the USAF Space Test Program (USAF STP). The satellite would consist of a 1200 pound, 150 cubic foot pancake-shaped structure capable of transporting up to 700 pounds of auxiliary payload related equipment; 100 cubic feet of the satellite was to be dedicated to payload uses. It would be integrated in the

Shuttle for launch to orbit with a projected first mission between 1980 and 1990. Attitude accuracies of +/- 0.1 degree were predicted. The spacecraft had a solid rocket propulsion system and a 900 watt power system.
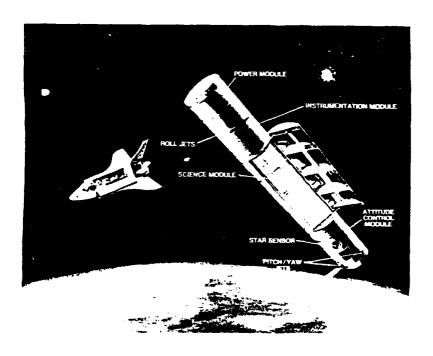
Figure 1-3

NRL Satellite for Small Payload Ejection and Recovery (SPEAR)
(Cruddace and Fritz, 1985, p.1)
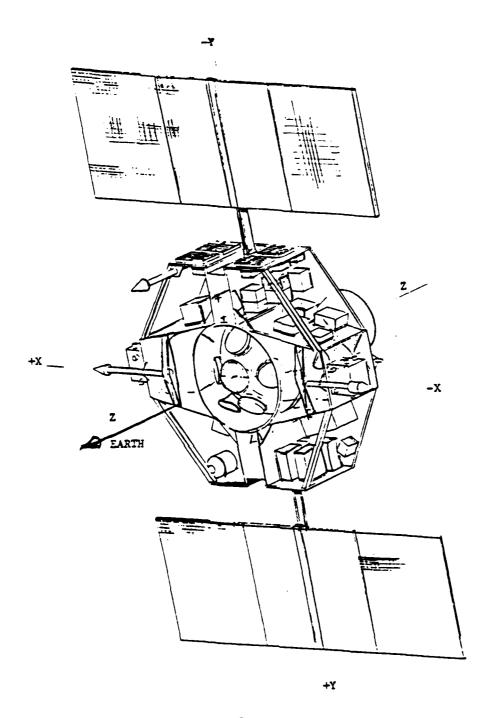
Figure 1-4

USAF Space Test Program Standard Satellite (STPSS)
(Aerospace Co., 1975, p.1)

The STPSS was never built. Budgetary considerations during the lean years of the mid-1970's were responsible in part for its cancellation. Some engineers have stated that it was excessively complicated, and thus too expensive, to suit the needs of a program that required a flexible, affordable, quickly procured spacecraft. Like the Shuttle, STPSS was designed as a complex spacecraft with multiply redundant systems whose construction would be overseen at the contractor and sub-contractor level. It is interesting to note that the (Air Force) STPSS design philosophy differed markedly from that of the (Navy) SPEAR concept. SPEAR was constrained to be simple, affordable and involve some degree of risk. It was to be developed in a small "skunk works" program that remained the responsibility of the sounding rocket scientists whom it was destined to serve. In contrast, STPSS was engineered in a classically complex fashion with a large corporation and military department influencing the design effort. The SPEAR "keep it simple" philosophy would ultimately result in an operational spacecraft, whereas STPSS never materialized.

In 1975 the Naval Research Laboratory and Goddard Space Flight Center Sounding Rocket Division began cooperating on the SPEAR concept. Their mutual interests in sounding rocket technology and low cost spacecraft were united between 1976 and 1979 in a transformation of the SPEAR design. That three year gestation period resulted in the SPARTAN general purpose scientific payload bus (Fig. 1-5) (Cruddace, 1977 and Olney, 1979). Although a three year cooperative effort had transformed the rocket-like SPEAR into a smaller rectangular SPARTAN, the sounding rocket philosophy of design remained intact. By 1982 the first satellite, SPARTAN-1, was manifested for

25

a 1984 X-ray astronomy observation mission on the Shuttle. The 3000 pound, 30 cubic foot rectangular vehicle was stabilized about three axes using cold gas jets with a pointing accuracy of +/- 10 arc seconds. The extreme accuracy required by the X-ray astronomy mission led to a very small attitude control dead band of 6 seconds, and a resultant lifetime (due to attitude control propellant usage) of only 2.5 days.
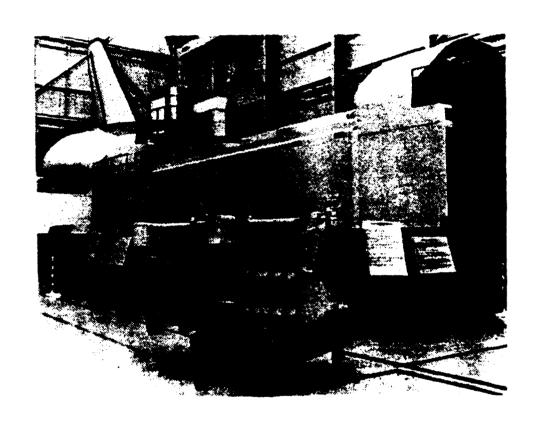
Figure 1-5

NASA Goddard SPARTAN Spacecraft
(NASA Photograph)
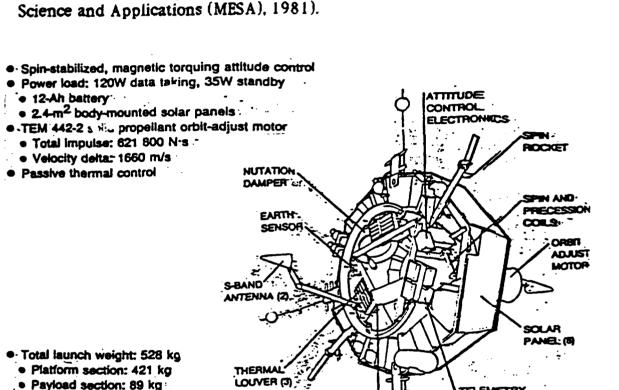
The SPARTAN data recorder was similarly limited, being capable of only 64 hours of data storage. SPARTAN was designed to be deployed from the Shuttle and allowed to perform as a free-flyer in formation flight with the Shuttle until the end of its mission. The satellite used a set of preloaded instructions to command pointing and internal operations during the 2.5 day mission. Although the 1984 flight was eventually postponed to May of 1985, the X-ray mission was a great success. SPARTAN-1 was to have been followed by SPARTAN-203/Halley on STS 51L, but that satellite was destroyed in the Challenger accident of 28 January 1986. A third SPARTAN has been readied for launch and the original SPARTAN-1 is being refurbished for future flights.

In the early 1980's Boeing submitted a proposal for a low cost spacecraft with its MESA (Modular Experimental Platform for Science Applications) design (Fig. 1-6). MESA was conceived as a low cost spin stabilized experiment platform and was based upon the VIKING satellite design. Using the 'companion spacecraft' concept, the satellite would ride an expendable booster with a primary mission payload achieving circular orbits as high as 900 nm. The 1000 pound disc shaped satellite would provide 170 pounds of payload capability in an 8 foot diameter volume. Spin stabilized pointing accuracies of +/- one degree would be possible using magnetic torquers. Solid rocket motors would provide up to 150,000 lbf-seconds of total impulse for orbital maneuvers. With regard to the MESA concept, Boeing Corporation states that

Satellites can be economically placed in orbit using already available (and otherwise wasted) launch vehicle space. MESA is a platform for carrying such satellites. The economies are realized when a MESA is joined with

27

another spacecraft in the unused payload volume of an existing launch
vehicle. Because the concept incorporates use of proven spacecraft
components and designs, MESA can be delivered to users at a cost that
might be as low as $10 million (1981 dollars) depending upon the specific
mission requirements. These costs are known because of the heritage
MESA now has (from VIKING); once mission requirements are firm, the
costs can be definitely established. (Modular Experimental Platform for
Science and Applications (MESA), 1981).

- Spin-stabilized, magnetic torquing attitude control
- Power load: 120W data taking, 35W standby
  - 12-Ah battery
  - 2.4-m^2 body-mounted solar panels
- TEM 442-2 solid propellant orbit-adjust motor
  - Total impulse: 621 800 N·s
  - Velocity delta: 1660 m/s
- Passive thermal control

- Total launch weight: 528 kg
  - Platform section: 421 kg
  - Payload section: 89 kg
  - Jettisonable items: 18 kg
- Octagonal platform: 1700 mm across flats
- Height: 490-mm main equipment section
- S-band communications

Figure 1-6

Boeing Co. MESA Spacecraft
Modular Experiment Platform for Science Applications
(Boeing Aerospace Co., 1981, p.12)

28

The MESA was initially produced for the Swedish Space Corporation's VIKING program. It was, like EURECA, designed for an Ariane expendable booster launch. Keyes (1982, p.1) points out that the affordability of the MESA spacecraft was

> achieved by staying as close to previous designs as possible. Low cost was achievable by using available components that the design cost had been previously paid for, and by maintaining a small experienced design and manufacturing team from previous small satellite programs. In addition, low cost (was) achieved by working with potential customers early in their mission planning to develop a satellite within the available budget. Sometimes this meant compromising some of the requirements to save money.

As with its predecessor, the S-3 spacecraft, MESA depended upon the use of proven technology and minimal redundancy to produce an affordable and fully capable satellite that met the users budget. In light of the cost of other satellite systems in the 1980-1982 timeframe, $10 million was considered to be low cost for a general purpose satellite.

The civilian quest for a generic, low cost satellite began in 1982 in Utah. Mr. Gil Moore of the Morton Thiokol Corporation and Dr. Rex McGill of Weber State College in Ogden, Utah organized a student and industry design team to begin the development of a 150 pound satellite which would be ejected from a standard Space Shuttle Get-Away-Special (GAS) canister. The standard GAS canister is a 5.0 cubic foot cylinder, with an optional opening lid assembly, which attaches to the side of the Shuttle cargo bay (Fig. 1-7). The GAS program was instituted in 1980 to transport small autonomous payloads to Shuttle orbits. Using GAS, low cost, space available payload
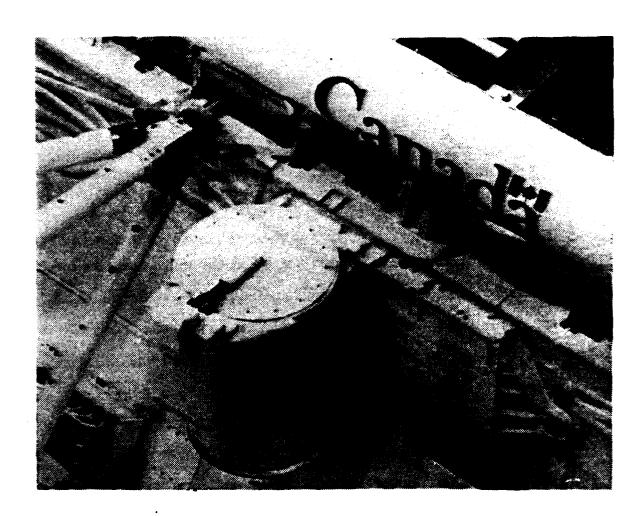
Figure 1-7

NASA Get-Away-Special (GAS) Canister
(NASA Photograph)

opportunities were provided for small experiments to fly on the Shuttle at low cost and with a minimum of documentation. Approximately two years after the institution of the GAS program, an opening lid was devised for the GAS canister (Fig. 1-8). The GAS canister was originally designed as a sealed unit, but the lid made possible the interaction of payloads with the space environment. It was this GAS canister and lid concept which Mr. Gil Moore sought to exploit as a means to transport and deploy small satellites. He proposed that the GAS canister be modified to include a spring launch mechanism (Fig. 1-9), and to transport up to 150 pounds of ejectable payload. The concept of ejecting spacecraft was initially met with disapproval by NASA. The persistence of Gil Moore and the NUSAT team led to a safety qualification of the concept and its adoption as a regular Get-Away-Special option.
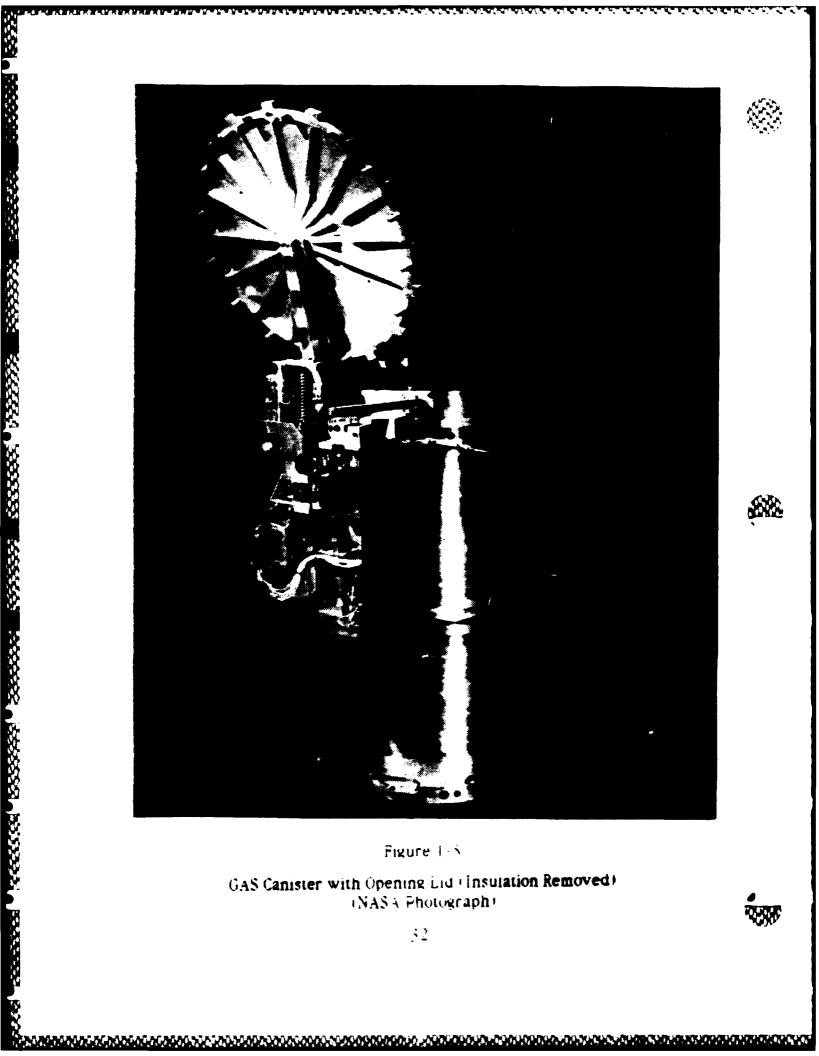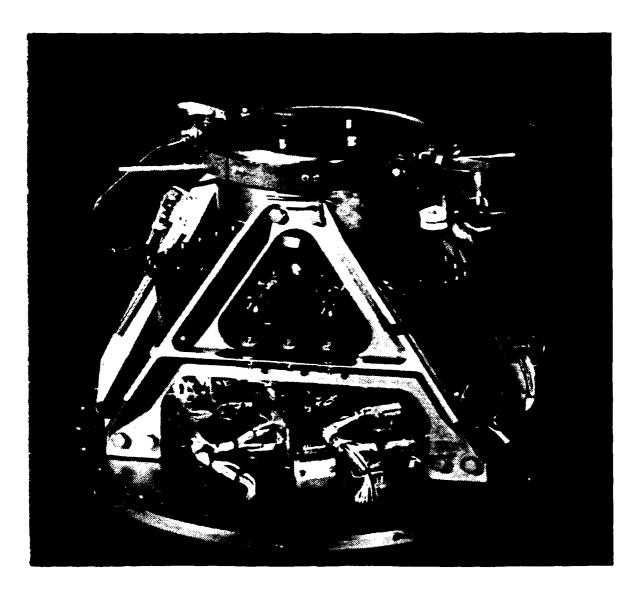
In the process of obtaining NASA sanction for the ejectable spacecraft concept, the NUSAT team accomplished a redesign of the GAS canister to include a launch mechanism and all of the required GAS-Shuttle interface circuitry. Following the qualification of that new canister configuration, NASA Goddard's GAS Program Office released the design as an approved method of ejecting payloads from the Shuttle. This was a monumental step for NASA and the GAS program because it conflicted radically with the previous "not-to-interfere" philosophy of Get-Away-Special operations. The change in NASA philosophy that enabled the transformation of the GAS "fixed payload" program into a satellite-capable program was made possible through support from the highest levels of the NASA organization. Mr. Chet

Figure 1-8

GAS Canister with Opening Lid (Insulation Removed)
(NASA Photograph)

32

Figure 1-9

NUSAT Get-Away-Special Satellite Launch Mechanism
(NASA Photograph)

Lee (Director, NASA Customer Services), Mr. Clark Prowty (NASA Customer Services), Mr. Jim Barrowman (NASA Headquarters), Mr. George Gerondakis (Director, NASA GSFC GAS Program Office), Mr. John Laudadio (NASA GSFC GAS Safety Officer) and Mr. Larry Thomas (NASA GSFC GAS Office) were the central NASA officers responsible for ensuring the approval of the NUSAT concept. Their efforts and those of Mr. Gil Moore and the NUSAT team provided history's first opportunity for the transportation and launch of low cost, technologically simple spacecraft. The NUSAT program brought satellites within the grasp of the common man.

NUSAT (Figs. 1-10 and 1-11) became an operational spacecraft in 1984 with a successful launch from Shuttle on an FAA radar calibration mission. The satellite was a multifaceted (20 sides) brass structure, 19 inches in diameter. It contained a small data storage unit, UHF and VHF telemetry units and a small solar power array. NUSAT was designed to tumble in orbit and did not possess attitude control or propulsion. The satellite performed beyond the most liberal of estimates remaining in orbit for over two years and operating for over 60% of that time. The satellite deorbited in December 1986. Because the spacecraft design was extremely simple and nonredundant, many professionals doubted that the NUSAT student effort would succeed. However, the great success of NUSAT only served to strengthen the contention of many small spacecraft proponents that a good satellite need not be complex. The NUSAT engineering mirrored, in many ways, the design philosophy of the Goddard Sounding Rocket Division and the Naval Research Laboratory. That is, the use of proven technology, the

Figure 1-10

NUSAT and Get-Away-Special Canister
(NASA Photograph)

Figure 1-11

Weber State College Northern Utah Satellite (NUSAT)
(NUSAT Promotional Artist Sketch)
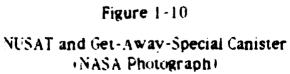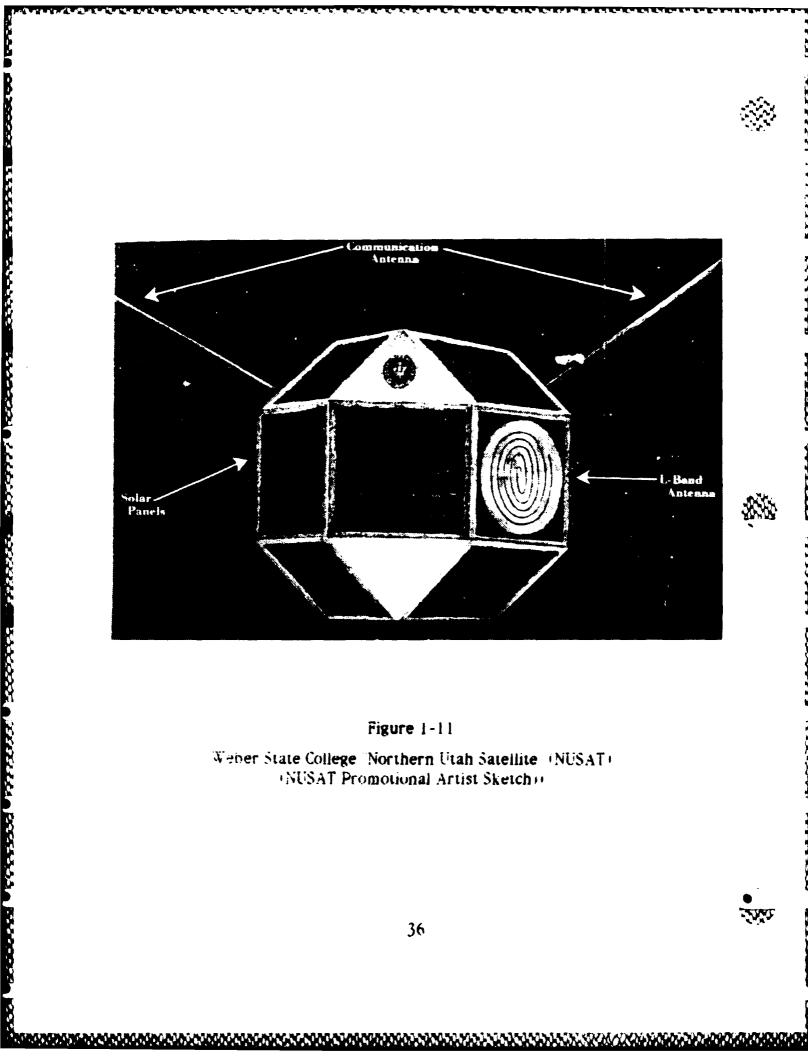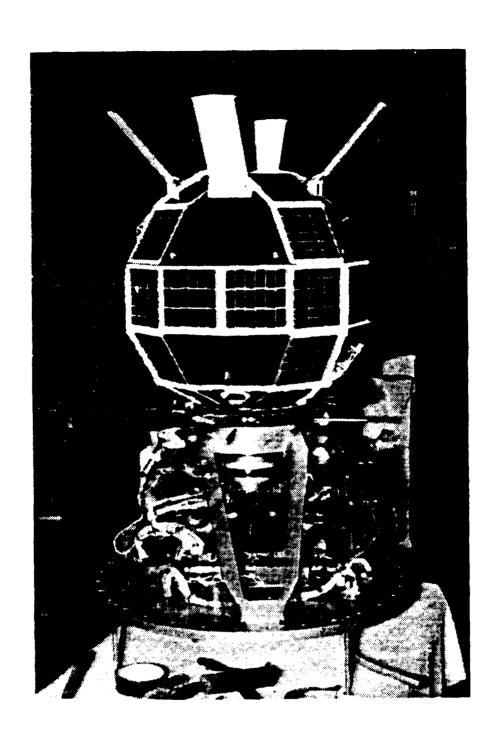
adherence to a simple affordable design, and the acceptance of risk combined to make a highly successful spacecraft. NUSAT proved that good satellites need not be costly and complex.

The approval by NASA to eject satellites from GAS canisters, and the design successes of the NUSAT program encouraged the Department of Defense to contribute to the GAS small satellite effort. In 1983 the Defense Advanced Research Project Agency (DARPA) began construction of the GLOMR (Global Message Relay) satellite, under a contract with Defense Systems Inc. (DSI) of McLean, VA. LTCOL Brian Bell, USAF, of DARPA and Dr. George Sebestyen of DSI led the effort to introduce the use of ultra-low cost spacecraft to the Department of Defense. DARPA and DSI could both foresee an increasing need for low cost space platforms which would permit the proliferation and reconstitution of military space assets. The GLOMR design (Fig 1-12) was patterned after that of the NUSAT spacecraft using the same launch mechanism. GLOMR was successfully deployed in 1985 as a forward message relay platform. The satellite deorbited in February 1987. GLOMR established a popular footing within DoD as a result of its low cost and operational performance.

In response to the success of small satellites, production of additional GLOMR and NUSAT style vehicles has been undertaken by DSI and Globesat, Inc. respectively. Globesat is a new company founded by Dr. Rex McGill and others is dedicated to the production of NUSATs and other spacecraft for commercial purposes. The Globesat founders have recently teamed with the American Rocket Company (AMROC) to provide multiple GLOBESAT launches on a commercial booster. DSI has also contracted to launch additional

37

Figure 1-12

DARPA Global Message Relay (GLOMR) Satellite
(NASA Photograph)

GLOMRs and other spacecraft for defense related missions. INTRASPACE Co. is developing a low cost cylindrical communication satellite designed to also use the NUSAT launch mechanism.

Unfortunately, none of these spacecraft nor their derivatives possess any propulsion. Attitude control is lacking in all but two. The GLOBESAT and GLOMR spacecraft are gravity gradient stabilized. While the lack of propulsion was not a hindrance for the NUSAT or GLOMR missions, these spacecraft cannot be considered general purpose without orbital boost capabilities or a more flexible form of attitude stabilization. Most satellite users require some form of payload pointing control. These vehicles have provided the proof of concept for small, simple, low cost satellites. However, the needs of a wider audience of users must now be considered, and a second generation of vehicles must be designed which can carry larger payloads to higher orbits with better attitude accuracy. Building upon the successes of the past, the time has come to integrate the best features of general purpose satellites (S-3, STPSS, MESA, SPARTAN, LDEF) and small low cost satellites (NUSAT, GLOMR) into a truly capable and affordable platform. The ORION general purpose satellite is just such a vehicle, with an increased payload relative to NUSAT, much higher orbits than NUSAT or SPARTAN, and pointing accuracies consistent with those of the Boeing S-3 and MESA. ORION draws upon the simple design philosophies of the sounding rocket engineers and improves upon the designs of NUSAT and GLOMR.

C. ORION HISTORY

Following the launch of NUSAT in the fall of 1984, Dr. Allen Fuhs of the Naval Postgraduate School (NPS) began to promote the concept of a larger, more capable general purpose spacecraft to be used in a wide variety of military operational roles. He assigned the design of a submarine launched "Cheapsat" satellite to a class of graduate space systems engineers at the Naval Postgraduate School in the spring of 1985. Based upon the success of that design assignment, Dr. Fuhs continued to promote the idea of a small general purpose spacecraft expanding the scope of the satellite to include compatibility with expendable boosters. This led to a number of promising second generation spacecraft designs generated by the next class of NPS space engineers in the fall of 1985.

On 8 December 1985, a proposal by the author for an improved GAS-deployed satellite was presented to DARPA, the sponsoring agency of GLOMR. This cylindrical, 150 lbm, satellite would use a spinning launch mechanism to deploy it from the GAS canister (Fig. 1-13). This design included a solid rocket motor to provide highly elliptic orbits, a 12 megabyte magnetic bubble memory data storage unit, and a spin stabilized attitude control system. Based upon inputs from LTCOL Chris Shade, USAF, of DARPA and Mr. Bob Mercer of the Strategic Defense Initiative Office (SDIO), a revised design was prepared for the USAF Space Division Space Test Program. On 23 April 1986, the updated concept (Fig. 1-14) was formally presented to the "Navy Call for Experiments" meeting of the Navy Space Test Program, and the Space Test Program office of the USAF Space Division. 1LT Mike Bitzer and Mr. Bert Ferger of Space Division (Code SD/YCM) suggested

40

additional improvements in the launch mechanism and presented a summary of the concept to their Space Division superiors.
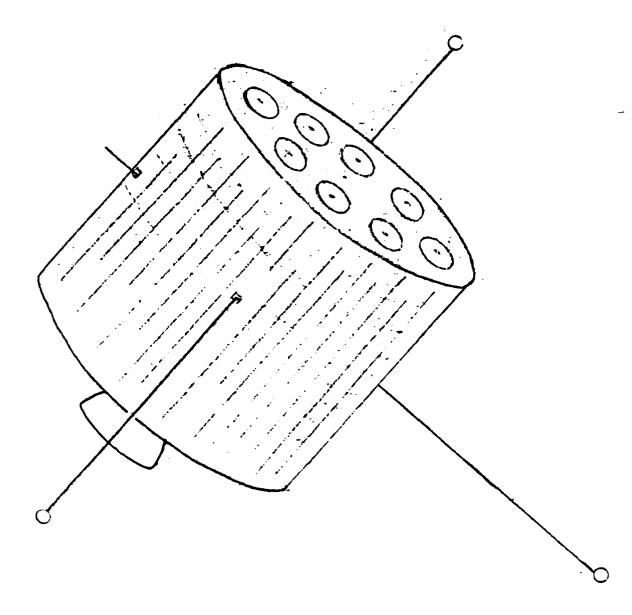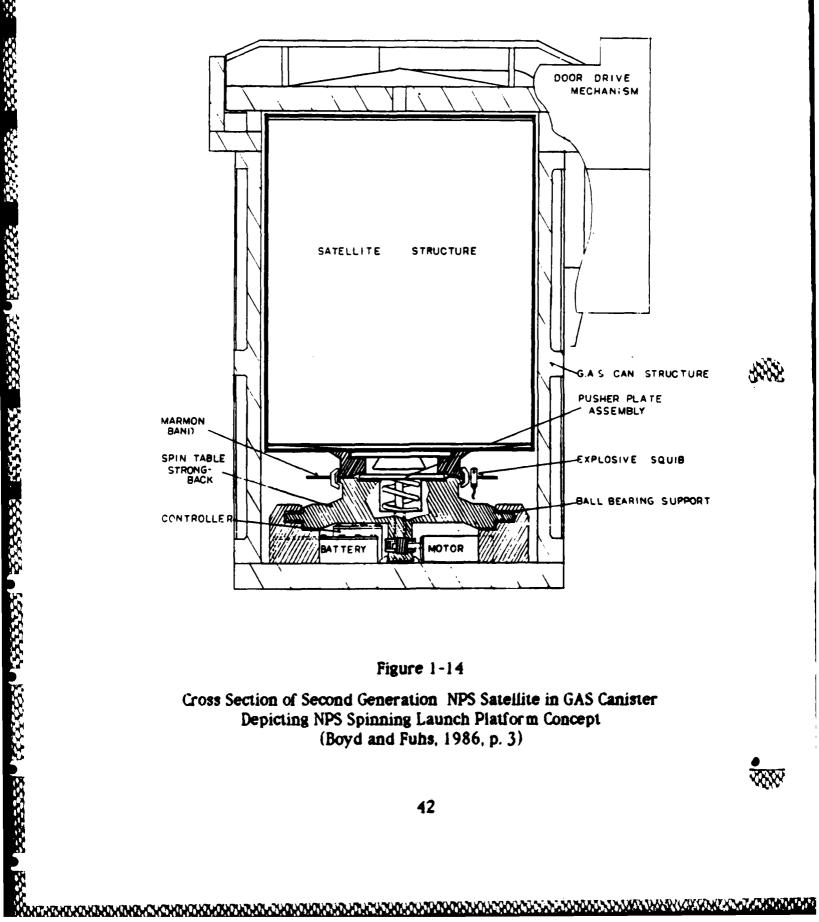
Figure 1-13

Sketch of a First Generation Naval Postgraduate School Satellite
(Boyd and Petersen, 1986, p. 47)

Figure 1-14

Cross Section of Second Generation NPS Satellite in GAS Canister
Depicting NPS Spinning Launch Platform Concept
(Boyd and Fuhs, 1986, p. 3)

As a result of the burgeoning interest in GAS deployable satellites, the USAF Space Division Space Test Program (STP) office committed $1 million to the development of an extended GAS canister and a much improved launch mechanism. Foreseeing the operational capability of GAS ejectable payloads, STP contracted the design of a much larger (250 pound payload, 5.7 cubic foot) canister and a low profile launch mechanism (Fig. 1-15) to the Ball Aerospace Co. of Colorado Springs, CO. in May 1986. This contract ensures the success of designs for larger and more capable GAS ejectable satellites. While initially dedicated to a classified military payload, the extended canister is expected to be available for use by DoD agencies as early as January 1989. Consequently, this extended GAS canister was formally adopted as the deployment mechanism for an NPS satellite. The NPS design effort was freed of the need to engineer an improved low profile launch platform. As a second benefit, the new canister would provide a larger payload volume and weight than was available in the standard canister. Based upon the use of the new canister, the NPS satellite would be 35 inches tall by 19 inches in diameter, and weigh up to 250 pounds. A detailed description of the extended canister is found in Chapter Two.

As a result of contacts through Mr. Bob Mercer of SDIO, the Space Vector Corporation of Northridge, CA was consulted in the spring and summer of 1986 with regard to the general purpose satellite design. Mr. Richard Rasmussen (President) and Mr. Clay Bushnell (Chief Engineer) were instrumental in helping the author evaluate lightweight spacecraft structures and various propulsion systems for a general purpose spacecraft design. Their experience in sounding rocket programs was extremely useful as the

NPS design was directed toward the use of proven, simple technologies and low cost spacecraft systems.

In June of 1986, 1LT Mike Bitzer of the USAF STP office promoted the NPS satellite concept to the USAF Headquarters at Patrick AFB for Air Force funding of a formal NPS preliminary design effort. As a result of 1LT Bitzer's
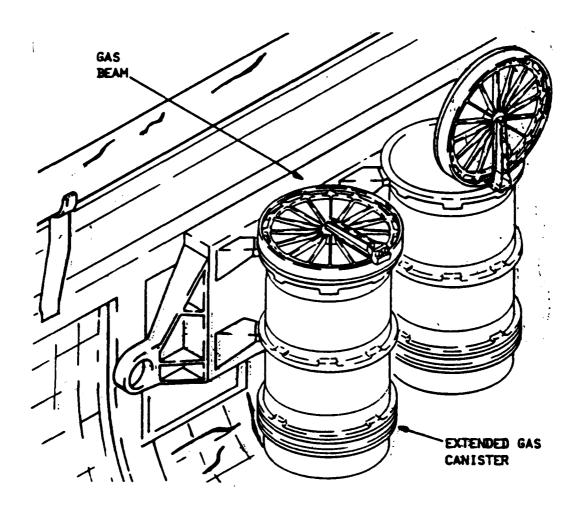
Figure 1-15

USAF/Ball Aerospace Extended Gas Canister
(Ball Aerospace Co. Artist Depiction, 1986)

recommendations, CAPT Joe Nicholas (USAF) committed $100,000 of Air
Force advanced concept funding to a four-month design study of a spin
stabilized GAS ejectable satellite. The NPS design effort was directed toward
the needs of a classified mission under development in cooperation with the
Aerospace Corporation and the USAF Space Division. That mission required
an elliptic orbit passing through the lower Van Allen radiation belt. Based
upon this mission requirement and a survey of available propulsion options,
a hydrazine propulsion system was identified for the NPS satellite. A target
date of July 1987 was set for the formal preliminary design report. With the
support of the US Air Force, the NPS concept for a low cost general purpose
spacecraft was now recognized as a feasible and potentially valuable
contribution to the DoD spacecraft program.

On 14 August 1986, a conceptual design review of the NPS satellite was
conducted at the Naval Research Laboratory. Dr. Fuhs and 10 NPS graduate
space engineers joined the USAF funding point of contact, CAPT Nicholas,
and a team of 12 NRL spacecraft engineers to critique the satellite design.
Dr. Robert Lindberg, then Branch Head for Concept Development in the NRL
Spacecraft Engineering Department, presided over the review of each of the
satellite systems. As a result of that review many priorities were
established for the satellite system designs. It also pinpointed special
attitude control requirements imposed by the decision to use spin
stabilization about the long axis of the vehicle.

The August conceptual design review was followed by a 5 day design
caucus with NRL engineers and NASA program managers during the week of
7-12 September 1986. Thermal, attitude control, power, propulsion,

45

structural, and telemetry systems were discussed in depth with NRL representatives. This caucus led to the adoption of a pressurized blowdown expulsion method for the hydrazine propulsion system, an S-band telemetry system, and a 15 volt electrical bus in the final design. Special nutation problems encountered by a prolate spinning spacecraft were discussed (See Chapter Five). The NPS concept was also formally presented to the GAS program office of NASA Goddard Space Flight Center (NASA GSFC). This meeting resolved many of the initial safety issues in the satellite design. In particular, assurances were obtained that the concept of hydrazine propulsion in a GAS ejectable satellite was technically feasible from the flight safety point of view providing that a detailed safety qualification was conducted. Mr. John Ledaudio (NASA GCFC GAS Safety) expressed that there would be hurdles encountered in the safety qualification process, but that none of the obstacles were insurmountable if thorough safety reviews were conducted early and updated frequently during the satellite program. In particular, the use of proven propulsion technology which had obtained prior NASA flight certification was considered crucial to the success of the NPS effort. A target date of spring/summer 1987 was set to begin the safety process with a NASA "Phase Zero" safety review.

Inputs from the conceptual design review and caucus confirmed the earlier decision to rely upon simple satellite systems rather than a complex, highly redundant architecture. Affordability, reliability and simplicity were stressed by many of the government and corporate engineers that critiqued elements of the NPS satellite design. By late September 1986, the concept had been briefed to over thirty separate military and civilian organizations.

More than twenty operational military missions were identified for the satellite, and several organizations expressed interest in the vehicle for their future payloads.

In October 1986 the NPS spacecraft was formally named the "ORION General Purpose Satellite". A complete description of ORION was presented to the 37th Congress of the International Astronautics Federation (IAF) in Innsbruck, Austria on October 8, 1986. The concept was extremely well received by the international community, being judged the most significant international contribution at the "New Concepts and Technologies" symposium of the IAF congress. Japanese, German and Italian representatives were particularly interested in the design as they made plans to deploy similar small satellite systems.
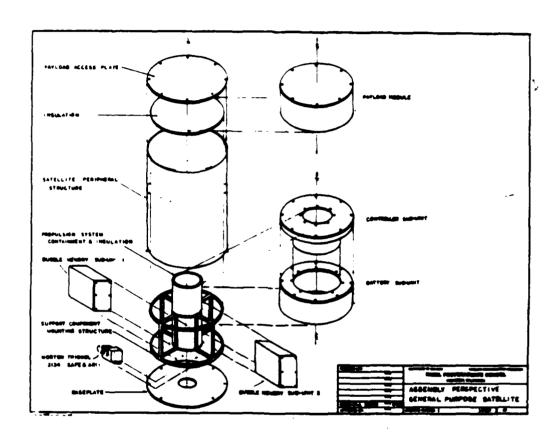
In November 1986 the pace of the ORION design project was quickened with the hiring of a full time engineer, Mr. Marty Mosier, to coordinate the design effort begun by the author. In late November formal presentations were made to the US Air Force Headquarters at Patrick AFB, the Strategic Defense Initiative Office (SDIO), and the Air Force Systems Command (AFSC). This informational program was designed to publicize the ORION program and the preliminary results of the Air Force design study (Figs 1-16, 1-17a). Shortly thereafter, CAPT Joe Nicholas arranged an ORION presentation for the SDI Office of Innovative Science and Technology (SDIO-IST). On 8 December 1986, Dr. Jim Ionson, Director of SDI IST, was briefed on ORION and its capabilities. Coordination at that meeting between Dr. Fuhs (NPS), COL Joe Angelo (USAF HQ), CAPT Joe Nicholas (USAF HQ) and Dr. Ionson (SDIO-IST) resulted in a decision by the SDI organization to cosponsor the

Figure 1-16

Cross Section of the Second Generation ORION Satellite Design
(Boyd and Fuhs, 1986, p.4)

Figure 1-17a

NPS ORION General Purpose Satellite
(Third Generation Design)
(Boyd and Fuhs. 1987. p.2)
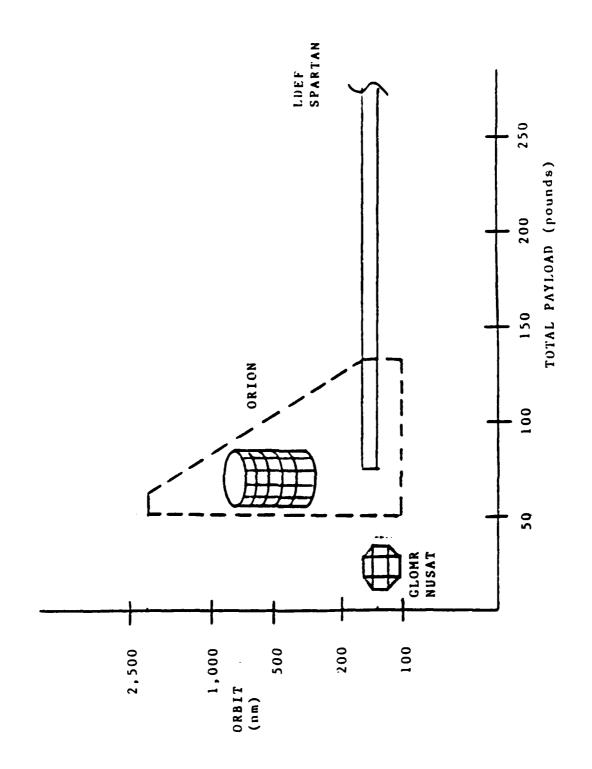
Figure 1-17b

Comparison of Small Satellite Capabilities

development of a flight ready ORION with the US Air Force. Tentative agreements were tendered to provide approximately $3 million in funding to NPS to build the first ORION flight unit. This satellite would be dedicated to an Air Force classified payload, contingent upon Naval Postgraduate School acceptance of the research funding. This decision to fund the actual construction of ORION would ensure the viability of this now popular small spacecraft concept. Curiously, the funding agreement was made exactly one year (and 45 briefings) after the satellite's first exposure to DARPA on 8 December 1985.

D. PARALLEL DEVELOPMENTS

The success of NUSAT and GLOMR provided the incentive to develop additional satellites at Globesat and DSI. Other companies have also ventured proposals to capitalize upon the interest in small satellites. Several government agencies have begun to promote the concept of small satellites as well. Like the NPS design team, those companies and agencies have recognized the need to improve upon the small volume and payload of the original NUSAT design.

Foreseeing the need to develop larger spacecraft and the potential market for such vehicles, three organizations began work in 1986 to develop satellites very similar to ORION. INTRASPACE Co. was formed in 1986 with the intention of marketing small modular GAS-ejectable spacecraft for communication purposes. The Intraspace concept is known as "T-SAT", (i.e. Model-T satellite) and has been promoted internationally as a platform for communication transponders and scientific payloads (Fig. 1-18). Most

51

notable is the T-SAT cooperation with the Philippine government as that country seeks to establish a low cost communication constellation that would serve the 5000 Philippine islands. T-SAT is a 200 pound, 3.5 cubic foot cylindrical spacecraft that would deploy from a standard GAS canister using the NUSAT launch mechanism. Employing cold gas jets for three axis attitude control, the satellite is expected to achieve +/- 1 degrees of pointing

ANTENNAS DEPLOYED

TT&C MODULE

ANGULAR SIDE VIEW
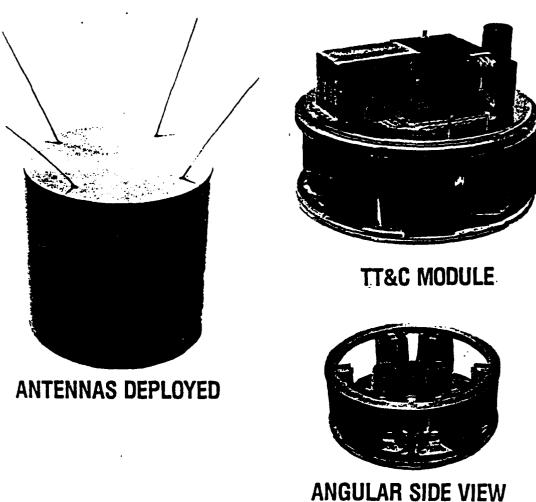
Figure 1-18

Intraspace "T-SAT" Satellite
(Reproduced from Intraspace Promotional Literature)

accuracy of +/- 1 degree. It has no orbital propulsion capability and will carry approximately 50 pounds of payload at Shuttle altitudes. Like ORION, T-SAT uses a structural aluminum skin upon which are mounted silicon solar cells. With 30-40 watts of power, the satellite can support two small transponders for the communicaiton mission. Intraspace Co. estimates that T-SAT can be marketed for approximately $600,000.

Dr. Rex McGill, Dr. Frank Redd and others of the original NUSAT team have proposed a second generation satellite design (Fig. 1-19) for the Weber State College space organization. Recognizing the need to redesign the original NUSAT launch platform and incorporate larger satellite volumes in a GAS canister, they have also chosen the Air Force extended GAS canister as the benchmark of their next satellite design. The satellite will be a 12 sided cylinder roughly the dimension of ORION, incorporating a gravity gradient boom and tip mass. The Utah team is a highly capable and motivated group of students, faculty and industry. Their significant groundbreaking success with NUSAT is no doubt a barometer of continued success in follow-on small spacecraft designs.

In late 1986 Dr. McGill of the NUSAT team formed a Utah based company, known as Globesat, to market their new vehicle commercially. Promoting their spacecraft to military and commercial audiences, the Globesat group has commanded considerable respect as a result of their past successes with NUSAT. In the spring of 1987 the company joined forces with the American Rocket Co. and formed a business group known as "Orbital Express" and combined the low cost Globesat spacecraft with unsubsidized commercial launch opportunities.
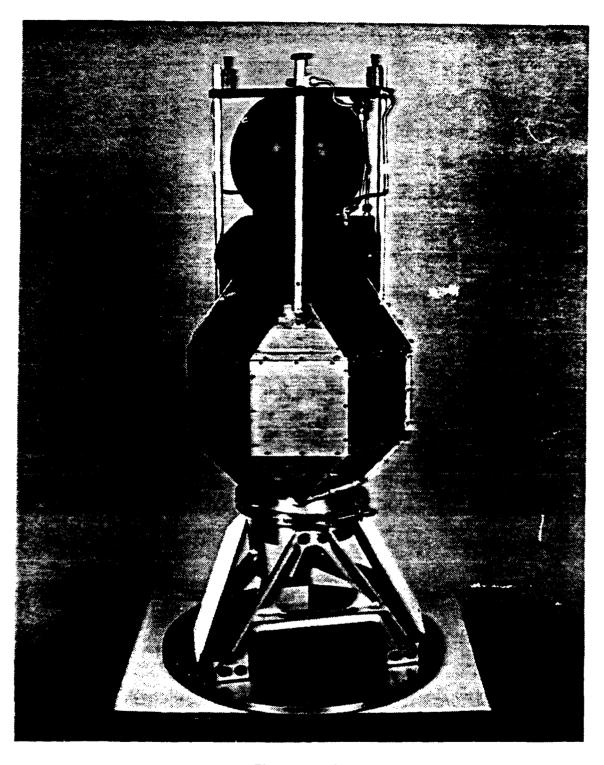
Figure 1-19

Weber State College Second Generation NUSAT Satellite
(Weber State College Photograph)

54

Figure 1-20

Orbital Express Concept
(Aviation Week and Space Technology, 11 May 1987, p. 97)

The TRW Co. has also fielded a design for a small multipurpose spacecraft. That design, like ORION, is based upon the use of the new Air Force extended GAS canister. The design includes a solid rocket propulsion system for establishing highly elliptic orbits. It would utilize gravity gradient stabilization for attitude control. Externally, this 250 lb vehicle is very similar to the ORION design. Defense Systems International (DSI) has also designed a cylindrical satellite that will be compatible with the extended canister. Like the TRW spacecraft, it will be gravity gradient stabilized. Orbital Sciences Co. of Fairfax, VA and Ball Aerospace Co. of Colorado Springs CO have also undertaken efforts in the field of small satellite design. The crippling setbacks in the US space launch effort during 1986 have highlighted the interest in small satellites. The recent small satellite design activity in many space oriented companies is testament to the serious attention being focussed by industry upon low cost reliable spacecraft.

Several government agencies have recently embarked upon programs involving the use of small satellites. The most ambitious government effort is being led by the Defense Advanced Research Project Agency (DARPA). Beginning in Fiscal year 1988, DARPA will initiate a basic and applied research program in the area of lightweight satellites and low cost launch vehicles. Of this program, the AIAA news service writes

The goal of the DARPA program, called Advanced Satellite Technology Program (ASTP) or LIGHTSAT, is to support technology development to allow the Department of Defense, in the early 1990's, to develop and field space-based systems which will provide support to operational field commanders for force planning and force execution. The basic premise of this initiative is that key military needs, partially fulfilled by existing U.S. space-based systems, can be more fully supported by alternative space-based platforms which complement these systems. Without ASTP, these

needs are unlikely to be fulfilled in the foreseeable future, due to cost
constraints and severe limitations in the current United States space launch
programs. The technology in the U.S. has advanced to the point, or will in
the very near future, where low-cost, lightweight satellite systems are
possible and that they can be placed in orbit by low-cost launch vehicles.

The first conference dedicated solely to small satellite technologies
occured in August 1987. The AIAA and DARPA jointly sponsored the
conference which was held on the Naval Postgraduate School campus. This
gathering enabled government, academic and industrial researchers to share
information on the parallel efforts described above in the furtherance of the
U.S. small satellite design effort.

The Naval Research Laboratory (NRL) and Strategic Defense Initiative
Office (SDIO) are also involved in small satellite research. The ORION
program is jointly funded by the SDIO, Air Force and DARPA, with
engineering support from NRL. NRL has been active in many small satellite
programs from the outset of the U.S. space program. SDIO is investigating
the benefits of small spacecraft for various sensor and test monitoring
missions.

NASA has begun several related efforts with regard to small satellites.
Overseeing most small satellite development, the NASA Goddard Space Flight
Center (GSFC) supports all Get-Away-Special (GAS) based spacecraft. The
GAS program office of GSFC monitors the safety qualification of GAS payloads
through two paperwork channels, the Payload Access Request (PAR) and the
Safety Data Package (SDP). The office also conducts safety reviews at various
levels of the design effort and oversees vibration/vacuum qualifications of
GAS payloads.

GSFC recently issued a "call for proposals" in several areas of space research through the Small Business Innovative Research Program (SBIR 87-1, 1987). A program solicitation in the spring of 1987 addressed a wide range of topics of interest to NASA, encouraging small businesses to submit proposals for grant support in the development of innovative technologies. Among these was a request for the development of a small spacecraft similar to the T-SAT and based upon the use of the NUSAT launch mechanism.

A simple, innovative, economical, expendable spacecraft is required to provide an orbiting platform for space based commercial use. This will be a single strand, one experiment free-flyer that can be ejected from an STS flight or an ELV. This ejected canister shall be an 18-inch high cylinder, 19-inches in diameter, weighing less than 150 pounds, and may have solar cells on the 18 inch-high cylinder walls. This subtopic solicits innovative approaches for the design, consturction and qualification of any or all of the following:

(1) GAS canister system: Assuming sufficient power collection in orbits with up to a 40 percent umbra, provision shall be made to store solar power and provide two watts average power to internal functions and 50 watt-hours per day to the single experiment with a peak power of 50 watts. The spacecraft shall contain an innovative propulsion system with a nozzle aimed at the cylinder axis at the bottom of the canister. One cubic foot and 50 pounds of the 150 pound total weight shall be reserved for the experiment.

(2) The spacecraft shall have VHF PCM convolutionally coded, phase modulated telemetry, UHF PCM commands, 24-hour stored command memory, 107 bit solid-state memory with EDAC for command telemetry data storage, passive thermal design, STS separation timer, end-of-life timer, omnidirectional antenna system, and ability to operate from a single ground station. This single ground station shall be simple, portable, user-owned and operated with an omnidirectional antenna and shall be designed, fabricated, and provided with this effort. NASA facilities may be used for qualification and acceptance activities. One hundred percent commercial solid-state parts shall be used with their only qualifications

being completion of 500 hour period of prelaunch satellite operation with no failures. (NASA SBIR 87-1, 1987, p. 52)

NASA is also involved in small spacecraft research at the Jet Propulsion Laboratory (JPL) in Pasadena, California. A JPL funded program is developing a Get-Away-Special launched satellite to be propelled by electric propulsion into a lunar orbit. Inspired by the success of the NUSAT/GLOMR programs and the imminent availability of of the extended GAS canister, JPL researcher K. Nock promoted a concept for interplanetary GAS launched satellites. Folowing two presentations on ORION capabilities, the JPL team refined the concept to the present Xenon ion engine propelled design, and optimized the design for use in the extended GAS canister.

The Lunar GAS mission employs a small hghly integrated and reliable spacecraft which can carry one or two small science instruments to the moon. Besides important science considerations, Lunar GAS is an ideal first mission to demostrate the potential of solar electric propulsion. In addition, in order to meet the challenge of placing this spacecraft, which has an 8 km/s delta-V capability and carries more than 2 kw of solar array, into the GAS canister, a new integrated approach to the design of the structure and electronics has been developed.

The primary attractions of the GAS program are: potential early launch, proven Shuttle safety path and a very low launch cost. It is important to point out that once developed, the spacecraft is not restricted to the Shuttle. The current spacecraft design has a 30% launch margin on the SCOUT launch vehicle. In addition, this spacecraft could be launched as a piggyback payload on many of the world's existing space launchers.

Key elements of this concept are GAS launch, a spin stabilized spacecraft with solar electric propulsion using Xenon ion engines, and a slow spiral
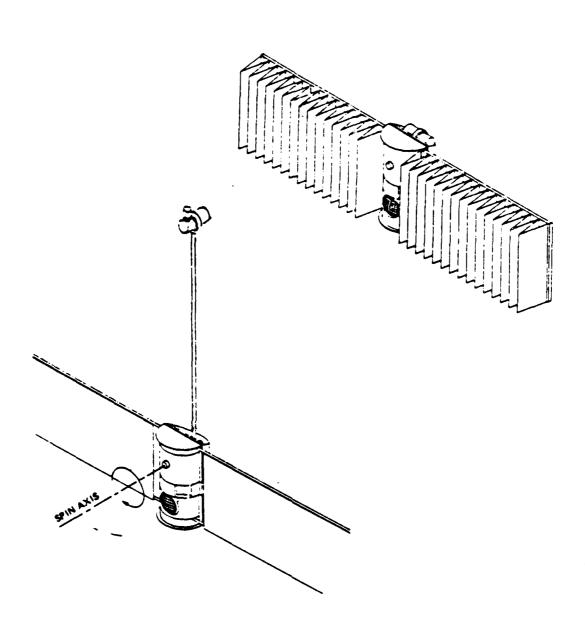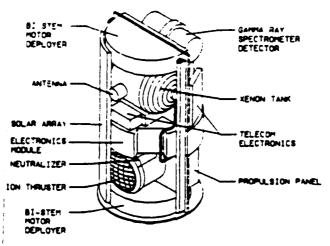
Figure 1-21

Lunar GAS shown with 2kw Solar Array Deploying/Deployed
(Nock. 1987. pp. 5-7)

B: STEM MOTOR DEPLOYER
GAMMA RAY SPECTROMETER DETECTOR
ANTENNA
XENON TANK
SOLAR ARRAY
ELECTRONICS MODULE
TELECOM ELECTRONICS
NEUTRALIZER
ION THRUSTER
PROPULSION PANEL
BI-STEM MOTOR DEPLOYER
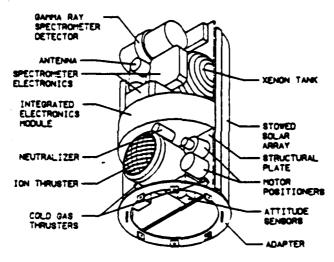
Equipment arrangement for stowed
configuration - view of sun side.

GAMMA RAY SPECTROMETER DETECTOR
ANTENNA
SPECTROMETER ELECTRONICS
XENON TANK
INTEGRATED ELECTRONICS MODULE
STOWED SOLAR ARRAY
NEUTRALIZER
STRUCTURAL PLATE
ION THRUSTER
MOTOR POSITIONERS
COLD GAS THRUSTERS
ATTITUDE SENSORS
ADAPTER
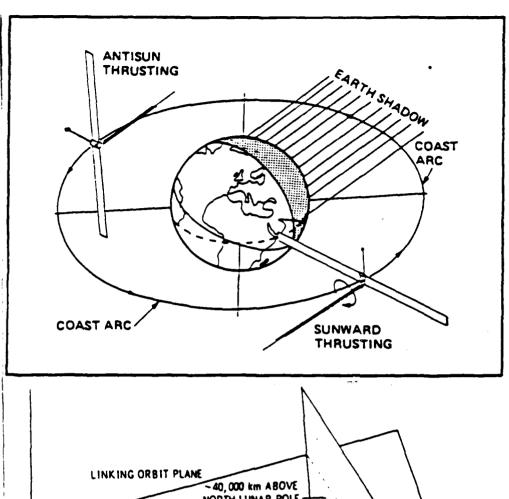
Equipment arrangement for stowed
configuration - view of anti-sun
side.

Figure 1-22

Internal Construction of Lunar GAS
(Nock, 1987, p. 6)

61

ANTISUN
THRUSTING

EARTH SHADOW

COAST
ARC

COAST ARC

SUNWARD
THRUSTING

LINKING ORBIT PLANE

~40,000 km ABOVE
NORTH LUNAR POLE

EARTH DEPARTURE SPIRAL

LINKING ORBIT

LUNAR CAPTURE
SPIRAL

- FLIGHT FROM SHUTTLE ORBIT TO 100 km, POLAR LUNAR ORBIT
  REQUIRES ~2 years
- LUNAR OPERATIONS FOR 1 year
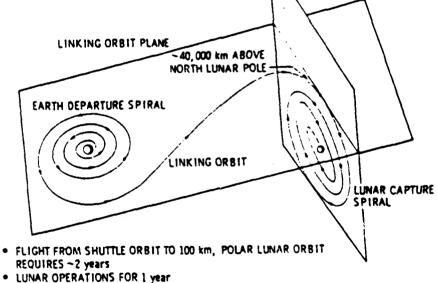
Figure 1-23

Orbital Path of Lunar GAS
(Nock, 1987, p. 2)

62

departure from low earth orbit to a 100 km circular polar Lunar orbit. A series of missions are contemplated having objectives related to Lunar surface composition, mineralogy, gravity shape, and internal density. (Nock, 1987, p.1).

The JPL design deserves considerable merit on three accounts. It is the first formal attempt to expand the application of GAS to interplanetary or Lunar travel. Visionary thinking such as this will do much to carry the United States into a new era of low cost interplanetary probes. It is also a first step toward the commercialization of Lunar space. Second, this GAS satellite concept is the only one of the parallel efforts listed above that will provide high quality pointing accuracy, signficant orbital propulsion and a full range of payload services. Such spacecraft are proof that attitude control, propulsion and a mission capable satellite can be integrated in a small package. Third, but no less important, JPL is to be commended for rapid and generous funding of Lunar GAS using only internal funds. This marks a serious consideration of the value of low cost spacecraft in a NASA organization other than GSFC.

Many other parallel efforts exist in the early concept phase, especially in various university programs. All of these efforts underscore the popular scientific and economic acclaim of the small spacecraft concept. The advent of the Space Shuttle and the Get-Away-Special program has made small satellites operationally feasible. However, concepts such as these have only become a reality in the recent past. The success of NUSAT was the impetus for numerous new concepts such as ORION between 1985-1987. The promotion of ORION and second generation NUSAT designs have been followed by a flurry of activity in small spacecraft design in the 1986-1987 timeframe. A groundswell of support for small satellites is changing the

focus of the spacecraft industry. Future concepts for affordable expendable booster launches using commercial launch services promise even more radical changes in the evolution of small, low cost spacecraft. Foreign interest in developing affordable satellites that will mate with new foriegn launch vehicles will broaden the scope of the low cost spacecraft effort considerably. Enabling technologies, economic pressures, motivated space entrepreneurs and dramatic events such as the loss of STS 51-L have combined, perhaps serendipitously, to encourage and foster the development of the low cost, general purpose spacecraft. As an outgrowth of those pressures and events, ORION surely represents a concept whose time has come.
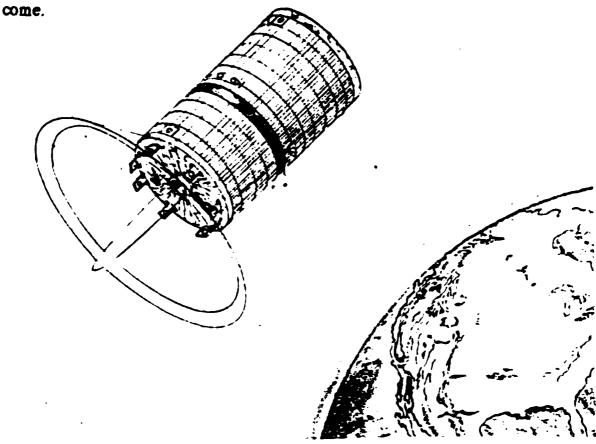
Figure 1-24

ORION Spacecraft During Orbital Transfer

Figure 1-25

LCDR Austin Boyd (left) and Mr. Marty Mosier (right)
With ORION Satellite Mockup

II. DESIGN CRITERIA

Spacecraft design is an iterative process that seeks to satisfy the physical and philosophic requirements of the user. Integrating physical constraints and limitations with the less tangible philosophy of a design, a spacecraft will emerge as a success or will fail being "not economically or physically realizable". This melding of physical and philosophical constraints begins as a mission definition for which the engineer seeks to produce a vehicle capable of satisfying an operational need. The design is then gently molded by philosophical goals and firmly guided by the mission, affordability and available technologies. The opposite approach is to conceive of the satellite from a philosophic perspective (i.e. the satellite should be low in cost or general purpose). Then, with a broadly defined concept of what the satellite should be, the design is painfully molded by the physical realities of mission definition, affordability, available technologies, safety and reliability. Very slowly, the concept emerges as a workable design.

Typically a satellite design begins with a defined physical goal and compromises of some philosophic constraints are made in order to achieve a physically realizable spacecraft. Molding a philosophic concept into a satellite, working under physical constraints that cannot be ignored, is a much more difficult design path. Such is the case of the ORION satellite where the driving force in the design is the concept of an affordable, general purpose satellite. Constrained by the realities of expensive aerospace systems, few space launch opportunities, and myriad mission requirements

imposed by potential users, the concept of a low cost general purpose satellite can be quickly compromised. Those compromises that satisfy the physical constraints but which do not abandon the philosophy must be sought. A design philosophy can mold a design but cannot direct it. ORION began as a concept without mission definition or design criteria. However, with careful attention to the compromises required and the end goal, a general purpose satellite design can be successfully accomplished that provides low cost access to space for many users.

This chapter will outline the steps in the satellite design process and specify several of the philosophic and physical constraints imposed upon the ORION design. Specific criteria have been adopted for the vehicle structure and volume based upon selection of the Space Shuttle Get Away Special canister as the deployment mechanism. Mission definition for the first vehicle has been provided by the US Air Force sponsor. Safety criteria have been specified by NASA. A price goal has been set to ensure affordability. More general criteria such as reliability and cost effectiveness have also been addressed. It may not be possible to satisfy all of the constraints which these criteria impose. In particular, the propulsion requirements of a general purpose satellite may not be compatible with the volume constraints of a small GAS deployed spacecraft. Therefore, a preliminary design study is required to prove the feasibility of the ORION concept. This thesis describes the specific ORION design criteria and evaluate various design options for the structure, propulsion and attitude control subsystems. Within the context of the design criteria and the design options, the concept

of a low cost general purpose satellite is demonstrated to be technically feasible and physically realizable.

A. THE SATELLITE DESIGN PROCESS

A satellite design often begins as a mission concept or a vehicle concept. For instance, a communication firm may desire to market a geosynchronous communication capability (mission) without specifying a vehicle design. Guidelines with respect to systems architecture and affordability supplement the design process, but the primary goal is to fill the communication mission need. Fuhs (1986) refers to this as the "clean sheet of paper approach" in which the "designer converts a space mission into a space system design ... including the following considerations:

1. Orbit selection
2. Number of satellites (i.e. constellation size)
3. Definition of spacecraft payload
4. Manned versus unmanned
5. Size, weight, spacecraft configuration
6. Launch vehicle needs
7. Ground support (sites, telemetry, recovery)
8. Cost estimates"

A spacecraft may also begin as a concept of a special vehicle without a clear picture of all the possible missions. The design process then integrates the needs of potential users, and forecasts possible missions and requirements. However, the vehicle concept, and not a particular mission, will be the major focus in such a design effort. To a certain extent the designer may even fit the mission to the vehicle.

An example of the mission oriented approach is found in the Apollo program. Each of the Apollo spacecraft were designed to meet a specific

need. The Apollo program was very strongly centered upon mission goals. The dedication of Apollo engineers and American taxpayers helped to overcome the technological and economic hurdles of putting a man on the moon. On the other hand, the Space Shuttle began as a vehicle concept. It was conceived as a spacecraft that could perform many different space transportation missions. The Shuttle designers assimilated the needs of many potential users in the design, attempting to create an affordable, reusable launch vehicle. Again, technological and economic challenges were painstakingly overcome in order to develop the first reusable spaceship. In both the mission and vehicle concept approach, strongly supported goals resulted in successfully deployed spacecraft.

The design of the ORION spacecraft began as a vehicle concept. Without a particular mission in mind but many potential users identified, the design effort focused upon construction of a low cost general purpose satellite. However, this concept was too general to enable the design to proceed to the component level. After eight months of preliminary work, the ORION design was critiqued at the August 1986 NRL conceptual design review. It was noted in that review that specific mission requirements were needed to progress further in the design effort. While it is reasonable to begin a design with a vehicle (rather than a mission) concept, at some point one or more specific missions must be identified to transition from abstract concepts to hardware. Similarly, the designer that starts with a mission concept is constrained to eventually choose some physical form for his vehicle. In one case (vehicle concept approach) several mission options and their requirements are considered as the vehicle design is refined. In the other

69

situation, many possible vehicle options are considered with a specific mission in mind.

IDEA	(PHILOSOPHY)
↓	↓
MISSION APPLICATION	(A REFINED OR "ENABLED" IDEA)
↓	↓
DESIGN CRITERIA	(A FUNCTION OF THE PHILOSOPHY, DESIGN CRITERIA & LAUNCH VEHICLE)
↓	↓
SUBSYSTEM DESIGN	(A FUNCTION OF DESIGN CRITERIA & BUDGET CONSTRAINTS)
↓	↓
TOTAL SYSTEM DESIGN	(ALMOST NEVER THE SAME AS ORIGINAL CONCEPT AFTER DESIGN ITERATIONS)
↓	↓
OPERATIONS	(DOES DESIGN MATCH ORIGINAL PHILOSOPHY AND MISSION?)

Figure 2-1

The Satellite Design Process

Once the mission or vehicle concept has been defined, the next step is to develop a set of basic design criteria for the physical system. These criteria include such items as basic structural limitations (volume, weight, launch vehicle loads), power budgets, payload mass budgets, telemetry/data budgets, thermal budgets, and economic budgets. Some considerations (Agrawal, 1986, p. 31) in the specification of those criteria are:

1. Provide support to equipment in a layout that minimizes signal losses and interconnections.

2. Provide the required electrical power within specified voltage tolerances.

3. Provide temperature control within the limits imposed by satellite equipment.

4. Keep the spacecraft attitude within allowable limits.

5. Provide telemetry and command services to permit ground monitoring.

6. Provide support to the total mass with adequate stiffness, alignment, and dimensional stability.

A selection of criteria that satisfy these provisions occurs early in the design as the mission specifications are identified. Often the first limitations on the design are imposed by the launch system and the payload. The vehicle structure is quickly constrained by choice of the launch system and the payload volume and mass. Within the physical limitations of that structure, an allotment of space is made for the support elements of the total satellite system. Payload critical elements are then added to the design and the iteration process begins.

71

A vendor survey is conducted early in the design process when specific criteria have been identified. The purpose of this survey is to identify proven technologies and commercially available components that can be integrated to form the spacecraft bus. The vendor survey may be supplemented by a Request For Proposal (RFP), particularly if the satellite requires the use of new technologies. The NASA Small Business Innovation Research (SBIR) solicitation is an example of such a request. The RFP process involves the solicitation of bids from various manufacturers for the construction of one-of-a-kind components, subsystems, or the entire spacecraft. A vendor survey or RFP provides an early indication of the feasibility of the design and determines if the design criteria are realistic. It will also initiate the iteration process from the standpoint of development costs and schedule timelines. These considerations will then be programmed into a revision of the design criteria, modifying the design where needed to meet schedule commitments and budget ceilings.

As the various spacecraft components are identified, the issues of reliability and cost effectiveness come into play. Reliability addresses the likelihood of the successful operation of key components as a function of demonstrated mean-time-between-failure (MTBF). Cost effectiveness is concerned with the use of the best component in terms of the overall performance, lifetime, redundancy, and affordability. For example, a military reconnaissance satellite with a mission lifetime of seven years and an important national security role may require a highly reliable propulsion system. However, a relatively inexpensive photographic satellite with a three month lifetime might not require the same quality propulsion system

72

PERFORMANCE
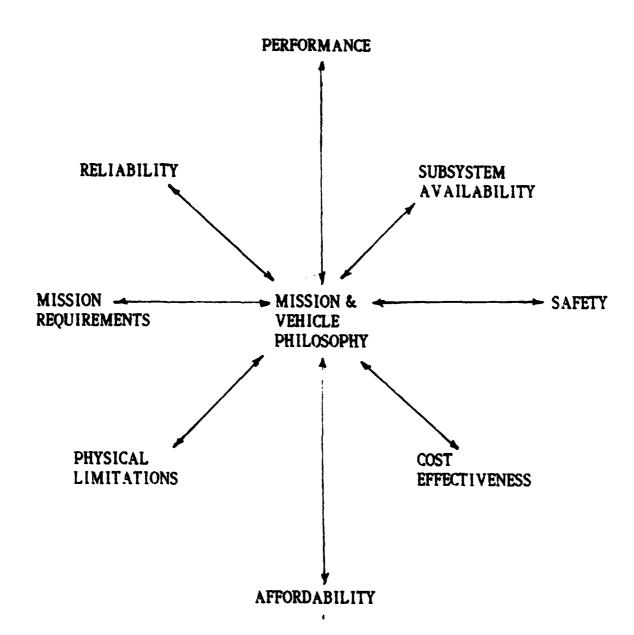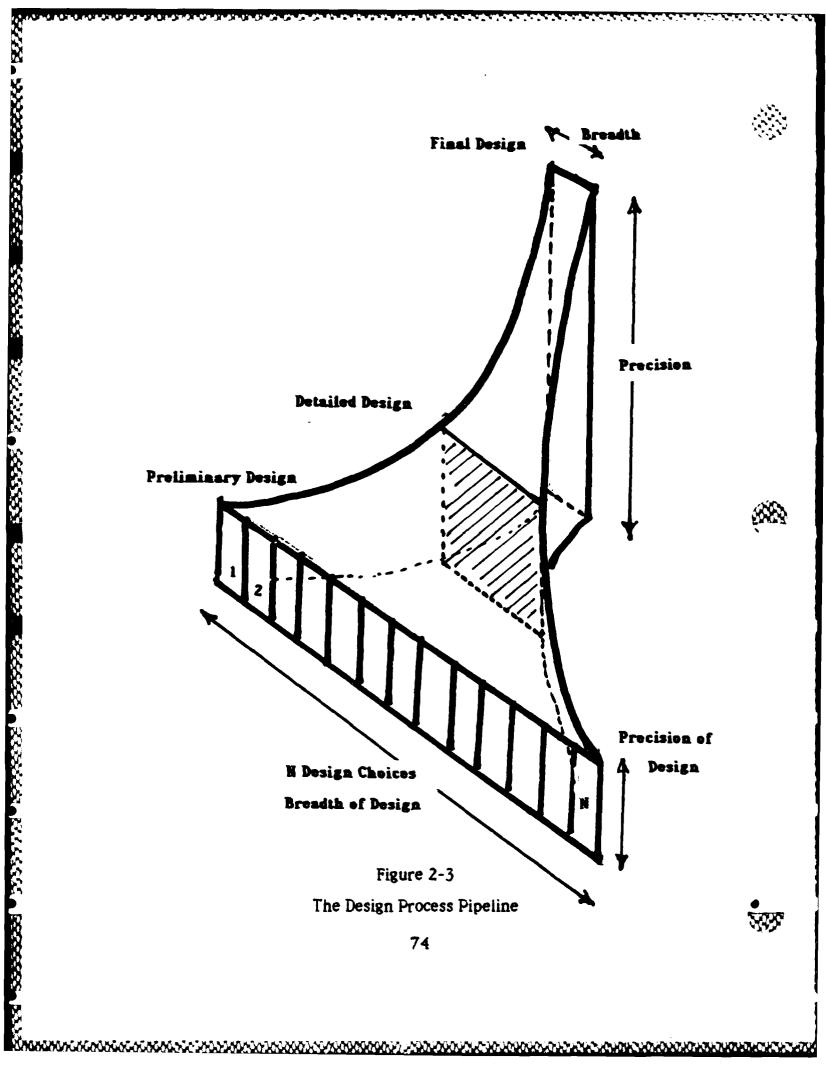
RELIABILITY

SUBSYSTEM
AVAILABILITY

MISSION
REQUIREMENTS

MISSION &
VEHICLE
PHILOSOPHY

SAFETY

PHYSICAL
LIMITATIONS

COST
EFFECTIVENESS

AFFORDABILITY

Figure 2-2

Satellite Design Considerations

73

Figure 2-3

The Design Process Pipeline

74

components. Use of less expensive and perhaps less reliable components may be more cost effective for the short lived satellite.

As the design is iterated to account for modifications to the design or the criteria, the technical precision of the design will be observed to increase while the breadth of the design choices is narrowed. Fuhs (1986) depicts this as a pipeline or funnel where the design is narrowly focused to a single design choice of great precision. With regard to this increase in precision, Agrawal (1986, p. 4) notes that

A spacecraft design is an iterative process. It can be broadly divided into three phases: preliminary (i.e. conceptual) design, detailed design, and final design. At first, a feasibility study is made to determine whether the mission performance requirements can be met within the mass and size constraints of the launch vehicle. The first step is to select a spacecraft configuration which provides a general arrangement of the subsystems. The mass and power requirements of the subsystems are estimated, based upon preliminary analysis and extrapolation of existing designs. After the feasibility of the mission is confirmed, a detailed design of the subsystems starts with detailed analyses and test carried out at the unit and subsystems levels. The spacecraft design is qualified at the subsystem and system levels by conducting performance, thermal and vibration tests. Units that do not meet the performance requirements during the tests are redesigned and retested. After successful completion of the qualification tests, the spacecraft design is finalized and the required number of flight spacecraft are fabricated. The flight spacecraft are subjected to acceptance tests to detect manufacturing and assembly defects .... A spacecraft configuration (will be) highly influenced be the performance requirements of the mission payload, the launch vehicle, and the attitude control stabilization system selected.

At each step of the process, the current design is evaluated to determine that it conforms to the original vehicle or mission concept. To the greatest extent possible, the designer seeks to prevent the design from manipulating the

vehicle or mission philosophy. The philosophy should mold the design and not vice versa. By the same token, mission concepts should not specifically define all of the technical aspects of the vehicle design. Some latitude must be provided to make compromises. Mission requirements should guide the design as it proceeds from the conceptual stage to the final design stage.

B. THE ORION DESIGN PHILOSOPHY

The ORION design began as a concept to provide low cost access to space aboard an easily deployed general purpose satellite platform. The concept has been guided by several philosophic and physical constraints over a period of fifteen months. This thesis is the result of a preliminary design process that sought to prove the feasibility of such a vehicle. The feasibility of a low cost general purpose satellite is dependent upon the ability to design a physically realizable space system subject to five broad constraints. Specifically, ORION should be:

1. Affordable
2. Cost effective
3. General purpose
4. Reliable
5. Safe

The issues of affordability and general purpose architecture were discussed in Chapter One. These constraints must be qualified, however, with respect to a particular audience's perception of "what is affordable?" and "what is general purpose?". The issue of reliability involves quantitative failure analyses as well as a subjective perception or acceptance of risk.

76

Safety, unlike the other issues, is not subject to perception and is well defined by NASA. These criteria are defined in greater detail below.

1. Affordability

Between March 1985 and December 1986 the author had the opportunity to survey many different DOD satellite systems and payloads. Through the annual Navy Space Test Program "Call For Experiments" forum, additional proposed Navy payloads were evaluated. As a result this exposure to a number of satellite and payload programs, some observations were made as to the perceived definition of "affordability" within NASA and the Department of Defense (DoD). The cost of satellite and launch systems has been observed to span a spectrum of 10^5 to 10^9 dollars. Systems whose total production and launch cost is in excess of approximately $100 million are generally considered to be "high cost". These include large military surveillance systems, complicated basic science missions (Space Telescope, Viking, Voyager), commercial geosynchronous communication platforms and large launch vehicles (Shuttle). Those systems whose total cost ranges approximately between $10 million and $100 million are considered to be "medium cost". They represent the median of the cost spectrum. Most space systems are implemented within this cost range. The "low cost" space systems are typically those costing less than $10 million. The ultra-low portion of the cost spectrum is occupied by those spacecraft which cost less than $1 million (NUSAT, OSCAR, TSAT, Get-Away-Specials).

It is difficult to list all of the subjective considerations involved in this classification. Many perceptions of affordability in aerospace are conditioned

ULTRA LOW COST	LOW COST	MEDIUM COST	HIGH COST

OSCAR   ORION   VIKING   SHUTTLE

G.A.S.   T-SAT   SPARTAN   SPACE TELESCOPE

NUSAT   NUSAT-2   LDEF
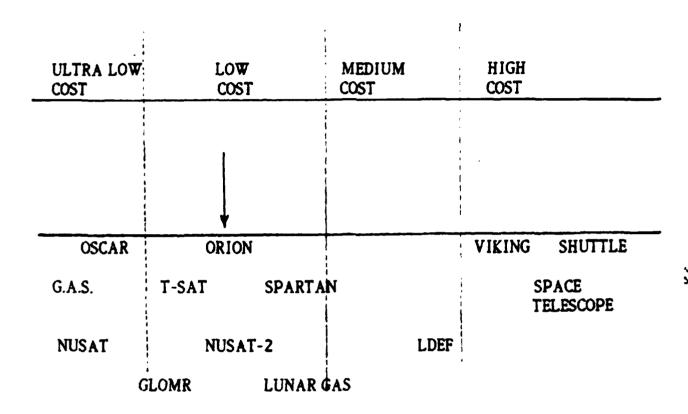
GLOMR   LUNAR GAS

Figure 2-4

Satellite Cost Spectrum

by what the market and the taxpayer will bear. Most of the author's observations as to cost perceptions are based upon DoD responses to various NPS funding proposals. There appears to be a rough consensus within DoD and the larger aerospace corporations that satellite systems of less than $10 million are "quite affordable" and those less than $1 million are "cheap". It should be stressed that this is primarily a psychological perception based upon the relatively high cost programs typically associated with military space. It is expected that the perceptions of a military space program manager and those of a private citizen will differ markedly with regard to affordability.

It should be noted that there are different program management and funding approval mechanisms within DoD and NASA for "high cost" and "low cost" programs. Often the "low cost" (less than $5 million) programs will be subjected to less scrutiny than "high cost" endeavors. Many experimental concepts or tests of unproven technology fall within the "low cost" category. In the words of one government official, "three million dollars is venture capital....and with it you are buying risk" (with reference to government spending for innovative space systems).

Based upon the subjective inputs listed above, "low cost" in the ORION context was defined to be approximately $1 million. This target cost for the acquisition and fabrication of an ORION spacecraft was selected to appeal to the "low cost" sensibilities of DoD agencies and aerospace corporations. The psychological goal of $1 million is a "soft" target of the ORION feasibility study. Economic criteria are often the most difficult to achieve and the most frequently compromised in aerospace programs. Therefore, "affordability"
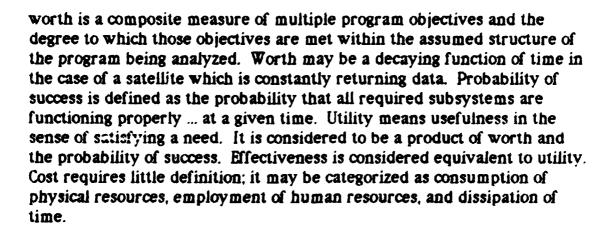
will relate to public (taxpayer) access to space through "affordable" national security and science missions that would use ORION. It is understood that a private investor may not share the perception that $1 million constitutes low cost access to space.

2. Cost Effectiveness

A corollary of "affordability" is "cost effectiveness". It is desirable to spend no more than necessary to produce ORION (affordability) and also to ensure that the money which is obligated is well spent (cost effective). Cost effectiveness is an approach to design which seeks to avoid the purely technological analysis that identifies a subsystem at any cost. In a cost effectiveness analysis, the designer considers such elements as worth, probability of success, utility, effectiveness, and total cost. With regard to these elements, Holcomb (JPL TR-32-1505 ,1972, p. 6) states that

> worth is a composite measure of multiple program objectives and the degree to which those objectives are met within the assumed structure of the program being analyzed. Worth may be a decaying function of time in the case of a satellite which is constantly returning data. Probability of success is defined as the probability that all required subsystems are functioning properly ... at a given time. Utility means usefulness in the sense of satisfying a need. It is considered to be a product of worth and the probability of success. Effectiveness is considered equivalent to utility. Cost requires little definition; it may be categorized as consumption of physical resources, employment of human resources, and dissipation of time.

Cost effectiveness methods are applied as a criterion for subsystem design trade-offs and design selections. They are valuable tools for impartially assessing the trade-offs of a design without the influence of subjective factors (such as intuition?) (Holcomb, JPL TR-32-1505, 1972).

Cost effectiveness analysis is not without criticism, however, as reflected in this quote from Rep. Mendell Rivers, Chairman of the House Armed Services Committee in 1966:

> All of this is being rationalized on the basis of cost/effectiveness studies. Do you know that the M-14 rifle costs more than a bow and arrow? From a cost effectiveness standpoint we obviously would be better off if we went back to bows and arrows. A beer bottle filled with gasoline and stuffed with a rag wick is a fairly effective weapon at close quarters, and it is cheaper than a land mine or a hand grenade. From a cost/effectiveness viewpoint, we should be collecting beer bottles and old rags.

From a technological perspective, the design of a general purpose low cost satellite represents a progression toward the "beer bottle and old rag" approach. That is, one question posed by the ORION design philosophy has been that "If a basic satellite will accomplish many of the needs of a large audience of users, why should complex and costly 'one-of-a-kind' units be created to support individual needs ?" As a system, the general purpose satellite would be "intuitively" cost effective. Yet a subjective analysis of cost utility is exactly what cost effectiveness analysis seeks to avoid. In the system perspective, a detailed cost analysis of ORION must be undertaken to define its usefulness for each mission. In this sense its usefulness as a short lived "cheap-sat" must be evaluated relative to the usefulness of longer lived high value satellites. On the subsystem level, individual component and integration decisions must be weighed in the light of their utility, cost, worth, etc. Such a cost analysis is provided by Holcomb (JPL TR-32-15u5, 1972) in an analysis of candidate propulsion systems for the ATS-H satellite It demonstrates that cost effectiveness analysis is very quantitative at the subsystem level.

A detailed cost effectiveness analysis is beyond the scope of this thesis. The cost breakdown in Table 2-12 indicates only estimated costs and does not attempt to evaluate the various cost effectiveness criteria. However, the expenditure of human resources is part of an evaluation of cost, and it is apparent that the design and construction of ORION at NPS using graduate student labor is certainly a cost effective element of the ORION design program. Consideration of all the cost effectiveness elements should be made at each step of the design process. Design decisions should be documented quantitatively as a function of cost, utility, probability of success, worth and effectiveness. Doing so, it will be easy to analyze past decisions and to document the overall value of the ORION concept.

What benefit can be gained from a cost effectiveness analysis of systems? Ultimately, when faced with a list of candidate systems and their associated mass, cost, reliability, and power, a selection of a single system for a given mission must be performed. These characteristics (weight, reliability, etc.) have different relative effects on the system capability depending on the particular mission in question. With cost effectiveness techniques these diverse characteristics can be normalized into one figure-of-merit, thereby establishing the quantitative relative importance of each characteristic. In the past, selections have too often been made on unclear and undefined criteria and have therefore been subject to conflicting personal opinions. Use of the proposed cost-effectiveness selection criteria, if nothing else, forces the decision maker to document his input data and assumptions; traceability is vastly increased.

3. General Purpose Architecture

In 1976 the Aerospace Corp. and Rockwell International were funded by the US Air Force to conduct a preliminary design study for the Space Test Program Standard Satellite (STPSS). The purpose of this satellite would be to provide support to the many scientific and military payloads proposed to the US Air Force and US Navy for spaceflight. Often these payloads were

developed by DoD research laboratories but without a specific launch assignment. One of the missions of the Space Test Program is to solicit launch opportunities for one-of-a-kind payloads and promising innovative concepts. The STPSS was to provide a Shuttle-deployed spacecraft capable of supporting many different payloads at various orbits. As a result of the stipulation that STPSS would be the common carrier of these payloads. the satellite design was constrained to be general purpose and flexible. Consequently, the Aerospace Corp. initiated a survey of the potential users of STPSS for their basic satellite requirements and attempted to integrate those needs into the STPSS design.
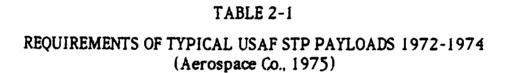
In a survey of 43 STP spaceflight requests between 1972 and 1974, the Aerospace Corp. identified a range of requirements for payload support in the areas of payload volume, payload mass, payload power consumption and data rate. The mean and range of these STP requests were compared to 60 Navy STP spaceflight requests made between 1985 and 1986. The Aerospace Co. survey showed that the mean and 90th percentile payload support requirements were as indicated in Table 2-1 and Figure 2-5. Compare these to the typical NASA requirements of Table 2-2. The Aerospace Co. survey and NASA data indicate that the average payload mass for 357 spaceflight requests is 32 pounds. The Aerospace survey of DoD payload requests indicates a need for a volume of 1500 in^3 and 14 watts power. This was only one third of the volume and power requested by the civilian sector. The data rate requirements of the two surveys are roughly similar. The 1985-1986 Navy payloads were not documented by the author but were subjectively observed to conform to the mean values indicated in

Table 2-3. These requirements are similar to those of the two quantitative surveys.

The Aerospace Corporation survey also addressed orbital, instrument and attitude control requirements of many potential STP payloads. Table 2-4 details the results of a survey of 40 payload requests. The orbital requirements vary widely, but the majority of the payloads require some sort of low orbit (below 500 nm). Table 2-5 illustrates the inclination requirements of 42 payload requests. Most payloads users requested near-polar orbits which was con;; tent with the STP role of support for deep space, sun and earth observation missions. Table 2-6 illustrates the diversity of potential STP payloads with regard to experimental apparatus. Note that the majority of payloads would use particle counters. The Navy

TABLE 2-1

REQUIREMENTS OF TYPICAL USAF STP PAYLOADS 1972-1974
(Aerospace Co., 1975)

Characteristic	Mean	90th Percentile
Data Rate, bits/sec	2000	40,000
Power, watts	14	50
Volume, cubic inches	1500	10,000
Weight, lb	30	200

Figure 2-5

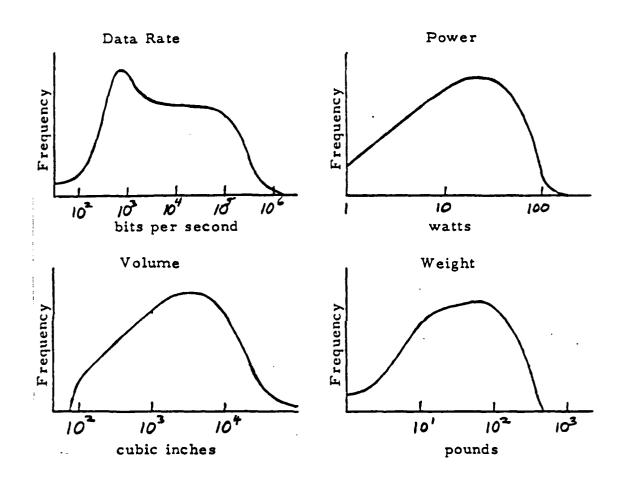Characteristics of STP Payload Requests 1972-1974
(Aerospace Co., 1975)

TABLE 2-2

REQUIREMENTS OF TYPICAL NASA PAYLOADS 1972-1976
(Aerospace Co., 1975)

Characteristic	Cases	Mean	80th Percentile
Data Rate, bits/sec	102	4000	5×10^8
Power, watts	208	38	56
Volume, cubic inches	139	4800	9000
Weight, lb	324	32	50

TABLE 2-3

REQUIREMENTS OF TYPICAL NAVY STP PAYLOADS 1985-1986

Mass	50 lbm
Volume	3 ft^3
Power	50 watts
Data Rate	10,000 bits/sec
Attitude Control	+/- 0.01° to 1.0° Three Axis
Orbits	200-800 nm circular
Inclinations	Primarily 28.5°

STP payloads of 1985-1986 were almost exclusively low earth orbit (less than 300 nm) missions at Shuttle inclinations (28.5 degrees). The majority of Navy STP requests are generated by the Naval Research Laboratory Space Sciences group. Their emphasis upon X-Ray astronomy and upper atmosphere research was reflected in the fact that most Navy STP requests proposed the use of particle counters or lenses, photomultipliers and microchannel-plate type instruments. In the Aerospace and Navy surveys, simple instruments that required only particle counter or lens mounting holes were predominant. This is advantageous from the satellite design point of view in that it simplifies the integration of the payload.

Finally, an attitude control requirements survey was conducted by Aerospace Corp. using 51 STP requests submitted between 1970 and 1978. Table 2-7 shows that, for major (or primary mission) payloads, the predominant requirement was for three axis stabilization. Minor payloads, or those meant to fly space-available, typically requested spin stabilization. A few minor payloads demonstrated no preference. Pointing accuracy requirements were more stringent for the three axis stabilized payloads. Minor payloads exhibited a wide variation in acceptable accuracies. The Navy STP survey conducted by the author reflected an almost unanimous choice of three axis stabilization, with pointing accuracy requirements commensurate with the astronomy and ultraviolet missions of the NRL experimenters (.01 to 1 degree).

The STPSS survey, the author's survey of Navy STP, and the popular success of the NUSAT, GLOMR and SPARTAN spacecraft were all considered in the selection of a general purpose design philosophy for ORION. In a
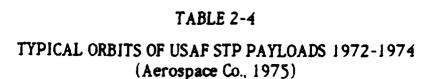
TABLE 2-4

TYPICAL ORBITS OF USAF STP PAYLOADS 1972-1974
(Aerospace Co., 1975)

Group	Usual Motivation of Group	Altitude Range (nmi)	Cases
1	Close to earth	70 to 200	5
2	Close to earth with longlife	200 to 500	13
3	High Altitude	1000 to 18,000	4
4	Earth-synchronous	19,323	4
5	Dip in and out of atmosphere	Low-elliptic 60 to 200	7
6	Dip in and out of magnetosphere	High-elliptic 200 to 10,000	7

TABLE 2-5

TYPICAL ORBITAL INCLINATIONS OF USAF STP PAYLOADS
(Aerospace Co. 1975)

Inclination requested (degrees)	No. of cases
60 - 120	26
30 - 60	0
0 - 30	7
Any orbit	9

TABLE 2-6

TYPICAL INSTRUMENTS OF USAF STP PAYLOADS 1972-1974
(Aerospace Co., 1975)

Measurements	Typical Instrument	Typical Requirement	Cases
Particles	Counter	Hole	46
Light	Spectrometer	Lens	19
E Fields	Receiver	Antenna	11
B Fields	Magnetometer	Coil	3
Gravity Fields	Accelerometer	Test Mass	3
Other	-	-	4
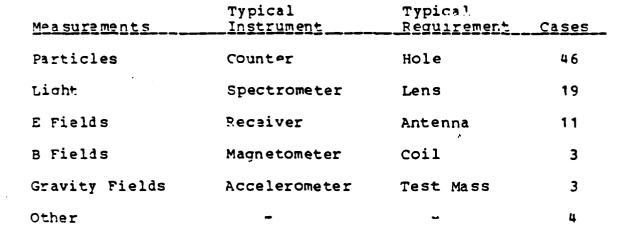
TABLE 2-7

ATTITUDE REQUIREMENTS OF TYPICAL STP PAYLOADS
(Aerospace Co., 1975)

Type of Control	Major Satellite Payload	Minor Satellite Payload
3-axis attitude control	13	8
Spinning attitude	3	18
Unconcerned	1	8
Total Number	17	34

Pointing Accuracy	Major Satellite Payload	Minor Satellite Payload
3-axis, degree	0.25 - 1 (Note 1)	1 - 10
Spinning, degree	approx 2	2 - 20

broad sense, a general purpose architecture was defined as the ability to successfuly integrate various payloads of the proper size while providing a propulsion, attitude control and standardized electrical, data and attitude control interfaces. By virtue of the need to accomodate various payload geometries, modular construction was selected for ORION with the provision to alter component placement as needed without significantly impacting the success of the design.

Physically speaking, "general purpose" was defined as accommodating the "mean" payload. Table 2-8 details the mean payload parameters extracted from the STP and Navy surveys. Because the orbital requirements of the surveyed payloads varied so widely, it was determined that the satellite should possess the propulsion capability to operate in circular orbits as high as 800 nm, which is coincidentally the lower limit of the lower Van Allen radiation belt. Although the majority of payloads surveyed requested three axis stabilization, ORION was initially targeted as a spin stabilized vehicle. In many cases, spin stabilization requires less propellant than the three axis. Thus a combination of high orbits and energy intensive attitude control may not be compatible in a small satellite. A general purpose architecture was pursued using a judicious propulsion system design with a future three axis system upgrade in mind. The attitude control goal of +/- 1° enables ORION to satisfy most STP mission requirements.

The design of a general purpose propulsion system is difficult. The lesson learned from NUSAT, GLOMR, and SPARTAN was that insufficient attention has been given to the propulsion needs of experimenters.

TABLE 2-8

SUMMARY OF TYPICAL NAVY/STP PAYLOAD REQUIREMENTS

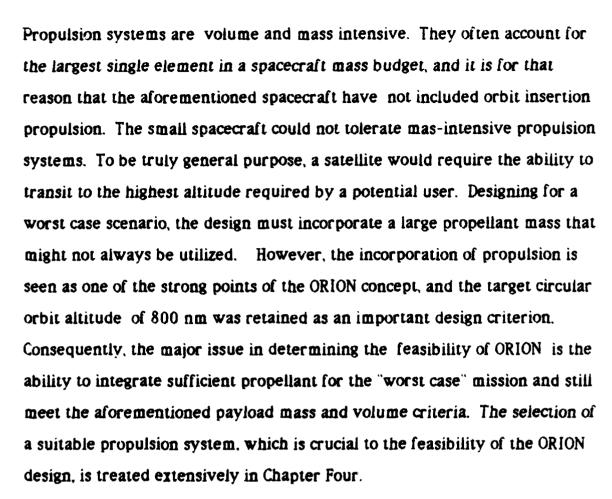|	
Mass	32 lbm
Volume	2.36 ft^3
Power	34 watts
Data Rate	5000 bits/sec
Orbit	200-800 nm circular
Inclination	0°-30° or 60°-120°
Instruments	Particle Counter or Lens
Attitude Control	3 Axis +/- 0.75°
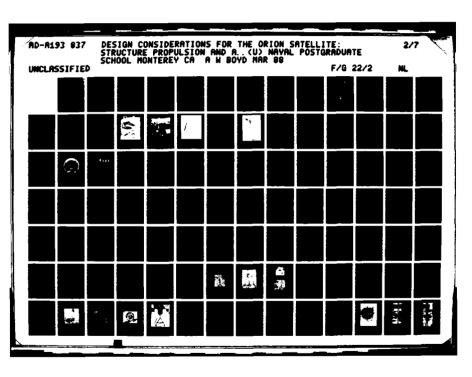
Propulsion systems are volume and mass intensive. They often account for the largest single element in a spacecraft mass budget, and it is for that reason that the aforementioned spacecraft have not included orbit insertion propulsion. The small spacecraft could not tolerate mas-intensive propulsion systems. To be truly general purpose, a satellite would require the ability to transit to the highest altitude required by a potential user. Designing for a worst case scenario, the design must incorporate a large propellant mass that might not always be utilized. However, the incorporation of propulsion is seen as one of the strong points of the ORION concept, and the target circular orbit altitude of 800 nm was retained as an important design criterion. Consequently, the major issue in determining the feasibility of ORION is the ability to integrate sufficient propellant for the "worst case" mission and still meet the aforementioned payload mass and volume criteria. The selection of a suitable propulsion system, which is crucial to the feasibility of the ORION design, is treated extensively in Chapter Four.

An accepted fact is that a satellite design cannot be all things to all people. However, with consideration given to the needs of the approximately 110 USAF and Navy payloads surveyed, a workable design can be produced that satisfies the requirements of most of the payloads most of the time. The "mean payload requirements" identified in surveys conducted by the author and the Aerospace Co. were adopted as a framework about which to structure the definition of a general purpose architecture. Most of the potential users contacted by the author expressed the opinion that the availability of a low cost satellite like ORION justifies compromises in one or more design areas. Experimenters in search of a

MICROCOPY RESOLUTION TEST CHART

launch opportunity sometimes sacrifice several payload support requirements rather than not fly at all. An ORION design that does not meet the specifications of every experimenter and military user may nonetheless be attractive to all of them by virtue of the satellite's low cost. Thus, satellite design is iterative because it is a process of repeated compromises.

4. Reliability

Of the five design constraints, reliability is the most difficult to define. Like affordability, reliability is quantifiable but is also strongly influenced by perception. Reliability involves the expectation that a component or system will perform dependably over a period of time. For a designer to accept a 0.9 reliability means two things: there is a 90% likelihood that the component or system will perform satisfactorily, and there is a 10% chance that it will fail. This is graphically illustrated by public frustration with the Shuttle accident of January 1986. Although the Shuttle system was advertised as 98% reliable, that figure also implied that 1 flight in 50 would fail. Few people realized that the quoted reliability figures applied to the lifetime of the Shuttle system, not each individual Shuttle launch performance. Although reliability is quantifiable through such methods as Mean-time-between-failure (MTBF) analysis, it is also conditioned by the designer's (and the public's) opinion of "acceptable performance". Reliability, therefore, implies an acceptance of risk.

To state that ORION should be reliable actually means that it should not fail more often than is acceptable from a mission and economic point of view. As affordability is stressed, the design may be guided toward the use of less reliable and less expensive components. If the satellite fails early in

its lifetime as a result of poor quality components, then it is no longer cost effective. However, ultra-reliable satellite systems require the selection of expensive space qualified materials and the use of redundancy. There must be a middle ground where some reliability is sacrificed to lower the vehicle cost but not so much as to incur an unacceptably high probability of failure.

No system can achieve its purpose more reliably than its least reliable component. For this reason it becomes the job of the engineer to develop hardware that is reliable and economical.

The development of reliable hardware can be divided into various phases. Each phase is as important as any other, and the final result is only as good as the least pursued phase of the development program. Components are designed to perform specific functions. The simpler the function the higher the reliability the individual component can achieve. Assignment of too broad a function for any one component can make its subassemblies too numerous and too complicated.

Another important ingredient which must go into the initial design of a reliable component or system is the ease of maintenance and installation. Unless some thought is given to these problem areas at the inception of the design, major problems and loss of time are inevitable.

Quality control programs must be put into effect. It is a fundamental fact that unless quality control standards are maintained throughout every phase of the manufacture, test and assembly of a component, reliability is impossible.

Testing is far and away the most important ingredient in the development of reliable hardware. Testing should be carried out during every phase of the development. Time utilized in test programs is worth its weight in reliability percentages. (Ring, 1964, pp. 155-156).

The overall reliability of a vehicle composed of many components is the product of the individual reliabilities. With a given component

97

population of 400, and individual reliabilities of 0.99, the total reliability is 0.99^{400}, or 1.8%. For this reason, many designs incorporate redundancy to circumvent the low product reliability. Doing so, the system reliabilities are made very high (i.e. 0.99999) and their products result in greater dependability. For example, 400 redundant components with individual reliabilities of 0.99999 would have a product reliability of 0.99999^{400} or 0.996. Unfortunately, as the designer resorts to redundancy, weight increases. The solution to this tradeoff is to use only a few simple components and ensure that their individual reliabilities are as high as possible consistent with affordability and cost effectiveness. Therefore, simplicity is synonymous with reliability.

The ORION mass budget has little room for ultra-reliable components and a weight and volume margin that permits redundancy is unlikely. Therefore, the ORION design was constrained to be ultra-simple, attempting to offset mass, volume and cost compromises through the use of a few simple highly reliable components. A total (product) reliability goal of no less than 0.95 was identified. This figure was based upon the perception that a 5% probability of failure would be acceptable in view of the satellite's low cost. Table 2-9 depicts the reliabilities of a Shuttle launched Air Force satellite and its subsystems. In order to achieve a combined reliability of 0.95, each of the 8 systems depicted in Table 2-9 require reliabilities of at least 0.95 $^{0.125}$, or 0.9936. Therefore the minimum reliability for each of the ORION subsystems is 0.9936. This will be easy to implement in all but

TABLE 2-9

BOEING CO. FLIGHT VEHICLE RELIABILITIES
(Boeing Aerospace Co., 1981)

- ASDS Flight Vehicle Reliability Prediction:
  - Fluid Systems (Pressurization, Feed, Fill, Dump)   0.999995
  - Reaction Control System (IUS Data Base)   0.999934
  - Avionics (IUS Data Base)   0.999540
  - Electrical Power & Distribution (IUS Data Base)   0.999946
  - Thermal Control (IUS Data Base)   0.999986
  - Main Propulsion Engines   0.99740
    - TVC System   0.99964

  Combined Reliability - 0.99644

the propulsion and attitude control systems due to the lower reliability values associated with mechanical systems (as opposed to electrical systems).

The Aerospace Co. survey did not identify the minimum useful lifetimes of the STP payloads. The author's survey of 1985-1986 Navy STP requests indicated that lifetime requirements of 30 days to 3 years were typical of most payloads. The short lived missions were usually military reconnaissance and imaging experiments. The scientific missions required much longer lifetimes for data collection. Based upon inputs from military and scientific satellite users. a design goal of up to three years was adopted for ORION dependent on the satellite orbit. That is. the lifetime goal was established independent of orbital drag considerations. As lower orbits and more atmospheric drag are encountered, the satellite's orbital lifetime will decrease. Orbital lifetime is not related to a reliability lifetime.

In summary. reliability is observed to consist of quantitative measurements and subjective perceptions. The reliability of a set of satellite subsystems can be combined to derive a total spacecraft reliability. Yet this value must be evaluated with respect to an acceptance of risk. High reliabilities for ORION may not be economically feasible. yet a high risk (10%) of failure may not be acceptable to the sponsor. A compromise of cost and reliability is possible where simple highly reliable but non-redundant components are used in the design. A goal of a total space system reliability of 0.95 has been set for the ORION design. Simple systems are to be used to the greatest extent possible to ensure a minimum lifetime of three years.

5. Safety

The first four of the design constraints have been observed to be sufficiently flexible that one can be compromised in favor of another. However. safety is not subject to compromise. In the ORION context. safety is defined as the prevention of hazards to the ground handling crew and the launch system. As mentioned in Chapter one. the satellite has been designed to mate with the Space Shuttle extended Get-Away-Special canister. Therefore. ORION must conform to the safety restrictions imposed by NASA for Shuttle payloads (KHB 1700.7a). The compromises that occur with regard to safety will be compromises of the other design constraints to ensure that the vehicle is safe. Particular attention must be given to this aspect of the design in the aftermath of the loss of the Challenger orbiter. No less important is the fact that GAS ejectable satellites have not been flown with a propulsion system. Consequently. it is reasonable to expect that considerable attention will be focused upon the safety aspects of the propulsion system design. All aspects of the ORION design are patterned after the safety requirements of NASA KHB 1700.7A safety document and the Get-Away-Special safety manual. No less will suffice.

C. DESIGN SPECIFICATIONS

The ORION design began with the five conceptual criteria described in the previous section. These criteria were specified in greater detail and led to the adoption of initial specifications for cost. payload mass and volume. data rate. payload power consumption. attitude control, and so forth. However. these criteria are too general to enable the design to specify component level

101

details. The purpose of this section is to document the choices made in the selection of even more stringent design criteria. The selection of a launch system was responsible for many of the ORION design decisions. Using the limitations imposed by the selection of the GAS canister as a deployment mechanism. many structural criteria were defined. US Air Force/SDIO sponsorship of a first satellite and provision of mission criteria additionally constrained the design. Mass. volume and power budgets were adopted to guide the design of the structure and power subsystems.

1. Launch Vehicle Options

Affordability was the primary consideration in the initial choice of a launch system for ORION. The expense of space transportation is so great that the benefit of an inexpensive satellite is soon overwhelmed by an expensive launch. It was desirable choose a launch method whereby the cost incurred would be small relative to the price of the satellite. However. in the wake of the Challenger explosion and numerous ELV failures. the reliability of a launch system has been seen to outweigh consideration of cost. While this thesis primarily addresses a Shuttle launched ORION. it is not unlikely that future ORION sponsors will want to tie development of this spacecraft to an expendable launch rather than make it dependent upon a transportation mechanism of questionable reliability (Shuttle).

The least expensive Expendable Launch Vehicle (ELV) in the US inventory is the SCOUT ELV. SCOUT will transport a 450 pound payload into a polar circular orbit of 100 nm. or 550 pounds to 100 nm at an inclination of 57.7 degrees. Shrouds 34˝ or 42˝ diameter will permit the integration of payloads as long as 61˝. The launch and range support costs for a single

SCOUT launch are approximately $15 million. Figures 2-6 through 2-9 depict the orbital performance and payload capabilities of SCOUT. There have been 106 successful missions using SCOUT since the late 1950's. Unfortunately. there are reportedly only five of these launch vehicles remaining that have not been manifested. A follow-on SCOUT upgrade program has been proposed to SDIO by the LTV Vought Aerospace Corp. (LTV, 1986) that would enable SCOUT to launch 600 pounds to a retrograde equatorial orbit at 100 nm. This program has not been funded at the time of this writing. Although SCOUT would be the least expensive ELV launch opportunity for ORION. it is significantly more expensive than the satellite.

Launch opportunities aboard the other American ELVs would be even more expensive and difficult to manifest. Commercial launch vehicles such as the AMROC ELV being develped by the American Rocket Co. of Camarillo. CA would be useful, but the launch price is equivalent to that of SCOUT. Foreign launch vehicles are equally expensive. Hence. the use of an ELV for typical ORION applications does not neccessarily complement the ORION affordability. ELVs are probably best suited to costly payloads and ORION launches to unusual orbits. There is little economic return to be realized by launching "cheap-sats" on expensive ELVs.

The other launch service available to ORION is the Space Shuttle. Deploying a satellite from Shuttle through conventional means involves the ejection of the spacecraft from a suitable cradle in the cargo bay. Payloads are charged pro rata for the volume or mass which they displace. Shuttle launch cost estimates range from $ 40 million to $100 million. depending upon the level of government subsidy considered. For a typical Shuttle
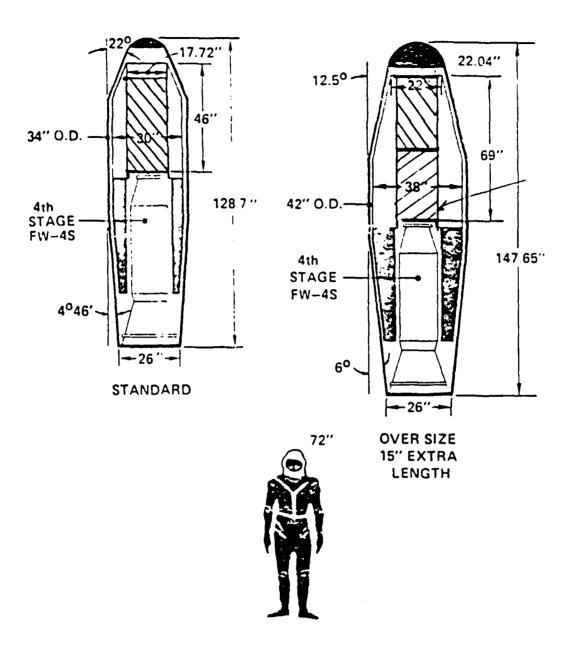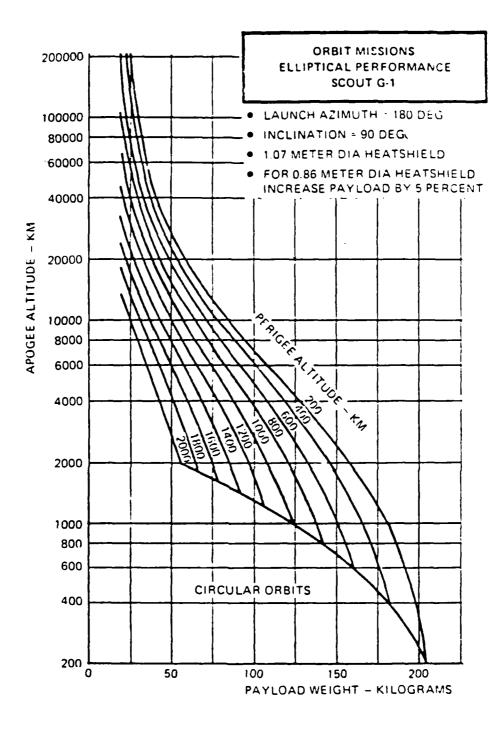
STANDARD

**OVER SIZE
15" EXTRA
LENGTH**

72"

Figure 2-6

SCOUT Payload Fairings and Payload Volume
(Vought Co., 1980)
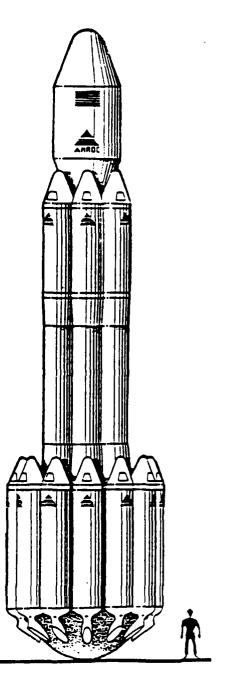
Figure 2-7

SCOUT Elliptic Orbit Performance - Vandenberg AFB Launch
(Vought Co., 1980)

105

Payload (135 mi circular orbit)
- Polar - 3,000 lbs.
- 28.5° inclination - 4,000 lbs.

Payload Interface
- 37 in diameter standard per Delta/PAM-D/Ariane

Nose Fairing
- Diameter - 90 in.
- Cylindrical length - 9 ft.
- Conical - 6 ft.

Maximum Acceleration (Longitudinal)
- Without throttling - 7.2 g
- With throttling - 5.8 g

American Rocket Company
847 Flynn Road
Camarillo, CA 93010
(805) 987-8970

For further information
please contact James C. Bennett

May 7, 1987

Figure 2-8a

American Rocket Company "Industrial Vehicle One" Specifications
(Reproduced from AMROC/GLOBESAT Promotional Literature)
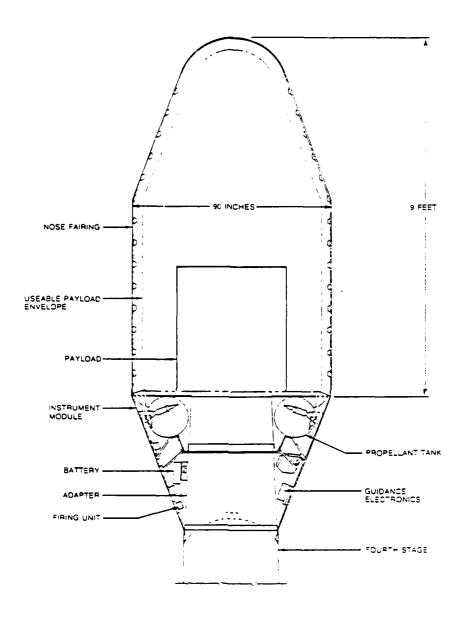
Figure 2-8b

American Rocket Company Launch Vehicle Fairing/Shroud
(Reproduced from AMROC Promotional Literature)

Vehicle Name	Company	Number of Orions (350 lb.)	Altitude Equatorial KSC	Polar VAFB
Super Starbird				
(Castor 4A)	SDC	1	360 NM	125 NM
(Algol 3A)	SDC	1	470 NM	220 NM
SDC Scout (star 20)	SDC	1	620 NM	340 NM
C-3A (star 20)	SDC	1	630 NM	350 NM
(star 30)		1 (2)	300 NM	960 NM
Pioneer (31)	SDC	1	740 NM	470 NM
LEO	ECR	1	800+NM	460+NM
		2	280+NM	--
Liberty 1	PAL	1	750 NM	155+NM

SDC = Space Data Corporation (602) 966-1440

ECR = Eagle Canyon Research (916) 644-1171

PAL = Pacific American Launch Systems (415) 595-6500

Figure 2-9

Expendable Launch Vehicle Options for ORION

payload of 50,000 pounds, the launch of a satellite will cost between $800 and $2000 per pound. Assuming a mass of 250 pounds for ORION, this equates to a launch expense of $200,000 to $500,000.

Satellites can also be ejected from Get-Away-Special (GAS) canisters mounted in the Shuttle cargo bay. There are two styles of GAS canisters available from which to deploy satellites. The first is the standard 5 cubic foot GAS canister that was used for NUSAT and GLOMR. This canister will transport a satellite payload of 150 pounds in an envelope 19" in diameter by 18.5" long. Launch costs for the standard canister are approximately $10,000. This equates to a per-pound cost of approximately $65. Although this is much less than the cargo bay expense, it comes at the penalty of reduced inflight support and a small payload mass. The NUSAT launch mechanism, depicted in Figure 2-13, uses a tripod style mount and Marmon band clamp apparatus to secure the prospective satellite. When a launch is commanded by an astronaut from the aft flight deck of Shuttle, the opening lid of the canister is deployed (Figures 2-14, 2-15), and the spring loaded Marmon clamp is released using two pyrotechnic bolts. A spring loaded plunger then separates the satellite from the tripod base at a velocity of 4 feet per second.

Although the NUSAT launch mechanism successfully deployed the NUSAT and GLOMR vehicles, it is excessively bulky to permit the integration of larger, more capable payloads. The small payload volume severely restricts satellite designs. In 1986, program managers at the US Air Force Space Test Program office recognized this deficiency and funded the development of a second generation GAS launch mechanism. USAF/STP

109
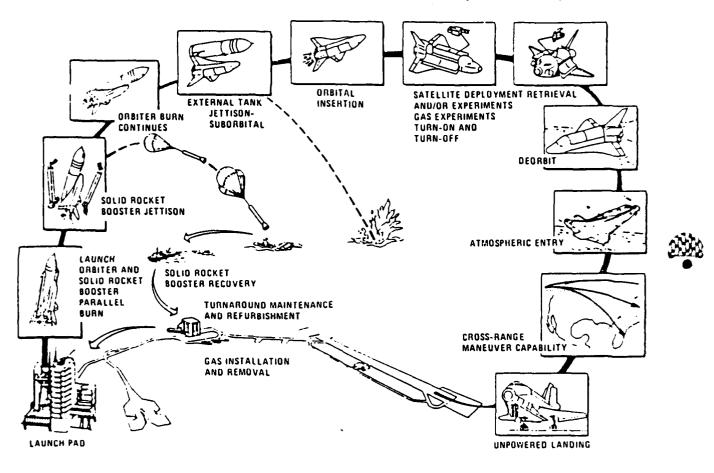
SPACE SHUTTLE MISSION PHASES (TYPICAL)

Figure 2-10

Space Shuttle Operations
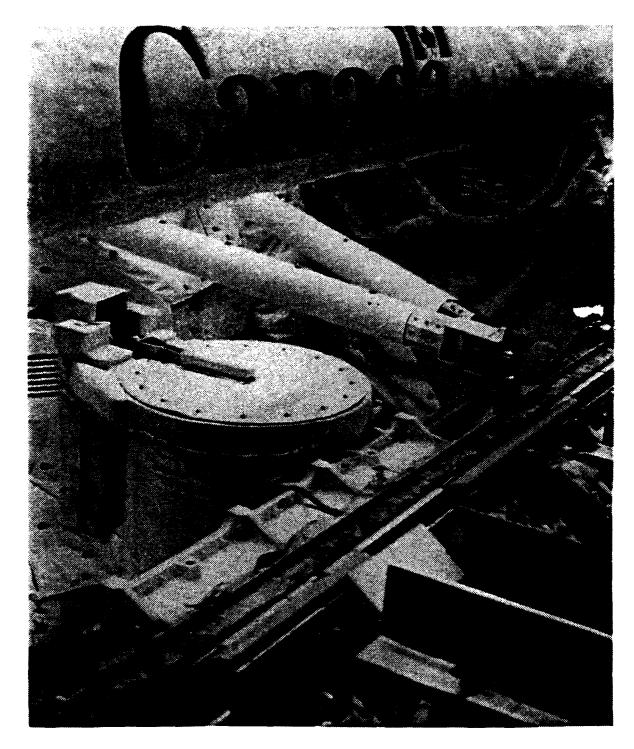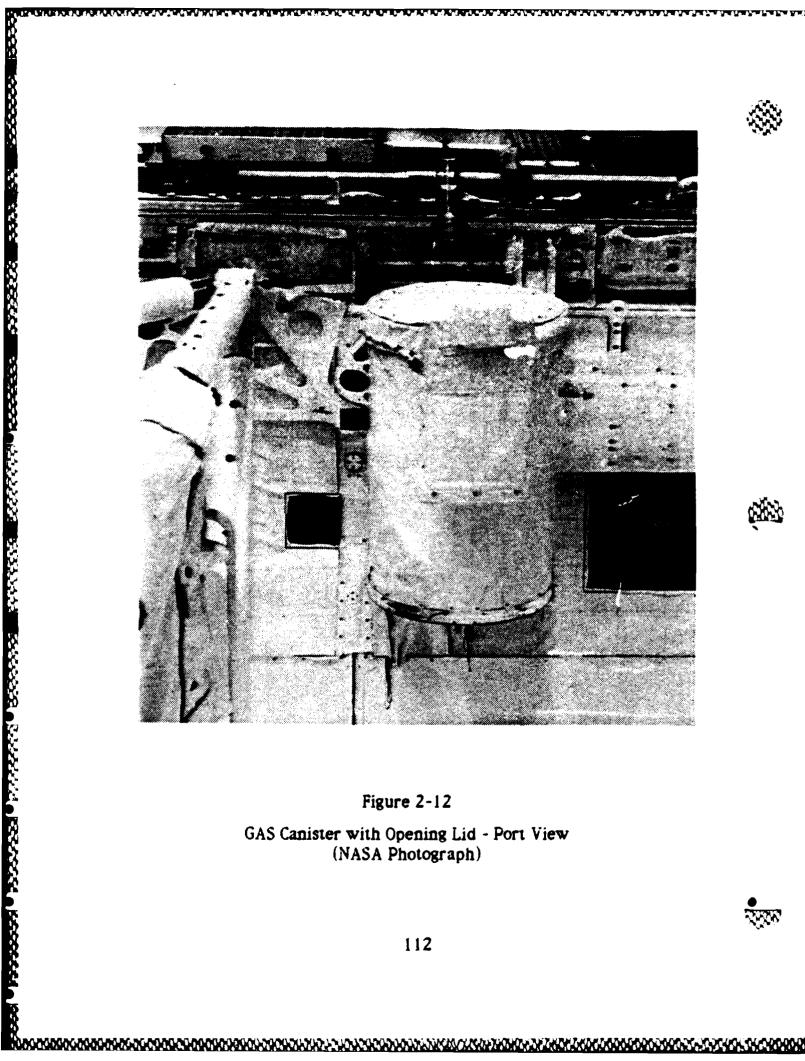(NASA GAS Experimenter Handbook, 1984, p.5)

Figure 2-11

GAS Canister with Opening Lid - Starboard View
(NASA Photograph)

111

Figure 2-12

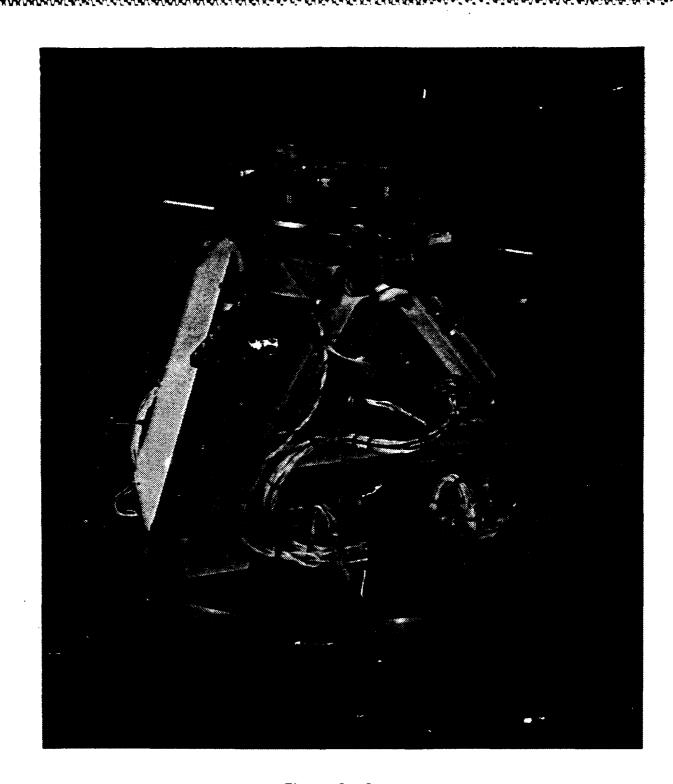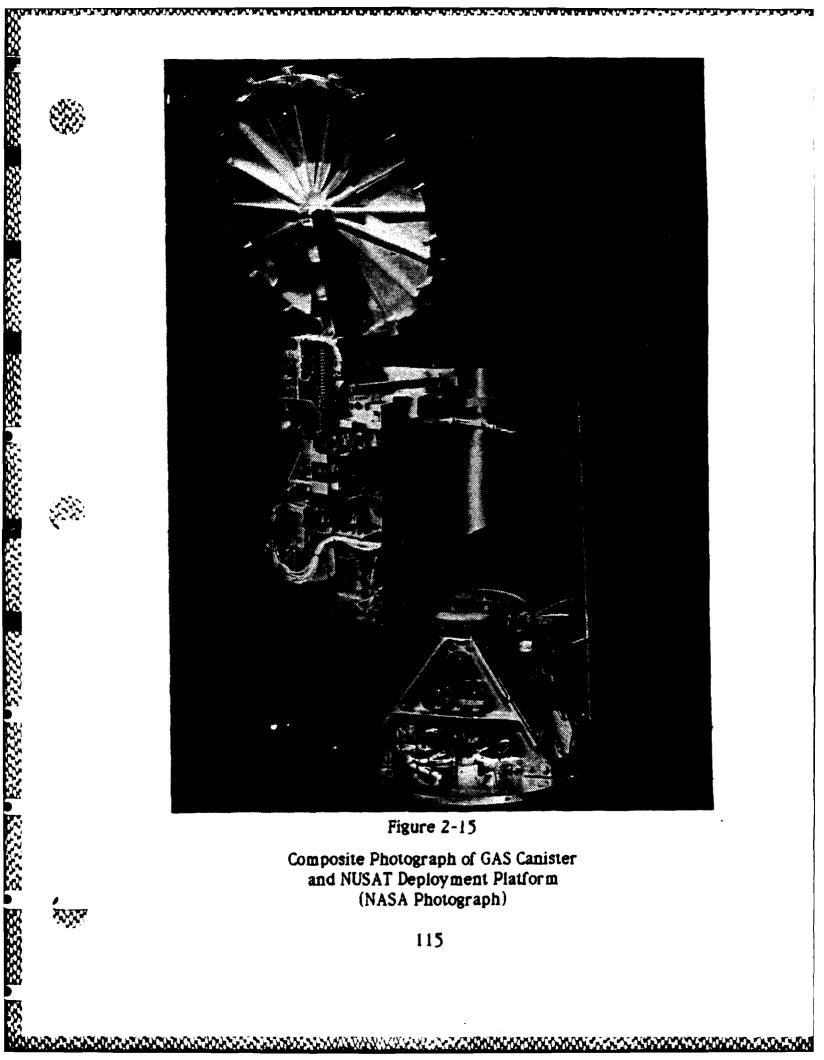GAS Canister with Opening Lid - Port View
(NASA Photograph)
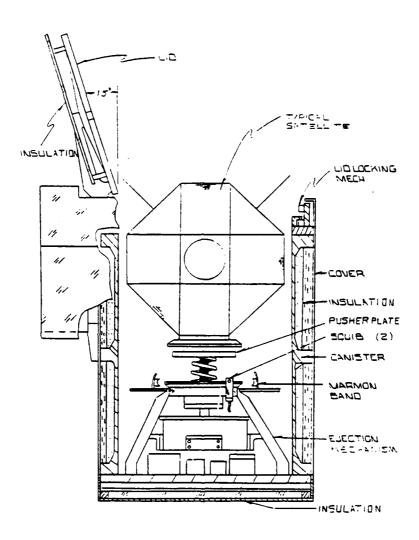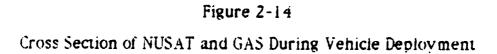
Figure 2-13

NUSAT Launch Tripod and Marmon Clamp Assembly
(NASA Photograph)

113

LID

15°

INSULATION

TYPICAL
SATELLITE

LID LOCKING
MECH

COVER

INSULATION

PUSHER PLATE

SQUIB (2)

CANISTER

MARMON
BAND

EJECTION
MECHANISM

INSULATION

Figure 2-14

Cross Section of NUSAT and GAS During Vehicle Deployment

114

Figure 2-15

Composite Photograph of GAS Canister
and NUSAT Deployment Platform
(NASA Photograph)

115

(Code SD/YCM) contracted Ball Aerospace Co. of Colorado Springs, CO. to develop an extension to the basic GAS canister that would house a low profile launch unit and the GAS interface electronics (Ball Aerospace, 1986). This GAS modification, known as the Extended GAS Canister, will enable the transport of much heavier (up to 250 pounds) satellites measuring 19" diameter by 35" long. A comparison of the volumes for the two deployment options is depicted in Figure 2-17. Because only one canister can be carried on a GAS adaptor beam in the cargo bay (as opposed to two for NUSAT), the launch costs are approximately $20,000, or $80 per pound.

Using either canister, a GAS deployment will provide a launch that is significantly less expensive than the satellite itself. Additionally, the use of a GAS canister enables the satellite to be "pre-packaged" and await Shuttle integration as a consolidated GAS-satellite unit. Classified satellites would be especially well suited to this package-launch concept. The disadvantage posed by the GAS deployment concept is that the available volume and mass are very restricted. The development of a general purpose satellite with a large propulsion reserve using the constraints of a GAS canister is a challenging task. However, in consideration of the GAS canister affordability, launches using an ELV or a Shuttle cargo bay cradle were rejected in favor of the GAS canister deployment. The extended GAS canister was adopted due to its larger volume capability.
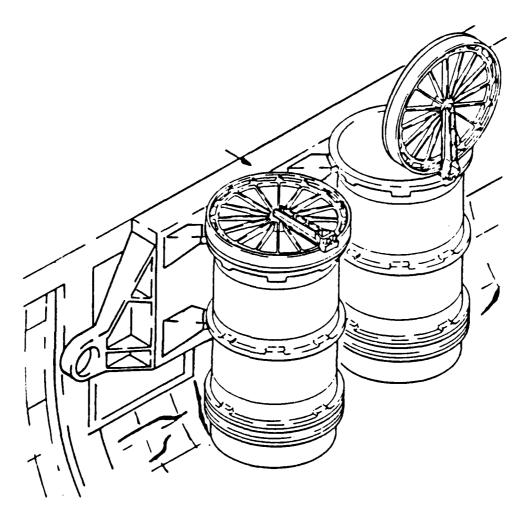
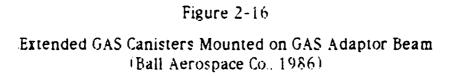## 2. Extended GAS Canister Specifications

The selection of the extended GAS canister for the deployment of ORION placed many specific constraints upon the design. Details of the canister and launch mechanism are included here to amplify upon design

Figure 2-16

Extended GAS Canisters Mounted on GAS Adaptor Beam
(Ball Aerospace Co., 1986)

117

CURRENT DESIGN

18.5"

19.0"

**EXTENDED
CONFIGURATION
89% INCREASED VOLUME**

35.0"

19.0"
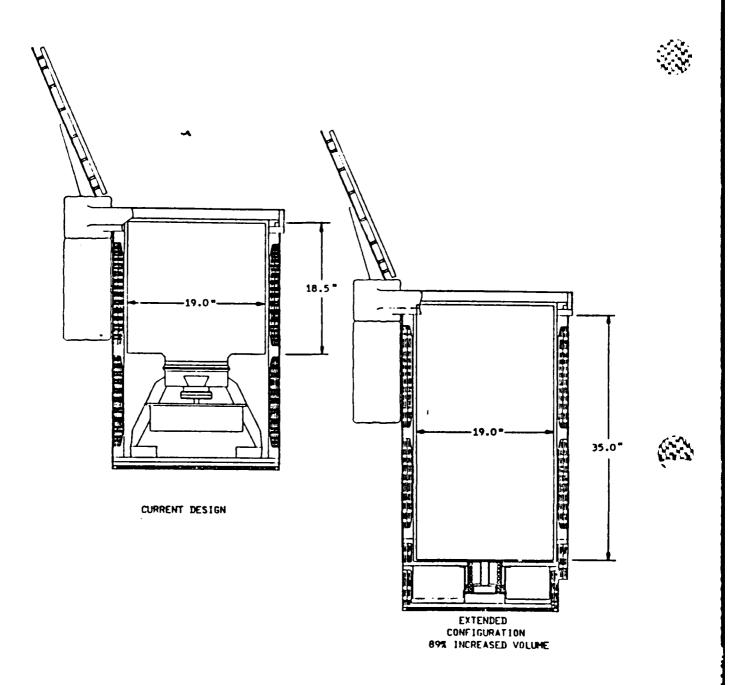
Figure 2-17

Extended GAS Canister Nearly Doubles Available Volume
(Ball Aerospace Co., 1986)

118

criteria for ORION. The construction details are extracted from the "Extended Get-Away-Special Canister Critical Design Review - 29 May 1986" manual distributed by Ball Aerospace to the USAF/STP offices. This preliminary document was superseded in the summer of 1987 and the reader is cautioned to consult USAF/STP program managers for specific construction details and interface requirements.

The objectives of the extended canister development were to increase the GAS payload envelope to the maximum extent possible while providing a suitable launch platform for satellite payloads. The designers sought to utilize existing GAS hardware to the maximum extent possible. The result of the Ball Aerospace design efforts is a 9.5" long extension ring which bolts to the base of a standard GAS canister sleeve. A cutaway view of the ring attached to the GAS sleeve is pictured in Figure 2-18. The extension ring provides a positive restraint for payloads using eight pins that lock a set of eight matching mounting flanges (lugs) projecting into the ring from the base of the satellite. In the center of the launch mechanism is a spring loaded plunger that forces the satellite out of the canister at approximately 3.5 feet per second. In the base of the ring are the various electronic modules responsible for interfacing with the Shuttle and sequencing the launch operation.

The electronic housing encloses five major components. Figure 2-19 depicts the GAS control decoder (GCD). Payload power Contactor (PPC). two battery boxes and a launch sequencing relay. The GCD and PPC are responsible for routing power to the launch mechanism and opening door after actuation by the Shuttle crew. The batteries and thru-bulkhead
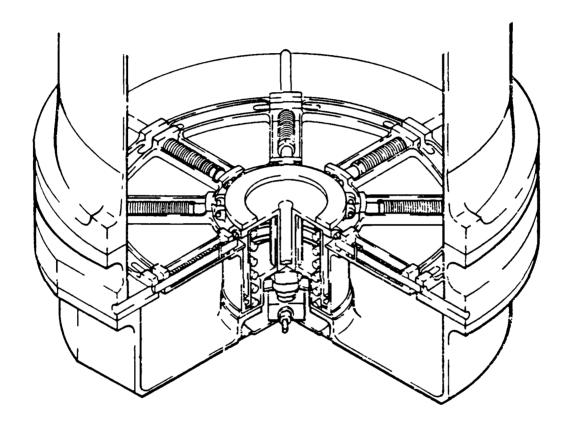
Figure 2-18

Cutaway View of Extended Canister and Launch Ring
(Ball Aerospace, 1986)

120

connectors are shown in a launch ring mock-up in Figure 2-20. Using a control box on the aft flight deck, an astronaut can activate the payload using one of three switches (see Figure 2-21). The astronauts' commands actuate relays in the GCD and PPC, directing power to the lid latches and motors, or the launch unit pyrotechnic nuts. There are no connections between the canister controls (on the aft flight deck) and the satellite. The satellite is inert until after launch separation. The extended canister functions only to control the launch. No satellite control is possible from the aft flight deck. This is also true for the NUSAT launch unit.

The extension ring restrains the satellite using eight retaining pins that mechanically lock the vehicle into the base of the canister (top of the extension ring). Eight receptacles for the satellite mounting lugs are spaced 45 degrees apart at a radius of 8" from the ring center. The retaining pins are compressed into the locking position by the plunger assembly in the center of the extension ring. Rollers are mounted on the periphery of the plunger and act as cams to hold the pins in the locked "ready to launch" position. The plunger is mounted on a guide pin and is compressed against a spring load. It is held in position beneath the satellite by a single pyrotechnic (explosive) nut. When the launch is commanded, the nut is explosively separated and the plunger is allowed to travel toward the payload. The upward movement of the plunger and rollers allows the springloaded pins to retract from the 8 satellite mounting lugs. The pins are fully retracted within 3 milliseconds after the pyrotechnic nut actuates. The plunger traverses the remaining 0.5" to the base of the satellite in the next 84 milliseconds. After contacting the base of the satellite, the plunger ejects
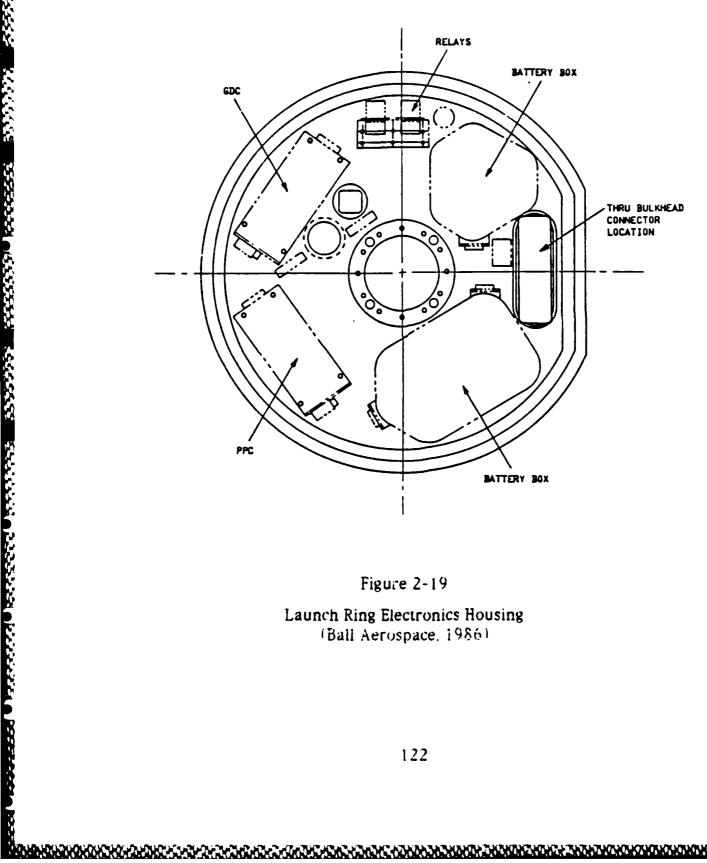
121

Figure 2-19

Launch Ring Electronics Housing
(Ball Aerospace, 1986)
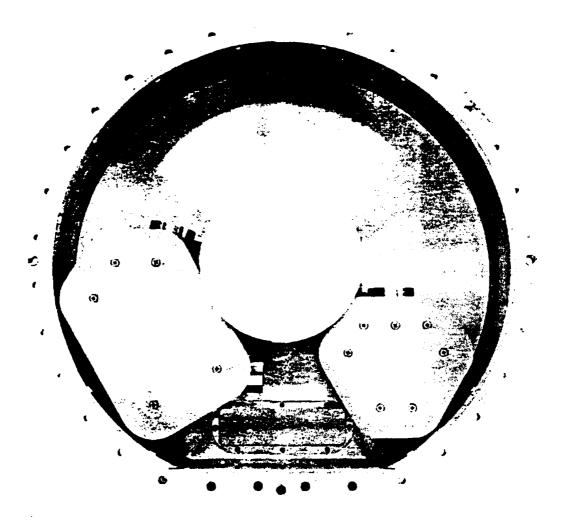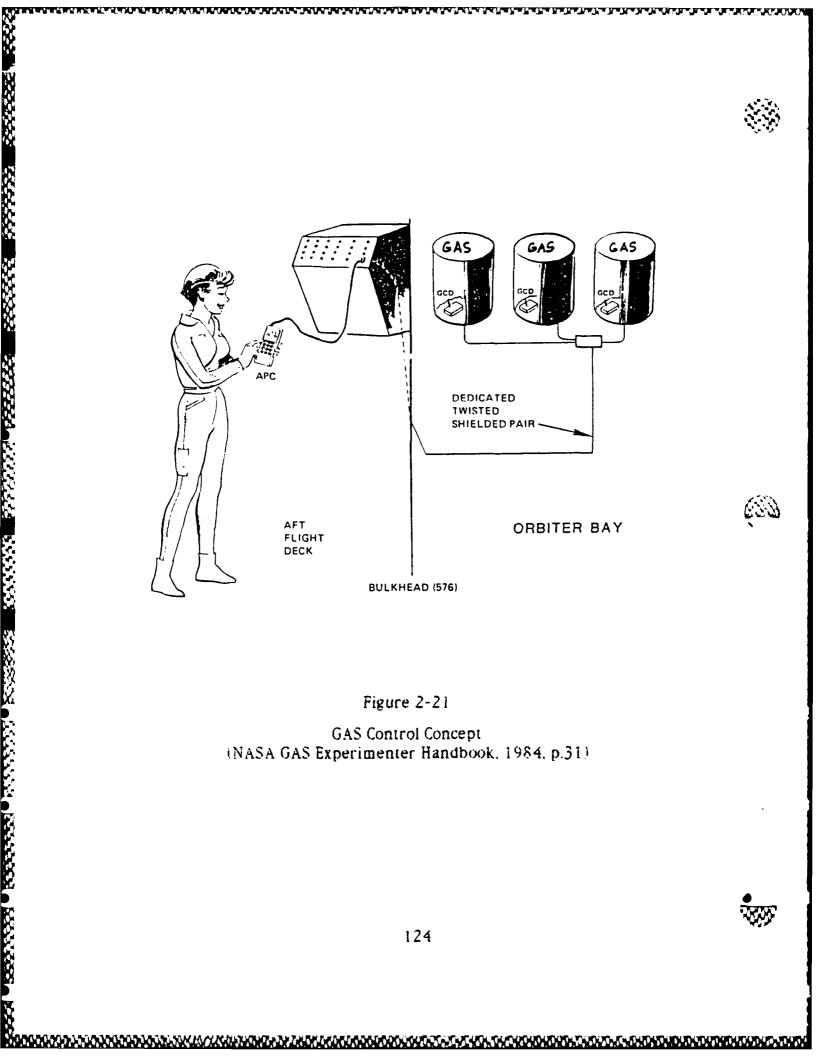
Figure 2-20

Electronics Housing Mock-up
(Ball Aerospace, 1986)

Figure 2-21

GAS Control Concept
(NASA GAS Experimenter Handbook, 1984, p.31)

ISOMETRIC CUT AWAY

Figure 2-22

Details of Ejection and Retaining Pin Assemblies - View #1
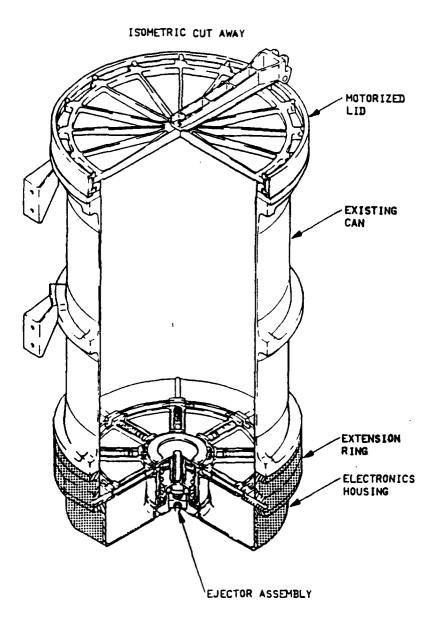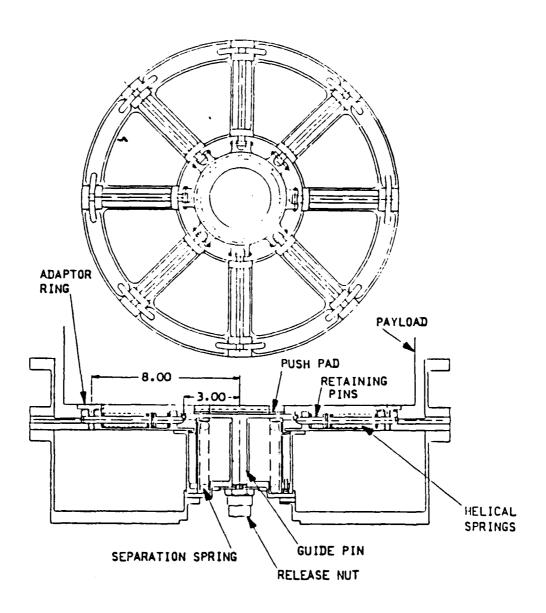(Ball Aerospace, 1986)

125

Figure 2-23

Details of Ejection and Retaining Pin Assemblies - View #2
(Ball Aerospace, 1986)

Figure 2-24

Details of Ejection and Retaining Pin Assemblies - View #3
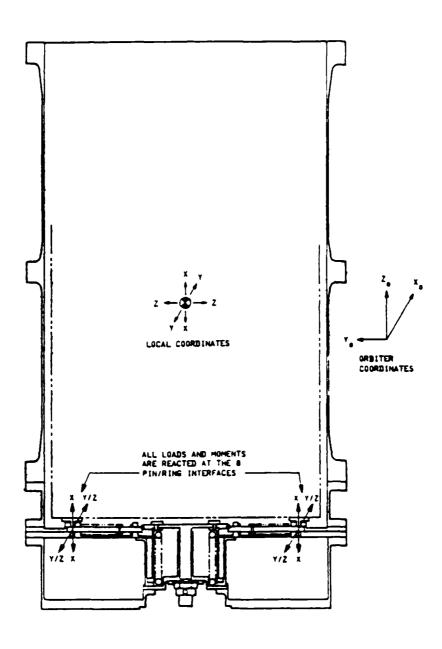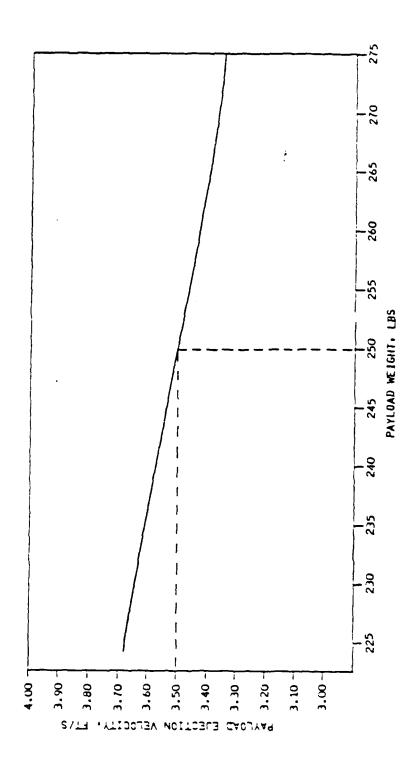(Ball Aerospace, 1986)

Figure 2-25

Satellite Ejection Velocity as a Function of Vehicle Mass
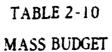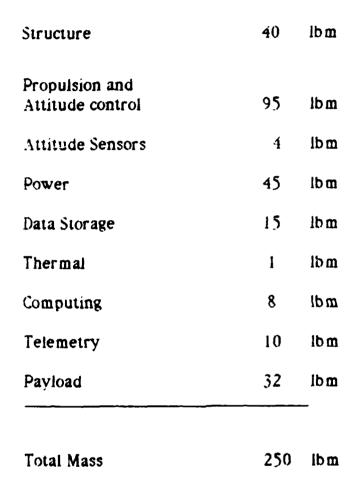(Ball Aerospace, 1986)

the payload at a nominal rate of 3.5 feet per second. Precise payload ejection velocities can be derived from the chart in Figure 2-25. Mechanical tolerances in the launch mechanism prevent tip off rates if the satellite center of gravity is on the axial center line. Thus, the payload will not contact the sides of the canister if ORION is designed properly.

3. Mass Budget

The ORION mass budget represents an estimate of the masses for the subsystems listed in Table 2-10. A detailed breakdown of these masses can be found in the mass properties section of Chapter Five. The majority of the structural mass is in the baseplate and structural skin (see Table 3-2). The majority of the propulsion subsystem mass is contained in the fuel (71.5 lbm). Attitude control subsystem masses are included in the mass of the propulsion subsystem in this table. The power subsystem reflects an estimate of 32 lbm for 24 NiCad cells and their containers, 6 lbm for power conditioning electronics and 7 lbm for solar cells. The data storage subsystem represents the mass of a 12 megabyte bubble memory solid state digital mass memory. Thermal management components account for 5 lbm. These include kapton thermal blankets, strip heaters and insulation. A general purpose computer of 8 lbm is proposed. Two telemetry units of 5 lbm each are also included. The remainder of the mass (32 lbm) is dedicated to the payload.

TABLE 2-10

MASS BUDGET

Structure	40	lbm
Propulsion and Attitude control	95	lbm
Attitude Sensors	4	lbm
Power	45	lbm
Data Storage	15	lbm
Thermal	1	lbm
Computing	8	lbm
Telemetry	10	lbm
Payload	32	lbm
Total Mass	250	lbm

4. Volume Budget

The volume budget in Table 2-11 represents a summary of data presented in Chapters Three, Four and Five. Subsystems are broken down into components in the same manner as for the the mass budget. These are representative values and are not exact. Note that the propulsion system is the most volume intensive subsystem of the satellite.

TABLE 2-11

VOLUME BUDGET

Structure	0.23	(ft^3)
Propulsion and Attitude control	2.00	
Attitude Sensors	0.02	
Power	0.39	
Data Storage	0.60	
Thermal	0.01	
Computing	0.30	
Telemetry	0.15	
Payload	2.00	
Total Volume	5.70	(ft^3)

5. Power Budget

The power budget for ORION is predicated on the provision of an end-of-life DC power of at least 60 watts. Solar cells are mounted on the curved periphery of the satellite skin. A total area of 1765 in² is populated with solar cells. Assuming that the sun line is normal to the satellite longitudinal axis, the projected area is 581 in² (with the empty boom recess accounted for). Using an assumed solar cell efficiency (E) of 14% and the solar constant of 125.6 watts/ft² (1350 watts/m²), the beginning of life power is

$$Power = (solar \; constant)(E)(Projected \; area)$$

$$= 70.8 \; watts$$

Assuming a typical degradation of 10% per year in the solar cell efficiency, the end of life power of 60 watts will occur after approximately 18 months. Note that the solar cell degradation is entirely a function of orbital altitude, inclination, and thus, radiation exposure; none of these have been specified for this spacecraft. The end-of-life value is attained much faster in regions of high radiation, such as the Van Allen belts.

Varying power demands are supported by a set of 24 Ni Cad cells, rated at 1.25 volts each. These cells are arranged in two stacks of 12 cells each, for a total of 15 volts per stack and 90 watt hours per stack. The total energy rating of the batteries is thus 180 watt-hours. The cells are mounted in four pressurized canisters containing 6 cells each. These containers are mounted on 90° centers near the periphery of the structure as indicated in

Figure 5-11. The power regulation components are mounted in two electronics housings and are located near the batteries.

D. SUMMARY

The concept of a general purpose low cost satellite established five broad criteria for the ORION design. Affordability, cost effectiveness. a general purpose architecture, reliability and safety are constraints that were chosen as the framework of the ORION design philosophy. These general requirements were refined by the choice of specific criteria such as price goals. structural limitations. performance specifications. system reliabilities and safety guidelines. The Space Shuttle was chosen as the primary launch vehicle to provide affordability and launch flexibility. The extended Get-Away-Special canister was chosen for the transport and deployment of the satellite aboard the Shuttle. The GAS canister provides an affordable method of deployment with the added advantage of simplified packaging and integration. The GAS canister constrained the satellite volume and mass to a 250 pound cylinder 19" in diameter and 35" long. These structural limitations will be the basis of detailed design choices with respect to attitude control. propulsion. power. payload mass/volume and telemetry.
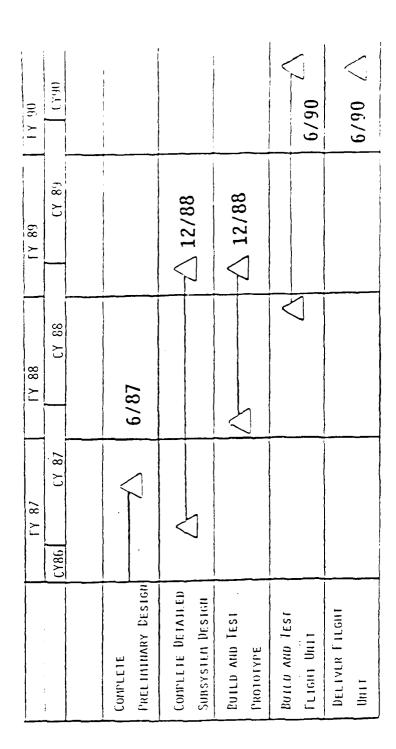
A feasibility study is now required to evaluate the likelihood that all of the necessary systems can be integrated within the given volume and provide the necessary performance. Specific design criteria will be provided for the design of each subsystem. The feasibility of meeting these specifications is critically dependent upon the successful design of tne structure. propulsion and attitude control subsystems. The power subsystem

133

nas been briefly described. The structure must be lightweight to permit integration of the many subsystems within the weight constraints of the GAS canister. The incorporation of a propulsion subsystem that will transport ORION from Shuttle orbits to 800 nm circular orbits will pose a significant challenge due to the volume constraints of the GAS canister. The decision to spin stabilize ORION for energy conservation necessitates that the attitude control subsystem be able to counter the nutation of a prolate spinning body. The thermal, telemetry and data handling subsystems are less crucial to the feasibility of the design. Chapters Three, Four and Five of this thesis demonstrate the feasibility of integrating the subsystems described above into a working ORION spacecraft. Figure 2-26 and TABLES 2-12 through 2-19 outline the proposed project schedule and anticipated budget for the fabrication and testing of the first ORION flight unit.

Figure 2-26

ORION Project Timeline

135

TABLE 2-12

ORION PROJECT SUMMARY BUDGET

Total Hardware Costs (Flight Unit) Description	Satellite Totals	
	Qty Reqd.	Ext. Cost
Structural Subsystem		$24,164
Attitude Control Subsystem		$135,000
Electrical Power Subsystem		$181,500
Computer Subsystem		$210,500
Propulsion Subsystem		$432,700
T T & C Subsystem		$288,000
Thermal Control Subsystem		$30,000
Totals		$1,301,864

TABLE 2-13

ORION PROJECT BUDGET (STRUCTURE)

Cost Item									Program Totals	
Structural Materials (Flight Unit) Description	Qty Rqd. Material per Sat.	Material	Material Required per unit	Estimated Material Cost (note 1)	Total Matl (each)	Est. Labor (M/D)	Labor Cost /Unit ($150/hr)	Total per Unit	Qty Satellite Reqd.	Total Cost
Bottom Plate	1	AL 7075	4.0 Sq ft, .5" plate	$77 per sqft	$308	4	$600	$908	1	$908
GAS Launch Mechanism	1	Purch.	--	--	--	--	--	$10,000	1	$10,000
Longitudinal Supports	4	AL 7075	4.0 ft of 2x2 bar	$48 per ft	$192	10	$1,500	$1,692	4	$6,768
Lower Mounting Plate	1	AL 6061	4.0 Sq ft, .20" plate	$21 per sqft	$84	2	$300	$384	1	$384
Tank Support Brackets	4	AL 7075	2.0 ft of 2x2 bar	$48 per ft	$96	1	$150	$246	4	$984
Upper Mounting Plate	1	AL 6061	4.0 Sq ft, .20" plate	$21 per sqft	$84	2	$300	$384	1	$384
Payload Interface Plate	1	AL 6061	4.0 Sq ft, .20" plate	$21 per sqft	$84	2	$300	$384	1	$384
Top Plate	1	AL 6061	4.0 Sq ft, .20" plate	$21 per sqft	$84	2	$300	$384	1	$384
Exterior Skin Panels	4	AL 6061	9.0 Sq ft, 0.05 plate	$15 per sqft	$135	2	$300	$435	4	$1,740
Boom Elements	8	AL 6061	4.0 ft of 1x1 bar	$24 per ft	$96	1	$150	$246	8	$1,968
Passivation Lot Charges	26	--		$10					26	$260
Totals										$24,164

Notes:
1. Material cost estimates include a 100% scrap/overage allowance.

137

TABLE 2-14

ORION PROJECT BUDGET (ATTITUDE CONTROL)

Attitude Reference Subsystem (Flight Unit) Description	Quantity Required per Sat.	Estimated Material Cost	Total Qty Reqd.	Satellite Totals Ext. Cost
Sun Sensor	1 each	$30,000 each	1	$30,000
Earth Sensor	1 each	$75,000 each	1	$75,000
Magnetometers	4 each	$5,000 each	4	$20,000
Mics. Hardware	--	$10,000		$10,000
Totals				$135,000

TABLE 2-15

ORION PROJECT BUDGET (POWER)

Electrical Power Subsystem (Flight Unit) Description	Qty Rqd. per Sat.	Est Mat Cost	Satellite Totals Qty Reqd.	Ext. Cost
Solar Cells	1400 2x4cm	$15 each	1400	$21,000
Solar Cell Shunt Regulator	1	$15,000 each	1	$15,000
Power Supply	1	$15,000 each	1	$15,000
Ni-Cad Batteries	2 packs	$30,000 each	2	$60,000
Cable	500 feet	$1 /ft	500	$500
Lot Chg for att. Solar Cells	4	$15,000 /pnl	4	$60,000
Mics. Hardware	--	$10,000		$10,000
Totals				$181,500

139

TABLE 2-16

ORION PROJECT BUDGET (COMPUTER)

Computer Subsystem (Flight Unit) Description	Qty Rqd. per Sat.	Est Mat Cost	Satellite Totals	
			Qty Reqd.	Ext. Cost
Main Computer	1 each	$40,000	1	$40,000
Attitude Con. Int. PCB Hard.	1 lot	$10,000	1	$10,000
Propulsion Int. PCB Hard.	1 lot	$10,000	1	$10,000
Analog Sensor Int. PCB Hard.	1 lot	$10,000	1	$10,000
Telemetry Inter PCB Hardware	1 lot	$10,000	1	$10,000
Payload Int. PCB Hardware	1 lot	$10,000	1	$10,000
Data Storage Unit	1 each	$70,000	1	$70,000
Pressure Sensors	10	$1,500	10	$15,000
Temperature Sensors	10	$300	10	$3,000
Status Sensors	10	$200	10	$2,000
Printed Circuit Boards	6	$1,500	6	$9,000
Enclosures, Etc	3	$500	3	$1,500
Mics. Hardware	--	$20,000		$20,000
Totals				$210,500
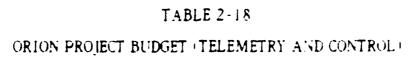
TABLE 2-17

ORION PROJECT BUDGET (PROPULSION)

Propulsion Subsystem (Flight Unit) Description	Quantity Required per Satellite	Est Cost /Mat		Satellite Totals	
				Qty Reqd.	Ext. Cost
Propellant Tank	1 tank	$45,000	each	1	$45,000
5.0 Lbf Thrusters	1	$45,000	each	1	$45,000
0.1 Lbf Thrusters	6	$40,000	each	6	$240,000
Pressurant Tank	2 tanks	$15,000	each	2	$30,000
Propellant Piping	20 feet	$10	/ft	20	$200
Pyro Valves	2	$5,000	each	2	$10,000
Misc Valves and Fittings	15	$500	each	15	$7,500
Lot Charge for Assem. of Pipe	1 lot	$30,000	lot	1	$30,000
Misc. Hardware	--	$25,000			$25,000
Totals					$432,700
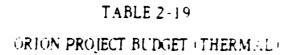
TABLE 2-18

ORION PROJECT BUDGET (TELEMETRY AND CONTROL)

T T and C Subsystem (Flight Unit) Description	Qty Rqd. per Sat.	Est Mat Cost	Satellite Totals Qty Reqd.	Ext. Cost
Transponder	1	$200,000 each	1	$200,000
Antenna	4	$15,000 each	4	$60,000
Power Combiner/Splitter	1	$10,000 each	1	$10,000
Mics RF Cables and Connectors	1 lot	$3,000 lot	1	$3,000
Mics. Hardware	--	$15,000		$15,000
Totals				$288,000

TABLE 2-19

ORION PROJECT BUDGET (THERMAL)

Thermal Control Subsystem (Flight Unit) Description	Qty Rqd. per Sat.	Est Mat Cost	Satellite Totals Qty Reqd.	Satellite Totals Ext. Cost
Strip Heaters	50	$200 each	50	$10,000
Heater Control Hardware	1	$5,000 each	1	$5,000
Insulating Blankets	1 lot	$10,000 lot	1	$10,000
Misc. Hardware	--	$5,000		$5,000
Totals				$30,000

III. STRUCTURAL SUBSYSTEM

A. INTRODUCTION

1. Background

The purpose of this chapter is to describe the structural subsystem of the ORION spacecraft. Although the structure is the least complex of the three major subsystems (structure, propulsion, and attitude control), this subsystem is important because it limits the volume, mass and physical layout of the other subsystems. Each subsystem component must integrate with the structure. The structure must withstand the launch and flight loads. This chapter will list the design considerations that must be addressed in the design, and then the specific design options will be described. Finally, the design of the structural subsystem will be discussed, supplemented by mechanical drawings of the proposed structure. The intent is not to provide a detailed mechanical engineering analysis of the structural subsystem. Such a treatment is beyond the scope of this preliminary study. However, basic design options are discussed which lead to the choice of a structure that demonstrates the feasibility of the ORION concept. Further refinement of the design is both expected and needed.

2. Design Criteria

There are fifteen constraints considered in the design of the ORION structure subsystem. They involve an assesment of:

1. Design philosophy (Chapter Two)

2. Requirements of the typical user

3. Mass and volume constraints of the extended GAS canister

4. Structural requirements of the other subsystems

5. Modular construction

6. GAS canister structural interface

7. Thermal conductive paths

8. Micrometeoroid protection

9. Assembly and integration requirements

10. Vibration sensitivity (resonant frequencies)

11. Launch loads

12. Ground and inflight maintenance requirements

13. On-orbit retrieval and refueling requirements

14. Manufacturing and production

15. Safety requirements

    a. Design Philosophy

In Chapter Two, five general design constraints were outlined for the ORION satellite. The satellite should be (1) affordable, (2) cost effective, (3) general purpose, (4) reliable and (5) safe. Although broad, these criteria should be considered as major design philosophies during the detailed design of elements of the structural subsystem. These criteria are the guiding principles of the ORION concept.

    b. Requirements of the Typical User

The needs of the typical user were identified using the Space Test Program surveys conducted by the Aerospace Corporation and the author (discussed in Chapter Two). With reference to the structural subsystem, the design requires that an accomodation be made for at least 32 lbm of user

145

payload mass and up to 2.0 cubic feet of user payload volume. The structure
must also support the various subsystems vital to the satellite operation.
such as the propulsion. attitude control. telemetry. power and data
processing subsystems.

c. Mass and Volume Constraints of the GAS canister

The extended GAS canister imposes a limit upon the total mass and
volume of its payload. The total satellite mass may not exceed 250 lbm
within a cylindrical volume of 19" diameter and 35" in length. The design
should minimize the percentage of the total mass dedicated to the structure.
An initial design goal of 15% (37.5 lbm) is established for the ratio of
structure to satellite weight. A ratio of 8 % is typical of other spacecraft
systems. as noted in Figure 3-1. As the design is refined in further iterations
the ratio (15%) is expected to decrease.

Subsystem	Mass (kg)
Communications	
Antennas	650
Electric power	
Structure	289
Thermal	54
Propulsion	80
Telemetry and command	39
Attitude control	98
Electric integration	77
Mechanical integration	28
Apogee motor inert	99
Mass margin	157
Dry spacecraft mass	1571
Propellant/pressurant	456
Apogee motor expendable	1413
Spacecraft mass at separation	3440

Figure 3-1

Summary of Typical Spacecraft Masses
(Agrawal. 1986. pp. 39/53)

146

d. Structural Requirements of other Subsystems

Specific structural requirements are imposed by the various
subsystems. Specifically, the propulsion subsystem requires a mounting
structure for the propellant tank and seven hydrazine thrusters (see Chapter
Four). The tank mount must restrain the 84.5 lb, 16.5" diameter propellant
tank during a 6 G load with a 1.4 factor of safety. The thruster mounts must
provide simple mounting for the rocket assemblies. These mounts must
withstand the impulsive loads imposed by the thruster operation. The twin
high pressure gas tanks which pressurize the hydrazine propellant and the
valves and piping associated with the propulsion system must be securely
mounted. The power subsystem requires four NiCad batteries (28 lbm) be
mounted near the periphery of the satellite cylinder. Solar cells are located
on the satellite exterior. The telemetry subsystem requires hard points for
the mounting of S-band conformal antennae on the satellite exterior.
Shelving must be provided to mount electronic modules and wiring
harnesses. The attitude control subsystem requires booms for spin stability
Therefore. a structural assembly must house and deploy the booms.

e. Modular Construction

Modular design eases assembly and reconfiguration of the satellite.
To the greatest extent possible, the design must permit a flexible placement
of components to suit the mission at hand. Modularity can be provided
through the use of several equipment shelves and a symmetrical equipment
layout. Since each mission imposes peculiar requirements upon the design.
complete modularity is not likely. Mass placement for stability restricts the
component layout. As in other aerospace applications the colocation of the

147

center of pressure and center of mass is desired. In the case of a cylindrical spacecraft the center of pressure due to miniscule aerodynamic drag is also near a plane which passes through the center of volume. Thus. mass properties dictate that the center of mass (CM) be located near the center of volume. This will restrict absolute modularity. The component layout proposed in Chapters Three and Five results in a center of mass location as depicted in Figure 5-19. With some consideration of equipment layout. volume requirements. and mass properties of several mission configurations a modular design can be pursued.

f. GAS Canister Structural Interface

The extended GAS canister imposes three specific structural requirements. To begin with. the satellite must be fitted with a set of eight mounting lugs that protrude from the vehicle base into the canister locking mechanism (Figure 2-22). These lugs are to be spaced on 45° centers at a radius of 8" from the canister center. Second. a base plate is required to connect the mounting lugs to the satellite frame. This baseplate supports the inertial loads due to the satellite components. During launch the satellite will be cantilevered such that the spacecraft longitudinal axis is orthogonal to the launch acceleration vector. Therefore. the baseplate supports the cantilevered 250 lbm load under as much as a 6 G acceleration with a safety factor of 1.4 holding the mounting lugs on one side and the vehicle frame on the other. Finally. the baseplate is used to mount the primary (40 lbf) hydrazine thruster. The thruster nozzle is flush to the exterior surface of the plate allowing the launch mechanism to contact the baseplate during launch
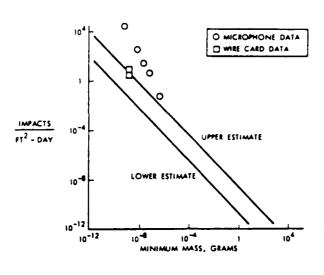
operations. Two attitude control thrusters also protrude through the baseplate near the outer edge.
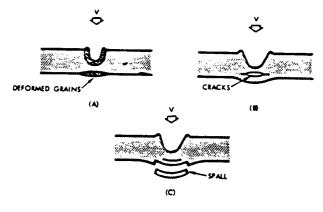
g. Thermal Conductive Paths

The thermal control subsystem requires thermal conduction paths from the electronic equipment and thrusters to the satellite exterior. This enables the vehicle to radiate heat generated within the satellite. Thermal paths can be provided by the use of cold plates" whereby the conductive metals used to mount the electronics are connected thermally to the satellite skin or thermal radiators. For the purpose of the ORION preliminary study, aluminum plates and honeycomb metal panels with heavy gauge face metals are utilized to provide a thermal path from components to the skin and endcaps of the satellite cylinder. A detailed thermal analysis that incorporates a nodal thermal model is required at a later stage of the satellite design.

h. Micrometeoroid Protection

Space debris and micrometeoroids range in size from microscopic particles to booster segments one hundred feet long. Consideration must be given to space debris and micrometeroid shielding for ORION. The distribution of debris is such that microscopic material exists in the greatest abundance and large "chunky" material is the least prevalent. Moving with relative velocities of up to 30.000 miles per hour (8.4 miles per second), most particles pose a threat to satellites. Even a small particle a fraction of a gram in mass can penetrate a thin satellite skin. A number of probability

$$d = C(mV)^{1/3}$$

where
    d = depth and radius of a hemispherical crater, cm

    m = particle mass, gm
    V = impact velocity, km/sec
    C = constant for a given combination of particle and target materials

        C = 1.04 for aluminum hitting aluminum
        C = 0.606 for iron hitting iron
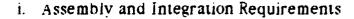 C = 1.3 for lead hitting lead

Figure 5-2

Distribution of Micrometeoroids
(AFSC DH 5-2, 1970, p. 13.6.4-2)

150

distributions for space debris have been calculated with sufficient accuracy to enable the designer to predict the time to impact for particles of various size at a given orbital altitude. The thickness of the micrometeoroid shielding is then a function of the desired lifetime until a destructive impact. The thicker the shielding, the longer the lifetime because the larger particles that can penetrate the thick shielding have lower distributions, and impacts are less frequent. Figure 3-1 depicts the relative frequency of impacts (at Shuttle orbits) as a function of particle size. Some maximum weight of shielding will exist as a function of the desired lifetime and the budget for the dryweight satellite mass. For ORION, the micrometeoroid shielding must provide a lifetime of at least 90 days at a 135 nm circular orbit, and up to 3 years at 800 nm. The shielding mass, when counted with the other structural masses, must not account for more than 15% of the total satellite mass (15% of 250 lbm = 37.5 lbm). The shielding will double as a structural skin providing much of the satellite support in the periphery of the structure.

i. Assembly and Integration Requirements

The structure must provide for ease of assembly and disassembly allowing easy removal of components from within the vehicle. To that end, the ability to remove panels from the side of the vehicle is advantageous. Fueling and defueling of the hydrazine tank during ground operations must not be hampered by the structural layout.

ACCELERATIONS
QUASI-STEADY STATE
LIMIT LOAD FACTORS

ACROSS
CONTAINER = ± **6.0 g's**
AXIS (ALL
DIRECTIONS)

OVERALL ROOT MEAN SQUARED
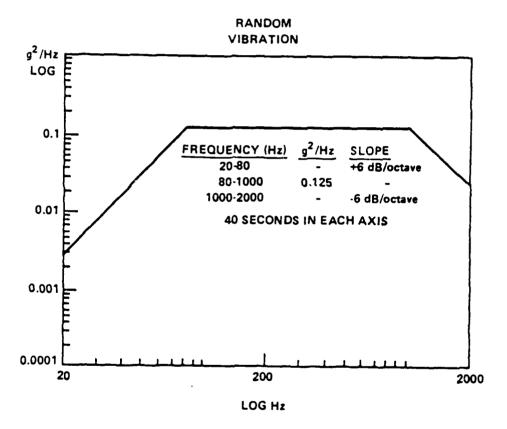RANDOM VIBRATION LEVEL IS
12.9 g's

ALONG
CONTAINER = ± **10.0 g's**
AXIS

RANDOM
VIBRATION

FREQUENCY (Hz)	g^2/Hz	SLOPE
20-80	-	+6 dB/octave
80-1000	0.125	-
1000-2000	-	-6 dB/octave

40 SECONDS IN EACH AXIS

LOG Hz

Figure 3-3

Random Vibrations and Maximum Accelerations for GAS Canisters
(NASA G.A.S. Manual, 1984, p. 57)

j. Vibration Sensitivity (Resonant Frequencies)

The structure must be capable of withstanding Shuttle launch vibrations and must avoid resonances below 35 Hz. Figure 3-2 depicts the GAS vibration test and the levels which a payload must endure to be qualified for space flight. Subsystem components which are vibration sensitive must be identified. and vibration isolation mountings must be provided.

k. Launch Loads

The satellite structure shall withstand a 6 G acceleration with a safety factor of 1.4 while cantilevered from the extended GAS canister launch mechanism. When subjected to this acceleration. the satellite may not deflect more than 0.375" in order to avoid contact with the canister walls. Figure 3-3 details specifics of the GAS canister vibration qualification which the satellite must endure during ground tests.

l. Ground and Inflight Maintenance

The structure shall be designed so as to enhance easy handling of internal components during ground operations. Ease of access to all portions of the vehicle shall be emphasized. The structural design must be coordinated with ground support equipment (GSE) requirements. Access to critical elements of the payload through the open end of the GAS canister is neccessary. Proper design permits the astronaut to access the payload on orbit during EVA operations. The end of the structural cylinder must be removable to accomplish this EVA access. Test points for critical vehicle functions and telemetry channels must also be accessible through the end

153

cap. Note that ideal component placement for accessibility is not always possible. A tradeoff exists between mass properties and payload placement.

m. On-orbit Retrieval and Refueling requirements

The success of the SOLAR-MAX retrieval and repair mission demonstrated the flexibility of the Shuttle and its crew in performing inflight maintenance. ORION should be fitted with a grapple fixture that is compatible with the Shuttle Remote Manipulator (RMS) to permit possible inflight retrieval. It is unlikely that ORION would be retrieved because the cost of such an operation approximates the cost of the satellite. However, advance planning for such a contingency may be valuable in the event of unforeseen requirements. Satellite recovery may be required for certain missions. External ports for refueling of the hydrazine tank and repressurization of the propellant pressurization system are also desirable. A grapple fixture that is conveniently located in conjunction with the refueling ports is advantageous.

n. Manufacturing and Production

The structure is needed for the integration of the satellite subsystems. Consequently, the manufacture of the structure should not be so complicated as to extend the timeline of the satellite assembly. A simple, lightweight and inexpensive structure that can be manufactured using standard machining tools is preferred. Aluminum may be the preferred structural material.

o. Safety Requirements

NASA document KHB 1700.7A details the safety requirements imposed upon Shuttle payloads. The structure must support the subsystems

during the acceleration and vibration-intensive Shuttle launch. Materials which are prone to outgassing, decomposition or embrittlement in the space environment are eliminated from the design. NASA requires a structural design which provides ultimate factors of safety equal to or greater than 1.4 for all Shuttle mission phases except emergency landings. When a failure of the structure can result in a catastrophic event, the design shall be based on fracture control procedures to prevent structural failure. The selection of materials used in the design of payload structures, support bracketry and mounting hardware shall comply with the stress corrosion requirements of MSFC-SPEC-522. To the greatest extent possible, the design will utilize proven spaceflight materials and fabrication practices.

The ORION design will incorporate the use of 7075-T6 aluminum and titanium or alloy-steel faced honeycomb metal panels, providing low weight and stiffness in the structure. Stainless steel aerospace fasteners will be used throughout the design. Welding of materials will be avoided as much as possible. Milling out of excess aluminum material will be accomplished on those structural elements where it does not impact the structural integrity of the component (i.e. baseplate). All structural components will be subjected to non-destructive inspection (NDI) to certify space worthiness. Exposed metal faces will be anodized or aladined as appropriate. Safety will not be sacrificed to provide for a low structural weight or cost.

3. Mass Estimation for Micrometeoroid Shielding

The likelihood of a micrometeoroid impacting ORION during a 90 day or 3 year mission is described by a probability distribution of

155

micrometeoroid particles in low Earth orbit. DeMeis (1987, p.11), Lucas (1961, p. 3-75), and Kaechele and Olshaker (1960, p.44-45) each describe the probability of a meteoroid impact as a function of satellite cross sectional area, particle mass (or size) and time. Figure 3-4a depicts the rate of flux of randomly distributed particles (per unit area per unit time) as a function of particle diameter. Figures 3-4b and 3-5 depict similar information gathered after the first satellite flights in the late 1950 s. cataloging the flux as a function of particle mass. De Meis (Figure 3-3) chooses to describe the rate of flux as a function of particle size because the older data in these figures do not reflect the accumulation of man-made space debris. The data of the latter graphs is for micrometeoroids only. These have a relatively constant density of 249 lb/ft^3 (4000 kg/m^3) yet today s space debris is composed of materials of various densities such as paint chips propellant byproducts metal booster fragments. and metal fasteners released during EVA operations.

Using the data in these figures. it is desirable to determine the size of particles from which ORION must be shielded to ensure a lifetime of 90 days to 3 years, as appropriate. Note that a determination of the shielding mass depends upon two assumptions. First, to estimate the flux from Figure 3-3
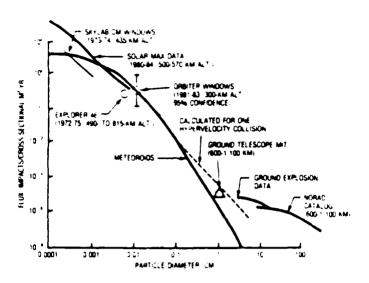
Figure 3-4a

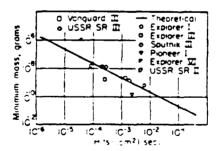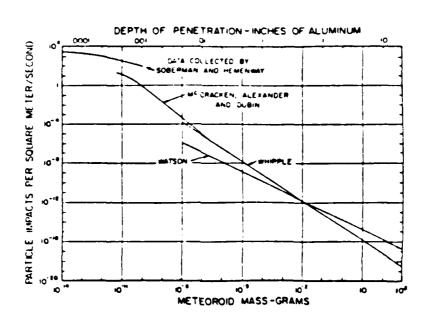Distribution of Space Debris
(De Meis, 1987, p. 11)

Figure 3-4b

Distribution of Micrometeorids
(Lucas, 1961, p. 3-75)

157

requires that the area of the satellite be determined. The total area of the satellite could be used, or only the projected area along the velocity vector. Choosing only the projected area presupposes that the debris is encountered only in the path of the satellite. This ignores faster moving debris overtaking the vehicle. For a conservative assumption, the total shielding area should be used in the determination of shielding mass. The total area of the cylindrical satellite is 16.1 ft^2 (1.49 m^2). This value does not include the base plate, however, because the 0.62" baseplate will act as shielding and not require supplemental protection.

Second, it is important to determine the relative velocity of the impacting particles in order to determine the depth of meteoroid penetration, and therefore, the thickness of shielding. There are some particles in solar orbit whose inertial velocities are as high as 22.6 miles per second (42 km/sec). Velocities in excess of this value are sufficient to escape the solar system, and it is reasonable to assume that particles moving faster than that value do not remain to impact ORION. The inertial velocity of a satellite orbiting Earth (and therefore the Sun) is approximately 16.2 miles per second (30 km/sec). Thus, the maximum closing velocity for such a solar orbiting particle would be 38.8 miles per second (82 km/sec). The minimum closing velocity for a solar particle would be 6 miles per second. An average closing velocity might then be 22.4 miles per second. If Earth orbiting space debris is considered, the maximum particle velocity in a 135 nm orbit must be 3.8 miles per second (7 km/sec). Velocities in excess of this value will result in a particle s escape to another orbit. In a circular orbit at the ORION altitude, the maximum closing velocity between the
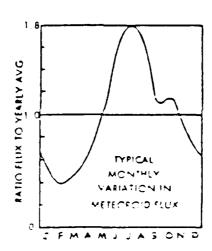
158

Figure 3-5

Distribution of Micrometeoroids
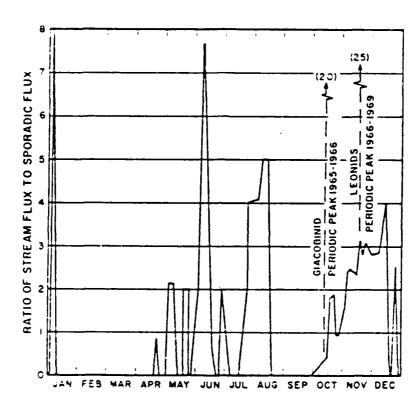(Space Planners Guide, 1965, p. 11-13)

satellite and Earth space debris is twice that value, or 7.6 miles per second.
Higher values may be encountered for particles in elliptic orbits whose
perigee is at the ORION altitude. Particles in such orbits are ignored in this
analysis. Note that De Meis predicts maximum impact velocities of 5.4
miles/sec. He notes that those particles most often intercept spacecraft at
angles of 90 degrees or less to their velocity vector. On a yearly average,
man made space debris is predominant in the Shuttle orbital region of 135
nm. However, periodic "directional meteoroid showers" occur as a function
of the time of year, exceeding the flux of the "sporadic showers" by a factor
of up to 8:1. Figure 3-6 depicts the seasonal frequency of such directional
showers. For the purpose of this analysis, the distribution of sporadic
showers will be used, assuming a conservative impact velocity of 22.4 miles
per second (41.5 km/sec). The De Meis value of 5.4 miles/sec may be more
realisitic because sporadic micrometeoroids and man-made debris
predominate in Shuttle orbits. The depth of penetration of a particle is
shown in Figure 3-7, and is expressed by

$$d = [[k] E / \rho \mathcal{H}]^{.333} \qquad (3.1)$$

where [k] is a constant, E is the kinetic energy of the particle based on
relative velocity, ρ is the density of the shielding material, and $\mathcal{H}$ is the heat
of fusion of the shielding material. The depth of penetration of a particle is
determined by the amount of energy released as a result of the sudden
conversion of kinetic energy to heat upon impact with the spacecraft.

Figure 3-6

Ratio of Meteoroid Shower Flux to Sporadic Meteoroid Flux
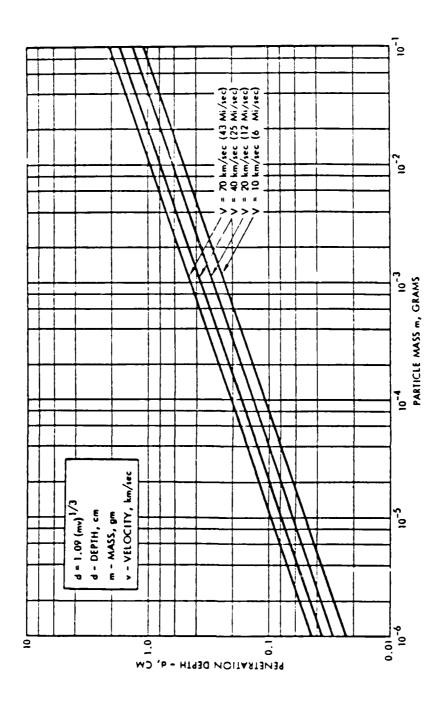(USAF-SC Space Planners Guide, 1965, II-13)

Figure 3-7

Penetration in Aluminum of Hypervelocity Particles
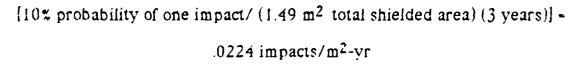(AFSC DH 3-2, 1964, p. 13.6.5 - 1)

162

The factor [k] depends upon an assumption of the type of crater which the impact creates. Lucas (1961, p. 3-75) presupposes that the crater would have the configuration of a right circular cone with a total apex angle of 53 degrees. Thus, k would be equal to [12 / π] or 3.82. Fuhs (1986) does not include the factor [k] in the depth penetration equation.

Figure 3-3 can be used to determine the probability of a micrometeoroid impact. Using the reliability goal of 90% stated in Chapter Two, it is neccessary to determine the particle size of debris that has a 10% probability of impacting ORION during a three year mission lifetime. Normalizing to the units (impacts per m^2 per year) the particle size can ce determined from Figure 3-3.

[10% probability of one impact/ (1.49 m^2 total shielded area) (3 years)] =

.0224 impacts/m^2-yr

Particle size = 0.06 cm diameter

Assuming an average micrometeoroid particle density of 4000 kg/m^3 (Fuhs, 1986), and assuming a spherical particle, the depth of penetration is determined.

$$\text{Mass} = [4/3][\pi][\text{radius}]^3[4000 \text{ kg/m}^3] = 452 \text{ E}^{-9} \text{ kg} \qquad (3.2)$$

$$\text{Energy} = [0.5][\text{Mass}][\text{Velocity}]^2 = 362 \text{ Joules} \qquad (3.3)$$

$$\text{Density 7075-T6 Aluminum} = 2801 \text{ kg/m}^3$$

$$\text{Heat of fusion 7075-T6 Aluminum} = 4 \text{ E}^5 \text{ Joules/kg}$$

$$\text{Depth of Penetration} = [[k] \text{ E} /\rho \text{ H}]^{.333} = 0.00686 \text{ m} = 6.86 \text{ mm}$$
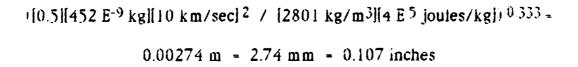
(Using the factor of [k] as Lucas reccommends, the depth of penetration would be 10.1 mm.) The required shielding mass for the satellite total area of 1.49 m² is

$$[1.49 \text{ m}^2] [0.00686 \text{ m}] [2801 \text{ kg/m}^3] =$$
$$28.63 \text{ kg } (63 \text{ lb}) \text{ aluminum}$$

Note that the conservative assumption using very fast closing velocities and the total exposed shielding area resulted in an unreasonably large shielding mass. If the particle impact velocities anticipated by De Meis are used (10 km/sec) and the maximum frontal area of the satellite is considered (0.429 m²), then a much lower depth of penetration results.

$$([0.5][452 \text{ E}^{-9} \text{ kg}][10 \text{ km/sec}]^2 \ / \ [2801 \text{ kg/m}^3][4 \text{ E}^5 \text{ joules/kg}])^{0.333} =$$
$$0.00274 \text{ m} = 2.74 \text{ mm} = 0.107 \text{ inches}$$

This results in a shielding weight of 11.4 kg, or 25.15 lb. If a 90% reliability is sought for a 90 day mission, the shielding mass can be further reduced to 4.8 kg (10.54 lb) based upon a depth of penetration of 1.143 mm (.045 inches). At a thickness of 0.05 " the 90% reliability can be achieved for mission durations of 120 days. Thus a material thickness of 0.05" is used in the design. Alternate shielding methods such as foam fillers could be used with the provision of lower shielding weights. This would free the structural

165

skin to be thinner and thus more closely match the industry average (8% of total mass) for the structural subsystem mass.

As mentioned earlier, this calculation ignores the monthly variation in micrometeoroid flux due to directional showers. If a mission date is known for the spacecraft, it is advantageous to calculate the shielding based upon the anticipated directional showers using the total spacecraft area and the sporadic showers using the frontal area. Additional refinements are possible by adjusting the exposure time of the vehicle to account for Earth shielding from directional showers. Finally, if solar cells are to be mounted on the periphery of the vehicle, their contribution to the shielding reduces the mass of aluminum required. Nonetheless, the calculations above provide a conservative estimate of the neccessary shielding. The author has observed that few satellites operating at Shuttle orbits are equipped with the 0.1" of solid metal plate recommended above for micrometeorite protection. Thus these calculations represent a very conservative assumption for particle shielding based upon current design practices.

B. STRUCTURAL SUBSYSTEM DESIGN OPTIONS

ORION has two options for a structural form. A framework for structural support of the vehicle can be provided by an internal skeleton of support members or by an "exoskeletal" skin that provides all of the structural integrity. Each option has merits. Consideration of the expected launch loads, payload and equipment geometries, and mass budget is required before a structure can be chosen for the satellite. This section provides a discussion of the various structural options and their relative merits.

1. Internal Framework

166

a. Frame and Skin

Most spacecraft structures are based on the use of an internal loadbearing frame with an overlay of protective skin and/or solar cells. The earliest satellites used this structural form almost exclusively and employed extruded metal tubing or channel to form the frame. Components are fitted between the frame members, and a removable skin of appropriate thickness is fitted over the frame. Figures 3-8 through 3-12 depict different internal frames. A modification of this structural form uses a combination of the frame and equipment shelves to provide loadbearing and stiffening support. The shelves enhance the ease of assembly, particularly when sufficient internal volume permits component layout on the "two dimensional" shelf. Shelves or platforms provide thermal paths to conduct heat to the periphery of the spacecraft. Intelsat V and VI use this form of construction as depicted in Figures 3-13 through 3-16. A semi-monocoque aluminum frame or central tube carries the majority of the vehicle load, and the equipment is mounted on shelves that surround the frame. On these dual spin satellites an external skin supports the solar cells and the remainder of the structural load .

Beams are also formed using bent sheet metal or milled aluminum ribs and panels. These provide an exceptionally stiff but lightweight
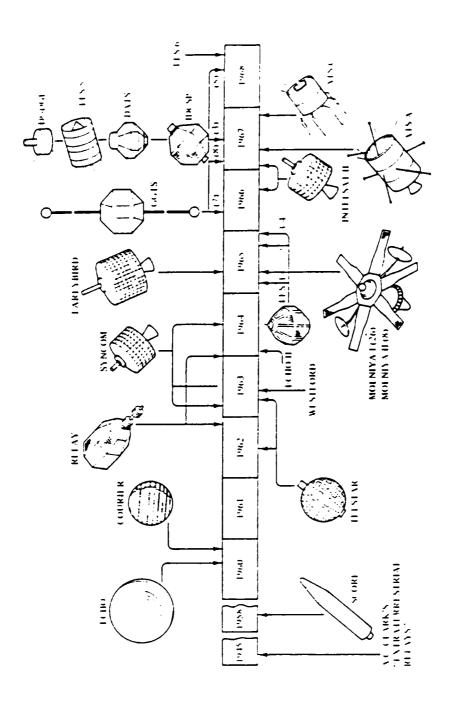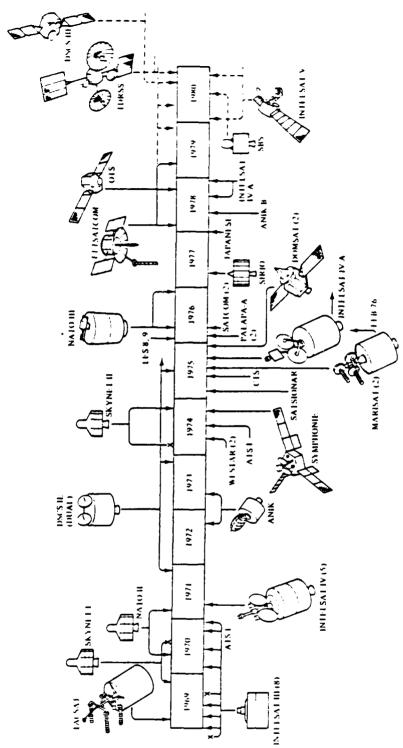
Figure 3-8

Evolution of Communication Satellite Structures
(Agrawal, 1986, pp. 11-12)

Figure 3-8 continued

Evolution of Communication Satellite Structures
(Agrawal, 1986, pp. 11-12)

Figure 3-9

Structure for the RELAY Communication Satellite
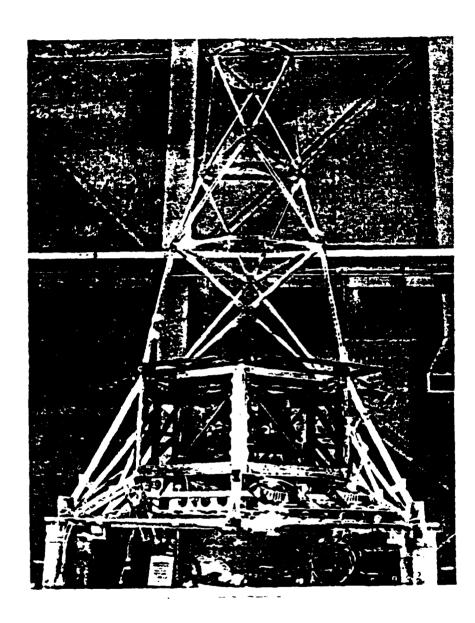(Adams, 1965, pp. 42-43)

Figure 3-10

Structure for MARINER II
(Adams, 1965, p. 45)

171

Figure 3-11

Structure for TRW Integrated Propulsion Stage (IPS)
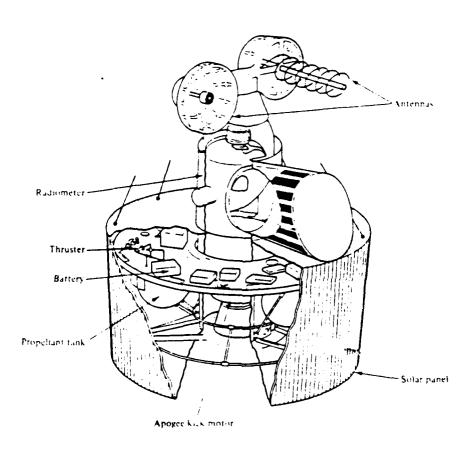(Reproduced from TRW Promotional Literature)

Figure 3-12

Structure for TRW LES-8/9 Ammonia Propulsion Subsystem
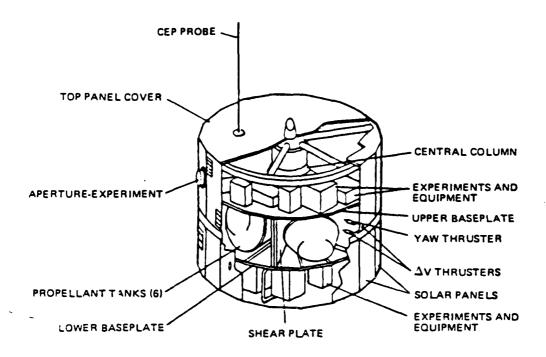(Reproduced from TRW Promotional Literature)

Figure 3-13

Structure for the Geostationary Meteorological Satellite (GMS)
(Agrawal, 1986, p. 6)

Figure 3-14

Structure for the Atmospheric Explorer Spacecraft
(Source Unknown)
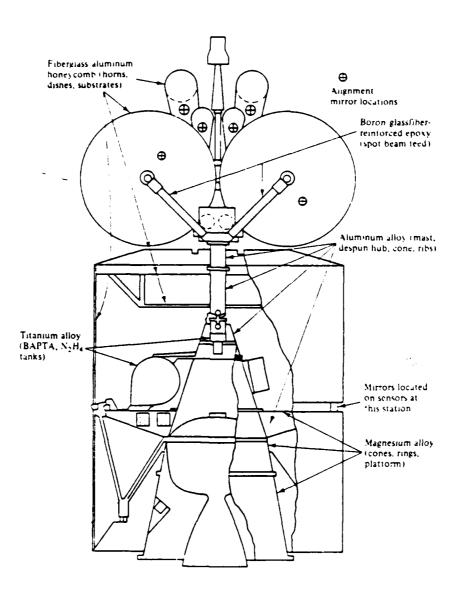
Figure 3-15

Structure of INTELSAT IV
(Agrawal, 1986, p. 182)

175

Antenna Support Structure

· Feed support structure
· Reflector support structure

Bus Structure

· Communications equipment support structure
· Support subsystems equipment structure

Adapter Structure
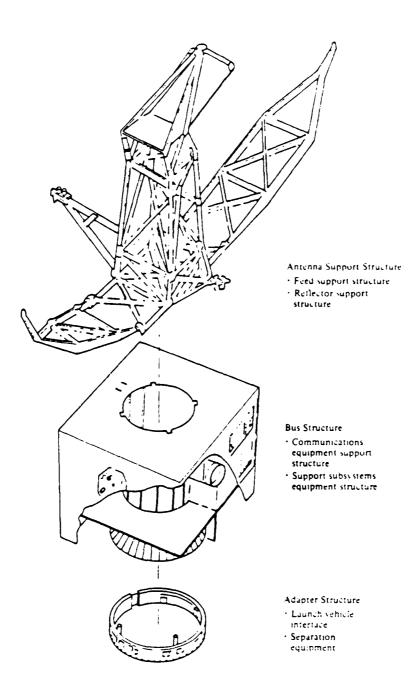
· Launch vehicle interface
· Separation equipment

Figure 3-16

Structural Elements of INTELSAT V
(Agrawal, 1986, p. 183)

but lightweight structure (Figure 3-17). As with the other internal framework options, however, this arrangement tends to preclude the availability of large unobstructed space within the vehicle.

b. Frame Only

A second version of the internal frame is the "uncovered" satellite without external skin. Three axis stabilization of a satellite allows the placement of solar cells on articulated panels. This eliminates the need to place a skin of solar cells about the vehicle as in spin stabilized satellites. Figure 3-18 shows the LANDSAT-D satellite configured box-like about an internal frame. Component shielding is provided by the individual equipment boxes.

2. Exoskeletal Structure

An external frame can be used when large portions of a satellite's internal volume must remain unobstructed for payload or equipment installation. Figures 3-19 through 3-21 depict satellites that use exoskeletal structures. The skin can double as the loadbearing element of the structure as in the NUSAT and TELSTAR satellites, or an external frame with a loadbearing skin can be used. Exoskeletal structures need not be cylindrical or circular as demonstrated by the box-like SPARTAN spacecraft (Figure 3-22). Cylindrical structures are particularly stiff and are well suited to spin stabilized satellites.

3. Materials

Aluminum is the material of choice for most aerospace applications. It is used in extrusions, milled ribs, panels, plates, shelves and pressure vessels. Many different alloys are available, and material selection depends
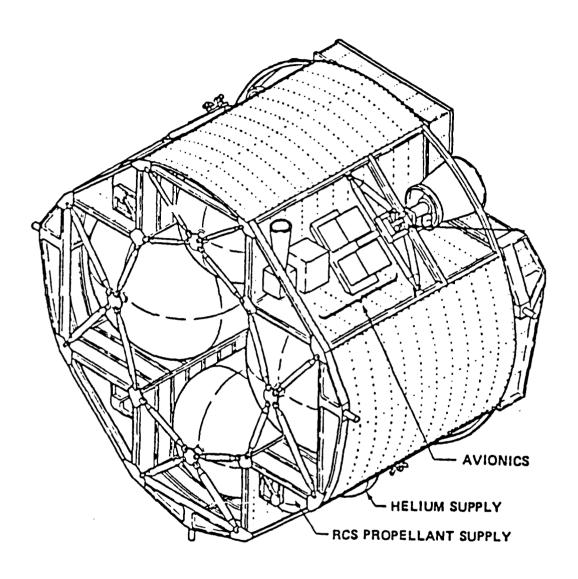
177

AVIONICS

HELIUM SUPPLY

RCS PROPELLANT SUPPLY

Figure 3-17

Structure for the Advanced Spacecraft Deployment System (ASDS)
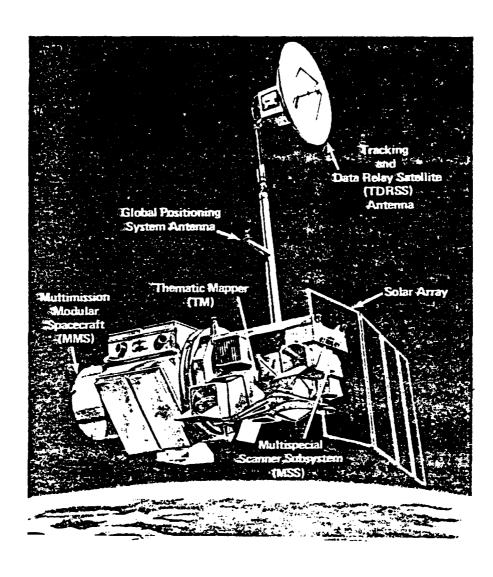(Boeing Co., 1976)

178

Figure 3-18

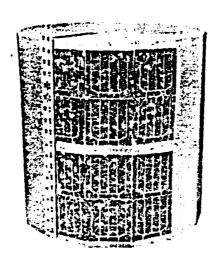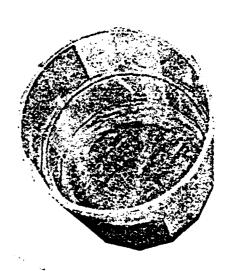LANDSAT D Satellite
(Agrawal, 1986, p. 8)

Figure 3-19

Exoskeletal Structure for the Intraspace Co. TSAT
(Reproduced from Intraspace Co. Promotional Literature)
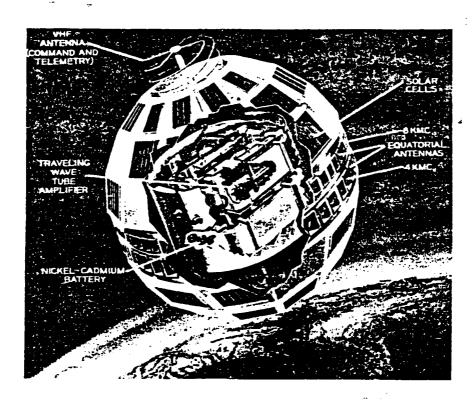
Figure 3-20

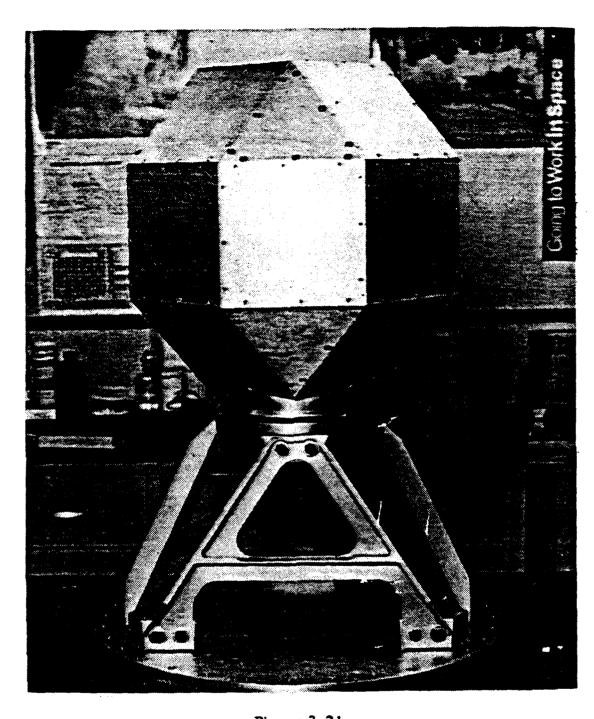Structure for the TELSTAR Satellite
(Adams, 1965, p.44)

181

Figure 3-21

Basic Structure of the NUSAT Satellite
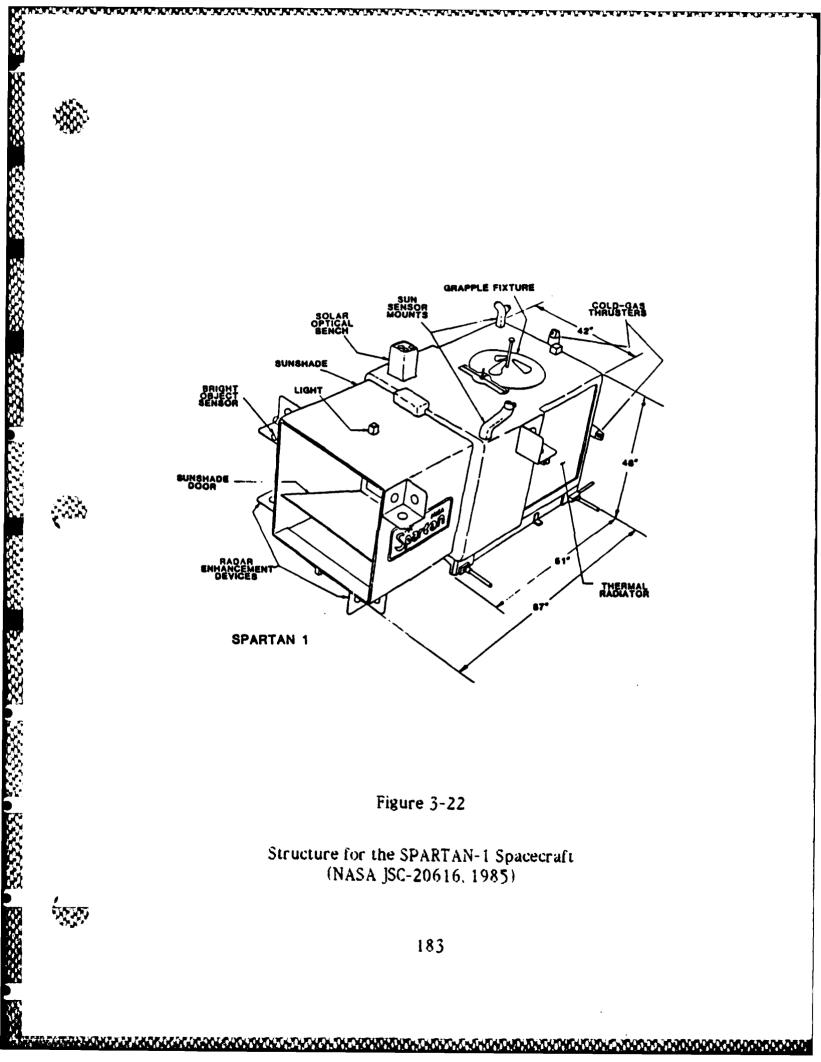(NASA Photograph)

182

SPARTAN 1

Figure 3-22

Structure for the SPARTAN-1 Spacecraft
(NASA JSC-20616, 1985)

TABLE 5-1

SPACECRAFT STRUCTURAL MATERIALS
(Adams, 1965, p. 24)

Materials	Tensile ultimate strength, F_u, ksi	Tensile yield strength, F_{ty}, ksi	Elongation, e, %	Young's modulus, E, lb/in.²	Density, W, lb/in.³	Conductivity, k, Btu/hr-ft-°F	E/W (approx.)	F_u/W (approx.)
Alloy steel, quenched and tempered, 4130, 4140	150	132	18.5	29.0×10⁶	0.283	22.0	102×10⁶	530×10³
Stainless, ½ hard, cold rolled, 301	150	110	15-18	26-28	.286	7.74	95	530
Stainless, 303, annealed	90	35	50	28.0	.286	8.0	95	315
Stainless, H-900 H.T., 17-4 PH	190	170	10	28.5	.282	10.3	101	672
Stainless, A-286	140	95	15	29.0	.286	8.68	102	495
Aluminum, sol'n H.T., 2024-T4	50-62	37-40	14	10.5	.100	70	105	620
Aluminum, ¾ hard, strain and stab, 5052-H36	37	29	3-4	10.1	.097	110	104	380
Aluminum, sol'n H.T., art. aged, 6061-T6	42	35	10-14	9.9	.098	96	100	430
Aluminum, sol'n H.T., art. aged, 7075-T6	77-81	66-73	5-7	10.3	.101	76	102	800
Magnesium, AZ31B	34	22	7	6.5	.064	56	101	530
Magnesium, art. aged, AZ80A-T5	48	33	4	6.5	.065	44	100	738
Magnesium, art. aged, ZK60-T5	45	36	4	6.5	.066	70	99	680
Titanium, 6Al-4V	130	120	10	16.0	.160	3.8	100	810
Beryllium copper, Be-Cu AT	180	130	3	16-18.5	.297	48.0	57	605
Beryllium	60-100	40-55	1-10	45.0	.067	100	670	1500
Fiber-glass laminate	70	--------	3	3.0	.067	.10	45	1050
Unidirectional fiber glass, S-glass	180	--------	3	7.8	.067	.16	116	2600
Lexan	9.5	--------	75	.345	.043	.11	8	220

on the structural stresses, mass budget and cost. Beryllium is used to a lesser extent due to high cost and the toxicity of the metal. It is a low density material exhibiting up to 6 times the stiffness of aluminum alloys. It is also very brittle and may fracture during machining processes. Titanium is used extensively to fabricate space qualified pressure vessels. Large structural panels and equipment shelves are often formed using honeycomb sandwich construction. The facing materials are typically aluminum, stainless steel alloy or titanium. These panels are extremely stiff and ultralight. Composite materials such as graphite/epoxy are also used for space applications. particularly when thermal dimensional stability is required. Agrawal (1986, p. 249) notes that "ultrahigh-modulus graphite/epoxy can surpass beryllium in specific stiffness". Composites provide great strength at low weight. Many forms of plastics. nylon. teflon and rubber materials are prone to outgassing in the vacuum environment of space. and only certain varieties are acceptable for space use. Table 3-1 details the characteristics of several materials for use in satellite structures.

C. ORION STRUCTURAL SUBSYSTEM

In consideration of the design criteria and structural options. a cylindrical structure has been adopted for the satellite design. Loadbearing support will be provided by the 0.05" thick cylinder and internal frame (Figures 3-23 through 3-26). The internal framework consists of four longitudinal recesses (longerons) that house four extendable booms. The semicylindrical structure is fastened to a baseplate and three equipment decks. The baseplate acts as an interface between the satellite cylinder and the launch apparatus. An

aluminum "strongback" supports the propellant tank and is fastened to the skin and longerons.
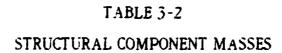
The use of a cylindrical structure provides for an unobstructed internal volume. The equipment shelves contribute significantly to the structural integrity and are placed according to equipment needs as well as for structural requirements. The lack of internal frame members enables the placement of the large 16.5" diameter propellant tank. The unobstructed volume also simplifies placement of the user payload. The propellant tank is placed in the lower two thirds of the cylinder, freeing the upper third for the user payload. Thus, the payload is easily accessible through the "top" of the satellite. The structure permits an unobstructed internal diameter of 14.5", with additional free space available on the arcs between the longerons. The total mass of the structure is 40.26 lbm. The individual component masses as listed in Table 3-2 represent a first iteration of the structural subsystem design. These masses are based upon the component designs of the following pages using 7075 T6 aluminum with a density of 0.101 lb/in^2. A finite element analysis of the structural design is required. After that analysis, the conservative estimation of masses in Table 3-2 will likely be reduced.
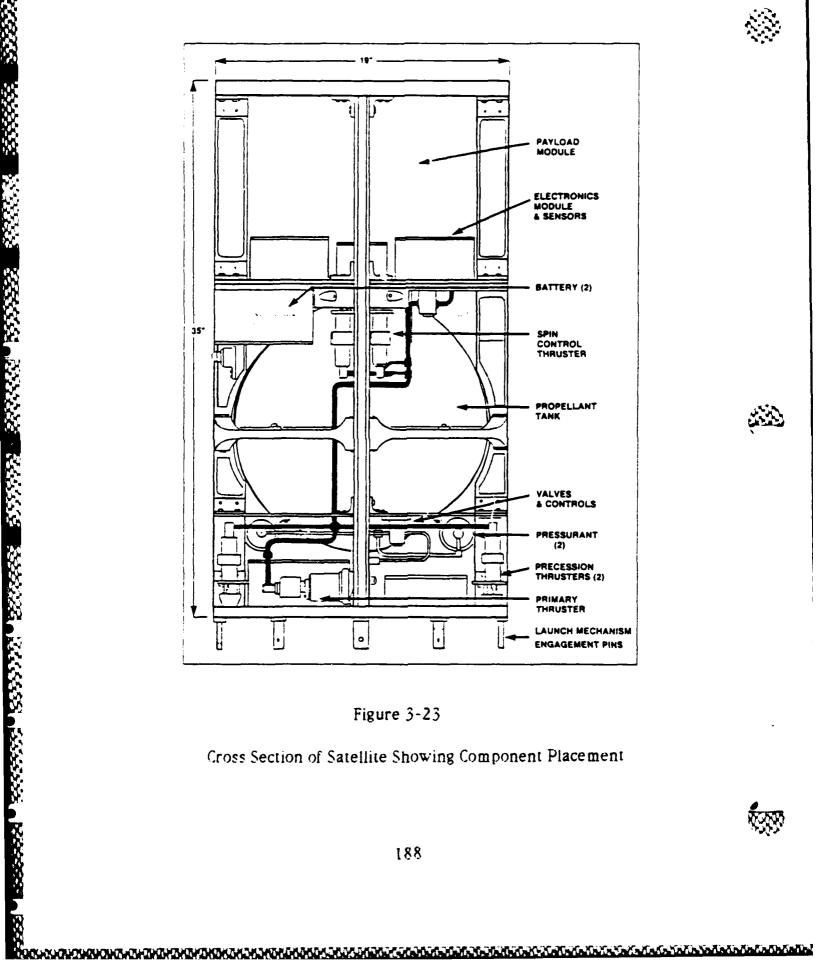
TABLE 3-2

STRUCTURAL COMPONENT MASSES

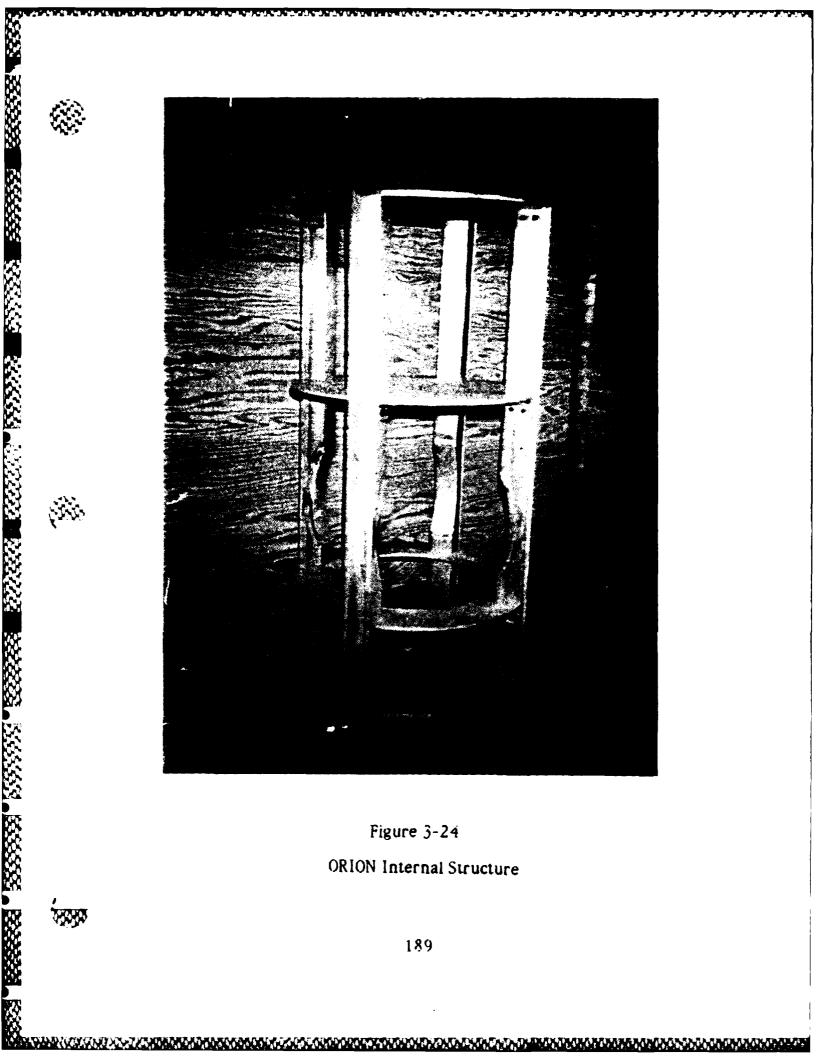|	
Top Deck	1.65 lbm
Equipment Deck	1.65
Propulsion Deck	1.05
Baseplate	9.75
Structural Skin	8.48
Longerons	5.80
Tank Strongback	2.20
Tank Supports	2.00
Booms	4.20
Fasteners (10% subtotal)	3.48
TOTAL	40.26 lbm

1. Baseplate

The baseplate (Figures 3-27 and 3-28) is the interface between the launch lugs and the satellite structural skin. It is constructed of 0.62" thick 7075-T6 aluminum plate. A 2.5" diameter hole in the center is provided for the nozzle of a 40.0 lbf hydrazine thruster. Two smaller holes of 0.5" diameter are placed on opposite sides of the plate at a radius of 8.55" from the plate center for the nozzles of the two precession thrusters. Four additional 0.25" diameter holes are provided near the edge of the plate for the inflight hydrazine and nitrogen servicing connections (fill and drain, each system). Eight launch lugs are attached to the bottom side of the plate, placed on 45 degree centers at a radius of 8" from the center. These lugs

Figure 3-23

Cross Section of Satellite Showing Component Placement

Figure 3-24

ORION Internal Structure

189
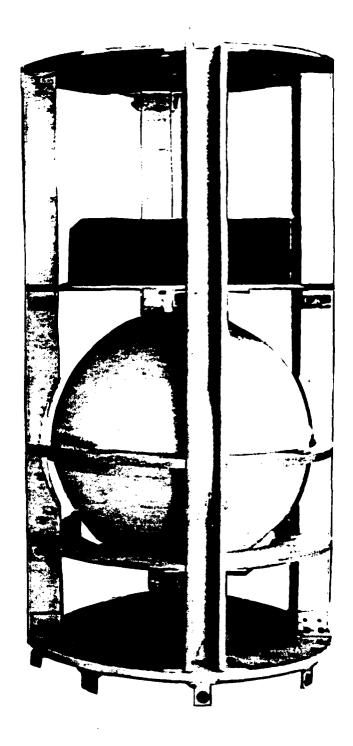
Figure 3-25

ORION Structural Mockup Showing Propellant Tank, Equipment Decks
and Structural Boom Housings (Longerons)
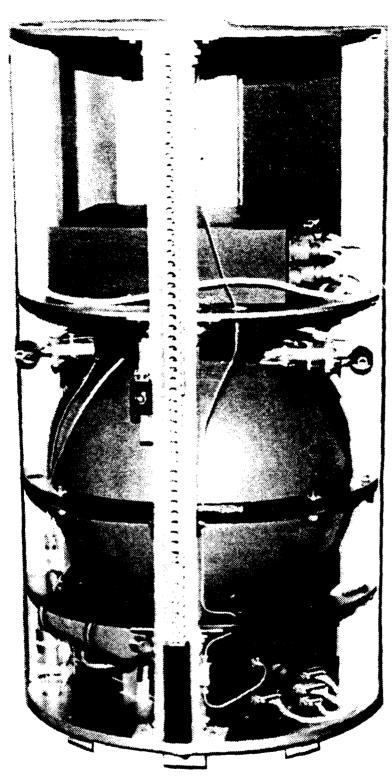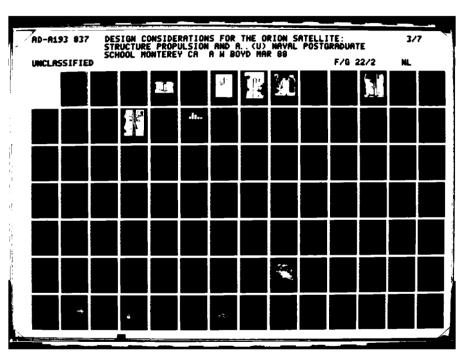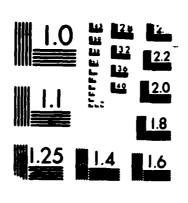
Figure 3-26

Complete ORION Structural and Equipment Mockup
(Less Payload)

191

AD-A193 837   DESIGN CONSIDERATIONS FOR THE ORION SATELLITE: 3/7
                 STRUCTURE PROPULSION AND A..(U) NAVAL POSTGRADUATE
                 SCHOOL MONTEREY CA A W BOYD MAR 88

UNCLASSIFIED   F/G 22/2   NL

MICROCOPY RESOLUTION TEST CHART

1.0

1.1

1.25   1.4   1.6

1.2   2.4
3.2
3.6   2.2
4.0   2.0

1.8

are used to restrain the payload when it is mounted in the GAS canister. The plate is lightened by milling out 40% of the aluminum. This creates the eight radial ribs that extend from the center to the launch lugs. The baseplate is tapped for various screw fittings to attach the structural skin, longerons, and equipment. Three hydrazine thrusters (two precession, one orbital boost), two telemetry units and the attitude control/data handling computer are mounted to the upper side of the baseplate. This enables these components to use the baseplate as a "coldplate" for thermal management.

2. Longerons

The longerons (Figures 3-29 to 3-31) serve a dual purpose. Foremost, they provide a longitudinal brace for fitting the equipment decks and baseplate, and create a frame on which to mount the structural skin. With the skin removed, the longerons enable the vehicle to retain its form without collapsing. This makes it possible to remove the structural skin for easy access to satellite components. The second purpose of the longerons is to form a housing for the extendable booms. The longerons and skin provide a continuous shield about the vehicle components.

The longerons are formed of extruded 1/16" thick 7075-T6 aluminum using milling processes or a custom extrusion die. This channel-like extrusion is 2" deep, 2" wide, and 34" long. A semicircular cutout for the hydrazine tank is made 13" from the base of the longeron, reducing the depth of the channel to 1" at the shallowest point. Brackets are used to mount the shelves and propellant tank strongback to the longerons at the hardpoint locations indicated. Solar cells may be mounted on the outward facing surface of the longeron channel to increase the solar cell surface area.

192

1.1

8.500

2.700

PRECESSION
THRUSTER
OPENING

PRIMARY
THRUSTER
OPENING

18.600

0.75

(DIMENSIONS IN INCHES)
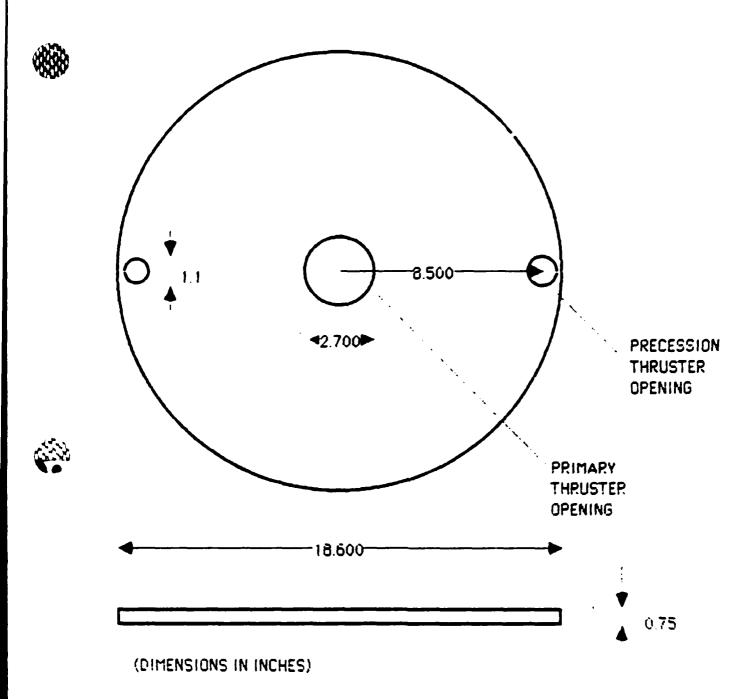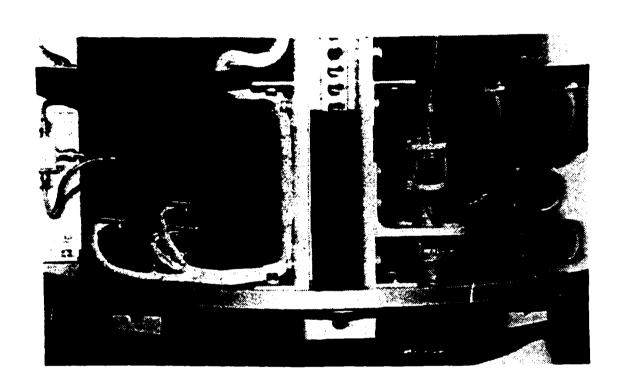
Figure 3-27

ORION Structural Baseplate

193

Figure 3-28

ORION Structural Mockup - Close-up View of Baseplate
and Propulsion Components

194

ISOMETRIC VIEW

2 0"

2 0"

END VIEW

0.1 "

1.8"

2.0"

0.1"

34"

17" RADIUS

FOR PROPELLANT TANK
CLEARANCE

Figure 3-29

ORION Structural Longerons

195
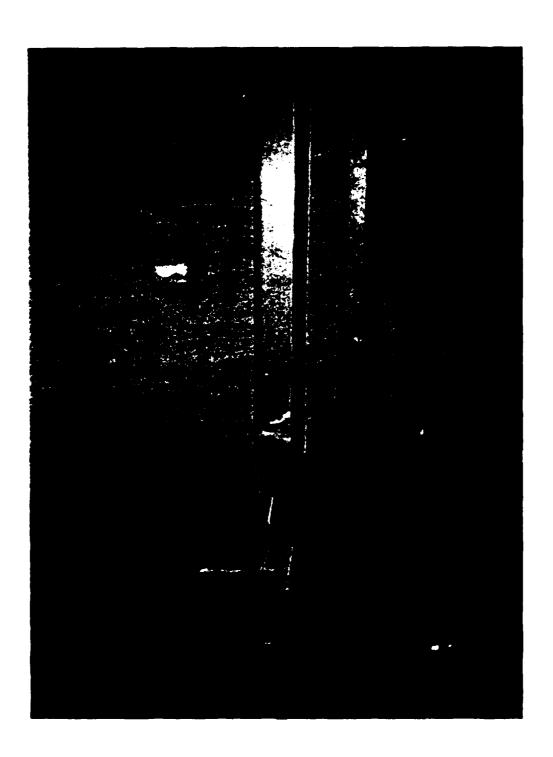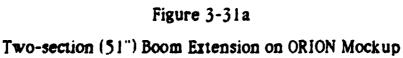
Figure 3-30

ORION   Longeron

196

Figure 3-31a

Two-section (51") Boom Extension on ORION Mockup

197

Figure 3-31h

Two-section (51") Boom Extension on ORION Mockup

170"

19"

35"

β 90°

α 180°
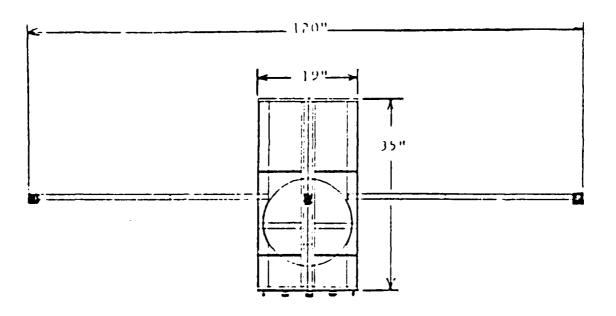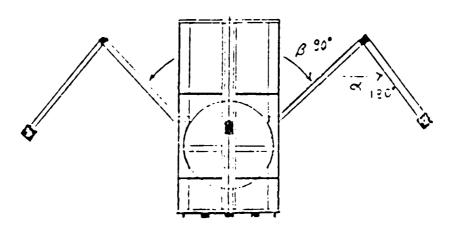
Figure 3-31c

ORION Spacecraft Depicted During/After Boom Deployment

3. Structural Skin

Aluminum sheet (7075-T6, 0.05" thick) is formed into four rigid semicircular panels that provide structural stiffness. The panels also provide sufficient shielding to ensure a 90% reliability of absorbing a micro-meteoroid impact as discussed in Chapter Two. Recall that a 0.107" thick micrometeoroid shield results in an unacceptably heavy structure (49.93 lbm). Consequently the 0.05" thick skin is a compromise between micrometeoroid protection and available mass. The skin is fastened to the longeron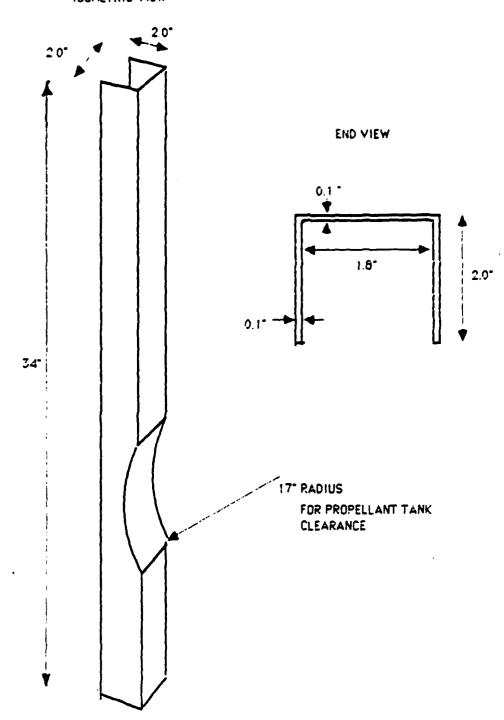s, shelf brackets and baseplate with removable fasteners to permit access to the satellite components. Ports are provided in the skin as indicated for attitude control thrusters, attitude control sensors, antennae and a set of refueling ports.

4. Equipment Decks

Three equipment decks are included in the design. These decks are constructed of 0.75" metal honeycomb panels using 0.02" titanium or stainless steel facing material. A lower propulsion subsystem deck is fitted around the hydrazine tank and supports two 12" long, 2" diameter nitrogen pressurant tanks. Various propellant valves, piping fixtures and pyrotechnic actuators are also installed on this deck. A power subsystem deck is placed above the propella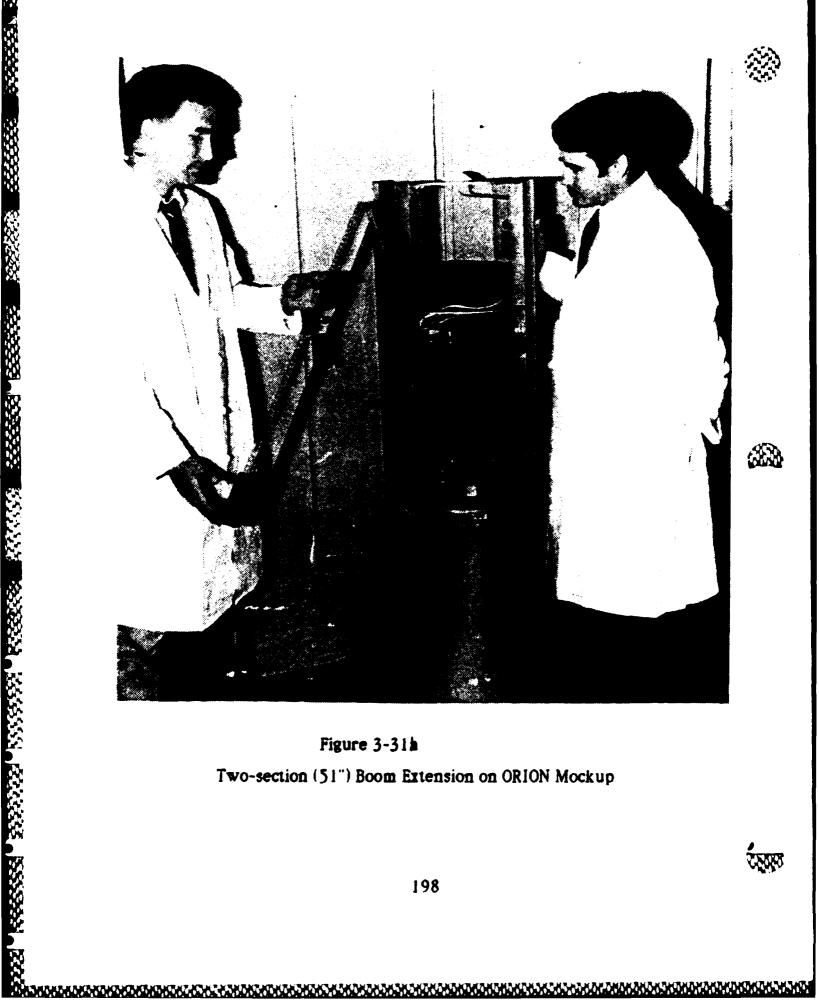nt tank. Two NiCad battery canisters are mounted to the lower side of this deck along with power conditioning and switching electronics. Four spin control thrusters are also mounted to the lower side of the deck. The area above the power subsystem deck is reserved for the user payload and data storage components. The payload subsystem deck also caps the "top" of the satellite structure. It is removable and provides

Figure 3-32

Close-up View of Electronics and Power Subsystem Deck

201

PRESSURANT TANK

HYDRAZINE TANK

FILTER

PRESSURANT TANK

CUTOUT FOR HYDRAZINE TANK

PYROTECHNIC VALVE

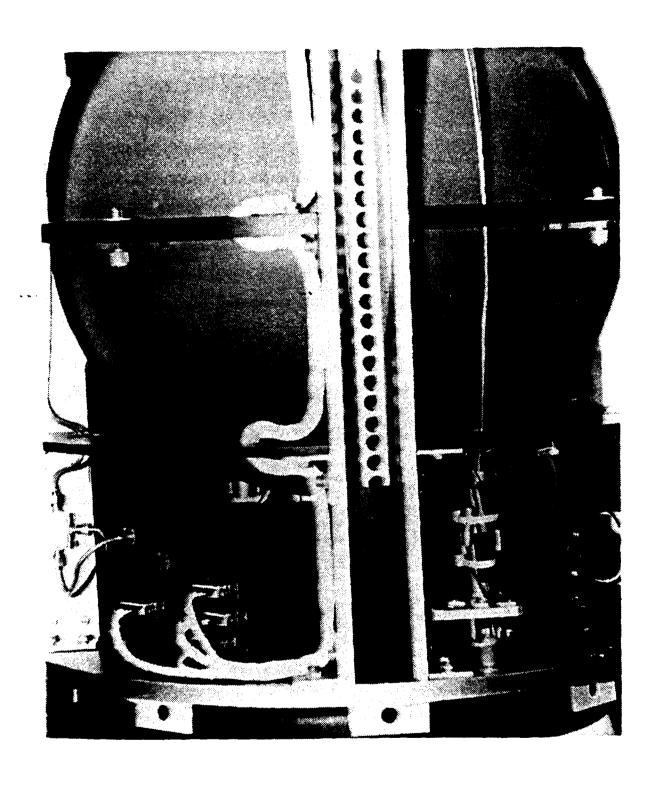HYDRAZINE LINE ACCESS TO PRECESSION THRUSTER
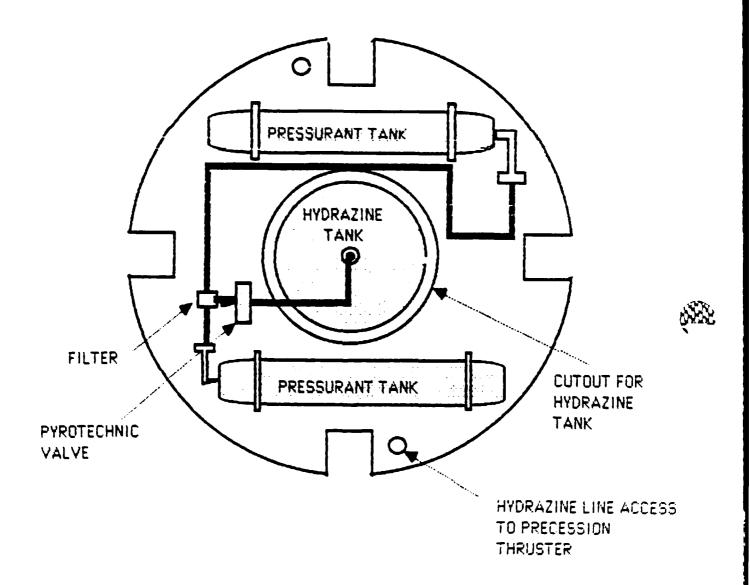
Figure 5-33

ORION Power Subsystem Deck - Lower Side

access to the payload components. The provision of an external surface for the payload allows the user to mount sensors such as particle counters and lenses. This plate provides a "coldplate" surface for payload elements that require thermal management. It is conceivable that a despun platform could be incorporated in the volume above the power subsystem deck, permitting the user to erect a despun antenna.

5. Propellant Tank Strongback
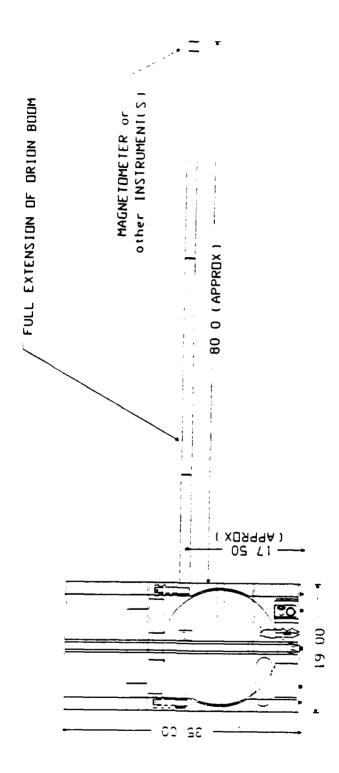
A brace for the support of the 16.5" diameter titanium propellant tank is mounted 13" above the baseplate, spanning four 90 degree arcs between the longerons. This 1" wide strongback is constructed of 1" thick honeycomb panel using a 0.04" stainless steel facing material. It is bolted to the longerons and skin. Four milled aluminum stanchions add additional support between the strongback and the baseplate. These stanchions support the propellant tank and strongback when the skin is removed for equipment access and the tank is filled. The tank is bolted to the strongback through four tank flanges that are spaced evenly between the four longerons.

6. Booms

Four 78.5" long booms are provided for mounting magnetometers or other small experimental devices. In the absence of sensors, each boom supports up to 2.0 lbm of balance weights to provide a stable spin about the longitudinal axis. The booms are constructed of 0.05" thick 7075-T6 aluminum, extruded into box beams 0.5" deep by 1.5" wide. The three-section booms are jointed such that the first 14.5" long segment is hinged to the longeron at a point 17.5" from the baseplate, in the plane of the satellite's center of volume. The center of mass will be observed in Chapter

203

:79 (approx)

35 00

80 0 (APPROX)

17 50 (APPROX)

19 00

ALL DIMENSIONS ARE IN INCHES

90 deg

180 deg   180 deg

Figure 3-34a

Three-section (78.5) Booms Deploying/Deployed

204
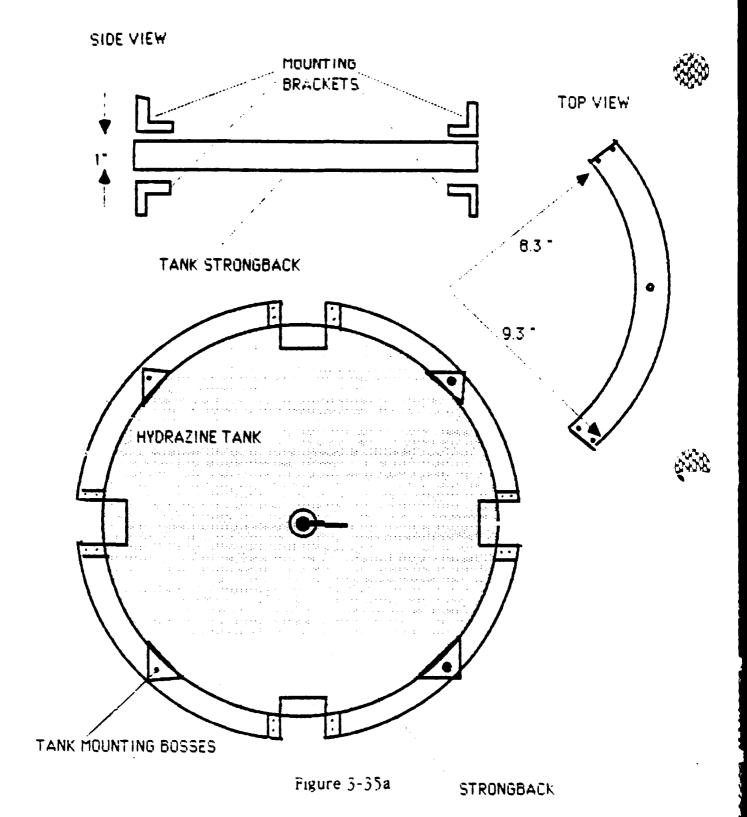
Figure 3-34b

Cross-section of ORION and a Three-section (78.5") Boom Deployed

205

SIDE VIEW

MOUNTING
BRACKETS

TANK STRONGBACK

TOP VIEW

8.3 "

9.3 "

HYDRAZINE TANK

TANK MOUNTING BOSSES

Figure 3-35a   STRONGBACK

ORION Propellant Tank Strongback and Tank Mount

206
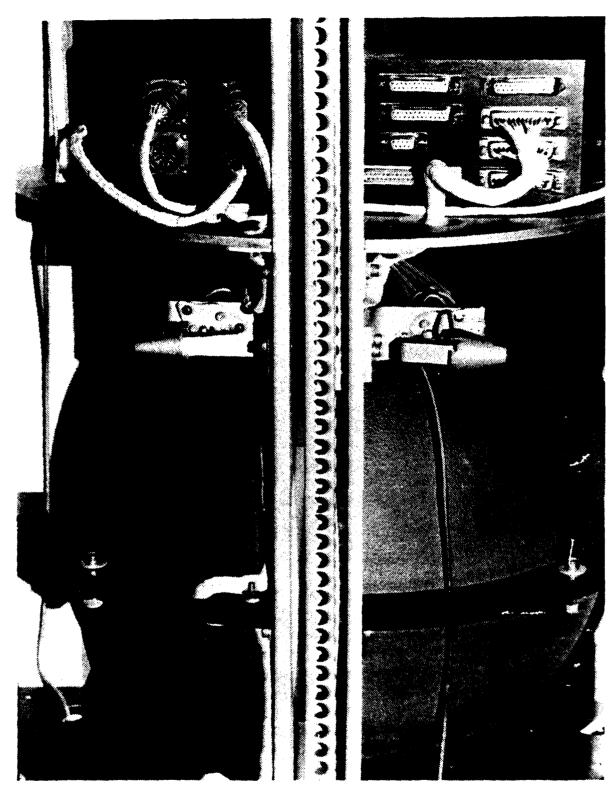
Figure 3-35b

Mockup of ORION Structure - Longerons, Decks and Strongback

Five to vary slightly on either side of that plane. The second section, 32" in length, is hinged such that the first mid-boom hinge recesses into the longeron near the top of the satellite. The 32" boom segment then folds over the 14.5" segment, nestling into the longeron housing. A third 32" segment folds back over the 32" section. The magnetometer or tip mass then recesses into a 3" tall, 2" deep and 2" wide volume at the top of the longeron. The booms are hinged using self locking devices that permanently lock the booms in an extended position when allowed to unfold under spring pressure. Pyrotechnic actuators restrain the spring loaded booms in their recessed positions until deployment.

D. STRUCTURAL DYNAMICS
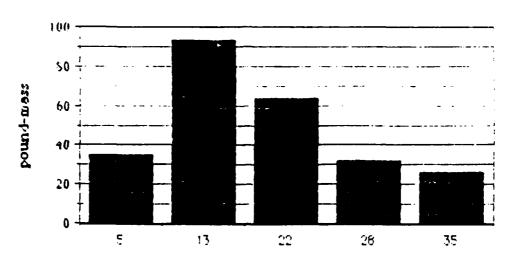
1. Deflection During Launch

An analysis for a cantilevered shell modeled as a beam was conducted to determine satellite deflection under launch loads. This analysis confirmed that the relatively stiff cylinder will not deflect more than 0.035" during launch while cantilevered from the GAS canister launch platform. Four critical assumptions are made in the analysis:

1. The mounting lugs will endure the stresses of launch during restraint of the cantilevered spacecraft. These lugs, which are being designed by the Ball Aerospace Co. for other payloads, are assumed to function properly.

2. The baseplate will support the spacecraft loads during launch. The standard GAS canister uses a 0.62" thick aluminum plate to cantilever payloads during launch. No attempt has been made to determine the stresses on the baseplate or on fasteners between the plate and the longerons or skin. The satellite cylinder is assumed to be rigidly mounted to the baseplate.

208

Mass Distribution at Structural Points

Distance from Baseplate

Moment Diagram for ORION at 10 G's

Distance from Baseplate (inches)
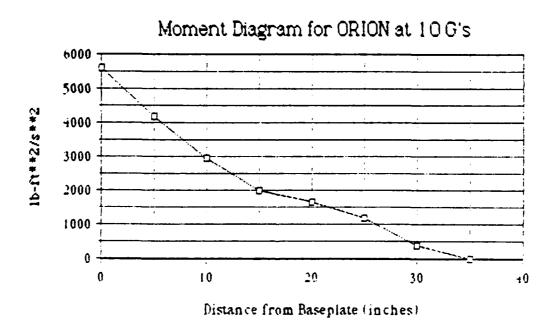
Figure 3-36

ORION Mass Distribution and Moment Diagrams

209

3. All of the launch loads act upon a point mass of 250 lbm at the end of the cantilevered shell. This is a very conservative assumption. The actual moment diagram is depicted in Figure 3-30. Using that diagram, the total moment is

$$M = \sum [\text{Weight}][\text{Moment Arm}][\text{G load}][\text{Safety Factor}]_i \qquad (3.4)$$

$$= 39941 \text{ lb-in}$$

For a point mass load on the end of the shell, using a moment arm of 35", the moment would be 71400 lb-in.

4. The cantilevered shell can be modelled as a cylinder. This is also a conservative assumption because the longerons contribute significantly to the longitudinal stiffness of the structure.

The moment of inertia of a right circular cylinder is:

$$I = \pi/64 [D^4 - d^4] \qquad (3.5)$$

$$D = \text{Outside diameter of cylinder} = 18.6"$$
$$d = \text{Inside diameter of cylinder} = 18.5"$$

$$I = 0.0491 [119688 - 117135]$$
$$= 125.3 \text{ in}^4$$

The radius of curvature of the deflection is:

$$R = [E][I] / M \qquad (3.6)$$

$$E = \text{Youngs Modulus of Elasticity} = 1 \text{ E}^7$$
$$M = \text{Moment} = 71400 \text{ lb-in}$$
$$I = \text{Moment of Inertia} = 125.3 \text{ in}^4$$

$$R = 17551 \text{ in}$$

The angle of deflection and displacement is:

$$\Theta = L \, / \, R = 0.002 \text{ radians} \qquad (3.7)$$

$$\text{Displacement} = R \, [1 - \cos(\Theta)] \qquad (3.8)$$

$$= 0.035''$$

$$\text{Stress} = \sigma = [M][D] / _{[I]} \qquad (3.9)$$

M = Moment = 71400 lb-in
D = outside diameter = 18.6"
I = Moment of Inertia = 125.3 in^4

$$= 10598 \text{ lb/in}^2$$

The deflection (0.035") is sufficiently small to ensure that the satellite does not deflect under launch loads. The maximum stress for 7075-T6 aluminum is 72000 lb/in^2 and thus the stress on the cylinder (10598 lb/in^2) is well below the maximum tolerable level. Note that a 19" diameter, 35" long cylinder is fairly short and stubby, which results in an exceedingly stiff structure. Contributions from the longerons and cross-structural decks will further stiffen the structure.

The actual deflection will likely be much less. Conservative assumptions were made for this study using a point mass loading on the satellite (at the end of a 35" cylinder) which also avoids consideration of longeron contributions to stiffness. For example, the actual moment will be approximately 50% less than the point mass moment of the assumption above. A finite element analysis is required which can accurately simulate the contributions of the longerons, equipment decks and structural skin.

2. Vibration and Resonant Frequencies

The structure must not exhibit resonances at frequencies less than 35 Hz in accordance with NHB 1700.7A safety specifications. To confirm that the satellite will resonate at frequencies significantly higher than 35 Hz, a NASTRAN model of the satellite was generated. This model was constructed using 48 points that model the satellite as a cylinder. The model simulates the contribution of four longerons and four structural panels longitudinally. It does not include the additional cross-cylinder contribution of the baseplate, equipment decks and tank strongback. This is a conservative model because these added contributions would stiffen the structure and lead to higher frequency resonances. High frequency resonances are desirable from the NASA viewpoint. The NASTRAN model indicates that resonance modes occur at 160.8, 178.3 and 244.6 Hz respectively. Figure 3-37 depicts the 48 point model. Figures 3-38 through 3-40 depict the exaggerated deformation of the cylinder as a result of these resonances. The NASTRAN simulation confirms the intuitive assumption that the cylinder does not exhibit low frequency resonances.

E. SUMMARY

The design of the structural subsystem was constrained by fifteen design requirements. Most of these have been addressed in the discussion of the structural subsystem. A design was chosen which employs an exoskeletal framework with transversely mounted equipment shelves and a four-piece skin. The shelves permit accessible mounting of equipment and provide thermal conduction paths. The exterior skin is removed in four sections and
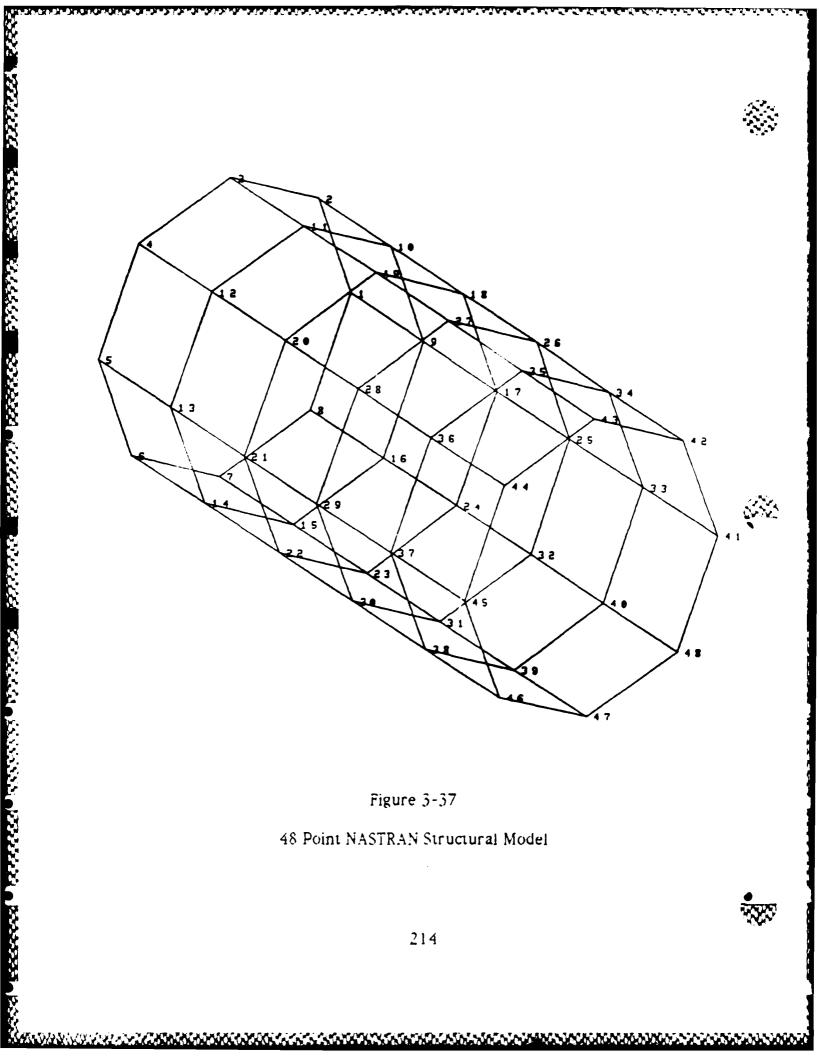
provides micrometeoroid shielding as well as a mounting surface for the solar cells. Longerons have been incorporated for longitudinal stiffness and for the storage of three-section booms approximately 80 inches long. The mass of the structure is approximately 40 lbm. The structure has been modeled as a cantilevered beam and shown not to deflect under the most conservative of launch loads. The resonant frequencies of the structure have been shown, through modelling, to exceed 35 Hertz as required by NASA 1700 series safety documents.

Figure 3-37

48 Point NASTRAN Structural Model
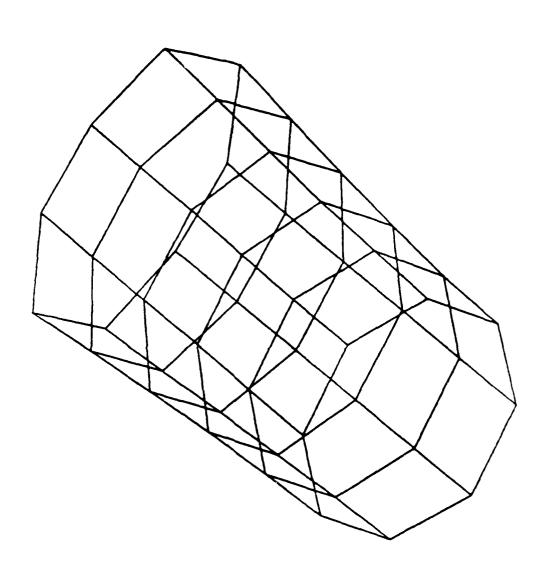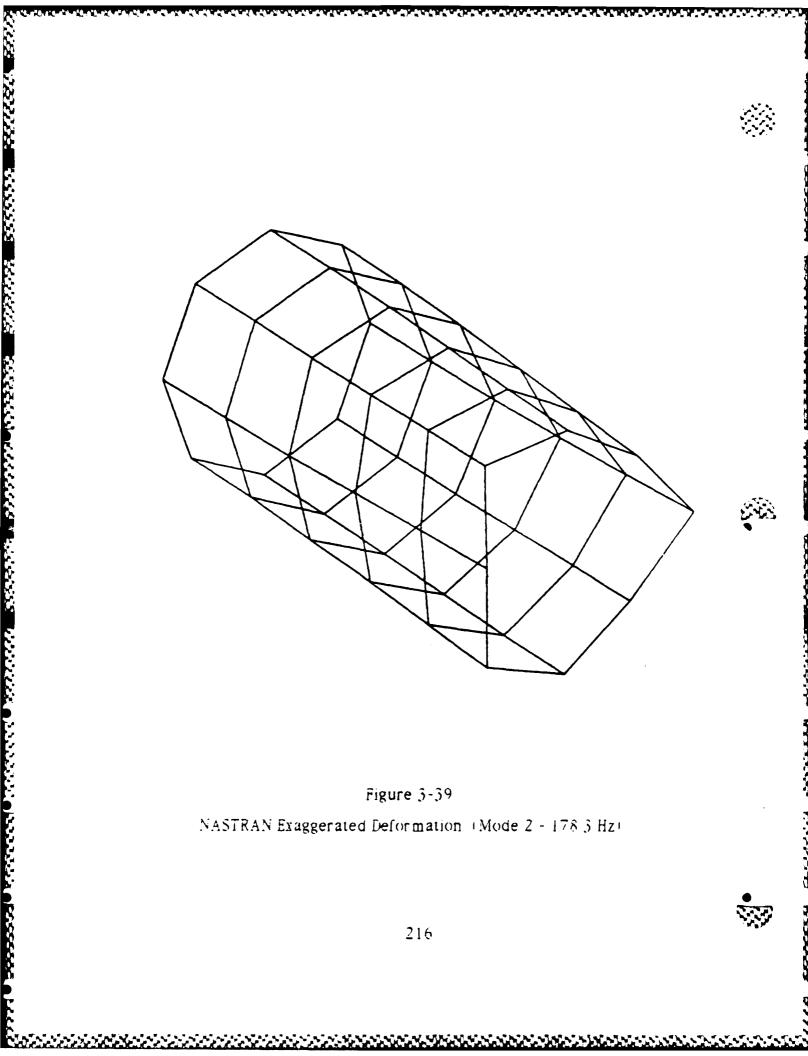
Figure 3-38
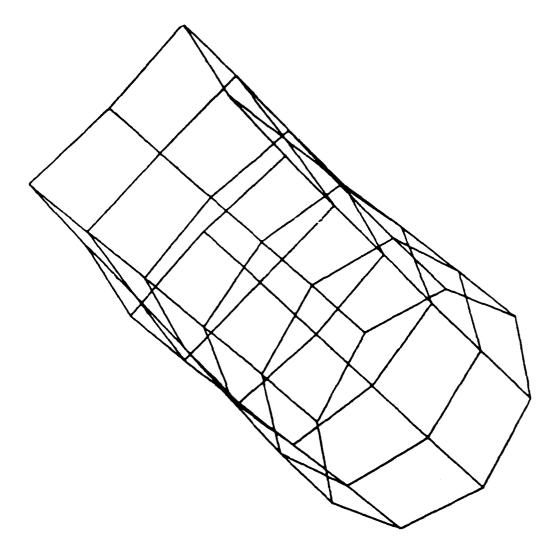
NASTRAN Exaggerated Deformation (Mode 1 - 160.8 Hz)

215

Figure 3-39

NASTRAN Exaggerated Deformation (Mode 2 - 178.5 Hz)

216

Figure 3-40

NASTRAN Exaggerated Deformation (Mode 3 - 244.6 Hz)

217
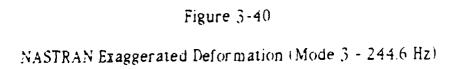
IV. PROPULSION

A. INTRODUCTION

1. Background

The proper choice of a propulsion subsystem is the most important consideration in the structural design and functional assembly of the ORION satellite. The propulsion subsystem which is used will dictate the volume and mass resources which are available for the remaining satellite systems. In addition, the choice of a propulsion subsystem will set the tone of the flight safety qualification process as the satellite is evaluated by NASA. Finally, the propulsion system fixes the orbit boost and attitude control capabilities of the ORION satellite. This is the first Get-Away-Special ejectable satellite to be configured with a capability to change orbits and with the additional provision of attitude control. The choice of a propulsion subsystem profoundly influences mission capabilities. As such, it will also affect the potential users. A tradeoff of various propulsion subsystems must be conducted to evaluate all possible propulsion options in the context of the missions, design constraints and safety issues. The structural design, mass and volume allocations for satellite components, and the mission effectiveness will all hinge upon a wise propulsion subsystem choice.

Satellite propulsion is divided between primary and auxiliary propulsion requirements. Primary propulsion is typically defined as that propulsion which is used only for orbit transfer insertion. Usually primary propulsion involves the use of engines with thrust levels above 5 lbf. Auxiliary propulsion is classically delegated to attitude control maneuvers and orbital

station keeping. Here, attitude control refers to the pointing requirements of the mission and corrections to that attitude to counter external torques. The required propulsive forces for ORION will be small in comparison to those of large satellites or missiles. In fact, all of the propulsion needs of this vehicle could be accomplished through the use of small engines which are normally employed only in attitude control roles on larger spacecraft. This is possible due to the small satellite mass and the small propulsive forces that are required to accelerate the spacecraft. For the purpose of this thesis, the primary propulsion system will encompass both orbit transfer and orbit station keeping using thrusts on the order of 5 to 50 lbf. Auxiliary propulsion will be defined to encompass only attitude control maneuvers using thrust levels of approximately 0.1 lbf.

The engineering tradeoff analysis which follows develops the propulsion subsystem design constraints. With these in mind, a detailed review of the various space qualified propulsion subsystems and their capabilities is presented. These subsystems will all be evaluated within the context of mission performance, adherence to design criteria, reliability, cost effectiveness and safety. A candidate subsystem is proposed based on the selection of pressure fed, catalytic hydrazine thrusters for both the primary and auxiliary propulsion requirements. A vendor survey of candidate hydrazine thrusters is presented along with recommended commercial thruster choices. Finally, a system design which implements those choices is presented and analyzed using propulsion system models. This preliminary design for the ORION propulsion subsystem may be modified as mission requirements and design criteria change. However, the choice of a new

219

candidate subsystem follows the same analysis process, and design decisions can be documented within the context of the applicable restraints.

2. Design Constraints

Twelve design constraints are considered in the selection of the ORION propulsion and attitude control subsystems. They are:

(1) Performance, i.e. I_{sp}
(2) Structural limitations
(3) Mission Delta-V requirements
(4) Simplicity of design
(5) Cost and availability
(6) Quality of the primary/auxiliary system interfaces
(7) Power requirements
(8) Thermal impact of thruster operations
(9) Operational cycles of the thrusters
(10) Contamination
(11) Reliability
(12) Safety requirements including toxicity

Decisions that impact the selection of a propulsion subsystem are documented within the context of these constraints. This allows subsequent review of the preliminary design with some feeling for the trade-offs involved in the use of the various propulsion options. These constraints have been developed through interactions with potential satellite users and system contractors. The constraints are the focal point of the trade-off analysis and are described in more detail below.

a. Performance

Performance is the most important criterion for selection of a propulsion subsystem. The subsystem must propel the satellite to higher orbits and accomplish attitude control for at least 90 days. Maximum propulsive impulse must be incorporated using minimum subsystem mass and volume. Performance is measured by the specific impulse (I_{sp}) of the propulsion subsystem. The ORION propulsion subsystem should demonstrate the highest I_{sp} possible consistent with a low subsystem mass and small volume.

b. Structural Limitations

(1) Volume. The propulsion subsystem must conform to the limitations imposed by the use of a cylindrical volume whose inside dimensions are 14.5" in diameter and 34" in length. In consideration of the longerons and baseplate, endplate, and surface skin thicknesses, these dimensions are less than the total GAS canister envelope. The total propulsion subsystem volume should be as small as possible while delivering a high total impulse. It is particularly important that the propulsion package occupy the smallest possible vertical dimension within the cylinder in order to accommodate the placement of other components. The subsystem may occupy the full girth of the internal volume.

(2) Mass. The total spacecraft mass is limited to 250 lbm. The propulsion subsystem should be of the minimum mass possible while accommodating a large propellant load. This will help to improve the mass fraction [mass $_{propellant}$ / mass $_{total}$] by reducing the dry weight mass. Reducing the mass fraction will lead to an improved delta-V capability of the

221

subsystem. It is undesirable to have useable spacecraft mass lost to excessively heavy subsystem components or trapped fuel. The subsystem should be capable of accommodating variable propellant loads in order to permit the total spacecraft weight to be trimmed to its 250 lbm maximum.

(3) Structure. The propulsion subsystem should be configured to permit a simple, lightweight substructure support. Propulsion components should not force a structural design using bulky platforms and braces. A simple, lightweight but stiff structure is required which can support the 250 lbm vehicle while cantilevered under 6 G acceleration.

c. Mission Delta-V Requirements

(1) Primary Propulsion. The propulsion subsystem should provide sufficient impulse to inject the satellite into an 810 nm circular orbit to permit a study of the lower Van Allen radiation belt region. This will require a delta-V of approximately 2100 feet per second (fps). The duration of the orbital transfer from the departure orbit to the destination orbit is not neccessarily a factor in the selection of a propulsion subsystem. Long transit times, and therefore low thrust devices, may be permissible but are not preferred.

(2) Auxiliary Propulsion. Based upon early design considerations with regard to thermal management, mission requirements, available total impulse and the desired simplicity of the attitude control subsystem, spin stabilization was chosen for the ORION satellite. Chapter Five describes the attitude control problem in detail. Proper spin management is best accomplished using coupled thrusters where two engines act in concert about the center of mass. The coupled thrust of two symmetric thrusters will

accomplish rotation of the satellite without translation. Attitude control for a spinning satellite will therefore require six thrusters, where a pair of thrusters provide spin-up, a pair provide despin, and a third pair precess the vehicle. The discussion of attitude control which follows this section will provide more detailed information with regard to the configuration of the thrusters.

The propulsion subsystem should provide the necessary impulse to accomplish spin up, despin, and commanded turns of the vehicle, as dictated by mission requirements. This subsystem should also enable active precession and nutation control to counteract the attitude disturbances due to external perturbing torques and internal energy dissipation. The commanded turns and torques can only be completely specified in terms of a fully developed mission plan. For the purpose of this preliminary design, the total impulse required to transition from a circular orbit at 135 nm to a circular orbit at 810 nm is approximately 14000 lbf-seconds. A preliminary analysis of mission attitude control requirements in Chapter Five indicates a need for approximately 1200 lbf-seconds of impulse. As the satellite orbital altitude increases, the the magnitude of perturbation due to aerodynamic drag, and thus the total impulse requirement for attitude correction, diminishes. The total impulse required is a function of the number of commanded turns, spin rate and the active nutation control in addition to the orbital insertion impulse. A detailed accounting of these impulse requirements is reported in the attitude control section.

d. Simplicity of Design

Simplicity enhances reliability. All subsystems of the satellite must possess the simplest design possible in order to achieve a highly reliable spacecraft design. The number of subsystem components and their failure modes must be minimized. Thoroughly tested, flight qualified components should be utilized.

e. Cost and Availability

Affordability is closely allied with simplicity. The lead time to manufacture a space qualified componen' i* often proportional to the design simplicity. Ease of access to space depends on affordable satellite subsystems with a relatively short production lead time. Therefore, the design emphasizes use of simple, affordable components. Use of proven off the shelf" technology should be emphasized in lieu of high priced, long-lead-time, new-product development.

f. Quality of the Primary/Auxiliary Subsystem Interfaces

Ideally, the primary and auxiliary propulsion subsystems should use the same propellant and feed system. If this is not possible, then the interface between the two systems should complement both systems. The commonality of the two systems should be maximized. Commonality, or the sharing of elements between the two systems, leads to a lower system mass and smaller system volume with the added benefit of enhanced reliability.

g. Power Requirements

The ORION satellite is limited to a maximum of 60 watts continuous power with a total of 180 watt-hours battery reserve. Thus the selection of propulsion subsystems is constrained to those that exhibit a very low power

consumption. These severe power constraints may exclude electric propulsion subsystems or electrothermal thrusters.

h. Thermal Impact of Thruster Operation

Due to the necessity for tight component packaging (a structural limitation) in the ORION satellite. the thruster components should permit operation of the thruster in close proximity to electronics and propellant feed lines. Optimization of the available satellite volume requires that the thruster nozzles be buried within the structure and not protrude beyond the outer envelope of the satellite. As a result. considerable emphasis must be placed on heat transfer from the operating thruster to nearby satellite components. Thrusters which must be mounted externally or which require a significant heat shielding mass must be avoided. Additionally. the rocket plumes of the primary or auxiliary propulsion subsystems must not impinge detrimentally upon the surface of the vehicle. Attitude control thrusters should be chosen so that exhaust gases do not contaminate the solar cells. In summary. a careful consideration of thermal management constrains the choice of candidate propulsion subsystems.

i. Operational Cycles

Both propulsion subsystems require a restart capability to accomplish their missions. The attitude control thrusters operate in a pulsed mode. The on/off time of a pulsed thruster will be random for a spin stabilized satellite as a function of commanded turns and vehicle perturbations. A small but accurate impulse is required of the thrusters. This impulse is a short duration (milliseconds) pulse of the thruster for which the start and stop of the pulse is well defined and repeatable.

Thrusters must exhibit pulse repetitions of at least 1000 cycles and be capable of long duration burns in excess of three minutes.

j. Contamination

The compact nature of the ORION design precludes the use of a large plume shield that protects the satellite from the impingement of exhaust gasses. The solar cells, attitude sensors and payload sensors require a clean environment to function properly. A propulsion subsystem must be chosen which will maintain a clean, non-corrosive environment near the satellite.

k. Reliability

The propulsion subsystem must exhibit an overall reliability of at least 0.90 for 90 days. Higher reliability is desirable, but not at the expense of extra mass and volume using redundancy. A simple and highly reliable non-redundant subsystem is the goal of this design.

l. Safety Issues

The ORION satellite will be the first Get-Away-Special ejectable satellite with attitude control and orbital transfer propulsion. Consequently, any subsystem choice must consider the safety of the Shuttle, its crew, and ground personnel. In the aftermath of the STS 51-L Challenger disaster, NASA engineers are reluctant to approve controversial propulsion subsystems for use on the Shuttle. The enclosure of explosive, caustic, or toxic propellants in a GAS canister is a sensitive issue which must be dealt with in small, well planned steps. Poor planning in the safety qualification of a propulsion subsystem for ORION likely will defeat the satellite project. Hence, the chosen system must be safe, reliable, and simple. The system design must conform to the propulsion safety guidelines detailed in NASA

Document NHB 1700.7A. "Safety Policy and Requirements". The provision of propulsion for GAS ejectable satellites is a big step for the user-friendly Get-Away-Special program. This advance will only be achieved through selection of a safe, reliable propulsion subsystem and a carefully orchestrated safety qualification effort accomplished in close conjunction with NASA engineers.

B. PROPULSION OVERVIEW

The application of propulsive thrusts to a spacecraft involves the use of mass expulsion devices that produce a reactive force opposite the direction of application. These devices exist in myriad forms producing thrusts over a range of millipounds to millions of pounds. A rocket propulsion system is a device that imparts energy to vehicle contained propellant or mass such that the mass, in being expelled, produces a directional thrust/force on the vehicle. The magnitude of this thrust is directly proportional to the weight flow and to the velocity of the expelled mass. To get more thrust, therefore, we must increase either the flow rate or the exit velocity of the ejected mass. This relationship is nothing more than our old friend momentum, defined as mass times velocity. Since the total momentum of any isolated system is constant in magnitude and direction, it follows that the ejection of mass imparts to the vehicle an equal and opposite momentum. (Ring, 1964, p.3)

Rocket propulsion depends on three elements to produce thrust. First, the mass must be expelled in a directed fashion. Second, the high-velocity propellant provides the momentum to which the satellite reacts. The choice of a propellant depends on the type rocket; there are more permutations to thruster and rocket designs than to the propellants themselves. The third element of the propulsion subsystem is the propellant storage and feed apparatus. The feed components deliver the propellant to the thruster at a

given rate which is proportional to the thrust of the rocket motor. The mass flow rate (dM/dt), exhaust gas exit velocity (V_e), thruster nozzle area (A_e) and thruster nozzle pressure differential ($p_e - p_a$) are used to describe the thrust.

$$F = (dM/dt) V_e + A_e (p_e - p_a)$$ (4.1)

Liquid propellant feed systems are either pressure fed or pump fed. Pressure fed systems are further classified as regulated (constant pressure) or blowdown (decaying pressure). These three elements form the basic propulsion subsystem. The design of a propulsion package for ORION involves the selection of thruster, propellant, and feed components. The choice of a subsystem is most often focussed on thrust and total impulse capability. More often than not, a class of thrusters is compatible with various propellants or feed systems. Hence, the choice of a propulsion system becomes a tradeoff of various component capabilities and design constraints to achieve an optimum design.

1. Rockets

Rockets are broadly classified in one of four categories: cold gas jets, heated gas jets, chemical (combustion or catalytic decomposition) rockets, and electric propulsion thrusters. Chemical rockets are subdivided into liquid, solid, or hybrid subsystems. Figure 4-1 shows the various types of mass expulsion subsystems. Of the chemical rockets, sublimation solid rockets achieve the highest specific impulse (up to 2000 seconds) but do so with a very low thrust level (01 to 0.000001 lbf). Bipropellants are capable of

specific impulse as high as 500 seconds and can produce thrusts in excess of 300,000 lbf such as in the current generation Shuttle main engine (SSME). Each F-1 engine on the Saturn V produced 1.5 million lbf. Solid rockets are used in both manned and unmanned space applications. They yield a slightly lower I_{sp} (250 - 300) but at thrust levels of up to one million lbf. The monopropellants are capable of moderate I_{sp} (220 seconds) and low to medium thrusts of 0.001 to 1000 lbf. Heated inert gas jets use electric resistance heaters to increase the temperature of a cold gas stream and exhibit an I_{sp} of up to 115 seconds at low thrusts (below 1.0 lbf). Liquid phase engines are another form of cold gas jets that utilize propane, methane, Freon-14, or ammonia liquids. These liquids are evaporated using electrical tank heaters to form a gas for use in an inert gas thruster. These engines demonstrate an I_{sp} of 80-100 seconds with added advantage of very high propellant storage densities. When the volume of propellant is the limiting factor in the spacecraft design, this type of system can be very attractive. Finally, the cold gas or inert gas thruster uses pressurized gas expanded from an appropriate nozzle to provide thrust with a very low I_{sp} of 65 to 85 seconds.

The chemical rocket engine is composed of two primary components, namely the combustion chamber and the rocket nozzle. In a typical bipropellant engine, the combustion chamber is that region of the rocket where propellants are mixed and burned to create thermal energy through the release of energy in chemical bonds. A monopropellant engine has only one propellant which must be decomposed by catalysis to release the chemical energy necessary for propulsion.

The second primary component of the rocket engine is the nozzle. The function of the nozzle is to convert the thermal energy generated by the reaction in the combustion chamber to kinetic energy. Nozzles may be configured in various shapes. A discussion of nozzle geometry is beyond the scope of this thesis but may be obtained from Sutton (1976) or Barrere (1960). Specification of the nozzle geometry is actually unnecessary at this level of the design effort because a commercially available rocket unit will be configured with a preset nozzle. The ORION design will use off-the-shelf propulsion units rather than custom products. The cold gas thrusters use a simple, uncooled, nozzle constructed for supersonic exhaust velocities. The high thrust bipropellant engines use regeneratively cooled nozzles. Monopropellant rockets, with lower chamber temperatures, are cooled radiatively. Solid rockets (not sublimation solids) often use ablative nozzles and depend upon radiative cooling. Thermal management is an important factor in the selection of a thruster and for mounting the thruster within the spacecraft.

2. Propellants

As with rocket engines, propellants may be classified and distinguished by several key characteristics. These include propellant type, performance and physical characteristics. Of the liquid propellants, there are monopropellants and bipropellants. With respect to liquid propellants, chemical compounds may be classified based upon their use. For example, note that hydrazine (N_2H_4) is used as a monopropellant when catalyzed by a Shell 405 iridium metal catalyst. Hydrazine is also a bipropellant when used in combination with various oxidizers, such as nitrogen tetroxide. Propellants
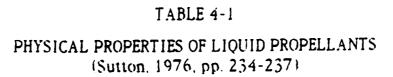
are evaluated on the basis of their performance. Specific impulse. effective exhaust velocity. specific propellant consumption. and ideal exhaust velocity are all parameters used to evaluate propellant performance. A propellant should yield large specific chemical energy per unit mass. This is accomplished using low molecular weight compounds which are highly energetic. Hydrogen is a good example. Note that the full value of the propellant energy is never fully realized due to incomplete combustion. friction losses. and exhaust gas disassociation.

Desirable physical qualities of a liquid propellant include a low freezing point. high specific gravity. shock insensitivity. and small variation in performance as a function of temperature. A low freezing point permits use of the propellant in the cold vacuum environment of space. A high specific gravity allows the storage of a large mass of propellant within a small volume. This is advantageous because, as storage volume is decreased. the storage system weight and spacecraft dry mass are also reduced. Various propellant specific gravities are tabulated in Table 4-1 and plotted in Figures 4-2 and 4-3. Shock-insensitivity relates to the ability of a propellant to withstand handling and shock without explosive decomposition. The use of shock-sensitive propellants is particularly undesirable in the ORION application. Long term storage stability is also important to avoid deterioration of the propellant or storage subsystem. Propellants must be chosen to be compatible with the storage tank and feed line materials ensuring that negligible chemical reactions occur even at elevated temperatures. The propellant should not absorb moisture and must tolerate the presence of small amounts of impurities. The stability of a propellant

TABLE 4-1

PHYSICAL PROPERTIES OF LIQUID PROPELLANTS
(Sutton, 1976, pp. 234-237)

Propellant	Red Fuming Nitric Acid	Nitrogen Tetroxide	Nitro-methane	Liquid Oxygen
Chemical formula	85% HNO_3 15% N_2O_4	N_2O_4	CH_3NO_2	O_2
Molecular weight	~60	92.016	61.04	32.00
Melting or freezing point, °F	-56.3	11.08	-20	-361.8
Boiling point, °F	—	70.1	214	-297.6
Heat of vaporization, Btu/lb	—	178*	242	91.6
Heat of formation, Btu/lb-mole	—	-12,240 (77 F)	—	-406(l) (-297 F)
Specific Heat, Btu/lb°F	0.416 (32 F) 0.424 (100 F)	0.367 (62 F)	0.41 (63 F)	0.4 (-343 F)
Specific gravity	1.573 (68 F) 1.529 (100 F)	1.447 (68 F) 1.37 (120 F)	1.15 (70 F)	1.14 (-297 F) 1.23 (-320 F)
Viscosity, centipoise	1.3 (68 F)	0.423 (68 F)	0.650 (70 F) 0.388 (160 F)	0.87 (-363 F) 0.19 (-297 F)
Vapor pressure, psia	2.0 (68 F) 9.4 (120 F)	13.9 (68 F) 60 (130 F)	0.1 (102 F)	0.75 (-300 F)

* At boiling point
(l) Liquid condition.

232

TABLE 4-1 (cont.)

PHYSICAL PROPERTIES OF LIQUID PROPELLANTS
(Sutton, 1976, pp. 234-237)

Propellant	Ammonia	Aniline	Chlorine Trifluoride	Ethyl Alcohol
Chemical formula	NH_3	$C_6H_5NH_2$	ClF_3	C_2H_5OH
Molecular weight	17.03	93.06	92.457	46.06
Melting or freezing point (F)	107.9	20	-117.4	-174
Boiling point (F)	-28	364	53.15	173
Heat of vaporization (Btu/lb)	590	187	—	360*
Heat of formation (Btu/lb-mole)	-29.900 (65 F)	-13.200 (77 F)	-80.100 (55.4 F)	-119.200 (65 F)
Specific heat (Btu/lb F)	1.05 (-76 F) 1.48 (212 F)	0.48 (50 F) 0.65 (300 F)	0.303 (53.15 F)	0.59 (68 F)
Specific gravity	0.604 (60 F) 0.524 (160 F)	1.0 (100 F)	1.85 (53.15 F) 1.77 (100 F)	0.79 (60 F) 0.74 (160 F)
Viscosity (centipoise)	0.27 (-76 F) 0.13 (68 F)	6.6 (50 F) 0.88 (200 F)	0.478 (53.15 F)	1.25 (68 F)
Vapor pressure (psia)	128 (60 F) 515 (160 F)	45 (200 F) 60 (500 F)	17.2 (60 F) 80.6 (140 F)	0.85 (60 F) 11.2 (160 F)

(1) Liquid condition
* At boiling point

TABLE 4-1 (cont.)

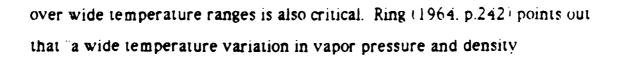# PHYSICAL PROPERTIES OF LIQUID PROPELLANTS
(Sutton, 1976, pp. 234-237)

Propellant	Monomethyl-hydrazine	Liquid Fluorine	Hydrazine	Liquid Hydrogen	Hydrogen Peroxide
Chemical formula	CH_3NHNH_2	F_2	N_2H_4	H_2	$H_2O_2(100\%)$
Molecular weight	46.08	38.0	32.05	2.016	34.02
Melting or freezing point (°F)	−62.3 F	−363	34.5	−434.5	31.4
Boiling point (°F)	189.5 F	−307	235.9	−423	302.4
Heat of vaporization (Btu/lb)	376.9 (at 77 F)	74.2*	602 (77 F)	192	653 (77 F)
Heat of formation (Btu/lb-mole)	23,600	0	21,600 (77 F)	−3420(l) (−423 F)	2745 (77 F)
Specific heat (Btu/lb °F)	0.688 (68 F) 0.725 (248 F)	0.366 (−306.2 F) 0.357 (−335 F)	0.736 (68 F) 0.758 (150 F)	1.75 (−423 F) —	0.628 (50 F) 0.672 (200 F)
Specific gravity	0.8788 (68 F) 0.8627 (100 F)	1.660 (−340 F) 1.431 (−285 F)	1.008 (68 F) 0.984 (120 F)	0.071 (−423 F)	1.442 (77 F) 1.375 (150 F)
Viscosity (centipoise)	0.855 (68 F) 0.40 (100 F)	0.299 (−320 F) 0.412 (−335 F)	0.97 (68 F)	0.024 (−434 F) 0.013 (−423 F)	1.02 (90 F)
Vapor pressure (psia)	1.0 (80 F) 100 (311 F)	23 (−300 F) 45 (−340 F)	0.2 (68 F) 7.2 (200 F)	1.2 (−435 F)	0.25 (150 F) 2.2 (200 F)

234

TABLE 4-1 (cont.)

PHYSICAL PROPERTIES OF LIQUID PROPELLANTS
(Sutton, 1976, pp. 234-237)

Propellant	Monomethyl-hydrazine	Liquid Fluorine	Hydrazine	Liquid Hydrogen	Hydrogen Peroxide
Chemical formula	CH_3NHNH_2	F_2	N_2H_4	H_2	$H_2O_2(100\%)$
Molecular weight	46.08	38.0	32.05	2.016	34.02
Melting or freezing point (°F)	−62.3 F	−363	34.5	−434.5	31.4
Boiling point (°F)	189.5 F	−307	235.9	−423	302.4
Heat of vaporization (Btu/lb)	376.9 (at 77 F)	74.2*	602 (77 F)	192	653 (77 F)
Heat of formation (Btu/lb-mole)	23,600	0	21,600 (77 F)	−3420(1) (−423 F)	2745 (77 F)
Specific heat (Btu/lb °F)	0.688 (68 F) 0.725 (248 F)	0.366 (−306.2 F) 0.357 (−335 F)	0.736 (68 F) 0.758 (150 F)	1.75 (−423 F) —	0.628 (50 F) 0.672 (200 F)
Specific gravity	0.8788 (68 F) 0.8627 (100 F)	1.660 (−340 F) 1.431 (−285 F)	1.008 (68 F) 0.984 (120 F)	0.071 (−423 F)	1.442 (77 F) 1.395 (150 F)
Viscosity (centipoise)	0.855 (68 F) 0.40 (160 F)	0.299 (−320 F) 0.412 (−335 F)	0.97 (68 F)	0.024 (−434 F) 0.013 (−423 F)	1.02 (90 F)
Vapor pressure (psia)	1.0 (80 F) 100 (311 F)	23 (−300 F) 0.95 (−340 F)	0.2 (68 F) 7.2 (200 F)	1.2 (−435 F)	0.25 (130 F) 2.2 (210 F)

over wide temperature ranges is also critical. Ring (1964. p.242) points out that "a wide temperature variation in vapor pressure and density
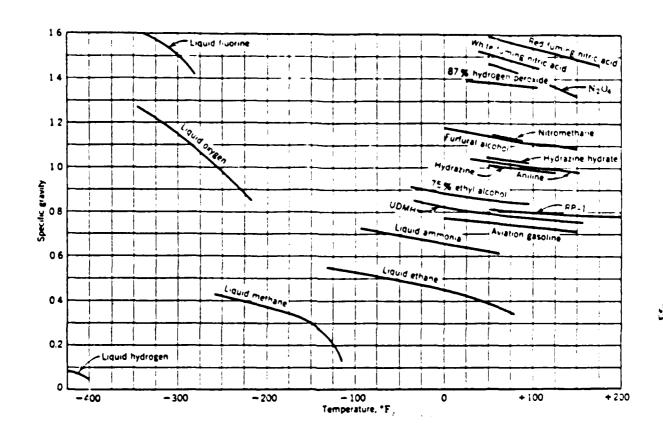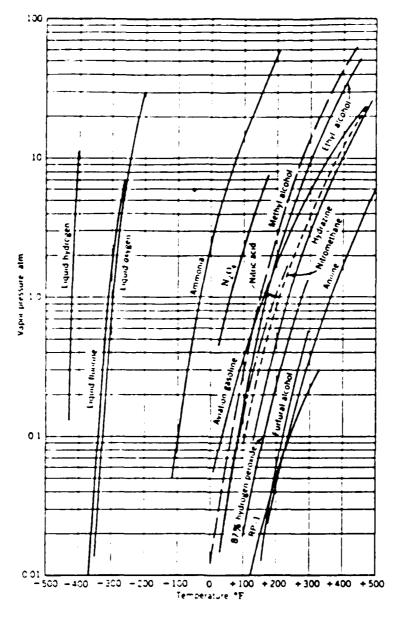
Figure 4-2

Specific Gravity of Liquid Rocket Propellants
(Sutton, 1976, p.238)

Figure 4-3

Vapor Pressure of Liquid Rocket Propellants
(Sutton, 1976, p. 239)

TABLE 4-2

A COMPARISON OF SELECTED MONOPROPELLANTS
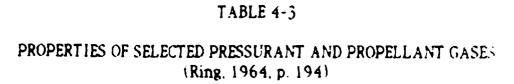### (Sutton, 1976, p. 254)

Propellant	Symbol	Molecular Weight	Specific Gravity	Theoretical I_s*	Combustion Temperature (R)	Operational and Handling Traits
Hydrogen peroxide (90 wt % solution)	H_2O_2	22.7	1.4	191.0	2296	Decomposes slowly during storage (<1% yearly) Decomposes rapidly above 280 F Explodes about 980 F Toxic as a vapor or spray
Ethylene oxide	C_2H_4O	12.3	0.9	226.6	1986	A gas at room temperature Boils at 51 F Stores well in sealed containers Compatible with mild steel, aluminum, and some stainless steels Vapors are toxic
Hydrazine	N_2H_4	11.6	1.0	285.91	2442	Stores well when sealed Compatible with many materials Vapors are very toxic Explodes at about 450 F
Nitromethane	CH_3NO_2	20.3	1.1	287.0	4408	Storable in plastic lined containers Vapors are very toxic Prone to detonate at about 800 F in liquid phase

* Chamber pressure of 1000 psia expanded to vacuum, nozzle area ratio 40:1.
† Approximately 40% NH_3 dissociation

238

TABLE 4-3

PROPERTIES OF SELECTED PRESSURANT AND PROPELLANT GASES
(Ring, 1964, p. 194)

Pressurant Gas	γ	Molecular Weight	Boiling Point at 1 Atm (°R)	Critical Properties		Compatibility with Propellant				Gas Specific Heat (Cp-BTU/lb °R) (Low Pressure)
				Temperature (°R)	Pressure (psia)	LO₂	LH₂	N₂O₄	50 UDMH	
Hydrogen	1.4	2	37	60	188	No	Yes	No	Yes	3.39
Helium	1.66	4	8	10	33	Yes	Yes	Yes	Yes	1.25
Methane	1.26	16	201	343	674	(Cond)	(Cond)	No	Yes	0.55
Ammonia	1.28	17	432	730	1640	(Cond)	(Cond)	No	Yes	0.523
Neon	1.61	20.2	50	80	394	Yes	(Cond)	Yes	Yes	0.25
Nitrogen	1.4	28	140	227	493	(Cond)	(Cond)	Yes	Yes	0.25
Air	1.4	29	142	239	547	Yes	(Cond)	Yes	Yes	0.24
Argon	1.67	39.9	15	271	706	(Cond)	(Cond)	Yes	Yes	0.125
Carbon dioxide	1.28	44	351	548	1073	No	No	Yes	No	0.18
Propane	1.13	49.2	415	666	617	No	No	Yes	Yes	0.25
Cyanogen	1.25	52	455	522	867	No	Yes	Yes	Yes	0.191
Vaporized Propellant										
Hydrogen	1.4	2	37	60	188	No	Yes	No	Yes	0.22
LO₂	1.4	32	162	279	737	(Cond)	(Cond)	Yes	No	0.1
2N₂O₄ = 2NO₂ + N₂O₄	1.14	46 92	530	776	1455	(Cond)	(Cond)	Yes	No	0.155

(Cond) = Condensible.

(thermal coefficient of expansion) or an unduly high change in viscosity with temperature makes it very difficult to calibrate a rocket engine system or predict its performance over any reasonable range of operating temperature. JPL TR 32-735 (1965, p.2) points out that propellants which are storable at near ambient temperatures are the best candidates for space based systems. This has led to their categorization as "earth storable" propellants. This term is used with reference to those fuels which exist in liquid phase at temperatures commonly encountered at the earth's surface (70° +/- 30° F). Propellants thus designated as earth storable have vapor pressures below some reasonable operating tank pressure (i.e. 300 psia) while in the prescribed (earth ambient) temperature range. JPL TR 32-735 (1965, p.3) tabulates the known Earth storable propellants. Finally, it is desirable to use propellants that yield the lowest possible molecular weight in order to develop a high I_{sp}. Fuels rich in hydrogen or other lightweight atoms are the best. Hydrazine, for example, dissociates with a large surplus of hydrogen atoms. Figures 4-2, 4-3 and Tables 4-1 through 4-3 summarize the characteristics of several propellant fluids and inert gases with respect to the desirable qualities detailed above.

3. Propellant Feed Subsystems

The two broad classes of propellant feed subsystems are "pump fed" and "pressure fed" subsystems. Solid propulsion subsystems do not use propellant feed components. Those propulsion subsystems which utilize gaseous propellants will obviously use only the pressure feed option. However, most propulsion subsystems that do not use solid rockets will utilize a fluid in some manner, and thus, either of the propellant feed

mechanisms listed above. The pump-fed subsystems are typically more complex than the pressure fed subsystems. These are employed in situations where very large propellant masses and/or high feed rates are encountered. An example of the pump-fed subsystem is the Shuttle liquid hydrogen and oxygen feed system. The volume of the Shuttle fuel tank is too great to pressurize the ullage with a gas, and the feed rate is higher than a pressurized feed subsystem could provide. The weight of a pressurized Shuttle tank would be enormous. On the other hand, most spacecraft deal in small quantities of fuel that are measured in the tens or hundreds of pounds. Feed rates rarely, if ever, exceed 0.5 lbm per second. This order of magnitude for fuel mass and feed rate is well within the range of pressurized feed subsystem capability. The added advantage of the simplicity and reliability of a pressurized feed subsystem make it the prevalent choice for many designs for spacecraft propulsion.

4. Attitude Control Subsystems

The attitude control (reaction control) system of a satellite imposes a number of constraints upon the design of a propulsion package. These constraints are often different than those placed upon the operation of the primary propulsion system. For example, primary propulsion is tasked with occasional orbit maintenance using medium to long duration propellant burns of one second or longer. The auxiliary propulsion system, on the other hand, is required to impart regular, minute control impulses for commanded turns, precision pointing, torque cancellation, and nutation control. The performance parameters of any rocket engine have upper and lower bounds which must be taken into consideration when choosing a subsystem for a

241

particular application. Often the parameters considered valuable for primary propulsion are of secondary concern for the auxiliary propulsion subsystems; hence, each subsystem requires a careful, separate design. A primary propulsion subsystem is responsible for high impulse operations which propel the vehicle into a new orbit. It will typically require a medium (5 lbf to 50 lbf) or high thrust (> 50 lbf) engine capable of long duration burns to enable orbit insertion maneuvers. Small, repeatable pulses are typically not required of the primary system engine. Thus, the lower bound on pulse width for a primary propulsion engine is of little concern. Auxiliary propulsion systems, on the other hand, are reaction control devices which orient the vehicle about the roll, pitch, and yaw axes using small, repeatable precision thrusts. Electrical signals from the spacecraft guidance system actuate flow control valves and regulate propellant flow to low thrust engines for precise attitude adjustments. This flow is regulated by an ON-OFF ("bang-bang") control using pulse width modulation or is metered via proportional flow control valves. The use of proportional flow control is a complicated process whereby the flow rate and thrust are proportional to the magnitude of the control signal. This type of control adds significant complexity and expense to the propellant feed control system. Using "bang-bang" control and pulse width modulation, the duration of propellant flow is varied as a function of time while the engine operates at a fixed thrust level. For three axis stabilization, the frequency of the thruster operation is fixed while the pulse width is modulated. Pulse frequency modulation is also utilized, with the pulse width and thrust fixed while the frequency of thruster operation is varied to accomplish the desired pointing. In each of these cases, error

sensing and attitude detection devices provide inputs to an attitude control computer as the desired attitude is obtained. The number and magnitude of attitude control maneuvers will dictate, in part, the total impulse of the propulsion system. Hence, an accurate assessment of the auxiliary propulsion requirements is needed to choose a propulsion package for a particular application. Parameters such as the smallest possible pulse width, fastest pulse repetition frequency, pulse width and thrust repeatability, total number of pulses, and total available system impulse weigh heavily in the selection of an auxiliary propulsion system. Before these requirements can be defined, all of the expected perturbing torques, vehicle moments of inertia, and nutation time constants must be quantified. Having defined the system dynamics of the satellite, the upper and lower bounds on the various performance parameters of the thrusters, propellant, and feed system can be identified.

5. Propulsion Requirements

The design requirements for the ORION satellite stipulate that a circular orbit of 809 nm (1500 km) be attainable for the purpose of operating in the lower reaches of the Van Allen radiation belt region. The total impulse to accomplish this maneuver can be determined using a model of the Hohmann transfer ellipse if the propulsive forces are assumed to be impulsive. Impulsive force applications infer that the period of force application is much less than the orbital period that results from that force application.

The initial orbit is assumed to be circular at 135 nm (250 km - nominal Shuttle deployment orbit), and a minimum energy orbital transfer (Hohmann

transfer) is to be used. Bate (1971, p. 163) provides a complete discussion of the calculations for such a transfer. Using the radius of the orbit (R) and the universal gravitational constant, k, the velocity of an orbit is

$$V = (k/R)^{0.5} \qquad (4.2)$$

Thus the Delta-V, or difference in orbital velocities, can be obtained from

$$\text{Velocity}_{250} = (k/(6378 + 250) \text{ km})^{0.5}$$
$$= 7.7588 \text{ km/sec}$$
$$\text{Velocity}_{1500} = (k/(6378 + 1500) \text{ km})^{0.5}$$
$$= 7.1167 \text{ km/sec}$$

$$k = 3.99 \times 10^5 \text{ km}^3/\text{s}^2$$

$$\text{Energy} = E = -k / (\text{Apogee} + \text{Perigee}) \qquad (4.3)$$
$$= -k / (6628 + 7878)$$
$$= -27.5058 \text{ km}^2/\text{sec}^2$$

$$V = (2[(k/R) + E])^{0.5} \qquad (4.4)$$
$$\text{Velocity}_{\text{Hohmann - perigee}} = (2[(k/6628] + \text{Energy}])^{0.5}$$
$$= 8.0862 \text{ km/sec}$$
$$\text{Velocity}_{\text{Honmann - apogee}} = (2[(k/7878] + \text{Energy}])^{0.5}$$
$$= 6.8032 \text{ km/sec}$$

$$\text{Delta-V} = V_p - V_a \qquad (4.5)$$

$$\text{Delta-V}_1 = 8.0862 - 7.7588 \text{ km/sec}$$

$$= 327.4 \text{ meters/sec}$$

$$\text{Delta-V}_2 = 7.1167 - 6.8032 \text{ km/sec}$$

$$= 313.5 \text{ meters/sec}$$

$$\text{Total Delta-V} = 327.4 + 313.5$$

$$= 640.9 \text{ m/sec}$$

$$= 2102 \text{ ft/sec}$$

$$M_p = M_0 \{ 1 - [e^{(\text{Delta-V}) / (\text{Isp} \times G)]} - 1 \} \qquad (4.6)$$

$$M_p = 250 \text{ lbm} \{ 1 - [e^{(640.9/(\text{ISP})(9.8))}] - 1 \}$$

$$\text{Total impulse} = (I_{sp})(M_p) \qquad (4.7)$$

Using the equations above, which are based upon the requirement to deliver a delta-V of 641 m/s (2102 ft/sec), the mass of propellant for primary propulsion can be derived. The total impulse for orbit insertion is seen to be a function of I_{sp} for the particular propellant in use. Propellants with a high I_{sp} require a smaller fuel mass.

The propellant mass for the auxiliary propulsion subsystem can also be defined using the total impulse equation. The total impulse is determined from an analysis of the attitude control requirements of a given mission. Knowledge of the impulse for the desired spin rate, spin rate changes, pointing requirements, perturbing torques, and active nutation control is needed to quantify the total amount of propellant required. The attitude control section of this thesis identifies those mission requirements in detail.

A conservative assumption of the total impulse is 1200 lbf-seconds (see Chapter Five) which represents a safety factor of 3 times the probable impulse requirement. The mass of propellant for attitude control purposes is then

$$M_p = (\text{Total impulse}) / I_{sp} \qquad (4.8)$$

The total propellant mass of the ORION satellite is the sum of the primary and auxiliary propellant masses. This value will vary widely depending upon the type propellant (and I_{sp}) which is chosen.

C. SUBSYSTEM DESIGN OPTIONS

With the advent of long life Earth-orbiting and interplanetary three axis stabilized spacecraft, the technology of low thrust (10^{-5} to 5 lbf) propulsion systems has received increased emphasis. The selection of the optimum (that is, most applicable based upon cost effectiveness) auxiliary propulsion system for a given mission is extremely important and can severely impact the spacecraft payload and probability of success. An auxiliary propulsion system can be characterized by parameters such as mass, power, performance, cost, volume, leakage, reliability, and others. The selection of an optimum system involves the tradeoff of these variables for the specific mission under consideration. Before a meaningful tradeoff of thruster systems can begin, an up to date survey of existing technology is necessary. An extensive survey of available thruster systems is required. (JPL TR 32-1505, 1971, p.1)

The evaluation of propulsion subsystem options for ORION involves the tradeoff of many parameters. In addition to the various thruster performance parameters, one must consider the design constraints, the mission requirements, and the less obvious but equally important subtleties

246

of product availability, spacecraft integration and subsystem component compatibilities. This section addresses the major advantages and faults of several types of propulsion subsystems. Consideration will be given to major parameters such as thrust, weight, volume, total impulse and power consumption. The intricate details of subsystem integration, product availability, and engineering specifications will not be discussed in this thesis. Instead, an evaluation of various propulsion options serves as a feasibility study to prove that ORION can be configured with a capable propulsion and attitude control subsystem.

The propulsion subsystems which are appropriate for ORION are listed below. The following discussions of those subsystems and their relationships. as summarized in Table 4-4, are adapted from JPL TR 32-1505.
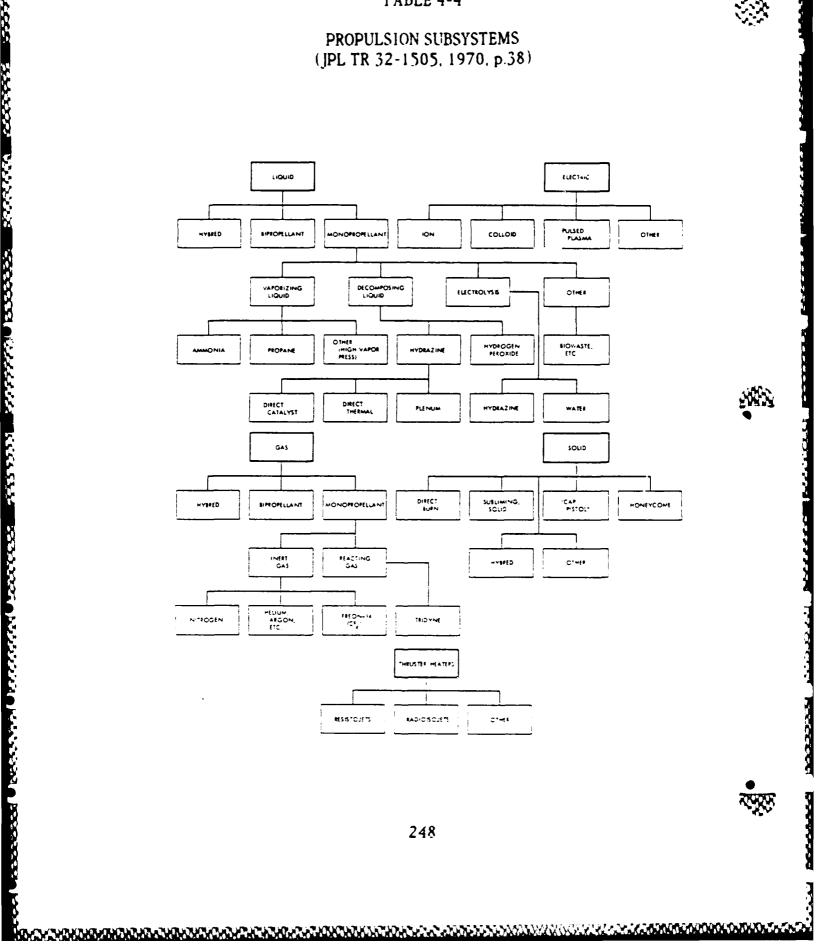
(1) Inert gas. H_2, He, N_2, A, Xe, CF_4, CH_4. The inert gas subsystems are characterized by the use of a high pressure gas which is reduced in pressure by a regulator and expelled through a nozzle.

(2) Hot gas. Inert resistojets. The resistojet is simply a thermal heater element which heats an inert gas increasing the exhaust temperature and thrust. Resistojets use nitrogen or other inert gas propellants that would normally yield low I_{sp}.

TABLE 4-4

PROPULSION SUBSYSTEMS
(JPL TR 32-1505, 1970, p.38)
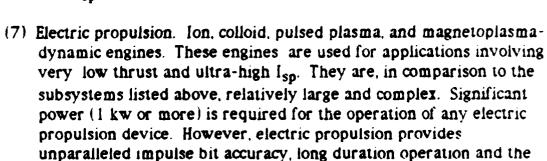
(3) Vaporizing liquid. NH_3, methane, Freon 14, and propane. The vaporizing liquids represent an increase in storage density and reduction in storage volume over the inert gas subsystems. These propellants do not substantially increase the available I_{sp}. Freon 14 and ammonia are the most common propellants. The equilibrium vapor pressure is used to pressurize the system, and inert gas nozzles are used for mass expulsion. Some heating of the storage tank may be used to accelerate the liquid vaporization.

(4) Monopropellants.

(a) Hydrazine direct catalyst. The hydrazine direct catalyst subsystem is composed of a liquid expulsion feed system and a catalytic thrust chamber that decomposes the hydrazine prior to expulsion.

(b) Hydrazine resistojet. This subsystem is similar to the hydrazine direct catalyst system. The fuel is decomposed by an electrically heated element in the thrust chamber.

(c) Hydrazine plenum. The hydrazine plenum subsystem uses liquid propellant feed components to supply a catalytic gas generator. The gases which are generated are stored in a plenum for later expulsion.

(5) Solid rockets. Solid rocket boosters, sublimating solid thrusters, and "cap-pistol motors". The solid rocket contains a propellant mixture with both fuel and oxidizer. It is capable of high I_{sp} and very high thrust. The thrust is not throttled, and each engine provides a single burn. Sublimating solids are thruster assemblies which use very small quantities of solid propellant. Using electric heaters, small thrusts are produced by vaporization of the solid fuel mixture, and subsequent expulsion of the gas through a nozzle. "Cap-pistol motors" are very small solid rocket charges stored in an array. Individual charges are ignited for the production of precise attitude control thrusts.

(6) Bipropellants. O_2 / H_2 or Hydrazine/Nitrogen tetroxide. The bipropellant engine, which provides the highest I_{sp} of any of the thruster systems listed above, has added complexity and potential

249

safety problems. Hypergolic mixtures (ignite on contact) are often used in long storage applications. Recent developments in gaseous bipropellant engines enables the storage of oxygen and hydrogen for high I_{sp} propulsion.

(7) Electric propulsion. Ion, colloid, pulsed plasma, and magnetoplasma-dynamic engines. These engines are used for applications involving very low thrust and ultra-high I_{sp}. They are, in comparison to the subsystems listed above, relatively large and complex. Significant power (1 kw or more) is required for the operation of any electric propulsion device. However, electric propulsion provides unparalleled impulse bit accuracy, long duration operation and the highest I_{sp} available.

The performance of the thruster subsystems presented above must be tabulated for various propellants, duty cycles, pulse width, pulse frequency repeatability, power requirements, cost, reliability and total impulse. The mass of the thruster, propellant feed and support components must be determined. Propellant or thruster interactions with the spacecraft, such as thruster plume impingement and heat transfer from the rocket, must be studied. In consideration of all of the system characteristics and design constraints, a proper system can be chosen. A summary of each of the aforementioned propulsion subsystems follows with an analysis of each subsystem and its merit as a propulsion element for the ORION spacecraft.

1. Inert Gas Thrusters

The inert gas monopropellant (cold gas) thruster subsystem is the most inexpensive and reliable propulsion subsystem available. Pressurized gas is stored in a suitable high pressure vessel. When a propulsive maneuver is commanded, the gas is vented from the supply vessel through a regulator and a solenoid-controlled valve. The gas is expanded through a suitable

250

nozzle for the production of thrust. Exothermic reactions do not occur, and as a result, the cold gas subsystem yields relatively low I_{sp}. The cold gas has little energy and, hence very little impulse. Large quantities of gas must be expended to produce thrusts of over 1.0 lbf. Typical gas storage pressures are in the range of 1000 to 6000 psi. The cold gas thruster subsystem, with its lack of catalysis or ignition processes, is inherently simple and reliable. However, a large mass of gaseous propellant is required due to the penalty of a low I_{sp}.

If <u>ideal</u> gases are compared with respect to the total impulse delivered, nitrogen (N_2) is the best propellant dased upon the gas molecular weight This result is due to the increase in gas density with increasing molecular weight which leads to reduced total tankage mass. Low molecular weight gases such as helium (He) and hydrogen (H_2) have a higher I_{sp} than nitrogen but must be stored at very high pressures to obtain a significant propellant density. At high pressures, the pressure vessel wall thickness is increased and, with it, the total tank weight. When heavy, <u>non-ideal</u> gases such as Freon-14 are considered, the effect of compressibility (Van der Waals forces) becomes important, and Freon delivers a larger total impulse per pound than nitrogen. For systems which are volume limited, the Freon-14 propellant is preferable. However, Freon-14 and other heavy gases such as ammonia and methane will liquify at the pressures and temperatures encountered in space applications. Consequently, these propellants are used in vaporizing liquid propulsion subsystems more often than in inert gas subsystems. For that reason, ideal gases, particularly nitrogen, are preferred for inert gas applications. In practice, for a given total impulse, the total system weight of

251

TABLE 4-5

PROPERTIES OF GASEOUS PROPELLANTS
(Sutton, 1977, p. 228)

Propellant	Molecular Weight	Density* (lb ft³)	Theoretical Specific Impulse (sec)
Hydrogen	2.0	1.21	296
Helium	4.0	2.37	179
Neon	20.4	11.56	82
Nitrgoen	28.0	17.37	80
Air	28.9	19.3	74
Argon	39.9	27.60	57
Krypton	83.8	67.20	39
Xenon	131.3	170.55	31
Freon 14	88.0	60.01	55
Methane	16.0	12.10	114
Carbon dioxide	44.0	Liquid	67

* At 3500 psia and 0 C.
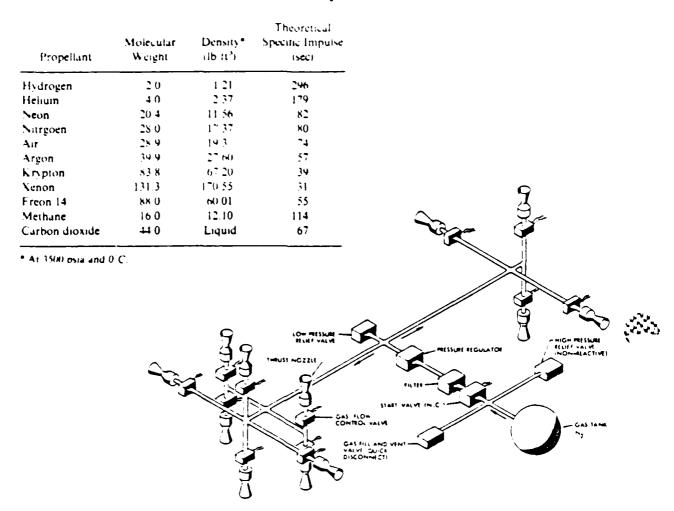
Figure 4-4

Inert Gas Attitude Control System
(AFSC DH 3-2, 1964, p.4.4-2)

propellant and tankage is roughly equivalent using nitrogen, Freon 14, or methane. With helium or hydrogen, the total system weight is much higher. The properties of several candidate gases (ideal and non-ideal) are outlined in Table 4-5.

Inert gas subsystems have flown on all Ranger, Mariner, Surveyor, Pioneer, and Nimbus spacecraft, as well as many others. However, inert gas subsystems are not a propulsion concept restricted only to early spacecraft. The European X-ray satellite, EXOSAT, which was launched in 1983, carried a methane cold gas subsystem. In addition, the ASAT missile uses a nitrogen cold gas thruster assembly for attitude control functions. As a result of their extensive use, the characteristics of inert gas subsystems are well known and highly reliable designs have been developed.

In JPL TR 32-1505 (1970, p. 37), Holcomb details the construction of a typical cold gas thruster unit.

The typical system consists of a propellant tank, fill valve, start valve, filter, regulator, low pressure relief valve, two pressure transducers, control valves, and nozzles. The fill valve is capped after filling to provide high reliability. The relief valve may be protected by a burst disc, set at a pressure slightly higher than the relief valve. This will prevent loss of gas caused by small relief valve leaks. System activation occurs with the firing of the squib start valve. A filter is employed downstream of the start valve to remove any contaminants which may have originated during squib firing. Line pressures are monitored by pressure transducers, the high pressure reading indicating the quantity of remaining propellant. Solenoid valves are provided for flow control.

The description above applies to all cold gas thruster subsystems. Each flight subsystem contains mission specific elements in its design with component duplication often provided for redundancy. The cold gas system is generic enough that a meaningful comparison of the systems on various

253

TABLE 4-6

SATELLITE INERT GAS SYSTEMS
(JPL TR 32-1505, 1970, p.37)

Spacecraft	Propellant	System weight, lbm	Storage pressure, psia	Thrust level, lbf	Specific impulse, $\frac{lbf\text{-}s}{lbm}$	Total impulse, lbf-s
Pioneer	nitrogen	9.6	3250	0.20	72	72
OGO A, B, C	argon	37.0	4000	0.050	52	880
OGO D	krypton	60.0	4000	0.050	37	1300
Vela III	nitrogen	9.6	4000	0.20	72	190
Nimbus D	Freon 14	275.0	2000	0.2-0.5	45	300
Discos	Freon 14	13.0	3000	0.001	45	200
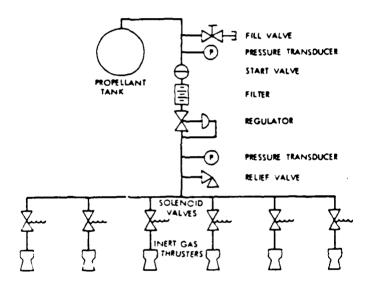
Figure 4-5

Typical Inert Gas Attitude Control Configuration
(JPL TR 32-1505, 1970, p.44)

FEED SYSTEM	COMPONENT	MASS, lbm
	FILL VALVE	0.25
	PRESSURE TRANSDUCER	0.25
	START VALVE	0.25
	FILTER	0.35
	REGULATOR	0.40
	PRESSURE TRANSDUCER	0.25
	RELIEF VALVE	0.30
	MISC. LINES	0.20
		2.15

COLD GAS THRUSTER	COMPONENT	MASS, lbm
	SOLENOID CONTROL VALVE	0.20
	LINES (1 PER THRUSTER)	0.20
	THRUSTER (0.01 TO 0.10 lbf)	0.10
	THRUSTER (0.20 TO 1.0 lbf)	0.20
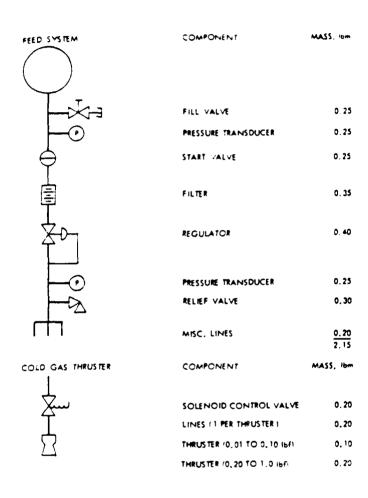
Figure 4-6

Inert Gas System
(JPL TR 32-1505, 1970, p.85)

255
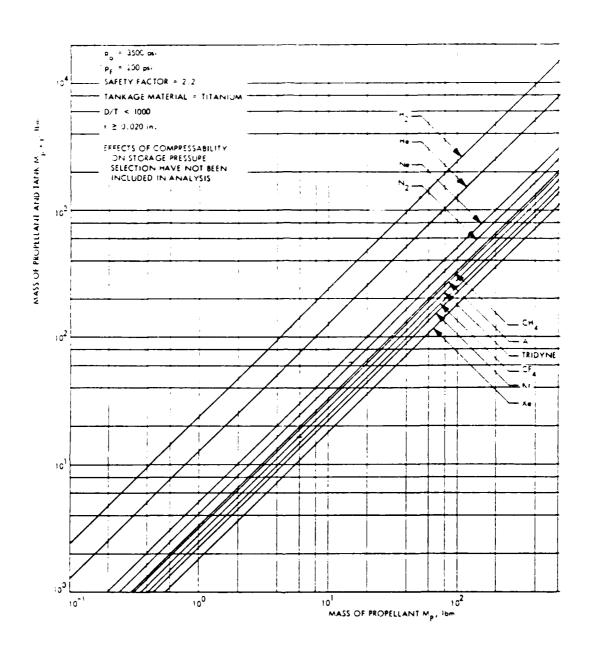
Figure 4-7

Inert Gas and Tankage Mass
(JPL TR 32-1505, 1970, p.86)

satellites can be made. Table 4-6 describes the various subsystem masses and characteristics of the early vehicles which used cold gas. Note the high storage pressures, low thrusts and low I_{sp} typical of this subsystem option. Despite subsystem masses as high as 275 lbm, the total impulse delivered is relatively low.

The mass of a complete system can be closely estimated based on past experience and knowledge of the type and total mass of propellant required. Figures 4-6 and 4-7 can be used to estimate the mass of a system when the propellant masses are large. For small propellant masses (less than 50 lbm) Figure 4-7 overestimates tankage mass by a factor of 2.0 to 3.0. Figure 4-7 is accurate only when propellant masses greater than 100 lbm are involved.

The most accurate assessment of the propulsion subsystem mass is made through a determination of the total propellant mass and volume required for each of several gases. The propellant requirement can then be used to determine the mass of the storage container. Using the values derived earlier for the required ORION orbital delta-V and attitude control total impulse, the masses of several candidate gases were determined. Table 4-8 lists these masses and the resultant total impulse for each gas selection. The I_{sp} of the selected gases ranges from 296 seconds for Hydrogen to 31 seconds for Xenon. It is obvious from the table that to accomplish the primary propulsion mission with cold gas requires an unacceptably large mass and volume of propellant. The attitude control requirements are within the capability of cold gas, however. Table 4-9 carries the analysis a step further through the determination of propellant volume and the necessary tankage mass to store the gas. For the purpose of the analysis, tankage mass is based upon the use

257

of 228 cubic inch spheres operating at storage pressures of 3500 psi. The 228 in³ sphere is 7.62" outside diameter, weighs 3.83 lbm. and can be nested in groups of three on 120° centers within the diameter of the ORION satellite. Each group of three tanks occupies a linear displacement of 7.6 in. and successive groups of three could be stacked as required. Obviously. a more effective utilization of the satellite volume is to use large storage vessels whose outside diameter is nearly that of the satellite. For the purpose of the comparison of gas storage requirements, however, a standard volume (228 in) has been selected. This represents a conservative assumption of the total tankage mass required.

Table 4-9 shows that. for the primary propulsion requirement of ORION. inert gas thrusters are unacceptable. An excessively large mass of propellant and tankage are required for the needed impulse. The auxiliary propulsion requirements could be satisfied using cold gas, however. On the basis of total system mass, Freon 14, methane and nitrogen are the best choices for attitude control. Tables 4-10 through 4-12 list the properties and physical constants associated with those three gases. Because Freon-14. carbon dioxide and methane will liquefy at high pressures. they must be used in the vaporizing gas propulsion system described later. Of the ideal gases. nitrogen is the best candidate, requiring six of the 228 in³ bottles. These

TABLE 4-8

INERT GAS - PROPELLANT MASS AND IMPULSE FOR ORION

Inert Gas	ISP (secs)	Primary Mass (lbm)	Primary Impulse (lbf-secs)	Auxiliary Impulse (lbf-secs)	Aux. Mass (lbm)
Hydrogen	296	49.6	14682.6	1200	4.1
Helium	179	76.5	13693.5	1200	6.7
Neon	82	137.4	11266.8	1200	14.6"
Nitrogen	80	139.6	11168.0	1200	15.0'
Air	74	146.7	10855.8	1200	16.2
Argon	57	170.6	9724.2	1200	21.5
Krypton	39	203.2	7924.8	1200	30.8
Xenon	31	219.7	6810.7	1200	38.7"
Freon-14	55	173.9	9564.5	1200	21.8
Methane	114	109.1	12437.4	1200	10.5*
Carbon Dioxide	67	155.8	10438.6	1200	18.0
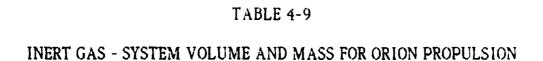
' Nitrogen is best overall choice among ideal gases.

" Neon, Xenon are expensive gases.

* Methane is flammable and liquefies at high pressures.

TABLE 4-9

INERT GAS - SYSTEM VOLUME AND MASS FOR ORION PROPULSION

Propellant	Mass (lbm)	Density (lbm/ft³)	Volume 3600 psi (ft³)	Tanks #	Total Tank Wt. (lbm)	System Wt. (lbm)
Hydrogen	49.6	1.2	40.99	311	1191.0	1240.7
	4.1		3.35	26	99.6	103.6
Helium	76.5	2.4	32.30	245	938.3	1014.9
	6.7		2.83	22	84.3	90.9
Neon	137.4	11.6	11.88	90	344.7	482.1
	14.6		1.26	10	38.3	52.9
Nitrogen	139.6	17.4	8.04	61	233.6	373.2
	15.0		0.86	6*	26.8	41.8
Air	146.7	19.3	7.60	58	222.1	368.8
	16.2		0.84	7	26.8	43.0
Argon	170.6	27.6	6.18	47	180.0	350.6
	21.5		0.78	6	23.0	44.5
Krypton	203.3	67.2	3.03	23	88.1	291.4
	30.8		0.46	4	15.3	46.1
Xenon	219.7	170.6	1.29	10	38.3	258.0
	38.7		0.23	2	7.7	46.4
Freon 14	173.9	Liquid	2.89	22	84.3	258.2
	21.8		0.36	3	11.5	33.3
Methane	109.1	Liquid	9.02	69	264.3	373.4
	10.5		0.87	7**	26.8	37.3
Carbon Dioxide	155.8	Liquid				
	18.0					

Note: First line of each entry is primary propulsion; second line is secondary

' Maximum satellite mass is 250 lbm
Inert gas unacceptable for primary propulsion

* Volume requires 6.4 tanks; could use 6 tanks at 3800 psi.
** Volume requires 6.6 tanks; could use 6 tanks at 3900 psi.

bottles would occupy a total linear displacement of 15.6" when stacked in sets of three within the spacecraft cylinder. Notice that Freon-14 requires more propellant mass than nitrogen, but that the density of Freon enables the storage of that gas in a significantly smaller volume than the other gases. In summary, inert gas cannot be used as a propellant for the primary propulsion of the satellite, but would be a possible choice for attitude control.

A vendor survey was conducted to determine the commercial availability of inert gas attitude control thrusters. Although inert gas saw significant usage in the Pioneer, Mariner, and Nimbus programs, few spacecraft have used inert gas since that time. Several domestic sources of inert gas thrusters were identified. European aerospace firms also manufacture inert gas thrusters, but information on foreign products was not obtained by the vendor survey.

The Hamilton Standard Co. of Windsor Locks, Connecticut manufactures a thruster triad for the attitude control system of the ASAT missile. This unit is the most recent of the commercially produced inert gas assemblies in the United States. The ASAT missile thruster package is shown in Figures 4-8 and 4-9. This triad of thrusters is rated for 1 lbf thrust in the X, Y, and Z axes and uses nitrogen as a propellant. The gas is fed from a set of 8000 psi spherical titanium tanks and is regulated to a thruster inlet pressure of 25 psi. The cluster price is $29,000 and requires a 12 month delivery time. ASAT requires large thrusts to control the missile and uses 1.0 lbf thrusters for attitude control as a result. Small spacecraft like ORION require less powerful thrusters to precisely control their manuvers. Thus, thrusters in the range of

TABLE 4-10

PROPERTIES OF GASES - ENGLISH ENGINEERING SYSTEM
(Zucker, 1977, p. 373)

Gas	Symbol	Molecular Weight	$\gamma = \dfrac{c_p}{c_v}$	Gas Constant ft-lbf/lbm-$^\circ$R	Specific Heats Btu/lbm-$^\circ$R		Viscosity lbf-sec/ft^2
				R	c_p	c_v	μ
Air		28.97	1.40	53.3	0.240	0.171	3.8×10^{-7}
Argon	Ar	39.94	1.67	38.7	0.124	0.074	4.7×10^{-7}
Carbon Dioxide	CO_2	44.01	1.29	35.1	0.203	0.157	3.1×10^{-7}
Carbon Monoxide	CO	28.01	1.40	55.2	0.248	0.177	3.7×10^{-7}
Helium	He	4.00	1.67	386	1.25	0.750	4.2×10^{-7}
Hydrogen	H_2	2.02	1.41	766	3.42	2.43	1.9×10^{-7}
Methane	CH_4	16.04	1.32	96.4	0.532	0.403	2.3×10^{-7}
Nitrogen	N_2	28.02	1.40	55.1	0.248	0.177	3.6×10^{-7}
Oxygen	O_2	32.00	1.40	48.3	0.218	0.156	4.2×10^{-7}
Water Vapor	H_2O	18.02	1.33	85.7	0.445	0.335	2.2×10^{-7}

Tabular values are for normal room temperature and pressure.

TABLE 4-11

PROPERTIES OF GASES - INTERNATIONAL SYSTEM (SI)
(Zucker, 1977, p. 375)

Gas	Symbol	Molecular Weight	$\gamma = \dfrac{c_p}{c_v}$	Gas Constant N-m/kg-°K	Specific Heats J/kg-°K		Viscosity N-s/m²
				R	c_p	c_v	μ
Air		28.97	1.40	287	1,000	716	1.8×10^{-5}
Argon	Ar	39.94	1.67	208	519	310	2.3×10^{-5}
Carbon Dioxide	CO_2	44.01	1.29	189	850	657	1.5×10^{-5}
Carbon Monoxide	CO	28.01	1.40	297	1,040	741	1.8×10^{-5}
Helium	He	4.00	1.67	2,080	5,230	3,140	2.0×10^{-5}
Hydrogen	H_2	2.02	1.41	4,120	14,300	10,200	9.1×10^{-6}
Methane	CH_4	16.04	1.32	519	2,230	1,690	1.1×10^{-5}
Nitrogen	N_2	28.02	1.40	296	1,040	741	1.7×10^{-5}
Oxygen	O_2	32.00	1.40	260	913	653	2.0×10^{-5}
Water Vapor	H_2O	18.02	1.33	461	1,860	1,400	1.1×10^{-5}

TABLE 4-12

GASEOUS PROPERTIES OF NITROGEN
(AFSC DH 3-2, 1964, p.12.2.4-4)
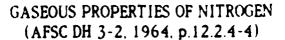
PROPERTY	VALUES		
Molecular Weight	28.02		
Critical Temperature, $^\circ F$	-233		
Critical Pressure, psia	491		
C_p, Btu/lb_m $^\circ F$	0.247		
C_v, Btu/lb_m $^\circ F$	0.1761		
Ratio of Specific Heats, C_p/C_v	$\dfrac{-100^\circ F}{1.404}$	$\dfrac{620^\circ F}{1.382}$	$\dfrac{980^\circ F}{1.360}$
Gas Constant, ft-lb_f/lb_m $^\circ F$	55.1		
Density, lb_m/ft^3	$\dfrac{-100^\circ F}{0.1068}$	$\dfrac{80^\circ F}{0.0710}$	$\dfrac{440^\circ F}{0.0426}$
Viscosity, lb_m/ft sec	$\dfrac{-280^\circ F}{1.41 \times 10^{-5}}$	$\dfrac{80^\circ F}{1.91 \times 10^{-5}}$	$\dfrac{440^\circ F}{2.39 \times 10^{-5}}$
Enthalpy, Btu/lb_m	$\dfrac{-100^\circ F}{89.0}$	$\dfrac{620^\circ F}{269.6}$	$\dfrac{980^\circ F}{364.5}$
Mean Free Path, cm	9.29×10^{-6}		
Thermal Conductivity, Btu/ft^2/hr/($^\circ F$/ft)	1 atm $\quad \dfrac{-100^\circ F}{0.01}$ 1000 psia $\quad$ 0.015	$\dfrac{80^\circ F}{0.015}$ 0.017	$\dfrac{500^\circ F}{0.023}$ 0.024
Compressibility Factor $Z = \dfrac{PV}{RT}$	1 atm $\quad \dfrac{-200^\circ F}{0.995}$ 1000 psia $\quad$ 0.51	$\dfrac{40^\circ F}{0.997}$ 0.990	
Velocity of Sound, ft/sec	1 atm $\quad \dfrac{-100^\circ F}{935}$ 100 atm $\quad$ 1040	$\dfrac{60^\circ F}{1135}$ 1237	$\dfrac{440^\circ F}{1490}$ 1588

264

TABLE 4-15
GASEOUS PROPERTIES OF NITROGEN
(Kit, 1960, pp. 328-330)

1. Molecular weight   28.02
2. Color   colorless
4. Freezing (melting) point   −346.2°F (−210.1°C)
5. Boiling point   −320.6°F (−195.9°C)

6. Density, liquid at
    −320.4°F (−195.8°C)   50.44 lb/ft³ (0.808 g/cm³)

   Density, gas at 14.696 psi (1.0 atm)

°F	°C	lb/ft³ × 10^{-3}	g/cm³ × 10^{-3}
−279.8	−173.2	217.26	3.480
− 99.8	− 73.2	106.82	1.711
80.2	26.8	71.04	1.138
440.2	226.8	42.64	0.683
1340.2	726.8	21.79	0.341
2240.2	1226.8	14.23	0.228
3140.2	1726.8	10.67	0.171
4040.2	2226.8	8.55	0.137
4940.2	2726.8	7.12	0.114

7. Critical temperature   −232.8°F (−147.2°C)
8. Critical pressure   491.0 psi (33.5 atm)
9. Critical density   19.414 lb/ft³ (0.311 g/cm³)

17. Vapor pressure

°F	°C	psi	atm
−341.0	−207.2	2.11	0.14
−333.8	−203.2	5.56	0.38

°F	°C	psi	atm
−315.8	−193.2	19.71	1.34
−207.8	−183.2	52.10	3.55
−279.8	−173.2	113.10	7.70
−261.8	−163.2	213.30	14.50
−243.8	−153.2	364.60	24.80
−233.0	−147.2	489.00	33.30

19. Heat of fusion at
    −395.7°F (−237.6°C) and
    14.7 psi (1.0 atm)   11.1 btu/lb (6.15 cal/g)
21. Heat of vaporization at
    −320.6°F (−195.9°C) and
    14.7 psi (1.0 atm)   85.7 btu/lb (47.6 cal/g)

22. Heat capacity, gas, constant pressure at
    14.7 psi (1.0 atm)

°F	°C	btu/lb mole°F	cal/g mole°C
−99.8	−73.2	6.984	6.984
620.2	326.8	7.199	7.199
980.2	526.8	7.513	7.513
1340.2	726.8	7.815	7.815
3140.2	1726.8	8.698	8.698
4940.2	2726.8	8.852	8.852

TABLE 4-13 (cont.)

GASEOUS PROPERTIES OF NITROGEN
(Kit, 1960, pp. 328-330)

23. Ratio of heat capacities, gas at
14.7 psi (1.0 atm)

°F	°C	
−99.8	−73.2	1.404
620.2	326.8	1.382
980.2	526.8	1.360
1340.2	726.8	1.341
3140.2	1726.8	1.301
4940.2	2726.8	1.289

33. Entropy, gas at 14.7 psi (1.0 atm)

°F	°C	btu/lb mole°F	cal/g mole°C
−99.8	−73.2	42.973	42.973
620.2	326.8	50.677	50.677
980.2	526.8	52.791	52.791
1340.2	726.8	54.501	54.501
3140.2	1726.8	60.214	60.214
4940.2	2726.8	63.756	63.756

34. Enthalpy, gas at 14.7 psi (1.0 atm)

°F	°C	btu/lb mole	cal/g mole
−99.8	−73.2	2,494.8	1,386.0
620.2	326.8	7,556.4	4,198.0
980.2	526.8	10,204.2	5,669.0
1340.2	726.8	12,963.6	7,202.0
3140.2	1726.8	27,883.8	15,491.0
4940.2	2426.8	43,621.2	24,234.0

35. Viscosity, gas

°F	°C	lb/ft sec × 10⁻⁴	centipoise
−459.7	−273.1	0.0111	0.0165
−279.8	−173.2	0.0141	0.0210
80.2	26.8	0.0191	0.0285
440.2	226.8	0.0239	0.0355

°F	°C	lb/ft sec × 10⁻⁴	centipoise
800.2	426.8	0.0282	0.0420
1160.2	626.8	0.0322	0.0481

36. Thermal conductivity, gas at
14.7 psi (1.0 atm)

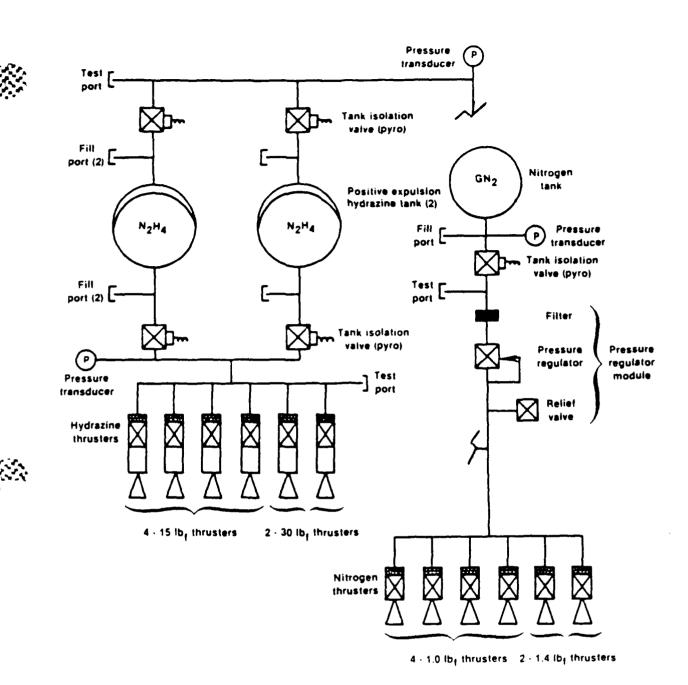| °F	°C	btu/ft hr°F	cal/cm sec°C × 10⁻⁵
−99.8	−73.2	0.006	2.478
80.2	26.8	0.008	3.304
260.2	126.8	0.013	5.369
800.2	426.8	0.018	7.434
1340.2	726.8	0.025	10.325
3140.2	1726.8	0.038	15.694

Figure 4-8

ASAT Missile Cold Gas Attitude Control Subsystem
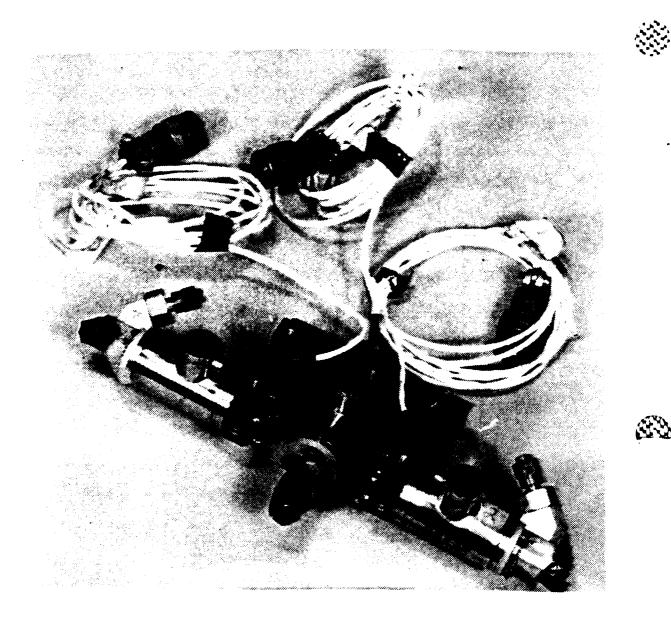(Hamilton Standard, 1986)

Figure 4-9

ASAT Missile Cold Gas Attitude Control Subsystem
(Hamilton Standard, 1986)

0.1 lbf each would be preferable for the ORION satellite. The ASAT thrusters could be modified by Hamilton Standard to adapt to the 0.1 lbf requirement.

2. Hot Gas Thruster Systems

The primary disadvantage of an inert gas propulsion subsystem is low specific impulse. This low I_{sp} leads to a large quantity of propellant and an associated heavy tankage. The low ISP of an inert gas is a consequence of the low energy level of the gas. Without heating, exothermic reaction, or ignition, the gas is limited in the amount of energy which can be converted to kinetic energy. A hot gas subsystem seeks to alleviate this lack of performance by increasing the chamber temperature. Heating of the gas can occur in one of two ways. Combustion can increase the temperature, or the necessary energy can be added by electrical or nuclear heaters. Using the second method, the advantages of an inert gas propulsion subsystem (simplicity, reliability, low cost) can be retained while improving the I_{sp}.

The hot gas subsystem, using electrical heaters, is termed a resistojet. This unit uses conductive and radiative heat transfer from a resistive thermal coil to the propellant gas. The resistojet is the simplest of all electric propulsion subsystems but is classified here as a subsystem of an inert gas thruster assembly. The specific impulse derived from the use of resistance heating is proportional to the square root of the temperature of the gas. The maximum attainable gas temperature is limited by the available satellite power and the heating coil materials. Use of a heating coil is a very effective way to enhance the gas temperature with minimum effort. The best propellants for use with the resistojet subsystem are those which dissociate below 2000° F. Ammonia, ammonium hydrosulfide, and ammonium

269

carbamate all dissociate between 1400° - 1800° F. Low molecular weight gases such as hydrogen and helium are also attractive as working fluids. (JPL TR 32-1505, 1970, p.70).
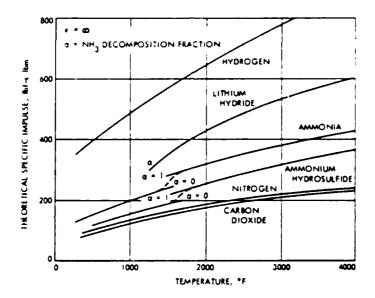

Figure 4-10

Theoretical Performance of Heated Propellants
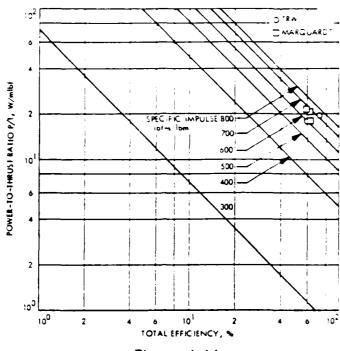(JPL TR 32-1505, 1970, p. 70)

Figure 4-11

Nitrogen Resistojet Efficiency versus Specific Impulse
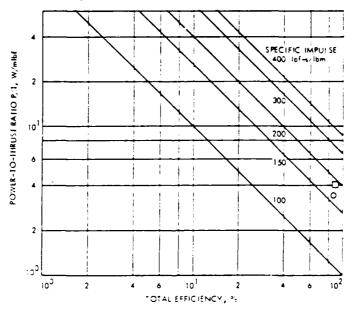(JPL TR 32-1505, 1970, p. 83)

Figure 4-12

Hydrogen Resistojet Efficiency versus Specific Impulse
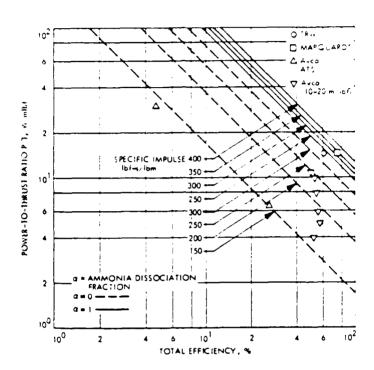(JPL TR 32-1505, 1970, p. 83)

271

Figure 4-13

Ammonia Resistojet Efficiency versus Specific Impulse
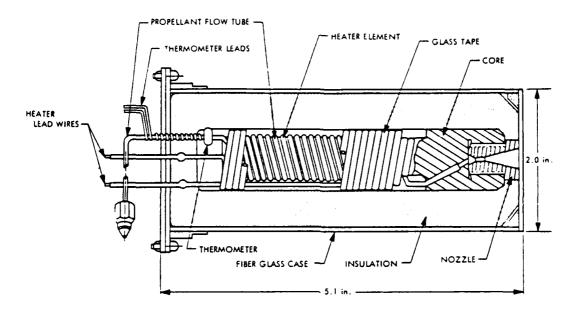
(JPL TR 32-1505. 1970. p. 83)

A plot of the theoretical performance of heated propellants is provided in Figure 4-10. The curves show that performance varies as a function of temperature. Thruster temperature varies as a function of heat loss in the thruster and the material thermal capacity. In particular, heat loss and the power consumption are not balanced by the increase in I_{sp} for operating temperatures above 3000° F. Being a thermal unit, a requisite heat up period occurs during a cold start. The initial power requirements are high and thermal cycling may be required to maintain the chamber at a high temperature when using a resistojet. Previous experience has shown that the use of resistojets is fine for small attitude control maneuvers, but that, as thrust levels are increased, the power consumption of the thruster becomes intolerably high. For example, on the Vela III spacecraft, a 0.043 lbf thruster required 92 watts of power simply to provide the gas heating for one thruster. This increased the observed I_{sp} from 80 seconds to 123 seconds but at the expense of a significant amount of power. Figures 4-10 through 4-12 depict the efficiencies of hydrogen, nitrogen, and ammonia resistojets respectively. With a knowledge of the desired propellant and thrust, the curves indicate the power required to attain a given specific impulse. For the ORION satellite, the restrictions on power usage are so severe that a resistojet subsystem is not feasible. For vehicles with access to large solar arrays, however, a resistojet may be ideal. Nock (1987) describes a GAS satellite capable of 2 kilowatts power generation that could be well suited for use with resistojets.

The vendor survey was not specifically targeted towards manufacturers of inert gas resistojets. Specifications of resistojets used in

Parameters	Characteristics
Thrust, lbf	0.042 (single nozzle)
Specific impulse, $\frac{lbf \cdot s}{lbm}$	123
Propellant	Nitrogen gas with 2% argon (vol)
Power requirement, W	92
Duty cycle capability	Continuous
Chamber pressure, psia	15
Operating temperature, °F	1000 (nominal)-1200 (max)
Thermal operating efficiency, %	93
Nozzle expansion ratio	100
Thruster weight, lbm	0.65
Thruster size envelope	See Fig. A-54
Demonstration service function	Velocity correction, Vela 3
Service total impulse requirement	200 lbf-s (80 min)

Figure 4-14

Vela III Electrothermal Reaction Control Thruster
and Specifications
(JPL TR 32-1505, 1970, p. 72)

the Vela III. Advanced Vela. and ATS III spacecraft as well as the Space Station are included as representative samples of the resistojet subsystem. The data for the Vela III thrusters indicate that a 0.043 lbf thrust and an
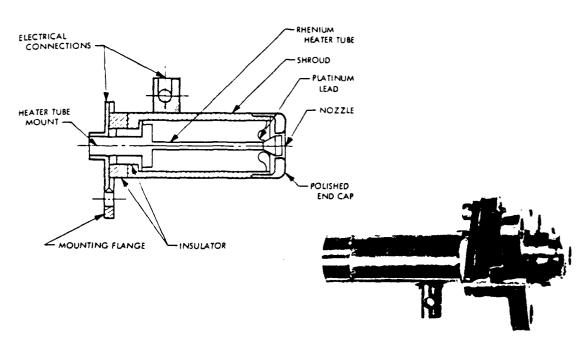

Figure 4-15

Advanced Vela III Electrothermal Thruster
(JPL TR 32-1505, 1970, p. 73)

275

TABLE 4-15

ADVANCED VELA-III THRUSTER SPECIFICATIONS
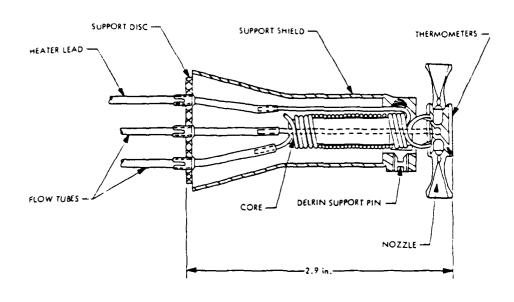### (JPL TR 32-1505, 1970, p. 73)

Parameters	Characteristics
Thrust, lbf	0.02 (each of 3 nozzles)
Specific impulse, $\frac{lbf\text{-}s}{lbm}$	132
Propellant	Nitrogen gas with 2% argon (vol)
Power requirement, W	30 W (steady state) 17 W, pulsing, 10% duty cycle
Duty cycle capability	Continuous
Chamber pressure, psia	30
Operating temperature, °F	1250 (nominal)-1425 (max)
Thermal operating efficiency, %	Greater than 90
Nozzle expansion ratio	67
Thruster weight, lbm	0.30
Thruster size envelope	See Fig. A-56
Demonstrated service function	Spin, attitude and velocity control, advanced Vela
Service total impulse requirement	1250 lbf-s

SUPPORT DISC
HEATER LEAD
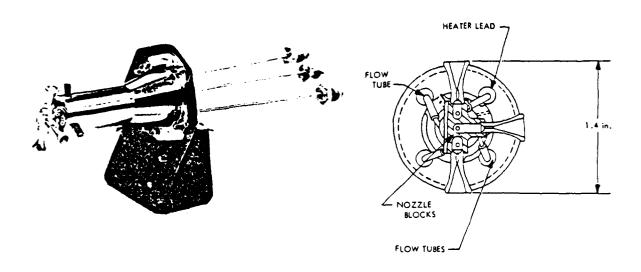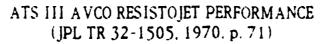SUPPORT SHIELD
THERMOMETERS
FLOW TUBES
CORE
DELRIN SUPPORT PIN
NOZZLE
2.9 in.

HEATER LEAD
FLOW TUBE
NOZZLE BLOCKS
FLOW TUBES
1.4 in.

Figure 4-16
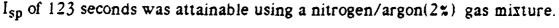
ATS III Avco Ammonia Resistojet
(JPL TR 32-1505, 1970, p.71)

277

TABLE 4-16

ATS III AVCO RESISTOJET PERFORMANCE
(JPL TR 32-1505, 1970, p. 71)

Operating conditions	Cold (~70°F)	Hot
Orbital test of thruster 1		
Thruster pressure,[a] psia	0.46	0.86
Plenum pressure,[b] psia	14.7	14.7
Thruster mass flow,[a] lbm/s	0.31×10^{-6}	0.29×10^{-6}
Thruster heater current, A	—	7.5
Thruster heater voltage, V	—	0.33
Thruster heater power, W	—	2.5
Thrust (laboratory), lbf	28×10^{-6}	41×10^{-6}
Thrust (flight), lbf	33×10^{-6}	38×10^{-6}
Specific impulse (lab), $\frac{lbf\text{-}s}{lbm}$	~1	135
Specific impulse (flight),[a] $\frac{lbf\text{-}s}{lbm}$	105	132

Orbital test of thruster 2		
Thruster pressure,[a] psia	3.12	4.65
Plenum pressure,[b] psia	15.0	15.0
Thruster mass flow,[a] lbm/s	2.77×10^{-6}	2.64×10^{-6}
Thruster heater current, A	—	8.0
Thruster heater voltage, V	—	0.45
Thruster heater power, W	—	3.6
Thrust (laboratory), lbf	255×10^{-6}	430×10^{-6}
Thrust (flight), lbf	238×10^{-6}	417×10^{-6}
Specific impulse (lab), $\frac{lbf\text{-}s}{lbm}$	90	150
Specific impulse (flight),[a] $\frac{lbf\text{-}s}{lbm}$	86	158

I_{sp} of 123 seconds was attainable using a nitrogen/argon(2%) gas mixture. The same mixture is used by the INTRASPACE "T-SAT" satellite for the inert gas propulsion subsystem. Using this thruster, the primary propulsion requirements of the ORION vehicle requires gas storage for 103 lbm which occupies a volume of 5.89 ft³ at 3500 psi. Unfortunately, this is equal to the entire volume of the satellite. The attitude control impulse requirement (1200 lbf-sec) could be supplied by 9.76 lbm of N_2, occupying a volume of 0.56 ft³ at 3500 psi. This is the equivalent of five standard spheres (228 in³) mentioned in the inert gas section. The total subsystem mass is 28.9 lbm. Contrast this to the Freon-14 subsystem mass of 33.3 lbm for an inert gas
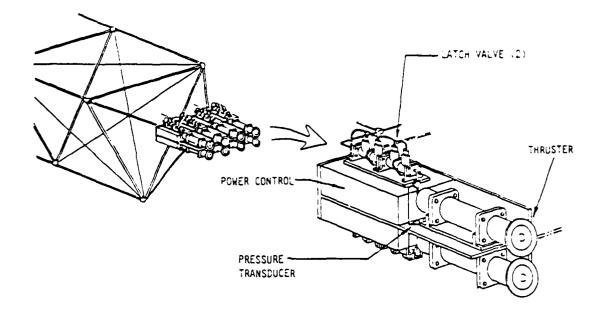
(vaporizing liquid) thruster. Using the Advanced Vela III thruster, with its higher I_{sp}, the subsystem mass could be further reduced to 24.4 lbm, using 4 storage bottles and 9.1 lbm of nitrogen propellant. The Vela III thruster exhibits a power to thrust ratio of 3.6 watts per millipound force. A 0.1 lbf thruster would therefore consume 360 watts while operating. The Advanced Vela III consumes only 30 watts in the steady state but is capable of only 0.02 lbf thrust.
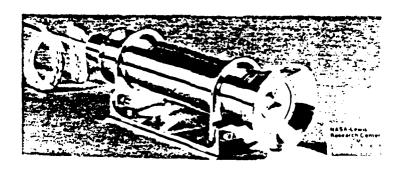
The hot gas thrusters listed above each represent late 1960's and early 1970's technologies. Because of low impulse and large gas storage volumes hot gas thrusters were not widely used during the past two decades. With the advent of Space Station, where volume is less critical the use of such thrusters has gained increased attention. Byproduct gases will be readily available on the Space Station, and power will be relatively plentiful. Hence, an inert gas resistojet is a sensible source of propulsion. The new generation thrusters are designed to use gases evolved from the Environmental Control and Life Support System (ECLSS). The gases include water vapor, carbon dioxide, methane, hydrogen, nitrogen, oxygen and trace inert gases. Because the volume of gas available for the thrusters will vary as a function of crew loading, these new thrusters have been designed to throttle for various gas flow rates. Electrical power throttling is also possible to control the thruster temperature during low gas flow rates, and thus, extend thruster lifetimes. A prototype thruster which is shown in Figure 4-17 exhibits a nominal thrust of 0.1 lbf and is rated for a design lifetime of 10,000 hours. Using platinum sheathed heaters the thruster achieves a 92% efficiency.

Figure 4-17

Space Station Inert Gas Resistojet
(Larson and Evans, 1986, pp. 8-10)

In summary, the resistojet is an effective addition to the inert gas thruster concept for attitude control of the ORION but requires large power consumption. If thrust levels for the attitude control were reduced below 0.1 lbf (i.e. 0.02 lbf), the resistojet concept would be workable within the power constraints of ORION (60 watts solar array peak output, 180 watt-hour battery).

3. Vaporizing Liquid Thruster Systems

A vaporizing liquid propulsion subsystem uses a liquid propellant that is pressurized by its own equilibrium vapor pressure. The resultant expulsion of that vapor through a suitable nozzle produces thrust. Inlet pressures of 40 psi at the thruster are typical; resistojet heating is often used to raise the gas temperature and improve performance. Only small improvements are possible in the I_{sp} relative to the specific impulse of an inert gas subsystem. However, considerable savings in tank mass are possible due to the high propellant density and low storage pressure of vaporizing liquids. This leads to the use of relatively lightweight tanks. Vaporization of the propellant is typically achieved through the addition of heat to the propellant by heater coils or heater strips which surround the propellant tank. Unfortunately, the requirement to add heat for the vaporization of propellant fixes the time response of such a subsystem. A measurable delay occurs between the initiation of heating and the time thruster actuation. Additionally, with the requirement to regulate heat transfer for the vaporization, the complexity is substantially increased relative to inert gas systems. The zero gravity environment also poses special problems for the propellant feed components.

In a typical subsystem. the liquid propellant flows into a vaporizer where heat transfer causes vaporization. The vaporizer typically works for liquid or mixed phase propellant flow. Downstream of the vaporizer. a pressure switch and control valve regulate the gas flow to a plenum for gas storage until it is used. Gas expulsion is controlled in the same manner as in
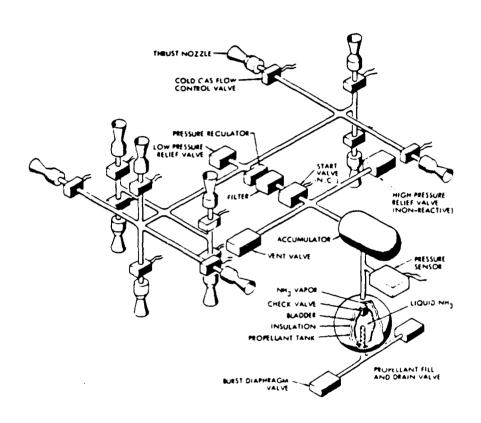

Figure 4-18

Liquified Gas Attitude Control Subsystem
(AFSC DH 3-6, 1964. p. 4.4-3)

an inert gas subsystem. Figure 4-18 diagrams a typical liquid gas subsystem.
Note its similarity to an inert gas subsystem. The liquid subsystem differs
only in its addition of an accumulator and a heated storage tank. The
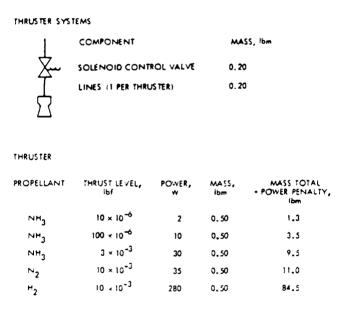breakdown of component masses for a liquid subsystem shows that the

THRUSTER SYSTEMS

COMPONENT	MASS, lbm
SOLENOID CONTROL VALVE	0.20
LINES (1 PER THRUSTER)	0.20

THRUSTER

PROPELLANT	THRUST LEVEL, lbf	POWER, w	MASS, lbm	MASS TOTAL + POWER PENALTY, lbm
NH_3	10×10^{-6}	2	0.50	1.3
NH_3	100×10^{-6}	10	0.50	3.5
NH_3	3×10^{-3}	30	0.50	9.5
N_2	10×10^{-3}	35	0.50	11.0
H_2	10×10^{-3}	280	0.50	84.5

Figure 4-19

Vaporizing Liquid Subsystem Component Mass
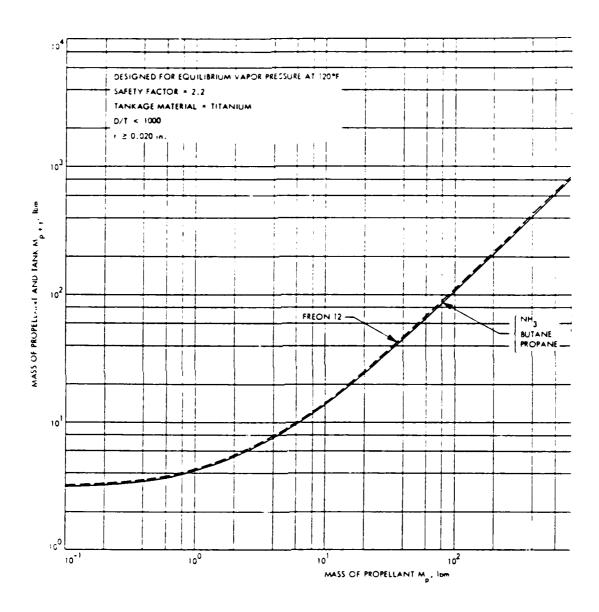(JPL TR 32-1505, 1970, p. 91)

283

Figure 4-20

Vaporizing Liquid Tank Mass
(JPL TR 32-1505. 1970. P. 92)

284

subsystem mass is not substantially altered from that of an inert gas
subsystem, except with regard to the propellant density and tank weight.

The vaporizing liquid subsystem is not marketed widely and is
typically a special modification of an inert gas subsystem design. The most
significant modification is the addition of a heated tank to enhance
vaporization of the liquid. and perhaps. a plenum chamber. A typical tank
and subsystem. developed at the Naval Research Laboratory. are depicted in
Figure 4-21. Using ammonia. the system provides specific impulse between
70 and 90 seconds with thrusts of 0.02 to 0.07 lbf. For the ORION auxiliary
propulsion subsystem impulse requirement of 1200 lbf-seconds. 17.1 lbm of
ammonia propellant is required. Using Figure 4-20. the subsystem mass is
calculated to be 22 lbm. The primary propulsion needs of the spacecraft
cannot be supported by a vaporizing liquid subsystem in as much as 152 lbm
of propellant are required. Using a density for ammonia of 37.6 lbm/ft^3. the
auxiliary subsystem propellant requires a volume of 758 in^3. This volume is
contained within an 11.4" diameter sphere. or four standard spheres of 228
in^3 each. For proper heat transfer. a single storage tank is preferred. Based
on the NRL subsystem. 3 to 5 watts of continuous power is required to
operate the subsystem. Use of the anhydrous ammonia vaporizing liquid
subsystem leads to an improvement in storage volume for the cold gas
thruster.

Ammonia is only one of several propellants is be suitable for a
vaporizing liquid subsystem. Freon-14 and methane have been mentioned
earlier as leading choices for vaporizing liquid subsystems. The selection of a
proper propellant is a complex process. however.

FEED SYSTEM

COMPONENT	MASS, lbm
PRESSURE TRANSDUCER	0.20
FILL VALVE	0.25
START VALVE	0.35
FILTER	0.10
CONTROL VALVE	0.40
VAPORIZER	1.00
PRESSURE SWITCH	0.25
PLENUM	0.30
FILTER	0.10
LINES	0.20
	3.05

COLD GAS THRUSTER

COMPONENT	MASS, lbm
SOLENOID CONTROL VALVE	0.20
LINES (1 PER THRUSTER)	0.20
THRUSTER (0.01 - 0.10 lbf)	0.10
THRUSTER (0.20 - 1.0 lbf)	0.20
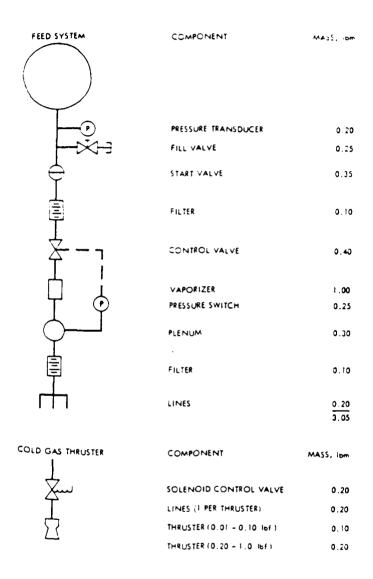
Figure 4-21

Typical Vaporizing Liquid Feed Systems
(JPL TR 32-1505, 1970, p.43)

WICKING FOR EVAPORATION

HEAT TRANSFER SURFACE

PROPELLANT TANK

PROPELLANT CONTROL BAFFLES

THRUSTER NO. 2

FILL LINE

THRUSTER NO. 1

LIQUID NH₃

VAPOR NH₃

LOW PRESSURE SWITCH

SOLENOID VALVE

ACCUMULATOR TANK

HIGH PRESSURE SWITCH

SOLENOID VALVE

FILTER
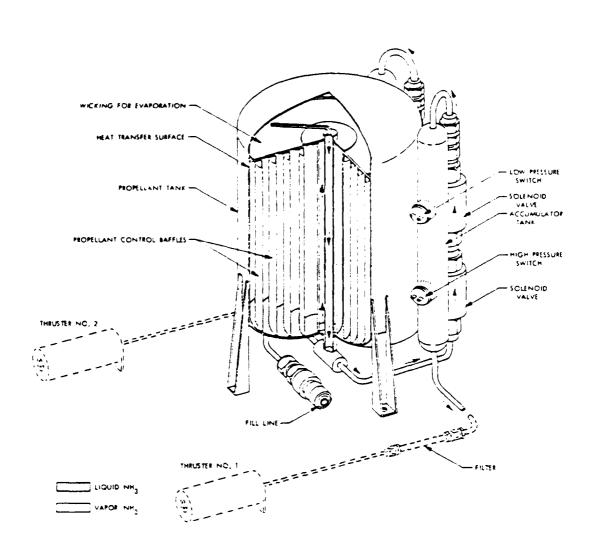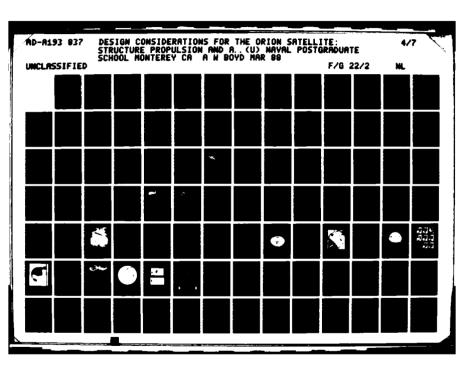
Figure 4-22a

NRL Microthruster Subsystem
(JPL TR 32-1505, 1970, p. 42)
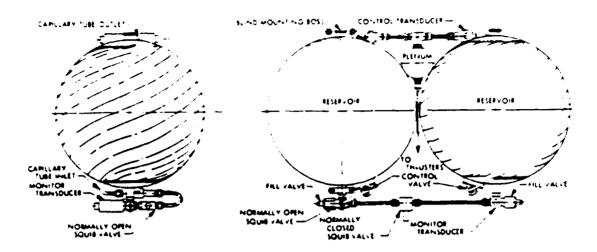
287

CAPILLARY TUBE OUTLET

BLIND MOUNTING BOSS   CONTROL TRANSDUCER

PLENUM

RESERVOIR   RESERVOIR

CAPILLARY TUBE INLET
MONITOR TRANSDUCER

TO THRUSTERS
CONTROL VALVE

FILL VALVE   FILL VALVE

NORMALLY OPEN SQUIB VALVE

NORMALLY OPEN SQUIB VALVE   NORMALLY CLOSED SQUIB VALVE   MONITOR TRANSDUCER

Parameters	Requirements
Propellant	Anhydrous ammonia
Thrust level, lbf	0.020 to 0.070
Specific impulse, $\frac{lbf\text{-}s}{lbm}$	70 to 90
Total impulse, lbf-s	~1000
Power requirements, W	3 (max)
Total system weight, lbm	15

*Developed by Philco Ford, Newport Beach, Calif., for NRL.

PROPELLANT STORAGE TANK

PRIMARY CONTROL VALVE

PREPLENUM
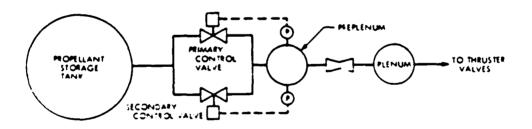
PLENUM   TO THRUSTER VALVES

SECONDARY CONTROL VALVE

Figure 4-22b

Vaporizing Ammonia Propulsion Subsystem
(JPL TR 32-1505, 1970)

TABLE 4-17

PROPERTIES OF AMMONIA
(AFSC DH 3-6, 1970, p. 12.2.1-3)

PROPERTY	VALUES			
Molecular Weight	17.036			
Boiling Point, °F	-28.03			
Freezing Point, °F	-107.95			
Critical Temperature, °F	271			
Critical Pressure, psia	1634.2			
Density, lb_m/ft^3	$\frac{68°F}{37.8}$ $\frac{160°F}{32.0}$ 42.5696 (liquid at NBP)*			
Vapor Pressure, psia	$\frac{68°F}{128}$ $\frac{77°F*}{145.45}$ $\frac{160°F}{515}$			
Heat of Vaporization, Btu/lb_m	588.16 (at NBP)			
Heat of Fusion, Btu/lb_m	142.75 (at MP of -107.95°F)			
Viscosity, Centipoise Viscosity, lb_m/sec ft	$\frac{-28.03°F*}{0.2527}$ $\frac{-28.3°F}{0.266}$ $\frac{41°F}{0.1818}$ $\frac{59°F}{0.1479}$ $\frac{77°F}{0.1350}$ 1.698×10^{-4} 17.9×10^{-5} 10.83×10^{-5} 9.88×10^{-5} 9.07×10^{-5}			
Specific Heat, Btu/lb_m °F	$\frac{160°F}{1.055}$ $\frac{-28°F}{1.066}$ $\left(\frac{-28.03°F*}{1.066}\right)$			
Enthalpy, Btu/lb_m	$\frac{-40°F}{0}$ $\frac{77°F}{128.5}$			
Surface Tension, lb_f/ft	$\frac{-68.8°F}{0.002683}$ $\frac{60.0°F}{0.00155}$ $\frac{138.16°F}{0.000887}$ 0.00233 (at NBP)*			
Thermal Conductivity $Btu/ft^2/hr/(°F/ft)$	$K = 9.9144 + 8.6230 \times 10^{-8}(R) - 2.4353 \times 10^{-10}(R)^2$ 0.912 (at NBP)			
Electrical Conductivity, mho/cm	0.13×10^{-6} (at -110.2°F)			
Bulk Modulus, psi				
Expansivity, $\frac{\Delta V}{V}$ per °F	$\frac{68°F}{1.3 \times 10^{-3}}$ $\frac{122°F}{1.74 \times 10^{-3}}$			
Velocity of Sound, ft/sec	615 psia $\frac{NBP*}{5679}$ $\frac{65°F}{4570}$ $\frac{135°F}{3800}$ $\frac{172°F}{3020}$			

TABLE 4-18

AMMONIA MATERIAL COMPATIBILITY
(AFSC DH 3-6, 1970, p. 12.5.3-1)

Valve Bodies
Stainless steels 302, 304, 316; alloy steels 4340, 4320, 4130;
aluminum alloys 2024, 356, 6061, 7075, 5052.

Springs
Stainless steels 302, 304; carbon steel 1075; Inconel.

Stems
Stainless steel 430.

Bellows
Stainless steels 302, 304; Inconel.

Bearings
Stainless steel 430.

Valving Units (seats and poppets)
Stainless steels 304, 316; alloy steel 4340; Teflon; Kel-F.

Seals
Teflon, Kel-F, polyethylene, ethylene propylene rubber,
butyl rubber, Neoprene, nitrile silicone.

Packing
Teflon, Kel-F, asbestos.

Lubricants
Fluorolube, dry films, silicone greases, refrigeration-grade
petroleum oil.

Bolts, Nuts, and Screws
Stainless steels 304, 321, 347, 17-7PH.

Thread Sealants and Antiseize Compounds
Fluorolube, silicone greases, Teflon tape.

Coatings
Gold, nickel, chrome plate.

Diaphragms
Teflon, ethylene propylene rubber, polyethylene, Neoprene,
stainless steels.

Any propellant choice must balance the following concerns: first, the liquid vapor pressure of the propellant must be sufficiently high to allow plenum pressures in excess of 10 psi while simultaneously being low enough to permit a small tankage mass. Suitable pressure boundaries are 20 to 500 psi. Second, the molecular weight of the vapor should be low in order to enhance the I_{sp}. Third, the heat of vaporization of the propellant must be low to limit the number of tank heaters and the power output. The propellant must be compatible with spacecraft materials, e.g., non-corrosive. Fourth, the propellant should possess high heat capacity and permit a high thermal storage capacity. The most popular propellants for the liquid vaporizing subsystem, in light of these constraints, are anhydrous ammonia and Freon-14. In particular, ammonia possesses high vapor pressure, low molecular weight, high heat capacity, and low heat of vaporization. It is also compatible with most spacecraft materials as indicated in Table 4-17. Propane and methane have also been used as propellants, although less extensively.

4. Monopropellant Hydrazine Propulsion Subsystems

Rocket subsystem designers have often longed for a magic liquid which, upon opening a single valve to a simple 'decomposer', would instantly change state into a clean, energetic gas that could be used to do work - propel or stabilize a vehicle, pump liquids, drive turbomachinery, etc. Monopropellant hydrazine systems, particularly those using the Shell 405 catalyst, are currently the closest thing to such a dream. (JPL TR 32-1227, 1968, p.1).

The monopropellant hydrazine (N_2H_4) thruster is perhaps the most widely used of all attitude control thrusters with thrust in the range 0.01 to

100 lbf. Hydrazine is used extensively in small attitude control rockets for the control of satellites and other spacecraft (Shuttle, missiles). 'Small' in this context refers to thrust levels of 5 lbf or less. A few applications exist for 50 lbf thrusters using hydrazine and at least one 100 lbf monopropellant subsystem has been developed as well. Dr. Shannon Coffee of NRL points out that, for many ORION orbital boost applications, thrusters rated above 5 lbf can be modeled as producing impulsive thrusts.

$$F = (m)(a) \qquad (4.9)$$
$$a = (40 \text{ lbf}) / (250 / 32.2)$$
$$= 5.15 \text{ ft/sec}^2$$

$$\text{deltaV} = 1184.2 \text{ ft/sec}$$
$$\text{Firing time} = t = (\text{deltaV}) / a \qquad (4.10)$$
$$= 230 \text{ seconds}$$

$$\text{Impulsive ratio} = \text{Firing duration/Orbital period} \qquad (4.11)$$
$$(\text{For a 90 minute orbit at 135 nm})$$
$$\text{Ratio} = 230 / 5400$$
$$= 0.0425 \ll 1.0$$

For the orbital transfer between 250 and 1500 km, a 40 lbf thruster would be modeled as impulsive by virtue of the fact that the ratio of burn time to orbit time would be much less than 1.0. Impulsive forces are required to model the orbital transfer of ORION using a Hohmann transfer.

As alluded to above, hydrazine is energetic, easy to use and provides the benefit of large I_{sp} using a simple thruster design. Three distinct concepts of monopropellant hydrazine thrusting systems exist. They are based upon:

(1) The expulsion of gases arising from direct <u>catalytic</u> decomposition of N_2H_4.

(2) The storage of catalysis gases in a plenum for later expulsion.

(3) The expulsion of gases as a result of the <u>thermal</u> decomposition of hydrazine.

All of these thrust producing methods depend on the exothermic reaction of hydrazine to produce hot exhaust gases and thrust. Each also requires a feed subsystem to provide the propellant flow. Hydrazine can be delivered by a pressurized feed subsystem or a pump-fed subsystem. The pressurized feed subsystem is the most reliable and most popular. Typically, the fuel is supplied from a positive diaphragm or surface tension tank.

Hydrazine is an attractive propellant for space applications for the following reasons:

(1) The decomposition products have a low molecular weight providing a high I_{sp}. On the basis of I_{sp}, hydrazine is one of the most useful fuels. It is second only to liquid hydrogen in terms of efficiency (low molecular weight exhaust gas versus ISP). The high percentage of hydrogen in the hydrazine molecule (N_2H_4) results in an excellent rocket performance.

(2) The decomposition of hydrazine, whether by catalytic or thermal means, is exothermic and results in a high gas temperature. The range of adiabatic gas temperatures for hydrazine is 1100° to 2500° F (1800° +/- 700°).

293

(3) Hydrazine will decompose when the fluid is relatively cool. This leads to prolonged life expectancies for the thruster and catalytic bed. Because decomposition is initiated at a low temperature. it can be decomposed thermally as well as catalytically. Thrust chambers can be built of low cost materials and operated without cooling.

(4) Hydrazine is a dense liquid and can be stored in a lightweight tank.

(5) Hydrazine is compatible with most spacecraft materials.

(6) Hydrazine is not shock sensitive.

(7) Hydrazine is thermally stable up to relatively high temperatures.

(8) The propellant feed and control subsystem associated with hydrazine is inherently simple to design and to operate.

The popularity of hydrazine systems is summarized in JPL TR 32-1227 (1968) where the author states that "basically, the advantage of monopropellant hydrazine is energetic simplicity. The added advantage of reliability (i.e. simplicity) cannot be overemphasized."

a. Properties of hydrazine

In order to evaluate the performance of a hydrazine subsystem in comparison to other thruster concepts. the properties of hydrazine fuel and its interaction with the catalytic or thermal decomposition elements are important to understand. A discussion of hydrazine properties is logically followed by an analysis of hydrazine thruster performance and engine thrust anomalies. Although hydrazine is an inherently simple fuel to use. its use is characterized by a more widely varied range of performance characteristics than the inert gas. hot gas. or vaporizing liquid systems. Many hydrazine thruster systems are available commercially. Therefore, a study of

294

construction and performance characteristics prior to a vendor survey of components for use on ORION is important. The use of hydrazine provides immense advantages in terms of impulse, simplicity, and commercial availability. Because of its superiority as a propellant, hydrazine and hydrazine thruster systems will be described in detail.

Hydrazine (N_2H_4) is an oily, hygroscopic liquid composed of nitrogen and hydrogen. It has a high boiling point, a low freezing point (35° F) and demonstrates thermal and shock stability. Table 4-19 describes various physical properties of anhydrous hydrazine covering a broad range of temperatures. Hydrazine freezes at 34.5° F which neccessitates that the thermal environment be controlled to prevent freezing of propellant within lines and catalytic beds. This can be accomplished through the integration of propellant line, tank, and chamber heaters, or by the addition of a freezing depressant to the propellant. Some suitable depressants include water, ammonia, lithium borohydrate, hydrazine cyanide, ammonia thiocyanate, and hydrazine nitrate (Kit, 1960, p. 106). These chemicals lower the freezing point of hydrazine without a significant performance penalty. Anhydrous hydrazine ignites spontaneously in the presence of any halogen compound as well as liquid oxygen, hydrogen peroxide, and other strong oxidizers. Because of this hypergolic reaction, hydrazine is also used in combination with an oxidizer in many rocket applications.

Hydrazine is compatible with most spacecraft materials, particularly stainless steel. It is not compatible with any organic compounds such as organic impurities in feed subsystems or organic seals. Tables 4-20 through 4-23 list the various materials which have been demonstrated to be

295

TABLE 4-19

PHYSICAL PROPERTIES OF ANHYDROUS HYDRAZINE
(Kit, 1960, p.102)

1. Molecular weight   32.05
2. Color   colorless
4. Freezing (melting) point   34.5°F (1.4°C)

5. Boiling point

psi	atm	°F	°C
14.7	1.0	235.4	113.0
28.94	1.96	274.3	134.5

6. Density, solid at 23.0°F (−4.4°C)   71.54 lb/ft³ (1.146 g/cm³)

Density, liquid

°F	°C	lb/ft³	g/cm³
32.0	0.0	64.041	1.0258
32.4	0.2	64.028	1.0256
68.0	20.0	62.961	1.0085

Density, saturated vapor

°F	°C	psi	mm Hg	lb/ft³	g/cm³
194.0	90.0	5.12	265.0	0.0228	0.000365
203.0	95.0	5.28	273.0	0.0228	0.000365
210.0	100.0	5.36	277.0	0.0228	0.000365
230.0	110.0	5.55	287.0	0.0228	0.000365
248.0	120.0	5.69	294.0	0.0228	0.000365
267.8	131.0	14.44	747.0	0.0594	0.000952

7. Critical temperature   716.0°F (380.0°C)
8. Critical pressure   2,135.0 psi (145.0 atm)
10. Critical volume 6.926×10^{-3} ft/lb
           (138.6 cm/g mole)

15. Coefficient of compressibility, liquid
    at 77.0°F (25.0°C) 1.572×10^{-6} in.²/lb
       adiabatic conditions   (22.36×10^{-6} cm²/kg)
    at 77.0°F (25.0°C) 1.746×10^{-6} in.²/lb
       isothermic conditions   (24.83×10^{-6} cm²/kg)

17. Vapor pressure, liquid

°F	°C	psi	mm Hg
32.0	0.0	0.0520	2.69
59.0	15.0	0.1479	7.65
68.0	20.0	0.2040	10.55
77.0	25.0	0.2781	14.38
86.0	30.0	0.3730	19.29
95.0	35.0	0.4964	25.67
104.0	40.0	0.6540	33.82
113.0	45.0	0.8524	44.08
122.0	50.0	1.1000	56.91
131.0	55.0	1.4090	72.85
140.0	60.0	1.7870	92.43
149.0	65.0	2.2490	116.30
158.0	70.0	2.8060	145.12

18. Surface tension

°F	°C	lb/ft × 10⁻³	dynes/cm
68.0	20.0	5.123	74.76
104.0	40.0	4.780	69.76

19. Heat of fusion at
    77.0°F (25.0 C)   170.1 btu lb (94.5 cal 9)

TABLE 4-19 (cont.)

PHYSICAL PROPERTIES OF ANHYDROUS HYDRAZINE
(Kit, 1960, p.102)

21. Heat of vaporization at
    77.0°F (25.0°C)　　　　601.88 btu/lb (10,700.0 cal/g mole)

22. Heat capacity, solid

°F	°C	btu/lb°F	cal/g mole°C
−437.8	−261.2	0.0022	0.07
−423.0	−253.2	0.0110	0.35
−387.0	−233.2	0.0666	2.13
−351.4	−213.2	0.1322	4.23
−315.0	−193.2	0.1864	5.96
−279.0	−173.2	0.2305	7.37
−207.4	−133.2	0.2991	9.57
−135.4	− 93.2	0.3550	11.36
− 99.4	− 73.2	0.3811	12.19
− 27.4	− 33.2	0.4333	13.86

Heat capacity, liquid

°F	°C	btu/lb°F	cal/g mole°C
35.0	1.7	0.728	23.20
44.6	7.0	0.730	23.37
62.6	17.0	0.735	23.51
77.0	25.0	0.738	23.62
80.6	27.0	0.739	23.65
98.6	37.0	0.744	23.80
116.6	47.0	0.749	23.96
134.6	57.0	0.754	24.14
152.6	67.0	0.761	24.34

24. Heat of formation, liquid at
    77.0°F (25.0°C)　　　　676.80 btu/lb (376.30 cal/g)

.5. Heat of combustion, liquid at
    77.0°F (25.0°C)　　　　8,346.0 btu/lb (4,640.4 cal/g)

28. Heat of sublimation　　　618.75 btu/lb (11,000.0 cal/g)

31. Free energy of formation, liquid at
    77.0°F (25.0°C)　　　　2,000.0 btu/lb (1,112.0 cal/g)

33. Entropy, liquid at
    77.0°F (25.0°C)　　　　0.9052 btu/lb°F (0.9052 cal/g°C)

34. Enthalpy, liquid at
    77.0°F (25.0°C)　　　　101.8 btu/lb (56.6 cal/g)

35. Viscosity, liquid
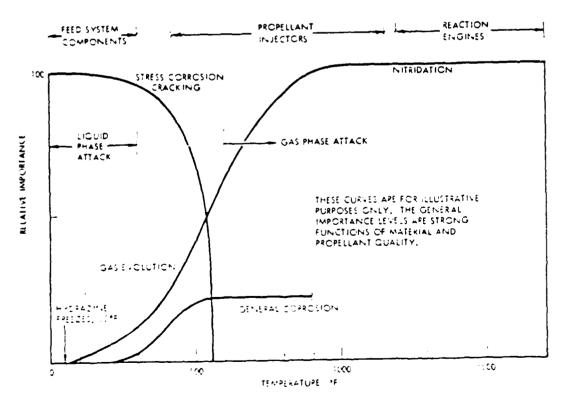
°F	°C	lb/ft sec	centipoises
32.0	0.0	0.0008830	1.314
33.8	1.0	0.0008689	1.293
35.6	2.0	0.0008548	1.272
37.4	3.0	0.0008407	1.251
41.0	5.0	0.0008111	1.207
50.0	10.0	0.0007513	1.118
59.0	15.0	0.0007016	1.044
68.0	20.0	0.0006543	0.974
77.0	25.0	0.0006081	0.905

TABLE 4-20

THERMAL STABILITY OF HYDRAZINE IN MATERIALS
(AFRPL TR 71-41, 1971, p. 27)

Material	Sample Temperature Range at Which Exotherms Were Initiated, °F	Bath Temperatures at Which Burst Disc Ruptured, °F
304L SS	450 – 460	520 – 530
316 SS	400 – 420	570 – 580
321 SS	485 – 495	530 – 560
347 SS	460	530 – 535
17-7PH	465 – 475	535 – 540
Inconel-X	490 – 495	535 – 540
Haynes-25	485	530 ·· 535
Hastelloy-X	385 – 420	510 – 545
2014-T6 Al	440	525 – 550
6061-T6 Al	410	502
1100-0 Al	--	500 Detonation

TABLE 4-21

MATERIAL COMPATIBILITY OF HYDRAZINE
(AFSC DH 3-6, 1970, p.12.5.5-2)

Valve Bodies

Stainless steels 304, 304L, 316, 321, 347; aluminum alloys 6061, 3003, 4043, 2024, 356T6, Tens 50; titanium 6A1-4V, B120VCA.

Springs

Stainless steels 301, 321, 347, AM 350, AM 355, 17-7PH; alloy steel A-286; Inconel, Inconel-X.

Stems

Stainless steels 321, 347, 403, 410, AM 350, AM 355, 17-7PH; alloy steel 8630.

Bellows

Stainless steels 303, 321, 347; Inconel, Inconel-X.

Bearings

Stainless steels 301, 301N, 403, 410, 440C.

Valving Units (seats and poppets)

Stainless steels 303, 321, 347, 440C, AM 350; Teflon; aluminum 1100; stellite 21; nylon; Kynar.

Seals

Teflon; aluminum 1100; butyl rubber compounds 805-70 (Parco), 613-75 (Stillman), 823-70 (Parco), B-480-7 (Parker), 60-61 (Bell), 9257 (Precision); propylene, polyethylene; Hypalon; Cis-4 polybutadiene; ethylene propylene rubber compounds EPR 132, EPT 10, E515-8 (Parker), 721-80 (Stillman), 724-90 (Stillman), 3015 (Uniroyal), Silicone rubber.

Packing

Teflon, Kel-F.

Lubricants

Teflon coatings and carbon graphite; DC-11, Krytox 240 fluorine grease.

Bolts, Nuts, and Screws

Stainless steels 303, 321, 347, 17-7PH; Inconel-X.

Thread Sealants and Antiseize Compounds

Unsintered Teflon; Redel UDMH Sealant, LOX Safe (exterior use only).

Coatings

Chrome plate, anodize (aluminum and magnesium), nickel plate.

Diaphragms

Stainless steels 304, 321, 347; Teflon; butyl rubber; SBR, ethylene propylene rubber E515-8 (Parker), SR 721-80 (Stillman), SR 722-70 (Stillman), SR 724-90 (Stillman).

TABLE 4-22

MATERIAL COMPATIBILITY OF HYDRAZINE
(Kit, 1960, p. 108)

Key:
1. Suitable for use with hydrazine
2. Believed to be compatible but verification is necessary.
3. Compatibility doubtful due to conflicting reports.
4. No information available.
5. Believed to be incompatible but verification is necessary.
6. Not suitable for use with hydrazine.

Metallic Materials

Aluminum alloys (in general)	2	Magnesium	6
2S Aluminum alloy	1	Molybdenum	3
14S Aluminum alloy	2	Monel	6
17S Aluminum alloy	2	Nickel	5
24S Aluminum alloy	1	Stainless steel-type	
		300 Series (in general)	2
40S Aluminum alloy	6	Stainless steel 303	1
43S Aluminum alloy	1	Stainless steel 304	1
52S Aluminum alloy	1	Stainless steel 316	6
61S Aluminum alloy	2	Stainless steel 317	6
75S Aluminum alloy	5	Stainless steel 321	1
356 Aluminum alloy	2	Stainless steel 347	1
Aluminum bronze	2	Stainless steel 400	3
Cadmium	1	Stainless steel 502	6
Chromium	2	Stainless steel W	1
Copper	3	Steel, low alloy	5
Hasteloy C	6	Steel, mild	6
Inconel	1	Stellite 21	1
Iron	6	Titanium and alloys	4
Iron, cast	6	Zinc	6
Lead	6		

Special Protective Coatings

Anodize	5	Iridite	4

Plating: If used to protect steel must afford complete protection to prevent rusting base metal.

Nonmetallic Materials

Elastomers			
Natural Rubber	3	Neoprene	5
Buna N	2	Silicone	2
Buna S	4	Thiokol	4
Butyl	2		
Plastics			
Acrylic	2	Polyamide	4
Alkyd	4	Polyester	4

TABLE 4-23

NON-METALLIC MATERIAL COMPATIBILITY WITH HYDRAZINE
(Kit. 1960. p. 109)

Identifying name	Manufacturer	Use	Remarks
Vinylite (poly-vinyl chloride)	Bakelite Co.	Packing, gasketing	Swells at 150°F after short-time contact; suitable up to 122°F for extended periods.
Koroseal (poly-vinyl chloride)	Goodrich Rubber Co.	Packing, gasketing, piping, and tubing	Swells at 150°F after short-time contact; suitable up to 122°F for extended periods.
Natural rubber	U.S. Rubber Co. and others	Packing, gasketing, piping, and tubing	Can be used up to 200°F for only intermittent use; satisfactory for extended use at ambient temperatures.
Silicone rubber (silastic elastomer)	Dow-Corning Corp. and many fabricators	Packing, gasketing, piping, and tubing	Satisfactory for extended use up to 300°F.
Synthetic rubber (Buna and poly-isobutylene types)	Various	Packing, gasketing, piping, and tubing	Suitable for long-time ambient temperature uses. Synthetic rubbers incorporating some sulfur are preferable.
L7825 (rubber-plastic copolymer-butadiene, styrene, acrylic)	U.S. Rubber Co.	Packing and gasketing	Suitable for long-time ambient temperature uses.
M20995 (rubber plastic copolymer-polyethylene-poly-isobutylene)	U.S. Rubber Co.	Packing, gasketing, and coating	Suitable for long-time ambient temperature uses. Suitable for linings and coatings.
DE-3422 (polyethylene)	Bakelite Co.	Piping and tubing	Satisfactory for ambient temperature uses.
Jescolite (poly-ethylene or Kel-F)	Jet Specialties Co.	Piping and tubing	For high-pressure applications (650-psi working pressure); a stainless steel armored hose is available with a liner extruded from Kel-F or polyethylene.
AN-C-53 Thread Compound	Socony-Vacuum and others	Pipe joint compound	
Oxyseal	Parker Appliance Co.	Pipe joint compound	
Thread-Tite	Armite Laboratories	Pipe joint compound	

301

compatible with hydrazine. Hydrazine can be stored in stainless steel, aluminum and titanium tanks, or glass carboys. Because it is very hygroscopic (absorbs water) it must be tightly sealed. Hydrazine will normally attack materials such as natural rubber, cork, mild steel, and most common metals. Polyvinyl chloride, teflon, butyl rubber, polyisobutylene, and asbestos are resistant at ambient and high temperatures. Stored for long periods of time (more than 1 year) at ambient temperatures, hydrazine shows no appreciable decomposition with the exception of the release of minute quantities of ammonia. However, at high temperatures, hydrazine decomposes at a rapid rate. It will explode in a sealed tank at 491° F (14.5 psia) after a rapid rise in its decomposition rate. It will also explode when sparked at temperatures above 212° F. Hydrazine reacts spontaneously in the presence of wool, rags, organic material, and the metal oxides of iron, copper, lead, manganese, or molybdenum. Kit (1960) is an excellent source of information for more detail on hydrazine compatibility with various aerospace materials. AFRPL TR 71-41 (1971), AFRPL TR 75-46 (1975) and The Handling and Storage of Liquid Propellants (1961) are also good sources of information on the results of hydrazine compatibility studies.

Hydrazine functions as a monopropellant through its catalytic or thermal decomposition within the combustion chamber of the thruster. Catalysis is the primary means of decomposing hydrazine. This process is accomplished using an active metal catalyst which dissociates the fuel into low molecular weight byproducts. Heater coils are also used to thermally decompose hydrazine by increasing the propellant temperature beyond 1800° F at which point dissociation occurs. In either case, the performance of
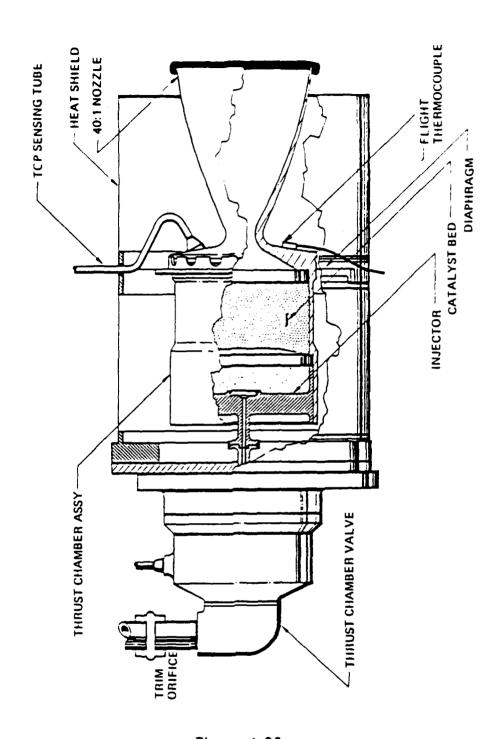
monopropellant hydrazine reactors can be measured in terms of the usual rocket parameters of thrust, characteristic exhaust velocity and specific impulse. For steady state operation, the I_{sp} of most hydrazine subsystems ranges between 220 and 235 seconds. When thrusters are operated in a pulsed mode, the measured I_{sp} may decrease to as low as 100 to 160 seconds.

Thrust levels for hydrazine engines are classified in three categories. Low thrust engines are all those engines up to 5 lbf thrust. Medium thrust engines encompass the range of 5 lbf to 100 lbf thrust. High thrust engines (typically bipropellant rockets using hydrazine as fuel) range from 100 to 10,000 lbf thrust. The low thrust engines are generally used for attitude control functions whereas medium to high thrust engines are designed for station keeping and orbit insertion. The choice of a particular thrust level for attitude control depends upon the angular accelerations which the designer wishes to impart to the vehicle. Most often, engines of less than 0.4 lbf thrust are used for fine angular control. In the ORION design, a 0.1 lbf engine will be used for attitude control, and a 5 to 50 lbf unit will be used for orbit transfer.

A fourth parameter unique to monopropellant hydrazine completely specifies the performance of hydrazine. This parameter is the amount of ammonia remaining in the decomposition products of the gas which leaves the catalytic chamber. The amount of ammonia completely specifies the composition of the decomposed hydrazine and is a function of the residence time of the hydrazine in the catalyst bed or heating element chamber. (JPL TR 32-1227, 1968, p. 2).

Figure 4-23

Hydrazine Thruster Assembly
(AFRPL TR 71-103, 1971, p. 4)

304
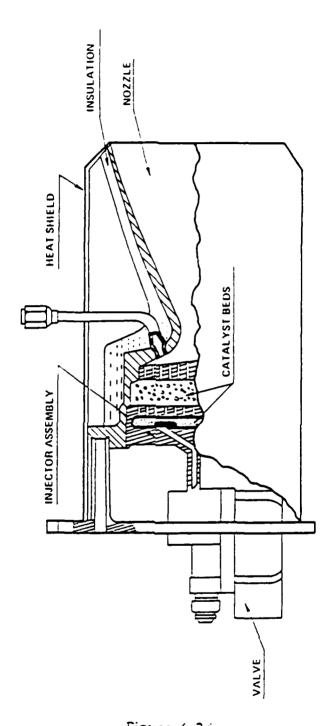
Figure 4-24

Rocket Research Co. Monopropellant Engine
(AFRPL TR 72-43, 1972, p. 4)

b. Hydrazine catalyst bed operation

A hydrazine catalyst decomposition chamber is used to produce gases for catalytic-thrust and catalytic-plenum engines. The chamber consists of an injector for distributing the hydrazine and a catalyst bed enclosed in a suitable container. Typical reactors are shown in Figures 4-23 through 4-25. The injectors and the chamber geometries vary as widely as their application. The injector atomizes and distributes the propellant within a catalyst bed as uniformly as possible.
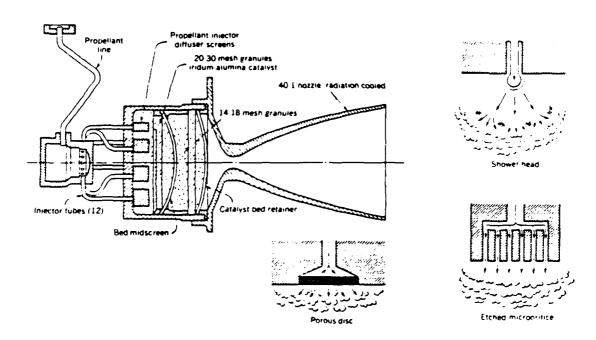
The catalyst is typically Shell 405 hydrazine catalyst which is composed of pelletized aluminum oxide and an active metal. iridium. Iridium is the byproduct of platinum mining and accounts for 30% of the Shell 405 mass. The catalyst, like hydrazine. is hygroscopic, and oxidizes on exposure to air. It is very responsive as a decomposer at low temperatures down to the freezing point of the fuel (35° F). The catalyst was developed by the Shell Oil Co. in the 1960's, and no other catalytic compound has been created since that time that is as effective.

Upon contact with the catalyst material. the hydrazine vaporizes due to the combined effect of catalysis and the heat produced by the earlier decomposition of propellant. In the next region of the catalyst bed. moving toward the outlet. a heterogenic catalytic decomposition of the vaporized hydrazine continues. Beyond that region, the decomposition continues but as a homogenous reaction. In its last region of decomposition, the hydrazine and vapor are further dissociated endothermically (absorbing energy) to form

Figure 4-25

Typical Hydrazine Rocket Design - Selected Injector Configurations
(Sutton. 1976. p. 296)

nitrogen and hydrogen. All of this action occurs within the first 10% of the catalyst bed under normal conditions (JPL TR 32-1227, 1968, p.5). The reactions which occur during catalysis are as follows:

$$N_2H_4 \rightarrow 4/3 \ NH_3 + 1/3 \ H_2$$
$$NH_3 \rightarrow 1/2 \ N_2 + 3/2 \ H_2$$
$$2N_2H_4 \rightarrow 2NH_3 + N_2 + H_2$$

The catalytic decomposition of ammonia then yields additional hydrogen in accordance with the equation

$$N_2H_4 \rightarrow 4/3 \ (1-X) \ NH_3 + 1/3(1+2X) \ N_2 + 2(X) \ H_2$$

in which X is the fraction of the original NH_3 that is subsequently dissociated. This quantity of dissociated ammonia specifies the temperature of the exhaust gas due to the absorption of energy during the ammonia dissociation phase. As the ammonia decomposes, energy is extracted from the exhaust gas, and more low molecular weight molecules (hydrogen) are introduced into the gas stream.

In JPL TR 32-348 (1962, p. 84-86), Lee presents the results of thermochemical performance calculations for hydrazine and describes the effect of ammonia dissociation on the performance of a monopropellant hydrazine subsystem. He presents performance data for various cases of dissociation (0%, 20%, 40%, 60%, 80%) and equilibrium ($N_2 - H_2$). These data, coupled with a knowledge of the nozzle expansion ratio (up to 200:1) and the

308

chamber pressure, allow a hydrazine subsystem user to completely determine the thruster performance as a function of ammonia dissociation. JPL TR 32-348 enables the determination of the thruster exhaust temperature, $I_{sp-vacuum}$, $I_{sp-optimum}$, and the characteristic exhaust velocity. Lee notes that for dissociation of ammonia above 30% at all chamber pressures, a sharp drop in the characteristic exhaust velocity of the thruster occurs. Hence, ammonia dissociation must be carefully considered in performance predictions and the analysis of any hydrazine thruster subsystem.

c. Hydrazine thruster performance

Unlike an inert gas or vaporizing liquid thruster subsystem. the hydrazine catalyst subsystem is subject to several performance anomalies. These include pressure overshoots during the start transient. pressure excursions during steady state operation, and loss of catalytic activity. The performance anomalies are functions of the duration of thruster operation with pulsed mode operations presenting some special problems for hydrazine units. Each of these thrust anomalies will be discussed with reference to the impact on pulsed mode operations. As such, then, the discussion applies mainly to the attitude control mission of the hydrazine subsystem.
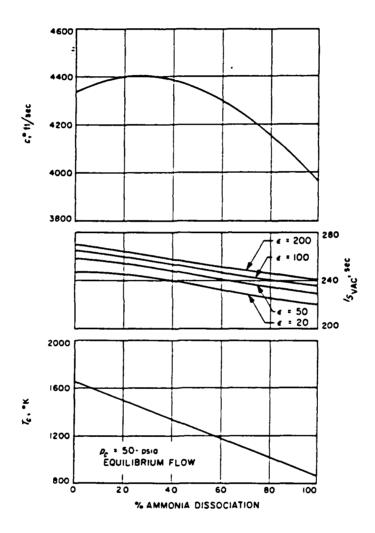
Figure 4-26

Hydrazine Performance - Chamber Pressure 50 psi
(JPL TR 32-348, 1962, p. 84)
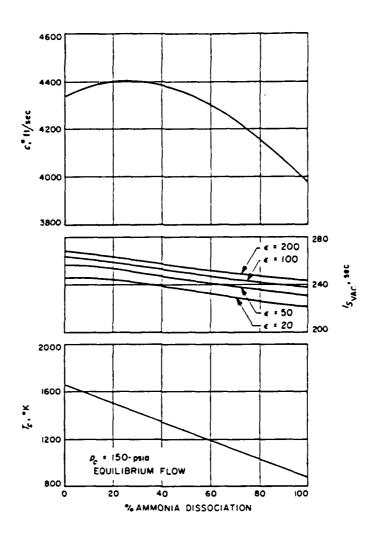
Figure 4-27

Hydrazine Performance - Chamber Pressure 150 psi
(JPL TR 32-348, 1962, p. 84)

311
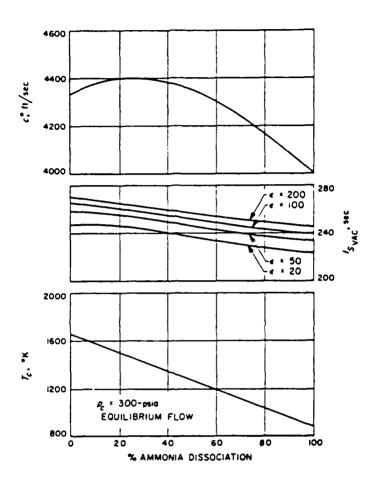
Figure 4-28

Hydrazine Performance - Chamber Pressure 300 psi
(JPL TR 32-348, 1962, p. 85)

(1) Pressure Overshoots. The start transient refers to the fluctuation of pressure during the startup of a cold rocket engine. This exhaust pressure anomaly is a function of the time required to initiate decomposition in the catalyst bed. Over a period of 200 ms. raw hydrazine will accumulate in the leading portion of the cool catalyst bed. When the raw hydrazine suddenly starts to decompose, the energy that is released furthers the rapid decomposition of the slug of fuel that has initially accumulated at the injector outlet. This sudden release of energy and rapid decomposition is the source of the transient pressure spike.

The start transient is usually described in terms of the time from arrival of the propellant electrical turn-on signal (at the valve) until the development of 90% of the steady state thrust value. Included in the response time are the valve opening time, the time to fill the propellant feed lines, the decomposition delay (time from introduction of fuel to decomposition) and the time required to increase the chamber pressure to its final value. The initial temperatures of the catalyst bed and propellant strongly influence the start transient and the shape of a pulse for the intermittently operated thruster. Therefore, thermal design and thermal management are critically important to the operation of a hydrazine subsystem. Excessively cold temperatures freeze the propellant in the lines or slow the bed reaction time to unacceptably low levels (JPL TR 32-1227. 1968, p.11). Use of the thruster in a pulsed mode depends upon knowledge and management of the pressure transient. As propellant temperatures decrease, and the subsystem response time rises, a certain minimum duration thrust pulse can be obtained. For a cold gas subsystem, the

313

minimum duration pulse is determined mainly by the response time of the solenoid valve controlling the gas flow. For a hydrazine subsystem, however, the determination of a minimum duration pulse is significantly more complicated.

(2) <u>Spiking</u>. In addition to the pressure overshoot during the startup transient, pressure spikes will also occur in the thrust chamber as the hydrazine decomposition process shifts from an initial state to a steady state condition. This can occur from between a few milliseconds to a full minute after reactor startup. Spiking critically affects operations where predictability of pulse duration is important. The impact upon pulsed mode operations is that the pulse duration may be variable or unpredictable if the reactor is not allowed to stabilize in a steady state operation. Reproducibility of pulses can also be a problem for short duration firings because of the strong dependence upon catalyst bed temperatures. Studies of thruster operation have shown that as repetitive thrusting cycles are conducted at close intervals, the residual heat within the thruster improves the thruster performance (JPL TR 32-1227, 1968). In summary, the impact of pressure spiking is that reproducibility of pulses is impossible due to the extreme dependence of the thrust upon the catalyst bed temperature.

(3) <u>Loss of Catalytic Activity</u>. The third anomaly observed in the operation of the hydrazine thruster subsystem is a loss of catalytic activity in the Shell 405 catalyst bed. The gradual crystallization of the active metal, iridium, within the catalyst material is the primary cause. Loss of catalytic activity may also occur as a result of the physical destruction of the catalyst (attrition) or contamination from outside sources. McCollough (1972, pp.97-

110) provides an excellent discussion of the catalyst degradation mechanisms. He notes, in short, that catalyst attrition is attributable to thermal shock, propellant impact with the catalyst granules, accumulation and "cook-off" of the propellant between the granules, gas erosion, crushing due to differential thermal expansion, and mechanical abrasion during pressure spiking. The crystallization of iridium is apparently a heat related problem resulting in a gradual loss of the active catalyst metal. Finally, contamination of the bed can be caused by gas poisoning (air leakage prior to the launch) or contamination by foreign metals within the feed subsystem.

(4) Thermal Considerations. In addition to thrust anomalies, the hydrazine thruster subsystem design must be chosen with thermal considerations in mind. Because the hydrazine propellant will decompose as a result of heat input, heat transfer from the thrust chamber to the propellant feed subsystem must be limited. Heat must not be conducted to regions where the propellant has stagnated. Although hydrazine is a relatively good conductor of heat before it decomposes, the thruster subsystem design must absolutely prohibit heat transfer to regions upstream of closed solenoid valves, where decomposition of the propellant would be catastrophic (explosive). With continuously operating systems, the flowing fluid absorbs the heat conducted by the upstream piping without ill effects. However, during pulsed mode operations the fluid does not continue to flow and enough heat transfer from the 2000° F thrust chamber to the upstream side of the propellant shutoff valve may be possible to cause local decomposition of the propellant (Schmidt, AFRPL TR 710103, 1971, pp. 20-27).

315

The solution to the thermal management of thruster operations is often to isolate critical parts of the liquid subsystem from the thrust chamber and catalyst bed ensuring that the feed subsystem is not heated while the propellant is stagnant. The usual treatment is to connect the shutoff valve and injector via a long thin capillary tube and thus introduce a high thermal resistance between the catalytic chamber and the solenoid. The valve may also be mounted upon a heat sink material, and seals may be used as thermal insulators in the thruster/feed subsystem interface. The drawback to thermal isolation is that the use of capillary tubes may increase the time for the startup transient of the thruster. Typically, however, the use of capillary tubes is fixed in the thruster design, and an engine is chosen with a given thermal characteristic. Propellant feed systems are often isolated from the thruster by low conductivity stainless steel tubing of a small inside diameter (0.125 or 0.25 in).

Note that one drawback to the use of pulsed mode operations with hydrazine thrusters is the loss of potentially available chemical energy due to cold catalyst beds in intermittently operated thrusters. A portion of the energy which would normally be available during steady state operations is lost to heat the catalyst bed with each successive, but delayed, pulsed burn. If the pulse is short and the duration between consecutive pulses is relatively long, the impulse derived from a given volume of hydrazine fuel will be low. Sutton (1976, p.295) lists the actual values of I_{sp} for hydrazine engines at various thrust durations. For steady state operation, the observed I_{sp} is as high as 92% of the theoretical I_{sp}. As thrust durations are decreased to 0.1 second, the observed-to-theoretical I_{sp} ratio drops to 75%-85%. For very

short pulses. (0.01 seconds), only 50% of the theoretical I_{sp} is attained. In several ways, thermal considerations in the operation of a hydrazine thruster are seen to be critically linked to the precise prediction of performance.

ELECTRICAL PULSE WIDTH = 80 ms
TIME BETWEEN PULSES = 520 ms
INITIAL BED TEMPERATURE = 70°F
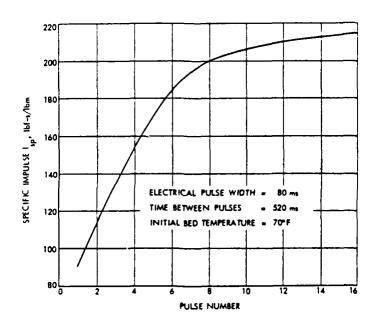
Figure 4-29

Specific Impulse Per Bit - Repeated Pulses Lead to Higher ISP
(JPL TR 32-1505, 1970, P. 53)

d. Subsystem Choices -- Thrusters

The discussion in this section lays a framework for the proper choice of a commercial thruster to be used on the ORION satellite. Feed subsystems. consisting of propellant storage and pressurization components. will be described in detail following the comparison of commercial thrusters and a selection of the best thruster candidates. Thrusters will be chosen within the context of the propulsion subsystem design criteria and will emphasize:

(1) Provision of the requisite total impulse
(2) Low mass for thruster, storage and pressurization components
(3) Small volumes for the thruster, storage and pressurization components
(4) Ease of integration; i.e., simple mounting schemes
(5) Simplicity of design

The choice of subsystems is based on the three different configurations of hydrazine thrusters which were discussed earlier and which are commercially available. The hydrazine plenum and hydrazine resistojet thrusters are not appropriate for the ORION due to their increase in complexity, power requirements, and/or cost. However, some background information on those systems is provided below.

(1) <u>High Temperature Augmented Thrusters</u>. The I_{sp} and thrust capability of a hydrazine thruster can be significantly improved through the use of an electrical heater. The typical temperature of hydrazine exhaust gas is $1800°$ F. This temperature can be increased to $3000°$ F using heater coils. As a result the I_{sp} increases from 225 seconds (average value) to over 300 seconds. The Air Force Rocket Propulsion Laboratory (AFRPL) has conducted tests to assess the lifetime of radiative and conductive wire heaters used in such thrusters (AFRPL TR 84-089). Long life thrusters have been developed

318

as a result of those studies, but the flightweight versions consume 380 - 400 watts of power which is beyond the capability of the ORION power supply except in very short infrequent bursts. Figure 4-30 diagrams a commercially available augmented thruster subsystem which delivers thrusts of 0.040 to 0.075 lbf. The unit delivers a specific impulse of 280 to 304 seconds with a large total impulse capability. The total mass is 1.8 lbm. and the continuous power requirement is 350 to 510 watts. Although a high I_{sp} is demonstrated at a relatively low weight, the power consumption of an augmented thruster is considered to be excessive for the ORION application.
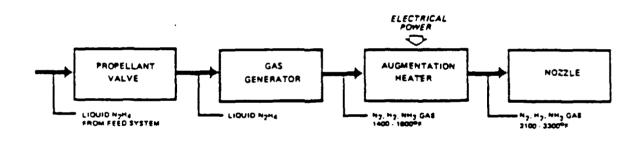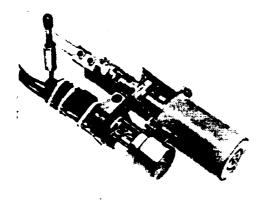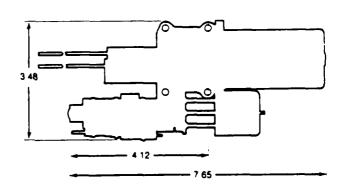
Figure 4-30

Augmented Thruster Concept
(AFRPL TR 84-089, 1984, p. 1)

Design Characteristics

- Propellant . . . . Hydrazine
- Catalyst . . . . Shell 405
- Thrust, Steady State (lbf) . . . . 0.075—0.040
- Feed Pressure (psia) . . . . 350—100
- Chamber Pressure (psia) . . . . 95—50
- Flow Rate (lbm/sec) . . . . 0.00028—0.00013
- Valve . . . . Wright Components Dual Seat
- Augmentation Heater Power . . . . 510—350 Watts
- Augmentation Heater Voltage . . . . 27.5—22 vdc Letdown
- Weight (lbm) 1.80

Demonstrated Performance

- Specific Impulse (lbf-sec/lbm) . . . . 280—304
- Total Impulse (lbf-sec) 70,000
- Total Pulses 500,000
- Minimum Off-Pulse Bit @ Max Feed Pressure (lbf-sec) 0.0005
- Steady-State Firing (hr) . . . . 1.7 — Single firing
  389 — Cumulative

Figure 4-31

Rocket Research MR-501 Augmented Catalytic Thruster
(Reproduced from Rocket Research Co. Promotional Literature)
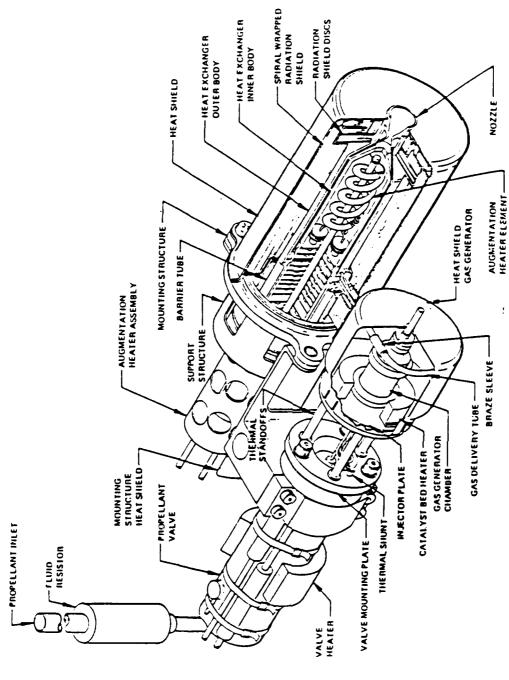
Figure 4-32

Augmented Thruster Cross Section
(AFRPL TR 84-089, 1984, p. A-2)

321

(2) Hydrazine Plenum Thruster. The plenum concept involves the storage of gas for future expulsion. In the hydrazine context, the gas is produced by a catalytic gas generator and is vented to a plenum storage bottle. The outlet pressure of the plenum is regulated, and the result is a constant pressure hot gas thruster. Figures 4-33 and 4-34 diagram a typical plenum subsystem and list the mass of components. The available I_{sp} is less than 220 seconds due to heat transfer from the gas to the plenum bottle. Specific impulses in the range of 130 to 200 seconds are typical for the plenum subsystem; 220 seconds is an average I_{sp} for a catalytic thruster. Essentially, the hydrazine plenum is a good way to carry very hot gases in a dense package. In effect, the satellite is storing the hot gas as unreacted hydrazine. Use of a hydrazine plenum subsystem enables the designer to use simple inert gas thrusters for gas control with only one catalyst bed. In situations where temperature control is likely to be critical, the use of only one catalyst bed may be advantageous. However, the plenum concept leads to the use of extra tanks and complicates thermal control. Figure 4-35 indicates the mass of various plenum systems. If this figure is compared to Figure 4-38 for a direct catalytic thruster, the increase in plenum mass for a given quantity of hydrazine propellant is apparent. Thus, the simplicity and low mass of a simple catalytic thruster subsystem is preferable to the plenum concept for the ORION application.

(3) Catalytic Thruster. The direct feed catalytic thruster, which was described earlier in Section C.4.a and C.4.b., is the preferable choice from the thruster options. The mass of a hydrazine subsystem for the primary and auxiliary missions will be less than that of any other propulsion

322

subsystem option presented heretofore. Typical catalytic thruster systems
are depicted in Figures 4-36 and 4-37.
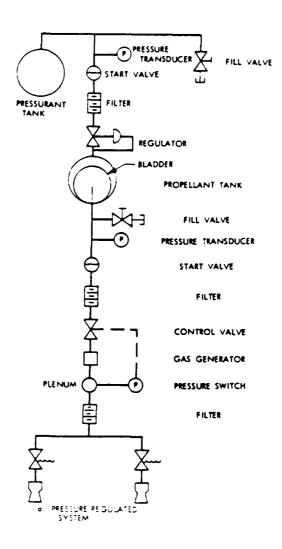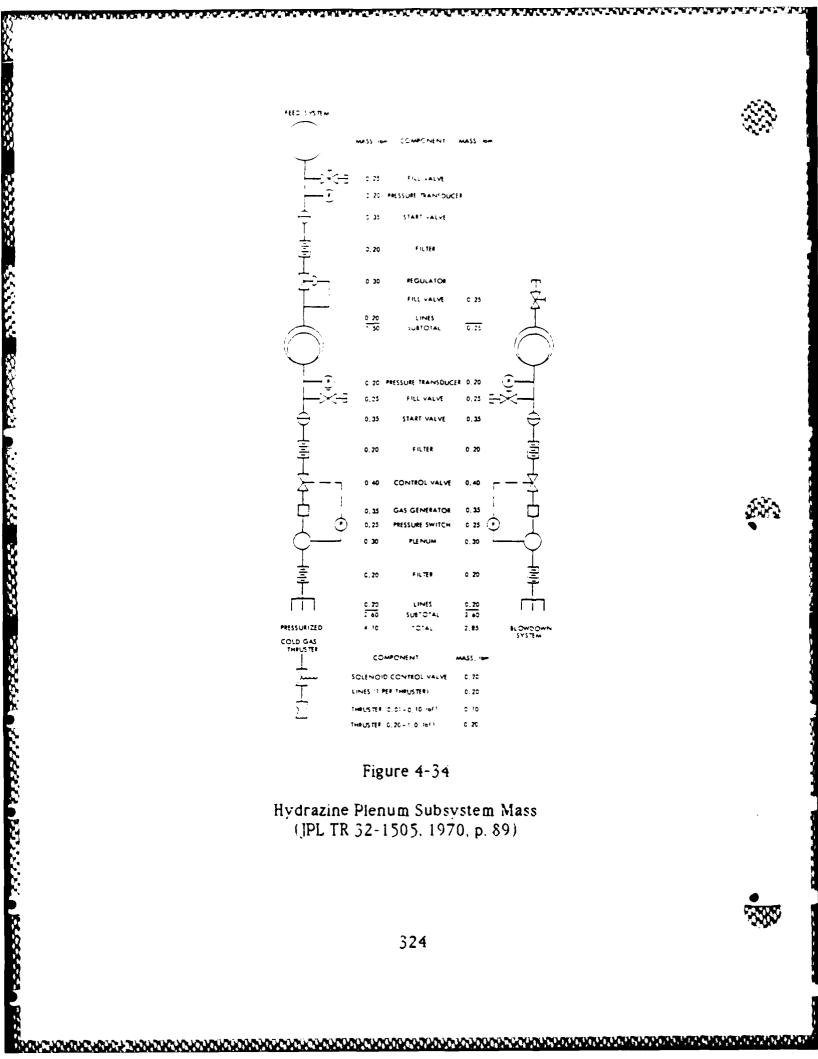
Figure 4-33

Typical Hydrazine Plenum Propulsion Subsystem
(JPL TR 32-1505, 1970, p. 47)

FEED SYSTEM

MASS lbm	COMPONENT	MASS lbm
0.25	FILL VALVE	
0.20	PRESSURE TRANSDUCER	
0.35	START VALVE	
0.20	FILTER	
0.30	REGULATOR	
	FILL VALVE	0.25
0.20	LINES	
1.50	SUBTOTAL	0.25
0.20	PRESSURE TRANSDUCER	0.20
0.25	FILL VALVE	0.25
0.35	START VALVE	0.35
0.20	FILTER	0.20
0.40	CONTROL VALVE	0.40
0.35	GAS GENERATOR	0.35
0.25	PRESSURE SWITCH	0.25
0.30	PLENUM	0.30
0.20	FILTER	0.20
0.20	LINES	0.20
2.60	SUBTOTAL	2.60
4.10	TOTAL	2.85

PRESSURIZED

COLD GAS THRUSTER

BLOWDOWN SYSTEM

COMPONENT	MASS, lbm
SOLENOID CONTROL VALVE	0.70
LINES (1 PER THRUSTER)	0.20
THRUSTER (0.01 – 0.10 lbf)	0.10
THRUSTER 0.20 – 1.0 lbf	0.20

Figure 4-34

Hydrazine Plenum Subsystem Mass
(JPL TR 32-1505, 1970, p. 89)

Figure 4-35

Hydrazine Plenum Feed Subsystem Mass
(JPL TR 32-1505, 1970, p. 90)
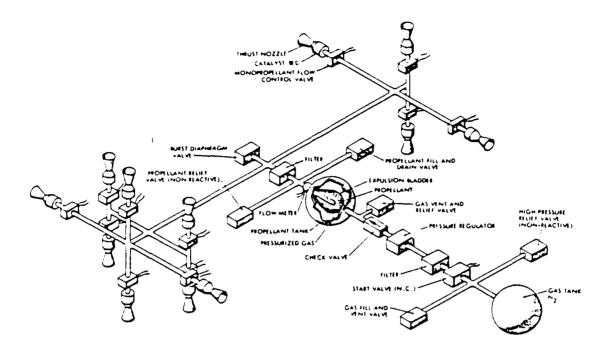
Figure 4-36

Monopropellant Attitude Control Rocket Subsystem
(AFSC DH 3-2, 1962, p. 4.4-4)

The selection of a hydrazine thruster for the ORION will be divided between primary propulsion and auxiliary propulsion systems as each has a different function and, thus, a different thrust requirement. The required delta-V for the primary propulsion package was determined earlier to be 641 m/s or 2102 ft/s. For a satellite mass of 250 lbm this equates to a hydrazine mass of 64.3 lbm. and a total impulse for primary propulsion of 14145 lbf-seconds.
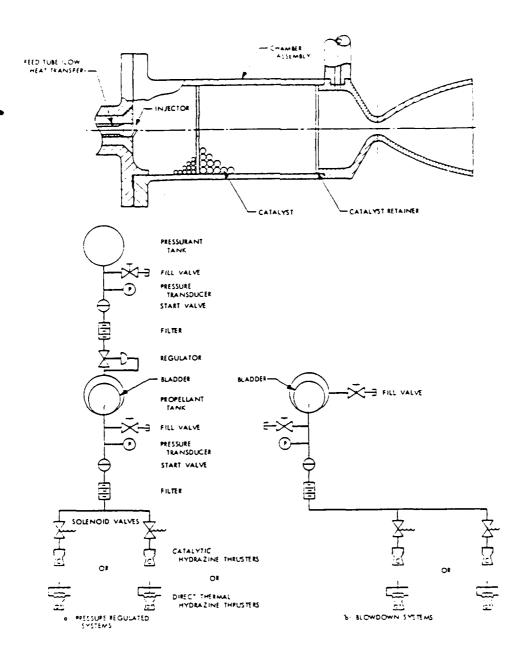
Figure 4-37

Direct Hydrazine Catalytic Thruster
(JPL TR 32-1505, 1970, p. 46)

The total impulse requirement for the auxiliary subsystem is 1200 lbf-seconds. With a knowledge of the total impulse required (15145 lbf-seconds), the Hohmann transfer delta-V and angular accelerations required by the mission, the proper size thrusters can be identified. Balancing the thrust and impulse requirements, a thruster can be chosen from commercially available units or can be designed to specifications that fit the particular need. For ORION, thrusters for the auxiliary subsystem will require small thrusts on the order of 0.1 lbf. Small thrust allows fine precision control of the spinning spacecraft. The primary propulsion subsystem should provide thrust levels of at least 5 lbf or greater. High thrust levels can then be modeled as impulsive forces in the Hohmann orbital transfer.

A vendor survey of candidate thruster units was conducted to determine what thrusters were commercially available and to compare their designs on a structural and propulsive basis. Approximate component costs and delivery times were also obtained. As a result of that vendor survey three firms were identified that are presently manufacturing thrusters appropriate for use in ORION. They are (1) Rocket Research Co., (2) Hamilton Standard Co., and (3) TRW. The products of those firms will be reviewed. Thruster systems in excess of 100 lbf thrust will not be considered. Likewise, thrusters of less than 0.001 lbf thrust will not be considered due to their inability to produce the necessary angular accelerations.

TABLE 4-24

ROCKET RESEARCH CO. PRIMARY PROPULSION THRUSTERS

Designator	MR 50 EJ	MR 50F	MR 50H	MR 50K	MR 50L	MR 50M	MRM 110
Programs	SMS, GOES, Meteosat	Viking	P-95 (Block III)	MJS	GPS	Intelsat V	Scatha
Design Characteristics							
(1) Thrust, steady state (lbf)	5.3—17	8.7—3.3	6.0—2.8	7.1—4.9	5.0—2.2	6.1—4.3	6.7—3.3
(1) Feed pressure (psia)	250—70	480—135	260—100	420—250	245—85	320—200	385—145
(1) Chamber pressure (psia)	97—32	166—65	115—50	133—86	106—43	115—80	125—60
(1) Expansion ratio	40:1	40:1	40:1	40:1	40:1	40:1	40:1
(1) Flow rate (lbm/sec)	0.023—0.008	0.0382—0.0149	0.026—0.013	0.031—0.022	0.0216—0.0103	0.0271—0.0193	0.0295—0.0151
(1) Valve	Parker Hannifin Single seal	Parker Hannifin Dual seal	Moog Single seal	Moog Single seal	Wright Component Dual seal	Parker Hannifin Dual bellar	Wright Component Single seal
(1) Valve power	19 W @ 28 vdc & 70°F	29 W @ 33 vdc & 35°F	29 W @ 33 vdc & 35°F	29 W @ 33 vdc & 35°F	29 W @ 33 vdc & 35°F	22 W @ 42 vdc & 40°F	13 W @ 28 vdc & 60°F
(1) Weight (lbm)	1.24	1.62	1.24	1.08	1.50	1.30	1.20
(1) Engine	0.84	0.80	0.84	0.68	0.90	0.82	0.80
(1) Valve	0.40	0.82	0.40	0.40	0.60	0.48	0.40
Demonstrated Performance							
(1) Specific impulse (lbf sec/lbm)	225—210	228—221	226—219	227—225	225—215	226—224	227—221
(1) Total impulse (lbf sec)	21,086	14,000	44,000	7,950	11,394	50,400	1,782
(1) Total pulses	21,452	20,000	471,000	15,100	12,300	24,000	1,350
(1) Minimum impulse bit (lbf sec)	0.36 @ 250 psia & 80 ms ON	0.09 @ 360 psia & 22 ms ON	0.055 @ 117 psia & 22 ms ON	0.15 @ 350 psia & 40 ms ON	0.075 @ 245 psia & 22 ms ON	0.46 @ 320 psia & 80 ms ON	0.30 @ 145 psia & 80 ms ON
(1) Steady state firing (sec)	300	3,504	300	30	600	4,620	60

TABLE 4-25

ROCKET RESEARCH CO. AUXILIARY PROPULSION THRUSTERS

Designator	MR-103	MR-103C	MRM-110	MR-103A	MR-103B
Programs	MJS	SATCOM, Spacenet, G-Star	SCATHA	GPS	I-V
Design Characteristics					
☐ Thrust, steady state (lbf)	0.252—0.042	0.252—0.042	0.231—0.087	0 180—0 042	0.240—0 054
☐ Feed pressure (psia)	420—70	420—70	385—145	300—70	400—90
☐ Chamber pressure (psia)	352—64	370—60	330—125	250—60	330—80
☐ Expansion ratio	100:1	100:1	100.1	100 1	100.1
☐ Flow rate (lbm/sec)	0.0011—0.0002	0.001—0.0002	0.001—0.0004	0.0008—0.00019	0 001—0 00023
☐ Valve	Moog Single seat	WCI Dual seat	WCI Single seat	WCI Dual seat	WCI Dual seat bifilar
☐ Valve power	5 W @ 31 vdc & 40°F	9 W @ 28 vdc & 45°F	4.1 W @ 28 vdc & 60°F	9 W @ 28 vdc & 45°F	12.2 W @ 42 vdc & 40°F
☐ Weight (lbm)	1.00	0.73	0 53	0 73	0 73
☐ Engine	0 33	0.28	0 28	0 28	0 28
☐ Valve	0 27	0.45	0.25	0.45	0 45
☐ Pressure transducer	0.40				
Demonstrated Performance					
☐ Specific impulse (lbf-sec/lbm)	227—206	227—206	226—214	223—206	226—208
☐ Total impulse (lbf-sec)	15,500	35,625	2.500	189	3.650
☐ Total pulses	750,000	410,000	5.000	1.059	161.000
☐ Minimum impulse bit (lbf-sec)	0.001 @ 150 psia & 8 ms	0.001 @ 150 psia & 8 ms	0 01 @ 145 psia & 80 ms	0.004 @ 165 psia & 20 ms	0 005 @ 100 psia & 25 ms
☐ Steady-state firing (sec)	64,800	64,800	60	120	180
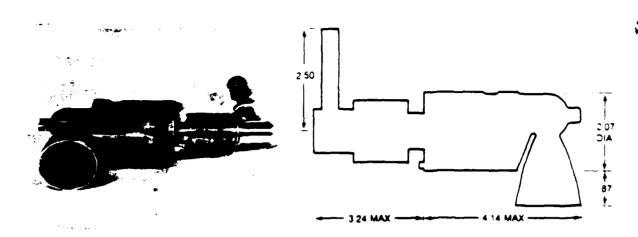
Specification sheets and cross sectional diagrams list the capabilities for two candidate Rocket Research thrusters. A table of Rocket Research Co. engines in the range of 0.1 lbf and 5 lbf is enclosed (Tables 4-24 and 4-25) to compare the performance of the various small engines sold by that company. The primary propulsion requirements of ORION could be satisfied using models MR-107B, MR-107E, or the MR-50 series. The MR-107B produces thrusts of 11 to 40 lbf over an inlet pressure range of 100 to 450 psi. This thruster uses a right angle nozzle and occupies an envelope 5.05" high by 7.38" long. Although the total impulse is listed as 4350 lbf-seconds, personal communication with Mr. Jim Bartron of the Rocket Research Co. indicates that impulses of 15000 lbf-seconds can be easily achieved with only slight modifications to the design. The MR-107E is an improved version of the MR-107B and is available in either a straight or right angled nozzle configuration. It is capable of thrust of up to 30 lbf and occupies roughly the same envelope as the MR-107B. The MR-107E is currently in production for the Titan II missile program. The MR-50 series engines represent a broad range of total impulse capabilities in the 5 lbf thrust category. Of these engines, the MR-50L is the only engine currently in production. It is being manufactured for the GPS Block II program. This engine is capable of 2.2 to 5.0 lbf thrust over an inlet pressure range of 85 to 245 psi. The total impulse of 11394 lbf-seconds is also subject to modification with only slight changes to the design. This 1.5 lbm unit occupies an envelope 7.21" high and 2.6 in diameter. The companion MR-50R is a right angle nozzle version with a reduced vertical clearance of 3.82"

Design Characteristics

☐ Propellant	Hydrazine
☐ Catalyst	Shell 405/LCH 202
☐ Thrust, Steady State (lbf)	40 — 11
☐ Feed Pressure (psia)	450 — 100
☐ Chamber Pressure (psia)	223 — 61
☐ Expansion Ratio	20:1
☐ Flow Rate (lbm/sec)	0.17 — 0.054
☐ Valve	Wright Components Single Seat
☐ Valve Power	50 Watts @ 28 vdc and 75 °F
☐ Weight (lbm)	1.95
Engine	1.35
Valve	0.60

Demonstrated Performance
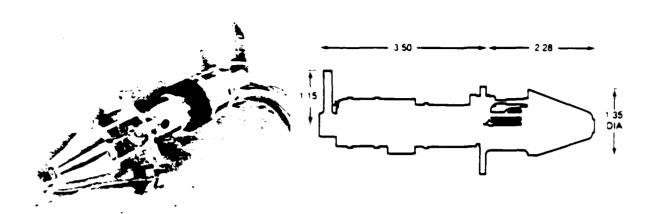
☐ Specific Impulse (lbf-sec/lbm)	235 — 203
☐ Total Impulse (lbf-sec)	4.350
☐ Total Pulses	2.258
☐ Minimum Impulse Bit (lbf-sec)	0.71 @ 450 psia & 20 ms ON
☐ Steady-State Firing (sec)	97

Figure 4-38

Rocket Research 40 lbf Thruster - Model MR 107B
(Reproduced from Rocket Research Co. Product Literature)

Design Characteristics

☐	Propellant	Hydrazine
☐	Catalyst	Shell 405
☐	Thrust, Steady State (lbf)	0.252—0.042
☐	Feed Pressure (psia)	420—70
☐	Chamber Pressure (psia)	370—60
☐	Expansion Ratio	100:1
☐	Flow Rate (lbm/sec)	0.001—0.0002
☐	Valve	Wright Components Dual Seat
☐	Valve Power	9 Watts Max. at 28 vdc and 45°F
☐	Weight (lbm)	0.73
	Engine	0.28
	Valve	0.45

Demonstrated Performance

☐	Specific Impulse (lbf-sec/lbm)	227—206
☐	Total Impulse (lbf-sec)	35,625
☐	Total Pulses	410,000
☐	Minimum Impulse Bit (lbf-sec)	0.001 @ 150 psia & 8 ms ON
☐	Steady-State Firing (sec)	64,800

Figure 4-39

Rocket Research 0.1 lbf Thruster - Model MR 103C
(Reproduced from Rocket Research Co. Product Literature)

333

and a span of 6.2". The MR-107P(E) or MR-50R engines are the preferable units for the ORION due to their compact size (in the right angle configurations) and due to their ready availability. Each of these thrusters will cost $45,000 each in lots of three and will require 14 to 18 months for delivery.
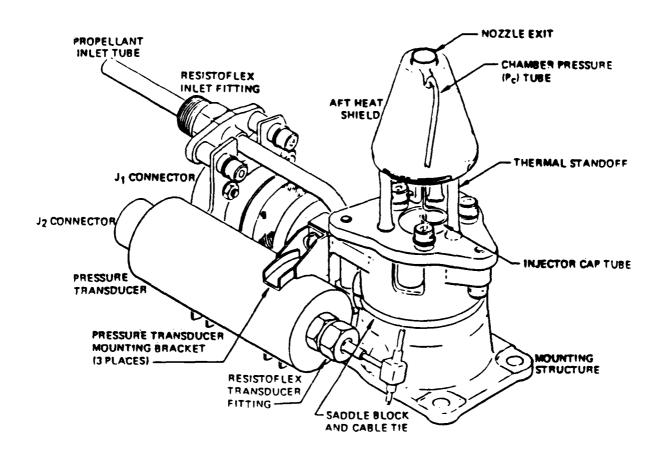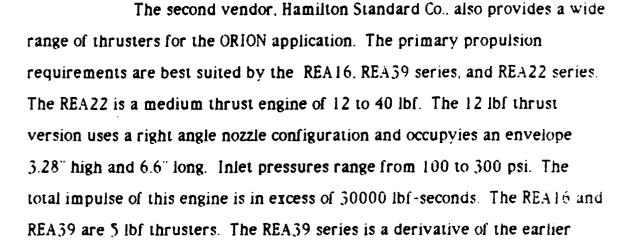
Figure 4-40

Rocket Research 0.1 lbf Thruster - Model MR 103C
(Reproduced from Rocket Research Co. Product Literature)

The auxiliary propulsion requirements could be satisfied using the MR-110, MR-111, or MR-103 series engines. The MR-111C may not provide the necessary fine angular control at 1.0 lbf thrust. The MR-111 and MR-111A provide approximately 0.5 lbf thrust with a total impulse in the range of 27000 lbf-second to 58000 lbf-seconds. The MR-103A and MR-103C are smaller engines of 0.1 and 0.2 lbf thrust respectively. The MR-103A is currently in production for GPS. Although it is specified for a limited total impulse of 189 seconds, the unit can be easily modified through the addition of extra catalyst to provide as much as 30000 lbf-seconds. Both of the engines occupy an envelope 5.78" long and 1.35" in diameter with a mass of 0.73 lbm. The MR-103A would be the best Rocket Research engine for the auxiliary propulsion needs due to its thrust level (0.042 to 0.18 lbf) and current production status. The engine must be modified to produce at least 1000 lbf-seconds total impulse. The purchase cost is also $ 45,000, with a 14 to 18 month delivery lead time.

The second vendor, Hamilton Standard Co., also provides a wide range of thrusters for the ORION application. The primary propulsion requirements are best suited by the REA16, REA39 series, and REA22 series. The REA22 is a medium thrust engine of 12 to 40 lbf. The 12 lbf thrust version uses a right angle nozzle configuration and occupyies an envelope 3.28" high and 6.6" long. Inlet pressures range from 100 to 300 psi. The total impulse of this engine is in excess of 30000 lbf-seconds. The REA16 and REA39 are 5 lbf thrusters. The REA39 series is a derivative of the earlier REA16 series. The REA39-1 uses inlet pressures of 70 to 350 psi and can be
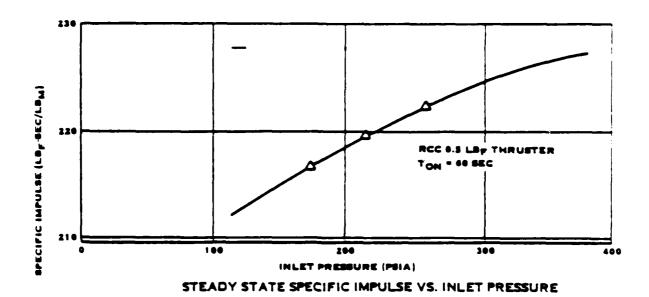
modified to provide the right angle nozzle configuration needed for the low profile mounting in ORION. The production status is unknown.

3.2 LB$_F$ THRUST CHARACTERISTICS

Figure 4-41a

Thrust Curves for Hamilton Standard Thrusters
(Hamilton Standard Co. Product Literature, 1986)

336

STEADY STATE SPECIFIC IMPULSE VS. INLET PRESSURE

0.5 LB_F THRUST CHARACTERISTICS
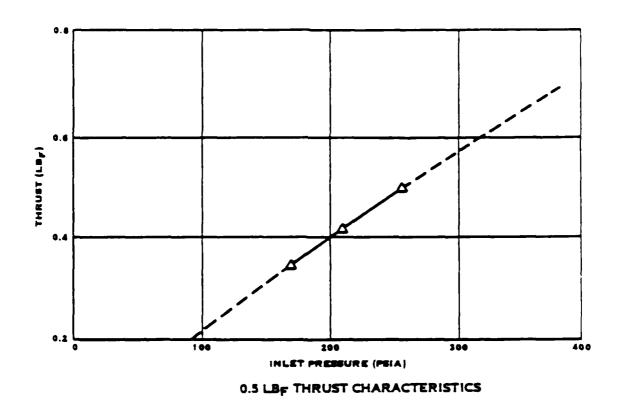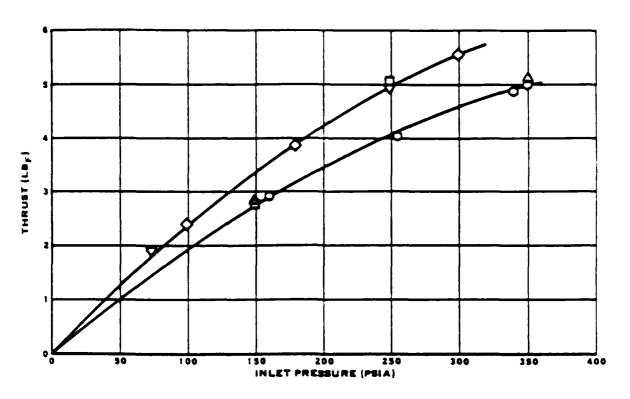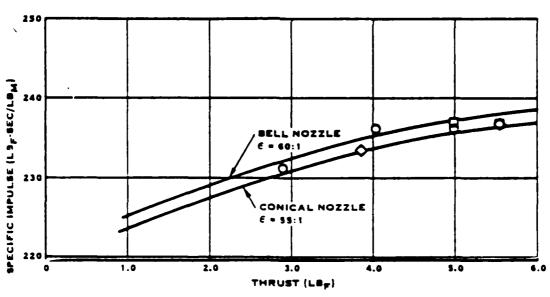
Figure 4-41b

Thrust Curves for Hamilton Standard C. Thrusters
(Hamilton Standard Co. Product Literature, 1986)

337

REA 16 THRUST CHARACTERISTICS WITH TWO DIFFERENT CALIBRATION ORIFICES
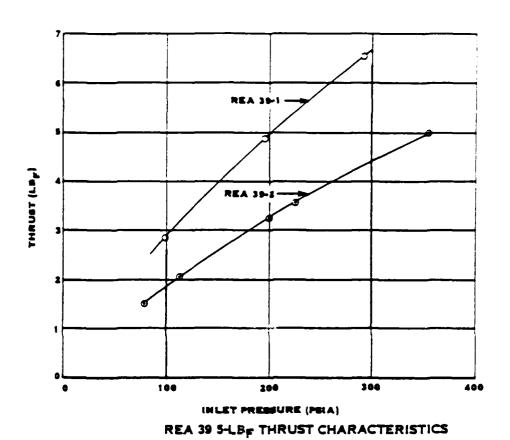
REA 16 STEADY STATE IMPULSE PERFORMANCE

Figure 4-41c

Thrust Curves for Hamilton Standard C. Thrusters
(Hamilton Standard Co. Product Literature, 1986)

338

REA 39 5-LB$_F$ THRUST CHARACTERISTICS
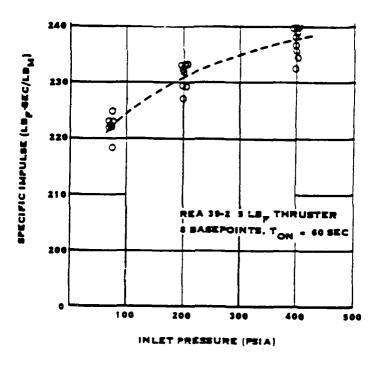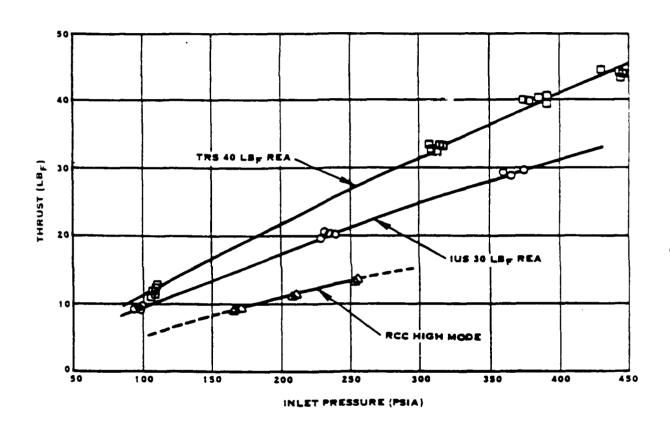
Figure 4-41d

Thrust Curves for Hamilton Standard C. Thrusters
(Hamilton Standard Co. Product Literature, 1986)

Figure 4-41e

Thrust Curves for Hamilton Standard C. Thrusters
(Hamilton Standard Co. Product Literature. 1986)

340
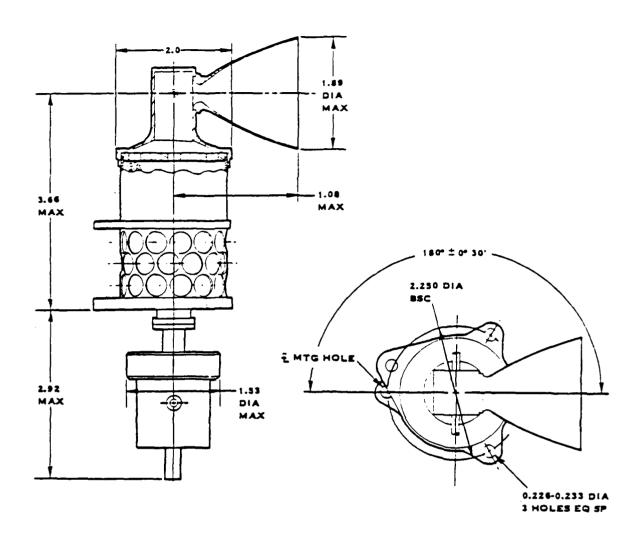
Figure 4-42

Hamilton Standard 12 lbf Thruster - Model REA 22
(Hamilton Standard Co. Product Literature, 1986)
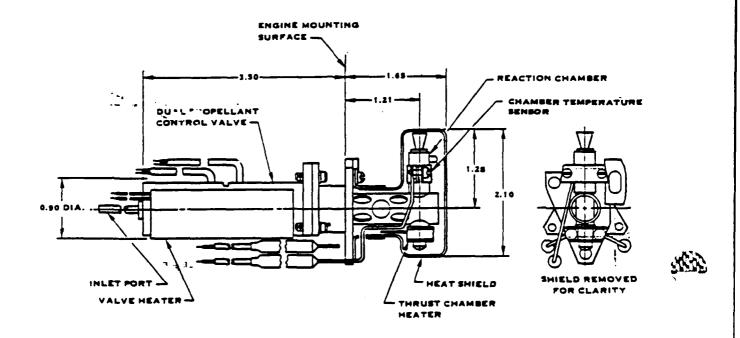
Figure 4-43

Hamilton Standard 0.1 lbf Thruster — Model REA 10-22
(Hamilton Standard Co. Product Literature, 1986)

342
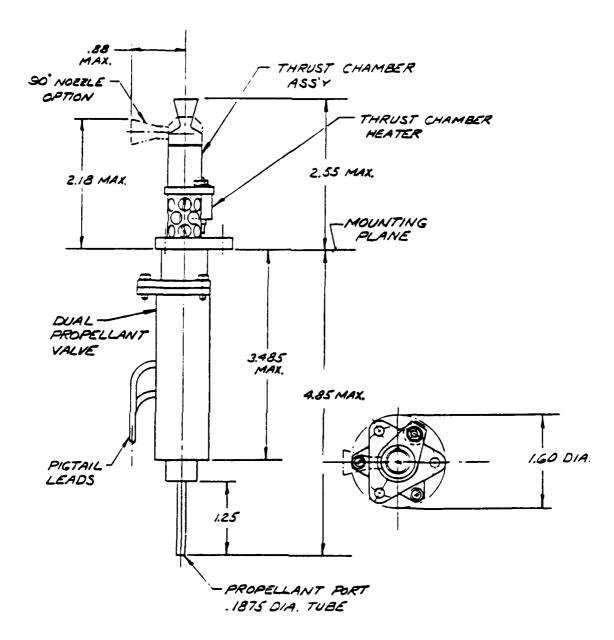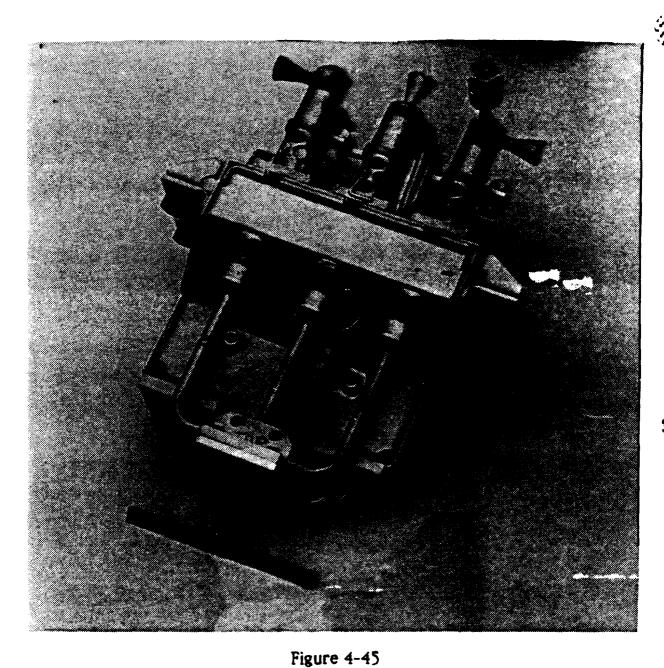
Figure 4-44

Hamilton Standard 0.4 lbf Thruster - Model REA 17-7
SEASAT Attitude Control Cluster

Figure 4-45

Hamilton Standard 0.4 lbf Thruster - Model REA 17-7
SEASAT Attitude Control Cluster
(Hamilton Standard Co. Photograph)

The auxiliary propulsion requirements could be satisfied using the REA-10 or REA-17 series engines. The REA10-22 is a 0.1 to 0.3 lbf thruster operating over an inlet pressure range of 70 to 350 psi. It is available in both a straight and angled nozzle configuration. The latter variety is 5.15" long and 2.1" in diameter and weighs 0.63 lbm. Of the REA17 series, the REA17-7 is a straight or angled nozzle thruster available in a three engine cluster as well as individually. The three engine cluster is marketed as part of the SEASAT program. Thrusts of 0.3 to 0.5 lbf are possible over an inlet pressure range of 100 to 300 psi. This thruster, like the REA10 series, has an excellent pulsed mode capability. A single REA17-7 unit is 7.4" long, 1.6" in diameter and weighs 0.68 lbm. Any of the Hamilton Standard engines will cost $35-45,000 each in lots of 3-6, with delivery times of 12 to 18 months.

TRW manufactures relatively few hydrazine thrusters in comparison to Rocket Research or Hamilton Standard. For the primary propulsion application. TRW offers a model MRE-5 or MRE-4. The MRE-5 is a 3 to 5 lbf unit operating over an inlet pressure range of 100 to 300 psi. This engine was last produced in 1984. It measures 8.2" long by 1.4" in diameter. Note that it is limited to burn durations of less than 10 seconds. The MRE-4 produces thrusts of 1 to 4 lbf over a wider inlet pressure range (50-500 psi) with a demonstrated total impulse of 115000 lbf-seconds. The engine is produced in a 45 degree angle nozzle configuration. Auxiliary propulsion requirements could be satisfied using the model MRE-0.1. The total impulse of this unit is 16000 lbf-seconds, and it is the smallest of all thrusters

examined in the vendor survey (3.5 in. long, 0.75 in. diameter). Prices or production data were not available for the TRW models.

The performance of the thrusters identified in the vendor survey are summarized in Tables 4-26 and 4-27. Of the primary propulsion thrusters, the Rocket Research Co. models MR-107E and MR-50R, and the Hamilton Standard models REA22 and REA39-2 are identified as the best thruster candidates. The REA39-2 would require modification for use in a right angle nozzle configuration. This choice of thrusters represents a selection from each of the major suppliers in the 5 to 12 lbf thrust categories. Rankings of the thrusters are provided indicating the preference for a high thrust, small, lightweight engine in a current production status. The auxiliary propulsion data are summarized in a similar manner and the Rocket Research MR-103C, Hamilton Standard REA17-7 and TRW MRE-0.1 are the best candidates. The Rocket Research and Hamilton Standard engines are the most preferable on the basis of production currency. The TRW unit is the smallest (size) thruster available. The Hamilton Standard REA 22/REA 17-7 or the Rocket Research MR-107E/MR-103C combinations would be the best choices on the basis that their inlet pressure ranges are most compatible with the propellant tank design selected in the next section.

e. Subsystem Choices - Feed Components

All hydrazine thrusters utilize identical feed systems. The purpose of the feed subsystem is to provide propellant to the engine in a reliable fashion at a predetermined flow rate and pressure. The two broad categories of feed systems are "pump-fed" and "pressure-fed". Pump-fed systems utilize turbopumps to provide a propellant pressure head to the thruster. For

small systems. the dry weight subsystem mass of the pump-fed subsystem will be much greater than that of the pressure-fed subsystem. The point beyond which the turbopump subsystem is lighter occurs as a function of mission duration, propellant performance, and propellant density. The Air Force Rocket Propulsion Laboratory generally considers the tradeoff of the two systems to occur between 8000 to 12000 pounds of propellant weight. The pump-fed systems are more complex, more expensive and less reliable than a pressure-fed network. For our application, where simplicity and reliability are focal points of the design, a pressure-fed subsystem is the most logical choice.

The pressurized subsystem uses a gas to provide the means to expel propellant from the feed tank and to provide the pressure head at the thruster inlet. Pressure fed systems typically generate thruster chamber pressures in the range of 100 to 300 psi, whereas single stage turbopumps are commonly capable of up to 1000 psi. The tradeoff of low chamber pressure (and thus, low thrust) is considered acceptable for small vehicles where long life, and not the massive thrust of a launch vehicle, is the dominant design parameter.

Pressurized systems use one of two methods to displace the propellant from the storage tank. Missiles, launch vehicles, and some spinning spacecraft often utilize a simple gas/propellant interface where the force of gravity or centrifugal acceleration forces the propellant toward the tank outlet. When spin or acceleration cannot be relied upon, a positive expulsion tank must be used. Without the benefit of positive expulsion tanks in zero gravity, the fuel would not be forced to a tank outlet, and gas bubbles

would be ingested by the free floating propellant. Ingestion of gas causes fluctuations in the propellant performance and results in poor feed performance. Positive expulsion tanks are predominantly used in satellites. Several types of tanks exist, including bladder tanks, diaphragm, surface tension, piston and bellows tanks. Variations of these tanks exist for reusable and one time use options. Tank selection depends on the structural geometry of the vehicle, internal tank volume, the expulsion technology desired, and propellant compatibility with the tank materials.

(1) <u>Propellant Storage Subsystem.</u> All of the positive expulsion tanks listed above are barrier type tanks with the exception of the surface tension tank. A barrier tank uses some form of device to physically separate the propellant from the pressurizing gas. Use of a barrier device is advantageous; in addition to bubble-free propellant, such a tank provides:

(1) The elimination of chemical reactions between the pressurant and propellant by preventing contact between the two media.

(2) The elimination of absorption of the pressurizing gas in the propellant.

(3) The elimination of propellant loss due to propellant vaporization in the pressurant free space.

(4) The elimination of corrosion in the propellant tank and the pressurization subsystem through the prevention of propellant backflow into the pressurization subsystem lines.

(5) Control of propellant slosh with the added provision of accurate center of mass control.

(6) The means to accurately measure tank volume. (JPL TR 32-899, 1966, p. 15)
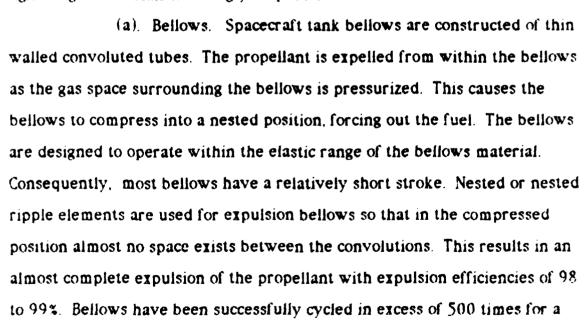
Five varieties of positive expulsion devices which are in use today for hydrazine subsystems are as follows:
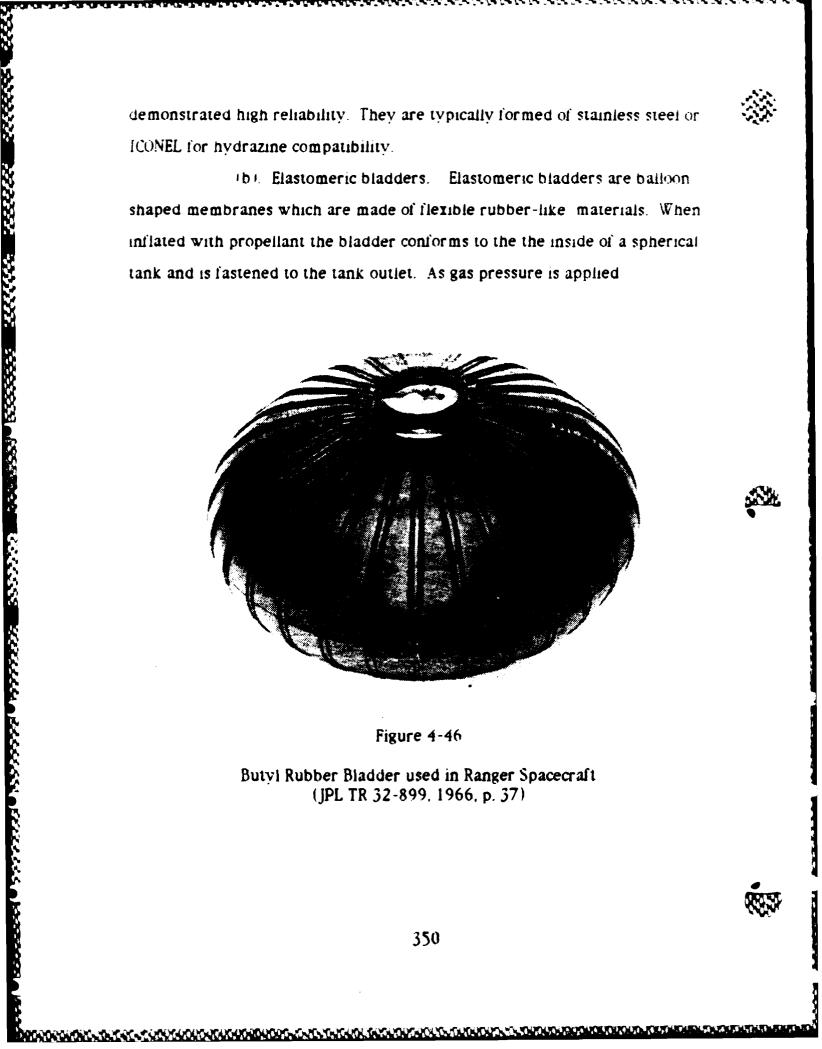
(1) Bellows
(2) Elastomeric/metal diaphragms
(3) Elastomeric bladders
(4) Surface tension tanks
(5) Pistons

The optimum shapes for propellant tanks are spherical or conospherical. These shapes are lower in weight than cylindrical tanks as a result of reduced stress. Consequently, elastomeric bladders, elastomeric/metal diaphragms, and surface tension tanks are the most commonly used. Piston devices do not lead to optimal use of storage volume or tankage mass and are rarely used. Spherical, (and to a lesser extent, conospherical and ellipsoidal) tanks are used almost exclusively in spacecraft propellant systems. Because the weight of spacecraft components is critical, the use of lightweight tanks and lightweight materials is strongly emphasized.

(a). Bellows. Spacecraft tank bellows are constructed of thin walled convoluted tubes. The propellant is expelled from within the bellows as the gas space surrounding the bellows is pressurized. This causes the bellows to compress into a nested position, forcing out the fuel. The bellows are designed to operate within the elastic range of the bellows material. Consequently, most bellows have a relatively short stroke. Nested or nested ripple elements are used for expulsion bellows so that in the compressed position almost no space exists between the convolutions. This results in an almost complete expulsion of the propellant with expulsion efficiencies of 98 to 99%. Bellows have been successfully cycled in excess of 500 times for a

demonstrated high reliability. They are typically formed of stainless steel or ICONEL for hydrazine compatibility.

(b). Elastomeric bladders. Elastomeric bladders are balloon shaped membranes which are made of flexible rubber-like materials. When inflated with propellant the bladder conforms to the the inside of a spherical tank and is fastened to the tank outlet. As gas pressure is applied

Figure 4-46

Butyl Rubber Bladder used in Ranger Spacecraft
(JPL TR 32-899, 1966, p. 37)

Figure 4-47

Filling Methods for Elastomeric Bladders
(JPL TR 32-899, 1966, p. 7)

to the outer surface of the balloon, the propellant is forced out of the flexible
bladder. Some residue is left in the bladder as the material collapses in two-
and three-corner folds. Mosher (1986) reports expulsion efficiencies of up to
98% although 90% may be more typical for stiff bladder materials. Cycle
limits of 100 to 200 cycles are typical of most elastomeric bladders due to
failures at the two- or three-corner folds. Figure 4-48 depicts a typical
collapsed bladder and the resultant folds. Bladder materials are carefully
chosen for long term monopropellant compatibility. In particular gas
permeability through the relatively thin membrane must be prevented.

351
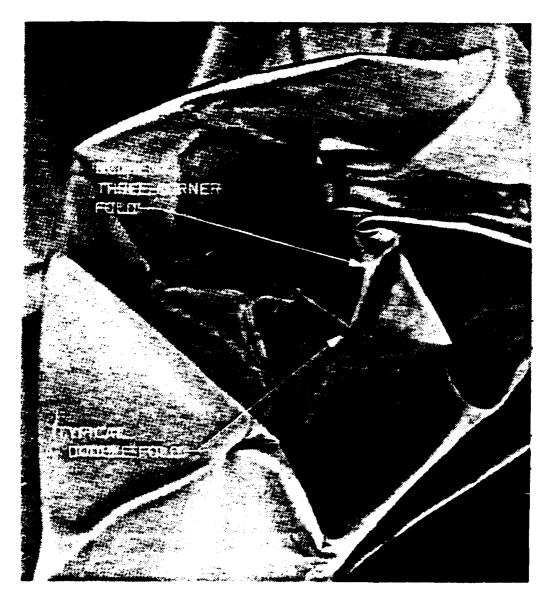
Figure 4-48

Double and Three-Corner Folds in a Bladder
(JPL TR 32-899, 1966, p. 9)
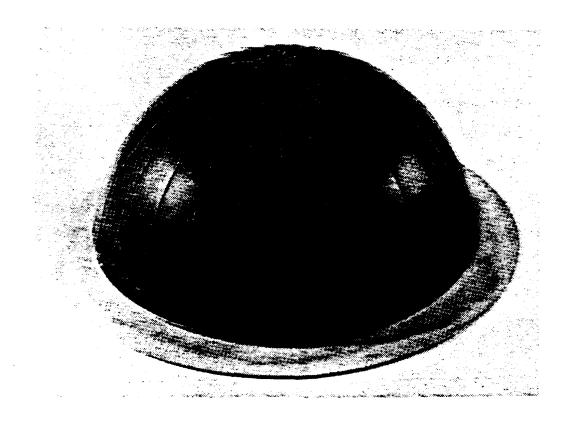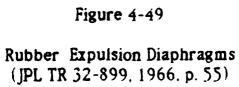
Also, hydrazine is readily decomposed by impurities and fillers such as carbon black that are common in rubber-like materials. Hence, the bladder material must be chosen carefully (JPL TR 32-862, JPL TR 32-899, 1966, p 22). Fabrication repeatability is a problem in the manufacture of any balloon-like device. Consequently, the reliability of elastomeric bladders is not as high as that of the aforementioned metal bellows.

(c). Diaphragms. The use of diaphragm positive expulsion devices represents a step toward eliminating the residue problem in positive expulsion tanks and the achievement of a 100% expulsion efficiency. A diaphragm is, ideally, a flexible surface that will expel any propellant through the effective displacement of the propellant volume. As an extensible membrane, it divides the tank into two compartments with the outer edge of the diaphragm attached to the inner surface of the tank. The shape of the diaphragm will begin as a mirror image of its final form, reversing midway through the expulsion. The diaphragm may also start at some intermediate snape and then fill the tank volume. The latter is known as a convoluted diaphragm. (JPL TR 32-899, 1966, p. 12). There are also dual diaphragms which expand in two directions about the mid plane of the propellant tank. Historically, diaphragm tanks were constructed of rubber or plastic due to the elasticity of those materials. However, recent developments by the ARDE Co. and others in the use of reversing and convoluted metal diaphragms have led to stainless steel expulsion barriers. The ARDE tanks are unique in their use of conospherical shapes to provide a volume for greater extension of these reversing convoluted diaphragms. Figure 4-50 demonstrates the extension process for an ARDE conospherical tank. Figure 4-51 depicts the flat convoluted metal diaphragm which expands to one half of a tank volume

353

Figure 4-49

Rubber Expulsion Diaphragms
(JPL TR 32-899, 1966, p. 55)
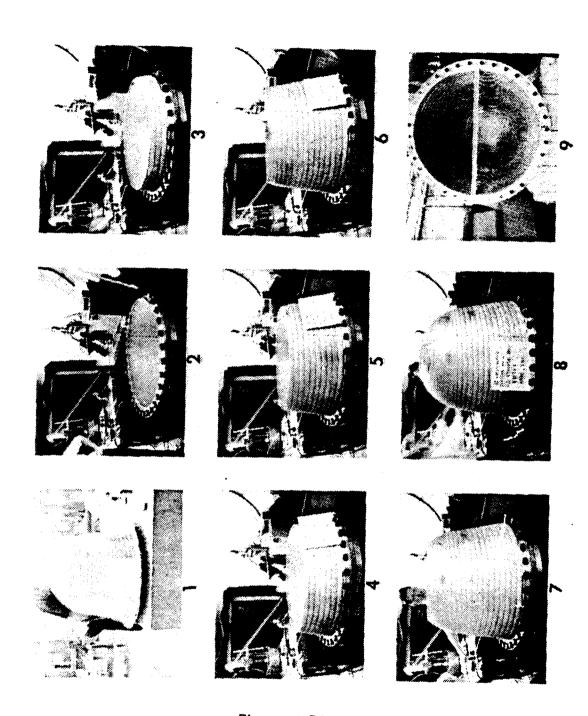
Figure 4-50a

Detail of ARDE Co. Metal Diaphragm
Reversing Model
(ARDE Co. Photograph)
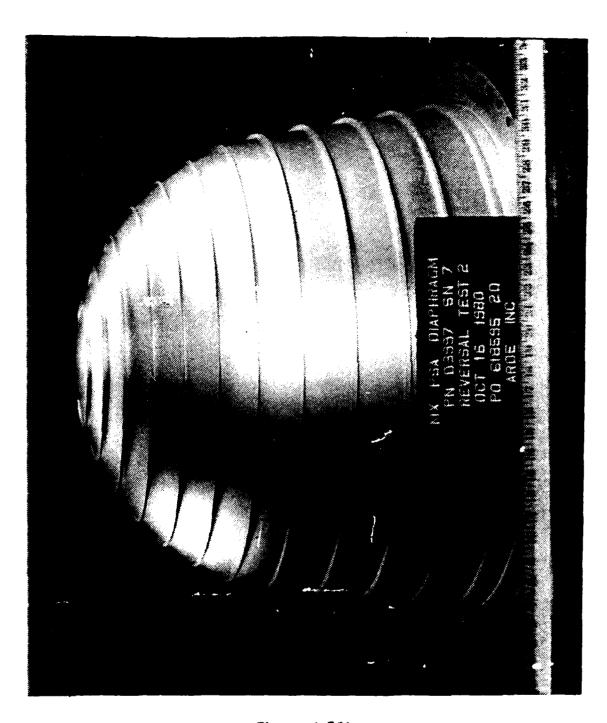
Figure 4-50b

ARDE Co. Conospherical Expulsion Diaphragm
Mirror Image Expulsion Process
(ARDE Co. Photograph)

356

FLUID OUTLET PORT

DIAPHRAGM FINAL POSITION AT END OF FLUID EXPULSION

INTERMEDIATE DIAPHR. A POSITION

DIAPHRAGM INITIAL POSITION

DIAPHRAGM REINFORCING RINGS

PRESSURANT PORT

TANK
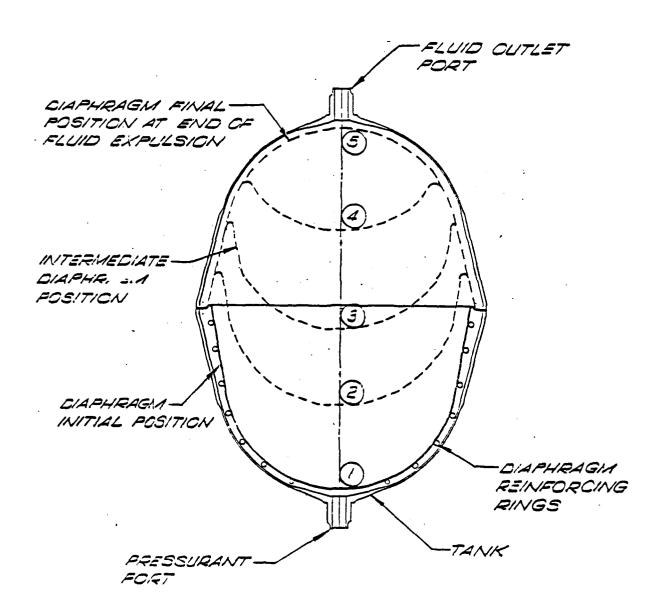
Figure 4-50c

Conospherical ARDE Co. Tank Diaphragm Positions
(ARDE Co. Promotional Literature, 1986)

357
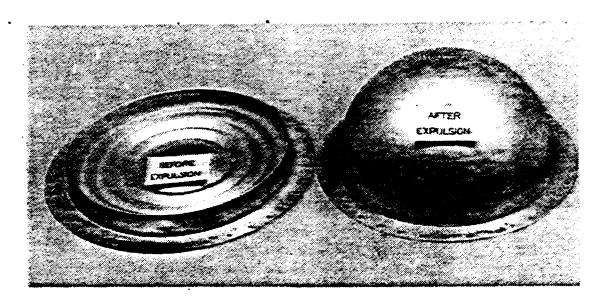
Figure 4-51

Hemispherical Convoluted Metal Diaphragm
Before and After Expulsion and After Refill Attempt
(JPL TR 32-899, 1966, P. 29)

This barrier is not recyclable. Although the metal diaphragm can be made
to reverse upon itself, it is not cyclable and is therefore not subject to cyclic
testing or reuse. Despite that fact, the use of metal diaphragms provides the
advantages of propellant compatibility and long life. Butyl rubber
diaphragms, while less resistant to highly reactive propellants, have been the
most commonly used due to their ease of reversal and subsequent recycling.
Woodruff (1972, p. 171-182) provides an excellent supplemental discussion
of diaphragm tanks, as does SSD-TDR 62-172 (1962, pp. 183-221). For more
detail in the analytical techniques of diaphragm design, consult Hulber, Keith
and Trainer in AFRPL TR 66-181 (1966).

(d). Surface tension devices. A surface tension positive
expulsion device consists of a fine mesh screen, capillary tubes, or closely

358
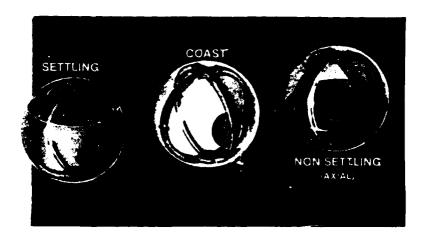
Figure 4-52
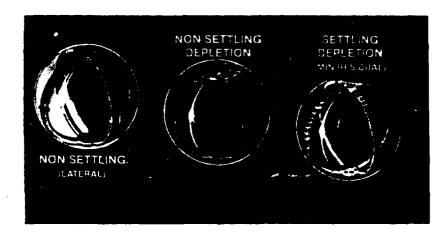
Lockheed Surface Tension Tank in Cross Section
(Reproduced from Lockheed Co. Product Literature)

359

Figure 4-53

Lockheed Propellant Management Subsystems
(Reproduced from Lockheed Co. Product Literature)

PISTON FLUID
FILL & BLEED

AIR BLEED FOR FILL

11.88

46.26 PISTON STROKE

GAS FOR PUSHING PISTON
EXPELS HERE AT END OF
PISTON TRAVEL

Figure 4-54

Experimental WAC CORPORAL Piston Tank
(JPL TR 32-899, 1966, P. 53)

361
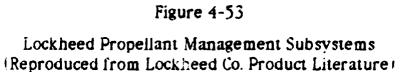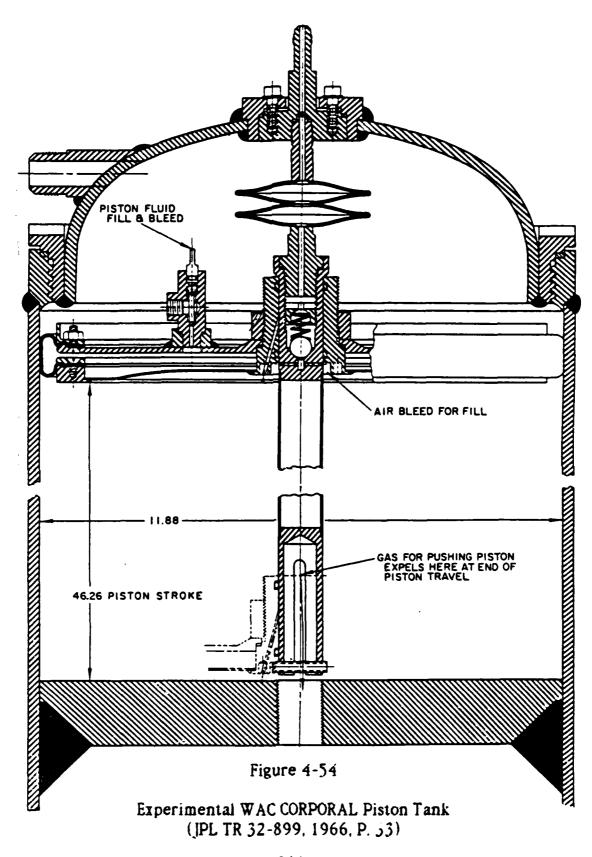
spaced baffles which use the forces due to propellant fluid surface tension to position a portion of the liquid adjacent to the tank outlet. This is a convenient method for use in situations which do not demand a rapid propellant feed rate. These types of tanks also separate the pressurization gases from the propellant and prevent premature exit of the pressurant gases prior to propellant depletion. Although this tank has application in certain instances, it is generally a more expensive component than the others listed so far. Use of the surface tension concept is especially valuable for tank geometries which are not suited to the use of bladders or diaphragms. For example, ellipsoidal and cylindrical tanks can be easily configured with surface tension fluid management devices. Expulsion efficiencies of 98% are attainable. Only recently have the life expectancies and reliabilities of surface tension tanks been competitive with the elastomeric expulsion devices.

(e). Piston devices. In a piston type tank, a rigid body is forced to travel the length of a cylindrical tank, expelling all of the propellant ahead of it. The piston can be sealed to the tank wall by rings or bellows. Except where special metal seals are incorporated, the piston unit is inherently recyclable. However, a piston-type tank is the most massive of the tank designs presented. A cross section of the WAC CORPORAL tank is shown for reference.

In summary, the elastomeric and reversing convoluted metal diaphragm tanks have the least weight. Many metal diaphragms are not recyclable. For the ORION application, recyclability is a design constraint in so far as the satellite should be configured for possible refueling on-orbit. Additionally, it is difficult to ascertain the reliability of a barrier device that

362

cannot be cycled. The elastomeric diaphragm is the most common expulsion barrier in use. It is also the least expensive and most reliable. The surface tension tank is inherently reliable but is also very expensive. The final choice of a tank design will be mission and vendor dependent, as it is not desired to develop new products for this ORION design. Hence, with a knowledge of expulsion device designs, the selection of an appropriate commercial product follows. Table 4-27 summarizes the performance of diaphragm, bladder, and surface tension tanks as a function of various criteria.

TABLE 4-27

COMPARISON OF HYDRAZINE EXPULSION METHODS
(Sutton, 1976, p. 312)

	Positive Expulsion Devices			
Selection Criteria	Elastomeric Diaphragm (hemispherical)	Inflatable Elastomeric Bladder (spherical)	Metallic Diaphragm (hemispherical)	Surface Tension Screens
Application history	Extensive	Extensive	Limited	Extensive in short-life satellites None in long-life satellites
Weight (normalized)	1.0	1.1	1.2	0.9
Expulsion efficiency	Excellent	Good	Fair	Good†
Long service life	Excellent	Excellent	Excellent	Unproven
Preflight check	Leak test	Leak test	Leak test	None

(2). <u>Analysis of a Propellant Storage Subsystem</u>. The delta-V
requirement of the propulsion subsystem needed to propel the satellite to a
1500 km circular orbit has been determined to be 641 m/s (2102 ft/sec).
Using the relationship

$$M_p = M_0(1 - e^{-(deltaV/(ISP)(G))})$$ \hfill (4.12)

and an assumed actual ISP of hydrazine of 220 seconds, the total primary
propulsion (delta-V) hydrazine requirement is determined to be 64.3 lbm.
The auxiliary propulsion requirement was determined in Chapter Five to
be 1200 lbf-seconds. This requirement corresponds to an additional 5.5 lbm
of hydrazine. Hence, a total of 69.81 lbm of propellant is required. The
density of hydrazine is 63 lbm-ft^{-3} at 62° F. At 40°F the material is slightly
more dense, being approximately 63.5 lbm-ft^{-3}. Assuming a conservative
fuel density of 63 lbm/ft^3, the total volume required to store 69.8 lbm of
propellant is 1.108 ft^3 (1915 in^3). Assuming a typical expulsion efficiency of
0.98 the total interior tank volume must then be

$$V = Propellant \ volume \ / \ efficiency$$ \hfill (4.13)

Hence, a positive expulsion tank must be chosen which is capable of storing
1954 in^3 of propellant. This volume assumes that:

(1) A maximum circular orbital altitude of 1500 km must be achieved.

(2) Both the primary and auxiliary propulsion systems are hydrazine
    propelled.
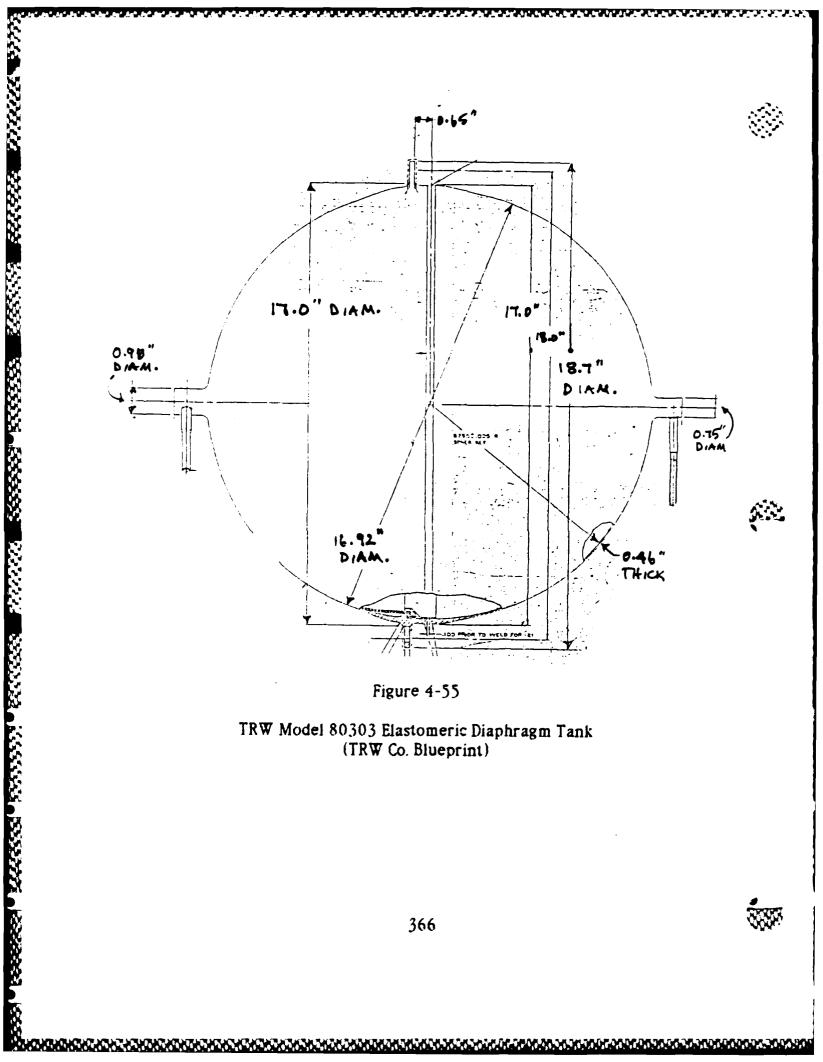
(3) The two propulsion systems use a common tank.

(4) Every ORION mission will not require the same fuel load. Smaller amounts of fuel may be carried on other missions. The tank should accommodate variable propellant loads easily. It should utilize a reliable positive expulsion device with a high expulsion efficiency

(5) The maximum outside diameter of the satellite is 19" and the tank should fit this restriction while occupying a small vertical dimension.

A vendor survey of available positive expulsion tanks was conducted. The results of this survey indicated that there are five companies actively involved in the manufacture of positive expulsion tanks. They are the TRW Co. subsidiary PSI (Pressure Systems Inc.), the ARDE Co., Bell Aerospace-Textron, Martin Marietta Co., and Lockheed Co.. The last two companies manufacture surface tension tanks exclusively and provided some details on their line of products. The ARDE and PSI companies each exhibited an active interest in the ORION program development. Bell Aerospace-Textron declined to participate in the design study.

The TRW PSI tanks use elastomeric diaphragms or surface tension devices. Most of the tanks sold by this company are spherical. The ARDE Co. uses both spherical and conospherical tanks equipped with either elastomeric diaphragms or convoluted metal diaphragms. Upon review of the vendor data, it was noted that the TRW PSI tank model 80303 provides 1963 in^3 of usable storage volume. The mass of this 16.5" diameter tank is 13 lbm and the maximum pressure is 340 psi. Four mounting bosses allow the tank to mount to a set of hard points at the tank midline on 90° centers. Other spherical tanks lack internal volume or have an excessively large outer

Figure 4-55

TRW Model 80303 Elastomeric Diaphragm Tank
(TRW Co. Blueprint)

diameter. The 80303 elastomeric diaphragm tank is currently being
manufactured for the Global Positioning Satellite program (GPS) and has been

Volume _____ 2060 inch^3 _____ $P_o/P_p/P_b$ _____ 600 _____ 900 _____ 1200 _____

Weight _____ 18.5 lbs. _____   Gas/Propellant Nitrogen/Hydrazine _____
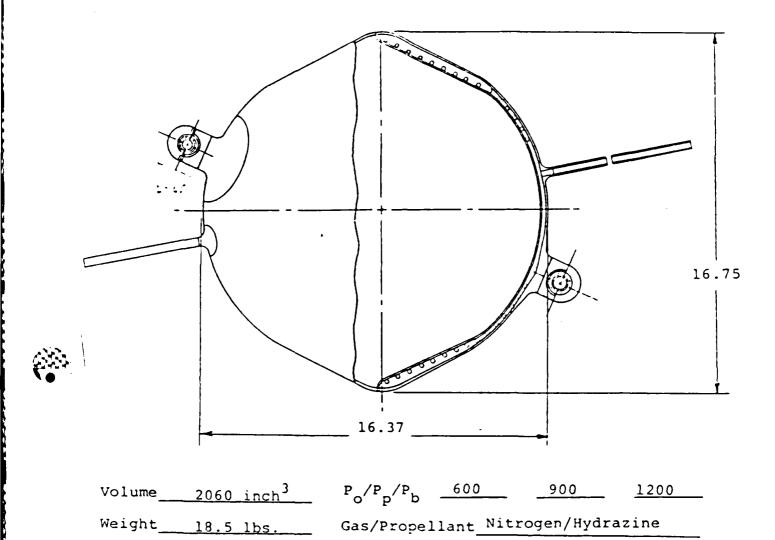
Figure 4-56

ARDE Co. Model E3840/56006
Convoluted Metal Diaphragm Positive Expulsion Tank
(Reproduced from ARDE Co. Sales Literature, 1986)

367

17.90

| Volume | 2775 inch^3 | $P_o/P_p/P_b$ | 350 | 525 | 700 |
| Weight | 18.8 lbs. | Gas/Propellant | | Hydrazine/Freon 13B | |
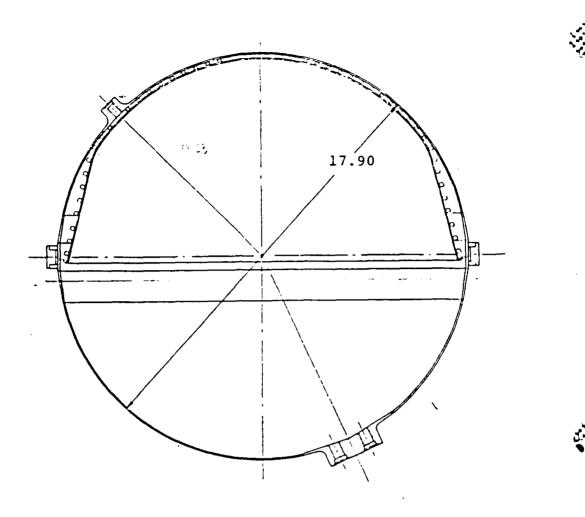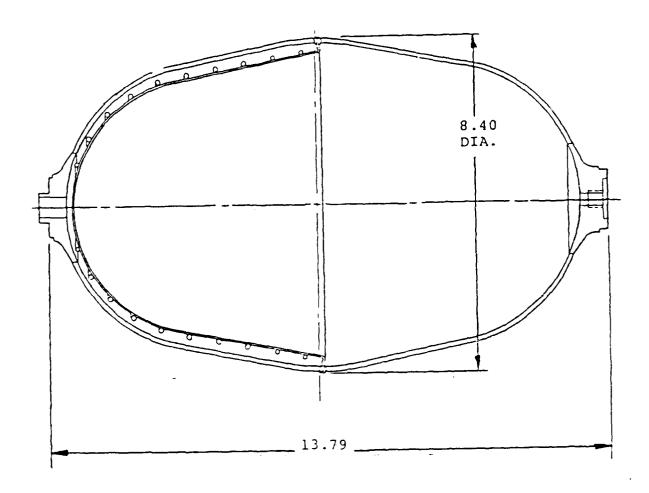
Figure 4-57

ARDE Co. Model E3848/56007
Convoluted Metal Diaphragm Positive Expulsion Tank
(Reproduced from ARDE Co. Sales Literature, 1986)

Volume 435 inch^3 $P_o/P_p/P_b$ 525   787   1050

Weight 11.25 lbs.   Gas/Propellant Helium or Nitrogen

Figure 4-58

ARDE Co. Model E3940/36002
Conospherical Metal Diaphragm Hydrazine Tank
(Reproduced from ARDE Co. Sales Literature, 1986)

purchased in lots of 50 by the Rockwell Co. of Los Angeles. CA. Procurement of this tank requires a minimum of retooling at TRW. In block purchases of three tanks, the tank will cost \$48,000 each. Delivery time, excluding environmental testing, is one year from receipt of order.

The ARDE Co. supplies two tanks which are good candidates for the ORION program. The Model E3840/56006 is a 2060 in^3 spherical tank. operating at pressures of up to 600 psi, has a 16.85" diameter. The model E3848-56007 is a 2775 in^3 tank has a 17.9" outer diameter and an operating pressure of 350 psi. Of the two, the E3840 is a better choice for ORION due to the higher operating pressure and smaller vertical clearance. ARDE also manufactures smaller tanks which could be arrayed to provide some propellant storage capacity, although not the required 1953 in^3. Up to 1305 in^3 could be provided using three of the model E3940/36002 conospherical tanks. These could be mounted on 120° centers, spanning 13.8" of vertical dimension in the satellite cylinder. These tanks are not in production for a current program but are available within 18 months of request.

The aforementioned tanks are depicted in Figures 4-55, 4-56, 4-57 and 4-58. The Lockheed and Martin Marietta surface tension tanks were not considered for ORION due to the extra expense of those tanks relative to the elastomeric tanks. However,these tanks are worthy of additional consideration when specific mission requirements and financial constraints favor the use of surface tension devices. Of the four tank designs mentioned above, the PSI Co. model 80303 is considered the best candidate. This choice is based upon the ability to use a single tank for the propellant storage while maximizing the use of the satellite inner diameter. This is also
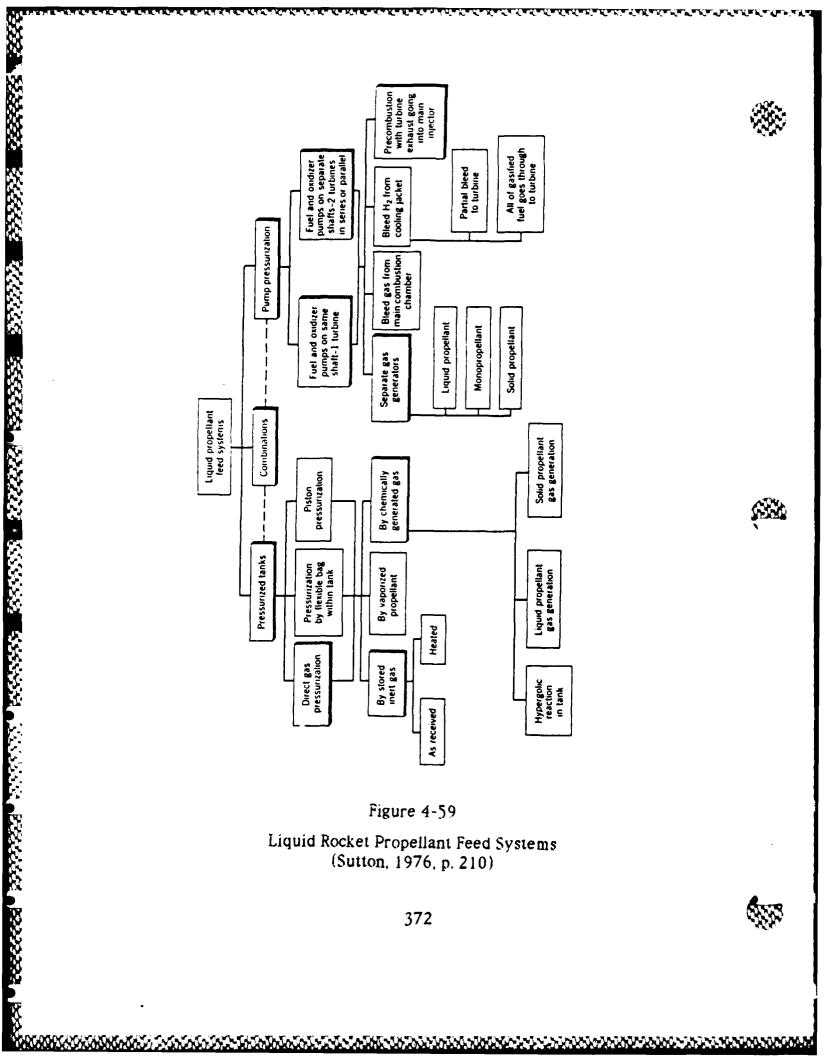
the lightest of the full capacity tanks. The mounting scheme for this tank is the simplest of the four considered. This is the only tank which is known to be in production. Use of readily procurable propulsion products that are currently in production is emphasized in the selection process of this thesis.

(3). **Pressurized Feed Subsystem.** Simple pressurized feed systems for the expulsion of fuel from the propellant tank are the logical choice for a small, compact satellite. Pressure fed propellant feed networks are to be preferred over the use of pump fed systems. Four methods currently used for the pressurization of a propellant tank are:

(1) Stored cold gas using nitrogen, argon, helium, freon or neon.

(2) Heated gas in which a stored cold gas passes over a heat exchanger prior to pressurizing the propellant tank.

(3) Hot gas generators which use solid or liquid combustibles for the production of hot pressurant gases.

(4) Autopressurization in which the vapor pressure of the fluid in the propellant tank provides the force to expel the propellant from the tank.

Of these four methods, pressurization using cold gas is the least costly, most reliable, and most commonly used. Heated gas is an effective means of pressurizing the propellant using smaller gas volumes but requires the consumption of considerable heater power. Gas generators are used when very little storage space is available for the pressurant. Use of a generator allows the pressurant gas to be stored as a high density combustible fluid or solid form. Hydrazine is often used as a fuel in gas generators. Autopressurization is less dependable than the other methods because the

371

Figure 4-59

Liquid Rocket Propellant Feed Systems
(Sutton, 1976, p. 210)

372

vaporization of the propellant is a strong function of temperature. For hydrazine systems, the stored gas method of pressurization is most highly favored due to its simplicity and resultant reliability.

To obtain the desired pressure history in the propellant tank using cold gas there are, again, several alternatives. With respect to the flow of the pressurant gas, the pressurization options involve:

(1) Variable mass flow
(2) Decreasing mass flow
(3) Constant mass flow
(4) No mass flow

Variable mass flow implies that the pressure of the pressurant gas is regulated at some fixed value to provide a fixed pressure head at the propellant tank outlet. Using decreasing mass flow, or an orifice blow down subsystem, the pressure drops as the pressurant gas occupies an increasingly larger volume during expulsion of fuel from the propellant tank. For hydrazine systems, blowdown ratios of up to 8:1 (initial pressure to final pressure) are not uncommon. The gas is supplied from a source external to the propellant tank. A constant mass flow subsystem combines a fixed orifice and regulator for the most precise control of the propellant output pressure. Using polytropic expansion, or "no mass flow", the propellant tank is prepressurized, and the pressurant gas is allowed to expand within the propellant tank volume as fuel is expelled. An external pressurant supply is not used.

The simplest and most reliable means of pressurizing the propellant tank is to use the "no mass flow" method. However, a regulated (variable or constant mass) output would be advantageous for the purpose of

373

maintaining a constant fuel pressure, and thus a constant thrust. An external gas supply and a regulator is required to implement such a subsystem. Unfortunately, regulators and valves decrease the reliability of any feed subsystem. Regulators will tend to fail open and must be configured in dual or quad connections to circumvent their failure mode. A regulated supply might be acceptable, however, because the "no mass flow" (polytropic expansion) method, while highly reliable, is often insufficient to expel the fuel at the desired pressures near the end of the expulsion process. When the majority of the fuel has been expelled using "no mass flow", the gas pressure in the expanding volume has been reduced to a fraction of its original value. Maintaining a high final expulsion pressure and simultaneously limiting the starting pressure to a reasonable value for a "no mass" flow application is difficult. Blow-down subsystems which vent directly from a storage container to the fuel tank without a regulator are the most reliable and the most commonly used for satellite applications. This method circumvents the problem of regulator reliability but also provides little control of pressure. Flexibility in the selection of initial and final tank pressures is provided through the choice of storage container volumes and pressures. The orifice blowdown method is not well suited to very large volume applications, such as in launch vehicles, due to the large volume of gas required to pressurize the fuel mass. However, for small applications such as ORION, a blowdown pressurized feed subsystem is ideal.

Ring (1964, pp. 192-193) points out that "at the outset it should be recognized that an optimum pressurization subsystem requires a high density pressurant storage and a low molecular weight gas." In general, the most desirable characteristics of pressurants are:

(1) Low molecular weight.

(2) Low specific heat ratio.

(3) High density storage which leads to low tankage weight.

These considerations are the same as those expressed as desirable for the propellant gas in section C.1. From the analysis in that section, we recall that nitrogen or Freon-14 is favored for use as a pressurant gas. Each of these gases is common in the pressurization of positive expulsion tanks.

(4) <u>Analysis of a Pressurized Feed Subsystem</u>. The purpose of a pressurization subsystem is to provide and control the gas pressure in the gas space of a propellant tank and thereby control the propellant feed pressure. This gas space is known as the ullage. A pressurization subsystem maintains the ullage at a preselected pressure history bounded by the thruster inlet feed pressure and storage tank structural requirements.

Propellant feed requirements are commonly expressed in terms of a "net positive suction head" (NPSH). This is defined as the total pressure at the thruster inlet minus the losses and the vapor pressure at the injector inlet. The tank pressure required to supply this NPSH is defined by

$$P_{tank} = NPSH + \text{Feed line frictional loss} + \text{vapor pressure} \quad (4.14)$$

The vapor pressure of hydrazine, as seen in Figure 4-51, is inconsequential at the tank temperatures normally encountered in space (70° F +/- 30° F). Hydrazine vapor pressure is a dominant factor in the previous equation only at thruster combustion chamber temperatures. It is not a factor in feed line pressure analyses. Likewise, the pressure loss due to friction is less than 1.0

375
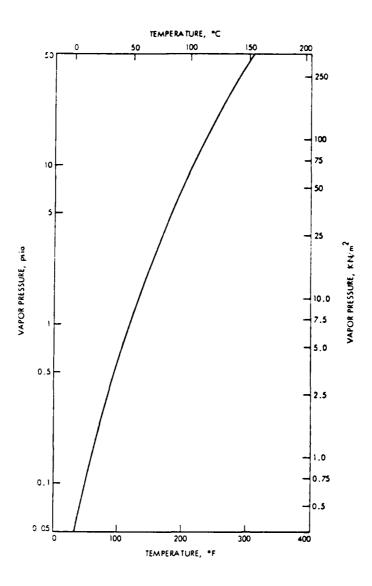
Figure 4-60

Vapor Pressure of Anhydrous Hydrazine
(JPL TR 32-1560, 1972, p. 5)

376

psi as a result of the non-regulated flow and the very short feed lines. As a result, NPSH can be equated to tank pressure in this subsystem with adequate accuracy.

Note that in a pressurized feed subsystem, the engine thrust is directly proportional to the thruster inlet pressure and, therefore, the tank pressure. Control of tank pressure and a predictable pressure history is critical to successful propulsion operations. In a pressure blowdown subsystem, the thrust will vary as the gas pressure decreases during fuel expulsion. The escaping fuel increases the gas volume within the propellant tank, and the fixed mass of gas expands with a corresponding pressure drop. Hence, regulation of the pressure is not possible and knowledge of the pressure history is required for the estimation of thrust. Pretesting and the use of pressure transducers permits prediction of thrust.

The volume of gas required to pressurize the tank can be approximated based upon the following assumptions:

(1) The temperature of the expanding gas is constant. This assumption is valid if heat is added to the propellant tank using external heaters. The heat input cancels the cooling effect caused by the expanding gas thus maintaining the isothermal relationship.
$T_{initial} = T_{propellant} = T_{gas} = T_i = T_p = T_g$

(2) The initial gas pressure (P_{gi}) is known.

(3) The propellant blowdown ratio (initial press./final press. $= P_{pi}/P_{pf}$) is known.

(4) Hydrazine is an incompressible fluid.

(5) The initial tank ullage (V_{pi}) is 340 in^3 for the TRW PSI 80303 positive expulsion tank. The total tank volume is 2300 in^3

(6) The tank ullage is initially unpressurized ($P_{p0} - 0$).

(7) The pressurant is an ideal gas.

(8) The propellant tank initial maximum operating pressure (P_{pi}) is 340 psi.

To accomplish the blowdown the propellant tank is pressurized by the opening of a pyrotechnic valve which is located between the storage bottle and the propellant tank. The gas in the storage bottle will be distributed between the storage bottle volume (V_g) and the ullage volume and the initial gas bottle pressure (P_{g0}) will decrease. Using the gas law relationship PV - nRT, we can state that

$$\frac{P_{initial} V_{initial}}{n R T_{initial}} - \frac{P_{gas} V_{gas}}{n R T_{gas}} + \frac{P_{propellant} V_{propellant}}{n R T_{propellant}} \qquad (4.15)$$

All variables refer to the pressurant gas in the respective tanks. R, n and T are assumed to be constant, where n is the number of moles pressurant gas, R is the individual gas constant of the pressurant, and T is the temperature of the pressurant. Combining the pressures and volumes of the pressurizing gas in the gas tank and the fuel tank, we have

$$P_{g0} V_g - P_g V_g + P_p V_{pi} \qquad (4.16)$$

The pressure in the storage bottle is assumed to reach equilibrium with the pressure in the ullage ($P_g - P_p$). Therefore,

378

$$P_{g0}V_g = P_g (V_g + V_{pi}) \qquad (4.17)$$

For the TRW PSI 80303 tank, the ullage (V_{pi}) is 340 in^3, or 0.1967 ft^3. The maximum operating pressure of the 80303 tank is 340 psi. This pressure is acceptable for use with the MR107 series thrusters (e.g., MR 107B) and all Hamilton Standard thrusters. Discussions with engineers at the Rocket Research and Hamilton Standard companies indicate that any of the auxiliary propulsion thrusters would function without degradation at an initial inlet pressure of 340 psi. Therefore, $P_{pi} = 340$ psi. The final pressure of the fuel tank, at the moment that it is emptied, is based upon the lowest acceptable inlet pressure for the thrusters. Discussions with the thruster vendors indicated that the reduction of inlet pressures below those in the vendor data would not adversely affect the thruster performance. Low inlet pressures may degrade the pulse repeatability of the small thrusters and will cause some fluctuation in the performance of the primary propulsion thruster (12 lbf +/- 4 lbf at 70 psi inlet pressure). Accurate primary propulsion burns will be required near the beginning of the satellite mission when the pressure is high and the thrust is predictable. The propellant tank pressure will be within the normal range of inlet pressures for the primary thruster at that time, and a pressure range of 340 psi to 70 psi is considered to be reasonable. The blowdown ratio is therefore 340/70 = 4.857.

With a knowledge of the pressure boundaries, the blow down ratio and the intial ullage volume, the storage bottle volume (V_g) and the initial storage bottle pressure (P_{gi}) can be determined. Using two simultaneous equations, these two unknowns can be solved for the initial and final fuel tank pressures.

$$P_{gi}V_{gi} = P_g V_g + P_p V_p$$

$$V_{gi} = V_g = \text{Pressurant storage bottle volume}$$

$$P_{gi} V_g = 340 V_g + 340 V_{pi}$$
$$P_{gi} V_g = 70 V_g + 70 V_{pf}$$

$$V_{pi} = 340 \text{ in}^3$$
$$V_{pf} = 2300 \text{ in}^3$$

$$340 (V_g + 340) = 70 (V_g + 2300)$$

$$V_g = 168.15 \text{ in}^3$$
$$P_{gi} = 1027.5 \text{ psi}$$

Alternatively, the equations can be combined into the following form:

$$P_{g0} = P_{gi} [(P_{gf} (V_{pf} - V_{pi})) / (P_{gf}V_{pf} - P_{gi}V_{pi})] \qquad (4.18)$$

From the equations above, for the isothermal assumption, an initial pressure of 1027.5 psi in a tank of 168 cubic inches provides the necessary volume to pressurize the propellant tank ullage. The ullage pressure begins at 340 psi and decreases to 70 psi at the end of propellant expulsion. This pressure/volume combination can be improved, however, by accepting an even lower final pressure to reduce the storage volume of the gas. Note that, of the pressurant tanks described in the text, the TRW PSI tank 80075-1 provides 85 in^3 of storage volume. Two of these 2.6 lbm tanks will provide all of the needed pressurant storage. The tank diameter is 5.7"; a smaller tank would be desirable for the purpose of nesting closely to the main hydrazine tank. The ARDE Co. manufactures a 28 in^3 high

10.0

.62

2.29

Volume __28 inch³__ $P_o/P_p/P_b$ __10,000__ __15,000__ __18,000__

Weight __1.54 lbs.__ Gas/Propellant __Nitrogen__

Material __Cryoformed 301 CRES__
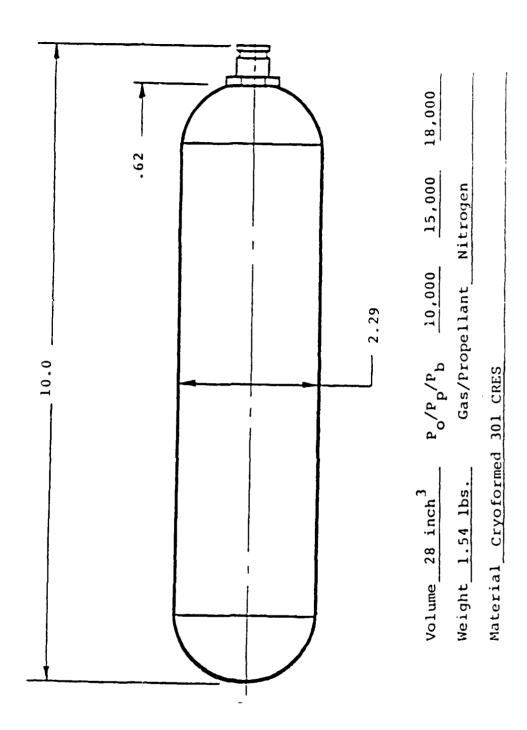
Figure 4-61

ARDE High Pressure Gas Resevoir
(Reproduced from ARDE Co. Sales Literature, 1986)

pressure cylindrical oxygen bottle that could also be used. These tanks are 2 in diameter and 12.3" long. Two such cylinders (56 in^3 total) would fit snugly below the large spherical propellant tank. With $V_g = 56$ in^3, the equations above indicate that an initial pressurant pressure of 2404 psi yields the initial propellant tank pressure of 340 psi. The final propellant tank pressure will then be 57.15 psi. Some degradation in attitude control thruster accuracy is to be expected as the last fuel is expended and the final gas pressure drops below 70 psi.

Attacking the problem from the other direction, the necessary storage bottle pressure can be derived to yield a final propellant pressure of 70 psi. In this case, for a 56 in^3 pressurant storage, the required initial pressurant pressure is 2945 psi. As before, note that the initial pressure of the propellant tank is no longer constrained to 340 psi. For a final propellant pressure of 70 psi and a pressurant storage volume of 56 in^3, the initial propellant pressure is <u>416 psi</u>. This exceeds the allowable operating pressure of the hydrazine tank. Therefore, the tradeoff is as follows: to achieve the initial and final fuel pressures (340 and 70 psi respectively), a relatively large storage bottle volume is required (168 in^3). If a lower final fuel pressure is acceptable (57 psi), then a much smaller pressurant storage volume can be utilized (56 in^3). The initial operating pressure limitation of the hydrazine tank (340 psi) cannot be exceeded. <u>Both the initial and final fuel pressures cannot be achieved if a pressurant storage bottle volume of less than 168 in^3 is used.</u> The final hydrazine feed pressure may be decreased to achieve a reduced pressurant storage volume.

An isothermal relationship was assumed to simplify the determination of tank pressures above. A constant pressurant temperature

382
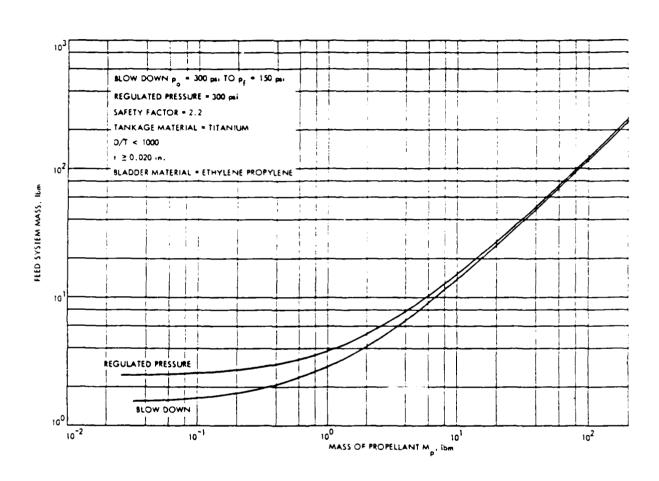
Figure 4-62

Mass of Direct Catalytic Feed Subsystem and Propellant
(JPL TR 32-1505, 1970, p. 88)

383

can be maintained using heaters on the propellant and pressurant tanks in conjunction with a slow pressurization rate. An alternative to this simple isothermal assumption is to use a constant pressure analysis for regulated flow of the pressurant gas. The use of a regulator degrades the subsystem reliability due to the "fail open" mode of that component. However, certain applications of the ORION vehicle may require a constant thrust application. and thus a constant thruster inlet pressure. For such situations, Ring (1964. p. 178) and Sutton (1976, p. 309) provide a constant pressure analysis and determine the total pressurant mass required to displace the contents of a hydrazine tank. It is for such analyses that nitrogen or Freon-14 are found to be excellent pressurizing gases. Unfortunately, Freon-14 may act as a plasticizer when it contacts the elastomeric material of positive expulsion tanks such as the TRW model 80303. However, nitrogen has been proven to be compatible with elastomerics over long durations and it is chosen as the pressurant for the ORION fuel expulsion application.

The mass of Nitrogen required is:

$$\text{Mass} = (\text{Volume})(\text{Density}) \qquad (4.19)$$

$$= (56 \text{ in}^3)(0.006895 \text{ lbm/in}^3_{@ 2404 \text{ psi}})$$

$$= 0.386 \text{ lbm Nitrogen}$$

5. Solid Rocket Propulsion Systems

Solid rocket propulsion uses propellants which are cast as a solid "grain" in a thrust chamber. The solid propellant typically cannot be restarted. Solid propellants have much higher specific impulse than the

liquid and gas subsystems described previously. For that reason, these rockets are often employed as boosters in the orbital transfer of spacecraft and missile stages. Three types of solid rocket motors are in use on spacecraft as follows: the solid rocket booster, the subliming solid motor, and the "cap-pistol" motor. The solid rocket booster ranges in thrust from a few tenths to millions of pounds-force (lbf), and is used almost exclusively for apogee kick (AKM) or perigee kick (PKM) orbit transfer applications. The subliming solid motor is composed of an electrothermal unit which sublimes a solid material into a gas for expulsion through a nozzle and the subsequent production of thrust. This type of motor provides multiple, repeatable burns. The "cap-pistol" arrangement uses a number of very small propellant grains which are individually sealed in separate chambers. Each of these individual rockets produces a calibrated thrust when fired. A nest of these motors can be transported for use in attitude control maneuvering, with a separate motor fired for each separate thrust application.

a. Solid Rocket Boosters

The "classic" solid rocket motor is a large solid propellant engine encased in a thrust chamber with an attached exit nozzle. For non-vectored thrust applications, the design of such a motor is inherently reliable. These rockets have a multitude of applications as high energy, compact engines for predetermined thrust applications. The solid rocket motor is a safe propulsion package. Its contents are not subject to leakage as in a liquid propellant subsystem and it is not typically shock sensitive. Solid rocket motors are thermaly stable over broad temperature ranges and are not easily ignited by accident. Most motors are incapable of multiple burns, and the engine requires little in the way of control hardware as a result. However,

because most solid rockets cannot be restarted, their use is restricted to spin up/spin down and apogee/perigee orbit transfer applications.
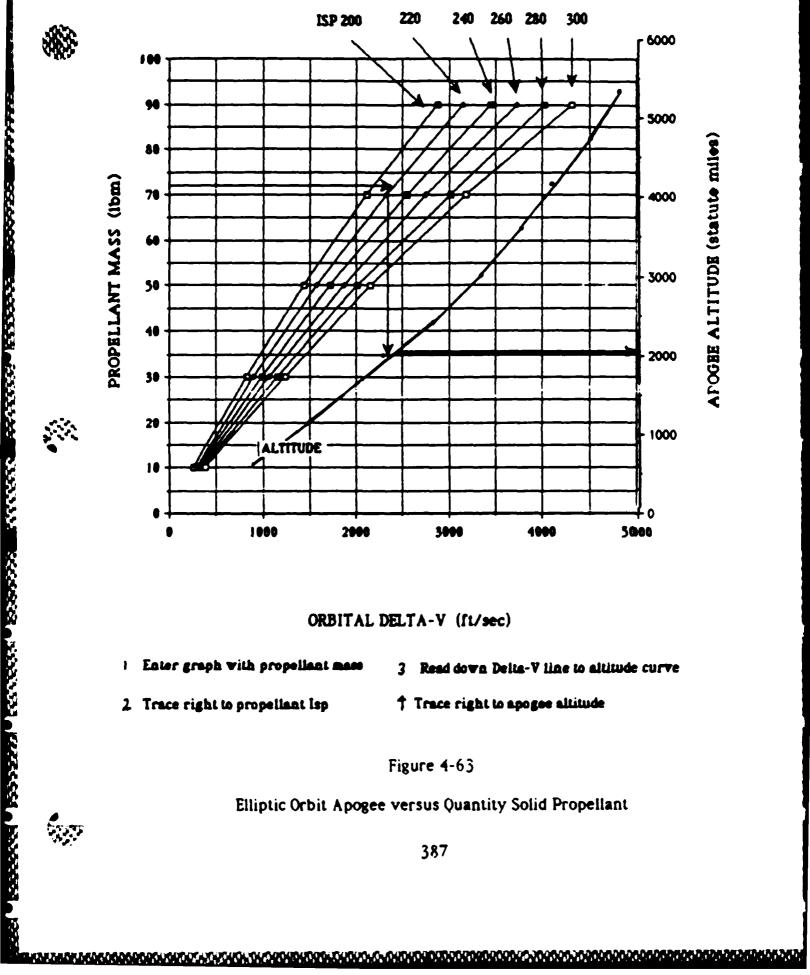
The I_{sp} of a typical solid propellant motor is 200 to 290 seconds. There are many varieties of propellants, propellant loads and thrust/nozzle designs. In general, the propellant, known as a "grain", is formed in a combustion chamber casing with an igniter and possibly a hollow core. If a core is not present, the engine is referred to as "end burning". The nozzle is typically made of an ablative material to withstand intense thermal loads. A booster is used in applications where a single burn for orbit insertion is required. If the vehicle is to attain a circular orbit, at least two burns are required for a Hohmann transfer orbit. Assuming that the initial orbit is circular and well defined, a single solid rocket motor can, at best, provide only elliptic orbits. The disadvantage is that, using the solid motor, stationkeeping propulsion does not exist because all of the rocket energy is expended in a single propulsion manuever. Additionally, provision is not made for an attitude control interface as with the hydrazine subsystem. The advantage of a solid rocket motor lies in its high impulse for a small propulsion package. It is not a flexible propulsion package, however. Excellent discussions of solid rocket motor design and performance can be found in Kit(1960), Sutton(1976), Barrere(1960), Koelle(1961), various NASA publications, and the United Technologies Co. "Pocket Rocket Reader".

Several solid rocket motor suppliers were identified in a vendor survey for the ORION application. Morton Thiokol Co., Aerojet-General CO., Hercules Inc., Lockheed Propulsion Inc., and the United Technology Chemical Systems division each manufacture solid rocket motors. However, only the Morton Thiokol Aerospace Group of Elkton, Maryland, manufactures a wide

386

Figure 4-63

Elliptic Orbit Apogee versus Quantity Solid Propellant

387

range of small solid rocket motors which can be adapted to the ORION requirements.

Table 4-29 is a representative sampling of the rocket motors identified in the vendor survey. Recognizing that a single solid motor can only provide an elliptic orbit, and that an impulse of approximately 15000 lbf-seconds is required for the propulsion subsystem, choice of several candidate engines is possible. These engines provide elliptical orbits whose apogees vary with the rocket engine total impulse. Figure 4-63 diagrams the magnitude of the elliptic orbit apogee as a function of the amount of propellant expended. This figure assumes that the satellite is initially established in a nominal Shuttle orbit of 135 nm (circular). The elliptic orbit capabilities of any of the engines described herein can be approximated using this graph.

TABLE 4-28

SURVEY OF SOLID ROCKET MOTORS

AGC = AEROJET GENERAL CORP   TCC = THIOKOL CHEMICAL CORP
HPC = HERCULES INCORPORATED   UTC = UNITED TECHNOLOGY CORP
LPC = LOCKHEED PROPULSION COMPANY

CONFIGURATION	MODEL NO.	MFR	PROGRAM	TOTAL WT (LB)	PROP WT (LB)	DIAM (IN)	LENGTH (IN)	TOT IMP VAC (LB-S)	THRUST (LB)	BURN TIME (S)	EXP RATIO
	SR9-1	233	HPC	SURVEYMAN & ATHENA RETRO	8.70	7.30	5.30	8.75	787	800	0.750	8.4
	TE-M-500	107	TCC	TRAIL BLAZER	6.35	3.0	5.07	7.7	705	457	1.7	8.7
	SRS-70	779	AGC	ULLAGE ORIENTATION	10.9	8.6	4.5	30.2	3490	130	10.8	10.0
	CO-70	780	LPC	ORBITAL BOOST MOTORS	18.79 TO 27.34	9.75 TO 18.34	8.5	8.7 TO 9.3	3410 TO 4296	230	16 TO 13.3	12.0
	TE-M-329	757	TCC	CLASSIFIED	68.6	48.3	12.0	12.0	10,390	1144	9.0	70.6
	TE-M-316	770	TCC	MERCURY	67	48	12.0	15.6	12,975	900	13.5	21
	TE-M-391	757	TCC	GEMINI	67.4	56.4	12.0	30.0	14,000	2100	6.7	23
	TE-M-345	781	TCC	TITAN III	83.7	63.3	13.5	16.6	16,200	830	21.4	38
	TE-M-458	779	TCC	AMP	78.6	60.3	13.5	21.2	16,500	910	21.0	41.7

389

TABLE 4-28 (Cont.)

SURVEY OF SOLID ROCKET MOTORS

CONFIGURATION	MODEL	SP S	MFR	PROGRAM	TOTAL WT (LB)	PROP WT LB	DIAM IN.	LENGTH IN.	TOT IMP VAC (LB-S)	THRUST (LB)	BURN TIME (S)	EXP RATIO
	TE M AAA	288	TCC	ANT	88 5	73 5	13 5	22 8	21 100	1 304	15 7	5.7
	TE M 516	288	TCC	SESP	83 8	73 70	13 5	22 8	21 200	1 350	15 0	5.7
	TE M 616	266	TCC	TRAIL BLAZER	100	90	15 80	21 4	24 000	5 121	4 6	9
	SVM 3	278	AGC	CLASSIFIED	110 6	137 7	18 0	24 7	28 110	1 706	24	45
	TE M 479	291	TCC	RAE	176 3	153 0	17 4	27 1	44 000	2 306	20 0	33 2
	SVM 5	288	AGC	INTELSAT IV	191 0	63 0	18 0	32 01	47 083	2 906	16 2	33 3

Note from Table 4-28 that the Morton Thiokol TEM-385 provides an impulse of 14000 lbf-seconds which is near that of the ORION total propulsion requirement. This 67.4 lbm Mercury-era motor occupies an envelope 12.8 in diameter by 20.8" long. The Morton Thiokol TEM 236-3 is a more recently produced engine capable of 13745 lbf-seconds total impulse. This engine is somewhat smaller, being 12.0" in diameter, and 12.8" long, at 74.6 lbm. Both motors have a smaller mass than the previously discussed 94 lbm hydrazine subsystem, but are decidedly inadequate as flexible propulsion options. Recall that one of the design constraints for the propulsion subsystem was maximum commonality of the primary and auxiliary propulsion subsystems. Such commonality allows the individual subsystems to share a common fuel source as in the hydrazine application. With a solid rocket motor, such commonality is impossible.
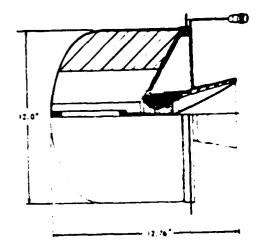
One solid rocket motor was identified which could be used for attitude control. The Morton Thiokol Co. manufactures the TEM 696/697 spin/despin motors that have been used in military reentry vehicle programs. These titanium encased motors provide a single shot spin/despin capability. Rated at 85 and 49 lbf thrust respectively, these thrusters produce 25 and 14.4 lbf-seconds of total impulse. These solid rockets are not capable of repeated firings and would not be a wise choice for the ORION application. In summary, several commercially available rocket motors will fit in ORION, but a solid rocket cannot provide the flexibility required by a general purpose spacecraft.

MOTOR PERFORMANCE, 60°F, vacuum

Burn Time, sec	7.5
Avg. Cham. Pres., psia	1,052
Total Impulse, lbf-sec	13.745
Burn Time Avg. Thrust, lb	1,630

PROPELLANT

TP-G3085F, Urethane binder, 13% Al

CASE

4130 Steel, 185,000 psi ult., 0.056" thick

TEMPERATURE LIMITS

Operational 0°F to 100°F

WEIGHTS, lbm

Total	74.0
Propellant	50.2
Case	10.9
Nozzle	10.8
Other	2.1
Burnout	23.1
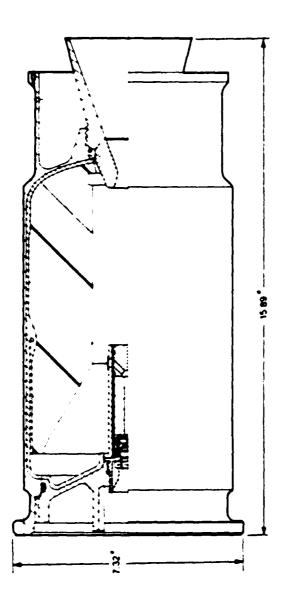
NOZZLE

Vitreous Silica Phenolic

Figure 4-64

Morton Thiokol Co. TE-M 236-3 STAR 12A Rocket Motor
(Morton Thiokol/Elkton Catalog, 1986)
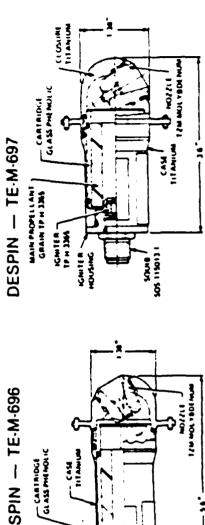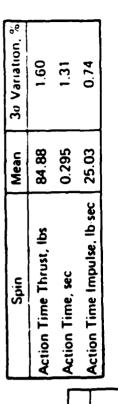
MOTOR PERFORMANCE, 70°F, vacuum

Burn Time, sec	5.9
Avg. Cham. Pres. psia	846
Total Impulse, lbf-sec	3,686
Burn Time Avg. Thrust, lb	565

PROPELLANT

TP-H3237A, CTPB binder, 2% Al

CASE

7050 Al Alloy, 66,000 psi ult., 0.067" thick

TEMPERATURE LIMITS

Operational + 30°F to 110°F

WEIGHTS, lbm

Total	22.62
Propellant	13.45
Case	6.02
Nozzle	0.80
Other	2.35
Burnout	8.92

NOZZLE

Carbon-Phenolic, Exp. Ratio = 32

CURRENT STATUS

Production

Figure 4-65

Morton Thiokol TE-M 790-1 STAR 6B Rocket Motor
(Morton Thiokol/Elkton Catalog, 1986)
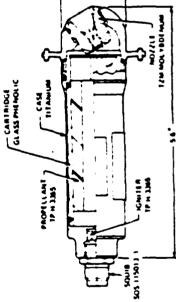
393

DESPIN — TE-M-697

SPIN — TE-M-696

Spin	Mean	3σ Variation, %
Action Time Thrust, lbs	84.88	1.60
Action Time, sec	0.295	1.31
Action Time Impulse, lb sec	25.03	0.74

Despin	Mean	3σ Variation, %
Action Time Thrust, lbs	49.27	3.70
Action Time, sec	0.292	3.26
Action Time Impulse, lb sec	14.39	0.77

	Spin	Despin
Case and Closure	Titanium	
Nozzle Insert	TZM Molybdenum	
Length, in.	5.6	3.6
Case Diameter, in.	1.38	1.38
Weight, lb	0.62	0.51
Propellant Weight, lb	0.102	0.057
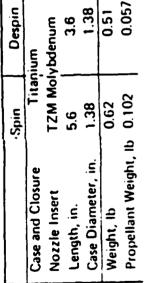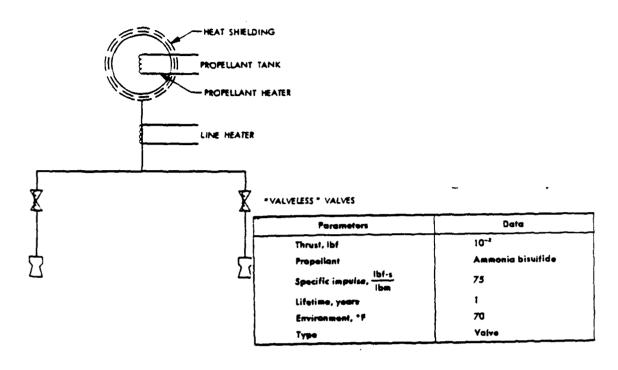
Figure 4-66

Morton Thiokol Co. TE-M 696/697 Spin & Despin Motors
(Morton Thiokol/Elkton Catalog. 1986)

b. Subliming solid thrusters

The subliming solid propellant thruster (Figures 4-67, 68) utilizes the thermal sublimation of a solid material and expulsion of the resulting hot

Parameters	Data
Thrust, lbf	10^{-2}
Propellant	Ammonia bisulfide
Specific impulse, $\frac{lbf\text{-}s}{lbm}$	75
Lifetime, years	1
Environment, °F	70
Type	Valve
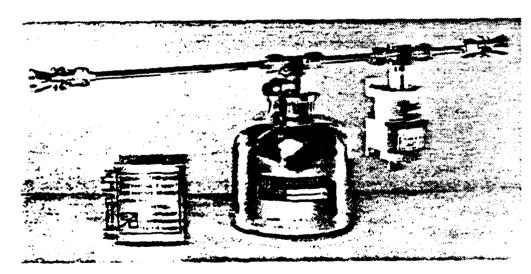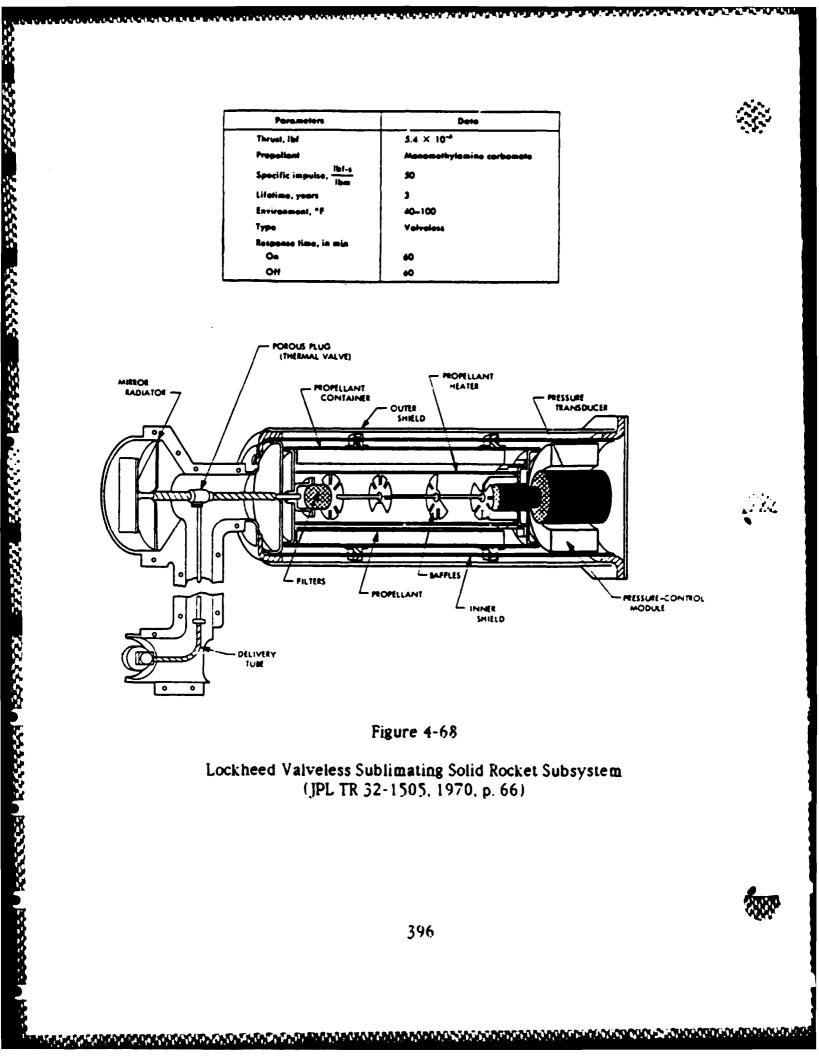
Figure 4-67

OV2 Respin Sublimating Rocket Subsystem
(JPL TR 32-1505, 1970, p. 63)

Parameters	Data
Thrust, lbf	5.4×10^{-6}
Propellant	Monomethylamine carbamate
Specific impulse, $\frac{lbf\text{-}s}{lbm}$	50
Lifetime, years	3
Environment, °F	40–100
Type	Valveless
Response time, in min	
On	60
Off	60

Figure 4-68

Lockheed Valveless Sublimating Solid Rocket Subsystem
(JPL TR 32-1505, 1970, p. 66)
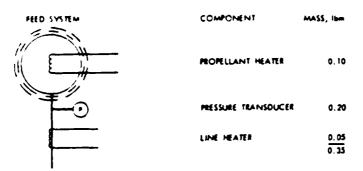
gases through a nozzle to produce thrust. The gas is contained within the subsystem by a valve prior to expulsion to control the thrust application. The vapor pressure of the sublimed material produces the chamber pressure and the needed thrust. When compared to an inert gas subsystem using nitrogen. no significant improvements in I_{sp} are possible. However. a substantial increase in the density of the stored propellant enables a more compact storage of the propulsion subsystem. A specific impulse of 50 to 80 seconds is attainable. In addition. the need to provide a propellant feed and storage subsystem is eliminated.

The specifications of several subliming solid propulsion units are provided in Figures 4-67 and 4-68; note that ammonia bisulfide and monomethylamine carbamate are used as propellants. Both of these propellants provide low molecular weight vapors. high equilibrium vapor pressure. high thermal heat capacity. low heat of vaporization and high solid density. Ammonium carbamate and ammonium sulfite are also commonly used. The thrust levels of these units are low indicating that subliming thrusters are best applied to auxiliary propulsion. Figures 4-69 and 4-70 detail the masses of typical subliming solid propulsion systems and their components. Note that superheated thruster configurations are possible where the vapor is heated after the sublimation much like an inert gas resistojet.

In consideration of the component masses outlined in Figures 4-69 and 4-70. the subliming solid subsystem is rejected as excessively massive relative to a comparable hydrazine subsystem. Six thrusters for attitude control. with a propulsive force of 0.01 lbf each. would weigh 31.2 lbm. The subliming solid concept is not applicable to the needs of the primary

397

FEED SYSTEM

COMPONENT	MASS, lbm
PROPELLANT HEATER	0.10
PRESSURE TRANSDUCER	0.20
LINE HEATER	0.05
	0.35

THRUST, lbf	PROPELLANT HEATER POWER, W	MASS PENALTY, lbm
10^{-2}	100	30
10^{-3}	10	3
10^{-4}	1	0.3

SUPERHEATED

10^{-2}	40	12
10^{-3}	4	1.2
10^{-4}	0.4	0.12

THRUSTER DATA:	COMPONENT	MASS, lbm	POWER, W	TOTAL MASS, lbm (MASS PLUS PENALTY)
	"VALVELESS" VALVE	0.55	5	0.70
	LINES	0.20	0	0.20
	COLD THRUSTER	0.10	—	0.10
	SUPERHEATED THRUST 10^{-2}	0.50	100	5.2
	10^{-3}	0.50	10	3.7
	10^{-4}	0.50	5	2.2
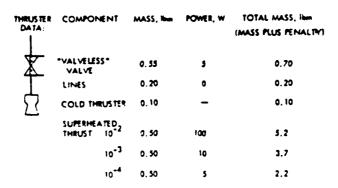
Figure 4-69

Subliming Solid Subsystem Masses
(JPL TR 32-1505, 1970, p. 95)
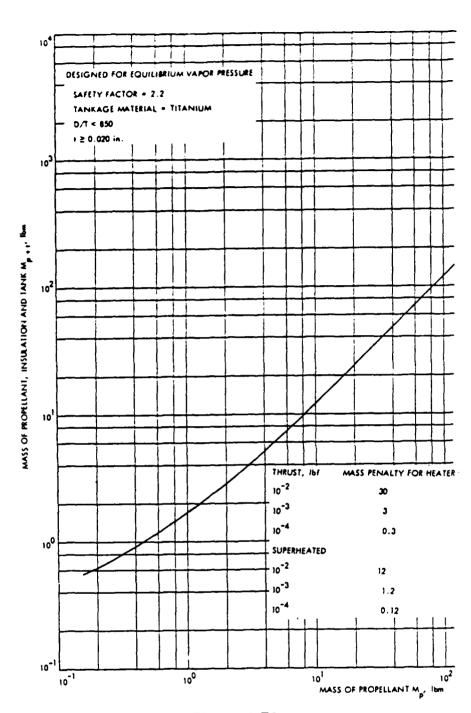
Figure 4-70

Subsystem Mass for Subliming Solid Thrusters
(JPL TR 32-1505, 1970, p. 96)

propulsion subsystem and also requires an unacceptable power drain (100 watts. each thruster) for the sublimation process.

6. Bipropellants

Two types of bipropellant thrusters are available for use on ORION. Liquid fueled bipropellant thrusters are most common. Gaseous bipropellants (gaseous oxygen and hydrogen) are also being developed. Of the liquids used in bipropellant rocket engines. there are hypergolic propellants and cryogenic propellants. Cryogenic liquid engines use liquified gases to improve propellant storage volumes. Cryogenics are not practical for long term storage of propellants as is required for ORION. Hypergolic fluids react exothermically when mixed (such as hydrazine and nitrogen tetroxide). High values for specific impulse (270 to 300 seconds) are attainable. and a combustion source is not required. Until recently such engines did not exist in a small package to allow integration in a spacecraft like ORION. However. recent advances by Aerotech Co. of Sacramento. CA. have resulted in small thrusters with a large thrust rating. These engines use regeneratively cooled nozzles and would be very effective for the ORION orbital transfer application. A bipropellant engine interfaces well with a hydrazine attitude control subsystem. requiring only the addition of the oxidizer (nitrogen tetroxide) for combustion. A typical small hypergolic bipropellant engine is shown in Figure 4-71. This Aerotech engine. which is marketed in conjunction with TRW Co.. is rated at 100 lbf thrust and has an I_{sp} of 275 seconds.

Using the engine of Figure 4-71. ORION would obtain a 25% (275/220) improvement in specific impulse over that of a hydrazine catalyst subsystem. The spacecraft would also exhibit a lower total impulse.

400

FLIGHT HERITAGE
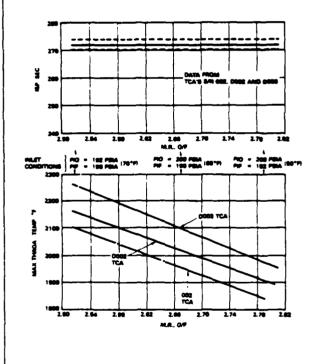
Program Usage:	Classified
Number Produced:	28
Maximum Time in Orbit:	Classified

QUALIFICATION SUMMARY
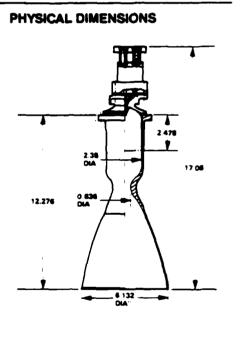
Propellants:	HDA and USO
Total Impulse:	1.6×10^6 Lbr-Sec.
Total Operating Time:	16,120 Sec.
Total Pulses:	300
Maximum Single Burn Duration:	570 Sec.
Minimum Single Burn Duration:	1 Sec.
Random Vibration:	13.9g rms
Inlet Pressure:	200 psia
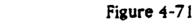
PERFORMANCE CHARACTERISTICS

PHYSICAL DIMENSIONS

Figure 4-71

100 lbf Hypergolic Liquid Bipropellant Thruster
(Reproduced from Aerotech Catalog, 1986)

401

The loss of total impulse occurs because the requirement for oxidizer results in a reduction of the available hydrazine propellant volume and, thus, the total impulse. Using the same propellant mass as in the hydrazine catalyst case, the total impulse of a bipropellant N_2H_4/N_2O_3 subsystem decreases 38% relative to a monopropellant hydrazine subsystem. These hypergolic thrusters are not suitable for the secondary propulsion requirements because they have not matured for small thrust, precise attitude control applications.
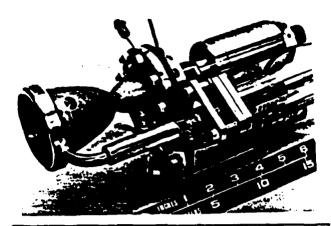
Gaseous propellants are also effective but require large propellant storage volumes. The density of the high energy, low molecular weight gases is such that the storage volumes are prohibitively large. The calculations for volume in the section on inert gas thrusters stressed that point quantitatively. Gaseous bipropellants are not feasible for the ORION application; however, such thrusters are appropriate for use on the Space Station where hydrogen and oxygen are natural byproducts of life support system operations. A prototype thruster has been developed by Rockwell that operates over a wide range of mixture ratios to deal with the variable quantity of gases available on Space Station. This 25 lbf thruster is pictured in Figure 4-72.

7. Electric Propulsion

Electric propulsion usea electric power to accelerate propellants to high exit velocities, thereby providing extremely high specific impulses at very low thrust. This propulsion mode is being utilized in several applications for both primary and auxiliary propulsion missions.

- Hydrogen/Oxygen Propellant

- Fuel-Cooled, Regenerative, Channel Wall Design
  - Copper Alloy Wall Material
  - Electrodeposited Closeout

- Coaxial Injector

- Independent Fuel and Oxidizer Valves

- Integrated Spark Igniter

- Operates at Mixture Ratios 3:1 to 8:1

- Operates Throttled 2:1

Design Characteristics	Design Goals	Demonstrated
Thrust, pounds	23 at ϵ = 30:1 25 at ϵ = 100:1	12.5 to 25
Chamber Pressure, psia	100	50 to 110
Mixture Ratio, o/f	3:1 to 8:1	3:1 to 8.2:1
Area Ratio	30:1 Regen Cooled	30:1
Specific Impulse (at MR =4.1 and ϵ = 30:1)	>400	405
Minimum Pulse Duration, milliseconds	30	30
Minimum Impulse Bit, lbf-sec	Less than 0.5	Under 0.5
Life	Meet 10 years Space Station Life	24.1 hours; 2M lb-sec
Pulse Capability	Over 1 million	Over 10,500
Weight, pounds	--	8.25

Figure 4-72

Prototype 25 lbf Gaseous Oxygen/Hydrogen Thruster
(Larson and Evans, 1986, p. 9)

While providing less thrust than any of the concepts previously outlined, electric propulsion subsystems have very long life and can be operated continuously. These subsystems provide propulsion benefits assuming that sufficient electric power is available and orbital transfer times are not constrained to be short. Several types of electric propulsion are being investigated including ion engines, colloid thrusters, magnetoplasmadynamic (MPD) thrusters, and pulsed plasma thrusters.

a. Ion Thrusters

An ion thruster is a device that electrostatically accelerates ions. The ionization can occur as a result of contact ionization or bombardment ionization. In contact ionization, a heated porous tungsten plug ionizes a flow of cesium propellant vapor. Gradual erosion of the heater element occurs due to the impact of ions and chemical reactions with the hot gas. This reduces the heater element efficiency and life expectancy. Bombardment ionization uses an anode and cathode arrangement to ionize mercury or cesium vapor and to accelerate the ions in an electrostatic field. In either method, the ions which are emitted from the thruster are later neutralized by an electron beam to prevent a charge build-up and subsequent static electrical discharge on the surface of the spacecraft. Contact engine ion thrusters yield very high specific impulse (40,000 to 80,000 seconds) as demonstrated in Table 4-29. However, this high specific impulse requires significant electrical power (on the order of 200 to 300 watts per millipound force). The bombardment ion thruster produces specific impulse of 980 to 98000 seconds over a wide range of thrust levels with power requirements of 100 to 1000 watts respectively. (JPL TR 32-

404
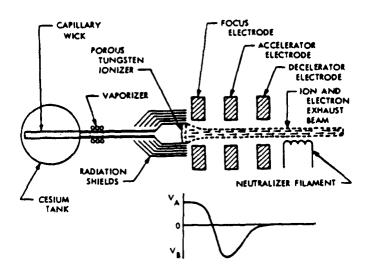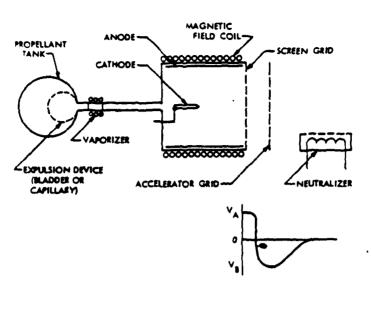
Figure 4-73

Contact Ion Thruster
(JPL TR 32-1505 Addendum, 1971, p. 2)

1505 Addendum, 1971). Figures 4-73 and 4-74 show conceptual diagrams of the contact ion and bombardment ion thrusters. Their specific impulse as a function of s osystem power is plotted in Figure 4-75.

Aston (1986) has developed several xenon ion engine propulsion units which would interface well with ORION if the satellite had a larger power supply. He has tested 10 cm and 30 cm diameter units which use mercury or xenon gas as a propellant. The 10 cm diameter engine requires 1 kilowatt. This large power demand could be satisfied through the use
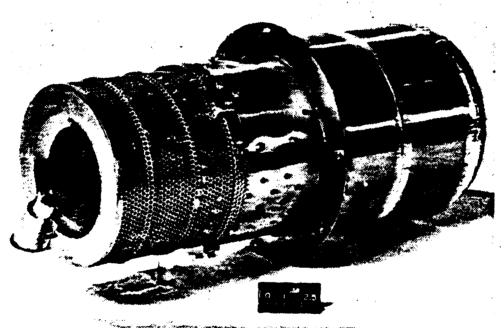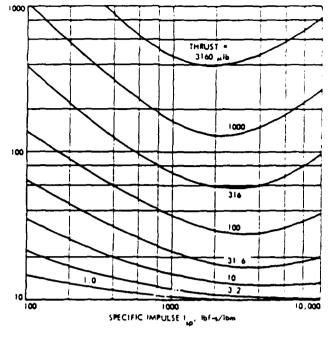
Figure 4-74

Electron-Bombardment Ion Thruster
(JPL TR 32-1505 Addendum, 1971, pp. 2/13)
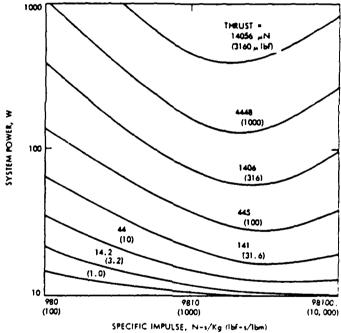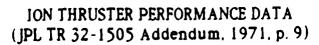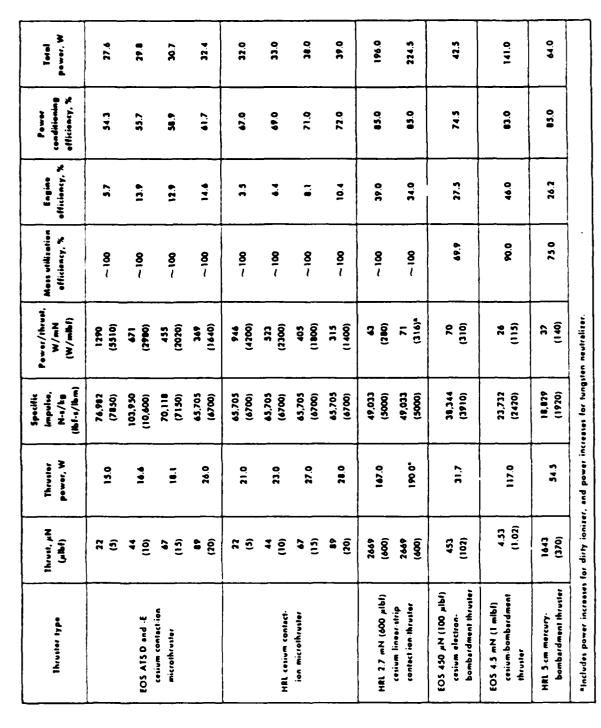
Figure 4-75

Specific Impulse versus Power for Ion Thrusters
(JPL TR 32-1505 Addendum, 1971, p. 5)

407

TABLE 4-29

ION THRUSTER PERFORMANCE DATA
(JPL TR 32-1505 Addendum, 1971, p. 9)

Thruster type	Thrust, μN (μlbf)	Thruster power, W	Specific impulse, N·s/kg (lbf·s/lbm)	Power/thrust, W/mN (W/mlbf)	Mass utilization efficiency, %	Engine efficiency, %	Power conditioning efficiency, %	Total power, W
EOS AISD and -E cesium contact-ion microthruster	22 (5)	15.0	76,982 (7850)	1290 (5510)	~100	5.7	54.3	27.6
	44 (10)	16.4	103,950 (10,600)	671 (2990)	~100	13.9	55.7	29.8
	67 (15)	18.1	70,118 (7150)	455 (2020)	~100	12.9	58.9	30.7
	89 (20)	26.0	65,705 (6700)	349 (1640)	~100	14.6	61.7	32.4
HRL cesium contact-ion microthruster	22 (5)	21.0	65,705 (6700)	944 (4200)	~100	3.3	67.0	32.0
	44 (10)	23.0	65,705 (6700)	523 (2300)	~100	4.4	69.0	33.0
	67 (15)	27.0	65,705 (6700)	405 (1800)	~100	8.1	71.0	38.0
	89 (20)	28.0	65,705 (6700)	315 (1400)	~100	10.4	72.0	39.0
HRL 2.7 mN (600 μlbf) cesium linear-strip contact-ion thruster	2669 (600)	167.0	49,033 (5000)	63 (280)	~100	39.0	85.0	196.0
	2669 (600)	190.0°	49,033 (5000)	71 (316)a	~100	34.0	85.0	224.5
EOS 450 μN (100 μlbf) cesium electron-bombardment thruster	453 (102)	31.7	38,344 (3910)	70 (310)	69.9	27.5	74.5	42.5
EOS 4.5 mN (1 mlbf) cesium-bombardment thruster	4.53 (1.02)	117.0	23,732 (2420)	26 (115)	90.0	46.0	83.0	141.0
HRL 5 cm mercury-bombardment thruster	1643 (370)	54.5	18,829 (1920)	32 (140)	75.0	26.2	85.0	64.0

aIncludes power increases for dirty ionizer, and power increases for tungsten neutralizer.

of a flexible solar array which would be stored as a panel wrapped about the ORION body cylinder and deployed as a despin yoyo on orbit. Nock (1987) describes a second method whereby two 0.5 kilowatt solar panels of rigid cells could be folded accordion style and recessed in the structure. The Jet Propulsion Laboratory is using the xenon ion engines developed by Aston in a prototype lunar mapping GAS satellite. See Chapter Two for details. The mass and power penalties of a single thruster are so great that the attitude control needs of a GAS satellite cannotbe supported by xenon ion engines. Nock (1987) proposes that sufficient xenon gas be transported to provide cold gas attitude control as well as working gas for the ion thruster. Like ORION, the JPL design is spin stabilized.

Based upon the JPL developments, ion engines may be a viable concept for future ORION applications. These engines could operate for a very long period of time and inject ORION into geosynchronous or interplanetary trajectory following thrust durations of 2 years or longer. While ion engines cannot match solid rockets for thrust, they are highly reliable over the long term and may well be the propulsion subsystem of choice for the first interplanetary GAS satellite. The value of this cost effective concept in interplanetary exploration deserves further consideration.

b. Colloid Thrusters

The colloid thruster is a device that electrostatically accelerates multi-atom or multi-molecule charged particles to high exit velocities. A liquid propellant is stored in a tank and fed on demand to a manifold. In the manifold an intense electromagnetic field causes the charged particle droplets to be electromagnetically sprayed from the engine.
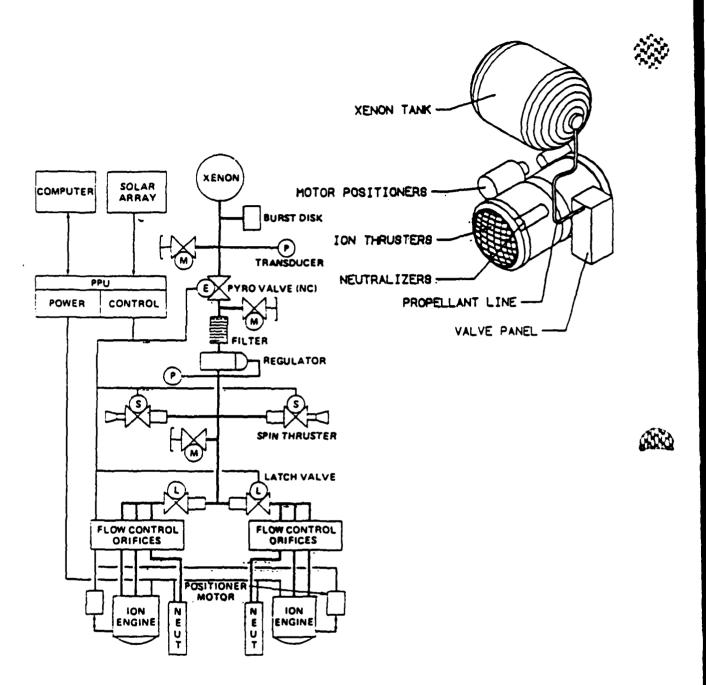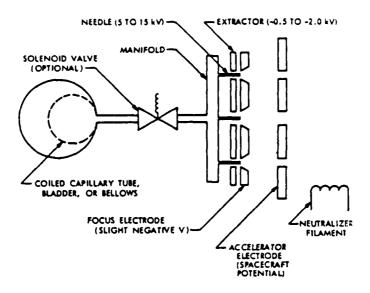
Figure 4-76

Jet Propulsion Laboratory "Lunar Gas" Satellite and
Xenon Ion Engine
(Nock, 1987, p. 4)

410

NEEDLE (5 TO 15 kV) — EXTRACTOR (~0.5 TO -2.0 kV)

MANIFOLD

SOLENOID VALVE
(OPTIONAL)

COILED CAPILLARY TUBE,
BLADDER, OR BELLOWS

FOCUS ELECTRODE
(SLIGHT NEGATIVE V)

NEUTRALIZER
FILAMENT

ACCELERATOR
ELECTRODE
(SPACECRAFT
POTENTIAL)

BELLOWS — ISOLATOR

FLOW CONTROL ASSEMBLY

PROPELLANT

PROPELLANT
MANIFOLD

MOUNTING PLATFORM

HEATER

EXTRACTOR

MODULE
ASSEMBLY (12 REQUIRED)

ZEOLITE AMMONIA
CANISTER

NEUTRALIZER ASSEMBLY

0.005 cm TUNGSTEN WIRE

UNIVERSAL FLEXURE
(OPTIONAL)

Figure 4-77

Colloid Thruster
(JPL TR 32-1505 Addendum, 1971, p. 20)

411

At the exit of the thruster, the positively charged propellant stream is neutralized by a beam of electrons to prevent charge build-up on the spacecraft. As with the ion engine, very high specific impulses can be attained, but the thrust level rarely exceeds 1 milli-pound. Very high power is required. Table 4-30 describes the various colloid thruster systems that were available in 1971. Recent colloid thruster data was not available for this report. Note from Table 4-30 that these engines are too large and have insufficient thrust for the ORION primary propulsion subsystem. As with the ion engines, the colloid thruster requires long transits to the desired orbital altitudes. The power requirement to support a colloid thruster operation is also excessively high for the current ORION power supply. Colloid thrusters deserve consideration for future applications, but are not acceptable for the first ORION missions.

    c. Magnetoplasmadynamic and Pulsed Plasma Thrusters

The magnetoplasmadynamic (MPD) thruster evolved from arcjet technology and a special magnetogasdynamic channel flow technology. In this application, an arcjet utilizes a very high current density discharge between a cathode and an anode to ionize a gas stream producing a plasma. This plasma is accelerated electromagnetically to produce thrust. Thrusts of milli-pound force require power input of 200 to 300 watts. Like the colloid thruster, the MPD thruster is too large and excessively power-hungry for the ORION application.

In one form, the pulsed plasma thruster uses rapid bursts of electrical energy to vaporize a solid material for the production of a plasma. The plasma wave is then accelerated and ejected as in the MPD concept. Pulsed

TABLE 4-30

COLLOID THRUSTER PERFORMANCE DATA
(JPL TR 32-1505 Addendum, 1971, p. 19)

Thruster type	Geometry	Thrust, μN (μlbf)	Thruster power, W	Specific impulse, N-s/kg (lbf-s/lbm)	Mass flow rate, μg/s	Reference	Power/ thrust, W/mN (W/mlbf)	Engine efficiency, %	Power conditioning efficiency, %	Total power, W
TRW colloid micro-thruster		39 (8.7)	1.39	9611 (960)	4.0	14	36 (160)	13.1	28.0	5.0
		23 (5.2)	1.43	16,867 (1720)	1.5	14	70 (275)	13.6	29.0	5.0
		48 (10.8)	1.38	7257 (740)	6.5	14	29 (128)	12.6	28.0	5.0
Typical colloid thrusters	36 needles	371.0 (83.5)	3.91	14,710 (1500)	24.9	Estimate	10.54 (46.8)	70.0		
	36 needles	383.0 (86.0)	3.80	14,691 (1498)	25.6	17	9.95 (44.2)	70.0		
	36 needles	306.0 (68.9)	3.30	14,318 (1460)	21.4	17	10.79 (47.9)	66.0		
	36 needles	345.0 (77.6)	3.80	14,837 (1513)	23.3	17	11.01 (48.9)	67.0		
	6 annular slit	534.0 (120.0)	5.54	15,200 (1550)	35.0	17	10.41 (46.2)	72.0		
	6 annular slit	512.0 (115.0)	5.52	14,906 (1520)	36.0	17	10.81 (48.0)	70.0		
	6 annular slit	489.0 (110.0)	5.22	14,514 (1480)	35.0	17	10.70 (47.5)	69.0		
	1 annular slit (EOS)	89.0 (20.0)	0.87	13,141 (1340)	6.8	18	9.90 (43.5)	73.0		
TRW 4.5-mN (1-mlbf) ADP colloid	(footnote)	4,450 (1000)	58.00	14,710 (1500)	298.8	Estimate	13.0 (58)	56.0f	85.0	68.2

Figure 4-78

MPD Thruster
(JPL TR 32-1505 Addendum, 1971, p. 24)

plasma thrusters are used in attitude control applications where pulse
repeatability and fine vernier control are required. Table 4-31 lists some
typical pulsed plasma systems. A common propellant for use in the thrusters
is Teflon. A rod of the material is forced into the path of the arcjet by a
springloaded mechanism, and the end of the rod is vaporized as needed.
Specific impulse up to 1000 seconds is attainable with this subsystem. The
Teflon pulsed plasma unit (24" diameter, 8" long, 40 lbm) is too large for the
ORION application but has found successful application in many other
satellite systems. If future pulsed plasma systems are engineered in smaller
packages, and if a large power subsystem were incorporated on ORION (i.e. 1
kilowatt) then this propulsion option may eventually be viable.

414

TABLE 4-31

PULSED PLASMA THRUSTER PERFORMANCE DATA
(JPL TR 32-1505 Addendum, 1971, p. 25)

Thruster type	Thrust, μN (μlbf)	Thruster power, W	Specific impulse, N-s/kg (lbf-s/lbm)	Power/ thrust, W/mN (W/mlbf)	Specific thrust, μN-s/J (μlbf-s/J)	Engine efficiency, %	Power conditioning efficiency, %	Total power, W
Low-power MPD arc thruster[a]	4181 (940)	193	3296 (340)	46 (206)			84.0	224.0
	9606 (2160)	345	12,425 (1267)	36 (159)		17.3	84.0	400.0
	14,437 (3250)	635	18,456 (1882)	44 (194)		21.3	84.0	727.0
Fairchild-Hiller LES 6 thruster	16.9[b] (3.8)	1.41[c]	3040 (310)	84 (371)	13.3 (3.0)	1.8	54.0	2.52
	17.8[d] (4.0)	1.41[c]	3040 (310)	80 (353)	14.2 (3.2)	1.9	54.0	2.52
	17.3[e] (3.9)	1.41[c]	1863 (190)	81 (361)	13.3 (3.0)	1.2	48.0	2.91
Fairchild-Hiller LES 7 thruster[f]	3996 (89.3)	19.6	10,081 (1028)	49 (219.0)	20.5 (4.6)	10.2	85.0	23.0
	3185[h] (716.0)	156.8	10,081 (1028)	49 (219.0)	20.3 (4.6)	10.2	85.0	184.0
	7325 (1646)[i]	237	12,200 (1245)	35 (156)	28 (6.4)	17.4	85.0	302.0
Fairchild-Hiller high energy pulsed plasma[g]	6470 (1434)[i]	244	13,000 (1328)	37 (164)	24 (5.9)	17.2	85.0	287.0
	6400 (1432)[i]	309	18,600 (1900)	46 (208)	21 (4.8)	19.9	85.0	344.0
	3515 (790)[i]	190	32,600 (3330)	54 (241)	19 (4.2)	20.2	85.0	224.0
General Electric Solid Propellant Electric Thruster (SPET)	9 (2)	1.2[j]	9807 (1000)	135 (600)	9.0 (2.0)	3.6	65.0	1.8
	13 (3)	1.2[j]	9807 (1000)	90 (400)	13.0 (3.0)	5.5	65.0	1.8

[a]Includes 48 W for edge wound magnet power and 2 W for a solenoid valve.
[b]Reference 27 at 0.667 ppr.
[c]0.1 W for telemetry.
[d]Reference 24 at 0.667 ppr.
[e]Tom Williams, NASA Goddard, at 0.69 ppr; one million pulses.
[f]Supplied by W. J. Guman, Fairchild-Hiller.
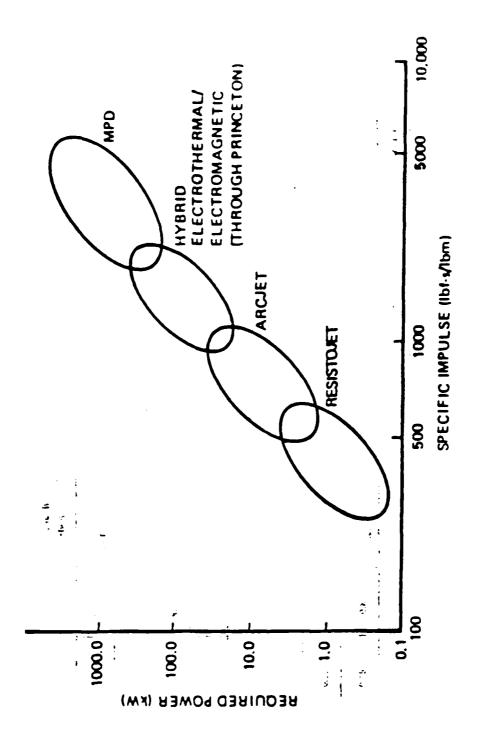
[a]At 1 ppr.
[b]At 8 ppr.
[h]At 0.931 ppr.
[i]At 0.971 ppr.
[j]At 1 ppr.
0.1 W for telemetry and 0.1 W for spark igniter.

415

Figure 4-79

Electric Propulsion Performance Spectrum

D. ORION PROPULSION SUBSYSTEM

Each of the candidate thruster subsystems has been described in detail with special emphasis placed on the suitability of a particular subsystem for use on ORION. The design criteria that most affect the choice of an ORION propulsion subsystem are performance, mass/volume utilization and power consumption. Among these, performance is the first consideration in the choice of a propulsion option. Table 4-32 summarizes many of the favorable and unfavorable characteristics of each propulsion option. Table 4-33 reviews the performance of many of the candidate subsystems.

Considering the available thruster options, a hydrazine catalyst subsystem was chosen. Specifically, a seven thruster hydrazine subsystem using a pressurized feed network was selected. One 40 lbf thruster and six 0.1 lbf thrusters are used. The 40 lbf thruster is used to conduct orbital transfer. It is mounted to the baseplate on the longitudinal centerline of the spacecraft. Two 0.1 lbf thrusters are used to precess the spacecraft and are mounted 180° apart on the baseplate. Their nozzles protrude through the baseplate and point along a line normal to that plate. The last four 0.1 lbf thrusters are mounted near the center of the structure on the cylinder periphery witht the nozzles aligned along a tangent to the structural cylinder, providing a pair of coupled thrusters to spin left and to spin right.

A pressurized feed subsystem using a positive expulsion tank supplies hydrazine to the thrusters. Pressurant nitrogen is provided by two

TABLE 4-32

GENERAL CHARACTERISTICS OF THRUSTER SUBSYSTEMS
(JPL TR-32-1505, 1970, p. 3)
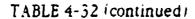
Thruster system	Favorable characteristics	Unfavorable characteristics
Inert gas	Inexpensive. Repeatable impulse bit. Flight experience.	Low specific impulse. Long-term leakage, for long missions. High-pressure tankage required. Excessive mass for high total impulse missions.
Tridyne (gaseous monopropellant)	Same feed system as inert gas. Increased performance over inert gas. Repeatable impulse bit.	Medium-to-low specific impulse. Long-te-n leakage, for long mission. High pressure tankage required. Low-power heater required.
Vaporizing liquid	Relatively inexpensive. Low-pressure storage. Repeatable impulse bit. Flight experience.	Relatively low reliability of present feed system designs. Medium-to-low specific impulse. Leakage for long missions.
Hydrazine catalyst	Relatively high reliability of feed system. Medium specific impulse. Flight experience. Low leakage of propellant for long-term storage.	Moderately expensive. Poor repeatability at very low impulse bit with cold catalyst bed. "Limited" catalyst bed life.
Hydrazine resistojet (liquid)	Relatively high reliability of feed system. Medium specific impulse. Low leakage of propellant for long-term storage.	Relatively expensive development. Poor pulse response at low thrust.
Hydrazine resistojet (gaseous)	Relatively high reliability of feed system. Medium specific impulse. Low leakage of propellant. Repeatable impulse bit.	Relatively expensive development. Thermal control of vaporizer required.
Hydrazine plenum	Relatively inexpensive. Repeatable impulse bit. Flight qualified system.	Relatively low reliability of nonpassive feed system. Medium-to-low specific impulse.

TABLE 4-32 (continued)

GENERAL CHARACTERISTICS OF THRUSTER SUBSYSTEMS
(JPL TR-32-1505, 1970, p. 3)

Thruster system	Favorable characteristics	Unfavorable characteristics
Subliming solid	High reliability. Low thrust.	Thermal control problems. Long on—off times. Moderately low specific impulse.
Ion	High specific impulse. Flight experience.	High voltages and large power requirement. Complex system. Exhaust neutralizer required. Expensive.
Colloid	High specific impulse. Low power-to-thrust ratio. Low propellant vapor pressure.	Some power required. High voltages. Complex system. Exhaust neutralizer required. Expensive.
Pulsed plasma	High specific impulse. Simple system. Flight experience. Relatively inexpensive.	Large power requirement. Limited thruster life. RF noise. Potential feed system problem.
Resistojet, NH$_3$	Low pressure storage. Repeatable impulse bit. Flight experience. Medium specific impulse.	Relatively low reliability of present feed system designs. Thruster heater power required. Leakage for long missions.
Resistojet, N$_2$	Relatively inexpensive. Repeatable impulse bit.	Medium-to-low specific impulse. Long-term leakage. Leakage for long missions.
Radioisojet, NH$_3$	Medium-to-high specific impulse. Repeatable impulse bit.	High cost. Isotope handling problems. Influence of isotopes on spacecraft and thruster design. Leakage for long missions. Relatively low reliability of present feed system designs.
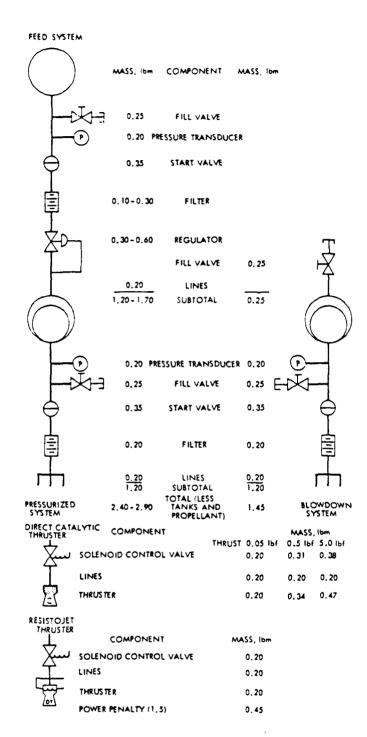
TABLE 4-33

PERFORMANCE CHARACTERISTICS OF THRUSTER SUBSYSTEMS
(JPL TR-32-1505, 1970, p. 82)

Systems	Thrust level, lbf	I_{sp} (vac), lbf-s/lbm	I_{min}, lbf-s
Inert gas (80°F)			
H₂	0.0001–1.0	272	10^{-6}
He	0.0001–1.0	165	10^{-6}
Ne	0.0001–1.0	75	10^{-6}
N₂	0.0001–1.0	72	10^{-6}
A	0.0001–1.0	52	10^{-6}
Kr	0.0001–1.0	37	10^{-6}
Xe	0.0001–1.0	28	10^{-6}
CF₄	0.0001–1.0	45	10^{-6}
CH₄	0.0001–1.0	105	10^{-6}
Tridyne (T = 1300°F)	0.1	143	10^{-3}
Hydrazine direct catalyst			
Steady state	0.05–0.10	200	5×10^{-4}
Cold pulse	0.05–0.10	100	5×10^{-4}
Hot (50h) pulse	0.05–0.10	170	5×10^{-4}
Steady state	0.5–5	225	5×10^{-3}
Cold pulse	0.5–5	110	5×10^{-3}
Hot (50h) pulse	0.5–5	210	5×10^{-3}
Hydrazine resistojet			
Initial pulse and steady state	10^{-3}	175	10^{-4}
Initial pulse and steady state	10^{-1}	200	10^{-3}
Initial pulse	0.1–5	210	10^{-3}

Systems	Thrust level, lbf	I_{sp} (vac), lbf-s/lbm	I_{min}, lbf-s
Hydrazine plenum Cold (80°F)	0.010–0.060	100	10^{-4}
Electrolysis			
Hot O₂/H₂ gas	0.05–5	350	5×10^{-2}
Hot O₂/H₂ gas (Marquardt)	0.05–5 (2500°F)	310	5×10^{-2}
Cold H₂O gas (80°F)	100×10^{-6} to 1.0	109	10^{-6}
Hydrazine cold (80°F)	100×10^{-6} to 1.0	116	10^{-6}
Vaporizing liquid (80°F)			
NH₃	10×10^{-6} to 50×10^{-3} lbf	97	10^{-7}
Freon	10×10^{-4} to 50×10^{-3} lbf	52	10^{-7}
Butane	10×10^{-6} to 50×10^{-3} lbf	84	10^{-7}
Propane	10×10^{-6} to 50×10^{-3} lbf	89	10^{-7}
Resistojets (2000°F)—Radioisojet (2000°F)			
NH₃	10×10^{-3} (3 W)	130	10^{-5}
	100×10^{-6} (3 W)	160	10^{-6}
	10×10^{-3} (10 W/mlbf)	230	10^{-4}

FEED SYSTEM

MASS, lbm	COMPONENT	MASS, lbm
0.25	FILL VALVE	
0.20	PRESSURE TRANSDUCER	
0.35	START VALVE	
0.10 - 0.30	FILTER	
0.30 - 0.60	REGULATOR	
	FILL VALVE	0.25
0.20	LINES	
1.20 - 1.70	SUBTOTAL	0.25

	MASS, lbm		MASS, lbm
0.20	PRESSURE TRANSDUCER	0.20	
0.25	FILL VALVE	0.25	
0.35	START VALVE	0.35	
0.20	FILTER	0.20	
0.20	LINES	0.20	
1.20	SUBTOTAL	1.20	
2.40 - 2.90	TOTAL (LESS TANKS AND PROPELLANT)	1.45	

PRESSURIZED SYSTEM

BLOWDOWN SYSTEM

DIRECT CATALYTIC THRUSTER

COMPONENT	MASS, lbm		
	THRUST 0.05 lbf	0.5 lbf	5.0 lbf
SOLENOID CONTROL VALVE	0.20	0.31	0.38
LINES	0.20	0.20	0.20
THRUSTER	0.20	0.34	0.47

RESISTOJET THRUSTER

COMPONENT	MASS, lbm
SOLENOID CONTROL VALVE	0.20
LINES	0.20
THRUSTER	0.20
POWER PENALTY (1.5)	0.45

Figure 4-79

Typical Hydrazine Direct Feed Propulsion Subsystem
(JPL TR 32-1505, 1970, p. 87)

421
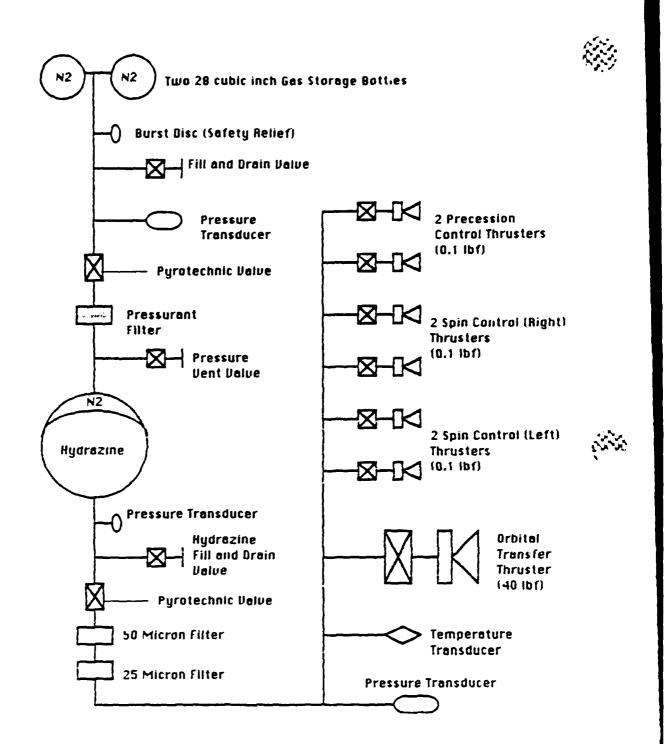
Figure 4-80

ORION Propulsion Subsystem

gas bottles. These 1028 psi bottles are vented first to a common fill and drain valve and then to a single pyrotechnic valve. The fill and drain valves are manually operated poppet valves which are used to load the pressurant and hydrazine tanks or to vent vapors during ground operations. The first pyrotechnic valve isolates the pressurant from the hydrazine tank. Pyrotechnic valves accomplish a one-time valve opening by shearing nipples off the ends of two adjacent tubing sections allowing gas or fluid to pass between the two. This is an irreversible operation. Once gas is vented as a result of pyrotechnic valve actuation. the hydrazine tank is pressurized to 340 psi.

The hydrazine is in contact with a fill and drain valve and a second pyrotechnic valve as diagrammed in Figure 4-80. Pressurant from the gas bottles forces the hydrazine through the pyrotechnic valve after actuation and downstream to the seven thrusters. The fill and drain valve is used to fill the hydrazine tank on the ground or in orbit. A third fill and drain valve on the pressurant side of the tank releases pressure on the gas side of the diaphragm barrier. Once the hydrazine has been released by the second pyrotechnic valve. an electrically-operated dual-seat control valve at each thruster will initiate thruster firing as appropriate. The NASA requirement for a three-point-safe design is fulfilled by the provision of a single pyrotechnic valve and the dual seat thruster valves. This is due to the fact that a pyrotechnic valve functions as two of the three points in the safety chain. NRL engineers (Mr. Paul Cary and Mr. Larry Mosher) have established the precedent for this policy in Navy satellite programs. Thus the ORION design exceeds the three-point-safe requirement using two pyrotechnic

423
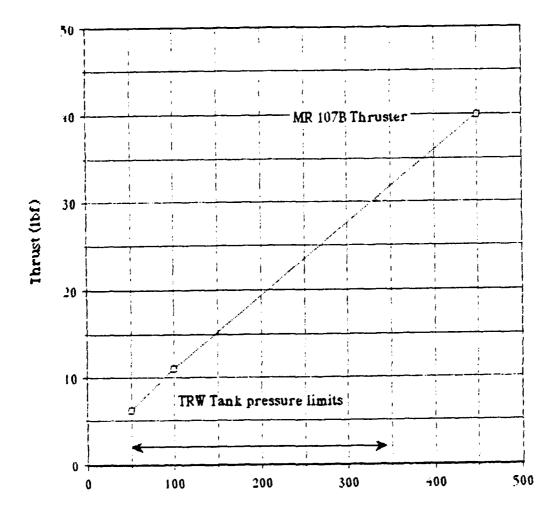
valves and the dual seat thruster control valves. ORION is five-point-safe with respect to propulsion subsytems.

Filters downstream of each pyrotechnic valve catch contaminants that are generated by the pyrotechnic cartridges and shearing of tubing nipples. Metal shards and some catalyzed explosive squib chemicals originate when a pyrotechnic valve is fired and would likely block the thruster valves if not screened by the filters. These filters incorporate two filter stages. The first stage is a set of two pleated screen-type filters of 50 micron absolute rating. The second stage consists of three stacked disc-type filters of 25 micron absolute rating. Pressure transducers sense the pressurant and propellant pressures. The pressure history of the subsystem must be known because the thrust is a function of thruster inlet pressure. Figure 4-81 depicts the approximate thrust of the primary and secondary thrusters as a function of inlet pressure. Thrust output in the last 10% of the pressure range may fluctuate considerably because thruster operation becomes less reliable at low pressures. Pressure histories are also used to evaluate the fill fraction of the hydrazine tank. Figure 4-82 depicts the tank volume as a function of the pressure of the subsystem.

Power consumption of the propulsion subsystem will be due to operation of the thruster inlet valves, pressure transducers, temperature transducers and line heaters. The line heaters are incorporated on all hydrazine wetted tubing and on the propellant tank to maintain the propellant above freezing temperatures. Temperature transducers provide signals to a system controller which cycles the electric heaters. The heaters are turned on when the transducer senses $42°$ F and turned off

424
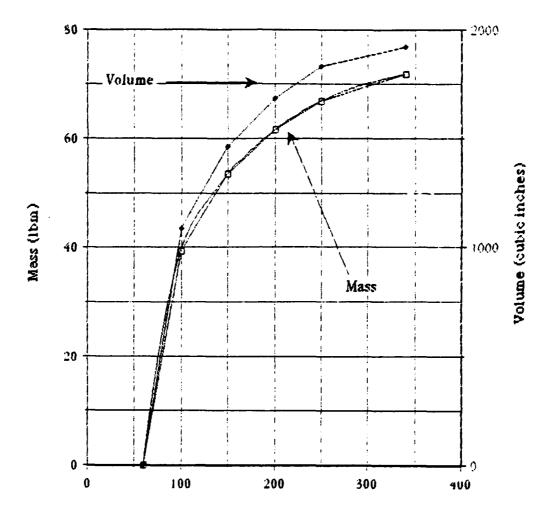
Figure 4-81

Thrust as a Function of Inlet Pressure
Rocket Research MR-107B Thruster

Figure 4-82

Hydrazine Volume and Mass as a Function of Inlet Pressure
TRW #80303 Tank Mass is not Included

426

at a temperature of no more than 98° F. A thermostatically controlled propellant tank heater maintains the hydrazine in the range of 47° to 58° F. All of the heaters are high resistance metallic strips overlayed on an adhesive backing. The propellant lines and heater strips are wrapped with NRC-2 super insulating blanket material to prevent heat loss. Heaters are also placed on the thruster inlet feed lines and are integral in the construction of the catalyst chamber. The thruster assemblies are surrounded by multilayer gold-plated stainless steel foil thermal shrouds.

The propulsion subsystem components are connected using brazed stainless steel tubing: 0.25" inside diameter (ID) tubing connects the pressurant tanks and associated valves to the pressurant side of the hydrazine tank. The outlet of the hydrazine tank also uses 0.25" ID tubing to feed propellant to the 40 lbf thruster. Smaller tubing (0.125 ID) taps off the 40 lbf thruster feed line to supply each of the 0.1 lbf thrusters. A solid brazed system is slightly more reliable than a non-brazed system. However, Paul Cary and Larry Mosher of NRL report that, for small systems like ORION, the reliability difference is insignificant. Gold-based brazing alloy is used with flared tubing ends. The subsystem will be brazed and pressure tested as a complete unit prior to delivery to NPS. Some interconnection of lines at the assembly site may be required for final integration.

A mass budget for this subsystem is provided in Figure 4-34. Note that the hydrazine mass is variable which permits up to 71.5 lbm of

TABLE 4-34

MASS BUDGET FOR ORION PROPULSION SUBSYSTEM
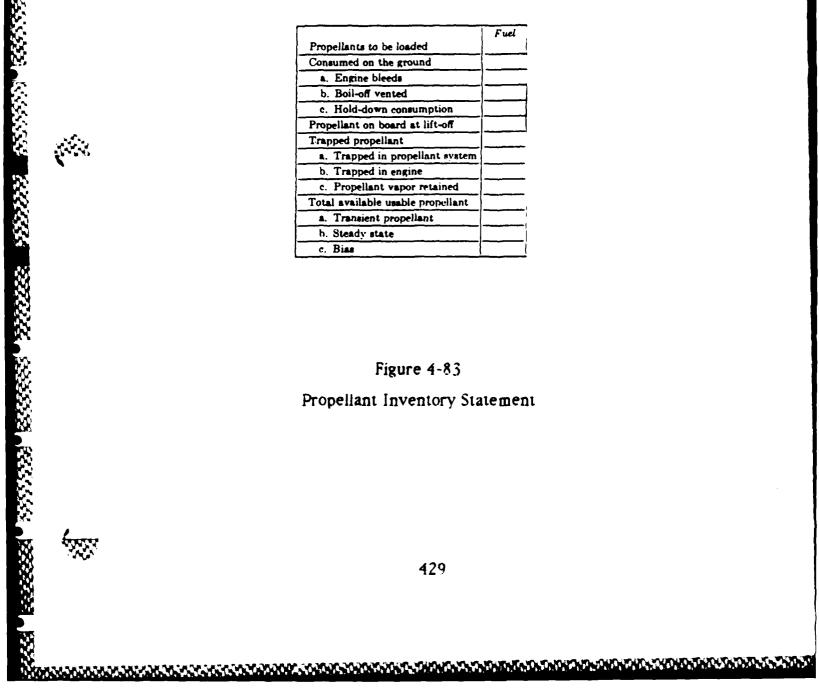
COMPONENT	TOTAL MASS lbm	UNIT MASS lbm
Hydrazine Tank	13.00	
Pressurant Tank (2)	3.08	1.54
Pyrotechnic Valve and Cables (2)	1.00	0.50
Fill and Drain Valve (2)	1.40	0.70
Pressure Vent Valve	0.70	
Tubing, Assorted	2.00	
Thruster (MR 107B)	1.93	
Thruster (MR 103C) (6)	9.18	1.53
Hydrazine (varies)	71.50	
Pressurant (varies)	0.39	

Total   104.18 lbm

	Fuel
Propellants to be loaded	
Consumed on the ground	
a. Engine bleeds	
b. Boil-off vented	
c. Hold-down consumption	
Propellant on board at lift-off	
Trapped propellant	
a. Trapped in propellant system	
b. Trapped in engine	
c. Propellant vapor retained	
Total available usable propellant	
a. Transient propellant	
b. Steady state	
c. Bias	

Figure 4-83

Propellant Inventory Statement

429

propellant to be transported. The propellant inventory table of Figure 4-83
points out the various propellant losses that must be accounted for in actual
propulsion subsystem management.

E. PERFORMANCE
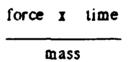
Using the data provided on components for the ORION propulsion
subsystem, specific aspects of the subsystem performance can be quantified.
The performance of various propulsion options was compared on the basis of
specific impulse (I_{sp}) and thrust. A best candidate for the subsystem, the
hydrazine direct catalyst thruster, was chosen because of the high I_{sp}, high
thrust, and low mass and volume compared to other options.

Specific impulse is defined as " the thrust in pounds resulting from the
expulsion of a pound mass of fuel in one second" (Goodger, 1970, p. 14).
Thus, it is an expression of

$$\frac{force \ x \ time}{mass}$$

Specific impulse has the units of poundforce-second per poundmass. For
convenience, specific impulse is usually specified in the units of seconds.
Thrust is expressed as

$$F = d(mV_e)/dt \qquad (4.20)$$

430

where V_e specifies the exit velocity of the exhaust gas leaving the thruster and m is the mass of propellant expended. This equation is usually simplified as

$$F = (dm/dt) I_{sp} = (dm/dt) g V_e \qquad (4.21)$$
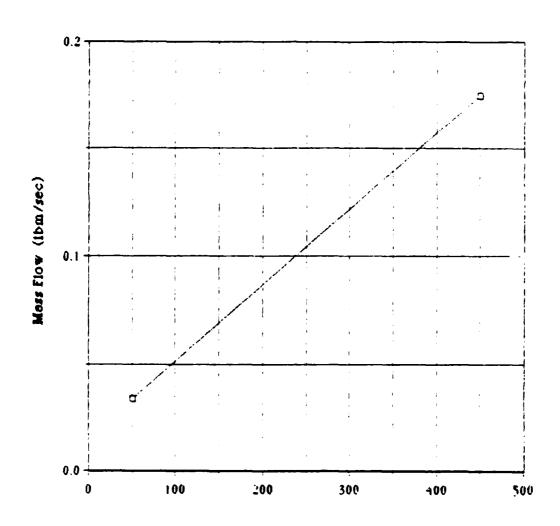
where (dm/dt) represents the mass flow rate of propellant and g is the gravitational constant. Recall that the MR-107B orbital transfer thruster exhibited a range of thrusts between 11 and 40 lbf as a function of propellant inlet pressures (See Figure 4-38). The inlet pressure yields a certain mass flow rate as a function of the propellant pressure head. Using a nominal I_{sp} for hydrazine of 220 seconds, the mass flow rate for this thruster lies approximately in a bound of

$$(dm/dt) = F/I_{sp} \qquad (4.22)$$
$$= 0.1818 \text{ to } 0.05 \text{ lbm/sec}$$

The actual measured mass flow rates for this thruster are seen in Figure 4-38 to be 0.17 to 0.054 lbm/sec. If a linear relationship between pressure and mass flow rate is assumed then Figure 4-84 results. Using these figures the pressure history of the propellant tank can be used to derive the thrust and mass flow rate at any instant. Assuming a nominal density for hydrazine of 63 lbm/ft³, the pressure history can be equated to the volumetric flow rate as depicted in Figure 4-85. Pressurant must replace the propellant in the hydrazine tank at the same rate that the propellant is

431

Figure 4-84

Hydrazine Mass Flow as a Function of Tank Pressure
Rocket Research MR107B Thruster

Figure 4-85

Thrust - Impulse - Flow Nomograph

433
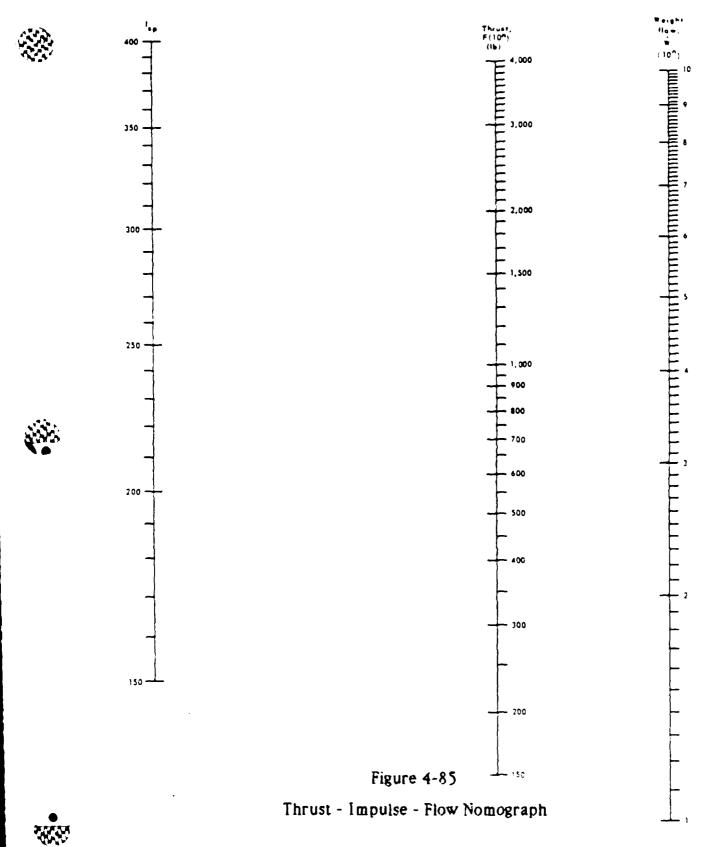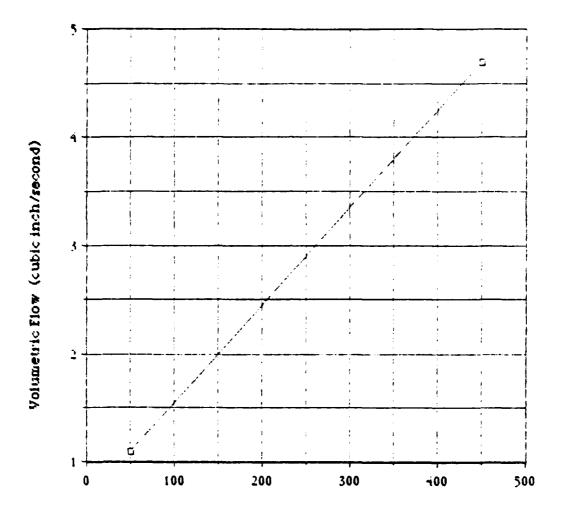
Inlet Pressure (psi)

Figure 4-86

Volumetric Flow of Propellant as a Function of Pressure
Rocket Research MR107B Thruster

434

expelled. At a maximum mass flow rate of 0.17 lbm/sec. a maximum volumetric flow of 0.0027 ft^3/sec. or 4.663 in^3/sec. is observed.

The total impulse (I_T) of the propulsion subsystem is expressed as

$$I_T = I_{sp} \, m_p \tag{4.23}$$

For ORION, the total impulse is approximately 15,730 lbf-sec.

The velocity of the spacecraft after a propulsive maneuver is expressed by

$$V = \left[(F \, t)/m_p\right] \, \ln\left[(m_p + m_{inert})/m_{inert}\right] \tag{4.24}$$

The velocity is a function of the thrust, F, which has been observed to decrease as a function of propellant pressure. If the full load of propellant (71.5 lbm) were expelled in a single propulsive manuever. the velocity imparted would be expressed by

$$V = g \, I_{sp} \, \ln(250/178.5) \tag{4.25}$$
$$= 2386 \, ft/sec$$

This exceeds the design criteria for 2102 ft/sec of orbital transfer delta-V. The acceleration of the spacecraft can also be determined using

$$a = F \, g/m_0 \tag{4.26}$$

The first propulsive burn ($F = 40$ lbf. $m_0 = 250$ lbm) using the MR-107B thruster will produce an acceleration of 5.15 ft/sec^2. The last burn of the thruster ($F = 11$ lbf. $m_0 = 178.5$ lbm) will produce an acceleration of 1.98 ft/sec^2.

F. RELIABILITY
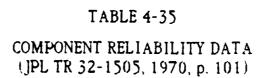
Reliability is one of the most essential elements in cost effectiveness evaluation of competitive system concepts or design options. Recommendations based on comparison of relative reliabilities (qualitative ranking) are useful in concept comparisons, but are not sufficient for a conclusive selection of component designs or subsystem redundancy requirements.

Reliability magnitude becomes important when systems are compared by cost effectiveness techniques. The magnitude of system mass and cost can be determined with reasonable accuracy. This is not the situation with reliability numbers for propulsion components which do not have the extensive statistical failure rate data typical of electronic components. Unless quantitative component reliabilities can be determined, the tradeoff of mass, cost, and reliability becomes erroneous, and can, at best, be only bracketed. (JPL TR 32-1505, 1970, p. 97)

It is important to analyze reliability in the selection of a subsystem to permit an accurate component tradeoff analysis. The tradeoff will be conditioned by the number of operational cycles to which the components will be subjected. As the number of cycles increases, and thus the component lifetime, reliability will be observed to decrease. Also, the configuration of a propellant feed network affects reliability. For example electrically operated solenoid valves and regulators are inherently unreliable compared with most other subsystem components. If solenoid valves fail, there is a historically proven likelihood (75%) that it will fail open. Like
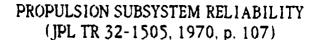
436

TABLE 4-35

COMPONENT RELIABILITY DATA
(JPL TR 32-1505, 1970, p. 101)

Component	Cyclic mode — Cycles				Passive mode
	1,000	5,000	10,000	100,000	
Bi-prop solenoid	0.9983	0.9915	0.983	0.830	0.9934
Solenoid valve	0.9987	0.9935	0.9871	0.871	0.9950
Regulator bi-prop thrust chamber	0.999	0.996	0.990	0.900	0.9963
Electrolysis cell pressure valve relief valve subliming solid "valve"	0.9992	0.996	0.9925	0.925	0.997
Spark generator catalysis thrust chamber direct thermal thrust chamber	0.9994	0.9981	0.9942	0.942	0.998
Lines and manifolds					0.9985
Fill valve (capped) Tridyne resistojet					0.9991
Pyro					0.9995
Bladders radioisojet source					0.99968
Pressure transducer					0.9998
Line heaters (low T)					0.99985
Inert gas (pressurized) plenum tanks					0.99988
Propellant tank inert gas thrust chamber					0.9999
Filter					0.9999

TABLE 4-36

PROPULSION SUBSYSTEM RELIABILITY
(JPL TR 32-1505, 1970, p. 107)

Parameters	Single systems			
	Single	Dual series	Quad	12 T/C dual series
Inert gas				
1,000	0.9513	0.9691	0.9878	0.9884
10,000	0.8822	0.9295	0.980	0.980
Hydrazine				
BD[a] 1,000	0.944	0.961	0.980	0.995
BD 10,000	0.853	0.899	0.947	0.991
PRS[b] 1,000	0.937	0.955	0.973	0.988
PRS 10,000	0.8391	0.884	0.932	0.9755
Hydrazine plenum				
BD 1,000	0.946	0.964	0.983	0.983
BD 10,000	0.8619	0.908	0.957	0.958
PRS 1,000	0.939	0.956	0.9748	0.9759
PRS 10,000	0.8473	0.8928	0.9409	0.9415
Vaporizing, NH₃				
1,000	0.949	0.9668	0.985	0.986
10,000	0.8689	0.9155	0.9648	0.965
Resistojet				
NH₃[c] 1,000	0.944	0.962	0.981	0.986
NH₃ 10,000	0.866	0.912	0.962	0.965
GN₂[d] 1,000	0.9468	0.964	0.983	0.988
GN₂ 10,000	0.8793	0.9266	0.977	0.980
Radioisojet				
NH₃ 1,000	0.948	0.9656	0.984	0.986
NH₃ 10,000	0.868	0.914	0.963	0.966
Electrolysis				
CGM[e] 1,000	0.948	0.966	0.984	0.985
CGM 10,000	0.872	0.919	0.969	0.969
HGM[f] 1,000	0.916	0.938	0.962	0.985
HGM 10,000	0.804	0.862	0.925	0.968
Subliming solid				
(2T)[g] 1,000	0.9918			
(2T) 10,000	0.9784			

[a] Blowdown system.

[b] Pressure regulated system.

[c] Ammonia feed system.

[d] Gaseous feed system.

[e] Inert gaseous expulsion system.

[f] Ignited propellant expulsion system

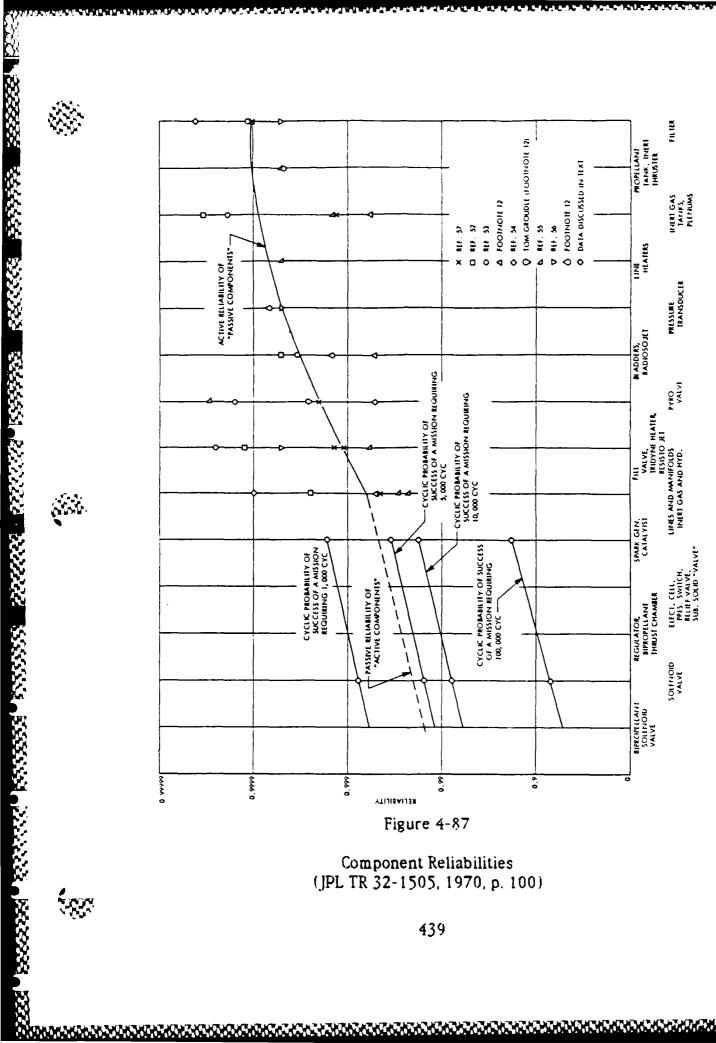[g] System containing only two thrusters.

Figure 4-87

Component Reliabilities
(JPL TR 32-1505, 1970, p. 100)

solenoid valves, regulators are likely to fail open. Hence the configuration of a subsystem (i.e., solenoid valves and regulators) will affect reliability. On the other hand, pyrotechnic valves and manual poppet valves are extremely reliable components. The comparative reliabilities of the these components are shown in Table 4-35 and Figure 4-87. Various subsystem reliabilities are summarized in Table 4-36.

The low reliability of solenoid valves, like those controlling the thruster inlet propellant flow, can be circumvented by using redundancy. Four valve redundancy configurations are pictured in Figure 4-88. The worst failure of a valve or regulator is a "fail open". For a thruster valve this results in an unregulated quantity of fuel being dispersed with associated uncontrollable attitudes or orbit adjustments. The dual series configuration provides redundancy against a "fail open" in one valve. The dual parallel configuration will circumvent a "fail closed" failure of one valve. The two concepts can be combined into quad or quad-connected arrangements.

The ORION propulsion subsystem does not employ solenoid valves upstream of the thrusters. The thruster-mounted solenoid valves cannot be made redundant without re-engineering the entire thruster unit. Pyrotechic valves are inherently reliable, and regulators are not used. Hence, little can be done to improve the reliability of the propulsion subsystem design with the possible exception of using redundant thrusters. Redundancy increases the mass of the subsystem and only protects against the "fail closed" mode of a thruster solenoid. It has been stated that there is a 75% likelihood that a valve will fail open. Hence, little is gained on ORION by using thruster

redundancy. Mathematically, the reliability of the propulsion subsystem is expressed as

$$R = R_f \ R_v^7 \ R_t^7 \qquad (4.27)$$

In this expression, the subscript f refers to the feed system, the subscript v refers to the valves and the subscript t refers to the thruster. By way of example, the reliabilities of a baseline inert gas subsystem and a hydrazine direct subsystem are shown in Figures 4-91 and 4-92. The reliability of the ORION subsystem, it is observed, exceeds the design criteria of 0.9 by a wide margin.
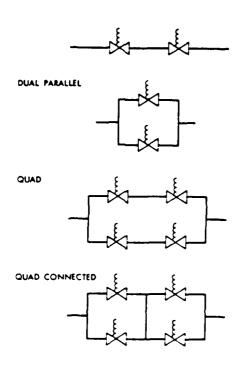
Figure 4-88

Common Valve Redundancy Configurations
(JPL TR 32-1505, 1970, p. 102)

441

(a) SINGLE SYSTEM
SINGLE SOLENOID

(b) SINGLE SYSTEM
DUAL-SERIES SOLENOID

(c) SINGLE SYSTEM
QUAD SOLENOID

(d) SINGLE SYSTEM
12 THRUST CHAMBERS (T/C)
DUAL-SERIES SOLENOID

Figure 4-89
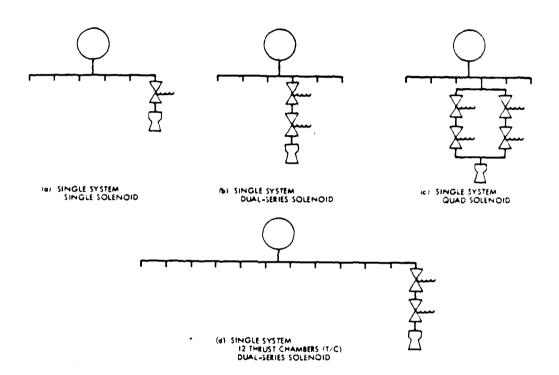
Common Thruster Redundancy Configurations
(JPL TR 32-1505, 1970, p. 5)
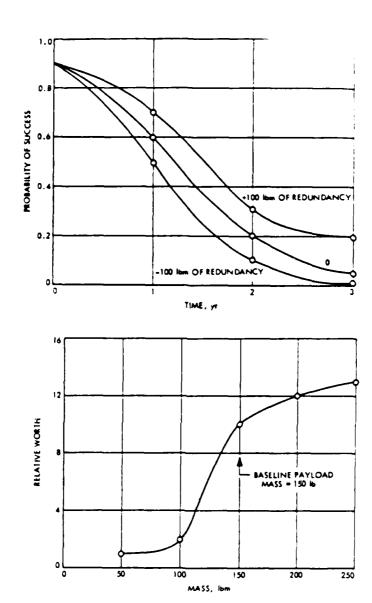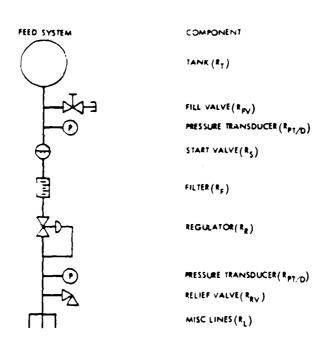
Figure 4-90

Effect of Redundancy on Mass and Probability of Success
(JPL TR 32-1505, 1970, pp. 10/15)
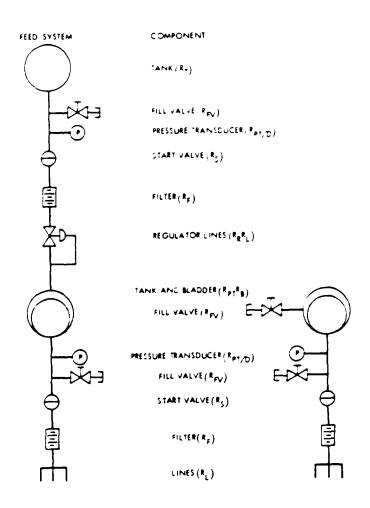
443

FEED SYSTEM

COMPONENT

TANK (R_T)

FILL VALVE (R_{FV})

PRESSURE TRANSDUCER $(R_{PT/D})$

START VALVE (R_S)

FILTER (R_F)

REGULATOR (R_R)

PRESSURE TRANSDUCER $(R_{PT/D})$

RELIEF VALVE (R_{RV})

MISC LINES (R_L)

$R_F = R_T R_{FV} R^2_{PT/D} R_R R_F R_L$

	BASELINE SYSTEM	BASELINE WITH PARALLEL REGULATOR
$R_{F_{1,000\ cyc}}$	0.9887	—
$R_{F_{10,000\ cyc}}$	0.9834	0.9871
$R_{F_{100,000\ cyc}}$	0.894	0.9765

Figure 4-91

Inert Gas Subsystem Reliability
(JPL TR 32-1505, 1970, p. 104)

444

FEED SYSTEM   COMPONENT

TANK (R_T)

FILL VALVE (R_{FV})

PRESSURE TRANSDUCER $(R_{PT/D})$

START VALVE (R_S)

FILTER (R_F)

REGULATOR LINES $(R_R R_L)$

TANK AND BLADDER $(R_{PT} R_B)$

FILL VALVE (R_{FV})

PRESSURE TRANSDUCER $(R_{PT/D})$

FILL VALVE (R_{FV})

START VALVE (R_S)

FILTER (R_F)

LINES (R_L)

$$R_{F_{PR}} = R_T R_{FV}^2 R_{PT/D}^2 R_S^2 R_R R_L^2 R_B R_F^2 R_{PT}$$

$$R_{F_{BD}} = R_{PT} R_B R_{FV}^2 R_{PT/D} R_S R_F R_L$$

	BASELINE SYSTEM	BASELINE WITH PARALLEL REGULATOR
$R_{F_{PR\ 1000\ cyc}}$	0.9885	—
$R_{F_{PR\ 10,000\ cyc}}$	0.9796	0.9833
$R_{F_{BD\ 1000\ cyc}}$	0.9954	—
$R_{F_{BD\ 10,000\ cyc}}$	0.9954	—

Figure 4-92

Hydrazine-Direct Subsystem Reliability
(JPL TR 32-1505, 1970, p. 104)

445

FEED SYSTEM   COMPONENT

TANK (R_{PT})

PRESSURE TRANSDUCER $(R_{PT/D})$
FILL VALVE (R_{FV})
START VALVE (R_S)

FILTER (R_F)

CONTROL VALVE (R_{CV})

VAPORIZER (R_V)
PRESSURE SWITCH $(R_{PS/W})$
PLENUM (R_P)

FILTER (R_F)

LINES (R_L)

$$R_F = R_{PT} R_{PT/D} R_{FV} R_S R_F^2 R_{CV} R_V R_P R_{PS/W} R_L$$

BASELINE SYSTEM

$R_{F_{1000\ cyc}}$ 0.9863

$P_{F_{10,000\ cyc}}$ 0.9683

Figure 4-93

Vaporizing Liquid Subsystem Reliability
(JPL TR 32-1505, 1970, p. 105)

446

FEED SYSTEM

COMPONENT

$$R_{F_{PR}} = R_T R_{FV}^2 R_{PT/D}^2 R_S^2 R_F^3 R_R R_L R_{PT} R_B^2 R_{CV} R_G R_P R_{PS/W}$$

TANK (R_T)

$$R_{F_{BD}} = R_{PT} R_B R_{FV}^2 R_{PT/D}^2 R_S R_F^2 R_L R_{CV} R_G R_P R_{PS/W}$$

FILL VALVE (R_{FV})

PRESSURE TRANSDUCER ($R_{PT/D}$)

START VALVE (R_S)

FILTER (R_F)

REGULATOR LINES ($R_R R_L$)

	BASELINE SYSTEM	BASELINE WITH PARALLEL REGULATOR
$R_{F_{PR}}$ 1000 cyc	0.9757	—
$R_{F_{PR}}$ 10,000 cyc	0.9443	0.9478
$R_{F_{BD}}$ 1000 cyc	0.9835	—
$R_{F_{BD}}$ 10,000 cyc	0.9606	—

FILL VALVE (R_{FV})

TANK AND BLADDER ($R_{PT} R_B$)

PRESSURE TRANSDUCER ($R_{PT/D}$)

FILL VALVE (R_{FV})

START VALVE (R_S)

FILTER (R_F)

CONTROL VALVE (R_{CV})

GAS GENERATOR (R_G)

PRESSURE SWITCH ($R_{PS/W}$)

PLENUM (R_P)

FILTER (R_F)

LINES (R_L)

Figure 4-94

Hydrazine Plenum Subsystem Reliability
(JPL TR 32-1505, 1970, p. 105)

none
none

447

G SUMMARY

The purpose of this chapter was to describe the design constraints which drive the selection of a propulsion subsystem and then to evaluate several propulsion options in light of those constraints. Twelve such constraints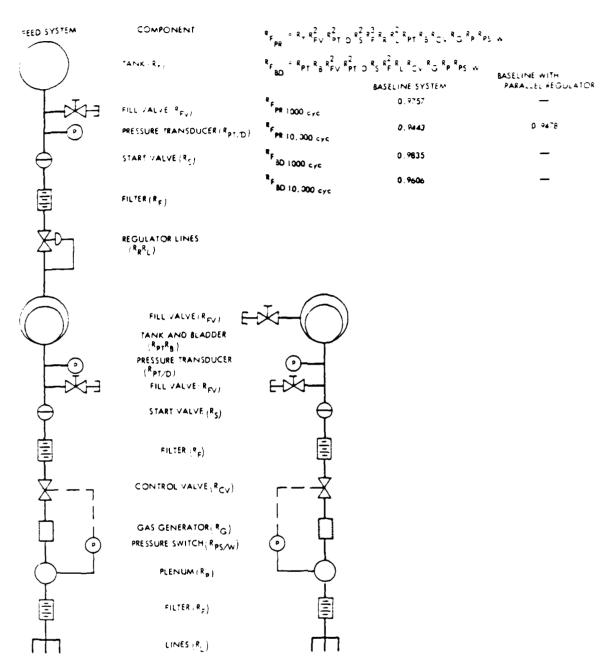 were identified, followed by a review of the mission of the propulsion subsystem and a description of rockets, feed subsystems and propellants. The difference between primary and auxiliary propulsion was highlighted and the required impulse for each was calculated. A total impulse requirement of 1200 lbf-secs for auxiliary propulsion and an orbital transfer deltav of 2108 feet-sec was identified.

Numerous propulsion subsystem options were evaluated for application to the ORION mission. Particular emphasis was placed upon cold gas- and hydrazine-based subsystems due to their simplicity and inherent reliability. The analysis of cold gas subsystems revealed that, because of low I_{sp}, excessively large storage volumes would be required to transport sufficient gas propellant for the primary and auxiliary propulsion missions. However, the hydrazine I_{sp} of 220 seconds was sufficiently large to accomodate all of the propulsion requirements within a propellant volume which was reasonable for the ORION structure. A vendor survey was conducted, and candidate thrusters were identified for primary and auxiliary propulsion roles. The Rocket Research Co. model MR107B was chosen as the primary propulsion thruster, rated for 12 to 40 lbf of thrust. Various options for propellant storage were also reviewed and a TRW spherical positive expulsion tank was selected on the basis of its storage capacity and size for the ORION structure. An analysis of pressurant requirements was also

conducted to determine the requisite pressurant storage volume based upon desired pressure boundaries for the propellant expulsion process. A pair of ARDE Co. high pressure cylinders was chosen to provide 56 in^3 of high pressure Nitrogen pressurant storage.

The design choices and the selected vendor products were integrated in a system summary with diagrams of the propulsion subsystem and a description of construction details. Performance charts were included for the prediction of thrust as a function of fuel pressure or propellant tank volume. The reliability of the hydrazine subsystem was reviewed in contrast to other propulsion options. It was noted that simplicity of design, rather than redundancy, was the best method to improve ORION reliability values consistent with the goal of a low cost, lightweight spacecraft.

V. ATTITUDE CONTROL

A. INTRODUCTION

The feasibility of the ORION concept is crucially linked to the development of a successful attitude control subsystem. The purpose of this chapter is to demonstrate that an accurate attitude control subsystem can be affordably implemented in concert with the hydrazine main propulsion subsystem. Various stabilization options (oblate spinner, prolate spinner, 3-axis, and gravity gradient) are discussed. A stable oblate spinner implemented using deployable booms is chosen for the ORION configuration. Energy dissipation due to internal hydrazine fuel slosh is analyzed with respect to its impact on spin stabilization.

Note that this thesis does not describe the design of the attitude control subsystem in detail. Instead, the goal of this chapter is to prove the feasibility of implementing an accurate hydrazine attitude control subsystem in a small satellite like ORION.   A detailed subsystem design which investigates specific sensor choices or models the dynamics of the vehicle is beyond the scope of this thesis. Each of those issues are to be covered in detailed design studies and follow-on theses. Attitude control feasibility, in of itself, is a large enough problem to justify its treatment in detail. This thesis also does not address the details of attitude dynamics which are outlined adequately by Wertz(1985), Hughes(1986), Kaplan(1976) and Agrawal (1986).

The feasibility of ORION is proven through (1) an analysis of ORION mass properties, (2) a detailed description of energy dissipation for oblate or prolate spinners and (3) and evaluation of methods to combat the problem of exponential nutation growth during energy dissipation. Options such as boom deployment that provide stability are discussed. Sufficient information is provided to allow future ORION designers to predict the performance of the satellite, and integrate specific mission requirements (spin rate, pointing accuracy, sensor utilization) with the data available in this chapter.

1. Design Criteria

Five criteria are important in the design of the attitude control subsystem. The criteria involve consideration of :

1. General Criteria (see Chapter 2)
   a. General purpose design
   b. Affordability
   c. Cost effectiveness
   d. Reliability
   e. Safety

2. Performance
   a. Pointing accuracy
   b. Low fuel usage and lifetime
   c. Low subsystem mass and small volume
   d. Repeatable attitude control burns

3. Mass Properties
   a. Minimal movement of center of mass (CM) as propellant is depleted
   b. CM placement near the center of volume.

4. Ease of Manufacture

5. Easily reconfigured to meet various attitude control requirements

a. General Criteria

The design philosophy of ORION is summarized in the discussions
of Chapter Two. Perhaps the most important of the five general criteria
listed above is that the subsystem design be general purpose. NUSAT, with
its tumbling attitude, possessed in a singular way a specialized attitude
control subsystem. That is, tumbling maneuvers suited the NUSAT mission
because its telemetry and sensors are omnidirectional. However, few other
missions can be implemented using a tumbling spacecraft. Thus, to be
general purpose, a spacecraft attitude control subsystem must accommodate
the needs of many users. Consideration must be given to the ability to
reconfigure a design rapidly and economically suiting the requirements of
different payloads.

A second important criterion is safety. As mentioned in Chapter
Four, GAS ejectable satellites have not been flown with an attitude control
subsystem. Hydrazine, in particular, has not been used in a GAS canister.
The first hydrazine stabilized GAS ejectable satellite must be carefully
designed to ensure safety of the Shuttle crew and success for future ORION
applications.

b. Performance

Several performance specifications for the attitude control
subsystem exist and reflect the requirements for the typical user as
documented in Chapter Two. Mission specifications have not yet been
identified (i.e. orbital altitude, spin rate, pointing requirements, lifetime).

452

(1) <u>Pointing Accuracy and Lifetime.</u>   In order to be general purpose the subsystem must provide a pointing accuracy of at least +/- 1.0 degrees (See Chapter Two for details). This is the accuracy which is attained after all sources of error have been accounted for. A pointing accuracy as fine as 0.1 degrees is desirable, if possible. Hopefully such an accuracy can be achieved by employing simple and inexpensive sensors with minimum redundancy. Achievement of this accuracy without the need for gyros is desirable.

The satellite must perform attitude control functions for at least 90 days in the event that stabilizing booms do not deploy, and an unstable spin is unavoidable. This requirement assumes that a full load of fuel is available for attitude control, and that orbital burns are not required.

(2) <u>Low Fuel Usage.</u> As a result of several spacecraft studies and conversations with NRL engineers, spin stabilization of a <u>stable</u> (oblate) body has been observed generally to require less fuel than three axis stabilization for the same attitude accuracy. Using spin stabilization, the spin axis of the satellite does not move relative to an inertial coordinate system until perturbed. For prolate (unstable) spinners the angular momentum vector shifts relative to a body-fixed coordinate system and requires active nutation control in order to maintain a fixed relation between the body coordinates and angular momentum vector. The fuel required to counter spin instability can be minimized through the selection of an efficient attitude control subsystem and optimization of the nutation time constant which determines the growth of the nutation angle. That is, through proper selection of fluid placement and with attention to mass properties, a design

453

can be achieved which is only slightly prolate,or possibly even oblate, when the spacecraft is spun about its longitudinal axis. This consideration of mass placement leads to a slower growth of the nutation angle. Optimally, the design effort should concentrate on the use of an oblate (stable) spinner, thereby avoiding active nutation control.

(3) **Low Mass and Small Volume**. As mentioned above (Section A-1-b-3), the volume and mass of the satellite can be reduced by consolidating propulsion and attitude control components. Minimum mass can be achieved by using a common fuel tank, fluid controls, piping, etc. Thrusters can also be shared between the propulsion and attitude control roles. Duplication of components for the separate roles is not desirable. Hardware decisions made in support of the attitude control subsystem should emphasize the dual roles for these components.

(4) **Repeatable Attitude Control Burns.** Accurate prediction of the performance of ORION in orbit is important. To do that, the output of the propulsion and attitude control thrusters must be predictable. The subsystem should be configured so as to provide repeatable attitude control thrusts whose performance can be controlled with a high degree of confidence.

c. Movement of Center of Mass

Prediction of the position of the spacecraft center of mass (CM) at any time during the satellite lifetime is necessary in order to model the satellite on-orbit performance. For example, coupled attitude control thrusters exert control forces about the satellite CM. The stability of the spacecraft may be adversely affected if the CM moves significantly as

454

propellants are expended. A favorable location for center of mass should be chosen, and the mass placement should then be structured so as to ensure that the CM moves only slightly over the course of the satellite lifetime. Control of the CM results in predictable performance and enhanced stability.

d. Ease of Manufacture

The design of the attitude control subsystem should be as simple as possible and focus on the use of simple, proven components. This design philosophy reduces cost, simplifies manufacturing and expedites repairs. Even a relatively simple 1.0 lbf hydrazine thruster requires a delivery time of almost two years from start of contract negotiations to receipt. More complicated components are prohibitively expensive and detract from the ORION "fast" design.

e. Reconfigurable

Specific mission requirements have not been identified for ORION. Instead, the satellite has been conceived to fulfill the needs of several different missions. Eventually, mission specific requirements must be provided to define mass properties, pointing accuracy, etc. Flexibility must be incorporated in the design to permit some reconfiguration prior to the "design freeze". A "stiff" design that will not tolerate some modification is not desirable.

2. Engineering Challenges

The design of the ORION attitude control subsystem faces several challenges. These challenges are attributable to (1) spinning ORION about its longitudinal axis and (2) the presence of "sloshing" liquid propellant. Note that the use of the GAS canister for spacecraft deployment leads to a

455

structure that is long axially with a relatively small radius. If such a rod shaped object (of uniform density) is spun about the longitudinal axis, it is known as a prolate spinner. Such an object is inherently unstable. The moment of inertia in the transverse axis (I_t) exceeds the moment of inertia in the longitudinal axis (I_s)
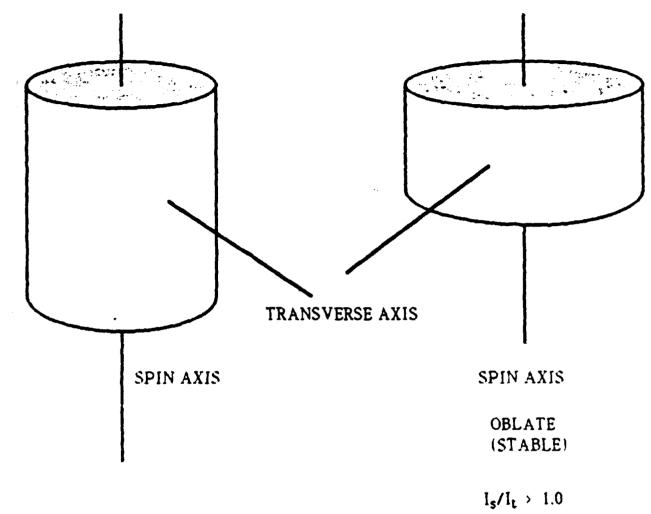
$$I_t \; > \; I_s$$

and the object will tend to nutate away from the initial spin attitude once it is perturbed. In a stable (or oblate) spinner the transverse moment of inertia does not exceed that of the spin axis. This results in a configuration that damps nutation rather than amplifying it. Figure 5-1 depicts the difference in the two geometries. The engineering challenge is to position mass in ORION so as to reduce the value of I_t to the smallest possible value. Minimum I_t can be accomplished by placing large masses close to the periphery of the structural cylinder. Massive components should be concentrated near the plane that passes through the center of mass and orthogonal to the longitudinal axis, as depicted in Figure 5-2. This mass distribution increases "oblateness" and thus increases stability.

The choice of hydrazine as a propellant also leads to a significant engineering obstacle. Recall that a 16.5 inch diameter positive expulsion tank was chosen to provide propellant storage. On orbit the propellant moves within the tank with a large wetted surface area. Note that for the positive expulsion bladder-tank in Chapter Four, the wetted surface area

TRANSVERSE AXIS

SPIN AXIS

SPIN AXIS

OBLATE
(STABLE)

$I_s/I_t > 1.0$

PROLATE
(UNSTABLE)

$I_s/I_t < 1.0$

Figure 5-1

Geometries of Spinning Bodies

will remain constant (ARDE, 1986) although the mass of fuel decreases during expulsion. As the spinning satellite begins to nutate, the axis of the spinning fuel and the tank will no longer be aligned, and hydrodynamic *forces will develop between the fluid and the tank wall*. These friction forces will act to further perturb the spin of the spacecraft as the spin kinetic energy of the satellite is dissipated. (The same problem holds true for three axis stabilization but the friction component is less noticeable due to the absence of high angular velocities.) For oblate spacecraft, energy dissipation enhances the stability of the satellite because it counteracts the rotation in the transverse axis which is due to nutation. Thus "fuel slosh" * damps nutation in an oblate spinner. The opposite is true in a prolate spinner, and the energy dissipation causes the spin about the longitudinal axis to decay. The satellite rapidly lapses into a flat spin about the transverse axis if the nutation is not actively countered by thrusters. Fuel will be consumed rapidly in an attempt to maintain the spin axis orientation. For medium to long lifetimes, the challenge of energy dissipation must be confronted if the satellite is to be deployed as a prolate spinner. Thus it is virtually imperative that a stable (oblate) design be pursued.

---

* "Fuel slosh" is used to describe dissipation due to the surface action of fuel in a tank without propellant management devices (PMD). Slosh also describes the dissipation due to internal wave resonances interacting with tank walls. The reader should consult Zedd (1985), Agrawal (1986), Dodge (1986) and Abrams in NASA SP-106 (1966) for further definition of internal wave resonances. Because ORION uses a positive expulsion tank, a free surface does not exist. However, there is a large wetted area against which hydrodynamic forces due to internal wave resonances can react. Unfortunately, "fuel slosh" is used too freely in the literature to describe both dissipation mechanisms.
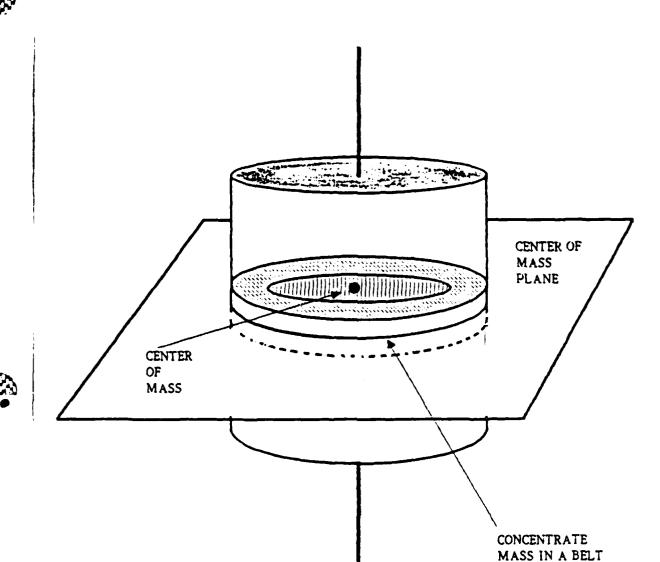
Figure 5-2

Mass Concentration in the Center of Mass Plane

The design of the attitude control subsystem is further complicated by the fact that energy dissipation cannot be predicted analytically. Efforts by Kaplan(1986), Vanyo(1986), Hubert and Goodzeit(1983), Agrawal(1986), Zedd(1985) and Dodge(1985) have all shown that the dissipation problem is not analytically tractable. Consequently satellite designers conduct scale model tests of proposed satellite systems in order to evaluate the effect of energy dissipation on stable and unstable spinners. Experimental values are scaled through dimensional analysis to predict satellite behavior. These tests determine the nutation time constant that describes the exponential growth or decay of the nutation angle. The nutation time constant is τ in the following equation.

$$\theta(t) = \theta_0 \, e^{t/\tau} \qquad (5.1)$$

Obviously, if t is increased or the time constant is decreased, the value of the nutation angle will change more rapidly. The time constant will be negative for stable spinners and positive for unstable spinners. A large time constant is desirable for unstable spinners and a short time constant (rapid nutation damping) is desirable for stable spinners.

The engineering challenge is to determine an accurate time constant. Some early scale model tests resulted in theoretical time constants that were in error by as much as a factor of 100. This is an unacceptably large margin of error in the prediction of transient behavior, and ultimately, lifetime of the satellite. Considerable effort is being devoted by the authors listed above to improve test facilities and devise advanced numerical analyses that

more accurately predict satellite spin behavior. As yet, however, methods have not been devised to predict the satellite time constant. Only actual spin tests and observations in the simulated space environment produce reliable values. The challenge, then, is to develop an accurate test protocol that results in a valid time constant for ORION. Fortunately, scale model tests by Vanyo (1986) and Hubert and Goodzeit (1983) have evaluated nutation time constants for on-axis tanks such as those in the ORION configuration. Their results can be interpolated for the ORION case with reasonable accuracy.

A number of minor challenges must be considered in the design of the satellite. First, with respect to the oblate vs. prolate spinner option, consideration must be given to the orientation of the sensors, payload, and solar cells. For solar cells, the best spin axis is the longitudinal axis. Spinning about this axis, the solar cells, which are distributed on the circular periphery of the structure, are provided with a time-averaged uniform distribution of light as the satellite rotates. A second consideration is the placement of components for thermal or operational requirements. Mass placement is critical to the stability of the spacecraft but must conform to equipment thermal and operational requirements as well as attitude control preferences.

A third challenge is the identification of specific mission requirements. The attitude control performance of the satellite cannot be modeled without knowledge of the spin rate, orbital altitude, payload mass and volume, pointing requirements, sensor accuracies and thermal constraints, to name a few. For the purpose of this thesis, certain assumptions are made regarding these parameters permitting an estimate of the satellite lifetime. A detailed

461

attitude control study can only be performed using actual mission parameters. Thus, this thesis serves the role of a feasibility study, and the challenge is to refine the parameters on which that study is based.

A fourth engineering challenge involves the choice of sensors for attitude determination. The type of sensors chosen depends upon the required pointing accuracy, cost and various physical constraints. Magnetometers, gyros, sun sensors, earth sensors and star sensors are all candidates for the attitude determination task. While specific sensor choices are highly dependent upon the mission, several general choices will be recommended. A pointing accuracy of +/- 1.0 ° is the design goal, although +/- 0.1° would be preferable. Very fine accuracy often requires expensive gyro suites which the design seeks to avoid because of cost. An excellent discussion of attitude sensors is provided in Wertz (1985).

B. ATTITUDE CONTROL BACKGROUND

Attitude control is a process of orienting the spacecraft in a specified, predetermined direction. It consists of two areas -- attitude stabilization, which is the process of maintaining an existing orientation, and attitude maneuver control, which is the process of controlling the reorientation of the spacecraft from one attitude to another. The two areas are not totally distinct, however. For example, we speak of stabilizing a spacecraft with one axis toward the Earth, which implies a continuous change in its inertial direction. The limiting factor for attitude control is typically the performance of the maneuver hardware and the control electronics...

Some form of attitude determination and control is required for nearly all spacecraft. For engineering or flight related functions, attitude determination is required only to provide a reference for control. Attitude control is required to avoid solar or atmospheric damage to sensitive components, to control heat dissipation, to point directional antennas and solar panels (for power generation) and to orient rockets

for orbit maneuvers. Typically, the attitude control accuracy necessary for engineering functions is on the order of 1.0 degree. Attitude requirements for the spacecraft payload are more varied and often more stringent than the engineering requirements. Payload requirements, such as telescope or antenna orientations, may involve attitude determination, attitude control, or both. Attitude constraints are most severe when they are the limiting factor in experimental accuracy or when it is desired to reduce the attitude uncertainty to a level such that it is not a factor in payload operation. These requirements may demand accuracy down to a fraction of an arc-second (1 arc-second equals 1/3600 degree). (Wertz, 1985, p. 2)

The field of attitude control is a broad one. A proper treatment of all attitude control, attitude prediction and attitude determination issues associated with ORION would be beyond the scope of this thesis. It is assumed that the reader has a working knowledge of attitude control theory. Several references are available that deal with the subject in great detail, notably Wertz(1985), Kaplan(1976), Hughes(1986) and Agrawal(1986). Most references in this chapter will refer to explanations in Wertz(1985).

1. Attitude Control Options

A convenient method for categorizing spacecraft is the procedure by which they are stabilized. The simplest procedure is to spin the spacecraft. The angular momentum of a spin-stabilized spacecraft will remain approximately fixed in inertial space for extended periods, because external torques which affect it are extremely small in most cases. However the rotational orientation of the spacecraft about the spin axis is not controlled in such a system. If the orientation of three mutually perpendicular spacecraft axes must be controlled, the spacecraft is three-axis stabilized. In this case, some form of active control is usually required because environmental torques, although small, will normally cause the spacecraft orientation to drift slowly. (However, environmental torques can be stabilizing in some circumstances.) Three axis stabilized spacecraft may be either nonspinning (fixed in inertial space) or fixed relative to a possible rotating reference frame, as occurs for an Earth satellite which maintains
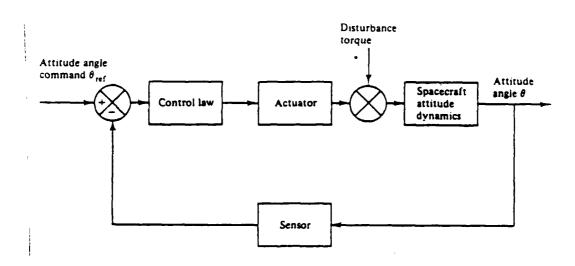
463

Figure 5-3

Attitude Control Block Diagram
(Agrawal, 1986, p. 106)

TABLE 5-1

ATTITUDE CONTROL OPTIONS
(Wertz, 1985, p. 503)

METHOD	ADVANTAGES	DISADVANTAGES
SPIN STABILIZED	SIMPLE; EFFECTIVE NEARLY ANYWHERE IN ANY ORIENTATION; MAINTAINS ORIENTATION IN INERTIAL SPACE	CENTRIFUGAL FORCE REQUIRES STRUCTURAL STABILITY AND SOME RIGIDITY; SENSORS AND ANTENNAS CANNOT GENERALLY REMAIN POINTED AT A SPECIFIC INERTIAL TARGET; WOBBLE (NUTATION) IF NOT PROPERLY BALANCED; DRIFT DUE TO ENVIRONMENTAL TORQUES
GRAVITY-GRADIENT STABILIZED	MAINTAINS STABLE ORIENTATION RELATIVE TO CENTRAL BODY; NOT SUBJECT TO DECAY OR DRIFT DUE TO ENVIRONMENTAL TORQUES UNLESS ENVIRONMENT CHANGES	LIMITED TO 1 OR 2 POSSIBLE ORIENTATIONS; EFFECTIVE ONLY NEAR MASSIVE CENTRAL BODY (E.G., EARTH, MOON, ETC.); REQUIRES LONG BOOMS OR ELONGATED MASS DISTRIBUTION; SUBJECT TO WOBBLE (LIBRATION); CONTROL LIMITED TO ~1 DEG—PROBLEM OF THERMAL GRADIENTS ACROSS BOOM
SOLAR RADIATION STABILIZED	CONVENIENT FOR POWER GENERATION BY SOLAR CELLS OR SOLAR STUDIES	LIMITED TO HIGH-ALTITUDE OR INTERPLANETARY ORBITS. LIMITED ORIENTATIONS ALLOWED
AERODYNAMIC STABILIZED		
MAGNETIC STABILIZED WITH PERMANENT MAGNET	SPECIAL-PURPOSE METHODS — HIGHLY MISSION AND STRUCTURE DEPENDENT IN ALL OF THEIR CHARACTERISTICS	
GAS JETS	FLEXIBLE AND FAST. USED IN ANY ENVIRONMENT; POWERFUL	USES CONSUMABLE (FUEL) WITH LIMITED SUPPLY AVAILABLE DUE TO FUEL WEIGHT. TOO POWERFUL FOR SOME APPLICATIONS (I.E., RELATIVELY COARSE CONTROL); COMPLEX AND EXPENSIVE PLUMBING SUBJECT TO FAILURE
MAGNETIC (ELECTROMAGNETS)	USUALLY LOW POWER; MAY BE DONE WITHOUT USING CONSUMABLES BY USE OF SOLAR POWER	SLOW; NEAR EARTH ONLY; APPLICABILITY LIMITED BY DIRECTION OF THE EXTERNAL MAGNETIC FIELD; COARSE CONTROL ONLY (BECAUSE OF MAGNETIC FIELD MODEL UNCERTAINTIES AND LONG TIME CONSTANTS)
REACTION WHEELS*	PARTICULARLY GOOD FOR VARIABLE SPIN RATE CONTROL; FAST, FLEXIBLE, PRECISE ATTITUDE CONTROL AND/OR STABILIZATION	REQUIRES RAPIDLY MOVING PARTS WHICH IMPLIES PROBLEMS OF SUPPORT AND FRICTION. MAY NEED SECOND CONTROL SYSTEM TO CONTROL OVERALL ANGULAR MOMENTUM ("MOMENTUM DUMPING") IN RESPONSE TO CUMULATIVE CHANGES BY ENVIRONMENTAL TORQUES. EXPENSIVE
ALTERNATIVE THRUSTERS (ION OR ELECTRIC)	PRIMARILY SPECIAL PURPOSE—LESS EXPERIENCE WITH THESE THAN WITH THOSE LISTED ABOVE. CHARACTERISTICS ARE HIGHLY MISSION DEPENDENT. SOME SYSTEMS MAY SEE MORE USE IN THE FUTURE AS FURTHER EXPERIENCE IS GAINED	
ACTIVE SOLAR, AERODYNAMIC, OR GRAVITY GRADIENT		

*REFERS TO ANY DEVICE THAT MAY BE USED IN A PROCESS TO EXCHANGE ANGULAR MOMENTUM WITH THE SPACECRAFT BODY.

CONTROL METHOD	REGIONS OF SPACE WHERE APPLICABLE	REPRESENTATIVE TORQUE	SATELLITES USING SYSTEM
GAS THRUSTERS	UNLIMITED	FOR A THRUSTER FORCE OF 0.1 N AND MOMENT ARM OF 2 M, TORQUE = 0.6 N-M	ISEE, OSO, ATS, CTS
MAGNETIC COILS	BELOW SYNCHRONOUS ORBIT (<35,000 KM)	FOR A 40,000 POLE-CM ELECTROMAGNET AT AN ALTITUDE OF 550 KM, TORQUE = 0.001 N-M	AEROS, OSO, SAS-3, AE
GRAVITY GRADIENT	NEAR MASSIVE CENTRAL BODY (EARTH, MOON, ETC.)	FOR AN 800-KM CIRCULAR ORBIT AND AN ELONGATED SATELLITE WITH A TRANSVERSE MOMENT OF INERTIA OF 1000 KG-M² TORQUE = 5 × 10⁻⁵ N-M/DEG OF OFFSET FROM NULL ATTITUDE	GEOS, RAE
MOMENTUM WHEELS	UNLIMITED	TYPICAL ANGULAR MOMENTUM = 10 KG-M²/S, TYPICAL TORQUE ABOUT THE WHEEL AXIS = 0.1 N-M	ATS-6, SAS-3, AE, OAO, GEOS

*E = ENVIRONMENT MODEL, H = HARDWARE, S = STABILIZATION; M = MANEUVERS.

one face toward the Earth and is therefore spinning at one rotation per orbit. Many missions consist of some phases in which the spacecraft is spin stabilized and some phases in which it is three-axis stabilized. (Wertz, 1985, p. 3)

A third form of attitude control uses gravity gradient stabilization. Using this procedure, mass distributions in the satellite are aligned with the local gravity vector to provide a relatively rough Earth orientation with an accuracy on the order of 3 degrees. Authors do not completely agree on the attitude accuracy of gravity gradient stabilization. Various authors quote accuracies of 1 to 5 degrees. Masses in the satellite must be segregated to enable the satellite to stabilize. "Tip masses" are often used to place a mass at the end of a boom away from the main body. This enhances the gravity gradient stability of a spacecraft through the provision of a moment arm and the presence of masses in slightly separate but distinct orbits.
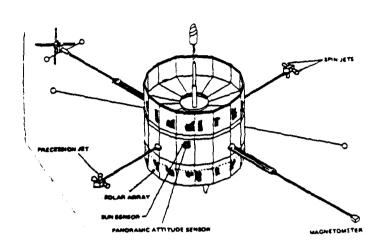
Several considerations are involved in the choice of an attitude control option. Pointing accuracy, fuel consumption, thermal constraints, power generation, satellite lifetime and design simplicity are all factored into the choice of spin stabilization for ORION. Three-axis stabilization was rejected for several reasons, one of which is thermal control. A first approximation of thermal loads and satellite thermal characteristics conducted by NRL engineers indicates that a severe overtemperature condition would result for the body mounted solar cells on ORION using three-axis techniques. A thorough thermal analysis for the specific ORION design is needed to confirm this. Conversations with NRL thermal engineers point out that, with little or no movement of the spacecraft relative to the sun line, the solar cells would quickly overheat on the sunlit side of the spacecraft. The cells will be

466

mounted to the aluminum skin of ORION, and, in the judgement of NRL

engineers, the skin of ORION would not conduct heat away from
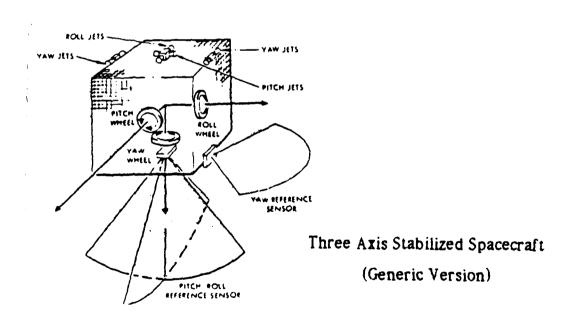

Spin Stabilized Spacecraft

(ISEE-1)

Three Axis Stabilized Spacecraft

(Generic Version)

Figure 5-4

Spacecraft Stabilization Options
(Wertz, 1985, p. 503)

467

the cells fast enough to counter the heat gain due to constant exposure to the sun. A detailed thermal analysis is required to evaluate the heat transfer characteristics of ORION. The thermal node model exhibits a complex geometry and cannot be evaluated analytically. Hot solar cells demonstrate a marked reduction in energy conversion efficiency. A low output, coupled with the continuous shade for those cells on the "dark side" results in unacceptably low power levels. Even with favorable sun orientations, production of more than 10 to 15 watts of power is unlikely. The overtemperature situation also affects internal electronics requiring the use of radiators and heat pipes to provide thermal management. By contrast, spin stabilized satellites that rotate at moderate RPM (less than 200 rpm) will absorb energy when exposed to the sun and then radiate much of that energy as portions cyclically rotate to face deep space. This constant absorption-radiation cycle leads to a balanced average surface temperature of approximately 70° F. Such a "room temperature" environment is conducive to high solar cell efficiency and provides an even exposure to all cells over a single period of rotation. As a result, power levels of 60-75 watts are attainable using spin stabilization.

Fuel considerations also weigh heavily against the use of three-axis stabilization. Using this procedure, jets fire to orient the spacecraft in a certain direction. An opposite jet firing of equal magnitude will stop the spacecraft at a precise orientation. However, any mismatch in the two jet pulses will result in some spacecraft motion. External torques will also perturb the satellite displacing it from the desired orientation. The jets must fire repeatedly to reorient, and a limit cycle develops in which thrusters fire

468

regularly to cancel motion in the three axes. For example, SPARTAN uses nitrogen gas jets to obtain arc-second accuracies and a limit cycle of 6 seconds is required. Short limit cycles lead to rapid propellant consumption: in the case of SPARTAN the lifetime is no greater than 3 days (Cruddace and Fritz, 1985). A stabilization scheme must be adopted that is fuel efficient to minimize fuel consumption in any spacecraft configuration (stable or unstable) and to achieve a minimum lifetime of 90 days for a prolate ORION (booms fail to deploy, or are not used). Three axis stabilization will very likely be more fuel efficient than spin stabilization for an unstable, prolate spacecraft. However. the goal of the design is to provide a stable platform: thus, fuel efficiency concerns are best served through the use of spin stabilization.

Finally, a consideration of the system design complexity weighs in favor of choosing spin stabilization. A key design criterion was to keep the design of ORION simple. That can best be accomplished using spin stabilization. Three axis stabilization requires more complex sensor and thruster systems; multiple sets of coupled thrusters and spin-scanning Earth sensors complicate the design of ORION unecessarily. Subsystems that provide arc-second pointing accuracies exceed the current ORION attitude criteria and involve unneccessary design complexity. Although future ORION derivations may require three-axis or dual-spin stabilization with fine attitude resolution, the "keep it simple" approach dictates the choice of an uncomplicated single spin stabilization for this first design.

Gravity gradient stabilization was also rejected as an option. The primary consideration was with regard to pointing accuracy. Using gravity

gradient, the best possible pointing accuracy is likely to be on the order of 3 degrees. Only one or two orientations of the spacecraft will be possible, and these will always be Earth-seeking. Inertial (heliocentric) pointing will not be possible. Furthermore, the elongated mass distribution required by gravity gradient stabilization can lead to significant structural challenges in the design of booms and optimization of the spacecraft structure for a GAS deployment.* Finally, this method of attitude control leads to thermal problems similar to those encountered in three-axis stabilization.

2. Spin Stabilization

Spin stabilization of a satellite can be accomplished using several different types of mechanisms. Most often, mass expulsion, or jet thrust, is used to initiate and control the spin of a vehicle or to accomplish precession and nutation. The range of spin rates and precession rates that can be accomplished using mass expulsion is virtually unlimited. These rates are simply a function of thrust level, thrust duration and available propellant. Several spacecraft have also been successfully flown using magnetic torquers to control both spin rate and precession. While a magnetic subsystem is lighter than a mass expulsion subsystem, it is incapable of

---

* At least one company, Defense Systems Incorporated of Washington, D.C., is investigating the use of gravity gradient stabilization for a GAS ejectable satellite. Because a separation of masses is required for this form of attitude control, a boom is typically deployed to carry a 'tip mass' some distance away from the main structure. Metal-memory booms which unroll like a tape rule into a cylindrical boom are often used. These booms typically occupy a relatively large volume (0.5 ft^3). Designing a miniature stiff boom for the GAS satellite applications has been a major engineering challenge in the DSI spacecraft development effort.
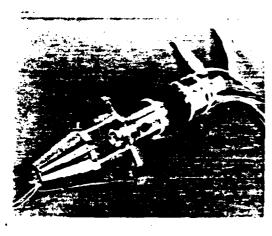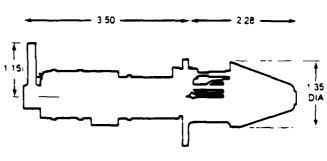
rapid control and has a limited range of spin rates which it can produce. For example, spin rates of 200 revolutions per minute are not uncommon for mass expulsion subsystems. Unfortunately, magnetic subsystems exhibit low torque which negates their use in fast slewing operations (Wong, 1985,401). Additionally, magnetic systems are only effective near the earth. As a third option, spin stabilization can be effected using momentum wheels. Fine angular control with rapid slew rates and smooth control is possible using momentum wheels.

Mass expulsion (hydrazine jet) is the best method of spin control for the ORION subsystem. Additional hydrazine jets are easily integrated with the propulsion subsystem and require the addition of little plumbing and only a small mass of thrusters. To accomplish spin stabilization, at least three thrusters are required. Two provide spin rate control (for spin-up and despin) and one provides both precession and nutation control. The spin rate control thrusters must be aligned so as to produce a thrust that is tangent to the circle of revolution. The precession/nutation control thruster is nominally aligned parallel to the spin axis being placed as far as possible from the spin axis to produce the greatest torque.

The ORION design incorporates a total of six attitude control thrusters as diagrammed in Figures 5-11 and 5-12 (components K and R). Each of these thrusters (Figure 5-5) weighs 1.53 lbm and produces 0.1 lbf thrust. Chapter Four describes these thrusters in detail. The spin rate thrusters (4) are arranged in two coupled pairs. Two diametrically opposed

Design Characteristics

- [ ] Propellant   Hydrazine
- [ ] Catalyst   Shell 405
- [ ] Thrust, Steady State (lbf)   0.240—0.054
- [ ] Feed Pressure (psia)   400—90
- [ ] Chamber Pressure (psia)   330—80
- [ ] Expansion Ratio   100:1
- [ ] Flow Rate (lbm/sec)   0.001—0.00023
- [ ] Valve   Wright Components Dual Seat Bifilar
- [ ] Valve Power   12.2 Watts Max. at 42 vdc and 40 °F
- [ ] Weight (lbm)   0.73
  - Engine   0.28
  - Valve   0.45

Demonstrated Performance

- [ ] Specific Impulse (lbf-sec/lbm)   226—208
- [ ] Total Impulse (lbf-sec)   3,650
- [ ] Total Pulses   161,000
- [ ] Minimum Impulse Bit (lbf-sec)   0.005 @ 100 psia & 25 ms ON
- [ ] Steady-State Firing (sec)   180

Figure 5-5

Hydrazine Thruster for Precession and Spin Control

thrusters provide spin control in one direction, and two in another. Using coupled spin control thrusters, all torques occur about the principal (longitudinal) axis without translation. One thruster could provide spin control; however, a single thruster results in some translation just as the propulsion subsystem thruster results in spacecraft movement. Also two precession thrusters (rather than one) provide redundancy. A coupled precession thruster pair must be placed so that one thruster fires from each "end" of the satellite cylinder, on opposite "sides". This is not possible for ORION because the payload end of the spacecraft has been dedicated to payload use alone. Two precession thrusters on one end, as in the ORION configuration, provide more rapid slewing and nutation control than one thruster. Two thrusters also provide redundancy for critical precession and nutation maneuvers.

The six thrusters are coupled with the propulsion subsystem as indicated in Figures 4-80 and 5-6. This design parallels that of other mass expulsion spin-stabilized spacecraft such as INTELSAT V (Figure 5-7). Note that the ORION design incorporates less redundancy than the INTELSAT design. This is due to the requirement that ORION be affordable, minimizing system mass and complexity. The fill/drain valves, pyrotechnically actuated in-line valves, filter, pressurant tanks, propellant tank and most of the plumbing are common to the propulsion subsystem.

3. Rotating Geometries and Moments of Inertia

Oblate and prolate spinner classifications are based on the moments of inertia of the spinning body. Assume that the spinner is axially symmetric and of uniform density(a right circular cylinder or sphere, for
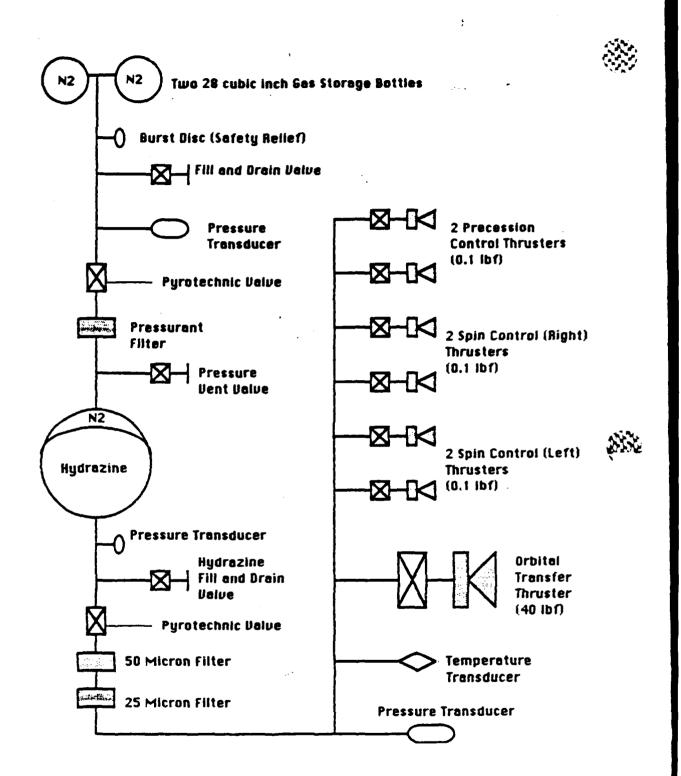
473

Figure 5-6
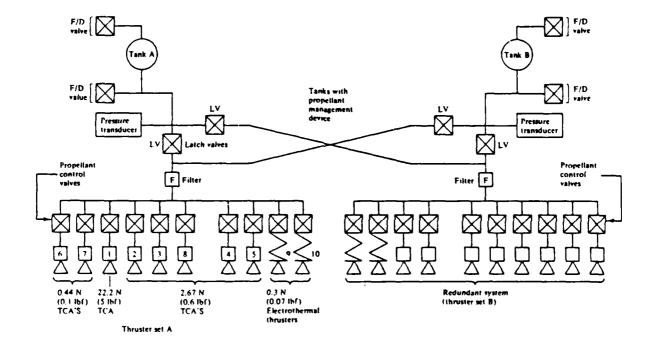
ORION Attitude Control Subsystem Block Diagram

Figure 5-7
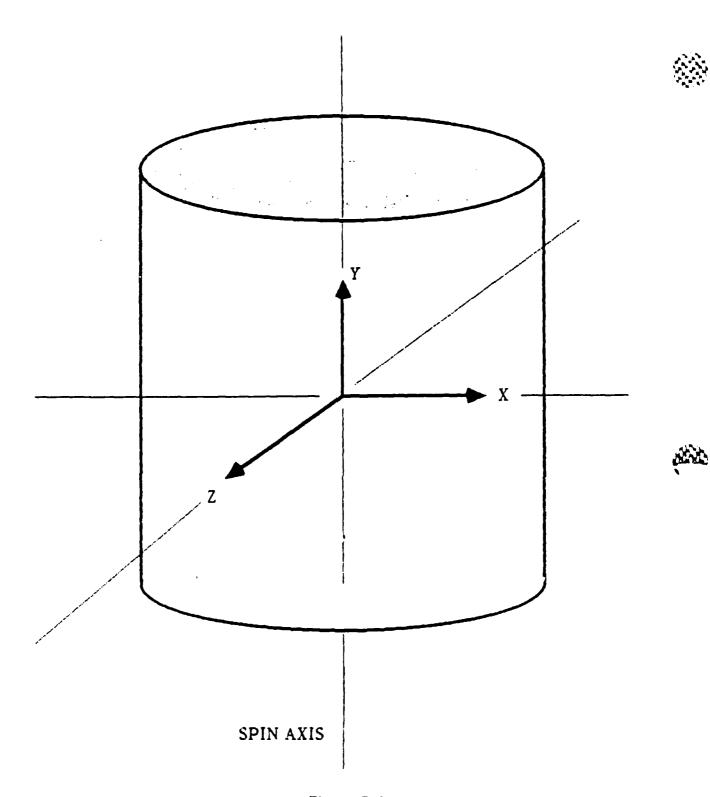
INTELSAT V Attitude Control Subsystem

475

SPIN AXIS

Figure 5-8

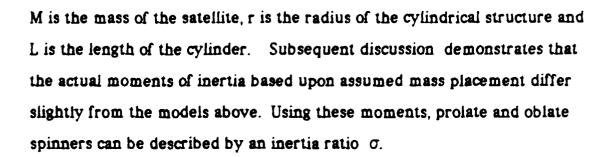Cartesian Coordinate System for Axes of the Moments of Inertia

476

example). For such a body, three principal moments of inertia (I_1, I_2, I_3) will be defined using the axes of Figure 5-8. (Note that for non-symmetric bodies a set of products of inertia will also exist.) These principal moments of inertia may also be termed I_x, I_y, and I_z using cartesian coordinates. If the body is axially symmetric and of uniform density then $I_1 = I_3$ (the moments of inertia about the longitudinal axis are equal). This simple case will be used for the ORION model assuming uniform density for a right circular cylinder. If the body is not axially symmetric and not of uniform density, then the axes should be labeled such that $I_1 < I_2 < I_3$. Such a body would be described using moments of inertia and products of inertia. Consult Wertz(1985), Kaplan(1976) and Hughes(1986) for further details. For the ORION design, mass symmetry will be assumed. An evaluation of the products of inertia will not be made. In actuality, the mass distribution of ORION is not uniform. When mass placement has been defined in the final design, the products of inertia, $I_1 I_2$, $I_2 I_3$, and $I_1 I_3$, will need to be evaluated to fully describe the moment of inertia tensor $\underline{I}$. The reader should consult Wertz (1985, pp. 516-521) for details regarding determination of the products of inertia and moments of inertia. The assumption of axially symmetric mass distribution for ORION is made here to simplify the feasibility study.

For the simple axial symmetry case, the transverse moment of inertia is defined as $I_T = I_1 = I_3$. Note that for spherical symmetry, $I_1 = I_2 = I_3$. The spin moment of inertia and the transverse moments of inertia for a right circular cylinder of uniform density are:

$$I_2 = I_s = 0.5 \, (M \, R^2) \qquad (5.2a)$$

$$\text{and} \quad I_1 = I_3 = I_t = M \, [\, (R^2/4) + (L^2/12) \,] \qquad (5.2b)$$

M is the mass of the satellite, r is the radius of the cylindrical structure and L is the length of the cylinder. Subsequent discussion demonstrates that the actual moments of inertia based upon assumed mass placement differ slightly from the models above. Using these moments, prolate and oblate spinners can be described by an inertia ratio σ.

$$\sigma = I_S / I_T \qquad (5.3)$$

If the transverse moment exceeds the spin moment, the inertia ratio will be less than unity. It is common to describe the degree of "oblateness" by the degree to which the inertia ratio exceeds 1.0; conversely, "prolateness" is observed to increase as the ratio decreases below a value of 1.0. For the simple case of a cylinder of uniform mass (Eqns. 5.2a and 5.2b), assuming a mass of 250 lbm and a cylinder radius of 9.5 inches, the spin moment of inertia is 2.45 slug-ft^2 and the transverse moment of inertia is 6.76 slug-ft^2. Thus, the inertia ratio is 0.36. When the spacecraft is spun about its longitudinal axis, the inertia ratio is observed to be a fraction of 1.0, confirming the "prolateness" of the spinner.

The actual satellite will not exhibit uniform density with regard to mass placement. In the final design, the mass distribution might also not be axially symmetric. If that is the case, the principal axes of inertia (along which I_1, I_2, I_3 are aligned) will not be aligned with the coordinate axes of
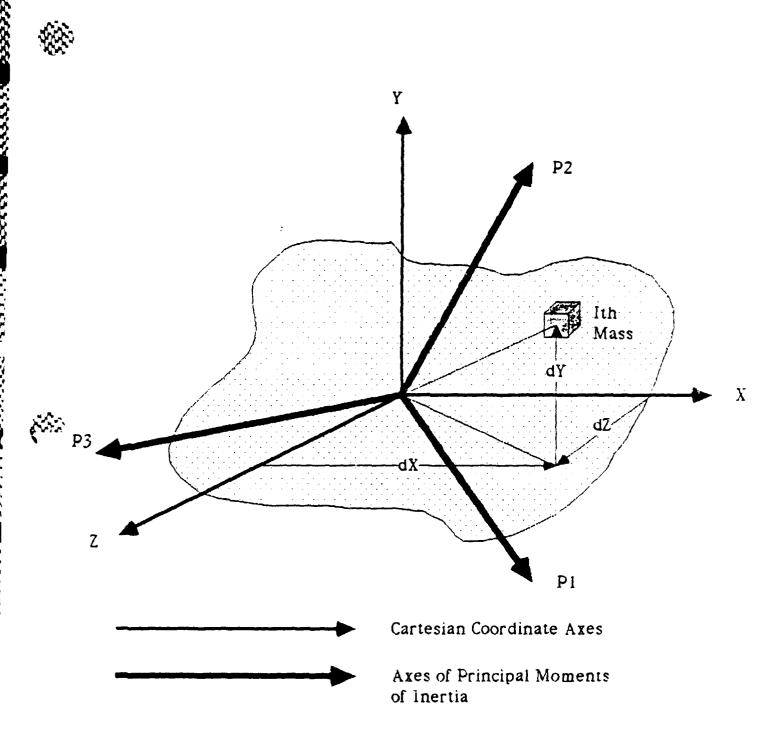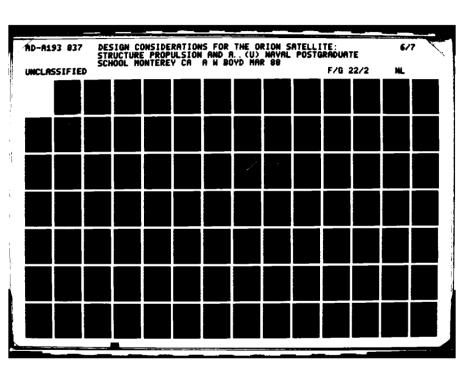
Y

P2

Ith
Mass

dY

X

dZ

P3

dX

Z

P1

→ Cartesian Coordinate Axes

→ Axes of Principal Moments
of Inertia

Figure 5-9

Coordinate Axes and Principal Axes of Inertia are not
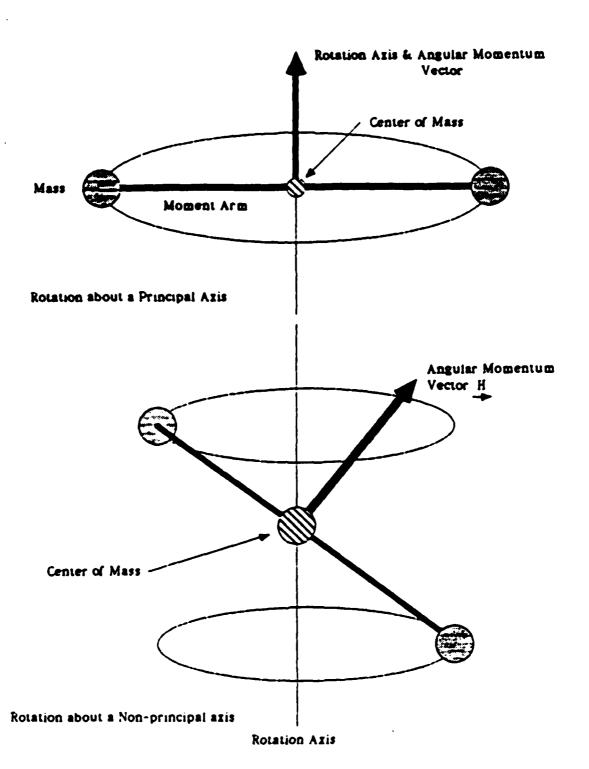Aligned for a Non-Symmetric Mass Distribution

479

MICROCOPY RESOLUTION TEST CHART

Figure 5-10

Rotation and Mass Symmetry
(Wertz, 1985, p. 488)

the spacecraft reference frame. This misalignment, however small, leads to the existence of products of inertia. The subsequent rotation of such a body (Figure 5-9) will be more complex than the simple case of rotation about the longitudinal axis that is assumed in this thesis.

Wertz (1985, p.489) points out that the angular momentum of a non-nutating body can be expressed by

$$H = I_p \, w \qquad\qquad (5.4)$$

where I_p denotes the dominant principal moment of inertia, and w is the spin rate about spin axis. In the case of a simple cylinder of uniform density, for example, I_S was observed to be the dominant principal moment of inertia. The moment is due to rotation about a principal axis. A principal axis is any axis P such that the resulting angular momentum is parallel to P when the spacecraft rotates about P. For rotation about a principal axis, the angular momentum vector is parallel to the spin vector. Figure 5-10 depicts rotation about a principal and a non-principal axis. Whenever the mass of an object is symmetrically distributed about an axis, the angular momentum generated by rotating about the axis of symmetry will be parallel to that axis. Thus any axis of symmetry is a principal axis.

The simple case for rotation is when the principal axis is aligned with the coordinate axis of the body. This occurs when the mass is symmetrically distributed about the coordinate axes of the spacecraft. In such a case, the three coordinate axes are also the principal axes. When the mass is not symmetrically distributed about the coordinate axes, the moments of inertia

481

must be resolved into moments of inertia and products of inertia. The products of inertia occur as a result of rotation about a non-principal axis. Representing the individual masses by m_i and the distance of the center of those masses from the spacecraft center of mass in each axis by dx, dy, and dz, Wertz(1985, pp. 518-519) defines these moments as follows[*].

$$I_{11} = \sum m_i [\, dy^2 + dz^2 \,] \tag{5.5}$$

$$I_{22} = \sum m_i [\, dx^2 + dz^2 \,] \tag{5.6}$$

$$I_{33} = \sum m_i [\, dx^2 + dy^2 \,] \tag{5.7}$$

$$I_{12} = I_{21} = -\sum m_i\, dx\, dy \tag{5.8}$$

$$I_{23} = I_{32} = -\sum m_i\, dy\, dz \tag{5.9}$$

$$I_{31} = I_{13} = -\sum m_i\, dx\, dz \tag{5.10}$$

The products of inertia are six components of the moment of inertia tensor, $\underline{I}$, which is a real, symmetric 3x3 matrix. This matrix has three real orthogonal eigenvectors and three real eigenvalues satisfying the equation
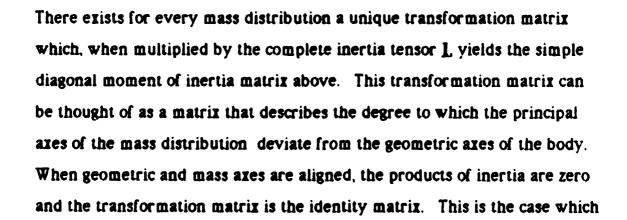
$$\underline{I}\, \underline{P}_i = I_i \underline{P}_i \qquad (i = 1,2,3) \tag{5.11}$$

where the scalars I_1, I_2, and I_3 are the principal moments of inertia and the unit vectors $\underline{P}_1$, $\underline{P}_2$, and $\underline{P}_3$ are the principal axes. The complete inertia tensor $\underline{I}$ looks like

---

[*] Kaplan(1976, p. 40) also defines the moments of inertia and products of inertia, but uses a cartesian coordinate nomenclature different than that adopted for this chapter. Kaplan, Wertz and Hughes are excellent references with regard to the determination of principal and non-principal axes of inertia.

$$
\mathbf{1} - \begin{vmatrix} I_{11} & I_{12} & I_{13} \\ I_{21} & I_{22} & I_{23} \\ I_{31} & I_{32} & I_{33} \end{vmatrix}
$$

The off axis elements are the products of inertia, $I_{12} - I_{21}$, $I_{23} - I_{32}$, and $I_{13} - I_{31}$. If the principal axes (axes of the principal moments of inertia) are used as the coordinate axes of a spacecraft reference frame, the moment of inertia tensor takes the diagonal form

$$
\mathbf{1} - \begin{vmatrix} I_{11} & 0 & 0 \\ 0 & I_{22} & 0 \\ 0 & 0 & I_{33} \end{vmatrix}
$$

There exists for every mass distribution a unique transformation matrix which, when multiplied by the complete inertia tensor $\mathbf{1}$ yields the simple diagonal moment of inertia matrix above. This transformation matrix can be thought of as a matrix that describes the degree to which the principal axes of the mass distribution deviate from the geometric axes of the body. When geometric and mass axes are aligned, the products of inertia are zero and the transformation matrix is the identity matrix. This is the case which is assumed for this study.

In the simplified matrix coordinate frame (coordinate axes - principal axes), and in only that frame, the angular momentum vector is resolved into the following components:

$$H_1 = I_1 w_1 \qquad\qquad (5.12)$$
$$H_2 = I_2 w_2 \qquad\qquad (5.13)$$
$$H_3 = I_3 w_3 \qquad\qquad (5.14)$$

where the components of $\underline{w}$ are w_1, w_2, and w_3, the rotations about the three principal (and coordinate) axes. "Thus", points out Wertz, "the principal axes can be thought of intuitively as axes around which the mass is symmetrically distributed. In particular, any axis of symmetry is a principal axis."
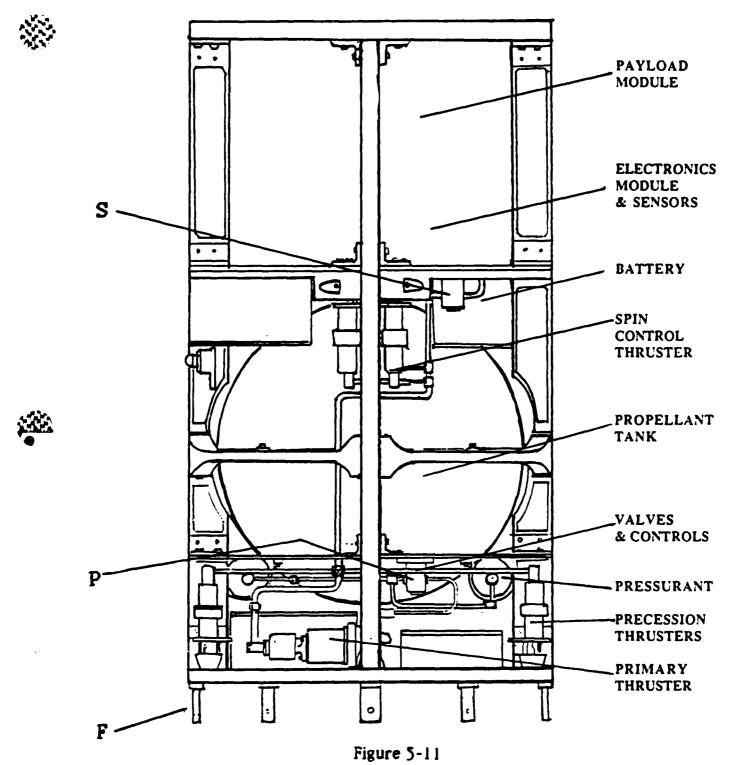
For the purpose of this feasibility study, mass placement was assumed to be symmetric about the longitudinal axis. The actual mass distribution about the spin axis was calculated using the component placement shown in Figures 5-11, 5-12, and Table 5-2,. The mass distribution is diagrammed in Figures 5-13 and 5-14 using density as a function of displacement from the spacecraft geometric centerline. Note that the density in the x-z plane shows that most of the mass is concentrated near the periphery of the cylinder. This is an ideal mass distribution due to the contribution of the heavy battery packages.

Mass placement was also approximated as being symmetric about the transverse axis. This assumption was made to simplify determination of the moments of inertia; specifically it was desired to make the products of inertia zero aligning the principal axes and the coordinate axes. The actual mass distribution is not symmetric, as indicated in Figures 5-15 and 5-16. However, contributions of the individual masses result in a center of mass which is near the geometric center the spacecraft center of mass. The

484

Figure 5-11

ORION Component Placement
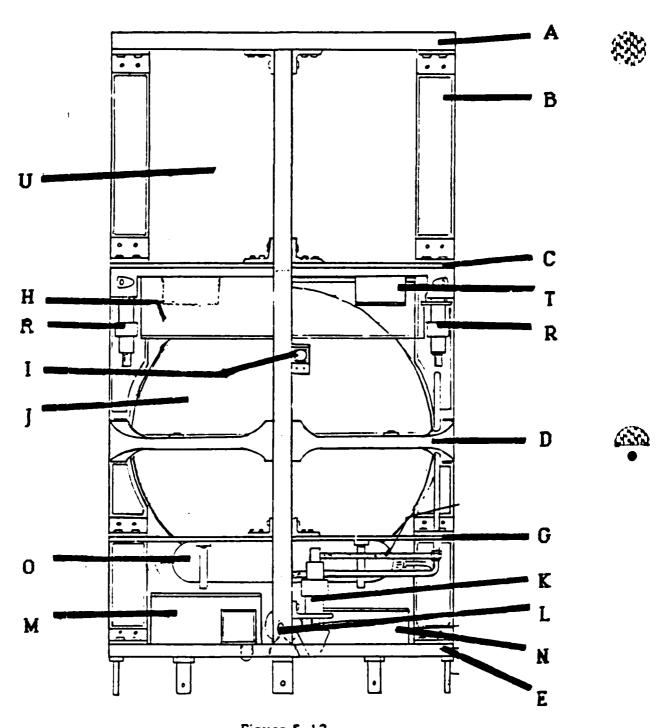Cross Section in the Y-Z Plane

485

Figure 5-12

ORION Component Placement
Cross Section in the X-Y Plane

486

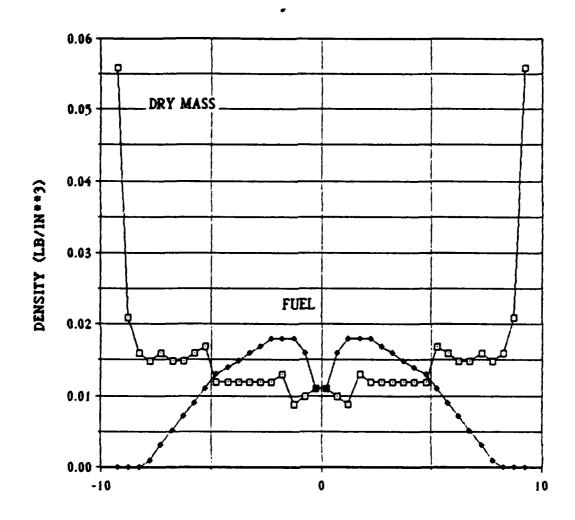# TABLE 5-2

MASSES OF ORION COMPONENT

Code	Component	Mass (lbm) Total unit
A	Top Plate, Aluminum	1.65
B	Longerons (4), Aluminum	5.80 (1.45)
C	Payload Midplate, Aluminum	1.65
D	Propellant Tank Strongback (4), Aluminum	4.20 (1.05)
E	Baseplate, Aluminum	9.75
F	Launch Restraint Pins (8)	0.80 (0.1)
G	Pressurant Mid-deck, Aluminum	1.05
H	Batteries and Battery Boxes (4)	28.0 (7.0)
I	Earth Sensor	0.30
J	Propellant Tank	13.0
K	Hydrazine Precession Thruster (2)	3.06 (1.53)
L	Hydrazine Orbital Transfer Thruster	1.93
M	Attitude Control and Payload Computer (2)	16.0 (8.0)
N	Telemetry Transmitter/Receiver (2)	10.0 (5.0)
O	Pressurant Gas Bottle (2) and Pressurant (1 lbm)	5.00 (2.0)
P	Fill and Drain Valve (3)	2.10 (0.7)
Q	Assorted Tubing for Propulsion	2.00
R	Hydrazine Spin Control Thruster (4)	6.12 (1.53)
S	Pyrotechnic Valve (2)	1.00 (0.5)
T	Power Conditioning Circuits (2)	4.00 (2.0)
U	Payload	32.0
V	Spacecraft Skin and Fasteners (not shown)	12.0
W	Solar Cells (not shown)	0.70
X	Booms, Aluminum (4) (not shown)	4.20 (1.05)
Y	Hydrazine Fuel (not shown)	71.5
Z	Magnetometers (4)	2.00 (8)
	Total Mass (lbm)	245.81
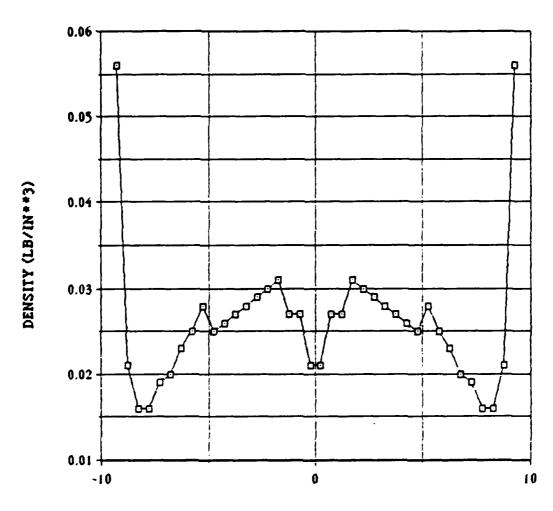
Figure 5-13

Fuel and Dry Mass Densities Along the X Axis

488
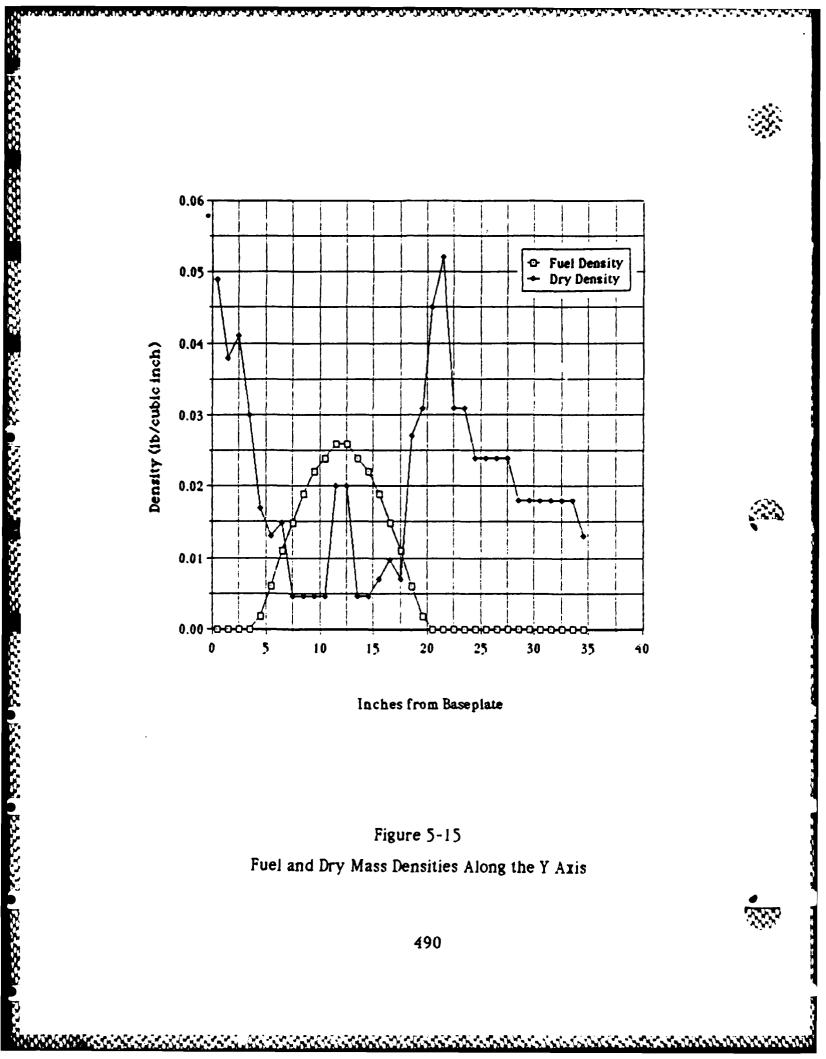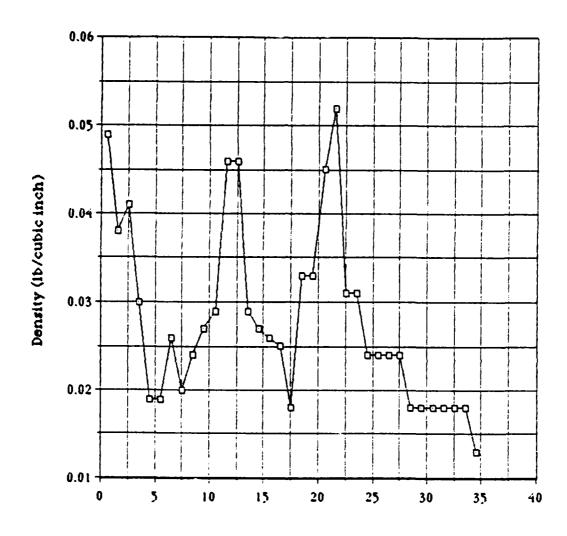
Figure 5-14

Total Density Along the X Axis

489

Figure 5-15

Fuel and Dry Mass Densities Along the Y Axis

490

Inches from Baseplate

Figure 5-16

Total Density Along the Y Axis

491

majority of the mass is concentrated in the baseplate region, equipment deck regions, propellant tank, and in the payload envelope. The propellant makes a variable contribution to the mass properties dependent upon the tank fill fraction. As fuel is expended from a full tank (Figures 5-17 and 5-18) the center of mass is observed to move from a position 17.8 inches above the baseplate to 17.1 inches as the tank empties. This movement of the center of mass is quantified in Figure 5-19. The effective center of mass is very close to the geometric center (17.5 inches), as desired. While the mass is not ideally distributed in a belt in the midplane, the aggregate effect does place the CM in the proper position. Were the mass concentrated as pictured in Figure 5-2, the satellite would have a value of σ close to unity.

The moments of inertia were also evaluated using an assumption of component masses and probable mass placement. Negating the influence of the products of inertia (symmetry assumed), the principal moments of inertia were evaluated for the point masses, where

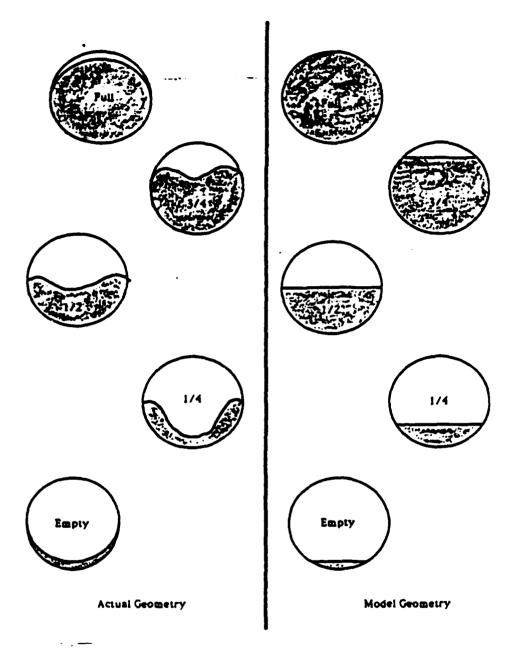$$I_p = \sum m_i \, \eta^2 \qquad (5.15)$$

The mass of each component is m_i and the radial distance of the center of mass of that component from the spacecraft geometric center is η. Using the component placements and masses, an assumed moment of inertia tensor I was derived. Consideration was given to the change in moments of inertia due to propellant expenditure. The varying mass of the propellant was calculated, and the tensor I was observed to change with the expulsion of fuel from the hydrazine tank. Figures 5-20 and 5-21 show the moments of inertia ($I_y = I_s$ and $I_x = I_z = I_t$) as a function of propellant usage. The
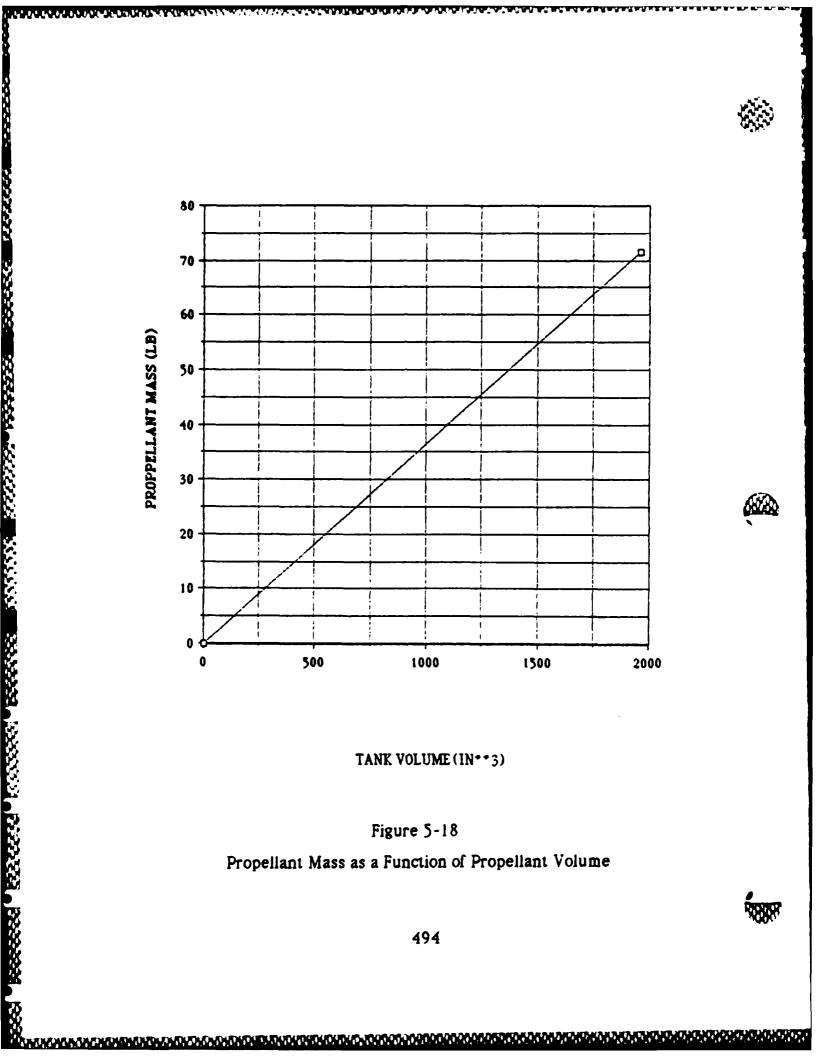
492

Figure 5-17

Fuel Expulsion from a Ribbed Diaphragm Tank
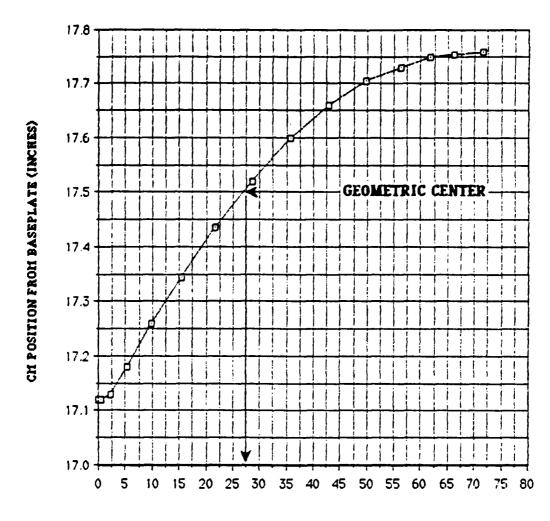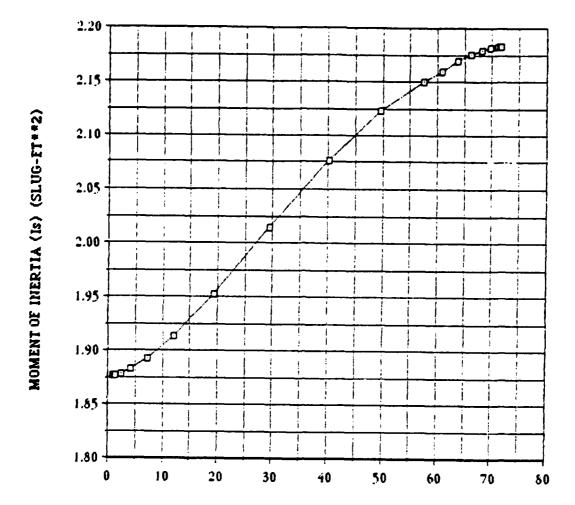Diaphragm Distension is Modeled by a Simple Volume Fraction
(ARDE, 1986)

TANK VOLUME (IN**3)

Figure 5-18

Propellant Mass as a Function of Propellant Volume

494

Figure 5-19

Movement of the Center of Mass Along the Y Axis

495
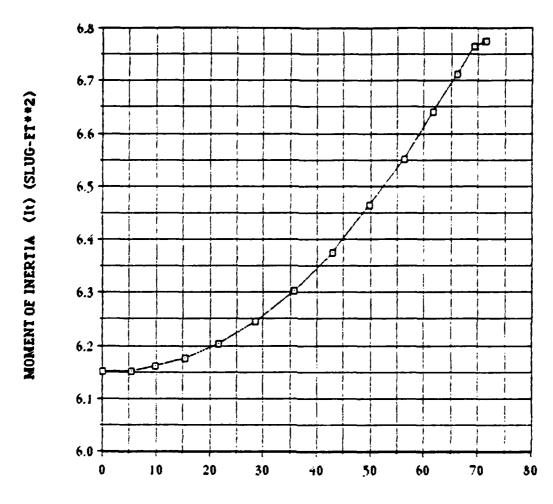
FUEL REMAINING (POUNDS)

Figure 5-20

Moment of Inertia (I_s) as a Function of Propellant Reserve

496
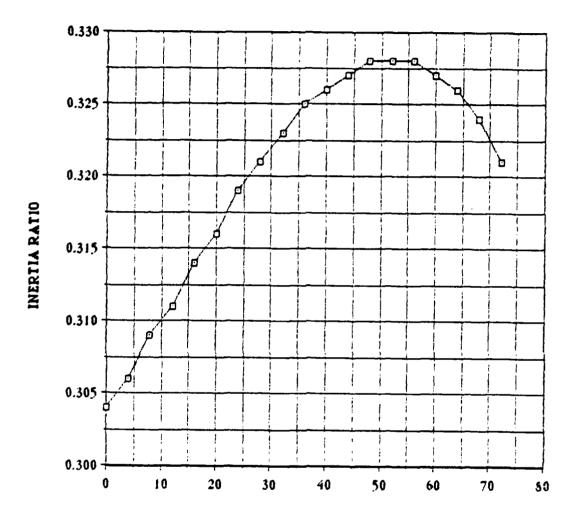
FUEL REMAINING (POUNDS)

Figure 5-21

Moment of Inertia (I_t) as a Function of Propellant Reserve
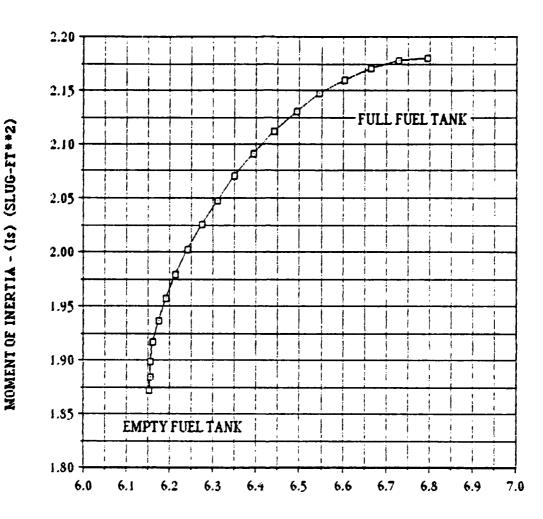
497

Figure 5-22

Inertia Ratio (σ) as a Function of Propellant Reserve

MOMENT OF INERTIA - (It) (SLUG-FT**2)

Figure 5-23

I_s versus I_t

inertia ratio was plotted in Figure 5-22 as a function of fuel remaining. Note that the inertia ratio is within a range of 0.303 to 0.326. Compare this to the inertia ratio for a right circular cylinder of uniform density (0.362). The actual satellite is slightly more prolate than the uniform density model predicted. This is partly due to the concentration of mass near the ends of the satellite cylinder.

Figure 5-20 indicates that the spin moment of inertia I_s with a full fuel tank is 2.18 slug-ft^2. This is less than the uniform density model of 2.45 slug-ft^2. As fuel is expended, the mass of the satellite is reduced. This leads to a reduction in both moments of inertia. The inertia ratio is observed to increase as propellant is expended from the full tank until 50 lbm of fuel remains. This is due to the fact that the rate of decrease of the transverse moment of inertia due to fuel expulsion is more rapid than the rate of decrease of the spin moment of inertia. Thus the inertia ratio increases until 21.5 lbm of propellant have been expended. For every I_s that existed due to various weights of propellant loads, a unique I_t occurs. Figure 5-23 plots I_s as a function of I_t.

Note that the purpose of this analysis was to derive the moments of inertia to be used in assessing the spin stability of the spacecraft. The goal was to derive an approximate inertia ratio which ultimately could be used to determine the time constant of nutation due to energy dissipation. The assumption of mass symmetry about the transverse axes, and the simplification of the tensor $\underline{I}$ is valid because the products of inertia do not affect the inertia ratio. Approximate inertia ratios of 0.303 to 0.326 were derived using the component masses and mass placement of Figures 5-11, 5-

12, and Table 5-2. These inertia ratios were observed to be less than that predicted by the uniform density model (0.362). This confirms that the satellite is extremely prolate when spun about the longitudinal axis.

The effect of supplemental booms was investigated in an attempt to improve the moment of inertia about the spin axis. The assumption was made that the booms would be placed in a plane through the center of mass and orthogonal to the longitudinal axis. Figure 5-19 indicates that the center of mass varies approximately 0.25" on either side of the geometric center as fuel is expended. This small change is ignored in the determination of the moments of inertia, and the center of mass is assumed to remain stationary. Consequently the booms are placed in a plane passing through the geometric center of the spacecraft and orthogonal to the longitudinal axis. It was further assumed that each boom would be tipped with a 2.0 lbm magnetometer.
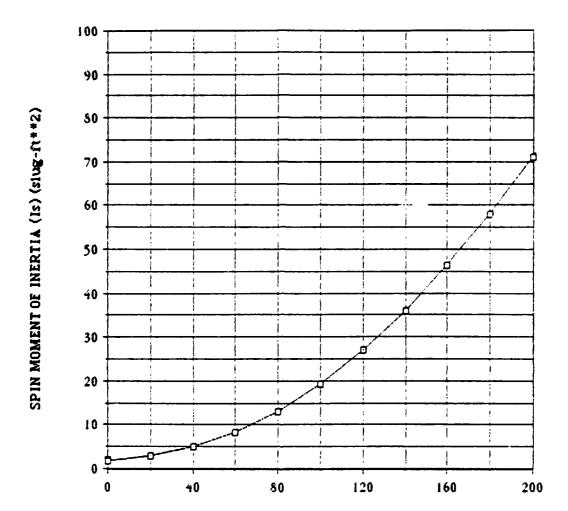
Several boom options were investigated. These included:

1. Nested-cylinder boom (similar to an automobile radio antenna)
2. Spring-loaded metal-memory boom
3. Dual- or single-wrap motor-deployed metal-memory boom
4. Spring-loaded whip
5. Spring-loaded scissors-boom
6. Spring-loaded "folding rule" boom
7. Self building truss

The metal-memory boom options require a large mass for the boom material and deployment mechanism. A whip antenna-like boom was deemed to be too flexible. The self building truss was too complex for the ORION concept. Consequently, a spring loaded "folding rule" style boom was chosen that would unfold from within a boom housing. The boom design is based on the use of 1.5" by 0.625" rectangular aluminum channel stock.

501

BOOM LENGTH (INCHES FROM Y AXIS)
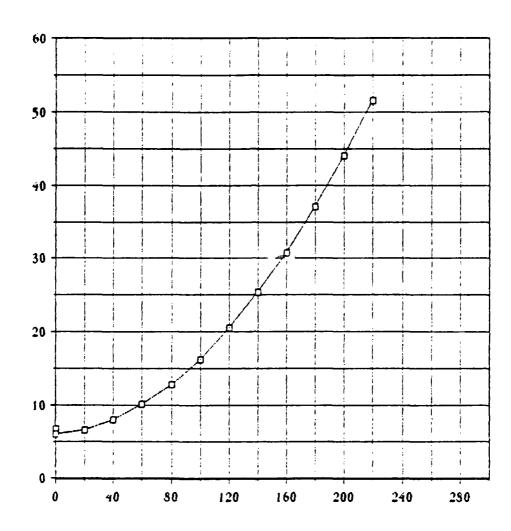
Figure 5-24

Moment of Inertia (I_s) as a Function of Boom Length
(Boom tip mass of 2 lbm assumed)

502

BOOM LENGTH (INCHES FROM Y AXIS)

Figure 5-25

Moment of Inertia (I_t) as a Function of Boom Length
(Boom tip mass of 2.0 lbm assumed)

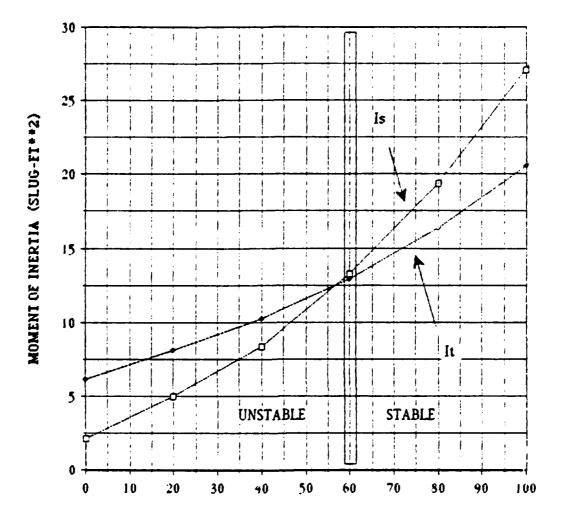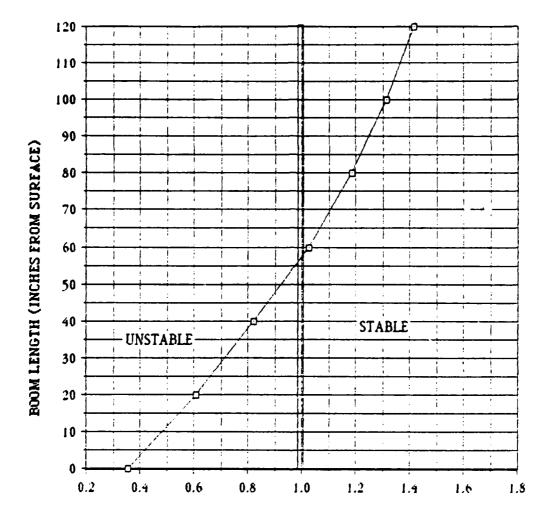Figure 5-26

Moments of Inertia (I_s and I_t) as a Function of Boom Length
(Boom tip mass of 2.0 lbm assumed)

INERTIA RATIO

Figure 5-27

Inertia Ratio as a Function of Boom Length
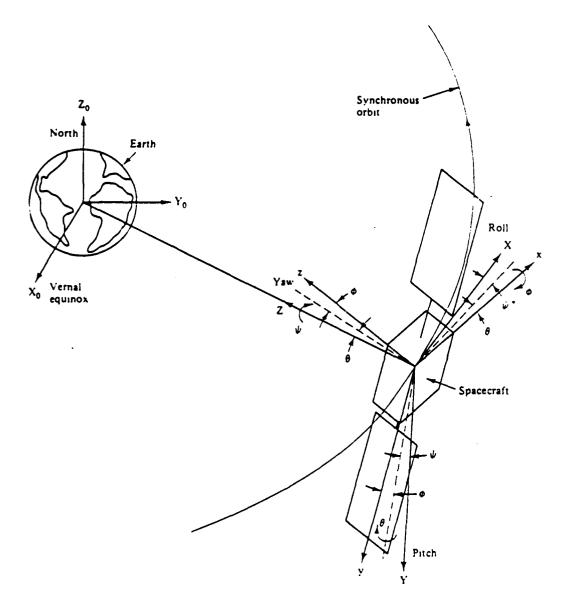(Boom tip mass of 2.0 lbm assumed)

Chapter Three describes the boom housing and the boom nesting method. Figures 5-24 through 5-27 were derived using equations 5.5, 5.6, 5.7, 5.15, and the geopmetry of Figure 5-1, assuming a boom tip mass of 2.0 lbm. From those figures a boom length of 80" was chosen. Note, in Figure 5-26, that the spin moment of inertia exceeds the transverse moment of inertia near a boom length of 60 inches. The spin moment of inertia I_s has contributions for all four booms and grows proportional to the length of the boom to the second power. However, only two booms contribute to the calculation of I_t. Beyond boom lengths of 20 inches the author observed that the propellant expenditure ceased to affect the moment of inertia value because the boom moment arm was dominant. With long booms the fuel, which is relatively close to the structural centerline, has little effect on the moments. The chosen boom length of 80 inches results in a stable spacecraft with an inertia ratio of 1.18.

4. Equations of Motion and Angular Rates
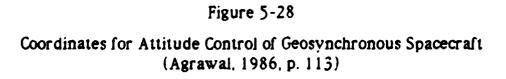
Figure 5-28, which depicts the movement of a spacecraft in three axes, has been labeled consistent with the nomenclature in Agrawal (1986, p. 113). Note that this figure depicts a geosynchronous spacecraft that is always earth oriented. For an inertially fixed spinning spacecraft, the orientation of the body relative to the Earth will change continuously. Thus the use of cartesian axes for spinning spacecraft is often arbitrary and subject to confusion. Unfortunately, a standard cartesian notation is not used by all authors. For that reason, numbered axes are chosen in the ORION analysis. The Greek notation in Figure 5-29 is common to controls literature.

Figure 5-28

Coordinates for Attitude Control of Geosynchronous Spacecraft
(Agrawal, 1986, p. 113)

Figure 5-29

Nomenclature for ORION Coordinate Axes

The basic equation of attitude dynamics is obtained from

$$\mathbf{H} = \sum \mathbf{H}_i = \sum r_i \times m_i v_i \qquad (5.17)$$

which expresses the angular momentum of the spacecraft as a sum over the spacecraft masses m_i moving with velocities v_i at a distance r_i from the spacecraft geometric center. Differentiating with respect to time gives
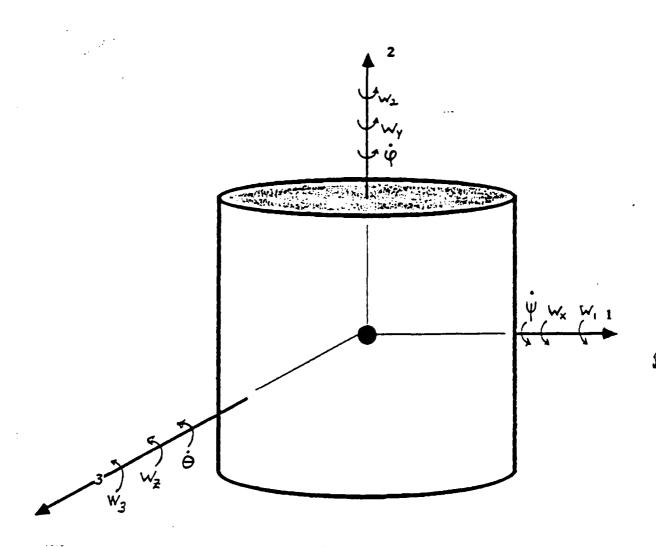
$$d\,\underline{\mathbf{H}}/dt = \sum d\underline{\mathbf{H}}_i/dt$$

$$= \sum d/dt\,(\underline{r}_i \times m_i\underline{v}_i)$$

$$= \sum \mathbf{M}_i$$
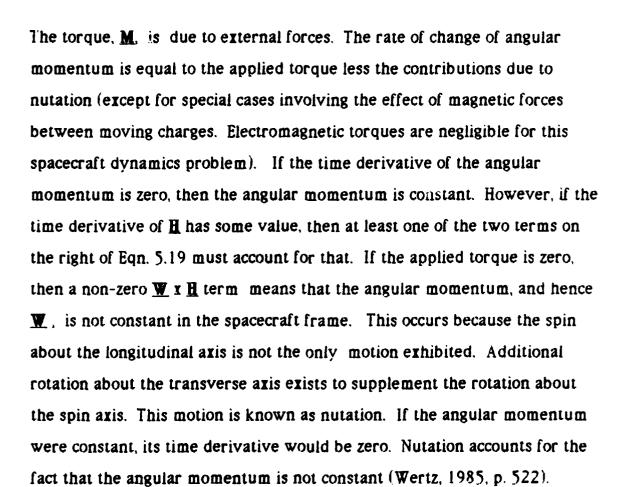
$$= \mathbf{M} \qquad (5.18)$$

Let the rotation about the three axes be denoted $\mathbf{w}_1$, $\mathbf{w}_2$, and $\mathbf{w}_3$. The ORION structure is assumed to be a rigid body. For the time being, energy dissipation due to "fuel slosh" is ignored. The equations of attitude dynamics (5.17 - 5.18) relate the time derivative of the angular momentum vector, $d\mathbf{H}/dt$, to the applied torque, $\mathbf{M}$. Combining these with equations (5.12 - 5.14) results in the fundamental equation of rigid body dynamics. (Note that this equation is only valid for the case of the rigid body; it is not valid for cases involving flexibility effects or propellant expenditure, both of which exist for the ORION design problem. Consult Agrawal [1986, p. 111], and Wertz [1985, p. 521] for more details.)

$$d\underline{\mathbf{H}}/dt = I\,d\underline{\mathbf{W}}/dt = \mathbf{M} - \underline{\mathbf{W}} \times \underline{\mathbf{H}} \qquad (5.19)$$

The torque, **M**, is due to external forces. The rate of change of angular momentum is equal to the applied torque less the contributions due to nutation (except for special cases involving the effect of magnetic forces between moving charges. Electromagnetic torques are negligible for this spacecraft dynamics problem). If the time derivative of the angular momentum is zero, then the angular momentum is constant. However, if the time derivative of **H** has some value, then at least one of the two terms on the right of Eqn. 5.19 must account for that. If the applied torque is zero, then a non-zero **W** x **H** term means that the angular momentum, and hence **W**, is not constant in the spacecraft frame. This occurs because the spin about the longitudinal axis is not the only motion exhibited. Additional rotation about the transverse axis exists to supplement the rotation about the spin axis. This motion is known as nutation. If the angular momentum were constant, its time derivative would be zero. Nutation accounts for the fact that the angular momentum is not constant (Wertz, 1985, p. 522).

The one case in which rotational motion can occur without nutation is when the angular momentum is constant. This occurs when rotation is about a principal axis of inertia. Note that there are three principal axes but only one major axis. Stable motion (motion without nutation) can occur about any of these three axes. However, when the motion about any principal axis is perturbed by some external torque, the spinning body will begin to nutate. Spin dynamics and internal effects in the satellite will then cause the nutation to grow or dissipate. If the rotation is about a minor axis (as in the case of ORION with no booms), the nutation angle will grow exponentially.

510

ORION or any other prolate body would spin about the minor axis indefinitely were it not for external torques which perturb the spin "off axis". This is known as "neutral stability" if the body spins purely about the minor axis without perturbation. For rotation about a major axis. the dynamics of the spinning oblate body will tend to resist external torques. This is readily demonstrated by the force needed to redirect the axis of a spinning gyro or top.

Energy dissipation effects due to liquid slosh or the movement of semi-rigid bodies will accelerate the damping of nutation in a stable spinner. These internal effects rapidly absorb the energy of rotation about the transverse axis due to nutation. Lacking any energy of rotation about the transverse axis, nutation does not occur. In a prolate or unstable spinner, rotation exists about a minor axis of inertia, and the satellite will seek to rotate about the major axis of inertia once it is perturbed. From a dynamics point of view, rotation about a minor axis is nothing more than rotation about a transverse axis. Energy dissipaters, such as sloshing fuel, will "absorb" rotational energy about a transverse axis. leading to an exponential growth in the nutation angle. In the case of a prolate spinner, a nutation angle is viewed as the body's angle of departure from an unstable attitude toward a stable one. Alternatively, one could view the spin about the minor axis as the largest possible deviation or "nutation angle" away from a stable spin. Energy dissipation reduces this "nutation angle" until the spin is again stable. The spinning body "seeks" to rotate about its major axis. and the dissipater speeds it on its way.

Equation (5.19) can be written in component form:

511

$$I_1 (dw_1/dt) = M_1 + (I_2 - I_3)w_2 w_3 \qquad (5.20)$$

$$I_2 (dw_2/dt) = M_2 + (I_3 - I_1)w_1 w_3 \qquad (5.21)$$

$$I_3 (dw_3/dt) = M_3 + (I_1 - I_2)w_1 w_2 \qquad (5.22)$$

In controls notation, the equations of motion are written as

$$M_x = I_x \ddot{\psi} + \dot{\phi}\dot{\theta}(I_z - I_y) \qquad (5.23)$$

$$M_y = I_y \ddot{\phi} + \dot{\psi}\dot{\theta}(I_x - I_z) \qquad (5.24)$$

$$M_z = I_z \ddot{\theta} + \dot{\psi}\dot{\phi}(I_y - I_x) \qquad (5.25)$$

These equations are known as Eulers equations of motion and can be used to discuss the stability of rotation about the principal axis of a rigid spacecraft. If the motion is assumed to be torque free ($\underline{M} = 0$) and if axial symmetry is assumed ($I_1 = I_3$), then equations (5.21-5.23) can be simplified as follows:
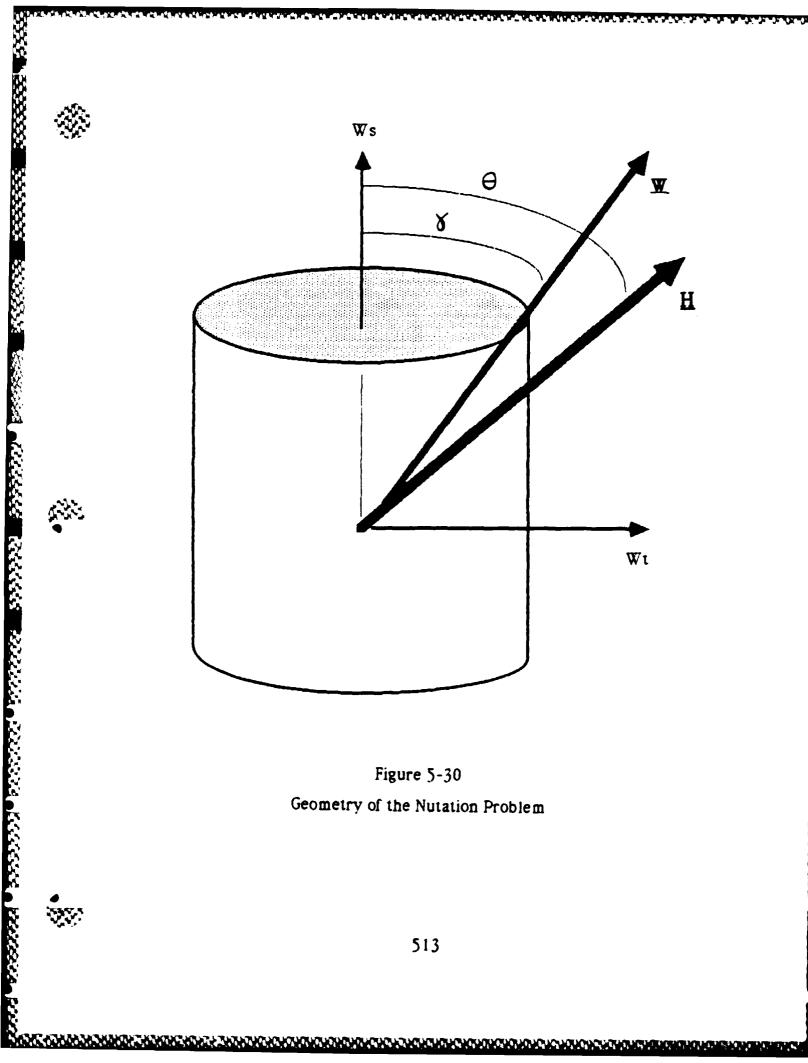
$$I_t (dw_1/dt) = (I_s - I_t) w_2 w_3 \qquad (5.26)$$

$$I_s (dw_2/dt) = (I_t - I_t) w_1 w_3 = 0 \qquad (5.27)$$

$$I_t (dw_3/dt) = (I_t - I_s) w_1 w_2 \qquad (5.28)$$

Equation (5.28) indicates that the time derivative of the spin rate, w_2, is zero. Thus the spin rate, w_2, must be constant in the absence of external torques. Wertz (1985, p. 525) and others define the transverse angular velocity w_t as the angular velocity about an axis perpendicular to the axis of symmetry, where

$$w_t = (w_1^2 + w_3^2)^{0.5} \qquad (5.29)$$

512

Figure 5-30

Geometry of the Nutation Problem

513
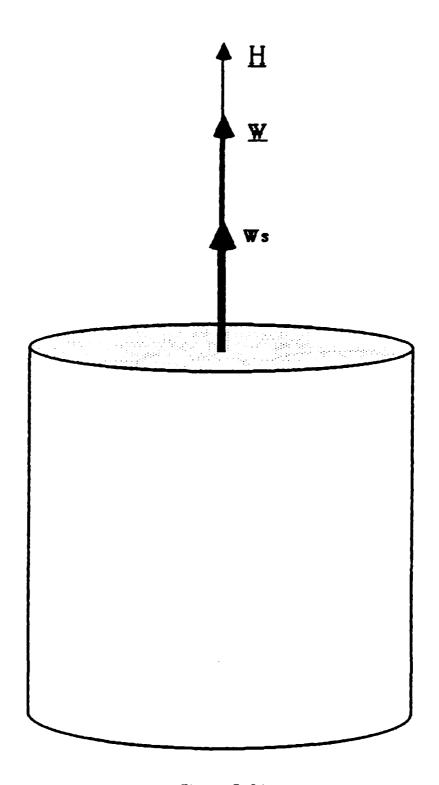
Figure 5-31

Geometry of Spin Without Nutation

514

In this context, w_t is a magnitude. As a two dimensional vector, w_t can be analyzed using real and imaginary components. Using the transverse angular velocity, the angular momentum is expressed in scalar notation as

$$H = I_s w_s + I_t w_t \qquad (5.30)$$

For the simple case of spin about the longitudinal axis of ORION without nutation,
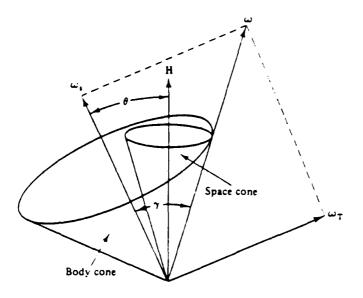
$$H = I_s w_s \qquad (5.31)$$

When the spacecraft begins to nutate, both components in equation (5.30) have values. The geometry of the angular momentum and spin vectors is depicted in Figure 5-30. The vector w_s denotes the spin axis of the vehicle at a precise moment. This vector is obtained using the right hand rule for the rotation of the satellite. Figure 5-30 also depicts w_t and the total spin vector $\underline{W}$. Note that $\underline{W}$ is offset from the spin axis by an angle γ. The nutation angle, Θ, denotes the angular displacement of the spin axis from the angular momentum vector. For the simple case where no nutation exists, the angles Θ and γ will be zero. The geometry of Figure 5-31 results. In this situation w_t will also be zero. Thus the goal for control of a spin-stabilized satellite is to collocate the spin axis and the angular momentum vector.

Two separate geometries exist for prolate and oblate spinners. Figures 5-32 and 5-33 depict stable and unstable spinners experiencing nutation. This motion is described as the interaction of a body cone and a space cone. For a stable spinner, the spin vector $\underline{W}$ is observed to rotate about the total
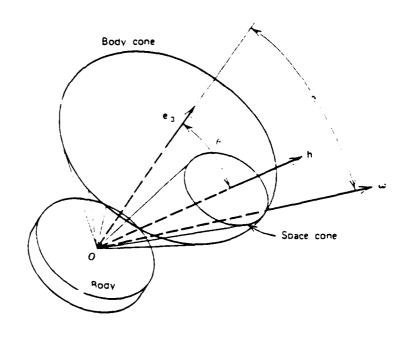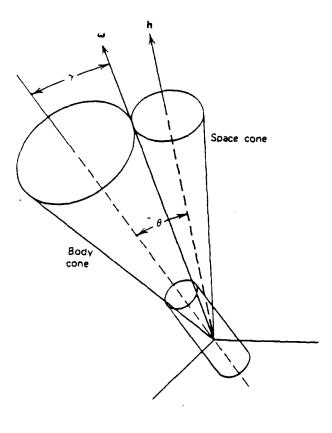
515

Figure 5-32

Geometry of a Stable Nutating Spinner
(Agrawal, 1986, p. 116; Kaplan, 1976, p. 52)

516
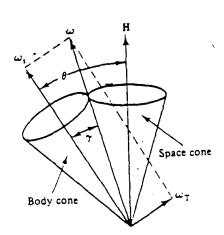
Figure 5-33

Geometry of an Unstable Nutating Spinner
(Agrawal. 1986. p. 116; Kaplan. 1976. p. 55)

517

angular momentum vector **H** and in the process generates the space cone. **H** is fixed in inertial space in the absence of external torques; the plane formed by w, w_s and w_T rotates about the **H** vector. The vector **W** is along the line of tangency of the angular momentum space cone with the body cone. The large body cone revolves about the smaller space cone. The two cone axes are displaced by the nutation angle θ, and the spin vector is further displaced from the spin axis by an angle γ. For an unstable spinner, Figure 5-33 indicates that the body cone revolves around the periphery of the space cone.

The nutation angle θ is defined by the relationship

$$\theta = \arctan [I_t \, w_t \, / \, H] \qquad (5.32)$$

Note that the magnitude of the nutation angle depends on the transverse angular velocity w_t. This angle must be observed at a specific time or predicted using the equations of motion because in real world applications θ is always growing or decaying exponentially. The angle between the spin axis and the spin vector **W** is γ and is defined as

$$\gamma \quad = \arctan [I_s \, \tan \theta \, / I_t] \qquad (5.33a)$$
$$= \arctan [\sigma \tan \theta] \qquad (5.33b)$$
$$= \arctan [w_t \, / \, w_s] \qquad (5.33c)$$

From the equations above, the nutation angle is zero whenever w_t is zero and vice versa. Equation 5.33b indicates that, for nutating spacecraft, $\gamma > \theta$

518

whenever $I_s > I_t$ (oblate spinner). For a prolate spinner, $\gamma < \Theta$. Finally, using the inertia ratio σ described in the previous section, the transverse angular velocity is defined as

$$w_t = \sigma \, w_S \, \tan\Theta \qquad (5.34)$$

The inertial spin rate (angular velocity) $\underline{\mathbf{W}}$ is defined as

$$\underline{\mathbf{W}} = \underline{\mathbf{w}}_p + \underline{\mathbf{w}} L \qquad (5.35)$$

The magnitude of $\underline{\mathbf{w}}_p$ is known as the body nutation rate. Wertz (1985, p. 490) defines this as the

"rotation rate of any point ... fixed in the body about the spin axis relative to the orientation of the angular momentum vector."

$$w_p = (1 - (I_s/I_t)) \, w_s = (1-\sigma) \, w_s \qquad (5.36)$$

$$\lambda = ((I_s - I_t) / I_t) \, w_s = - w_p = (\sigma - 1) \, w_s \qquad (5.37)$$

$$w_L = H / I_t \qquad (5.38)$$

Some authors (Zedd and Dodge) use the rotor nutation frequency λ, rather than the body nutation rate, w_p, to describe the frequency of nutation. Note that the "rotor" nutation frequency and "body" nutation rate are identical but of opposite sign. In a prolate spinner, λ will be negative rotating fixed in body coordinates opposite to the direction of spin. The inertia ratio for a prolate spinner is less than unity, and thus λ is opposite the sign of w_s. The

inertial nutation rate, w_L, is the rotation of w_s about **H** relative to an inertial frame of reference. In review, several angular velocities are of interest in the study of ORION, namely

W	-	inertial spin rate
w_s	-	spin rate about the spin axis
w_t	-	transverse angular velocity $= (w_1{}^2 + w_3{}^2)^{0.5}$
w_p	-	body nutation rate $= (1 - (I_s/I_t))\ w_s = (1-\sigma)w_s$
λ	-	rotor nutation frequency $= ((I_s - I_T) / I_t)\ w_s = -w_p$
	-	$(\sigma - 1)w_s = -w_p$
w_L	-	inertial nutation rate $= H / I_t$

5. Response to Torques

The torques, **M**$_i$, on the individual points in a rigid body are due both to forces between the points and externally applied forces....Internal torques sum to zero (for the general case) and the resultant torque **M** is simply due to external forces. The external forces are of two kinds: (1) Disturbance torques caused by environmental effects such as aerodynamic drag and solar radiation pressure and (2) deliberately applied control torques from devices such as gas jets or magnetic coils. If a spacecraft is initially spinning about a principal axis, a torque applied parallel or antiparallel to the angular momentum vector will cause an increase or decrease in **H** without affecting its direction. (For example, spin up or spin down of a satellite.) A torque component perpendicular to **H** will cause the direction of **H** to change without altering its magnitude. The change in direction of the angular momentum vector due to an applied torque is called precession. (Note that the definition of precession, which has been adopted in spacecraft dynamics, is somewhat different from the definition usually assumed in physics. Such a precession might be caused by a jet firing (as indicated in Figure 5-34.)) The special case of slow precession due to a small applied torque (such that the magnitude of the integral of the torque over a spin period is much less than **H**) is known as drift. Environmental torques are a common source of attitude drift. (Wertz, 1985, p. 498)

Using the geometry of Figure 5-34 the rotation angle through which the spin axis precesses per thruster engine pair pulse is given as

$$\theta_p = 2 [E F L (\theta' / w_s)] / I_s \qquad (5.39)$$

where E is the efficiency of the thruster pulse, F is the thrus, L is the moment arm from the principal axis to the thruster, and θ' is the fraction of a spin cycle (in radians or degrees) when the thruster was firing. θ' is normally less than $180°$ of arc, and $90°$ is typical. Efficiencies of 90% are typical and E is expressed analytically as

$$E = (2 \sin[\theta' / 2])/ \theta' \qquad (5.40)$$

For a pulse application over $90°$ of arc, we have

$$E = (2 \sin[\pi/4]) / [\pi/2]$$
$$= 90\%$$

Substituting the expression for E (Eqn. 5.40) in the precession equation (5.39), we have

$$\theta_p = (4 F L \sin[\theta' / 2]) / (I_s w_s^2) \qquad (5.41)$$

The fuel mass required to slew the spacecraft through a given angle, θ_p, using a single thruster, is

$$F (\Delta t) = E^{-1} I_s w_s L^{-1} \theta_p \qquad (5.42)$$

$$\text{Fuel} = F(\Delta t)/ I_{sp} \qquad (5.43)$$

521

Assuming a pure coupled spin control thruster pair, the fuel required to conduct a spin change maneuver is obtained using

$$2\,F\,L\,(\Delta t) = I_s\,\Delta w_s \tag{5.44}$$

$$\text{Mass} = 2F\,(\Delta t)\,/\,I_{sp} \tag{5.45}$$

The term Δt is the duration of the pulse, and Δw_s is the change in spin rate. The time required to spin up to a given rate is given by

$$\Delta t = (I_s\,\Delta w_s)\,/\,2\,F\,L \tag{5.46}$$

If only one thruster is used in lieu of a coupled thruster pair, the time to spin up doubles, but the fuel mass required remains unchanged.

Finally, the fuel mass required to cancel nutation can be determined from the equations above using an iterative process. Note that this is only required for the unstable spinner. In a stable spinner, nutation is resisted by dynamics and is damped by energy dissipation effects. Recall that during nutation, the transverse angular velocity, w_t, has a value. In order to cancel nutation, w_t must be reduced to zero. This is done most effectively if the control inputs occur when w_t is at its maximum value. These control inputs use the same thruster pairs as used for precession control. Recall that

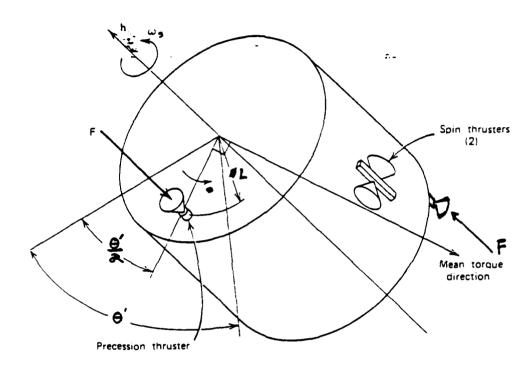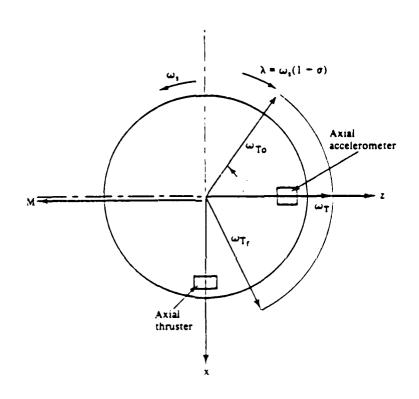$$w_t = \sigma\,w_s\,\tan\theta$$

Figure 5-34

Precession Geometry
(Kaplan, 1976, p. 126)

Figure 5-35

Active Nutation Control Requires the Cancellation of W_t
(Agrawal, 1986, p. 125)

Correct phasing of the control pulse requires a pulse duration encompassing $45°$ of arc on either side of the position of maximum w_t; the duration of the torque application is

$$w_s \, \Delta t = \pi / 2 \tag{5.47}$$

or for $1/2$ of the body nutation period, T, where

$$T = \pi / \lambda \tag{5.48}$$

$$|w_{t \text{ final}}| = |w_{t \text{ initial}}| - ((2 \; F \, L \, \Delta t) / I_t \, \lambda) \tag{5.49}$$

If one application of the coupled thrusters over an arc of $\pi/2$ does not cancel the nutation angle, then additional pulses will be needed. Equation (5.49) can be iterated until the desired nutation angle is obtained. Fuel mass can also be obtained using equation (5.45). It is important to note that this set of equations for active nutation control must be considered in concert with the destabilizing forces that are acting upon the spacecraft. For example, if energy dissipation is present in a prolate spinner, the nutation angle grows exponentially. This angular growth will be present even as the thrusters are firing to reduce w_t. The next section shows that, for energy dissipation problems, the time required to cancel nutation involves a consideration of the exponential

$$\theta = \theta_0 \, e^{t/\tau} \tag{5.50}$$

where τ is the time constant of the spacecraft, θ_0 is the original nutation angle and the new angle after some time t is θ. If the time constant is negative, as it is for stable spinners, the nutation angle will diminish. For unstable spinners, however, the angle will be growing even as the thrusters are firing. In the next section, energy dissipation effects are discussed, and efforts are made to predict the nutation time constant for the unstable ORION satellite.

6. Energy Dissipation Effects

A successful spacecraft design -- spin stabilized about the axis of minimum moment of inertia and having a large liquid propellant mass fraction -- depends on long term vehicle control. Liquid motion in a nutating spacecraft results in kinetic energy dissipation that increases coning motion in the prolate spinner. This coning motion, if not controlled, results in a flat spin, or spin about the axis of maximum moment of inertia (major axis). Coning motion must be minimized by active nutation control to maintain the original attitude. Consequently, the maximum energy dissipation rates from the propellant motions must be known to size in order to compensate an active nutation control system for these losses. (Zedd and Dodge, 1985, p.1)

Although internal torques do not change the value of the angular momentum in inertial space, they can affect the behavior of $\underline{H}$ in spacecraft fixed coordinates. Additionally, if the internal forces between the components of a spacecraft lead to energy dissipation (through solid or viscous friction or magnetic eddy currents, for example) the rotational kinetic energy of the spacecraft will decrease. (Wertz, 1985, pp. 498-499)

A major source of destabilizing energy dissipation in spinning spacecraft is liquid fuel. The amount of liquid fuel, expressed as the ratio of liquid mass to total mass, has become larger with the advent of integral liquid apogee propulsion systems. This ratio will increase dramatically with liquid perigee propulsion stages currently being studied. The simplicity of spin stabilization still means that spinning liquid fueled spacecraft will
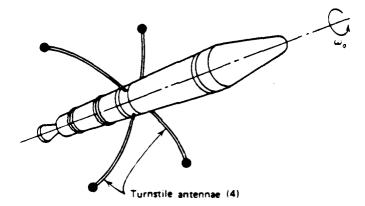
be a challenging problem in attitude dynamics and control. The challenge
may in fact become greater. (Vanyo, 1982, p.357)

The design of the ORION propulsion system is predicated upon the use
of hydrazine fuel which is stored in a 16.5 inch diameter positive expulsion
tank located on the longitudinal axis of the spacecraft. Past experience with
liquid fueled spacecraft has shown that liquid motion within the satellite is a
significant source of energy dissipation. This dissipation acts to stabilize an
oblate spinner causing the nutation angle to diminish. In a prolate spinner,
however, the dissipation will lead to a rapid exponential growth of the
nutation angle ultimately resulting in a flat spin about the transverse axis.
This nutation divergence was first proved by Dr. Owen Garriot and others
(Bracewell and Garriot, 1958, pp. 760-762) in a theory which accounted for
the tumbling motion of Explorer I shortly after orbital insertion of that first
United States satellite. The satellite (Figure 5-36) was spun about its
longitudinal axis and had a value of σ significantly less than unity. Four
flexible antennas acted as dissipative mechanisms. Shortly after deployment
external torques (such as orbital drag) began to perturb the spin. The
energy dissipation of the flexible antennas led to a rapid increase in nutation
angle, and the satellite entered a flat spin and tumbled end over end about
the transverse axis in a stable spin configuration. Garriott and Bracewell
deduced the tumbling, but stable, spin orientation from the cyclical fading of
radio transmissions from the satellite.

Later spacecraft were designed with the energy dissipation problem in
mind, particularly when the spacecraft carried liquid fuel or semi-rigid
components. However, design estimates of satellite lifetime as a function of

527

Figure 5-36

Explorer I with Dissipative Flexible Antennas
(Kaplan, 1976, p. 63)

attitude control propellant reserve were found to be in error by as much as two orders of magnitude. Modeling techniques, particularly those methods used in the late 1960's and early 1970's, were rejected as inadequate for predicting satellite performance. The energy dissipation problem was discovered to be untractable analytically.

Prediction of the effects of liquid motion in a spinning spacecraft is extremely difficult if not impossible. For that reason, the study of dissipation effects has given birth to ingenious physical models. Scale model spacecraft complete with liquid propellant tanks are subjected to various spin rates while free-falling into bins of grain; these experiments enable researchers to observe nutation angle divergence due to energy dissipation. These studies have led to dimensional analysis techniques that succeed in predicting actual satellite nutation time constants within a factor of 2-3.

Advances by Vanyo at the University of California (Santa Barbara), Hubert and Goodzeit at RCA, Zedd at NRL, and Dodge at Southwest Research Insitute (SWRI) have led to increasingly sophisticated modeling apparatus and computer models that accurately determine time constants for future spacecraft. The Vanyo spinning tank and the NRL spin table are used extensively to observe the growth of nutation angles for various spacecraft flight configurations and propellant fill fractions. The observed data are fit to exponentials that describe the exponential nutation growth. Using the methods of these researchers, short time constants can be observed for highly dissipative or very prolate spacecraft. However, no one has yet established a satisfactory modeling mechanism to observe nutation growth in nearly stable spinners which exhibit large time constants. In addition to

529

time constant investigations, these researchers have also identified various fuel dissipation "modes". Not all tank configurations exhibit dissipation for the same reason. Significant strides have been made in separating influences due purely to "fuel slosh" from those due to complicated wave action at the fluid-tank wall boundary. The dissipation contribution of propellant management devices (i.e. vanes) has also been successfully quantified. Dodge (1985) has begun to develop a sophisticated model that will numerically predict dissipation effects; the model is based on the NRL experimental analyses of the past 5 years. The interested reader is commended to Zedd and Dodge (1985) and NASA SP-106 (authored by Dodge) for illustrative details of the energy dissipation problem.

The following excerpt from Zedd and Dodge (1985, pp. 1-3) describes the fluid dynamics responsible for energy dissipation (emphasis is author's own).

A complete theory of the kinds of motion that can occur in a spinning spherical tank is not available, but differential equations of motion suggest that two kinds of natural oscillations are possible. They are:

(1) Sloshing waves (free surface oscillations) and
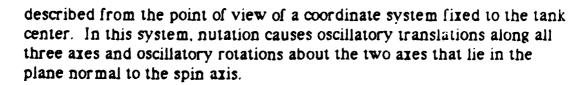(2) Inertial waves (inertial liquid oscillations)

In general, both kinds of waves produce oscillating forces and moments about the center of an arbitrary shaped tank. But for a spherical tank, liquid pressure can create only a force; thus any moment exerted about the tank center can only be due to viscous shear at the wall. Ordinarily, viscous shear is negligible compared to the effects of pressure. Similarly, an oscillating rotation of a spherical tank about its own center is transmitted to the liquid only by viscous shear at the wall. For other tank shapes, viscous shear is ineffective compared to the oscillating wall motion normal to the wall surfaces. One of the items of interest is to determine if viscous shear could cause significant inertial waves in a spinning spherical tank. The following discussion of liquid motion is

530

described from the point of view of a coordinate system fixed to the tank center. In this system, nutation causes oscillatory translations along all three axes and oscillatory rotations about the two axes that lie in the plane normal to the spin axis.

Sloshing waves are characterized by oscillations of the free surface and center of mass location such as to change the potential energy of the liquid relative to the effective gravity force. The effective gravity is a vector combination of the true gravity and centripetal accelerations. Sloshing is a dynamic interaction between effective gravity forces and inertial forces. There must be a free surface and it must move up and down through the gravity field. Mathematically, sloshing can be analyzed on the basis of an ideal liquid executing an irrotational motion, that is, as potential flow. The effects of viscosity may be considered later as a boundary layer at the wall; the effect is to provide some damping of the motion, but viscosity does not significantly change the slosh modal characteristics or the natural frequencies. When one of the lower frequency modes is driven at resonance, the damping of an ordinary low viscosity liquid is so small that the wave becomes unstable. For an axisymmetric tank, the instability causes the free surface wave to rotate around the symmetry axis but the bulk of the liquid has an irrotational potential type of motion. A sloshing wave is primarily excited by unsteady tank translation - not rotation - in a spherical tank.

When the tank spins, the liquid spins with it after some initial transient motion. The liquid motion is thus rotational, and a conventional analysis would not apply. There are some indications that a potential flow-like sloshing can exist in this rotational field and that all the slosh resonant frequencies are greater than twice the spin rate. Assuming that sloshing can be created in a spinning tank, sloshing resonances can be excited only if the excitation frequency, λ, is more than twice the spin rate.

Inertial waves do not require a free surface and can occur in a completely full tank. The center of mass oscillations are small even if the free surface oscillates. The resonances represent a dynamic interaction between Coriolis forces and pressure forces in the bulk on the liquid interior. Inertial waves are circulatory or to-and-fro motions in the liquid interior, and there may or may not be any apparent motions at the free surface. They are excited by unsteady tank rotations. Inertial wave

Boundary layer shear is the coupling of liquid motion to tank walls via the viscous liquid itself. This in an energy transfer mechanism, and the greater viscosity liquids induce both greater shear and energy dissipation rates. Although the boundary layer is a source of damping, it may drive an inertial wave to resonance in a spherical tank in addition to driving bulk motions.

(Figure 5-37) shows an equivalent mechanical model based on the liquid motion characteristics previously described. A pendulum is proposed to represent the predominant mode on inertial oscillations. For sloshing, the primary effect of the steady spinning is similar in form to that for a nonspinning spherical tank in a gravity field. The oscillations of the pendulum mass simulate the oscillations of the liquid center of mass. In a spinning tank, however, the pendulum has two natural frequencies, which correspond to oscillations in the circumferential direction and in the transverse direction. For inertial wave oscillations the steady spinning is crucial since such oscillations do not occur in a nonspinning tank. The equivalent mechanical element must also spin and should be in the form of a rotor. The natural frequency of the rotor is chosen by proper selection of the inertias, I_1, I_2, and I_3 to duplicate the natural frequency of the inertial oscillation mode of interest. A rotational viscous dashpot connects the rotor to the tank to simulate the indirect excitation of the liquid caused by viscous shear. The moment exerted on the rotor by the dashpot is not, however, a simple angular rate dependency since it must simulate an unsteady Ekman boundary layer. (Zedd and Dodge, 1985, pp. 2-3).

In the absence of rotation, and with a uniform acceleration field impressed by gravity or the thrust of a rocket motor, the propellant senses only a translational excitation. If the excitation is oscillatory and of small amplitude, the liquid center of mass moves as if it were a simple pendulum, with a natural frequency that is a function of the background acceleration field, the container geometry and the fill fraction. If the exciting force is large or abrupt, as in the case of a satellite being suddenly ejected from the Space Shuttle bay, the response of the fluid will be of large amplitude, and (ejection) clearance problems may arise. These slosh problems must nearly always be handled on a case by case
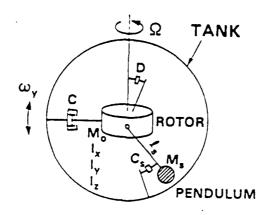
532

Figure 5-34

Mechanical Model of Propellant Effects in Energy Dissipation
(Zedd and Dodge, 1985, p. 3)

basis because of the unique forcing function and container geometries that prevail in each case. Incompressible flow problems prevail in each case and because of that the results of each problem are usually three dimensional as well as unsteady.... Currently most work is being performed by treating the fluid as a lumped mass and making worst case assumptions about reaction forces.

The concern is then whether the excitation frequency ... is near a slosh resonance frequency. The state of the art for theoretically calculating fluid natural frequencies in tanks of simple shapes such a spheres, cylinders and cones is well developed and abundant experimental data exist. <u>However, if the fluid is held beneath a positive expulsion diaphragm or bladder, no similar theoretical treatment is presently available, and one can only refer to experimental measurement of natural frequency. The development of a technology for analyzing the coupled mechanics of an elastomeric diaphragm in continuous contact with a contained liquid would be an important contribution to the science of propellant dynamics,</u> and it is a task that should be addressed in the near future because of the frequent reccurrence of tanks with diaphragms in spacecraft applications. (Aerospace Co. Vol. VII, 1983, p.23)

The author conducted an extensive literature search between October and December 1986 to determine the extent of the energy dissipation problem for ORION. Dr. Brij Agrawal (INTELSAT) and Mr. Michael Zedd (Naval Research Laboratory) were contacted personally about problems unique to the ORION design. Specifically, how could energy dissipation be predicted in a prolate spinner that contains an on-axis spherical positive expulsion tank? Responses from both Agrawal and Zedd, who are leaders in the field of off-axis tank dissipation studies, confirmed that the problem was not analytically tractable. In addition, Agrawal noted that the ORION case was actually the simple case of many more complicated on-axis studies conducted by Vanyo of UC Santa Barbara and Hubert & Goodzeit of RCA. He suggested that, with data from the dissipation studies of those researchers,

costly scale model laboratory tests of an ORION tank and structure might be avoided in this feasibility study. Unfortunately, most studies have been conducted to ascertain dissipation effects due to off-axis propellant tanks. Most of the satellite designs referenced used the central volume of a structure for apogee and perigee motors. Hence, an on-axis attitude control propellant tank was usually rejected in favor of tanks dispersed around the periphery of the vehicle. Peripheral tanks in a spinning satellite also demonstrate a natural positive expulsion capability as a consequence of centrifugal force. Figure 5-38 depicts a typical off-axis tank configuration in INTELSAT spacecraft which led to the emphasis on tank energy dissipation studies. Figures 5-39 and 5-40 diagram the spin tables used by INTELSAT and NRL to observe the nutation divergence of scale model tanks.

Zedd of NRL confirmed the emphasis by researchers upon off-axis tank studies noting that the data from those studies is incompatible with the ORION requirement. On-axis tanks do not exhibit the same fluid resonances as off-axis tanks. Thus the experimental methods and equations of Agrawal, Zedd and Dodge, while enlightening, are not applicable to this feasibility study.

On the suggestion of Dr. Agrawal, the author referenced studies conducted by J. P. Vanyo of the University of California, Santa Barbara. Many investigations were conducted by that researcher between 1978-1986 using an experimental device (Figure 5-41) that tests the nutational instability of on-axis tanks. In particular, one study (Vanyo, Garg and Furomoto, 1986, pp. 357-362) was conducted for a tank subjected to spin on a platform with an

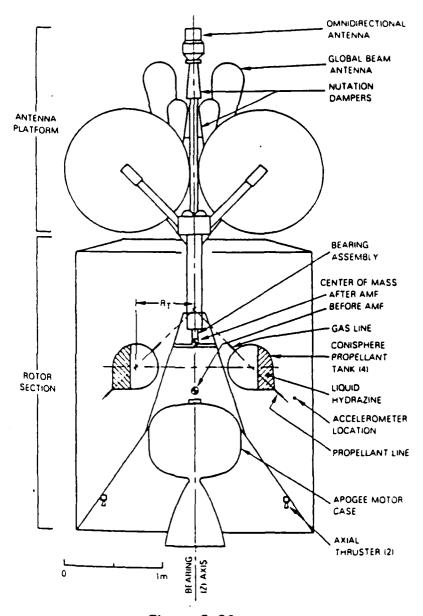Figure 5-38

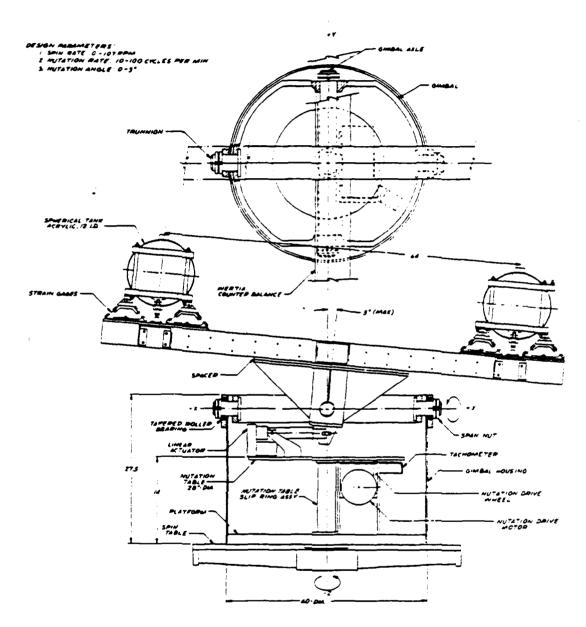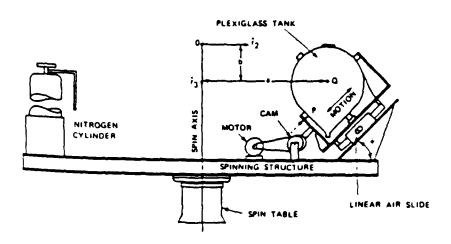INTELSAT Structure Depicting Off-Axis Propellant Tanks
(Slabinski, 1978, p. 21)

536

Figure 5-39

Naval Research Laboratory Forced Motion Spin Table
(Zedd and Dodge, 1985, p. 5)

Figure 5-40

INTELSAT Spin Table
(Martin, 1971, p.5)

538

inertia ratio of 0.324. Without booms deployed, ORION exhibits an inertia ratio of 0.324 or greater when the fuel tank is over half full. Tests were conducted at various spin rates between 20 and 70 RPM. A second pair of researchers, C. Hubert and N. Goodzeit of RCA Corporation (1983, p. 669) conducted on-axis spin studies at 60 RPM for a full 16 inch diameter tank. This spherical tank was spun on a platform which possessed an inertia ratio of 0.54. These two studies provided valuable insight into possible nutation time constants for the ORION satellite.

The time constant of nutation is related to the rate of kinetic energy dissipation in the propellant tank. The kinetic energy of a body is described by

$$E = 0.5 \ M \ V^2 \qquad (5.51)$$

For a rotating body, this is expanded to

$$E = 0.5 \ [I_t \ (w_1^2 + w_3^2) + I_2 \ (w_2^2)] \qquad (5.52)$$

Kaplan (1976, p. 130) shows that the time rate of change of the kinetic energy (also known as the rate of energy dissipation) is expressed as

$$dE/dt = H^2 \ I_s^{-1} \ [(I_s/I_t) - 1][\sin\theta \cos\theta][d\theta/dt] \qquad (5.53)$$

where θ is the angle of nutation. One of the difficulties in predicting energy dissipation is pointed out by this equation. The rate of dissipation is coupled to the magnitude of the nutation angle and its rate of change. For small

539

nutation angles, the value of dE/dt will likewise be small. Rearranging terms, the rate of change of the nutation angle can be expressed as

$$d\theta/dt = H^{-2} [\sin 2\theta]^{-1} [2 \ I_t \ I_s \ (I_s - I_t)^{-1}] [dE/dt] \qquad (5.54)$$

Kaplan, Agrawal and Vanyo further point out that the rate of energy dissipation (dE/dt) is a function of a number of the parameters shown in the following equation.

$$dE/dt = f \ (t, \omega, m_s, m_p, I_t, I_s, r, \rho, \mu, g, s, \theta) \qquad (5.55)$$

where t is the time, ω is the spin rate, m_s is the mass of the satellite, m_p is the mass of the propellant fluid, r is the radius of the tank, ρ is the fluid density, μ is the fluid kinematic viscosity, g is the gravitational constant, s is the liquid surface tension and θ is the nutation angle. Note that many of these values are constant. Notably, the liquid surface area does not change in a diaphragm tank. As the diaphragm reverses upon itself, the wetted area remains constant. Thus the friction due to liquid contact with the tank and diaphragm is likely to remain constant. However, the fuel mass and thus the satellite mass will change, and the moments of inertia with them.

Vanyo (1986, p. 358) relates energy dissipation to a time constant, τ, using an energy sink model. Figure 5-42, adapted from Vanyo (1986, p. 360), shows a range of time constant values for the experimental apparatus of Figure 5-41. These data were obtained for various fuel and oxidizer fluids using an initial nutation angle of $5°$. From these data points Vanyo
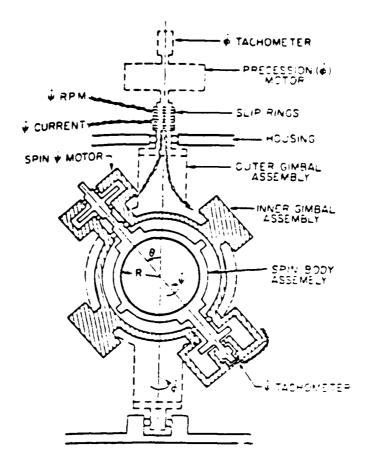
540

Figure 5-41
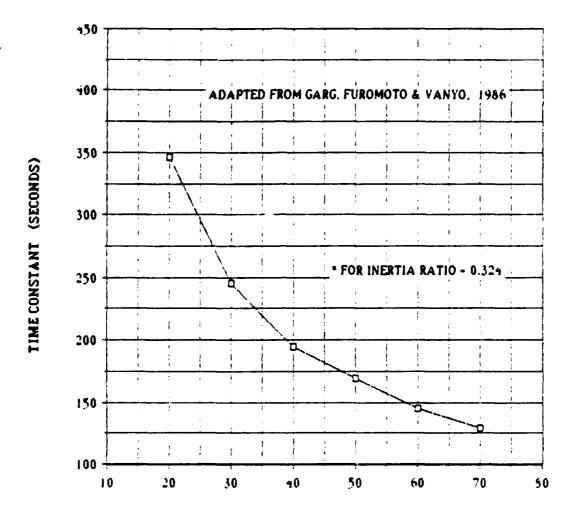
Vanyo Experimental Apparatus
(Vanyo, 1986, p. 359)

RPM

Figure 5-42

Effect of Spin Rate on the Nutation Time Constant

542

conducted a dimensional analysis and determined that τ was proportional to the spin rate multiplied by some constant C.

$$\tau \approx C \omega^{-0.74} \qquad (5.56)$$

Using Vanyo's data, a range of τ values for various RPM are plotted. At 60 RPM, for example, the time constant for nutation is 175 seconds. At 20 RPM the time constant is 350 seconds.

Hubert and Goodzeit also predict the time constant using dimensional analysis based upon experimental investigations. One particular test of a 16 inch diameter spherical aluminum tank accurately modeled the ORION hardware. However, the tank was subjected to a platform inertia ratio of 0.54, which is higher than that of the no-boom ORION configuration.[*] These tests utilized a special platform at the Goddard Space Flight Center (GSFC) which is described by Peterson (1976) in NASA-TN-D8346. The test accurately simulated ORION flight conditions using a full propellant tank, thus eliminating all slosh resonances as a dissipation effect. (From the standpoint of "fuel slosh", the ORION tank will always appear to be full due to the ribbed, compressive diaphragm which provides positive displacement.) Water was used as a test fluid because its density is very close to that of hydrazine. The dissipation mechanism in tests of tanks with or without propellant management devices (i.e. vanes) was found to be linear in nature. Using regression analysis to fit the test data to an exponential, Hubert and Goodzeit developed a range of energy dissipation

---

[*] If the booms are deployed to a length of approximately 15 inches (see Figure 5-27), the satellite exhibits an inertia ratio of 0.54.

rates as a function of the inertial nutation frequency of the tank. Here, inertial nutation frequency refers to the spin rate of the test apparatus, Ω added to the nutation frequency, λ

$$\lambda + \Omega = \lambda_i \qquad (5.57)$$

In order to correlate data from test runs of different platform inertias, the nutation time constants were used to calculate the average energy dissipation rate for each test case and a normalization technique was applied. The averaging was performed over a nutation cycle. For an inertially symmetric platform, with a linear dissipation mechanism, the average energy dissipation is given by

$$dE/dt = H \lambda \theta^2 / \tau \qquad (5.58)$$

...For a platform coning about its minor axis, λ is negative and τ is positive. For a platform coning about is major axis the signs are reversed. In either case, dE/dt is negative, indicating that kinetic energy is being lost from the system.

In developing an appropriate normalization technique, it was discovered that tanks driven at the same inertial nutation frequency do not undergo the same motion if attached to bodies with different inertia ratios. To normalize the data to account for the motion differences of ... various test conditions, the dependence of energy dissipation rate on nutation angle squared was eliminated. This was performed by dividing the equation above by the square of the amplitude of the transverse angular acceleration.

$$\alpha_t^2 = (\theta \Omega \lambda \sigma)^2 \qquad (5.59)$$

Here, Ω is the (test) platform spin rate, and σ is the platform inertia ratio. Taking the absolute value of the result yields the normalized energy dissipation parameter

$$K_n = | H (\lambda \tau \Omega^2 \sigma^2)^{-1}| \qquad (5.60)$$

544

The last step in correlating data from various test cases was to plot the values of the normalized energy dissipation parameter against the inertial nutation frequency, λ_i ... (Hubert and Goodzeit, 1983, pp. 670-671).

Figure 5-43 depicts the energy dissipation rate dE/dt as a function of the inertial nutation frequency. Hubert and Goodzeit suggest a relationship between the normalized dissipation parameter and the inertial nutation frequency where

$$K_n = C \lambda_i^\epsilon \qquad (5.61)$$

C is a scale factor. For the full 16 inch diameter test tank in their study, $C = 0.014$ and $\epsilon = -1.18$. Hence

$$K_n = (0.14)(\lambda + \Omega)^{-1.18}$$

Knowing w_s, H and the inertia ratio, the ORION time constant can be predicted. Assuming a spin rate of 60 RPM (6.283 rad/sec) and a full tank ($\sigma_{ORION} = 0.303$), for example

$$\lambda = (\sigma - 1)(w_s) = -4.379 \text{ rad/sec} \qquad (5.62)$$
$$\lambda_i = \lambda + w_s = 1.904 \text{ rad/sec}$$

$$K_n = 0.14\,(1.904)^{-1.18} = 0.0655$$
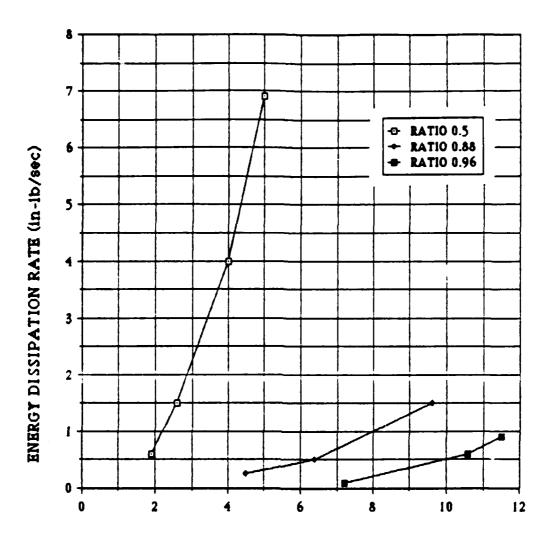
$$K_n = |H\,(\lambda \tau \Omega^2 \sigma^2)^{-1}|$$
$$0.0655 = |I_s w_s\,(\lambda \tau \sigma^2 w_s^2)^{-1}|$$
$$\tau = 1897.4 \text{ seconds}$$

545

Figure 5-43

Energy Dissipation Rates for a 16" Spherical Tank
(Hubert and Goodzeit, 1983, p. 671)

This value differs markedly from that obtained with the Vanyo data because it is based upon tests conducted with an inertia ratio of 0.54. Larger inertia ratios, and thus more stable spinners, result in larger time constants. A comparison of τ for the two studies confirms this.

Recall that the nutation angle grows according to the relationship

$$\theta(t) = \theta_0 \, e^{t/\tau}$$

If the nutation angle for a prolate spinner is permitted to grow, the spacecraft ultimately reverts to a flat spin about the major moment of inertia (the transverse axis). Stable spin results. Consequently, if the satellite is designed as a prolate spinner, active control of the nutation angle is required. As Wertz (1985, p. 2) points out, most engineering functions of a satellite can be accomplished using attitude control accuracies on the order of 1°. Specific payload requirements may dictate even greater accuracy. The exponential relationship for θ shows that relatively small changes will be made in the nutation angle for a given time period when θ_0 is very small. If θ_0 is very large, growth is much faster in the same period of time. For example, if τ is 175 seconds (Vanyo data @ 60 RPM) and if the observation time t is 60 seconds, consider the nutation angle growth for three separate values of θ_0.

TABLE 5-3

NUTATION GROWTH TIME AS A FUNCTION OF INITIAL ANGLE

$$t = [\ln(\theta/\theta_0)]\tau$$

$$\Theta(t) = \theta_0 \, e^{t/\tau}$$

t	θ_0	θ	$\Delta\Theta$
60 seconds	0.1°	0.141°	0.041°
60 seconds	1.0°	1.409°	0.409°
60 seconds	10.0°	14.09°	4.09°

Obviously, from a control point of view, nutation growth from a very small angle is preferrable to growth from a large angle. Suppose that a satellite conducts active nutation control when the nutation angle attains a maximum of 5.0°. The time to reach 5° from a starting nutation angle of 0.1° and 1.0° is shown in Table , using the equations below.

$$t = [\ln(\theta/\theta_0)]\tau \qquad (5.63)$$

Active nutation control will be required much less frequently if it is applied at small nutation angles and if the value of the initial nutation angle is as small as possible. It will be seen that active nutation control is most efficient when the initial and final nutation angles are very small. Intuitively this is reasonable when one considers the expression for t and the equations for active nutation control. Eradication of large nutation angles is not fuel efficient. Instead, fine control of the wandering $\underline{w}$ vector is desirable.

There is a limitation to the efficiency with which one can conduct active nutation control. While the maximum value of θ is subject to the designers choice (based on factors such as time between control applications and certain sensor constraints), the value of the starting angle, θ_0, is less arbitrary. The design goal is to make θ_0 as small as possible during active nutation control. However, this initial angle is limited by the accuracy of the control system. If the attitude determination sensor has a minimum resolution, then that is also the minimum value for θ_0. Resolution of small

549

angles is important for active nutation control considerations and payload requirements.

Once the two limits of nutation growth are set and a spin rate has been established, the designer can use the equations above to determine the fuel requirements of the attitude control subsystem for a prolate spinner. Satellite propellant mass is a limiting factor that determines satellite lifetime. Note that the angular bounds, i.e. θ_0 and θ_m, and the spin rate are mission dependent parameters. Specific values have not been chosen for ORION. A set of performance charts were created to provide a quick reference in determining fuel consumption and lifetime. The charts are based on an ORION worst-case inertia ratio of 0.303 and assume that only one nutation control thruster is available. Using these charts the thruster-on-time and the worst-case lifetime-per-pound-of-fuel can be determined. The charts provide data for various values of θ_m, θ_0 and w_s. Figures 5-44 through 5-51 depict the thruster pulse time required to actively decrease the nutation angle from a value of θ to θ_0.

Figures 5-44 to 5-51, the legend in the lower right corner refers to the graphs for particular values of θ_0. Various values of θ_0 were evaluated across a range of final nutation angles and spin rates. The value of the abscissa in each graph refers to the value of the nutation angle when the active nutation control is first applied. For example, at a spin rate of 20 RPM, assume that the best attitude control resolution is 1.0°. From Figure 5-45, note that after the nutation angle is allowed to increase to a value of 10.0°, an accumulated nutation control pulse of 13.2 seconds will be required to reduce the angle back to 1.0°. The time constant from Figure 5-42 is

550

350 seconds at 20 RPM. Thus the nutation angle will grow from 1.0° to 10.0° again in 805.8 seconds. After that time another nutation control pulse will be required. Recall that each pulse is executed over a 90° arc of rotation. At 20 RPM this arc is traversed in 0.75 seconds. To accumulate 13.2 seconds of active nutation control thrusting, the total number of separate pulses and total time to correct the nutation using a single thruster is approximated by

$$13.2 / 0.75 - 17.6 \text{ pulses}$$
$$(17.6 \text{ pulses})(3 \text{ seconds per revolution}) - 52.8 \text{ seconds}$$

These values would be less if both precession thrusters were used accomplishing the nutation control in half the time. Thus, the length of the nutation cycle is approximately

Active Nutation Control Cycle Period - thruster-on-time + thruster-off-time
$$A.N.C.P. = t + \Delta t \qquad (5.64)$$

$$t - \ln(\theta/\theta_0)\tau$$
$$\Delta t - (\#\text{pulses})(60 \, w_s^{-1})$$
$$A.N.C.P. - 805.8 + 52.8 - 858.6 \text{ seconds}$$

The nutation cycle appears as a function of time in Figure 5-52. Note that the nutation angle grows exponentially up to some predetermined limit. At that point the angle is actively controlled and reduced to the minimum resolvable angle. The angle continues to grow and the cycle repeats itself.

The actual cycle period is slightly longer because the nutation angle is increasing between thruster applications. The actual period must be solved for iteratively considering the nutation angle growth during the portion of the cycle when the thrusters are pulsing. Using the example above, the thrusters are applied 17.6 times over a span of 52.8 seconds. During those 52.8 seconds the rate of nutation angle growth will vary as a function of the starting angle (which is rapidly being diminished by the thrusting of the precession thruster). Hence, a computer program must be used to solve for the exact period of the cycle; the contribution of nutation angle growth during the thrusting portion of the cycle must be determined iteratively. For the example above, Eqn 5.65 indicates that the nutation angle will grow approximately $1.6°$ during the thrusting portion of the cycle. The actual growth will be less because this value assumes that the nutation angle grew from $10°$ for 52.8 seconds, when in reality the angle was constantly diminished by the active nutation control.

Note that if the time constant of nutation is short and the nutation angle is allowed to grow to a relatively large value (i.e. $> 10.0°$), the nutation control pulse will also be of long duration. Because the off-duty portion of the thruster cycle is three times longer than the on-duty portion, the nutation angle has a relatively long period of time to grow during the correction pulses. Thus, for short time constants and corrections from large nutation angles it may be difficult if not impossible to eliminate the nutation angle. Again, using the example above, if the time constant had been 60 seconds instead of 350 seconds, and if the correction portion of the nutation cycle had remained 52.8 seconds, Eqn 5.65 shows that the nutation angle

would have grown almost 8° during the control application. This is due to the exponential character of nutation angle growth; the angle grows most rapidly when it starts at large values, and beyond some value, the nutation angle will grow faster than the thruster can correct. Thus, it is critically important to maintain small nutation angles between correction applications, not only for fuel efficiency, but for stability as well.
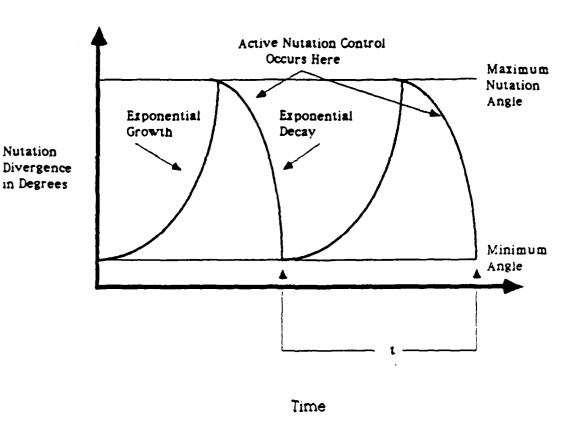

Figure 5-52

Active Nutation Control Cycle
(Assumes a Control Pulse of $\pi/2$ Duration)

553

Figure 5-44

Nutation Control Pulse Duration - 20 RPM

Figure 5-45

Nutation Control Pulse Duration - 20 RPM

555

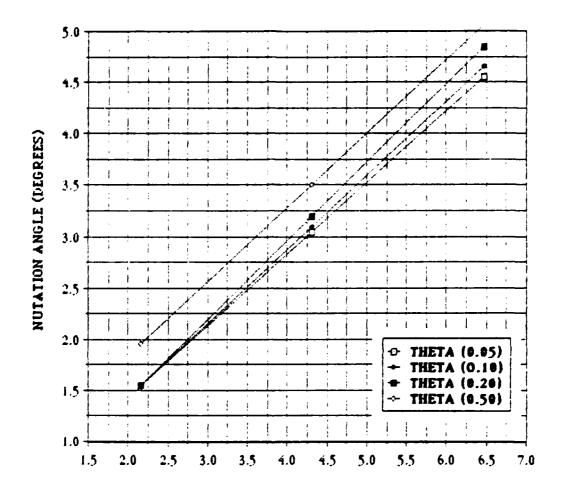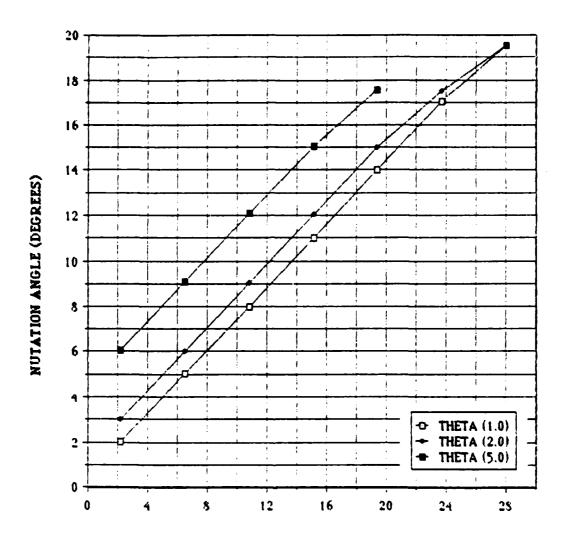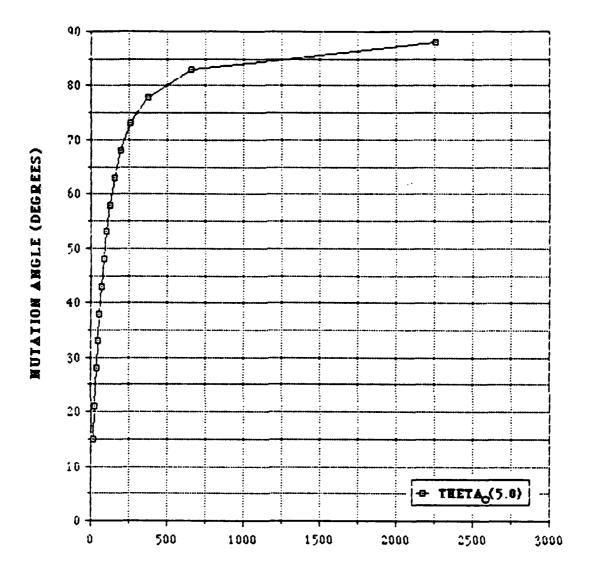**ACCUMULATED PULSE DURATION (SECONDS)**

Figure 5-46

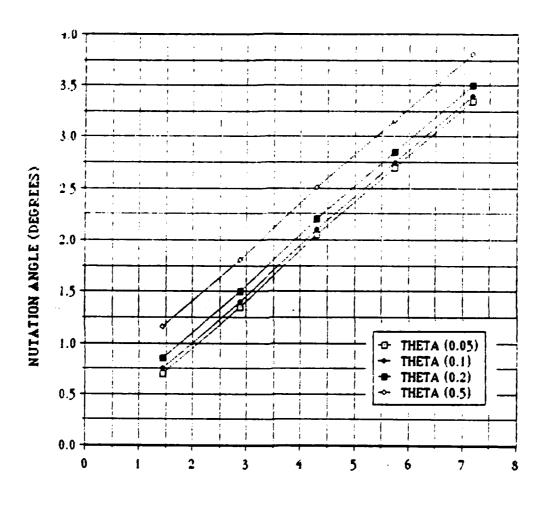Nutation Control Pulse Duration - 20 RPM

Figure 5-47

Nutation Control Pulse Duration - 30 RPM
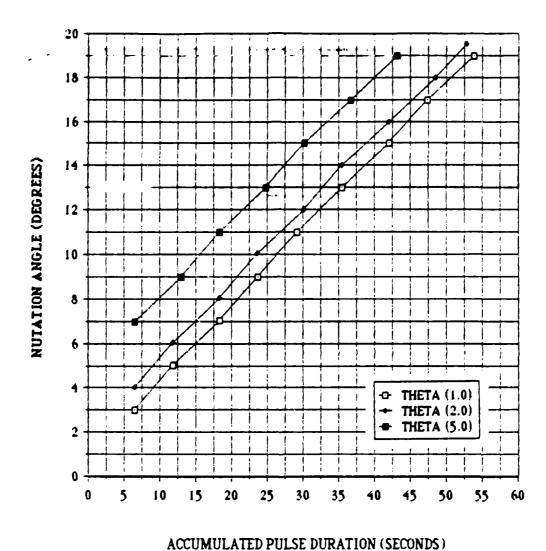
Figure 5-48
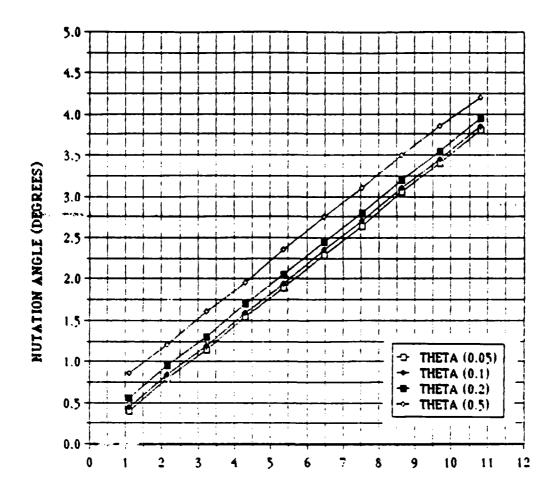
Nutation Control Pulse Duration - 40 RPM
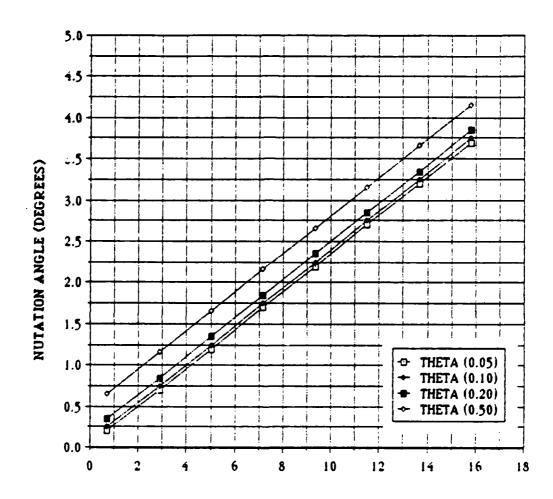
Figure 5-49

Nutation Control Pulse Duration - 40 RPM

559

Figure 5-50

Nutation Control Pulse Duration - 60 RPM
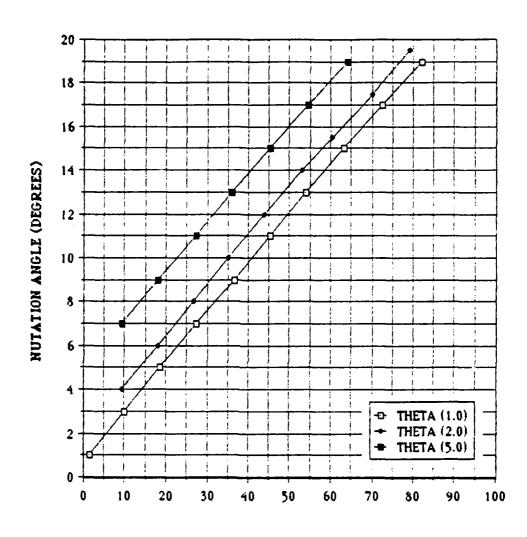
Figure 5-51
Nutation Control Pulse Duration - 60 RPM

The fuel expended per control pulse follows from Eqn. 5.43. The performance of the control system can be predicted where the lifetime of the spacecraft using active nutation control is a function of the quantity propellant available.
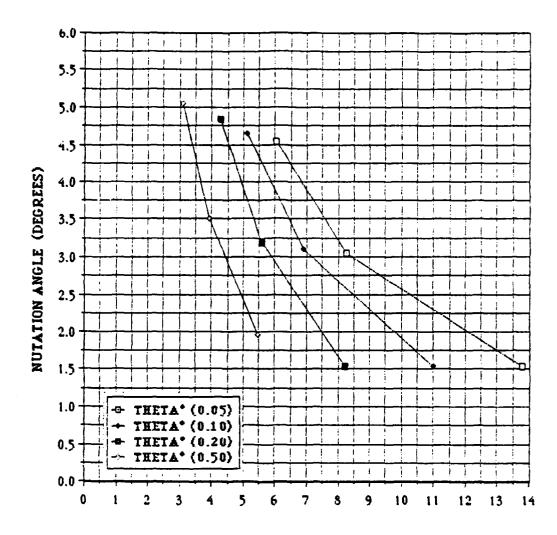
$$\text{Lifetime} = \frac{[\text{Total fuel available}] [\text{Period of Control Cycle}]}{\text{Fuel utilized each control cycle}} \qquad (5.65)$$

. Figures 5-53 through 5-60 enable the designer to calculate the worst-case lifetime-per-pound-of-fuel for spin rates of 20, 30, 40, and 60 RPM. With a knowledge of the total usable attitude control propellant (71.5 lbm maximum), these charts permit a rapid determination of lifetime for the prolate ORION. For example, if the initial nutation angle is 1.0° and the final nutation angle is 10.0°, the lifetime-per-pound-of-fuel can be determined by referencing Figure 5-54. Note that approximately 1.48 days duration-per-pound-hydrazine will be achieved. Thus the design goal of 90 days in orbit could be met using approximately 61 lbm of hydrazine for active nutation control. The propellant lifetime would be significantly reduced at 60 RPM for these nutation angle values. Figure 5-60 indicates that only 0.22 days-per-pound would be achieved at 60 RPM between the nutation angle bounds listed above.

These are approximate values because they are subject to the innacuracies of a large scale performance chart. The exact lifetime for a given quantity of propellant (assume 61 lbm. from example above) can determined using the following equations, where T_L refers to the lifetime and m_T is the total mass of attitude control propellant.

562
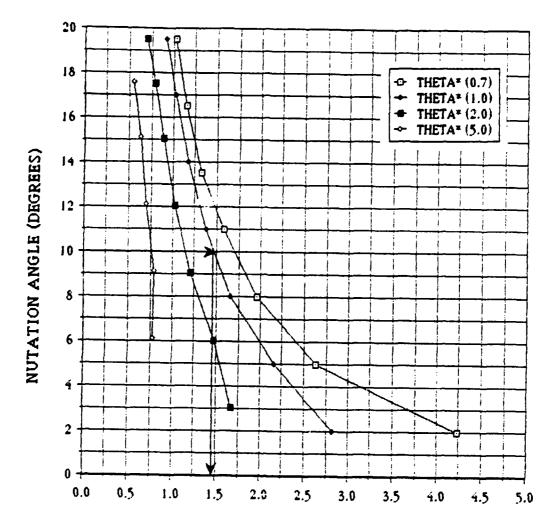
DURATION PER POUND FUEL (DAYS)

Figure 5-53

Mission Duration Versus Nutation Angle - 20 RPM

563
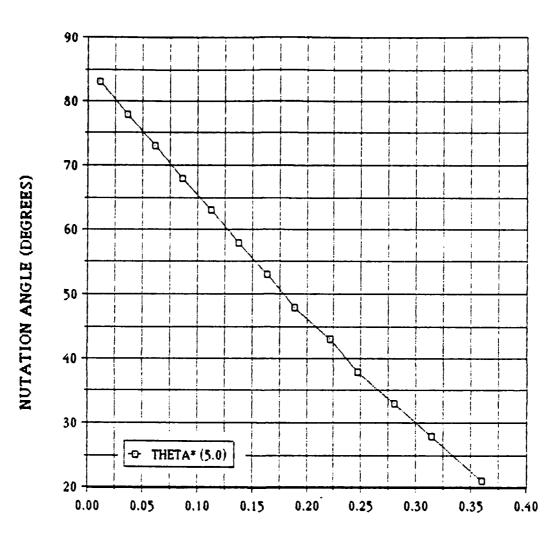
Figure 5-54

Mission Duration Versus Nutation Angle - 20 RPM
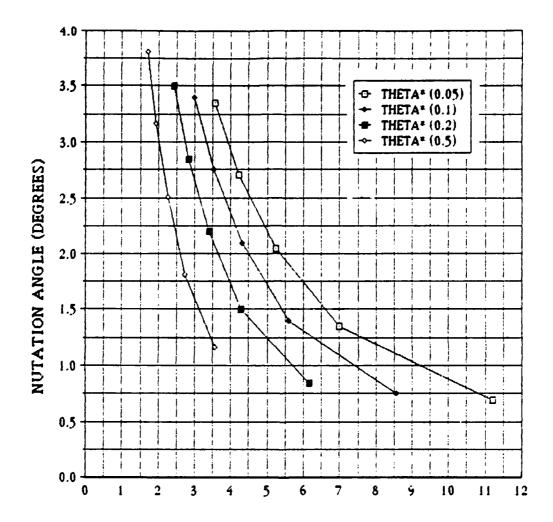
Figure 5-55

Mission Duration Versus Nutation Angle - 20 RPM

DURATION PER POUND FUEL (DAYS)

Figure 5-56

Mission Duration Versus Nutation Angle - 30 RPM

566
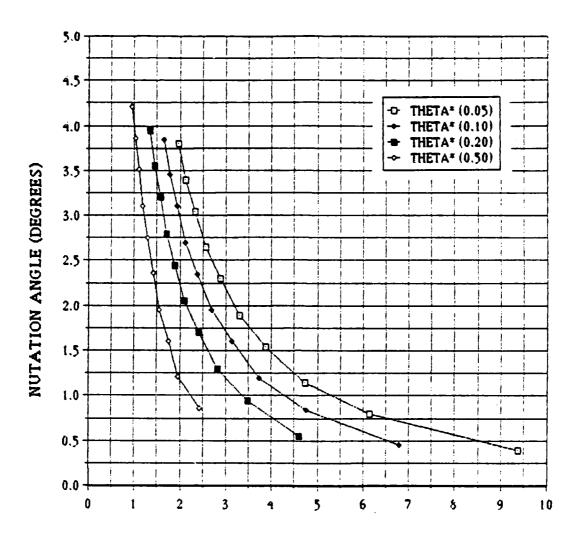
Figure 5-57

Mission Duration Versus Nutation Angle - 40 RPM

567
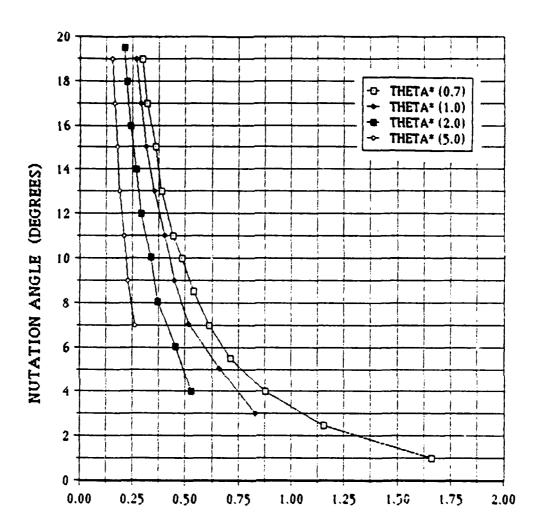
Figure 5-58

Mission Duration Versus Nutation Angle - 40 RPM

568
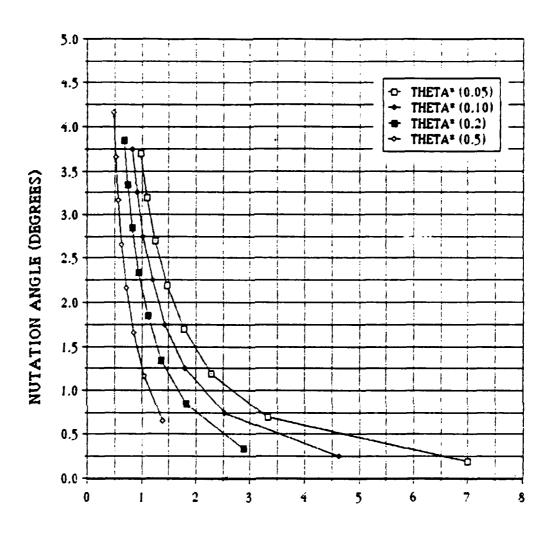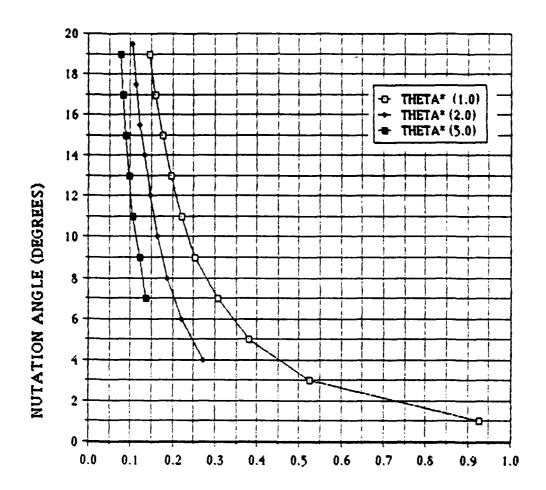
Figure 5-59

Mission Duration Versus Nutation Angle - 60 RPM

569

Figure 5-60

Mission Duration Versus Nutation Angle - 60 RPM

$$T_L = (ISP)(m_T)(F \Delta t_{thrust})^{-1} \Delta t_{cycle} \qquad (5.00)$$

$$T_L = (220 \text{ s})(61 \text{ lbm}) [(0.1 \text{ lbf})(17.6 \text{ pulses})(0.75 \text{ sec-pulse}^{-1})]^{-1} (858.7 \text{ s})$$

$$= 8,730,116.7 \text{ seconds} = 101.4 \text{ days}$$

In conclusion, the performance calculations point out that the efficiency of a control system increases as the values of θ_m, θ_0, and $\Delta \theta$ are diminished. More important, the lifetime of an attitude control system is relatively short for a satellite as prolate as ORION. However, the design goal of 90 days in orbit without the aid of booms could be achieved if a large portion of the spacecraft propellant were dedicated to attitude control requirements, and if the bounds of nutation angle growth (θ, θ_0) remain small. Therefore, even if the booms are not deployed, spin stabilized attitude control for ORION is a feasible concept. The use of booms and the subsequent transformation of ORION to a stable spinner renders the issue of active attitude control academic. With the booms, energy dissipation enhances stability through rapid damping of nutation angles. A boom-configured ORION satellite would be "rock steady" and long lived.

C. SENSOR OPTIONS

The attitude control design criteria stipulate that an accuracy on the order of $1.0°$ is the design goal. The performance calculations of the previous section underscore the importance of achieving a fine degree of accuracy in attitude control and attitude determination. The accuracy of a subsystem is a function of the accuracy of the thrusters (control) and the resolution of the sensors (determination). While the purpose of this thesis is not to choose

specific sensor and attitude computer components, an analysis of various sensor capabilities is warranted. Armed with a knowledge of sensor capabilities, one can address the feasibility of an attitude determination/control subsystem with a 1.0° resolution. Consequently, the goal is to demonstrate that affordable, simple sensors do exist which can be successfully integrated to provide an ORION attitude control subsystem of the requisite accuracy. Some conclusions with regard to feasibility are based on an analysis of previous attitude control subsystems in existing satellites. However, details of specific sensor selection will be left to subsequent design studies.

At least five types of sensors can be selected to provide a composite accuracy of 1.0° as follows:

1) Sun sensors
2) Earth sensors
3) Magnetometers
4) Gyros
5) Star sensors

Each of these sensors has particular limitations, and most spacecraft use more than one type to accomplish the attitude determination mission as well as to provide redundancy. The discussion which follows will analyze each type commenting upon typical accuracies and affordability.

The control of a spin stabilized system is diagrammed in Figure 5-61. Note that the sensors must function in spite of the rotation of the spacecraft. For that reason, sensors which scan an environment rather than dwell upon a point usually are best suited for spin stabilized control systems. Sun

TABLE 5-4

COMPARISON OF ATTITUDE SENSORS

SENSOR	ABS. ACCURACY	ORBIT	NULL AXIS	COMMENT
Horizon Sensor	1-4 min.	synchronous	local vertical	Accuracy is limited by horizon definition and degrades at low alt.
Interferometer	10-40 sec.	syohronous	beacon LOS	Accuracy is limited by antenna thermal distortion
Stellar	1-4 sec.	all	star LOS	Improved accuracy (e.g., 0.005 second) when target star is object of payload.
Sun	1-4 sec.	all	sun line	Improved accuracy (e.g., 0.01 second) when sun is object of payload
Rate Int. Gyro	.01-.04 deg/sec	all	spin vector	Requires update from primary sensor for drift offset.
Gravity Gradient	1-2 degree	low	local vertical	Accuracy is limited by thermal distortion of GG boom
Magnetic Field	1-2 degree	low	field line	Accuracy is limited by field shift during solar activity

573
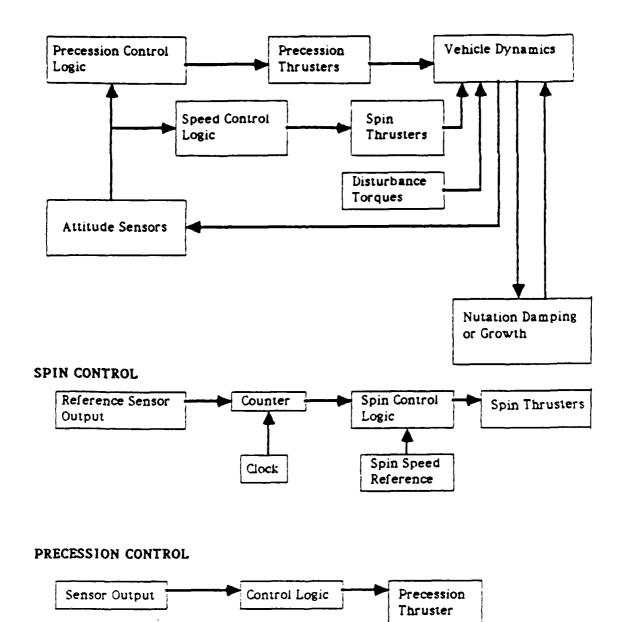
Figure 5-62

Block Diagram of Spin Stabilized Attitude Control
(Sabroff. 1968. p. 1380)

sensors and Earth sensors that detect the passage of the respective body through a field of view are the most commonly used. Figure 5-62 depicts typical sensor fields of view on two spinning spacecraft. Because the sensor is rotating with the satellite, a fan-shaped field of view will rotate to describe a cone or a donut-shaped three dimensional field of view. Intersections of two or more cones at discrete times will be used to provide a solution to the inertial orientation of the angular momentum vector.

Sun sensors are by far the most common attitude sensor in use. Digital sun sensors detect the presence of sunlight and provide a digital signal that indicates the direction of the light source. This signal is processed by an attitude control computer to determine the spacecraft orientation relative to the sunline. Digital detectors are particularly valuable for spinning spacecraft because their binary or gray-code digital outputs are an immediate representation of the rapidly changing sunline orientation. Figure 5-65 depicts a typical digital sun sensor in which sunlight enters a narrow slit and illuminates the photocells. Wertz (Table 5-4) observes that sun sensors display a resolution of 0.1° to 0.5°. These sensors are very light and are quite affordable (approx. $30K each).

Although sun sensors are accurate, affordable and compact, attitude determination cannot be accomplished single-handedly. At best, a combination of sun sensors provides attitude information in two orthogonal axes. The location of the third axis must be measured by some other sensor and reference source. Earth sensors which detect infrared emissions of the Earth are commonly used in conjunction with sun sensors. Like the sun sensor, these detectors note the passage of the Earth through their fanshaped

Figure 5-63

Sensors on Spin Stabilized Spacecraft
(Sabroff. 1968. p. 1380)
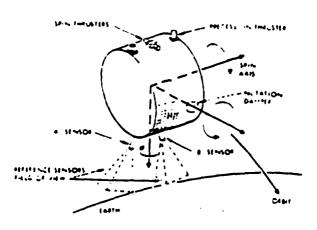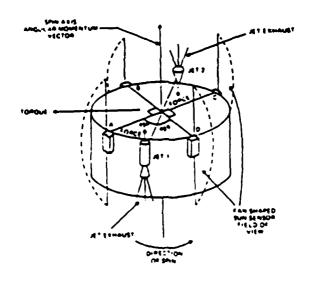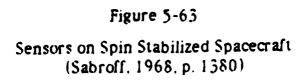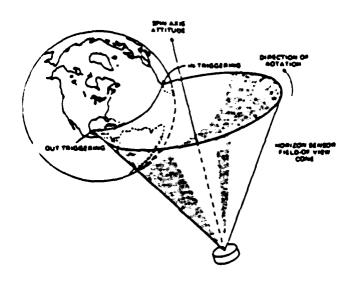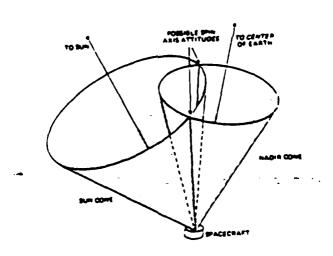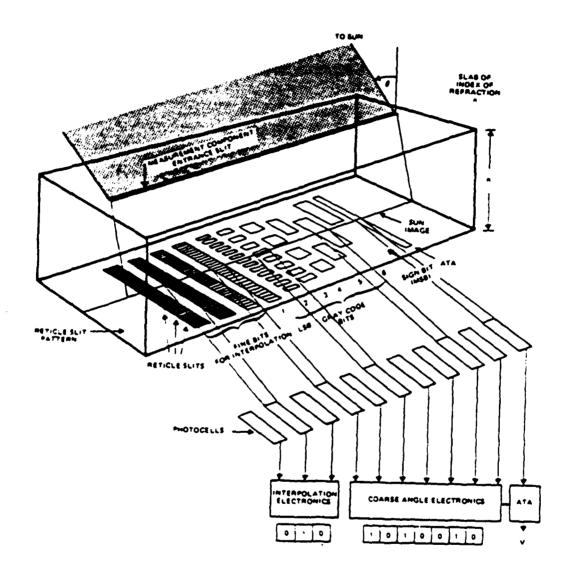
Figure 5-64

Sensors on Spinning Spacecraft Describe a Cone-Shaped Field of View
(Wertz, 1985, p. 11)

Figure 5-65

Digital Sun Sensor
(Wertz, 1985, p. 163)

field of view. However, they use more costly infrared detectors in lieu of photocells. Unlike the sun sensor they can function on the shaded side of an orbit, detecting a backlit "limb" of the Earth. Table 5-6 lists a representative sampling of Earth sensors. Note that an attitude resolution accuracy of 0.0015° to 0.1° is typical. These sensors are significantly more expensive than sun sensors, on the order of $70k - $250k each.
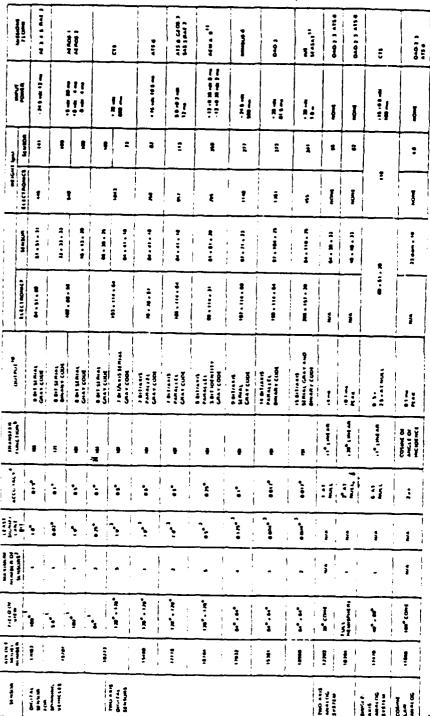
Magnetometers are a third source of attitude information. There are two types of these sensors, namely induction magnetometers and quantum magnetometers. The first measures the local magnetic field and is based upon Faraday's Law of Magnetic Inductance. The second measures nuclear magnetic resonance or Zeeman splitting in the magnetic field. Magnetometers are good sensors from the standpoint of their reliability (no moving parts), but are not highly accurate because the magnetic field in orbit is not completely known. In addition, the mathematical models used to predict the magnetic field strength and direction at the spacecraft position are subject to substantial errors in comparison to the output of other sensors. Because the earth's magnetic field decreases as the third power of the orbital radius, use of magnetometers is generally limited to orbital altitudes of less than 600 nautical miles. These sensors are often arrayed in triplets to evaluate field strength and direction in three orthogonal axes. The placement of one on each of the four ORION booms will increase the stability of the spacecraft and provide the requisite axis coverage with one redundant sensor. Tables 5-7 and 5-8 indicate that these lightweight, affordable sensors are capable of accuracies on the order of 1.0°.

579

TABLE 5-5

REPRESENTATIVE SUN SENSORS
(Wertz, 1985, p. 157)

TABLE 5-6

REPRESENTATIVE EARTH SENSORS

MANUFACTURER	TYPE	ACCURACY	SIZE	WEIGHT	POWER	LIFE REL	COST RECURRING	REMARKS
BARNES ULOCK VD 13-401	STATIC	±0.1° @ 450	6X" DIA	7.5 LB	1W @ 28V	.9961/2 YRS	290 390K	ORBIT MUST BE CIRCULAR — LOW ALT APPLICATION
BARNES GPS SENSOR 13-202/13-1690J	STATIC & HCI	±0.05° (NULL) ±0.05° 140 100 INFAN FIXED ALTITUDE	8.6" x 14"	130 LB	36W @ 28V	.9934/6 YRS	300K SINGLE BUY	DESIGNED FOR 12 HR ORBIT (10-20 KM) ADAPTABLE TO SYNCH
BARNES 13-164	CONICAL SCAN	±0.05°	8" DIA x 8.3" L 3 1/8 x 8 1/2 x 10 7/8	21.2 LB	20W @ 24.8V	64,850 HRS MTBF	180K	HIGHER VERSION FOR FEU & POS PILLBRAS CAPABILITY
LOCKHEED	EARTH DISC SCAN	±0.05° SYNCH ALT	4.1" x 6.1" x 6.5"	3.0 LB	4W @ 28V	0 818/8 YRS	180K	CAN BE ADAPTED TO 12 HR ORBIT. @ DELIVERED TO RCA
QUANTIC MOD IV	LANDED GE TRACKER	±0.015° (NULL)	10.1" x 6" x 5.5" (TRACKER)	20 LB ELEC 23 LB HEADS	38W @ 28V	.92386 NO REDUNDANT WITH SELF TEST	450K	PLUS DEMONSTRATED ACCURACY WITH 3 HEAD VERSION • ALT ALTITUDE SENSOR: DO 25,000 NMI
QUANTIC 6087	STATIC	±0.05° (NULL) SYNCH ALT	5.1" x 6.1" x 7.0	7.3 LB	0.35W @ 28V	390K MTBF	260K	• 8 YRS OF CLASSIFIED APPLICATION • 125 SENSORS • GE CNIS
TRW FLT SATCOM	EARTH DISC SCAN	±0.05°	HEAD: 4.6" x 0 x 9.7 ELEC 2.1 x 7.3 x 8.0	HEAD: 5.0 LB ELEC: 4.7 LB	10.8W	3 YR OPER	110K	QUALIFIED & 24 FLOWN
LOCKHEED TYPE 8	HORIZON CROSSING INDICATOR	±0.14°	3 x 3.6 x 4.0	1.3 LB	1.2W	3.0 x 10⁻⁶/HR	90K	USED ON P72-1 AND CLASSIFIED PROGRAMS
LOCKHEED TYPE 8	HORIZON CROSSING INDICATOR	±0.137°	2.2 x 2.75 x 6.5	1.2 LB	1.6W	3.0 x 10⁻⁶/HR	90K	P150
BARNES 13-211	HORIZON CROSSING INDICATOR	±0.14°	6.7 x 2.6 x 2.13	1.1 LB	0.6W	3.5 x 10⁻⁶/HR	70K	USED ON E3 SATELLITES AND TACSAT

TABLE 5-7

REPRESENTATIVE MAGNETOMETERS

MANUFACTURER	RANGE	ACCURACY	ZERO FIELD ACCURACY	LINEARITY	SIZE	WEIGHT	POWER	COST	REMARKS
SCHONSTEDT INST. CO. (SAM 83C-1)	±100 AND ±600 MG	LOW RANGE: ±1% OF READING HIGH RANGE ±1% OF READING	±1.6 MG	0.1% OF FULL SCALE	SENSOR: 4.7 x 2.8 x 2.8 ELECTRONICS 6.4 x 5.3 x 2.9	SENSOR 0.6 LB ELECTRONICS 1.6 LB	1.1W	21K	FLOWN ON S3
DEVELCO, INC.	±600 MG	±1% FULL SCALE	±2 MG	0.1% OF FULL SCALE	2 x 4 x 3	1 LB	0.3W	2K	DEL TO NRL AND APL

Figure 5-66

Magnetometer Block Diagram
(Wertz, 1985, p. 181)

A fourth type of sensor is the rate gyro (RG). A RG detects the rate of change of spacecraft orientation and provides an output proportional to spacecraft angular rate about an axis. Three RGs provide indications of the spacecraft motion in the Cartesian coordinate frame. An improved version of the RG is the rate integrating gyro (RIG). This gyro uses an electrical signal proportional to the spacecraft angular rate to torque the gyro to a null position. A RIG provides angular outputs or can provide rate outputs similar to a RG if it is a rate integrating gyro operating in the rate mode (Wertz, 1985, pp. 198-199). Because of its high accuracy and low drift rate. the RIG is the type most often used in spacecraft attitude control. While RGs and RIGs are highly accurate, sensing rates on the order of 0.01° per second. they are also costly and relatively bulky, as Tables 5-8 and 5-9 indicate. However, recent advances in gyro design have led to the advent of sensors accurate to 0.1° per second at a fraction of the cost and mass of those in these tables. For example, the Space Vector Corporation of Northridge. CA markets a RIG for approximately \$5K with an angular resolution of 0.1° and mass less than 1 lbm.

Finally. star sensors are used to provide extremely accurate positioning information on platforms which typically maintain a fixed inertial direction. They are rarely used on rotating spacecraft. When star sensors are used the field of view axis must be aligned with the spin axis. and nutation is not permitted. Star sensors are rejected as unsuitable for ORION for reasons of payload accessibility and cost, as well as the significant mass and volume penalty associated with their use. For the interested reader, Figure 5-67

TABLE 5-8

CHARACTERISTICS OF BENDIX Co. CLOSED LOOP RATE GYROS
(Wertz, 1985, p. 199)

CHARACTERISTIC	VALUE
SIZE	~ 7.8 x 30 x 48 CM
WEIGHT	0.34 KG
ANGULAR MOMENTUM	15.000, 30.000 OR 60.000 GM.-CM^2/SEC
MAXIMUM GIMBAL DISPLACEMENT	±0.6 DEG
INPUT RATE RANGE (FULL SCALE)	5 TO 1.000 DEG/SEC
GYRO OUTPUT (FULL SCALE)	±10 VOLTS
TEMPERATURE SENSITIVITY	< 0.02%/°K
LINEARITY	0.5% FULL SCALE TO ½ SCALE 2% FULL SCALE FROM ½ TO FULL SCALE
RESOLUTION	< 0.01 DEG/SEC
HYSTERESIS	< 0.01% FULL SCALE
LINEAR ACCELERATION SENSITIVITY	< 0.03 DEG/SEC/G

TABLE 5-9

REPRESENTATIVE STRAPDOWN RATE GYROS

MANUFACTURER	MAX INPUT RATE	LONG TERM STABILITY	SIZE (IN.)	WEIGHT (LB)	POWER (WATTS)	LIFE—REL	COST RECURRING	REMARKS
HAMILTON STANDARD (1139 S GYROS)	100°/SEC	±0.2°/HR	8 x 11 x 8	23.6	25 MAX	2.1 x 10⁶/HR	250K	DIGITAL PULSE REBALANCE VIKING LANDER
KEARFOTT ARU	1°/SEC	±0.3°/HR/3 YR	11 x 7 x 3	8.0	40 MAX 18 STEADY	17 x 10⁶/HR	100K	CLASSIFIED APPLICATION ANALOG REBALANCE
DRIRU (3 2 AXIS PKGS)	8°/SEC	±0.3°/HR/3 YR	36 x 7 x 7 / 3 x 7 x 16	20.0	2 3W/PLG/SEC 21 STEADY	33 x 10⁶/HR	262K	ANALOG VIII VIF P&SA S1D JPL IUS ATT'L REDUNDANT GYROS
BENDIX 2 AXIS RGA	35°/SEC	±0.003°/HR	6 x 8 x 8	29.4	20	.886/1 YR	350K	HEAD PULSE REBAL
IRA 8 SKEWED GYRO	600 SEC/SEC	0.5 SEC/SEC	10 x 8 x 3 / 10 x 7 x 8	33.4	60	908/6 YEARS	1000K	PULSE REBALANCE IUE GODDARD
NORTHROP 2 AXIS GRA (CICSS)	200°/SEC	0.05°/HR	6.6 x 5.6 x 3.6	4.3 FOR 2 AXIS	10	33 x 10⁶/HR	25K FOR 2 AXIS	PHILCO FORD
NORTHROP 1 AXIS GRA	60°/SEC	0.15°/HR	5.0 DX	6.0	12	2.8 x 10⁶/HR	60K/AXIS	DIGITAL REBALANCE LOOP OSO AND CLASSIFIED PROGRAMS
HONEYWELL HAU	60°/SEC	0.15°/HR	9.8 x 11 x 7	21	30	.9664/2 YEAR	200K	BLOCK VD USES NORTHROP GIK7G

TABLE 5-10

PARAMETERS FOR REPRESENTATIVE STAR SENSORS
(Wertz, 1985, p. 187)

SENSOR	DETECTOR	CONFIGURATION	SENSITIVITY (VISUAL MAGNITUDE)	FOV (DEG)	CALIBRATED ACCURACY-1σ	REFER-ENCE
APPLIED PHYSICS LABORATORY STAR SENSOR FOR SAS 1, 2 AND 3	PHOTO-MULTIPLIER	N	BRIGHTER THAN +4	5 BY 10	±1 ARC-MIN	1
BBRC[5] CS-103 STAR SCANNER FOR OSO-8	PHOTO-MULTIPLIER	V	+3.5 TO -2.0	5 BY 10	±0.1 DEG	2, 3
BBRC[5] CS-201 STAR SCANNER	SOLID STATE (SILICON)	V	+1.4 TO -1.4	EACH SLIT 25.0 BY 0.41	±0.5 DEG	–
HONEYWELL SPARS STAR SENSOR	SOLID STATE (SILICON)	6-SLIT	BRIGHTER THAN +3.15	8.8 WIDE	±2 ARC SEC	4
HONEYWELL BLOCK 5D/DMSP STRAPDOWN STAR SCANNER	SOLID STATE (SILICON)	6-SLIT	BRIGHTER THAN +3.7	10.0 WIDE	±2 ARC SEC	–
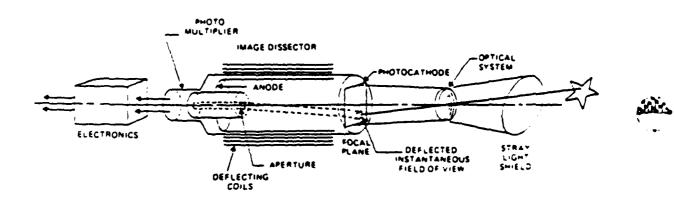
. Figure 5-67

Block Diagram of Typical Star Sensor
(Wertz. 1985. p. 189)

TABLE 5-11

REPRESENTATIVE STAR SENSORS

MANUFACTURER	ACCURACY	POWER (WATTS)	WEIGHT (LBS)	LIFE-REL	COST RECURRING	REMARKS
ITT GILF	20 SEC	12	14	N.D.	75 K	STRAPDOWN TRACKER ELMS
BBRC CS 200	1.0 MIN	0.5	3	.994/180 DAYS		SCANNER 3 8 BIT WORDS PER STAR CROSSING DEVELOPED FOR OSO
BBRC CT 401*	10 SEC	3.0	11	N.D.	120 K	STRAPDOWN TRACKER DEVELOPED FOR SAS C
TRW POLARIS	30 SEC	7.0	9.0	.94/YR	100 K	STRAPDOWN TRACKER ACQUISITION FOV: 25° CIRC TRACKING FOV: 34 MIN
TRW SRA	0.5°	0.5	2.5	.98/3 YRS	100 K	PIONEER SCANNER SOLID STATE
MARTIN MARIETTA AEROSPACE	1.0 SEC	30 PEAK 7 ON 2% DUTY CYCLE	25 INCLUDING ELEC-TRONICS	5 YRS, 90% CONFIDENCE	250 K INCLUD-ING DRIRU PKG	SPACE SEXTANT IS PLANNED FOR FLIGHT TEST IN 1979. DESIGNED FOR CISLUNAR MISSIONS

* NASA STANDARD

depicts the operation of a typical star sensor, and Tables 5-10 and 5-11 list typical accuracies and costs.

D. SUMMARY

The purpose of this chapter was to demonstrate the feasibility of the ORION attitude control subsystem. Specifically, spin stabilization was investigated within the constraints of a prolate body and limited propellant. Five broad design criteria were established at the outset, and particular attention was focussed on the performance and mass properties of the spacecraft. With regard to performance, ORION was constrained to function as a prolate (unstable) spinner, without boom deployment, for at least 90 days at Shuttle orbital altitudes. The spacecraft mass distribution must favorably impact performance and enhance the spacecraft stability. The mass distribution of spacecraft components was evaluated and moments of inertia and center of mass movement were quantified. The impact of boom deployment on stability was also assessed. Boom lengths of 80" were chosen to provide a stable inertia ratio of 1.18.

Nutation in a prolate spacecraft is a natural occurence, and much attention was devoted to an analysis of the causes and effects of this phenomenon. Specifically, the impact of fuel slosh on nutation divergence was discussed, noting that the large wetted area of the positive displacement ORION propellant tank would contribute to rapid growth of the nutation angle. Spacecraft nutation time constants were evaluated for various spin rates using the data of Vanyo (UC Santa Barbara) and Hubert and Goodzeit (RCA). Fuel slosh will contribute to rapid nutation damping in a stable

590

satellite, such as ORION with booms. However, the goal of this chapter was to prove the feasibility of spin stabilization if the booms failed or were deliberately not deployed. It was demonstrated that, within the limits of propellant reserve, ORION could be successfully spin stabilized about the longitudinal axis for more than 90 days without the use of booms. This would require approximately 61 lbm of propellant. While stabilization of a prolate ORION is possible, it is not desirable due to a short propellant-limited lifetime and frequent nutation control. Spin stabilization of an oblate ORION, with four 80" booms deployed, would be preferable and would be successful over the long term.

The discussion of sensors for ORION has shown that the goal of 1.0° for attitude accuracy is feasible. Several mechanisms, particularly sun and Earth sensors, rate gyros and magnetometers, are capable of this resolution. A finer resolution on the order of 0.1° is perhaps attainable with higher quality sun and Earth sensor suites, or almost any rate integrating gyro package. For the purpose of the mass property analysis conducted earlier in this chapter, an assumption was made that only sun and Earth sensors would be used. The conclusion that an attitude determination accuracy of 1.0° is feasible is confirmed by the success of previous satellites using sensor suites similar to those described herein. Wertz (1985, pp. 788-795) lists a number of satellite systems and their sensors. These satellites predominantly employ sun sensors and horizon scanners (Earth sensors). Most, if not all of the spin stabilized platforms exhibit accuracies on the order of 1.0°. Indeed, an accuracy of this order is feasible for ORION.

591

VI. SUMMARY AND CONCLUSIONS

The purpose of this thesis is to report on the author's work in the development of ORION, a low cost, general purpose lightweight spacecraft. Specifically, this thesis demonstrates the feasibility and preliminary design elements of three major spacecraft subsystems, namely structure, propulsion and attitude control. These subsystems are particularly critical in the successful implementation of a small, low cost spacecraft. The design of these subsystems has been based on five design criteria, being affordability, cost effectiveness, general purpose architecture, reliability and safety. Each subsystem has been structured around these and other more detailed design drivers. The subsystem descriptions are augmented by a historical perspective referencing the development of similar subsystems in earlier small satellites. The descriptions of each subsystem point out that the concept of a general purpose small satellite is feasible as implemented in the ORION design. ORION is a logical next step in the development of lightweight spacecraft, providing a vehicle for numerous small civilian and DoD payloads at orbital altitudes of up to 800 nm.

The ORION design criteria were described in detail in Chapter Two. Research of 375 NASA and DoD small payload requests revealed an average payload mass and volume within the capability of a small spacecraft. Average power needs, attitude accuracies, orbit requirements and data rates were likewise within the capability of a small host satellite. Based on these requests and a survey of recent DoD payload proposals, design targets for

payload mass, volume, data rate, attitude control accuracy, power and orbit requirements were drafted. Specifically, payload mass and volume goals of 32 lbm and 2.0 ft^3 were set to support "average" payload needs. Design efforts were constrained to develop a low cost, general purpose host spacecraft capable of meeting these target criteria. Following an evaluation of available launch vehicles, the Space Shuttle was chosen to transport ORION to low earth orbit and the Get Away Special canister was chosen to restrain and deploy the spacecraft. Mass and volume budgets for the spacecraft subsystems were established based on the provision of 250 lbm total GAS payload mass and 5.7 ft^3 volume, in a cylindrical structure. The choice of a GAS canister to deploy ORION from Shuttle was consistent with target design criteria in support of the "average" payload. A cost goal of $1.5 million was established for the fabrication of the first spacecraft. Analysis of forecast acquisitions and material costs demonstrated that the spacecraft could be constructed within the target budget constraints. In comparison with other spacecraft of similar capabilities, ORION is at least an order of magnitude less expensive. Thus, the design constraint of affordability was met and the satellite is qualitatively termed "low cost".

The design of the structure subsystem reflected NASA requirements to meet GAS volume, mass, launch load and vibration specifications. The design of the structure was also directed by payload, thermal, propulsion and attitude control considerations. The structures of many small satellites were reviewed for design options, and a cylindrical framework of "longerons" and circular "decks" was chosen. An external skin of 0.05" thick aluminum was chosen to provide micrometeoroid protection, availing a 90% reliability of

withstanding a "probable" micrometeoroid impact for at least 120 days. A mass budget was determined based on the provision of approximately 40 lbm mass for structural components. The majority of the structural mass was devoted to a structural baseplate, four longerons and the protective external skin. Component placement within the structure was estimated based on this first order structural design. A design for boom housings (longerons) was described, providing storage for four 80" stabilizing booms and their magnetometer tip masses. A full-size mockup of the vehicle was constructed to validate the structural design and aid in the determination of component placement. Finally, the structural dynamics of the satellite were analyzed. Specifically, the deflection of the cylindrical structure under launch and landing G loads was predicted to be much less than the maximum deflection allowed by NASA. The resonant frequencies of the vehicle were predicted to be well above the NASA minimum of 35 Hz. The conclusion of the structural design effort was that a sturdy structure can be implemented within the design goal of 40 lbm mass, optimizing use of the volume in the GAS canister and providing convenient spacious access to the satellite payload and spacecraft subassemblies.

Propulsion is essential for a general purpose spacecraft. Previous low cost spacecraft such as NUSAT and GLOMR did not provide a propulsion capability and their application to many small payloads was thus diminished. A low cost, high thrust, simple propulsion subsystem design was sought for ORION. Numerous propulsion options were investigated in detail because it is the provision of propulsive capability that sets ORION apart from other non-propelled lightweight spacecraft. Considerable emphasis was placed on

594

the choice of a subsystem design that will readily interface with the attitude control subsystem, providing commonality, enhanced reliability and lower total spacecraft cost. A hydrazine-based subsystem was chosen and a vendor survey was conducted to identify specific subsystem components. Seven Rocket Research Co. hydrazine thrusters, a TRW Co. positive displacement hydrazine tank and two ARDE Co. nitrogen pressurant tanks were chosen for the mockup design. A nitrogen-pressurized blowdown propellant feed network was chosen to supply hydrazine to the thrusters. The performance of the propulsion subsystem was analyzed based upon these component and feed subsystem choices. Specifically, thrust was predicted as a function of blowdown pressure, and the total impulse was calculated. It was demonstrated that an attitude control impulse of 1200 lbf-secs and an orbital transfer Delta-V of 2108 ft/sec can be provided within the mass and volume design constraints of this subsystem. These impulse and Delta-V capabilities will enable ORION to transit to 800 nm orbital altitude from a nominal Shuttle deployment altitude of 135 nm as well as conduct a reasonable number of attitude control manuevers for one year. The design of this subsystem was deliberately constrained to be simple and non-redundant, consistent with the goal of developing a low cost, lightweight spacecraft.

The feasibility of the ORION concept is also closely tied to the provision of an attitude control capability. Many of the small payloads surveyed in Chapter Two require attitude control accuracies on the order of 1°, yet previous small satellites have lacked attitude control due to the mass and volume constraints of those small spacecraft. Various methods of attitude

control were evaluated; spin stabilization was chosen for ease of implementation and efficient propellant utilization. Spin stabilization, with the deployment of stabilizing booms, is extremely efficient, enhances the thermal characteristics of the spacecraft, and is capable of attitude accuracies on the order of 1° (the design goal). Based on the mass and structural layout of Chapter Two, a first order approximation of mass distribution and moments of inertia was conducted. This analysis confirmed that ORION is extremely prolate when spun about the longitudinal axis without booms. As an unstable, prolate spinner, ORION exhibits an inertia ratio of approximately 0.320; the nutation angle is subject to a rapid growth due to the destabilizing effect of sloshing propellant in the hydrazine tank. However, the mission duration design goal of 90 days was shown to be attainable even if the booms do not deploy and active nutation control is required to inhibit nutation angle growth. Attitude control subsystem performance was specified as a function of spin rate, initial nutation angle and final nutation angle to permit users to calculate worst case attitude control performance without the benefit of stabilizing booms. If four 80" booms are deployed with 2.0 lbm magnetometer tip masses, a stable inertia ratio of 1.18 results, and the fuel slosh enhances stability by reducing the nutation angle. For a stable spinner, propellant will only be required to change spin rate or pointing direction, and the satellite will be long lived. Various sensor options which could provide 1° of pointing accuracy were evaluated. The performance predictions and subsequent sensor evaluations indicated that an attitude control accuracy on the order of 1° was indeed reasonable and, even with the failure of the stabilizing booms, can be maintained for at least

90 days. Thus, the feasibility of spin stabilized attitude control for ORION was confirmed.

The design of ORION was initiated during a period of transition for the United States space program. Prior to the Space Shuttle Challenger accident in early 1986, there was little commercial or government support for small satellite development. However, with the loss of many of the United States' space launch capabilities and grounding of expensive one-of-a-kind spacecraft, attention was rapidly focussed on low cost, proliferable lightweight satellites. The ORION satellite emerged in response to the need for such spacecraft. Numerous parallel proposals arose for small satellites of the ORION volume and mass category, yet these spacecraft lacked propulsion and attitude control subsystems, and thus could not fill the needs of many potential space users. Those same subsystems were evaluated at length for a cylindrical spin stabilized spacecraft like ORION, and affordable effective designs were proposed. Performance predictions indicated that those subsystems could be implemented successfully within the ORION design constraints. Thus, the design efforts reported on in this thesis confirm that a fully capable low cost, general purpose spacecraft is feasible.

LIST OF REFERENCES

Abramson, H. N., "Liquid Sloshing in Spherical Tanks", AIAA Journal, vol. 1, n. 2, February 1963.

Adams, N. J. and Melton, R. G., Orbital Transfer Error Analysis for Multiple Finite Perigee Burn, Ascent Trajectories, presented to the American Astronautical Society Astrodynamics Specialist Conference, Vail, Colorado, 12-15 August 1985.

Aerojet TechSystems Co. Letter, LOWTHRUS.918, to Austin Boyd, Subject: Attitude Control Thrusters, 18 September 1986.

Aerospace Corporation, Conceptual Design Study for the Space Test Program Standard Satellite (STPSS), 30 May 1975.

Aerospace Corporation, Experiment Planning Directorate, Conceptual Design Study for the Space Test Program Standard Satellite, 30 May 1975.

Aerospace Corporation, Report No. TOR-0083(9975)-1 Vol. 1, Vehicle Engineering State of the Art - Volume I: Design Technology, 19 August 1983.

Aerospace Corporation, Report No. TOR-0083(9975)-1 Vol. 2, Vehicle Engineering State of the Art - Volume II: Satellite Thermal Control Technology, 19 August 1983.

Aerospace Corporation, Report No. TOR-0083(9975)-1 Vol. 3, Vehicle Engineering State of the Art - Volume III: Design Analysis Technology, 19 August 1983.

Aerospace Corporation, Report No. TOR-0083(9975)-1 Vol. 4, Vehicle Engineering State of the Art - Vol. IV: Structural Dynamics Technology, 19 August 1983.

Aerospace Corporation, Report No. TOR-0083(9975)-1 Vol. 5, Vehicle Engineering State of the Art - Volume V: Structural Technology, 19 August 1983.

Aerospace Corporation, Report No. TOR-0083(9975)-1 Vol. 6, <u>Vehicle Engineering State of the Art - Volume VI: Ground System and Test Technology</u>, 19 August 1983.

Aerospace Corporation, Report No. TOR-0083(9975)-1 Vol. 7, <u>Vehicle Engineering State of the Art - Volume VII: Fluid Mechanics Technology</u>, 19 August 1983.

Aerospace Corporation, Report No. TOR-0083(9975)-1 Vol. 8, <u>Vehicle Engineering State of the Art - Volume VIII: Rocket Propulsion Technology</u>, 19 August 1983.

Agrawal, B. N., <u>Stability of Spinning Spacecraft with Liquid Filled Tanks</u>, AIAA Paper 81-0172, presented to AIAA 19th Aerospace Sciences Meeting, St. Louis, Missouri., 12-15 January 1981.

Agrawal, B. N., <u>Design of Geosynchronous Spacecraft</u>, Prentice-Hall, Inc., 1986.

Agrawal, B. N. and James, P., "Energy Dissipation Due to Liquid Sloshing in a Spinning Spacecraft", <u>Proceedings of the 3rd Symposium on Dynamics and Control of Large Flexible Spacecraft</u>, Blacksburg, Virginia, pp. 439-452, 15-17 June 1981.

Agrawal, B. N., ed., <u>Proceedings of the First INTELSAT/ESA Symposium on the Dynamic Effects of Liquids on Spacecraft Control</u>, Washington, DC, 25-26 April 1984.

AIAA News Service report on LIGHTSAT Lightweight Satellite in Monterey California, no date.

Air Force Rocket Propulsion Laboratory Technical Report AFRPL-TR-64-138, <u>Location and Control of Center of Gravity of Spacecraft</u>, October 1964.

Air Force Rocket Propulsion Laboratory Technical Report AFRPL-TR-66-181, <u>A Summary on the Development of Analytical Techniques for Bellows and Diaphragm Design</u>, by L. E. Hulbert, R. E. Keith, and T. M. Trainer, August 1966.

Air Force Rocket Propulsion Laboratory Technical Report AFRPL-TR-71-41, Propellant/Material Compatibility Study, by E. M. Vander Wall and others, December 1971.

Air Force Rocket Propulsion Laboratory Technical Report AFRPL-TR-71-103, Long Life Monopropellant Hydrazine Engine Development Program, by B. W. Schmitz and W. W. Wilson, September 1971.

Air Force Rocket Propulsion Laboratory Technical Report AFRPL-TR-72-43, Monopropellant Hydrazine Engine Evaluation with Shell 405 and Shell X-4 Catalysts, by F. N. Fredrickson, November 1972.

Air Force Rocket Propulsion Laboratory Technical Report AFRPL-TR-75-46, Hydrazine Compatibility Design and Handling Criteria, by E. A. Burns, R. A. Carlson, R. G. Gilroy, and R. N. Porter, December 1975.

Air Force Rocket Propulsion Laboratory Technical Report AFRPL-TR-75-69, Hydrazine Engine Cold Start Evaluation, by J. A. Quirk, February 1976.

Air Force Rocket Propulsion Laboratory Technical Report AFRPL-TR-82-036, Advanced Spacecraft Propulsion Design, Vol. I, by A. J. Scobin and W. R. Bissell, January 1983.

Air Force Rocket Propulsion Laboratory Technical Report AFRPL-TR-82-049, Advanced Spacecraft Propulsion Design, by C. T. O'Brien, and A. W. McPeak, April 1983.

Air Force Rocket Propulsion Laboratory Technical Report AFRPL-TR-84-089, High Temperature Augemented Hydrazine Thruster, by D. L. Emmons and L. E. Saltz, April 1985.

Air Force Space Systems Division Technical Documentary Report, SSD-TDR-62-172, Development of Exculsion and Orientation Systems for Advanced Liquid Rocket Propulsion Systems, December 1962.

Air Force Systems Command Design Handbook, DH 3-2, Revision 1-5 reprint, Space and Missile Systems Series: Space Vehicles, 10 April 1980.

Air Force Systems Command Design Handbook, DH 3-3, Revision 1-5 reprint, Space and Missile Systems Series: Ground Equipment and Facilities, 12 July 1984.

Air Force Systems Command Design Handbook, DH 3-6, Volume I, Revisions A-D, Space and Missile Systems Series: Fluid Components, 10 May 1985.

Air Force Systems Command Design Handbook, DH 3-6, Volume II, Revisions A-D, Space and Missile Systems Series: Fluid Components, 10 May 1985.

Anderson, P. N., Design Considerations for the Explorer VI Payload Structure, presented to the American Rocket Society Conference on Structural Design of Space Vehicles, Santa Barbara, California, 6-8 April 1960.

ARDE Corporation, Background on Cryogenically Formed Propellant Tankage Using Ring Stabilized Diaphragm Design, catalogue publication, Mahwah, New Jersey, 1986.

Aston, G., and others, A Xenon Ion Propulsion Module for Enhanced Spacecraft Capability, paper presented to the AIAA/ASME/SAE/ASEE 22nd Joint Propulsion Conference, Huntsville, Alabama, 16-18 June 1986.

Ball Aerospace Co., Extended Get-Away-Special (GAS) Canister Critical Design Review, Colorado Springs, Colorado, 28-29 May 1986.

Bangsund, E. L. and Caluori, V. A., Vehicle Design for Low Cost Operations, presented to 37th Congress of the International Astronautic Federation, Innsbruck Austria, 4-11 October 1986.
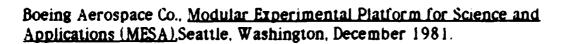
Barrere, M., Jaumotte, A., Fraeijs, B., and Vandenkerckhove, J., Rocket Propulsion, Van Nostrand Company Inc., 1960.

Bate, R. R., Mueller, D. D., and White, J. E., Fundamentals of Astrodynamics, Dover Publications, 1971.

Baumeister, T. and Marks, L. S., ed., Standard Handbook for Mechanical Engineers, 7th Ed., McGraw-Hill, 1967.

Beyer, W. H., ed., CRC Standard Mathematical Tables, 27th Ed., CRC Press, 1984.

Boeing Aerospace Co., Modular Experimental Platform for Science and Applications (MESA),Seattle, Washington, December 1981.

Boeing Aircraft Co. Document D2687-10656-1, Large Diameter Shuttle Launched-AEM (LDSL-AEM) Study, Contract No. NAS 5-23537, 28 April 1976.

Boyd, A. W., The Perturbation of Orbits : A Tutorial on Orbit Disturbing Effects and Basic Perturbation Theory, Department of Mathematics, Naval Postgraduate School, Monterey, California, December 1985.

Boyd, A. W., "LIGHTSAT Power Systems", Aerospace America, April 1988.

Boyd, A. W. and Petersen, S. E., A Design for a General Purpose Low Earth Orbit Satellite, Final Report for Naval Postgraduate School Space System Engineering design course AE 4792, Naval Postgraduate School, Monterey, California, March 1986.

Boyd, A. W. and Fuhs, A. E., A Design for Small, General Purpose, Low Earth Orbit Satellites, presented to 37th Congress of the International Astronautic Federation, Innsbruck Austria, 4-11 October 1986.

Boyd, A. W. and Fuhs, A. E., General Purpose Satellites: A Concept for Affordable Low Earth Orbit Vehicles, presented to AIAA Aerospace Sciences Meeting, Reno, Nevada, 12-16 January 1987.

Boyd, A. W., Kosinski, B. P. and Weston, R., "Autonomous Measurement of Space Shuttle Payload Bay Acoustics During Launch", Naval Research Reviews, Volume 39, pp. 9-17, November 1987.

Bracewell, R. N. and Garriott, O. K., "Rotation of Artificial Earth Satellites", Nature, vol. 182, pp. 760-762, 20 September 1958.

Brown, M. P., ed., Compendium of Communication and Broadcast Satellites 1958 to 1980, IEEE Press, 1981.

Cary, P. and Mosher L., Naval Research Laboratory, personal communication, 11 Sep 1986.

Chemical Propulsion Information Agency, Liquid Propulsion Design and Data Handbooks: An Annotated Bibliography, CPIA publication 143, April, 1967.

Chemical Propulsion Information Agency, Monopropellant Hydrazine Technology: An Annotated Bibliography, CPIA Publication 267, August 1975.

Chemical Propulsion Information Agency, JANNAF Compilation of Propulsion Technology Programs FY 1986, CPIA Publication 441,1986.

Cochrane, C. D., Gorman, D. M. and Dumoulin, J. D., ed., Space Handbook, AU-18, Air University Press, January 1985.

Collicott, H. E. and Bauer, P. E., ed., Spacecraft Thermal Control, Design and Operation, AIAA Progress in Aeronautics and Astronautics Volume 86, 1983.

Colladay, R. S. and Sadin, S. A, Technologies for Affordable Access to Space, presented to 37th Congress of the International Astronautic Federation, Innsbruck Austria, 4-11 October 1986.

Cooper, D. L. and others, A Proposal for a Satellite Communications System, US Naval Postgraduate School, 1965.

Corliss, W. R., Space Probes and Planetary Exploration, Van Nostrand Co., 1965.

Cruddace, R. G. and Fritz, G. G., Space Research and Spartan, paper presented to the AIAA 23rd Aerospace Sciences Meeting, Reno, Nevada, 14-17 January, 1985.

Cruddace, R. G., Fritz, G. G., and Shulman, S., "SPEAR: Small Payload Ejection and Recovery for the Space Shuttle", Astronautics and Aeronautics, p. 42, January 1977.

DeMeis, R., "Space Debris", Aerospace America, February 1987, pp. 8-11.

Dodge, F., Progress Letters 1 and 2 for Contract N00014-85-C-2417 of SWRI Project 06-8790, to Mr. Samuel Hollander, Naval Research Laboratory, Subject: Support for Shuttle Launch Dispenser, 15 January 1985.

Dodge, F. T., Proceedings of the Second Symposium on Fluid Transients in Fluid Structure Interaction, pp. 11-17, 17-22 November 1985.

Dumas, L. N., "Temperature Control of the Mariner V Spacecraft", Aviation and Space: Progress and Prospects: Proceedings of the ASME Annual Aviation and Space Conference, Beverly Hills, California, pp. 573-579, 16-19 June 1968.

Ellis, J., "Entrepreneurs in Space", Air and Space, vol. 1, n. 5, December 1986, pp. 98-102.

Fermelia, L. R., The Design and Development of GOES, unpublished paper, 1981.

Fisher, R. and McCabe, J., "Effects of Thermal Interface on Engine Thermal Characteristics", Proceedings 1972 JANNAF Propulsion Meeting: Monopropellant Hydrazine Propusion System Sessions, Chemical Propulsion Information Agency Publication 228, vol. 4, pp. 121-132, December 1972.

Fishlock, D., A Guide to Earth Satellites, American Elsevier Publishing, 1972.

Freeman, H. R. and Longanecker, G. W., The International Ultraviolet Explorer (IUE) Case Study in Spacecraft Design, AIAA Professional Study Series, AIAA, August 1979.

French, J. R. and Griffin, M. D., Spacecraft Systems Design and Engineering, private tutorial notes, 1984.

Fthenakis, E., Manual of Satellite Communications, McGraw-Hill, 1984.

Fuhs, A. E., course notes for Spacecraft Systems Design course AE 4792, Naval Postgraduate School, Monterey, California, 1986.

Gagliardi, Satellite Communications, Van Nostrand and Rheinholdt, 1984

Gale, A. J., Trilling, L., McKay, W. and Finston, M., Orbital and Satellite Vehicles, Vol. 2, Massachusetts Institute of Technology, 1956.

Garg, S. C., Furomoto, N., and Vanyo, J.P., "Spacecraft Nutational Instability Prediction by Energy Dissipation Measurements", Journal of Guidance, Dynamics and Control, vol. 9, n. 3, pp. 357-362; May-June 1986.

Garg, S. C., Furomoto, N., and Vanyo, J.P., Measurement of Energy Dissipation in Forced Precession Compared to Flight Data, AIAA Paper 84-1841, 1984.

Garrison, P. W., Advanced Propulsion Activities in the USA, presented to 37th Congress of the International Astronautic Association, Innsbruck Austria, 4-11 Ocotber 1986.

Garrison, P. W., and Stocky, J. F., Future Spacecraft Propulsion, presented to AIAA Space Systems Technology Conference, San Diego, California, 8-12 June 1986.

Gee, A. C., "OSCAR: Amateur Radio Satellites and Spacecraft", AMSAT.

Gemmel, R. A., Criteria for Meteroid Protection, presented to American Rocket Society Conference on Structural Design of Space Vehicles, Santa Barbara, California, 6-8 April 1960.

General Electric Company Letter to LT Austin Boyd, Subject: NiCd Battery Cells GE Quotation Q8635, 14 August 1986.

George, D., Advanced Space Propulsion Concepts, presented to 37th Congress of the International Astronautic Federation, Innsbruck Austria, 4-11 October 1986.

Get-Away-Special Payloads Safety Manual, NASA GSFC, November 1983.
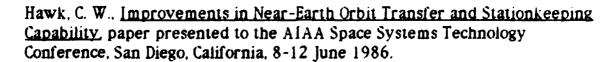
Get-Away-Special (GAS) Small Self-Contained Payloads Experimenter Handbook, NASA GSFC, July 1984.

Goldman, N.C., Space Commerce, Ballinger Publishing Co., 1985.

Goodger, E. M., Principles of Spaceflight Propulsion, Pergammon Press, 1970.

Gray, C. S., American Military Space Policy, Abt Books, 1982.

Hawk, C. W., Improvements in Near-Earth Orbit Transfer and Stationkeeping Capability, paper presented to the AIAA Space Systems Technology Conference, San Diego, California, 8-12 June 1986.

Hayashi, T. and others, Feasibility Study on the Ultra-Small Launch Vehicle, presentedto 37th Congress of the International Astronautic Federation, Innsbruck Austria, 4-11 October 1986.

Hill, P. G. and Peterson, C. R., Mechanics and Thermodynamics of Propulsion, Addison-Wesley Co., 1965.

Holloway, P. F. and Zersen, W. F., Future Space Transportation Options -- Overview, presented to AIAA Space Systems Technology Conference, San Diego, California, 8-12 June 1986.

Hord, M. J., CRC Handbook of Space Technology, CRC Press, 1985.

Hough, W. W. and Elrod, B. D., "Solar Array Performance as a Function of Orbital Parameters and Spacecraft Attitude", Aviation and Space: Progress and Prospects: Proceedings of the ASME Annual Aviation and Space Conference, Beverly Hills, California, pp. 123-131,16-19 June 1968.

Huang, H., "The Research of Liquid Sloshing under Low Gravity Environments", Journal of the Chinese Society of Astronautics, vol. 1, pp. 71-84, 1980.

Hubert, C. and Goodzeit, N., "The Effects of Propellant Motion on a Spinning Satellite with Vaned Tanks", AIAA Paper 83-2262, Proceedings of the AIAA 1983 Guidance and Control Conference, Gatlinburg, Tennessee., pp. 669-674, 17 August 1983.

Hughes, P. C., Spacecraft Attitude Dynamics, John Wiley and Sons, 1986.

Jet Propulsion Laboratory Interoffice Memorandum 312/84.3-2656, A New Propulsion Strategy for Round Trip Missions, by C. L. Yen. 18 September 1984.

Jet Propulsion Laboratory Technical Report 32-348, Performance Calculations for Monopropellant Hydrazine and Monopropellant Hydrazine-Hydrazine Nitrate Mixtures, by D. H. Lee, 3 December 1962.

Jet Propulsion Laboratory Technical Report 32-735, On the Evolution of Advanced Propulsion Systems for Spacecraft, by D. F. Dipprey, J. H. Rupe, R. N. Porter, and D. D. Evans, 15 July 1965.

Jet Propulsion Laboratory Technical Report 32-862, Some Design Considerations, Large Expulsion Bladders for Nitrogen Tetroxide and Hydrazine, by A. J. Bauman, 15 January 1966.

Jet Propulsion Laboratory Technical Report 32-899, Propellant Expulsion in Unmanned Spacecraft, by R. N. Porter and H. B. Stanford, 1 July 1966.

Jet Propulsion Laboratory Technical Report 32-953, Mariner Mars 1964 Basic Structure, Design and Development, by J. D. Schmuecker and R. J. Spehalski, 1 May 1967.

Jet Propulsion Laboratory Technical Report 32-955, Mariner Mars 1964 Temperature Control Hardware Design and Development, by W. Carroll, G. G. Coyle, and H. von Delden, 1 June 1967.

Jet Propulsion Laboratory Technical Report 32-957, Mariner Mars 1964 Temperature Control Subsystem, by D. W. Lewis, D. C. Miller and L. N. Dumas, 15 September 1967.

Jet Propulsion Laboratory Technical Report 32-960, Systems Engineering Considerations in Spacecaft Design, by A. G. Conrad, 15 June 1966.
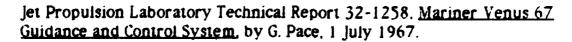
Jet Propulsion Laboratory Technical Report 32-1029, A Sensitive S-Band Noise Receiver Developed for the Mariner Mars 1964 Spacecraft Program, by L. H. Keeler, A. J. Nalbandian, and A. A. Olbeter, 15 November 1966.

Jet Propulsion Laboratory Technical Report 32-1039, Storage Tests of Nitrogen Tetroxide and Hydrazine in Aluminum Containers, by L. P. Hollywood, T. R. Metz, and R. N. Porter, 15 January 1967.

Jet Propulsion Laboratory Technical Report 32-1227, The Status of Monopropellant Hydrazine Technology, by T. W. Price and D. D. Evans, 15 February 1968.

Jet Propulsion Laboratory Technical Report 32-1258, Mariner Venus 67 Guidance and Control System, by G. Pace, 1 July 1967.

Jet Propulsion Laboratory Technical Report 32-1353, A Method for Calculating Steady-State Thrust and Flow-Rate Levels for Mariner IV Type Attitude Control Nitrogen Gas Jets, by J. D. Ferrera and P. M. McKown, 1 December 1968.

Jet Propulsion Laboratory Technical Report 32-1461, Attitude Control and Structural Response Interaction, by J. Abel, 15 November 1970.

Jet Propulsion Laboratory Technical Report 32-1505, Satellite Auxiliary Propulsion Selection Techniques, by L. B. Holcomb, 1 November 1970.

Jet Propulsion Laboratory Technical Report 32-1505, Appendum, Satellite Auxiliary Propulsion Selection Techniques: Survey of Auxiliary Electric Propulsion Systems, by L. B. Holcomb, 15 July 1971.

Jet Propulsion Laboratory Technical Report 32-1505, Supplement 1, Satellite Auxiliary-Propulsion Selection Techniques: Apllications of Selection Techniques to the ATS-H Satellite, by L. B. Holcomb, 1 October 1972.

Jet Propulsion Laboratory Technical Report 32-1560, Attitude Propulsion Technology for TOPS, by P. J. Moynihan, 1 November 1972.

Jones, R. M., Railgun Launched Planetary Science, Jet Propulsion Laboratory Interoffice Memorandum 312/85.3-3085, 8 July 1985.

Kachele, ___, and Olshaker, ___, "Micrometeoroid Distribution", excerpted from Space Systems Engineering and Design Notes, by Dr. Allen E. Fuhs, 28 October 1985.

Kane, T.R., Spacecraft Dynamics, McGraw-Hill, 1983.

Kaplan, M. H., Modern Spacecraft Dynamics and Control, John Wiley and Sons, 1976.

Kaplan, M. H. and Beck, N. M. Jr.,"Attitude Dynamics and Control of an Apogee Motor Assembly with Paired Satellites", Journal of Spacecraft and Rockets, vol. 9, n. 6, pp. 410-415, June 1972.

Keyes, G. W., Low Cost Spacecraft - A Private Sector Approach, AAS Paper 82-232, 1982.

Kit, B. E. and Evered, D. S., Rocket Propellant Handbook, MacMillan Co. , 1960.

Koelle, H. H., ed., Handbook of Astronautical Engineering, McGraw Hill, 1961.

Kreith, F., Radiation Heat Transfer and Thermal Control of Spacecraft, Oklahoma State University Publication No. 112, April 1960.

Langton, N. H., ed., Rocket Propulsion, American Elsevier Co., 1970.

Larson, V. R. and Evans, S. A., Propulsion for the Space Station, presented to 37th Congress of the International Astronautic Federation, Innsbruck Austria, 4-11 October 1986.

Ledford, O. C. and Blakely, R. L., "Spacecraft Radiator Analysis", Aviation and Space: Progress and Prospects: Proceedings of the ASME Annual Aviation and Space Conference, Beverly Hills, California, pp. 77-85, 16-19 June 1968.

Leondes, C.T., ed., Guidance and Control of Aerospace Vehicles, McGraw-Hill Co., 1963.

Logan, J. T., "Market Demand for Small Satellites Spurs COmmercial Efforts at GLOBESAT", Commercial Space, pp. 61-63, Oct/Nov 1986.

LTV Aerospace Corporation, NASA/DOD Scout Program, notes from a presentation on SCOUT launch vehicle upgrades to the Strategic Defense Initiative Office, June 1986.

Lucas, W. R., "Engineering Fundamentals", Handbook of Astronautical Engineering, Ed. by H.H. Koelle, pp. 3-75, McGraw Hill Inc., 1961.

Lucas, W. R., "Environmental Effects on Materials", Handbook of Astronautical Engineering, Ed. by H. H. Koelle, pp. 365-376, McGraw Hill Inc., 1961.

Mantell, C., Batteries and Energy Systems, 2nd Ed., McGraw-Hill, 1983.

Marec, J. P., Optimal Space Trajectories, Elsevier Scientific Publishing Co., 1979.

Martin, E. R., Experimental Investigation on the Fuel Slosh of Dual-Spin Spacecraft", COMSAT Technical Review, vol. 1, n. 1, pp. 1-19, 1971.

Martin, H. L., Micrometeoroid Distribution Measured by Several Rockets and Satellites, ABMA Report DV-TN-4-60, Huntsville, Alabama, 1960.

Mavrogenis, J. D. and Brill, Y. C., "Orbit Adjust Propulsion Subsystem Aboard Atmosphere Explorer", Proceedings 1972 JANNAF Propulsion Meeting: Monopropellant Hydrazine Propusion System Sessions, Chemical Propulsion Information Agency Publication 228, vol. 4, pp. 1-7, December 1972.

McCartney, LTGEN F. S., What We Need... When We Need It: The Complimentary Expendable Launch Vehicle, presented to AIAA Space Systems Technology Conference, San Diego, California, 8-12 June 1986.

McCullough, F. Jr., "Engine Life Considerations", Proceedings 1972 JANNAF Propulsion Meeting: Monopropellant Hydrazine Propusion System Sessions, Chemical Propulsion Information Agency Publication 228, vol. 4, pp. 97-110, December 1972.

Meirovitch, L. and Nelson, H. D., "On the High-Spin Motion of a Satellite Containing Elastic Parts", Journal of Spacecraft and Rockets, pp. 1597-1602, November 1966.

McKinley, J. L. and Bent, R. D., Powerplants for Aerospace Vehicles, McGraw-Hill Co., 1965.

Milligan, T., Modern Antenna Design, McGraw-Hill, 1985.

Morton Thiokol letter ECO-4252, to Austin Boyd, Subject: Spin/Despin Motors, 6 March 1986.

Mosher, L., "Pressurant and Propellant Tanks", personal communication, 15 September 1986.

NASA Contract Publication NAS 5-9042, Gravity Gradient Stabilization System for the Advanced Technology Satellite, 1964.

NASA CP-2401, Proceedings 1985 Get-Away-Special Experimenters Symposium, by L. Thomas and F. Mosier, ed., 8-9 October 1985.

NASA CP-2438, Proceedings 1986 Get-Away-Special Experimenters Symposium, by L. Thomas and F. Mosier, ed., 7-8 October 1986.

NASA CR-903, Stabilization System Analysis and Performance of the GEOS-A Gravity Gradient Satellite (Explorer XXIX), by V.L. Pisacane, P. P. Pardoe, and B. J. Hook, 1967.

NASA Get-Away-Special (GAS) Small Self Contained Payload Experimenter Handbook, NASA Goddard Space Flight Center, July 1984.

NASA JSC-14021 Rev. D, Get-Away-Special Payload Integration Plan, October 1984.

NASA JSC-20616, Cargo Systems Manual: SPARTAN-203/Halley - (STS 51-L), 18 October 1985.

NASA KHB 1700.7A, Space Transportation System Payload Ground Safety Handbook, (also USAF SAMTO HB S-100), 30 November 1984.

NASA NHB 1700.7A, Safety Policy and Requirements: For Payloads Using the Space Transportation System (STS), 9 December 1980.

NASA SP-19, Chemical Rocket Propulsion, by D. L. Nored and E. W. Otto, December 1962.

NASA SP-66, Space Technology: Volume II, Spacecraft Mechanical Engineering, by J. L. Adams, 1965.

NASA SP-106, The Dynamic Behavior of Liquids in Moving Containers, ed. by H. N. Abramson, 1966.

NASA SP-125, Design of Liquid Rocket Propellant Rocket Engines, 2nd Ed., by D. K. Huzel and D. H. Huang, 1971.

NASA SP-133, Scientific Satellites, by W. R. Corliss, 1967.

NASA SP-8009, Propellant Slosh Loads, August 1968.

NASA Technical Memorandum 83105, Historical Data and Analysis for the First Five Years of KSC STS Payload Processing, by J. R. Ragusa, September 1986.

NASA TN D-1175, The Structure of the Explorer X Magnetometer Space Probe, by E.D. Angulo and R. K. Browning, April 1962.

NASA TN-D-2143, Attitude Determination for TIROS Satellites, by J. W. Siry, June 1964.

NASA TN D-2468, The Micrometeroid Satellite Explorer XIII: Collected Papers on the Design and Performance, by C.T. D'Aiutolo, November 1964.

NASA TN D-4284, The Explorer XXIII Micrometeroid Satellite, by R. L. O'Neal, June 1968.

NASA TN-D-4945, Minimum Thrust for Correcting Keplerian Orbits with Application to Interplanetary Guidance, by F. W. Boltz, December 1968.

NASA TN D-8135, ATS-6 Spacecraft: In-Flight Antenna Pattern Measurement, by L. W. Nicholson and others, January 1976.

NASA TN D-8346, Air-Bearing Spin Facility for Measuring Energy Dissipation, by R. L. Peterson, October 1976.

NASA TR R-131, Final Report on the TIROS Meteorological Satellite System, 1962.

NASA TT-F-586, Calculation of the Motion of a Low Thrust Spacecraft, NASA Technical Translation of Russian paper "Raschet Dvizheniya Kosmicheskogo Apparata s Maloy Tyagoy" by V. N. Lebedev, 1968.

NASA TT F-794, Principles of Technical Planning for Satellite Communication Systems, by A.D. Fortushenko and others, August 1974.

NASA X-732-83-8, Get-Away-Special (GAS) Thermal Design Summary, by D. Butler, July 1983.

Naval Research Laboratory Report 7408, <u>The SOLRAD 10 Satellite, Explorer 44, 1971-058A</u>, by D. N. Horan and R. W. Kreplin, 12 July 1972.

Naval Research Laboratory Report 8932, <u>Energy Dissipation of Liquids in Nutating Spherical Tanks Measured by a Forced Motion Spin Table</u>, by M. F. Zedd and F. T. Dodge, 30 October 1985.

Naval Space Systems Activity, <u>U.S. Space Launch Systems</u>, 2nd Ed., Report Number NSSA-R-20-72-2, 1 July 1977.

Nellesen, W., "The EURECA Design Concept", <u>ESA Bulletin</u>, n. 45, pp. 7-14, 1986.

NOAA Technical Memorandum NESS 35, <u>Modified Version of the Improved TIROS Operational Satellite (ITOS D-G)</u>, by A. Schwalb, April 1972.

Nock, K. T. and others, <u>Lunar Get-Away-Special (GAS) Spacecraft</u>, AIAA Paper 87-1051, presented to 19th AIAA/DGLR/JSASS International Electric Propulsion Conference, Colorado Springs, Colorado, 11-13 May 1987.

Northrup, R. W., <u>Structural Design of the TIROS Meteorological Satellite</u>, presented to the American Rocket Society Conference on Structural Design of Space Vehicles, Santa Barbara, California, 6-8 April 1960.

OAO Corporation, <u>Thermal Design Guide for Get Away Special/ Motorized Door Assembly Users</u>, OAO Corporation Report to NASA GSFC, by C. D. Butler, January 1985.

Olney, D. J. and Cruddace, R. G., "Free-Flying Shuttle Payloads, an Extrapolation of Sounding Rocketry into the Shuttle Era", AIAA Paper 79-0485, 1979.

O'Lone, R. G., "U.S. Planning New Emphasis on Lightweight Satellite Systems", <u>Aviation Week and Space Technology</u>, pp. 22-23, 10 August 1987.

Peters, R. L., <u>Design of Liquid, Solid and Hybrid Rockets</u>, Hayden Book Co., 1965.

<u>Pioneering the Space Frontier: An Exciting Vision of Our Next Fifty Years in Space</u>, Report of the President's National Commission on Space, Bantam Books, 1986.

Pocha, J. J., "Propellant Slosh and Spacecraft Stability", Space Communications and Broadcasting, vol. 3, pp. 233-240, September 1985.

Quirk, J. A., "Life Evaluation of Monopropellant Hydrazine Thrusters", Proceedings 1972 JANNAF Propulsion Meeting: Monopropellant Hydrazine Propusion System Sessions, Chemical Propulsion Information Agency Publication 228, vol. 4, pp. 133-170, December 1972.

Ragusa, J. R., Historical Data Retrieval Study Results for the First Five Years of KSC STS Payload Processing, presented to 37th Congress of the International Astronautic Federation, Innsbruck Austria, 4-11 October 1986.

Rathbone, R. P., Communicating Technical Information, 2nd Ed., Addison-Wesley Publishing Co., 1985.

Register, B. M., "Boosting Business into Space", High Technology, Oct. 1985, pp. 53-54.

Reiss, K. W. and O'Neill, J. C., "Tracking the GLOMR Satellite", Proceedings, 1986 Get-Away-Special Experimenters Symposium (NASA-CP-2438), Greenbelt, Maryland, pp. 1-8, October 1986.

Riley, F. E. and Sailor, J. D., Space Systems Engineering, McGraw-Hill, 1962.

Ring, E., Rocket Propellant and Pressurization Systems, Prentice-Hall, Inc., 1964.

Rocket Research Company Letter 64100JB-86-032 to Naval Postgraduate School, Subject: Hydrazine Propulsion Information, 28 August 1986.

Rockwell International Space Division Report SD 75-SA-0135, Final Report Contract F04701-75-C-0127, Space Test Prgram Standard Satellite Launch Optimization Study, by M. A. Cantor, 15 September 1975.

Sabroff, A. E., "Advanced Spacecraft Stabilization and Control Techniques", Journal of Spacecraft and Rockets, vol. 5, n. 12, pp. 1377-1392, December 1968.

Sandorf, P. E., Wrigley, W. and Strughold, H., Orbital and Satellite Vehicles - Volume I, Massachusetts Institute of Technology, 1956.

Sarychev, V. A. and Sazonov, V. V., "Spin Stabilized Satellites", The Journal of Astronautical Sciences, vol. 24, n. 4, pp. 291-310, October-December 1976.

Sercel, J. C., Solar Thermal Propulsion for Planetary Spacecraft, Jet Propulsion Laboratory memorandum, 1985.

Sercel, J. and Krauthamer, S., Multimegawatt Nuclear Electric Propulsion: First Order System Design and Performance Evaluation, presented to AIAA Space Systems Technology Conference, San Diego, California, 8-12 June 1986.

Shepherd, D. G., Aerospace Propulsion, American Elsevier Co., 1972.

Shivanand, B., Spacecraft Attitude Perturbation Torques due to Space Environmental Sources, AIAA Paper 85-329, presented to AAS/AIAA Astrodynamics Specialist Conference, Vail, Colorado, 12-15 August 1985.

Shute, N. "Homemade Satellites", Air and Space, vol.1, n. 5, December 1986, pp. 76-84.

Singer, S. F., ed., Torques and Attitude Sensing in Earth Satellites, Academic Press, 1964.

Slabinski, V. J., "INTELSAT IV In-orbit Liquid Slosh Tests and Problems in the Analysis of the Data", COMSAT Technical Review, vol. 8, n. 1, pp. 1-39, 1978.

Smith, W. W., "Hydrazine Status Report", Proceedings 1972 JANNAF Propulsion Meeting: Monopropellant Hydrazine Propulsion System Sessions, Chemical Propulsion Information Agency Publication 228, vol. 4, pp. 53-70, December 1972.

Space Planners Guide, U.S. Air Force Systems Command, 1 July 1965.

Space Vector Corporation, Development, Fabrication, Test and Delivery of Six Mini-RMS, Volume I- Technical, Technical Proposal in Response to Sandia Laboratories Document No. 71-2540, 29 June 1983.

Stutzman, W. L. and Thiele, G. A., Antenna Theory and Design, John Wiley and Sons, 1981.

Sutton, G. P. and Ross, D. M., Rocket Propulsion Elements, 4th Ed., John Wiley & Sons, 1976.

Talaga, P., "NUSAT 1 Attitude Determination", Proceedings 1986 Get-Away-Special Experimenters Symposium (NASA CP-2438), Greenbelt MD, pp. 187-191, October 1986.

The Handling and Storage of Liquid Propellants, Office of the Director of Defense Research and Engineering, March 1961.

The U.S. Civil Space Program - An AIAA Assessment (Executive Summary), AIAA Draft of 12 September 1986.

Thomson, W. T. and Reiter, G. S., "Attitude Drift of Space Vehicles", Journal of the Astronautical Sciences, pp. 29-34.

TRW Pressure Systems Inc. Letter, to Austin Boyd, Subject: Positive Expulsion Tank Designs, 29 August 1986.

Turabian, K. L., A Manual for Writers, 4th Ed., The University of Chicago Press, 1973.

U. S. Air Force Systems Command, Space Planners Guide, 1 July 1965.

U. S. Congress, Solar Power From Satellites, Hearings before the Subcommittee on Aerospace Technology and National Needs, 94th Session, 19-21 January 1976.

US Dept. Commerce PB-283 859, The TIROS-N/NOAA A-G Satellite Series, March 1978.

United Technologies Hamilton Standard Co., Letter to Naval Postgraduate School, Subject: Hydrazine Propulsion Systems for Satellite Applications, 27 August 1986.

Urash, R. G., SCOUT Planning Guide, LTV Aerospace and Defense Company, May, 1986.

Vanyo, J. P., "An Energy Assessment for Liquids in a Filled Precessing Spherical Cavity", _Journal of Applied Mechanics_, pp. 851-856. December 1973.

Vanyo, J. P., "Cavity Radius versus Energy Dissipation Rate in Liquid-Filled, Precessing, Spherical Cavities", _AIAA Journal_, vol. 11, n. 3, pp. 261-262, March 1973.

Vanyo, J. P. and Likins, P. W., "Measurement of Energy Dissipation in a Liquid Filled, Precessing, Spherical Cavity", _Transactions of the ASME_, pp. 674-681, September 1971.

Vanyo, J. P. and Likins, P. W., "Rigid Body Approximations to Turbulent Motion in a Liquid-Filled, Precessing, Spherical Cavity", _Transactions of the ASME_, pp. 18-24, March 1972.

Vanyo, J.P., Garg, S.C., and Furomoto, N., "Spacecraft Nutational Instability Prediction by Energy-Dissipation Measurements", _AIAA Journal of Guidance, Dynamics and Control_, vol. 9, n. 3, pp. 357-362; May-June, 1986.

Vogel, J. M., _The Pocket Rocket Reader_, Chemical Systems Division of United Technologies Co., 1985.

Vought Corporation, _SCOUT Users Manual_, 1 January 1980.
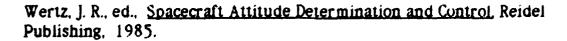
Wadleigh, K. H., Galloway, A. J. and Mathur, P. N., "Spinning Vehicle Nutation Damper", _Journal of Spacecraft and Rockets_, vol. 1, n. 6, pp. 588-591, November-December 1964.

Walberg, G. D., Gasperich, F. J., and Scheyhing, E. R., _National Space Transportation and Support Study/Technology Requirements and Plans_, presented to AIAA Space Systems Technology Conference, San Diego, California, 8-12 June 1986.

Wang, Z. L. and Deng, Z. P., "Sloshing of Liquid in Spherical Tanks at Low Gravity Environments", _Chinese Journal of Space Science_, vol. 5, pp. 294-302, October 1985.

Weast, R. C., ed., _CRC Handbook of Chemistry and Physics_, 66th Ed., CRC Press, 1986.

617

Wertz, J. R., ed., Spacecraft Attitude Determination and Control, Reidel Publishing, 1985.

Weydandt, J. and others, The Evolution of a Serviceable Eureca, IAF Paper no. 86-38, presented to 37th Congress of the International Astronautic Federation, Innsbruck Austria, 4-11 October 1986.

Wolff, E. A., Spacecraft Technology, Spartan Books, 1962.

Wong, E. C., "Attitude Control System for the Extreme Ultraviolet Explorer Satellite", Journal of the Astronautical Sciences, vol. 33, n. 4, pp. 401-416, October-December 1985.

Woodruff, W. L., "An Experimental Evaluation of Metallic Diaphragms for Positive Fuel Expulsion in the Atmosphere Explorer Hydrazine Propulsion Subsystem", Proceedings 1972 JANNAF Propulsion Meeting: Monopropellant Hydrazine Propusion System Sessions, Chemical Propulsion Information Agency Publication 228, vol. 4, pp. 171-182, December 1972.

Yenne, B., The Encyclopedia of US Spacecraft, Exeter Books, 1985.

Zedd, M., Personal notes on "Spin Dynamics of SLD", Naval Research Laboratory, 27 December 1982.

Zedd, M., Personal notes on "Preliminary summary of energy dissipation equations for NRL GDMS test data conversion to fluid mechanical model", Naval Research Laboratory, 5 November 1986.

Zedd, M. F. and Dodge, F. T., Energy Dissipation of Liquids in Nutating Spherical Tanks Measured by a Forced Motion Spin Table, Naval Research Laboratory Report 8932, 225488/// 30 October 1985.

Zucker, R. D., Fundamentals of Gas Dynamics, Matrix Publishers, Inc., 1977.

Zuoyi, H., The Launching Opportunities for Small Satellites, presented to 37th Congress of the International Astronautic Federation, Innsbruck Austria, 4-11 October 1986.

INITIAL DISTRIBUTION LIST

No. of Copies

1. Defense Technical Information Center   2
   Cameron Station
   Alexandria, VA 22304-6145

2. Library, Code 0142   2
   Naval Postgraduate School
   Monterey, CA 93943-5002

3. Distinguished Professor Allen E. Fuhs (Emeritus)   2
   P.O. Box 3258
   Monterey, CA 93942

4. Professor Harold Titus   1
   Code 62TI
   Naval Postgraduate School
   Monterey, CA 93943-5000

5. Professor Rudolph Panholzer   5
   Code 62PZ
   Naval Postgraduate School
   Monterey, CA 93943-5000

6. Chairman, Dept. of Electrical & Computer Engineering   1
   Code 62
   Naval Postgraduate School
   Monterey, CA 93943-5000

7. Director of Research Administration   1
   Code 012
   Naval Postgraduate School
   Monterey, CA 93943-5000

8. United States Space Command   1
    Attn: Technical Library
    Peterson AFB, CO 80914

9. Naval Space Command   2
    Code N13
    Dahlgren, VA 22448

10. Commander, Naval Space Surveillance Activity   1
    Attn: D. Diaz, CAPT, USN
    Dahlgren, VA 22448

11. Commander   5
    Naval Military Personnel Command
    Sea Duty Component
    Attn: Austin Boyd, LCDR, USN
    P. O. Box 16134
    Arlington, VA 22215-1134

12. Air Force Systems Command   1
    HQ/AFSC - XRB
    Attn: Mark Foster, CAPT, USAF
    Andrews AFB, DC 20334-5000

13. Headquarters, United States Air Force   5
    AFTAC/TXN
    Attn: Joseph Nicholas, CAPT, USAF
    Patrick AFB, FL   32925

14. Office of Naval Research   1
    Patent Office
    Attn: Mr. John Forrest
    Code 00c-P-11
    800 North Quincy Street
    Arlington, VA 22217-5000

15. Commander, Naval Space Systems Activity   1
    P. O. Box 92960
    Worldway Postal Center
    Los Angeles, CA 90009

16. Defense Advanced Research Projects Agency   1
    ASTP Program Office
    Attn: Dr. Bill Marquitz
    1400 Wilson Blvd.
    Arlington, VA 22209

17. Commander, United States Air Force Academy   1
    Department of Astronautical Engineering
    USAF/DFAS
    Attn: Nancy Rhoades, CAPT, USAF
    Colorado Springs, CO 80840

18. Dr. Peter Wilhelm   1
    Director, Space Systems Division
    Code 7700
    Naval Research Laboratory
    Washington, DC 20375

19. Commander, United States Air Force Space Test Program 1
    USAF/STP Code YC
    Attn: Michael Bitzer, CAPT, USAF
    P. O. Box 92960
    Los Angeles, CA 90009

20. National Aeronautics and Space Administration   1
    Director, Customer Services
    NASA/HQ
    600 Independence Avenue
    Washington, DC 20546

21. National Aeronautics and Space Administration   1
    Technical Library
    NASA Headquarters
    600 Independence Avenue
    Washington, DC 20546

22. Mr. Michael Michaud   1
    Director, Advanced Technology Office
    United States Department of State
    Washington, DC   20301

23. Mr. Karry Nock   1
    Jet Propulsion Laboratory
    Station 4-2153
    Mail 301-1700 Section 132
    4800 Oak Grove Blvd.
    Pasadena, CA 91109

24. Space Vector Corporation   1
    Attn: Mr. Clay Bushnell
    19631 Prairie Street
    Northridge, CA 91324

25. Public Affairs Officer   1
    Attn: Mr. John Sanders
    Naval Postgraduate School
    Monterey, CA 93943

26. Mr. Marty Mosier   2
    Space Systems Academic Group
    Code 072
    Naval Postgraduate School
    Monterey, CA 93943

27. National Aeronautics and Space Administration   1
    Technical Operations Branch
    Attn: Harold Moffitt, Technology Development Officer
    National Space Technology Laboratories
    NSTL Station. MS 39529

28. Professor Peter Banks   1
    Director
    STAR Laboratory
    Department of Electrical and Computer Engineering
    Stanford University
    Stanford, CA 94305

29. Mr. Richard Rasmussen   1
    President
    Eagle Canyon Research Corp.
    4520 Eagle Canyon Road
    Placerville, CA 95667

30. Dr. Joseph Angelo, Jr.   1
    Director, Advanced Technology
    BG&G, Inc.
    100 Byster Boulevard
    Rockledge, FL 32955

31. Mr. James Bartron   1
    Manager, Business Department
    Rocket Research Company
    P. O. Box 97009
    11441 Willows Road, N.E.
    Redmond, WA 98073-9709

32. Mr. Harry Bixby   1
    Manager, Advanced Programs - New Business
    Lockheed Astronautics Division
    O/50-20 B/102
    1111 Lockheed Way
    Sunnyvale, CA 94089-3504

33. Mr. Gary Hudson   1
    President
    Pacific American Launch Systems
    10 Twin Dolphin Drive
    Redwood City, CA 94065

34. Dr. Francois Martel   1
    Vice President - Marketing/Sales
    Spacecraft Instrumentation & Marketing Division
    Ithaco, Inc.
    735 W. Clinton St.
    Ithaca, NY 14850

35. Mr. Jack Schwartz   1
    Head, SSPO Program Branch
    Strategic Systems and Sciences Division
    Naval Weapons Station
    Seal Beach, CA 90740

36. Commander   1
    Space and Naval Warfare Systems Command
    (PMW-145)
    Attn: J. Fontana, CAPT, USN
    Washington, DC 20363-5100

37. Strategic Defense Initiative Office   2
    Innovative Science and Technology (SDIO/IST)
    Attn: Dr. James Ionson
    Pentagon
    Washington, DC 20301

38. Mr. Robert D'Austilio   1
    President
    Intra-Space, Inc.
    16354 Grayville Rd.
    La Marada, CA 90638

39. Dr. Robert Lindberg   1
    Director, Advanced Projects
    Orbital Sciences Corporation
    12500 Fair Lakes Circle
    Fairfax, VA 22033

40. Mr. Bill Crook   1
    Program Development Manager
    Secure Systems
    Motorola, Inc.
    Government Electronics Group
    2501 South Price Road
    Chandler, AZ 85248-2899

41. Mr. George Pieper   1
    United States Naval Academy
    Aerospace Engineering Department
    MS 11B
    Annapolis, MD 21402

42. Mr. Bruce Bollerman   1
    Space Data Corporation
    1333 W. 21st Street
    Tempe, AZ 85282

43. Chief of Naval Operations   1
    Director, Navy Space Systems Division
    (OP-943)
    Attn: B. Cargill, RADM, USN
    Pentagon
    Washington, DC 20301

44. Chief of Naval Operations   1
    Director, Tactical Air, Surface and EW Division
    (OP-982)
    Attn: R. Shumaker, RADM, USN
    Pentagon
    Washington, DC 20350-2000

45. Commander   1
    Space and Naval Warfare Systems Command
    (PD-80)
    Attn: C. Dorman, RADM, USN
    Washington, DC 20361-5100

46. Commander   1
    Space and Naval Warfare Systems Command
    (PMW-181)
    Attn: J. Sabatini, CDR, USN
    Washington, DC 20361-5100

47. National Aeronautics and Space Administration   1
     Director, Shuttle Operations
     Attn: R. Truly, RADM, USN
     600 Independence Avenue
     Washington, DC 20546

48. Commander   1
     Space and Naval Warfare Systems Command
     (PDW 106-5)
     Attn: R. Betterton, RADM, USN
     4555 Overlook Drive, SW
     Washington, DC 20375

49. Commander   1
     Space and Naval Warfare Systems Command
     (PDW 106-5)
     Attn: B. Kosinski, LT, USN
     4555 Overlook Drive, SW
     Washington, DC 20375

50. Robert Springer, COL, USMC   1
     Astronaut Office
     Code CB
     Johnson Space Center
     Houston, TX 77058

END

DATE
FILMED

8-88
DTIC